

(NASA-TM-84557) AERODYNAMIC CHARACTERISTICS
OF A SERIES OF SINGLE-INLET AIR-BREATHING
MISSILE CONFIGURATIONS (NASA) 363 F
HC A16/MF A01 -

N83-18666

CSCL 16D

Unclas

G3/02

02920

NASA Technical Memorandum 84557

**Aerodynamic Characteristics
of a Series of Single-Inlet
Air-Breathing Missile
Configurations**

Clyde Hayes
Langley Research Center
Hampton, Virginia



National Aeronautics
and Space Administration

Scientific and Technical
Information Branch

1983

SUMMARY

A series of air-breathing missile configurations has been investigated to provide a data base for the design of such missiles. The model could be configured with either a single axisymmetric or a two-dimensional inlet located at the bottom of the body. Two tail configurations were investigated: a tri-tail and an X-tail. The tail surfaces could be deflected to provide pitch control. A wing could be located above the inlet on the center line of the model. Tests were made at supersonic Mach numbers with the inlet open and internal flow, and at subsonic-transonic Mach numbers with the internal duct closed and no internal flow.

At supersonic Mach numbers, the body-inlet and the body-inlet-wing configurations were unstable longitudinally, had a negative pitching moment at an angle of attack, α of 0° but had a linear pitching-moment curve up to about $\alpha = 10^\circ$. The body-inlet-tail configuration was longitudinally stable, had a positive pitching moment at $\alpha = 0^\circ$, and also had a linear pitching-moment curve up to about $\alpha = 10^\circ$. Also at supersonic Mach numbers, the body-inlet-wing-tail configuration was longitudinally stable, had a positive pitching moment at $\alpha = 0^\circ$, and had a nonlinear pitching-moment curve at low angles of attack. The body-inlet-wing-tail configuration, with either inlet or either tail, trimmed at $\alpha = 20^\circ$ with -12° or less of pitch-control deflection. However, the pitch-control effectiveness was greater with the X-tail than with the tri-tail. Only with the X-tail was the body-inlet-wing-tail configuration directionally stable for the entire angle-of-attack range, although the X-tail had a detrimental effect on the lateral stability compared to the tri-tail.

At subsonic-transonic Mach numbers, the nonlinearity of the pitching-moment curves for the body-inlet-wing-tail configuration was greater than at supersonic Mach numbers and was greatest for the X-tail configuration. The body-inlet-wing-tail configuration with the X-tail was stable both laterally and directionally for the entire angle-of-attack range. At both supersonic and subsonic-transonic Mach numbers, the effect of inlet configuration was small.

INTRODUCTION

During the past several years, several air-breathing missile configurations have been investigated in the Langley Unitary Plan Wind Tunnel. These include one-, two-, and four-inlet configurations with various wing and tail arrangements. The results of these investigations have been reported in references 1 through 7. While the data from these specific missile programs have contributed to an air-breathing configuration data base, a broader data base is needed to better predict the aerodynamic characteristics of candidate configurations and to better design an air-breathing configuration to meet desired aerodynamic specifications. Therefore, to provide a broader data base, a series of models has been designed and tested incorporating a wider range of configuration variables.

The model could be configured with either axisymmetric or two-dimensional (2-D) single or twin inlets. The single inlet was located at the bottom of the body, while the twin inlets could be located circumferentially from 90° to 135° from the top center. Two vertical wing locations were available to properly locate the wing relative to the inlets at orientation angles of 115° and 135° to provide favorable inter-

ORIGINAL PAGE IS
OF POOR QUALITY

ference between the wing and inlet at positive angles of attack. Tail surfaces could be mounted on the inlet fairing and/or on fairings on the body to provide several tail configurations. The tail surfaces could be deflected to provide pitch control. The 2-D inlets could be configured with extended compression surfaces in order to improve the angle-of-attack performance of the inlets for the wingless configuration.

The present investigation covers tests of the single-inlet configurations for both axisymmetric and 2-D inlets at supersonic and subsonic-transonic Mach numbers. The results of the twin-inlet investigation are presented in references 8, 9, and 10.

Two tail configurations were investigated: a tri-tail and an X-tail. The tests included body-inlet, body-inlet-wing, body-inlet-tail, and body-inlet-wing-tail configurations.

The supersonic tests were performed in the high Mach number test section of the Langley Unitary Plan Wind Tunnel at Mach numbers of 2.50, 2.95, 3.50, and 3.95. To simulate ramjet operation, the inlets were operating with flow through the model. The subsonic-transonic tests were conducted in the 7- by 10-Foot Transonic Wind Tunnel at the David Taylor Naval Ship Research and Development Center at Mach numbers of 0.60, 0.80, and 0.95. To simulate rocket boost, the internal ducts were closed with no internal flow through the model.

Longitudinal aerodynamic characteristics, lateral-directional stability, pitch-control effectiveness, and trim characteristics were obtained.

SYMBOLS

The coefficients of forces and moments are referred to both the body-axis and stability-axis systems, where appropriate. Aerodynamic moments are taken about a point on the model center line at a distance downstream of the model nose equal to 52 percent of the body length (fig. 1). All coefficients are based on the cross-sectional area and diameter of the body.

A	cross-sectional area of basic body, 0.00456 m ²
C _A	axial-force coefficient, $\frac{\text{Axial force}}{qA}$
C _{A,i}	internal-flow axial-force coefficient, $\frac{\text{Internal-flow axial force}}{qA}$
C _D	drag coefficient, $\frac{\text{Drag}}{qA}$
C _L	lift coefficient, $\frac{\text{Lift}}{qA}$
C _{l_β}	effective-dihedral parameter, $\left(\frac{\Delta C_l}{\Delta \beta} \right)$ (β = 0°, 5° at M < 1; β = 0°, 3° at M > 1)
C _m	pitching-moment coefficient, $\frac{\text{Pitching moment}}{qAd}$

C_N	normal-force coefficient, $\frac{\text{Normal force}}{qA}$
$C_{n\beta}$	directional-stability parameter, $\left(\frac{\Delta C_n}{\Delta \beta}\right)$ ($\beta = 0^\circ, 5^\circ$ at $M < 1$; $\beta = 0^\circ, 3^\circ$ at $M > 1$)
$C_{y\beta}$	side-force parameter, $\left(\frac{\Delta C_y}{\Delta \beta}\right)$ ($\beta = 0^\circ, 5^\circ$ at $M < 1$; $\beta = 0^\circ, 3^\circ$ at $M > 1$)
d	body diameter, 0.0762 m.
L/D	lift-drag ratio
M	free-stream Mach number
$M.S.$	model station
m/m_∞	inlet mass-flow ratio (ratio of inlet mass flow to mass flow at free-stream conditions through a stream tube of cross-sectional area equal to inlet projected area)
q	free-stream dynamic pressure, Pa
x, y, y_1, y_2, y_3	model coordinates (figs. 1(c) and 1(d))
α	angle of attack, deg
β	angle of sideslip, deg
δ_p	tail deflection in pitch direction, (positive deflection with leading edge up) deg
2-D	two-dimensional (rectangular-type inlet)

Configuration designations (various components are shown in fig. 1):

B_1	body
I_4	circular inlet (axisymmetric)
I_5	rectangular inlet (2-D)
I_{5c}	rectangular inlet with inlet covers installed
T_1	tri-tail
T_2	X-tail
W_1	wing

MODEL DESCRIPTION

Details of the models are presented in figure 1, and photographs in figure 2. The body was an ogive cylinder approximately 14 diameters long. A single-inlet of either the axisymmetric or rectangular type (2-D) was located beneath the body and separated from the body by a boundary-layer diverter. The internal duct extended downstream of the inlet to a point where it would turn and dump into the combustor. Beyond this point, the external geometry of the inlet consisted of a tapered fairing extending back to the base.

On the model, the duct dumped into a passage within the body. The internal flow was kept separate from the balance cavity to facilitate measurement of the internal-duct and balance-cavity axial-force and drag corrections. A rake at the exit of the internal duct was used to measure flow conditions needed to compute the axial force due to internal flow.

The design of the inlets was identical to that of the twin inlets of references 8, 9, and 10, except that the size of the single inlet was increased so that the total capture areas were the same (Capture area = $0.50A$). The 2-D inlet had a boundary-layer bleed slot which removed the boundary layer from the compression surface and dumped it overboard. The axisymmetric inlet had no boundary-layer control.

The tail surfaces were attached to the body by means of fairings, which provided the necessary support and represented the volume that would be required for the tail-control actuators. Two tail configurations were used: a tri-tail and an X-tail. The tri-tail had a vertical surface at the top center and horizontal surfaces at circumferential locations of 90° and 270° . The X-tail had four surfaces: two at the upper 45° locations and two at the bottom 45° locations. For pitch control, the two horizontal surfaces of the tri-tail were deflected, while all four surfaces of the X-tail were deflected. Tail-surface deflections were measured in the plane normal to the hinge line.

TESTS

Supersonic Tests

The supersonic part of the investigation was conducted in the high Mach number test section of the Langley Unitary Plan Wind Tunnel at Mach numbers of 2.50, 2.95, 3.50, and 3.95. The tunnel is a variable-pressure continuous-flow facility having two test sections each approximately 1.2 m square and 2.1 m long. The nozzles leading to the test sections are of the asymmetric sliding-block type, which gives continuous variation in the supersonic Mach number range. A description of the facility is given in reference 11. A rake having eight total-pressure tubes and four static-pressure tubes was used to measure the flow conditions at the internal-duct exit. Base-pressure measurements were made with static orifices on the model base, and balance-cavity pressures were measured with two static-pressure tubes attached to the sting and terminating near the balance. Forces and moments were measured with a six-component, sting-mounted, strain-gage balance. Separate runs were made for the internal-flow measurements; force data from these runs are not presented herein. However, typical internal-flow data computed from these measurements are presented in figure 3.

Tests were made at angles of attack ranging from about -5° to $+20^\circ$. To obtain lateral-directional stability, runs at angles of sideslip of 0° and 3° were made.

Angles of attack and sideslip were corrected for tunnel-flow angularity and for deflection of the sting and balance due to aerodynamic loads. The axial-force and drag data were adjusted to free-stream static pressure acting over the model base and balance chamber areas. An adjustment was made to remove internal drag, that is, the drag associated with the streamwise momentum and buoyancy of flow passing internally from the free-stream to exit conditions. The Reynolds number was maintained constant at 6.56×10^6 per meter. The stagnation dew point was maintained below 239 K to avoid condensation effects.

All tests were made with the boundary-layer transition point fixed by means of transition strips. The transition strips were located 3.05 cm aft of the body nose and 1.02 cm in a streamwise direction from the leading edges of the wings, tail surfaces, and inlets. The transition strips consisted of No. 35 sand grains individually spaced.

Subsonic-Transonic Tests

The subsonic-transonic part of the investigation was conducted in the 7- by 10-Foot Transonic Wind Tunnel at the David Taylor Naval Ship Research and Development Center. The tunnel is a continuous-flow closed-loop facility capable of operating over a Mach number range from 0.4 to 1.17 and a dynamic pressure range corresponding to altitudes from sea-level to 40 000 ft. A description of the facility is given in reference 12. The tests were performed at Mach numbers of 0.60, 0.80, and 0.95.

The internal ducts were closed at the point where flow would enter the body, so that there was no internal flow for the subsonic-transonic tests. The tube used in the supersonic tests to separate the internal flow from the balance cavity was removed and the entire cavity was treated as a balance chamber. The cavity pressure was measured by two static-pressure tubes attached to the sting, terminating near the balance. Forces and moments were measured by a sting-mounted, six-component balance furnished by NASA.

Tests were made at angles of attack ranging from about -5° to $+28^\circ$. Some runs were terminated at lower angles of attack because of the balance limits. To obtain lateral-directional stability, runs at angles of sideslip of 0° and 5° were made. Angles of attack and sideslip were corrected for deflection of the sting and balance due to aerodynamic loads. The axial-force and drag data were adjusted to free-stream static pressure acting over the model base, including the data measured in the balance cavity and at the internal-duct exit.

The Reynolds number of the tests was 8.5, 9.5, and 10.0×10^6 per meter at Mach numbers of 0.60, 0.80, and 0.95, respectively. All tests were made with the boundary-layer transition point fixed by means of transition strips. The transition strips were located 3.66 cm aft of the body nose and 1.78 cm in a streamwise direction from the leading edges of the wing, tail surfaces, and inlets. The transition strips, 0.325 cm wide, consisted of No. 90 grit on the aerodynamic surfaces and No. 100 grit on the nose.

PRESENTATION OF RESULTS

The results of this investigation are presented in the figures listed in the following tables:

ORIGINAL PAGE IS
OF POOR QUALITY

Supersonic Mach Numbers

The following table lists figures presenting results of tests made at supersonic Mach numbers with the inlet open and internal flow:_____

Wing	Tail	δ_p , deg	Variable	Effect measured	Figure
Axisymmetric inlet, I_4					
On-off	T_1	0	Model components	Longitudinal	4
On-off	T_2	0	Model components	Longitudinal	5
Off	Varies	0	Tail configuration	Longitudinal	6
On	Varies	0	Tail configuration	Longitudinal	7
Off	T_1	Varies	δ_p	Pitch-control effectiveness	8
Off	T_2	Varies	δ_p	Pitch-control effectiveness	9
On	T_1	Varies	δ_p	Pitch-control effectiveness	10
On	T_2	Varies	δ_p	Pitch-control effectiveness	11
On-off	T_1	0	Model components	Lateral-directional	12
On-off	T_2	0	Model components	Lateral-directional	13
Off	Varies	0	Tail configuration	Lateral-directional	14
On	Varies	0	Tail configuration	Lateral-directional	15
Two-dimensional inlet, I_5					
On-off	T_1	0	Model components	Longitudinal	16
On-off	T_2	0	Model components	Longitudinal	17
Off	Varies	0	Tail configuration	Longitudinal	18
On	Varies	0	Tail configuration	Longitudinal	19
Off	T_1	Varies	δ_p	Pitch-control effectiveness	20
Off	T_2	Varies	δ_p	Pitch-control effectiveness	21
On	T_1	Varies	δ_p	Pitch-control effectiveness	22
On	T_2	Varies	δ_p	Pitch-control effectiveness	23
On-off	T_1	0	Model components	Lateral-directional	24
On-off	T_2	0	Model components	Lateral-directional	25
Off	Varies	0	Tail configuration	Lateral-directional	26
On	Varies	0	Tail configuration	Lateral-directional	27

Subsonic-Transonic Mach Numbers

The following table lists figures presenting results of tests made at subsonic-transonic Mach numbers with the internal duct closed and no internal flow:

Wing	Tail	δ_p , deg	Variable	Effect measured	Figure
Axisymmetric inlet, I_4					
On-off	T_1	0	Model components	Longitudinal	28
On-off	T_2	0	Model components	Longitudinal	29
Off	Varies	0	Tail configuration	Longitudinal	30
On	Varies	0	Tail configuration	Longitudinal	31
Off	T_1	Varies	δ_p	Pitch-control effectiveness	32
Off	T_2	Varies	δ_p	Pitch-control effectiveness	33
On	T_1	Varies	δ_p	Pitch-control effectiveness	34
On	T_2	Varies	δ_p	Pitch-control effectiveness	35
On-off	T_1	0	Model components	Lateral-directional	36
On-off	T_2	0	Model components	Lateral-directional	37
Off	Varies	0	Tail configuration	Lateral-directional	38
On	Varies	0	Tail configuration	Lateral-directional	39
Two-dimensional inlet, I_5					
On-off	T_1	0	Model components	Longitudinal	40
On	T_1	0	δ_p	Pitch-control effectiveness	41
On-off	T_1	0	Model components	Lateral-directional	42
Off	Off		Inlet cover	Longitudinal	43
Off	Off		Inlet cover	Lateral-directional	44

DISCUSSION OF RESULTS

Supersonic Tests

The effects of the various model components on the longitudinal aerodynamic characteristics are shown in figures 4 and 5 for the axisymmetric inlet and figures 16 and 17 for the 2-D inlet. With the assumed pitching-moment center location (50 percent of body length), the model was unstable without the tail, and stable with either tail (T_1 or T_2). The pitching-moment curves were linear for the model without tails up to about $\alpha = 10^\circ$ and then at $M = 2.50$ the slope decreased as the angle of attack was increased further. As the free-stream Mach number was increased, the curves tended to straighten and at $M = 3.95$ the slope increased as the angle of attack was increased above about 12° . Yet, when either tail was added, without the wing, the opposite occurred. The slope changed in the positive direction as the Mach number was increased at the high angle-of-attack end of the curves.

Without the tail, either with or without the wing, the model had a negative pitching moment at $\alpha = 0^\circ$. This effect was greatest for the axisymmetric-inlet configuration, for which $C_m \approx -1$, while for the 2-D inlet configuration, $C_m \approx -0.5$. Although longitudinally unstable at $M = 2.50$, the axisymmetric-inlet configuration trimmed at $\alpha = 2^\circ$ and 4° with and without the wing, respectively, and the 2-D inlet configuration trimmed at $\alpha = 1^\circ$ either with or without the wing. These trim angles of attack remained approximately consistent through the supersonic test Mach number range.

The configurations with tails were longitudinally stable and had pitching-moment increments at $\alpha = 0^\circ$ of about the same magnitude as the configurations without tails, but of the opposite sign. All configurations trimmed at small positive angles of attack. The pitching-moment curves were linear, except for the $B_1I_5T_1$ configuration, for which the slope of the pitching-moment curve tended to decrease (becoming less stable) at high angles of attack. Configurations $B_1I_4W_1T_1$ and $B_1I_5W_1T_1$ both had a nonlinearity of the pitching-moment curves for a range of angle of attack near 0° .

A better comparison of the effect of tail configurations is seen in figures 6 and 7 for the axisymmetric-inlet configurations and figures 18 and 19 for the 2-D inlet configurations. With the X-tail, T_2 , the nonlinearity of the pitching-moment curves begins and ends at higher angles of attack than with the tri-tail, T_1 . The relatively small differences in longitudinal aerodynamic characteristics of the two tail configurations without the wing are apparent as well as the relative location of the nonlinearities of the pitching-moment curves for configurations with the wing. This effect occurs only with both the wing and the tail in place and can be assumed to be a wing-tail interference effect. While these nonlinearities exist, they are not as extreme as those encountered with the twin-inlet configurations of references 8, 9, and 10.

To consider the effect of the various model components on the lift or normal force, the pitch-control and trim characteristics were considered. Pitch-control data are presented in figures 8 through 11 for the axisymmetric inlet configurations and figures 20 through 23 for the 2-D inlet configurations and include longitudinal characteristics with pitch-control deflections δ_p of 0° , -10° , and -20° except where limited by balance limits or model fouling.

Configurations $B_1I_4T_1$ and $B_1I_5T_1$ (figs. 8, 9, 20, and 21) trimmed at $\alpha = 20^\circ$ with $\delta_p > -20^\circ$, while the configuration with T_2 , $B_1I_4T_2$ and $B_1I_5T_2$, trimmed at $\alpha = 20^\circ$ with much less pitch-control deflection. With $\delta_p = -10^\circ$, tail T_2 trimmed

the model at about $\alpha = 15^\circ$ with I_4 , and with T_5 from $\alpha = 18^\circ$ to 20° at $M = 2.50$ and 3.95 , respectively. At $\alpha = 20^\circ$, the body-inlet-tail configuration with the axisymmetric inlet had a trimmed C_N of about 4 at $M = 2.50$ and 3.7 at $M = 3.95$; with the 2-D inlet, it had a trimmed C_N of 5 and 4.2, respectively. These values were independent of tail configuration.

With the wing added (figs. 10, 11, 22, and 23), the longitudinal stability level was decreased and less pitch control was required to trim the model at a given angle of attack. Configurations $B_1I_4W_1T_1$ and $B_1I_5W_1T_1$ trimmed at $\alpha = 20^\circ$ with $\delta_p > -12^\circ$ and the X-tail configuration had even greater pitch-control effectiveness. At $\alpha = 20^\circ$, the body-inlet-wing-tail configuration with the axisymmetric inlet had a trimmed C_N of about 9 at $M = 2.50$ and 7 at $M = 3.95$; with the 2-D inlet, it had a trimmed C_N of 10 and 8, respectively. As with the wing-off configurations, these values were independent of tail configuration.

The effect of the various model components on the lateral-directional stability characteristics is shown in figures 12 and 13 for the axisymmetric inlet and figures 24 and 25 for the 2-D inlet. Without the tail the model was unstable both laterally and directionally, although the body-inlet configuration became directionally stable at very high angles of attack (above about $\alpha = 16^\circ$). Adding the tri-tail, T_1 , resulted in a large increase in both lateral and directional stability. At $M = 2.50$, the model became directionally stable up to about $\alpha = 6^\circ$ and laterally stable up to about $\alpha = 9^\circ$ with the wing and $\alpha = 5^\circ$ without the wing, with the values decreasing with increasing Mach number.

Replacing T_1 with the X-tail, T_2 , increases directional stability not only at low angles of attack, but also at high angles of attack. The model was directionally stable for the entire range of angle of attack with or without the wing. A direct comparison of the two tail configurations is shown in figures 14 and 15 for the axisymmetric inlet and shown in figures 26 and 27 for the 2-D inlet. Not only is a large effect on directional stability apparent, but also the unfavorable effect of the X-tail on the lateral stability. With T_1 , there was a small range of angle of attack near 0° at which there was a margin of lateral stability; however, at higher angles of attack the model became unstable. With T_2 , the model was unstable laterally for the entire range of positive angle of attack.

Comparison of the lateral-directional stability data of figures 12 through 15 with that of figures 24 through 27 shows that while there was a small difference in individual data points and level of the data curves, the effects of inlet configuration were generally small and the overall trends were the same regardless of inlet configuration.

Subsonic-Transonic Tests

The effect of the various model components on the longitudinal aerodynamic characteristics are shown in figures 28 and 29 for the axisymmetric inlet and figure 40 for the 2-D inlet. The trends for the body-inlet, body-inlet-wing, and body-inlet-tail configurations were similar to those at $M = 2.50$ at angles of attack up to about 15° . With the body-inlet-wing-tail configuration, however, the nonlinearity of the pitching-moment curves was greatly increased. The result was that the model was longitudinally unstable for a range of angle of attack near 0° ; however, as the angle of attack was increased, a decrease in slope was apparent and the model became longitudinally stable. While there was little effect of inlet configuration on the longitudinal stability, the effect of tail configuration was significant.

A comparison of the effects of the two tail configurations is shown in figures 30 and 31 with the axisymmetric inlet. Apparent in the figures are the extended range of angle of attack at which the X-tail configuration with the wing was unstable and the resulting difference in the trim angle of attack for $\delta_p = 0^\circ$.

With T_2 the range of angle of attack at which the model was unstable was increased; and whereas the model with T_1 trimmed with $\delta_p = 0^\circ$ at about $\alpha = 11^\circ$, with T_2 the trim angle of attack was about 16° . The configuration with the wing had a break in the pitching-moment curves and to a lesser extent in the normal-force curves at about $\alpha = 16^\circ$. The boost configuration would not be expected to be required to operate at angles of attack as high as 16° .

A better comparison of the characteristics of the two tails can be seen in figures 32 through 35 for the axisymmetric inlet and figure 41 for the 2-D inlet which show the trim and pitch-control effectiveness of the various configurations. Without the wing and with inlet I_4 and tail T_1 , pitch control was effective, but because of a high stability level, the model trimmed at about $\alpha = 8^\circ$. Replacing T_1 with T_2 reduced the stability level and increased the pitch-control effectiveness; the model trimmed at about $\alpha = 13^\circ$. Adding the wing to form configuration $B_1 I_4 W_1 T_1$ resulted in trim characteristics that required positive pitch-control deflections for trim at angles of attack less than about 12° . Figure 34 shows data for this configuration with $\pm 10^\circ$ of pitch-control deflection. A rough estimate would indicate that the model would trim at $\alpha = 0^\circ$ with a pitch-control deflection of about $+5^\circ$. At this condition, the model would be slightly unstable longitudinally. Increasing the angle of attack to about 4° or above, and the pitch-control deflection to trim accordingly, would render the model stable. The data of figure 41, for the 2-D inlet configuration, although for only -10° of pitch-control deflection, indicated a similar trend. With tail T_2 , however, configuration $B_1 I_4 W_1 T_2$ (fig. 35) had an extended range of neutral stability or slight instability; and if the model was trimmed at angles of attack of about 10° or less, the model would be neutrally stable or slightly unstable. The X-tail, T_2 , provided greater pitch-control effectiveness than the tri-tail, T_1 , and the T_2 configuration was slightly less stable longitudinally than the T_1 configuration.

The lateral-directional stability characteristics shown in figures 36 through 39 for the axisymmetric inlet and figure 42 for the 2-D inlet show trends similar to those at supersonic Mach numbers. Whereas at supersonic Mach numbers none of the configurations were stable both laterally and directionally, the configuration with the X-tail, $B_1 I_4 W_1 T_2$, was at subsonic-transonic speeds. Whereas the X-tail configuration became unstable laterally at high angles of attack at supersonic Mach numbers, the same configuration at subsonic-transonic Mach numbers retained a small margin of lateral stability throughout most of the angle-of-attack range. Considering the lateral-directional stability characteristics both at supersonic Mach numbers with the inlet open and at subsonic-transonic Mach numbers with the inlet closed, the X-tail configuration would be a preferred configuration.

The effect of inlet covers on the lateral-directional stability of the 2-D inlet configuration, shown in figures 43 and 44, was insignificant.

CONCLUDING REMARKS

A series of air-breathing missile configurations has been investigated to provide a data base for the design of such missiles. The model could be configured with either a single axisymmetric or a two-dimensional inlet located at the bottom of the

body. Two tail configurations were investigated: a tri-tail and an X-tail. The tail surfaces could be deflected to provide pitch control. A wing could be located above the inlet on the model center line. Tests were made at supersonic Mach numbers with the inlet open and internal flow, and at subsonic-transonic Mach numbers with the internal duct closed and no internal flow.

As a result of the investigation the following general trends may be observed:

1. At supersonic Mach numbers, the body-inlet and the body-inlet-wing configurations were unstable longitudinally, had a negative pitching moment at an angle of attack α of 0° but had a linear pitching-moment curve up to about $\alpha = 10^\circ$.

2. At supersonic Mach numbers, the body-inlet-tail configuration was longitudinally stable, had a positive pitching moment at $\alpha = 0^\circ$, and had a linear pitching-moment curve up to about $\alpha = 10^\circ$.

3. At supersonic Mach numbers, the body-inlet-wing-tail configuration was longitudinally stable, had a positive pitching moment at $\alpha = 0^\circ$, and had a nonlinear pitching-moment curve at low angles of attack.

4. At supersonic Mach numbers, the body-inlet-wing-tail configuration, with either inlet or either tail, trimmed at about $\alpha = 20^\circ$ with -12° or less of pitch-control deflection. However, the pitch-control effectiveness was greater with the X-tail than with the tri-tail.

5. Only with the X-tail was the body-inlet-wing tail configuration directionally stable for the entire angle of attack range, although the X-tail had a detrimental effect on the lateral stability compared to the tri-tail.

6. At subsonic-transonic Mach numbers, the nonlinearity of the pitching-moment curves for the body-inlet-wing-tail was greater than at supersonic Mach numbers and was greatest for the X-tail configuration.

7. At subsonic-transonic Mach numbers, the body-inlet-wing-tail configuration with the X-tail was stable both laterally and directionally for the entire angle-of-attack range.

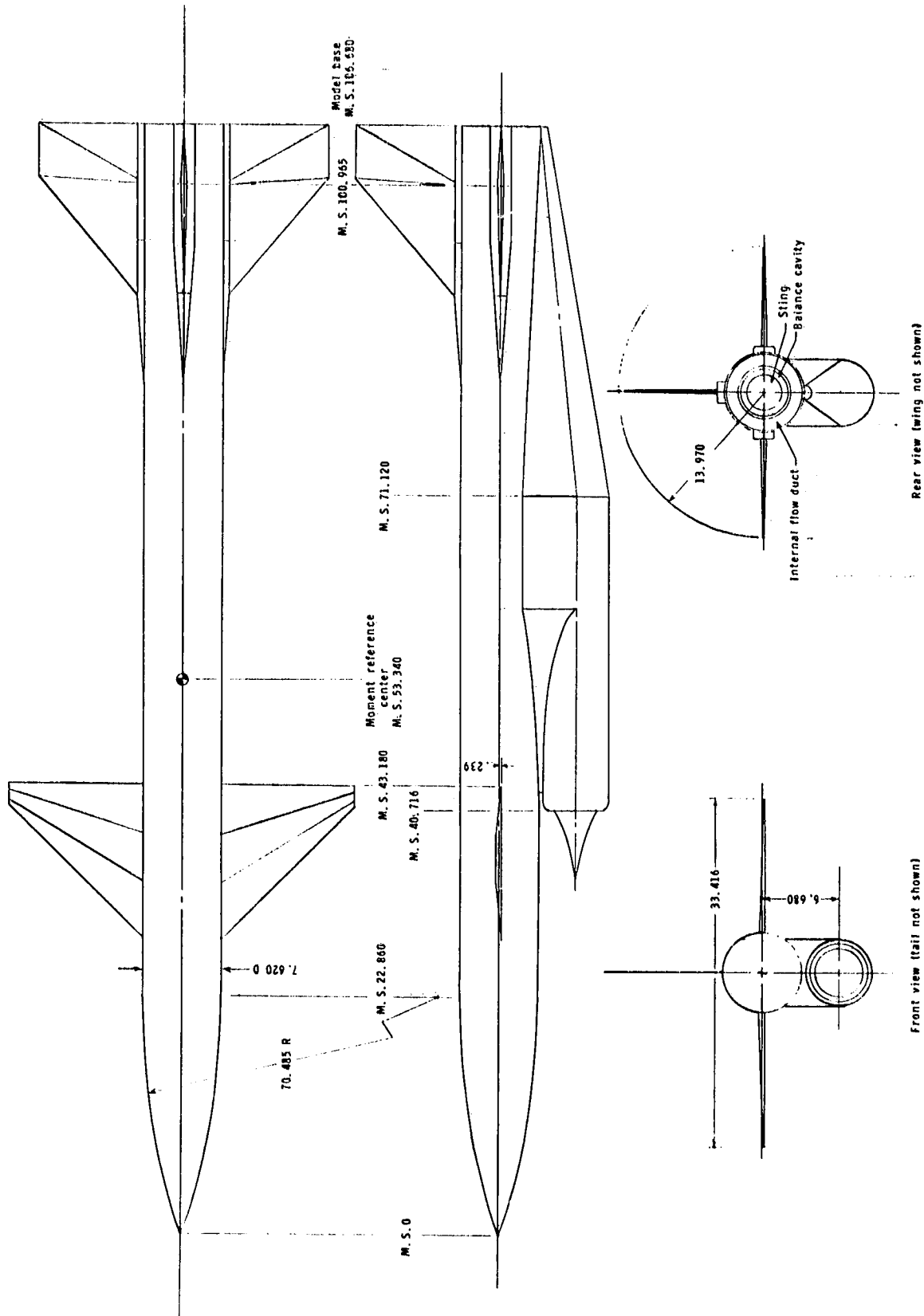
8. At both supersonic Mach numbers and subsonic-transonic Mach numbers the effect of inlet configurations was small.

Langley Research Center
National Aeronautics and Space Administration
Hampton, VA 23665
November 17, 1982

REFERENCES

1. Sawyer, Wallace C.; and Hayes, Clyde: Stability and Control Characteristics of an Air-Breathing Missile Configuration Having a Forward Located Inlet. NASA TM X-3391, 1976.
2. Hayes, Clyde; and Monta, William J.: Aerodynamic Characteristics of a 1/4-Scale Model of MORASS Missile Configurations at Supersonic Speeds. NASA TM X-3354, 1976.
3. Hayes, Clyde: Aerodynamic Characteristics of 1/4-Scale Model of ALRAAM Missile Configuration at Supersonic Speeds. NASA TM-74075, 1977.
4. Hayes, Clyde; and Sawyer, Wallace C.: Aerodynamic Characteristics of a Model Simulating the Gainful (SA-6) Missile at Supersonic Mach Numbers. NASA TM X-3493, 1977.
5. Hayes, Clyde; and Sawyer, Wallace C.: Aerodynamic Characteristics of a Series of Air-Breathing Missile Configurations Investigated as Part of the SASS Program. NASA TM-80139, 1979.
6. Hayes, Clyde: Supersonic Aerodynamic Characteristics of a Twin-Inlet Advanced Intercept Air-to-Air Missile (AIAAM) Configuration. NASA TM-83178, 1981.
7. Hayes, Clyde: Aerodynamic Characteristics of a Supersonic Single-Inlet Missile Configuration Investigated as Part of the Advanced Intercept Air-to-Air Missile (AIAAM) Program. NASA TM-83177, 1981.
8. Hayes, Clyde: Aerodynamic Characteristics of a Series of Twin-Inlet Air-Breathing Missile Configurations. I - Axisymmetric Inlets at Supersonic Speeds. NASA TM-84558, 1983.
9. Hayes, Clyde: Aerodynamic Characteristics of a Series of Twin-Inlet Air-Breathing Missile Configurations. II - Two-Dimensional Inlets at Supersonic Speeds. NASA TM-84559, 1983.
10. Hayes, Clyde: Aerodynamic Characteristics of a Series of Twin-Inlet Air-Breathing Missile Configurations. III - Axisymmetric and Two-Dimensional Inlets at Subsonic-Transonic Speeds. NASA TM-84560, 1983.
11. Jackson, Charlie M., Jr.; Corlett, William A.; and Monta, William J.: Description and Calibration of the Langley Unitary Plan Wind Tunnel. NASA TP-1905, 1981.
12. AS&D Staff: Transonic Wind-Tunnel Facility at the Naval Ship Research and Development Center. Rept. AS&D 332, U.S. Navy, June 1975.

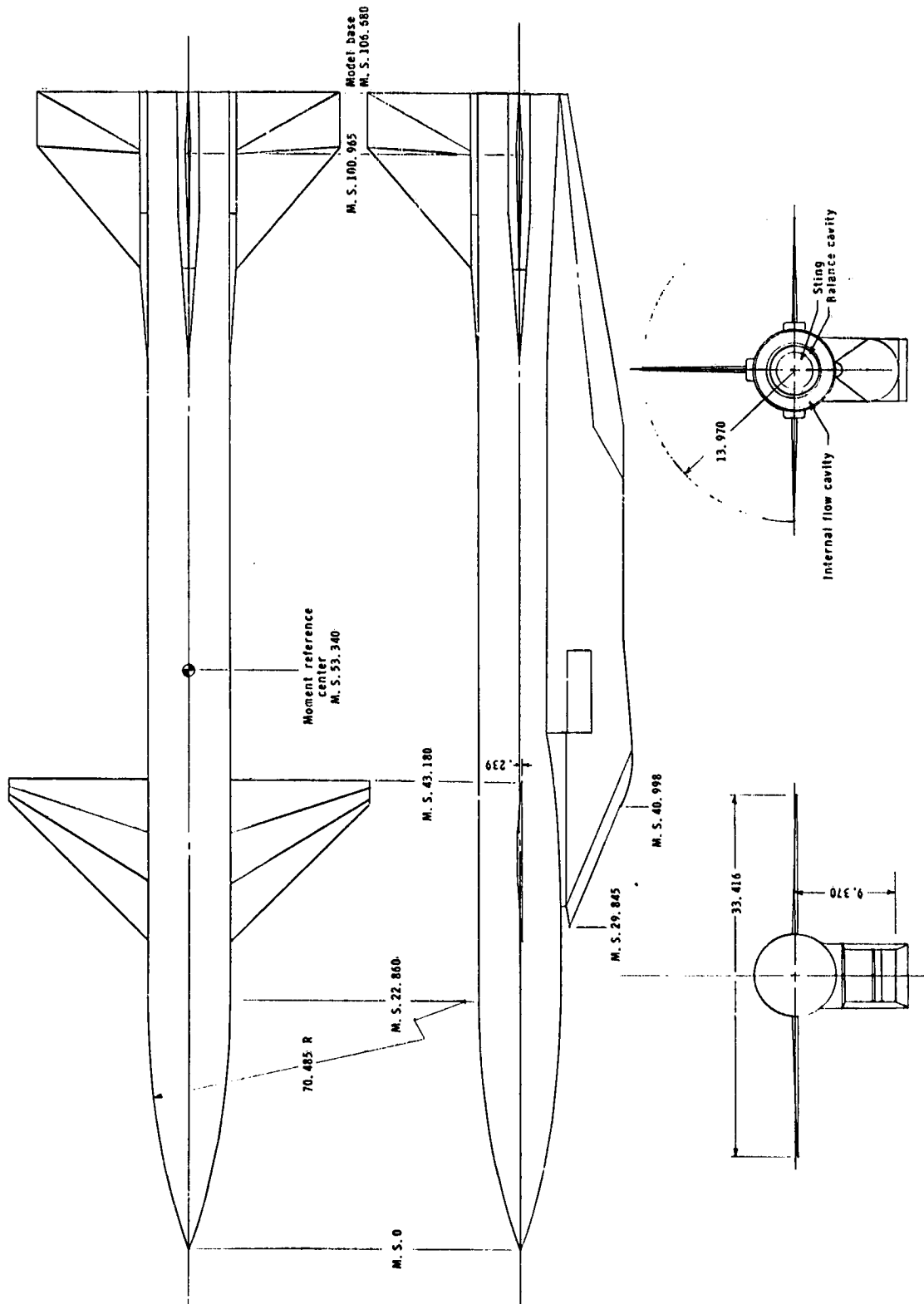
ORIGINAL PAGE IS
OF POOR QUALITY



(a) General arrangement of single axisymmetric inlet model.

Figure 1.- Details of model. All dimensions are in centimeters unless otherwise noted.

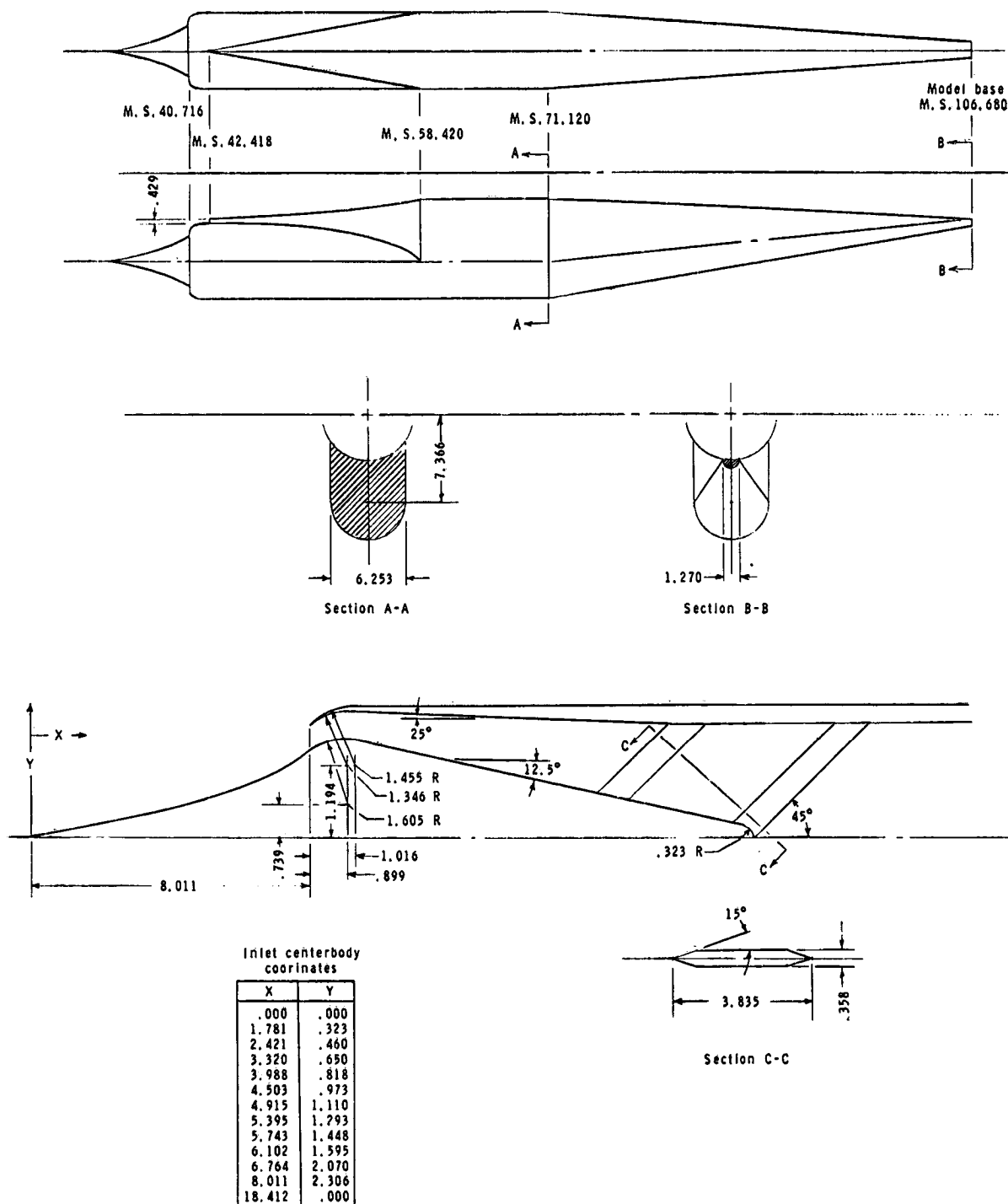
ORIGINAL PAGE IS
OF POOR QUALITY



(b) General arrangement of single 2-D inlet model.

Figure 1.- Continued.

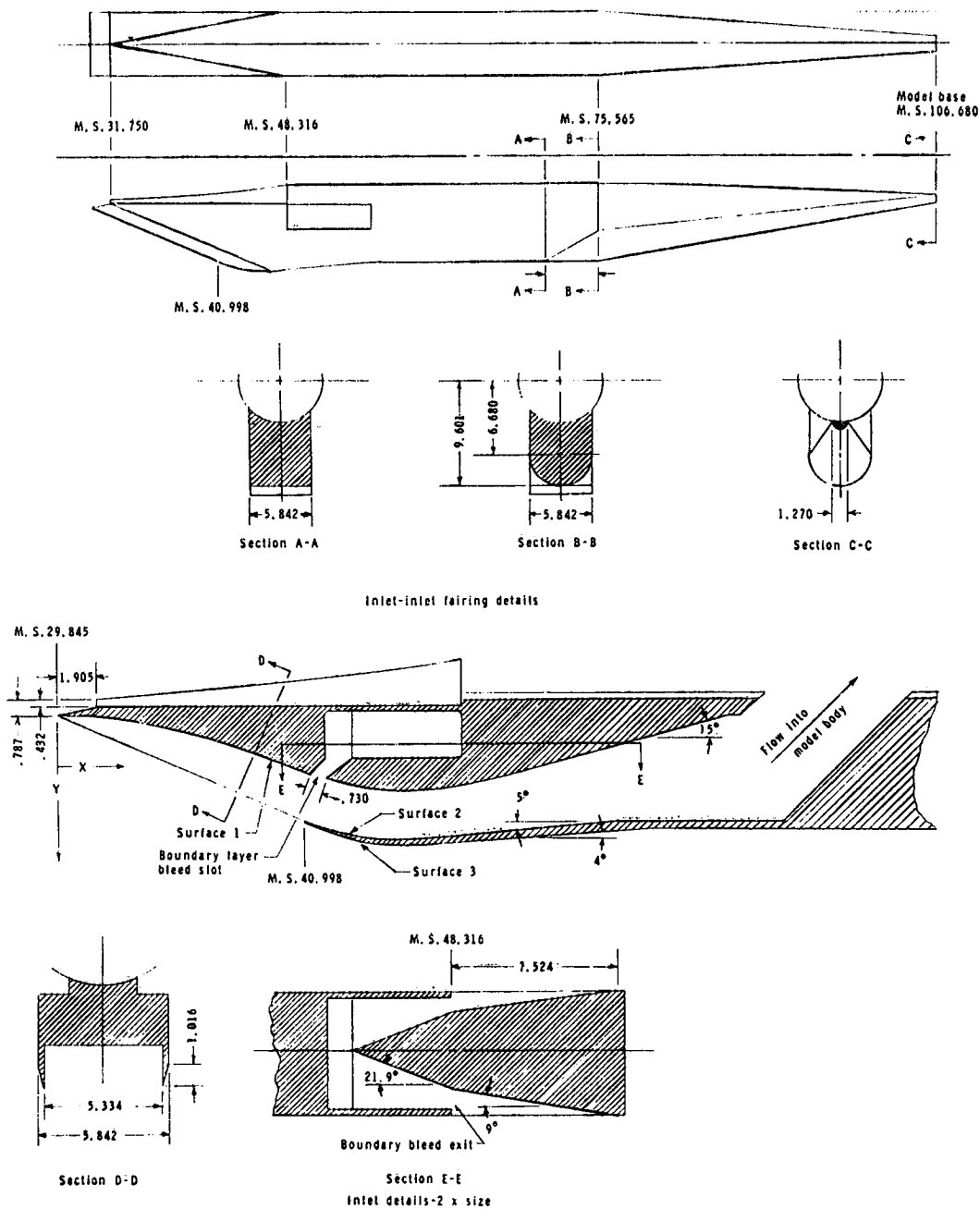
ORIGINAL PAGE IS
OF POOR QUALITY



(c) Single axisymmetric inlet and inlet fairing.

Figure 1.- Continued.

ORIGINAL PAGE IS
OF POOR QUALITY

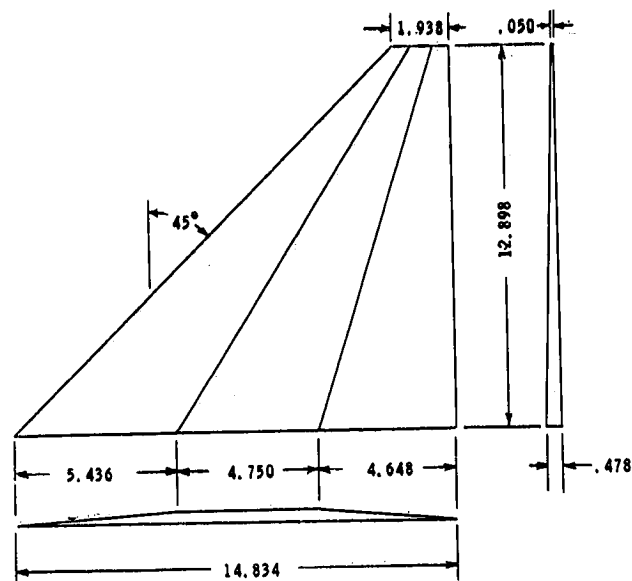


Surface 1		Surface 2 and 3		
X	Y ₁	X	Y ₂	Y ₃
.000	.000	11.153	4.773	4.773
1.829	.000	11.661	4.950	5.052
4.572	.330	12.169	5.103	5.255
5.464	.653	12.677	5.235	5.415
6.241	.938	13.185	5.347	5.550
6.919	1.013	13.693	5.441	5.662
7.508	1.196	14.201	5.509	5.743
8.049	1.377	14.709	5.555	5.799
11.791	2.743	15.217	5.585	5.839
13.005	3.048	15.725	5.585	5.865
14.529	3.302	16.233	5.565	5.865
15.982	3.409	16.741	5.519	5.839
18.543	3.073			

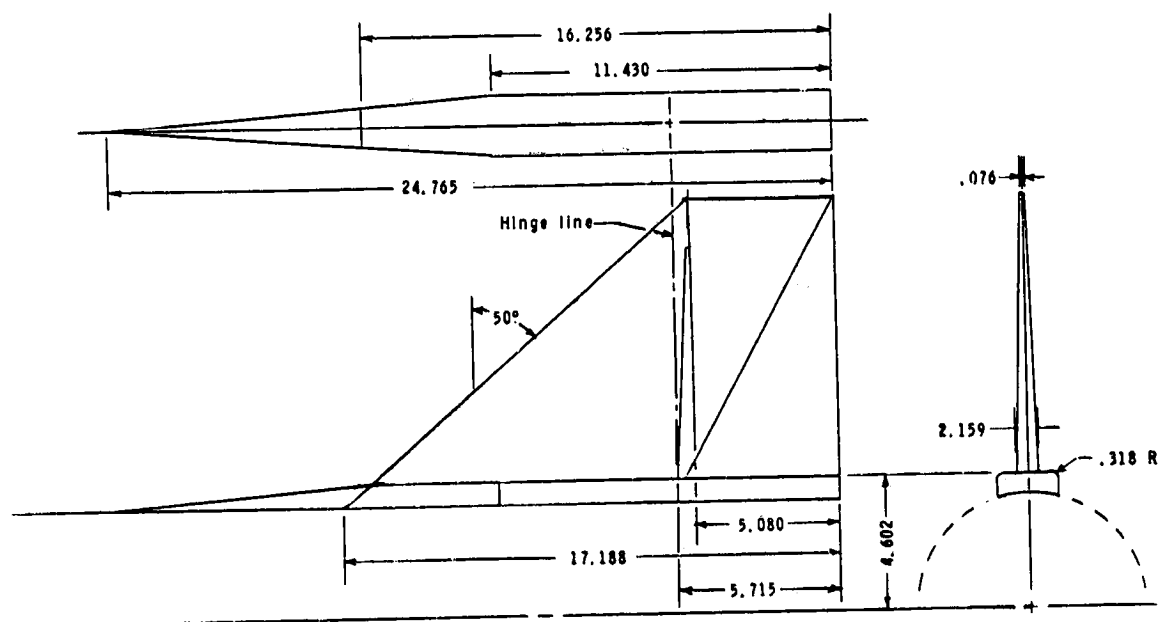
(d) Single 2-D inlet and inlet fairing.

Figure 1.- Continued.

ORIGINAL FACE IS
OF POOR QUALITY.



Wing details

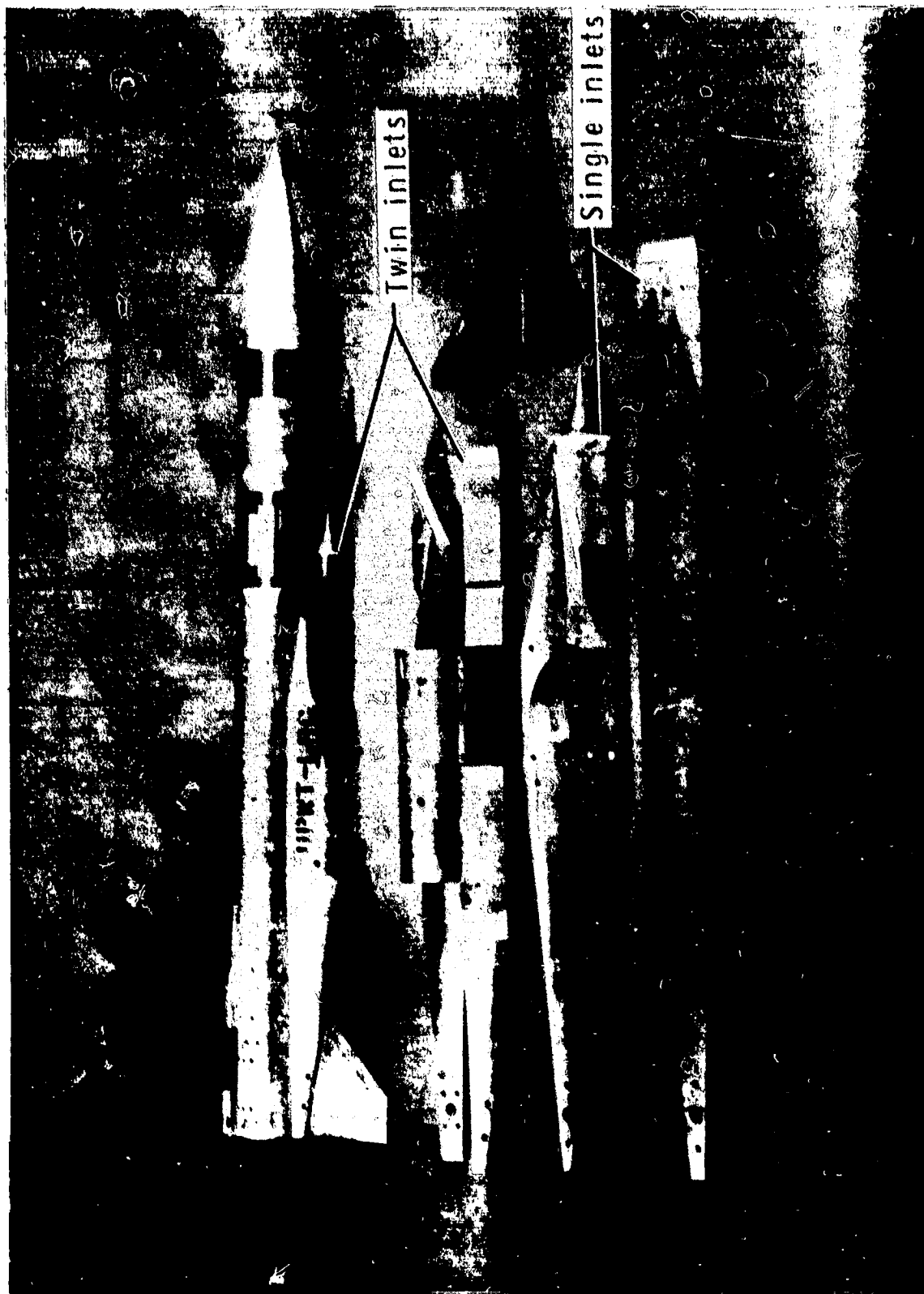


Tail-surface details

(e) Aerodynamic surfaces.

Figure 1.- Concluded.

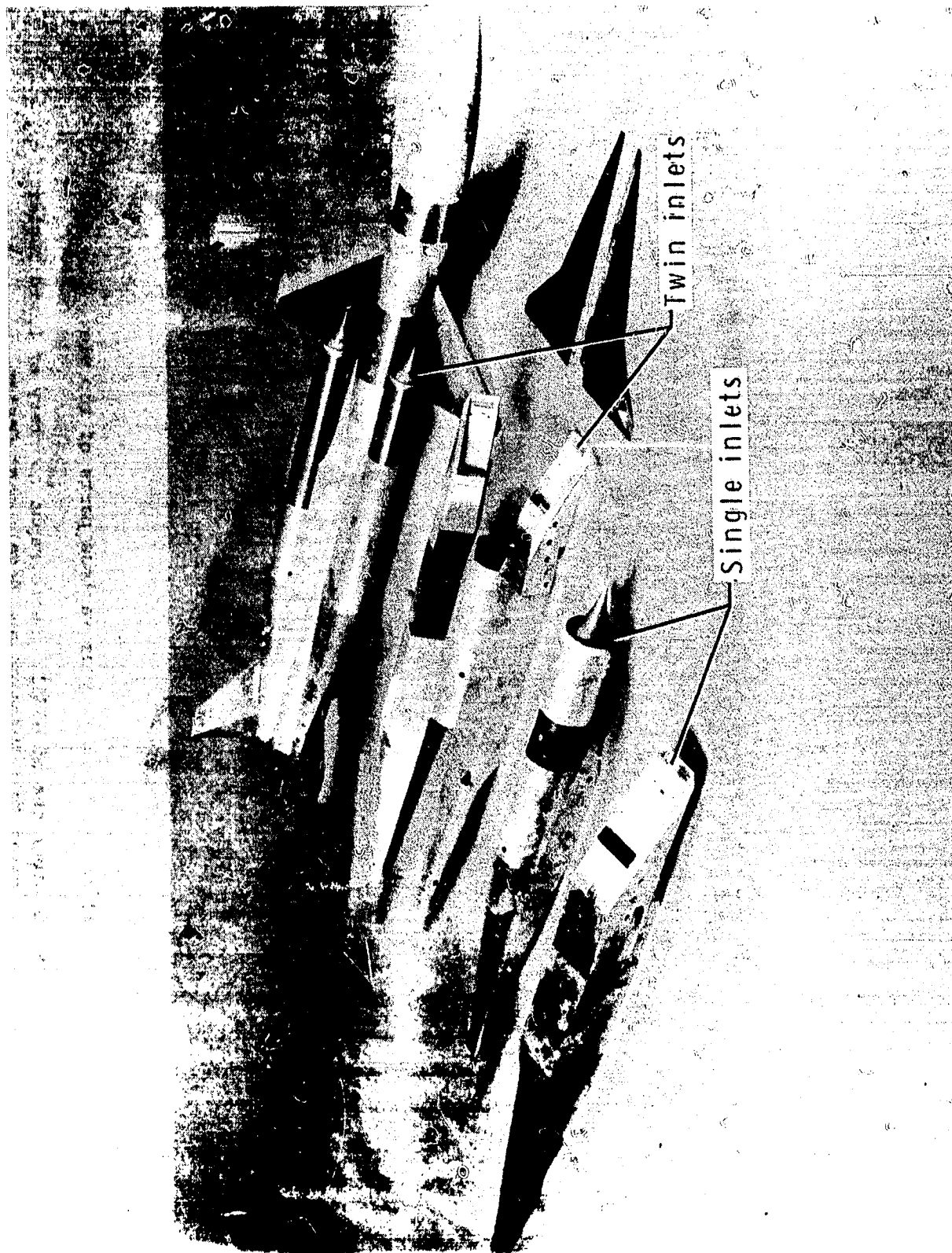
ORIGINAL PAGE IS
OF POOR QUALITY



(a) Assembled model plus various parts of top view.

Figure 2.- Photographs of model. Photographs courtesy of David Taylor
Naval Ship Research and Development Center.

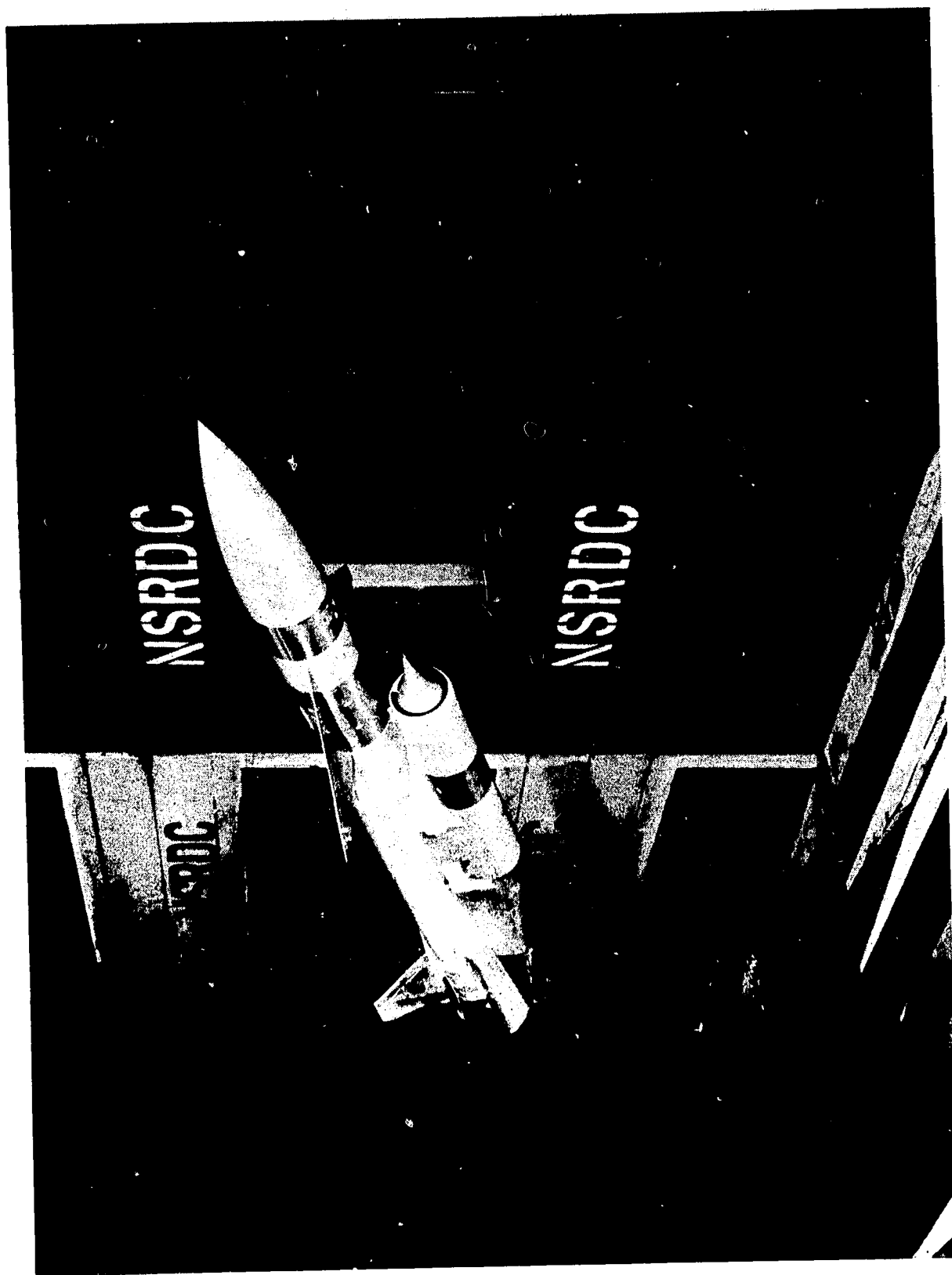
ORIGINAL PAGE
BLACK AND WHITE PHOTOGRAPH



(b) Assembled model plus various parts of bottom view.

Figure 2.- Continued.

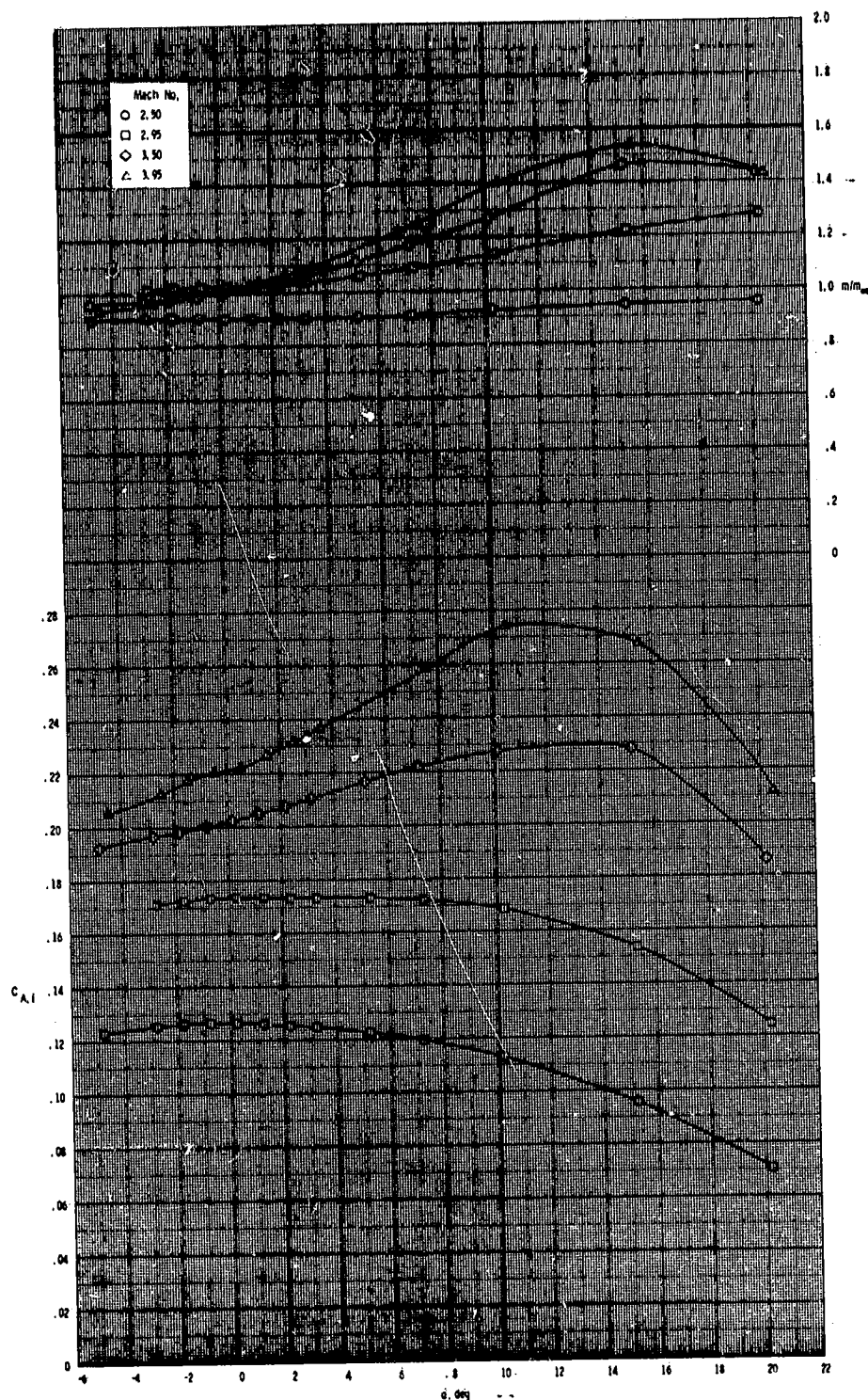
ORIGINAL PAGE
BLACK AND WHITE PHOTOGRAPH



(c) Model installed in David Taylor Naval Ship Research and Development Center
Transonic Wind Tunnel.

Figure 2.- Concluded.

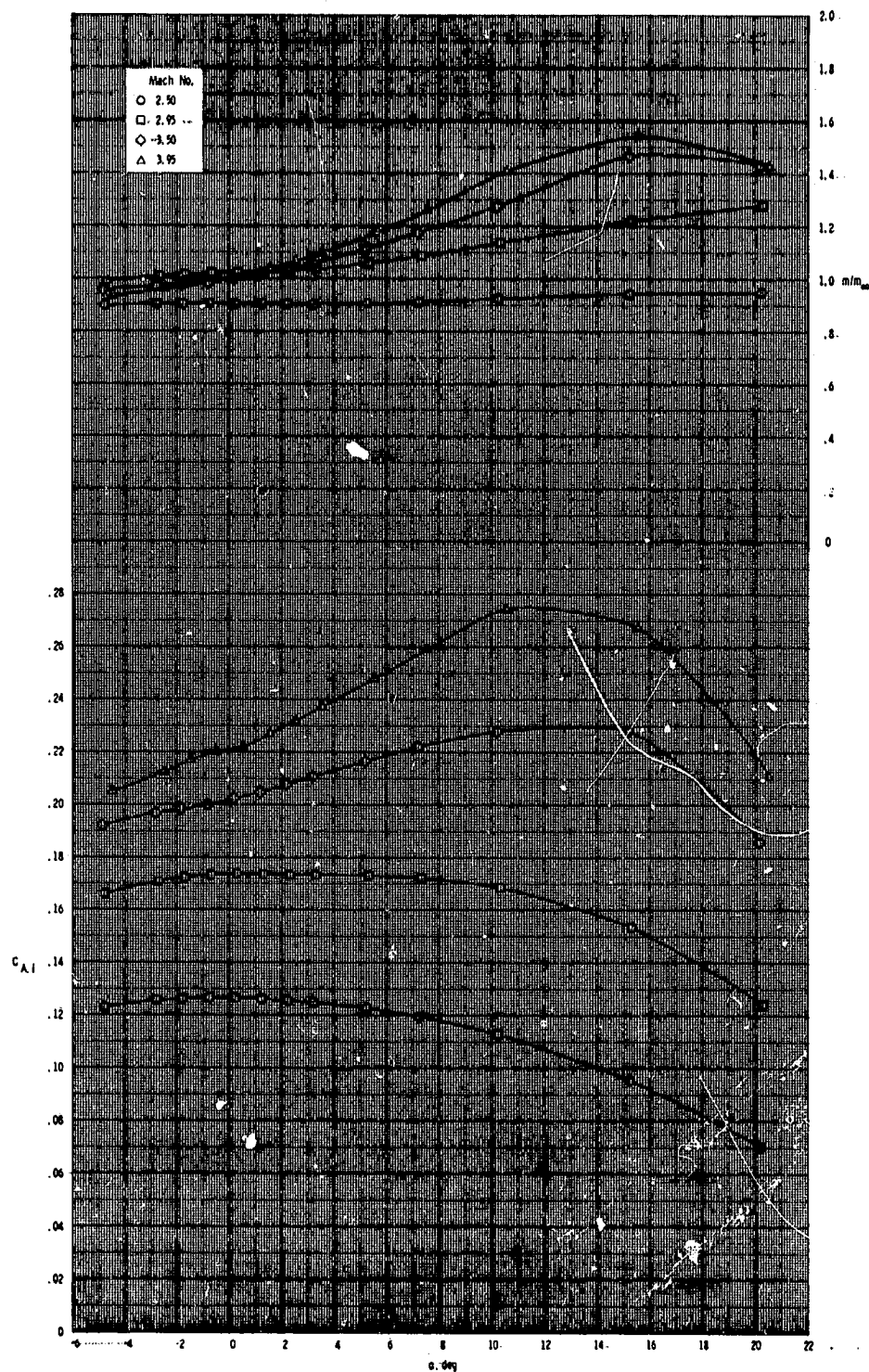
ORIGINAL PAGE
BLACK AND WHITE PHOTOGRAPH.



(a) Configuration B₁I₄.

Figure 3.- Internal-flow characteristics of various configurations.

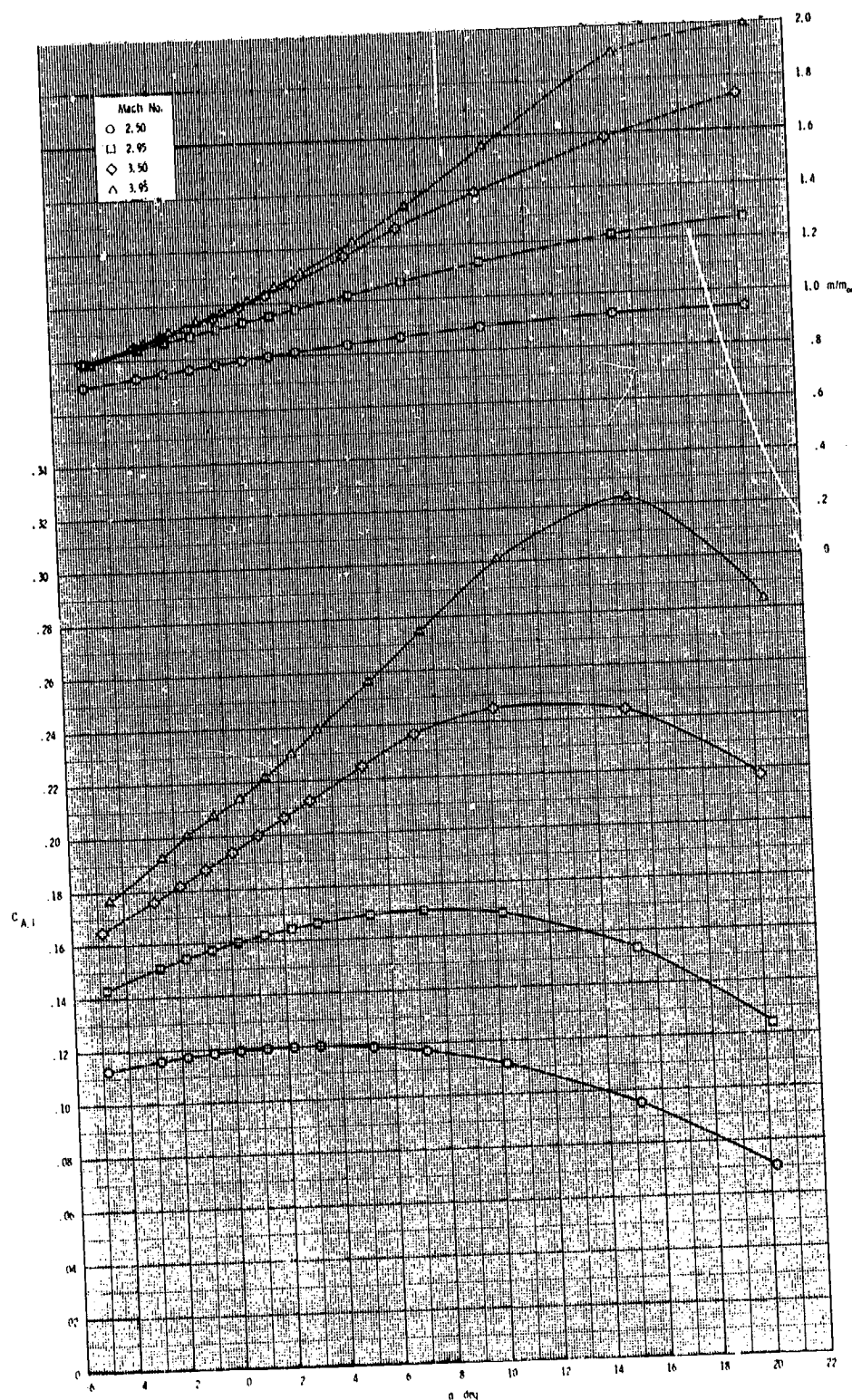
ORIGINAL PAGE
BLACK AND WHITE PHOTOGRAPH



(b) Configuration $B_1I_1W_1$.

Figure 3.- Continued.

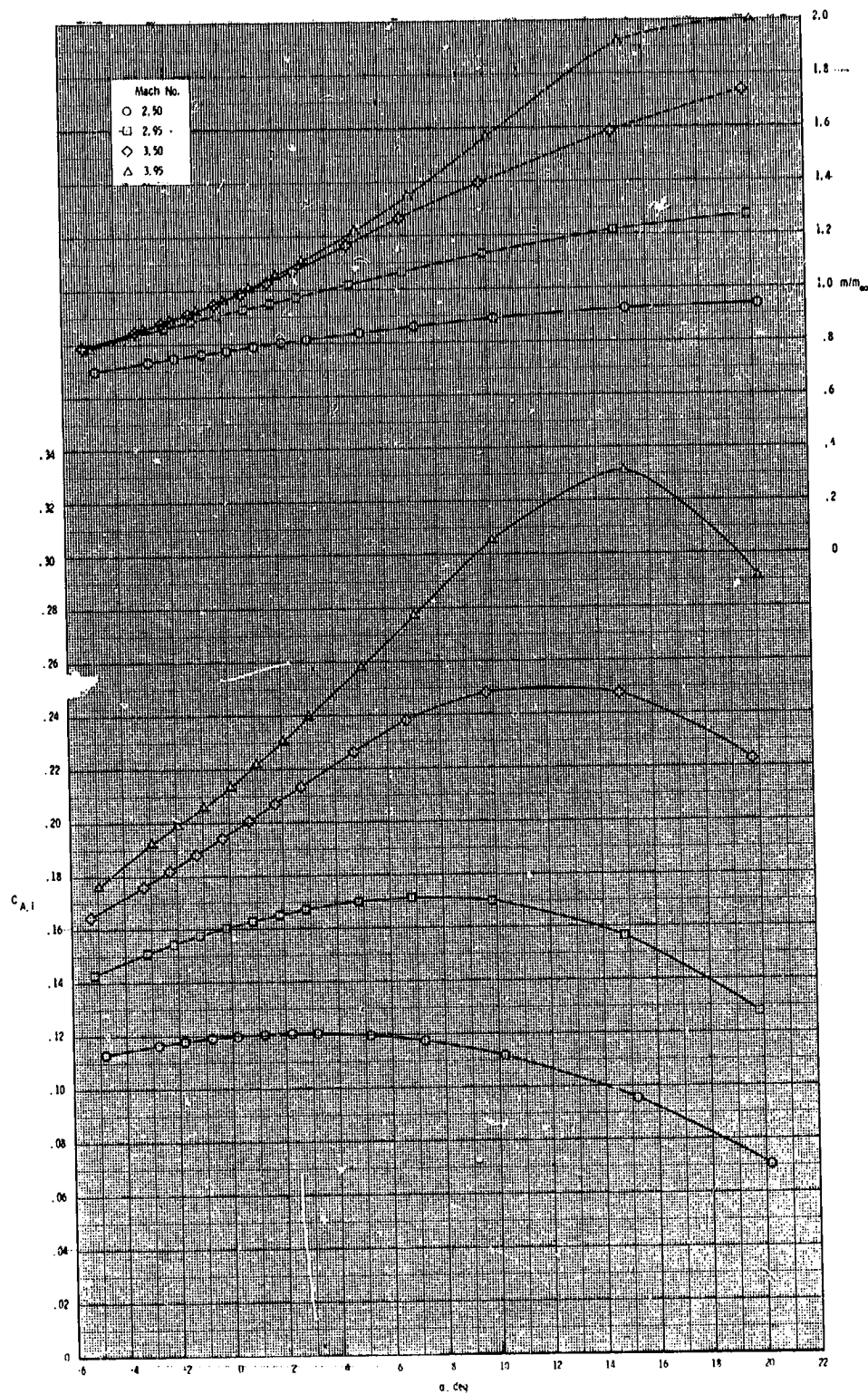
ORIGINAL PAGE
BLACK AND WHITE PHOTOGRAPH



(c) Configuration B₁I₅.

Figure 3.- Continued.

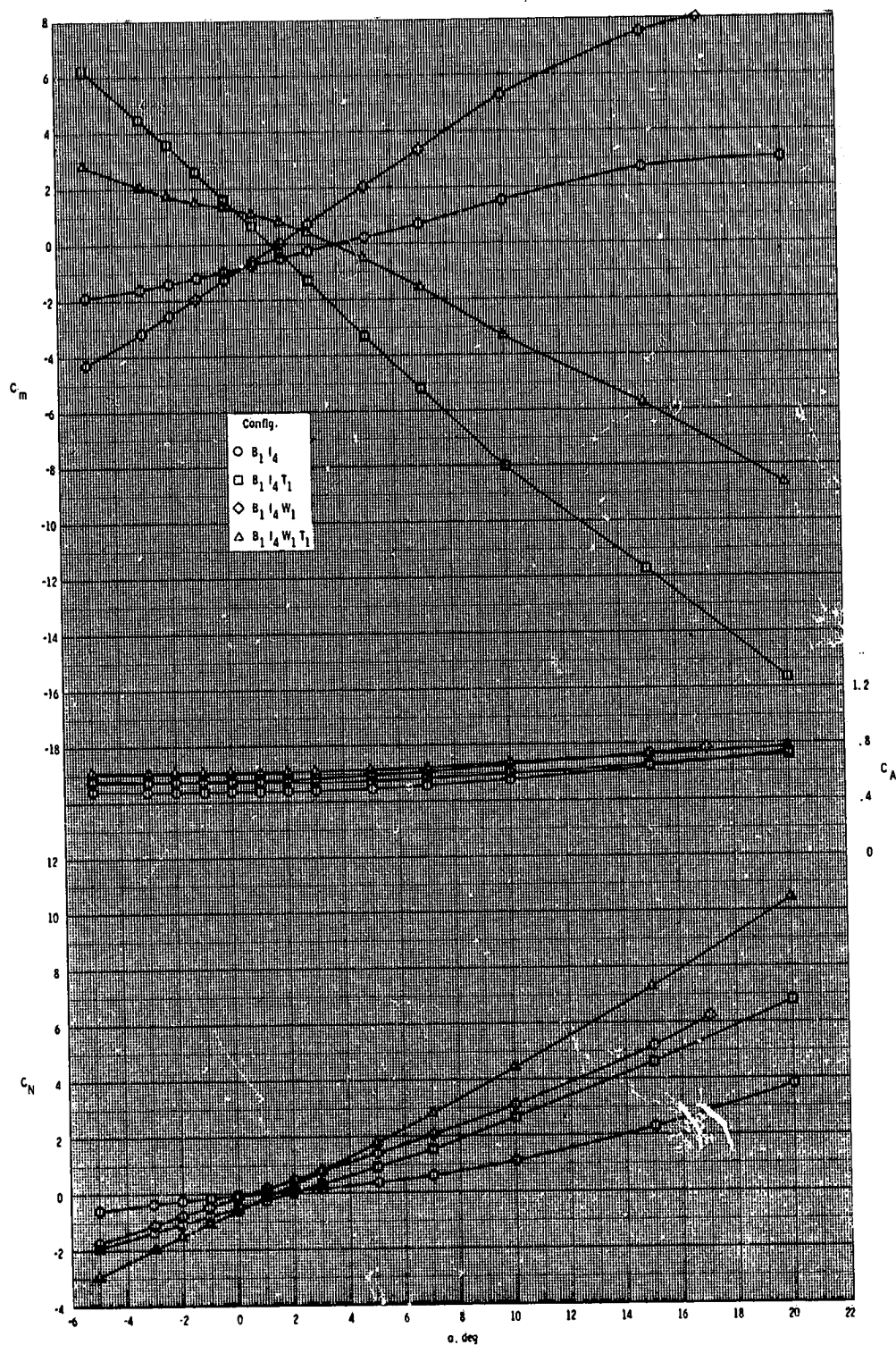
ORIGINAL PAGE
BLACK AND WHITE PHOTOGRAPH



(d) Configuration B₁I₅W₁.

Figure 3.- Concluded.

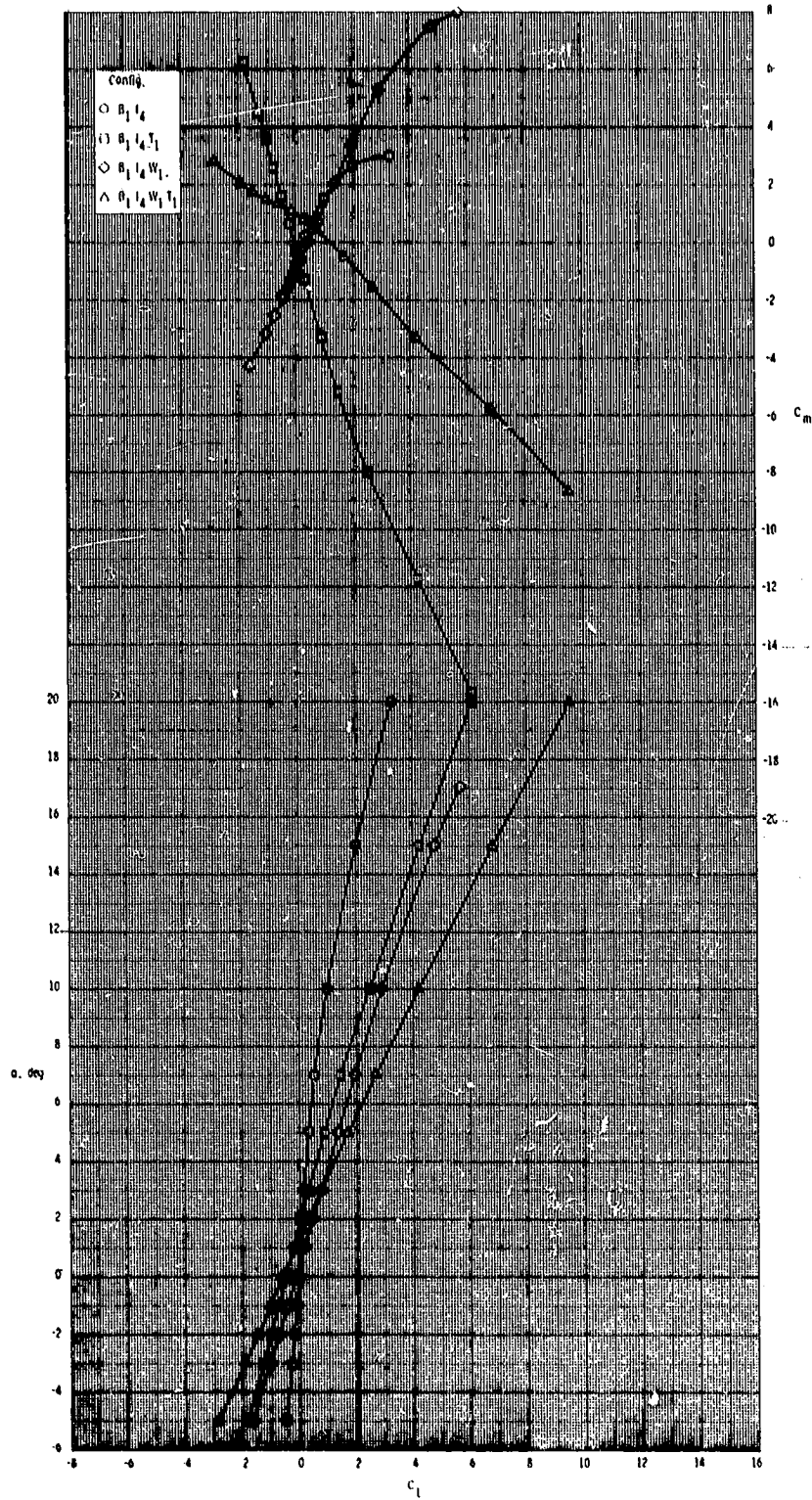
ORIGINAL PAGE
BLACK AND WHITE PHOTOGRAPH



(a) $M = 2.50$.

Figure 4.- Effect of various model components on longitudinal aerodynamic characteristics for axisymmetric inlet with T_1 .

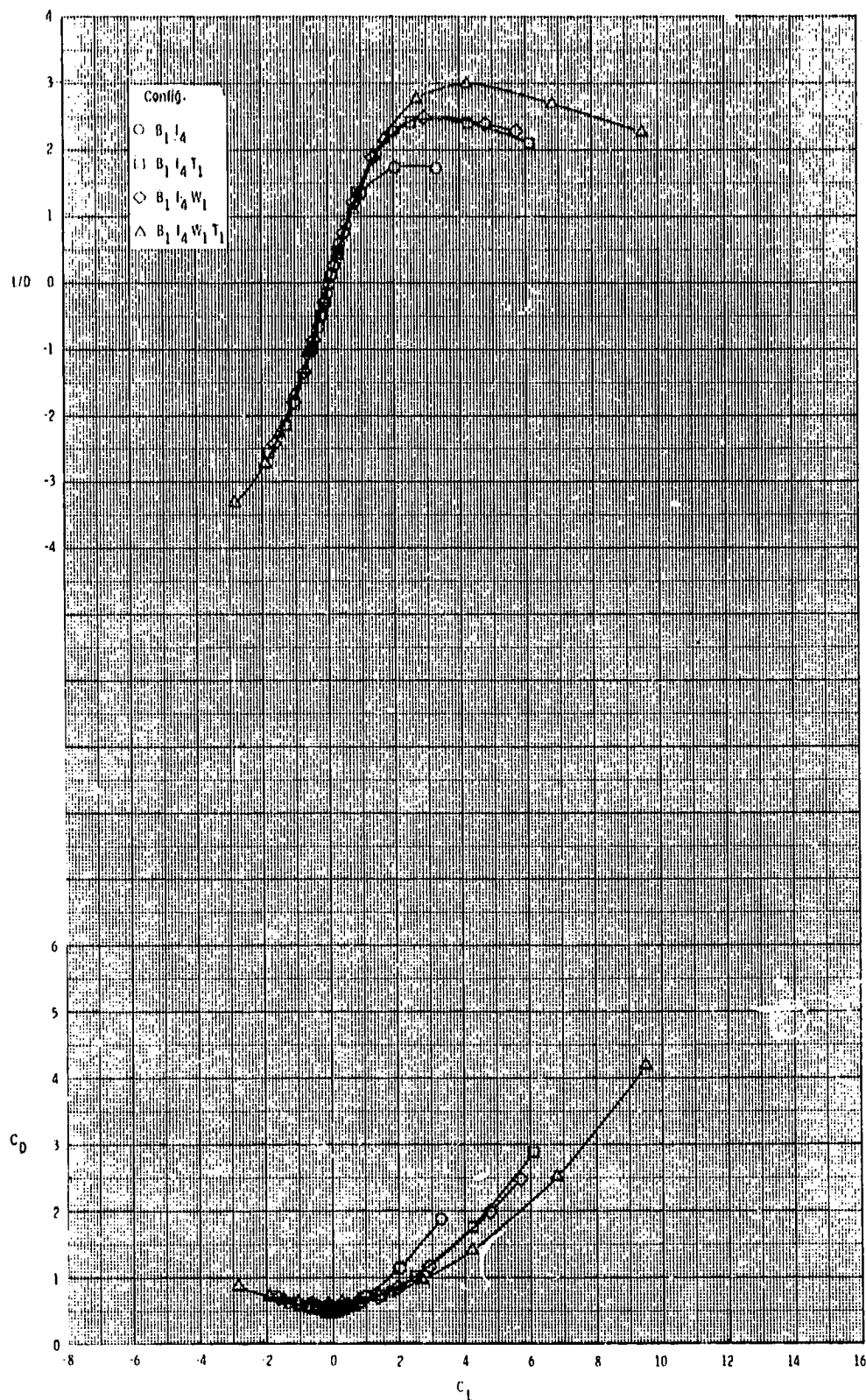
ORIGINAL PAGE
BLACK AND WHITE PHOTOGRAPH



(a) Continued.

Figure 4.- Continued.

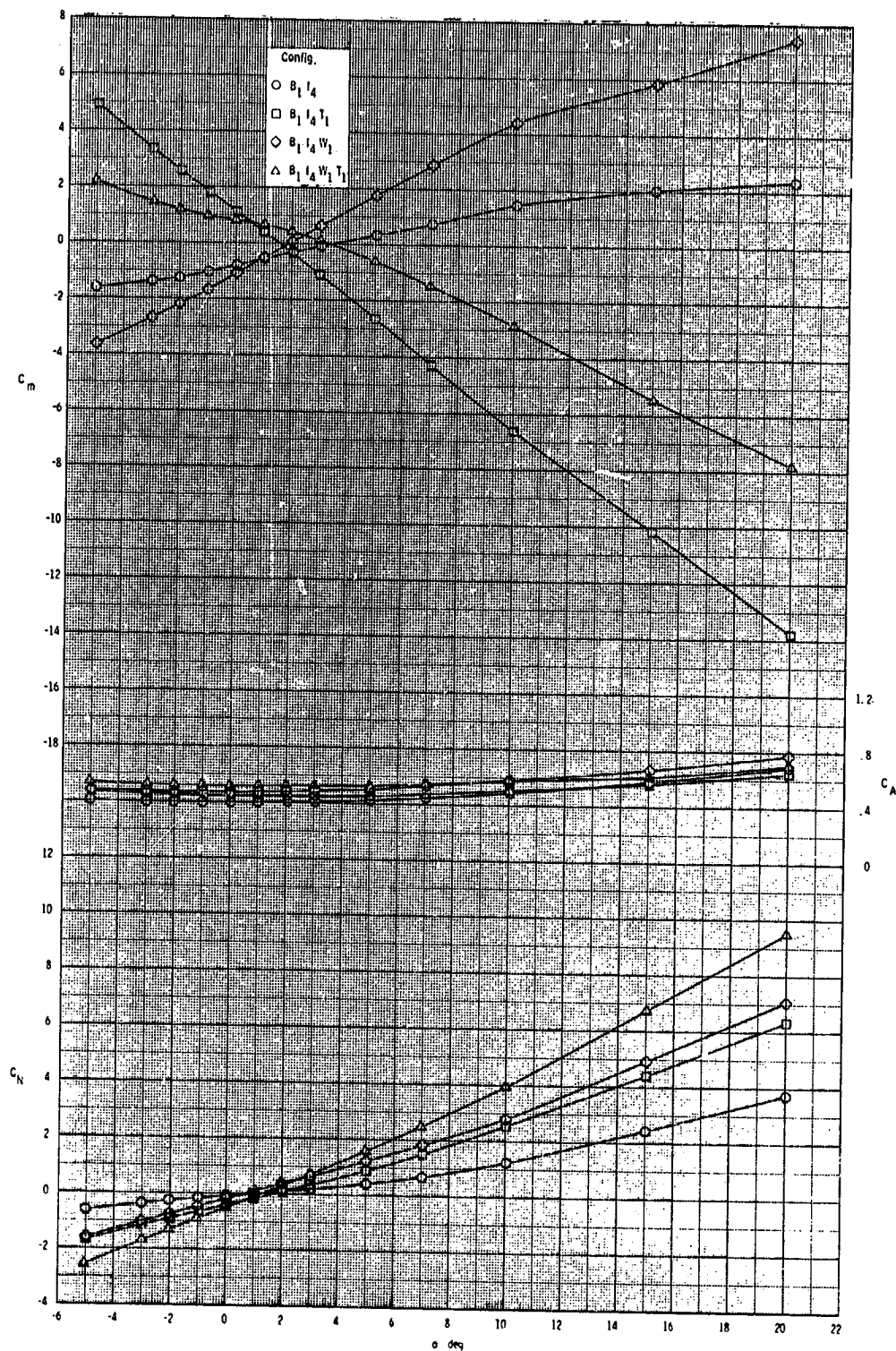
ORIGINAL PAGE
BLACK AND WHITE PHOTOGRAPH



(a) Concluded.

Figure 4.- Continued.

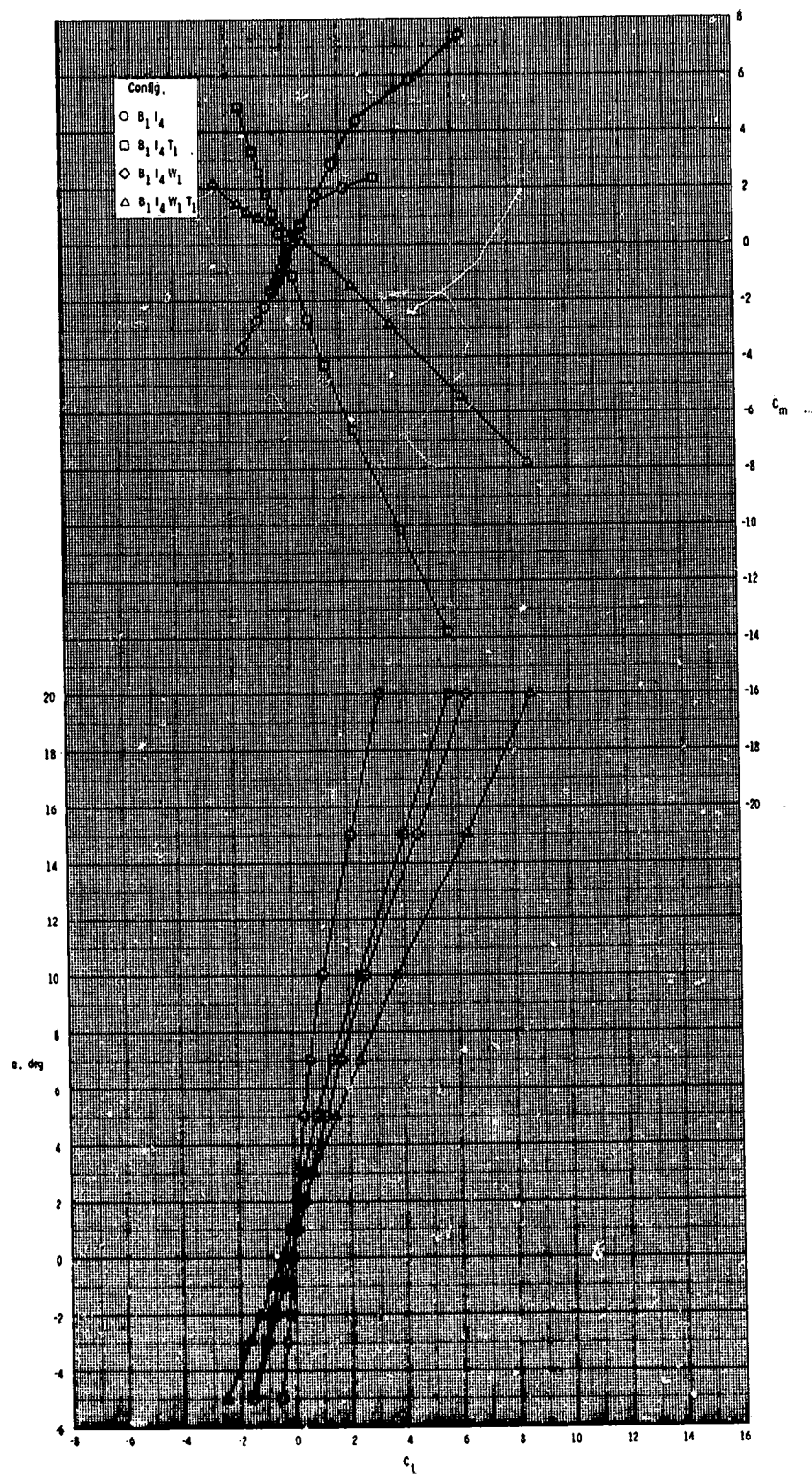
ORIGINAL PAGE
BLACK AND WHITE PHOTOGRAPH



(b) $M = 2.95$.

Figure 4.- Continued.

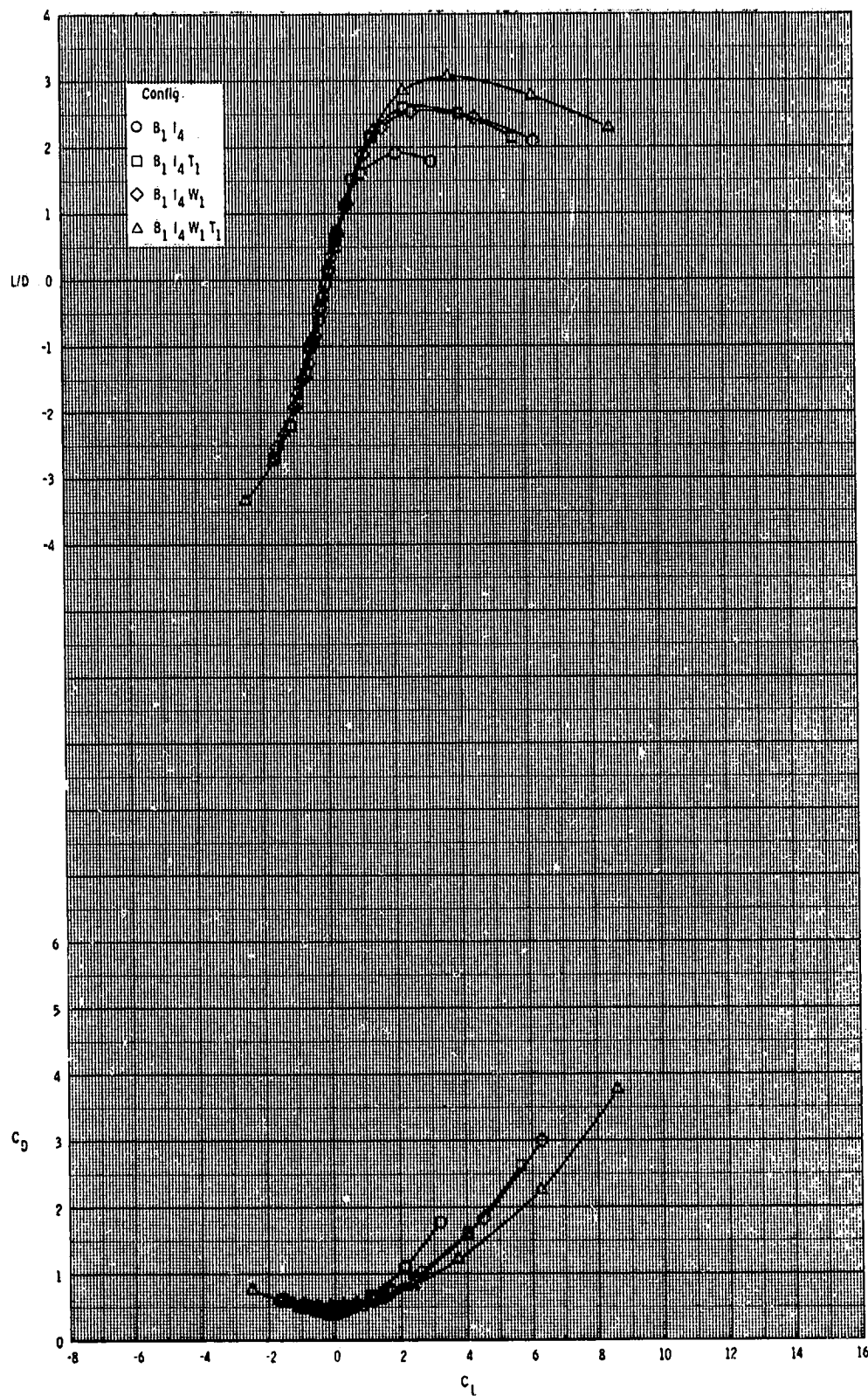
ORIGINAL PAGE
BLACK AND WHITE PHOTOGRAPH



(b) Continued.

Figure 4.- Continued.

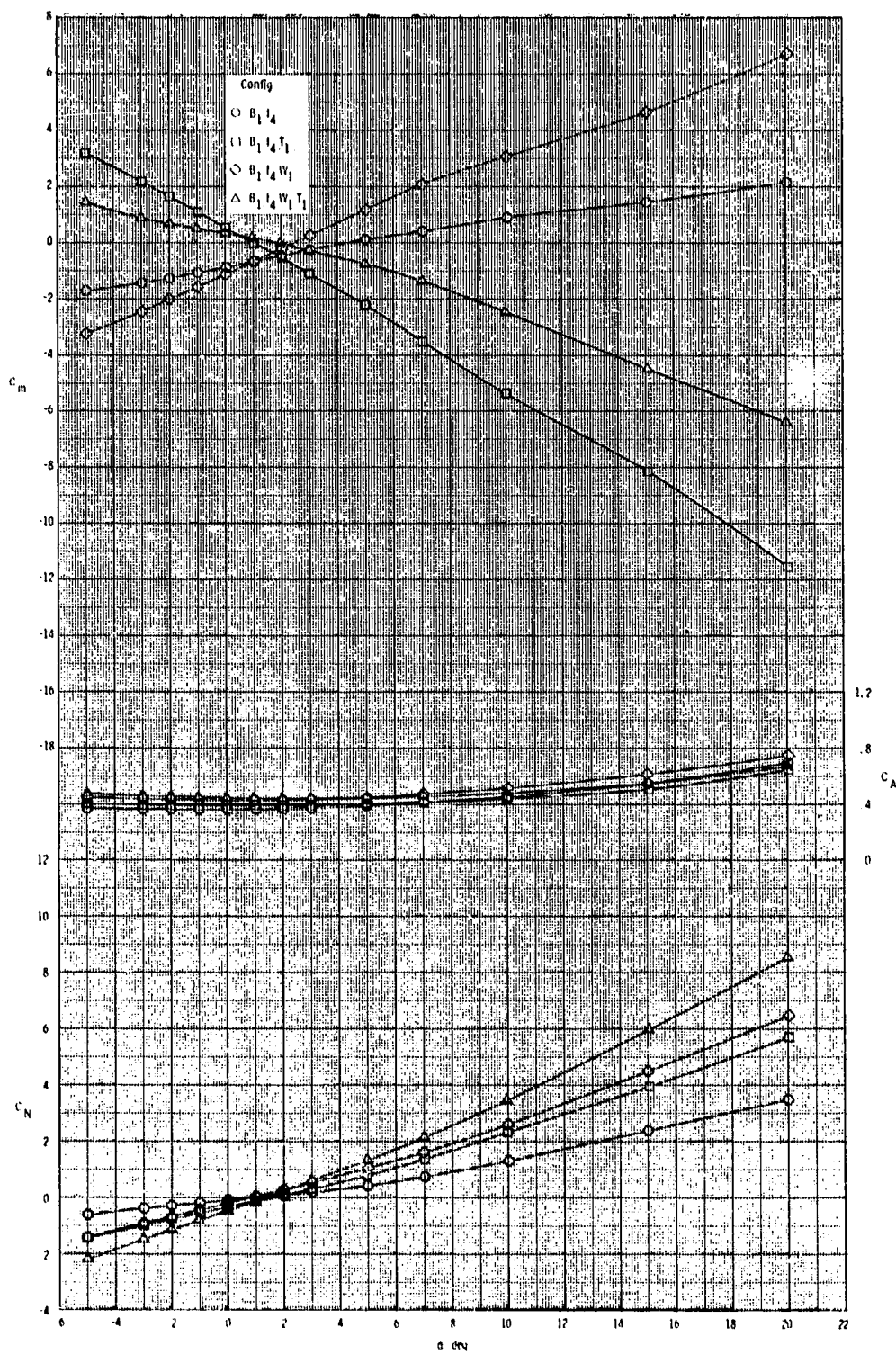
ORIGINAL PAGE
BLACK AND WHITE PHOTOGRAPH



(b) Concluded.

Figure 4.- Continued.

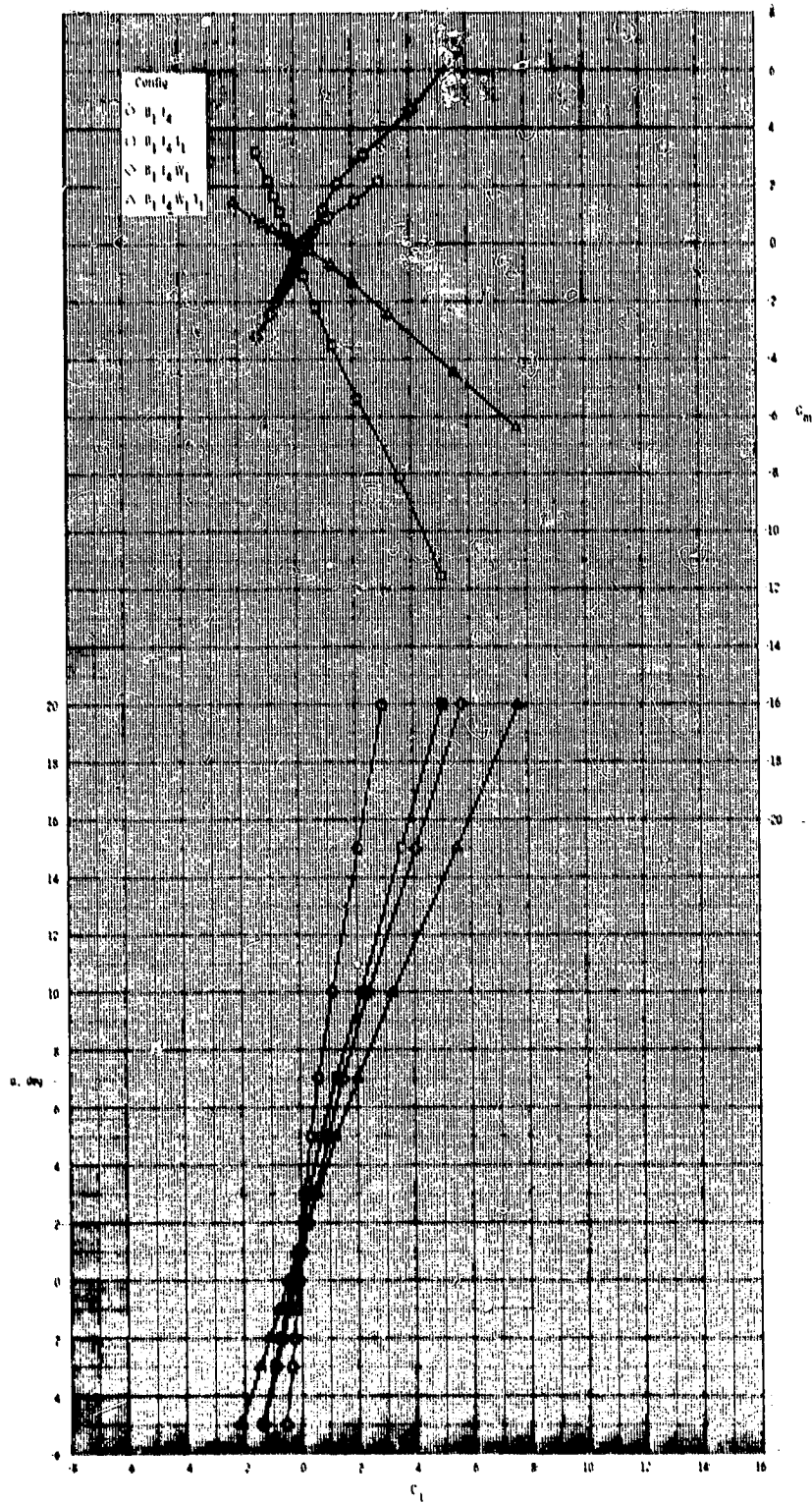
ORIGINAL PAGE
BLACK AND WHITE PHOTOGRAPH



(c) $M = 3.50$.

Figure 4.- Continued.

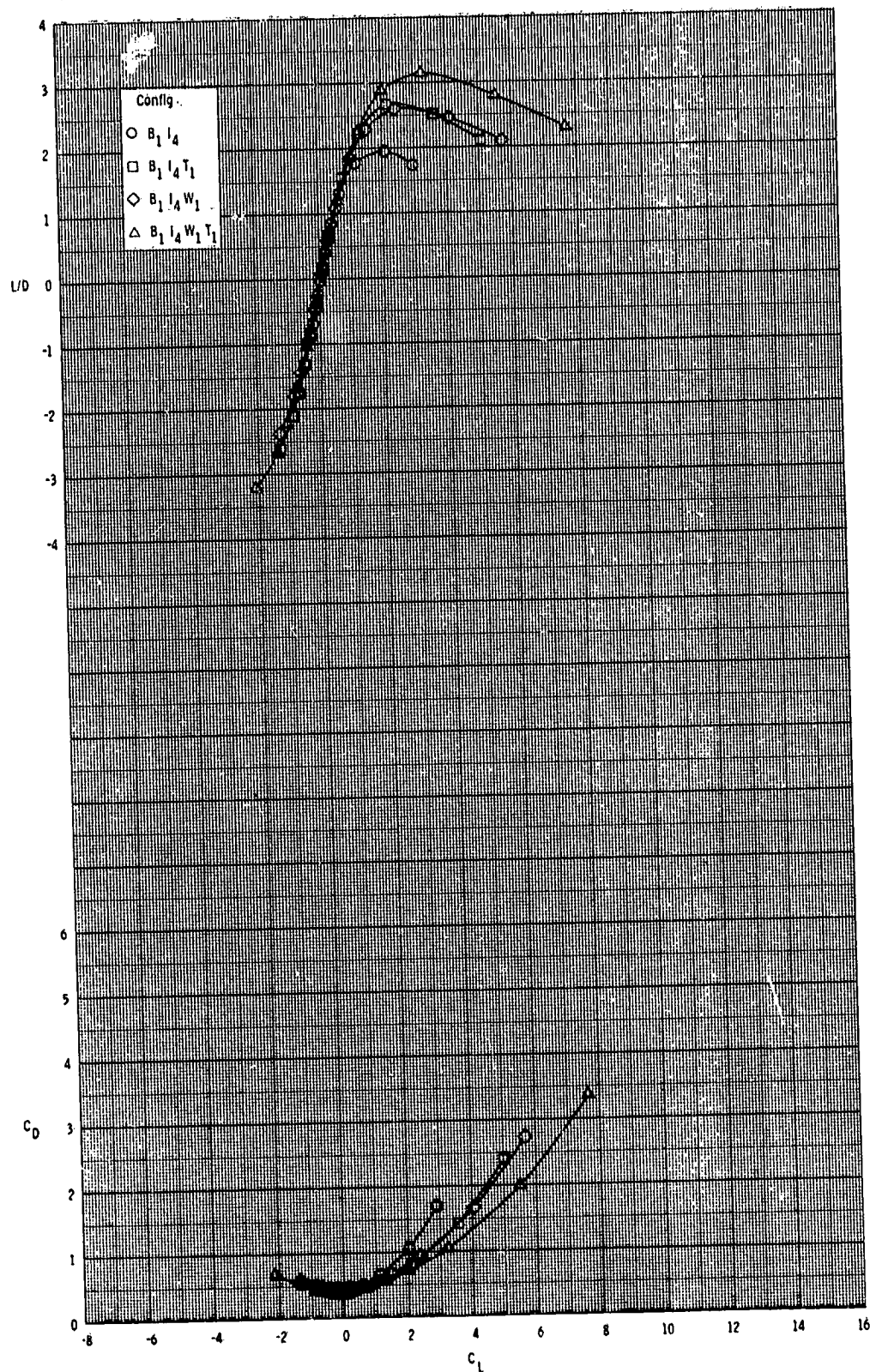
ORIGINAL PAGE
BLACK AND WHITE PHOTOGRAPH



(c) Continued.

Figure 4.- Continued.

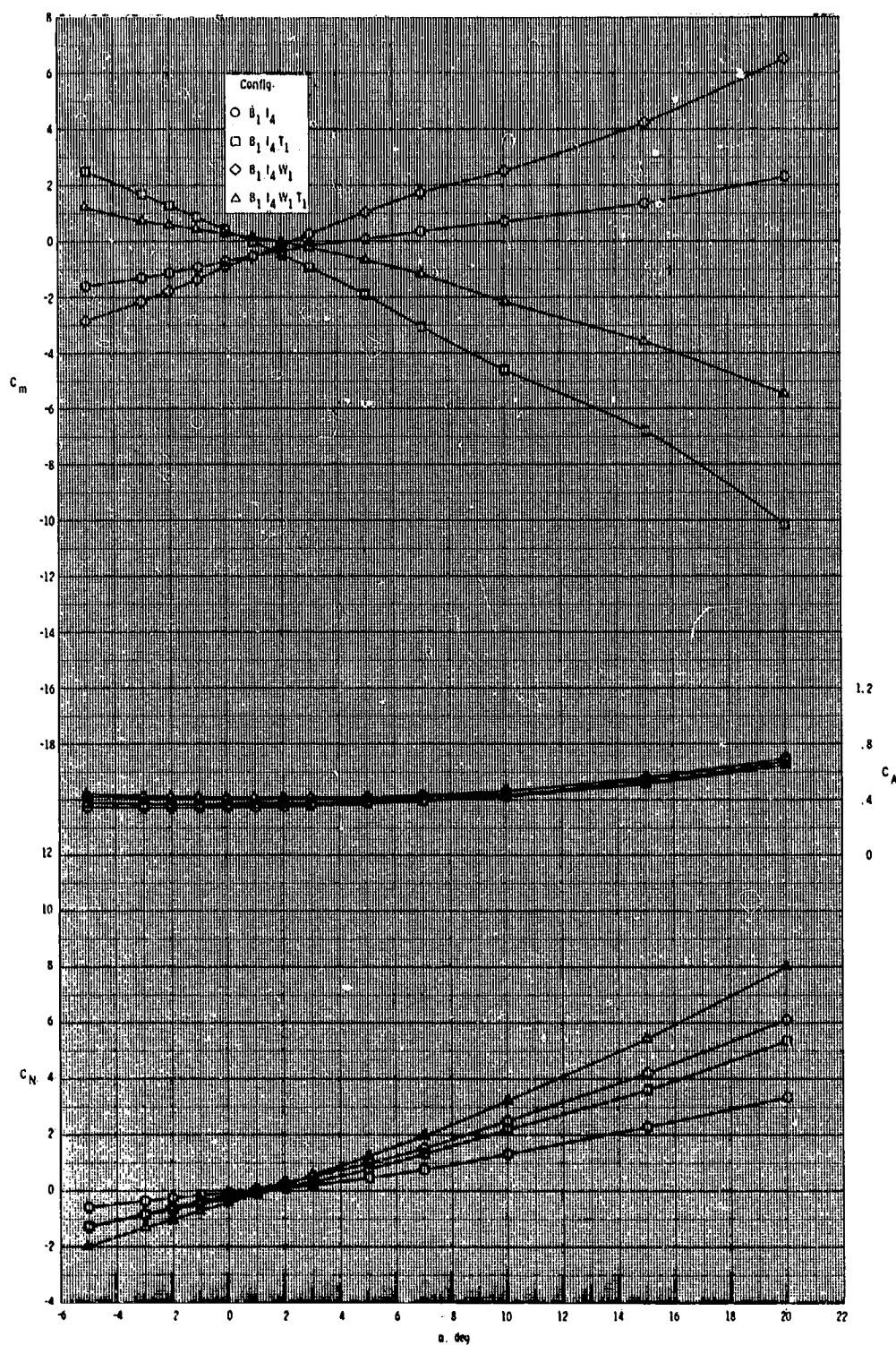
ORIGINAL PAGE
BLACK AND WHITE PHOTOGRAPH



(c) Concluded.

Figure 4.- Continued.

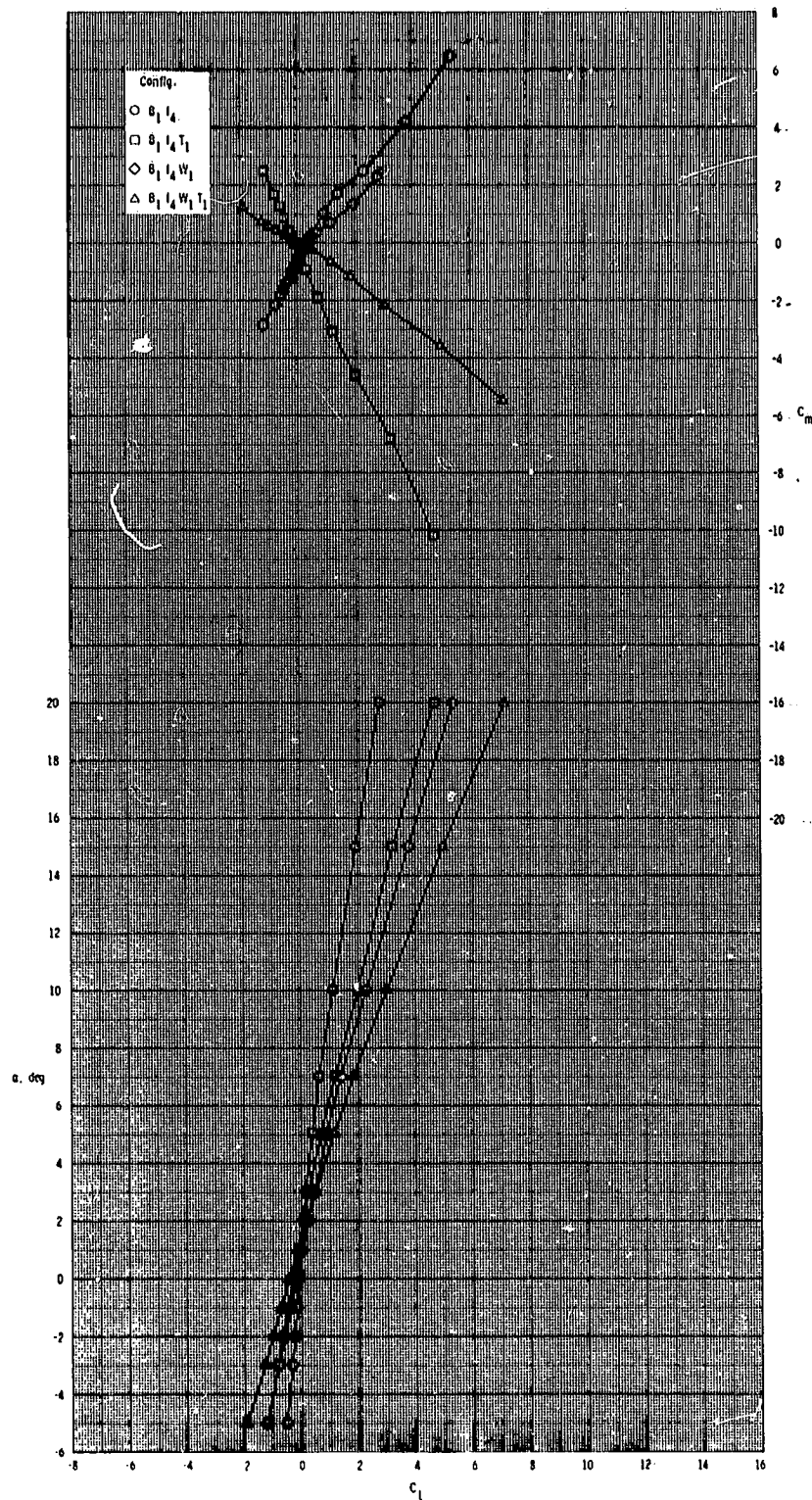
ORIGINAL PAGE
BLACK AND WHITE PHOTOGRAPH



(d) $M = 3.95$.

Figure 4.- Continued.

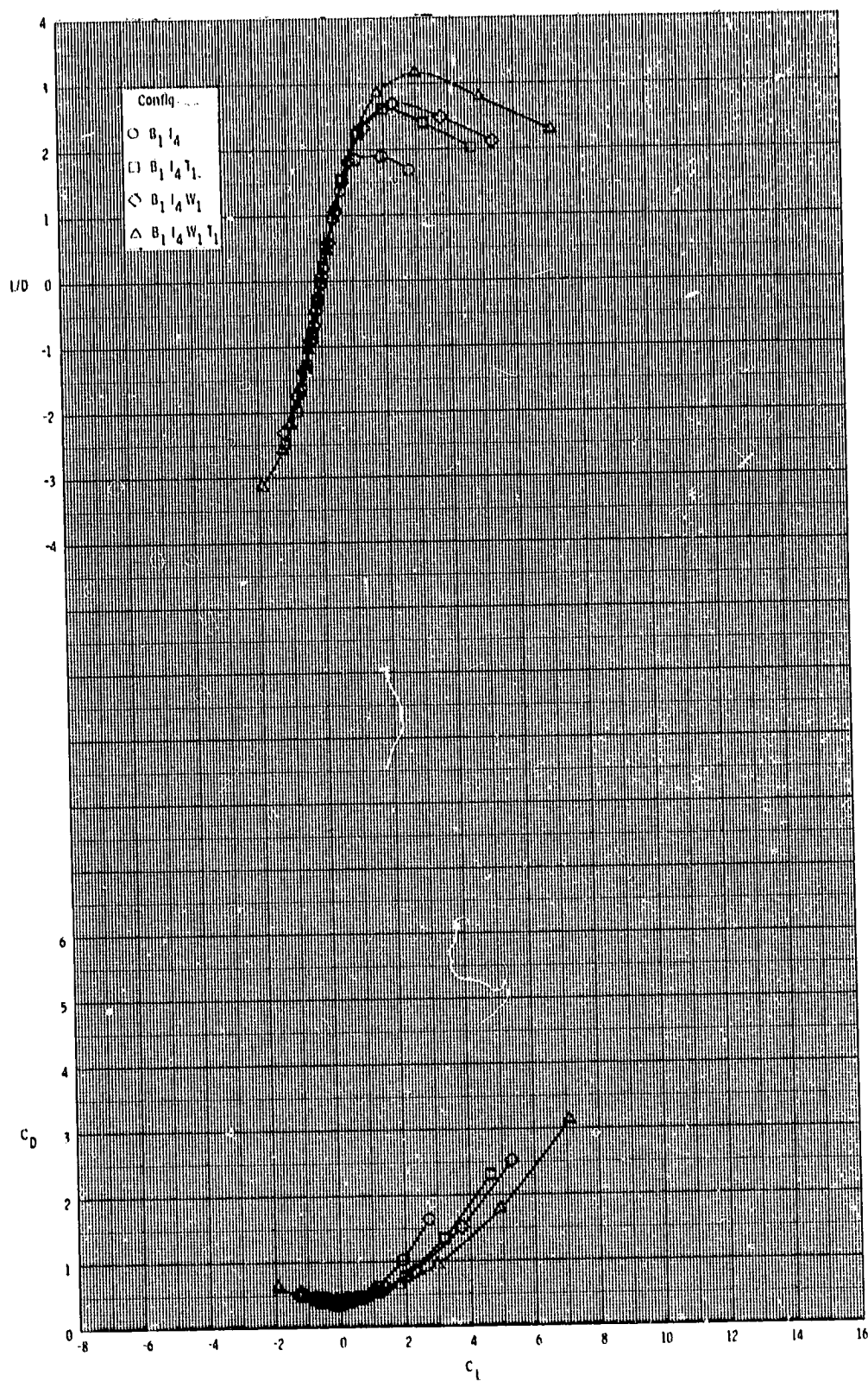
ORIGINAL PAGE IS
OF POOR QUALITY



(d) Continued.

Figure 4.- Continued.

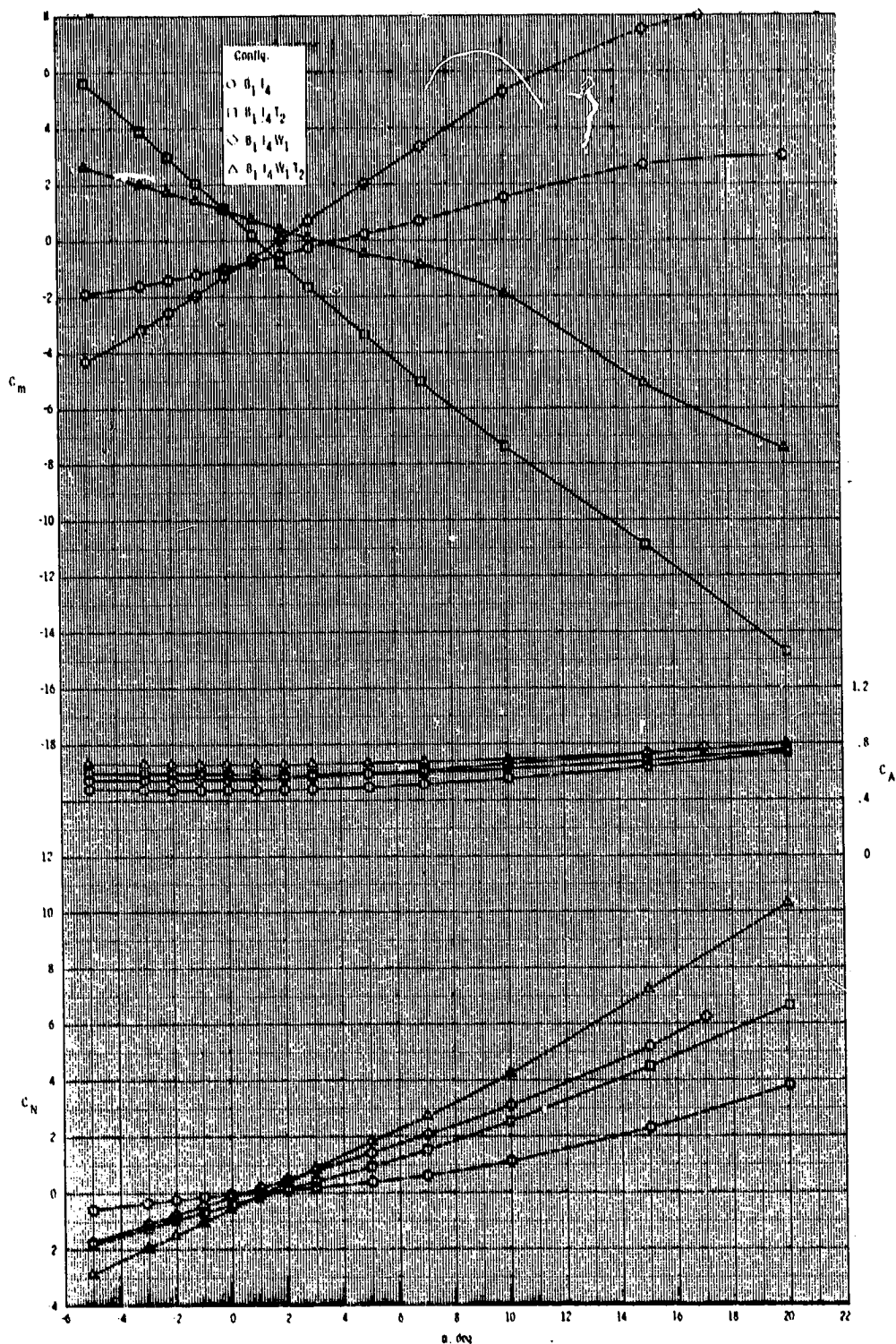
ORIGINAL PAGE IS
OF POOR QUALITY



(d) Concluded.

Figure 4.- Concluded.

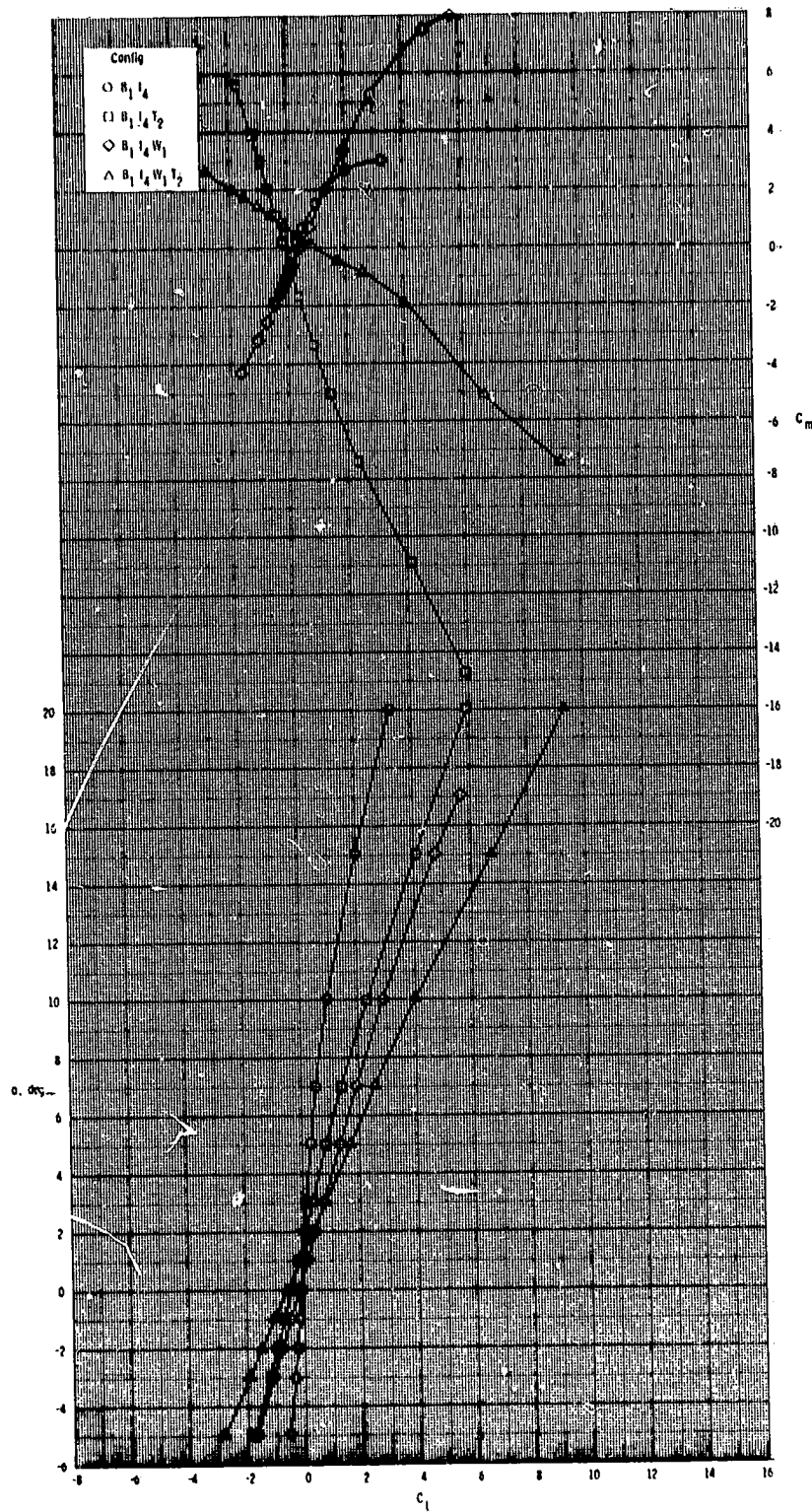
ORIGINAL PAGE IS
OF POOR QUALITY



(a) $M = 2.50$.

Figure 5.- Effect of various model components on longitudinal aerodynamic characteristics for axisymmetric inlet with T_2 .

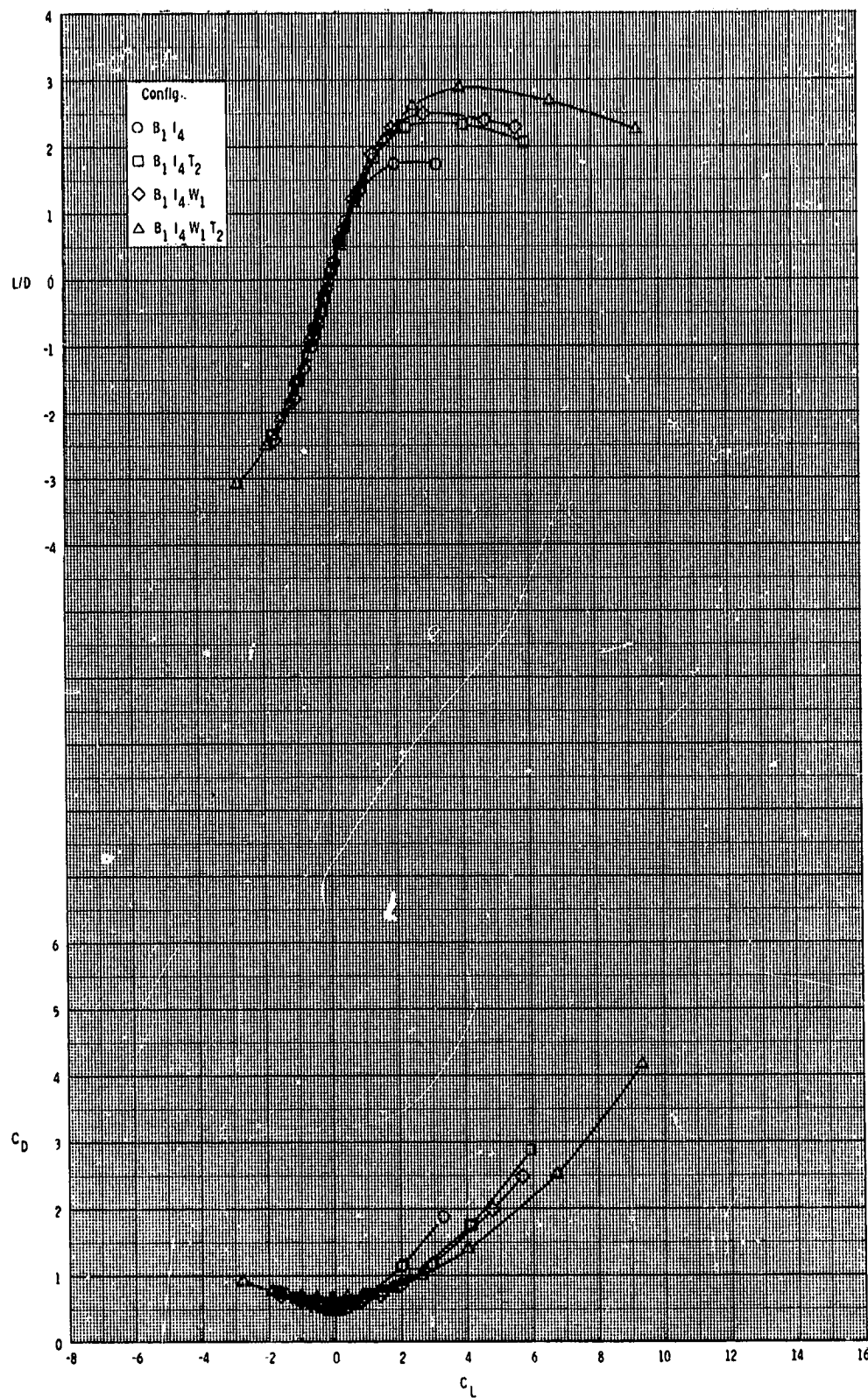
ORIGINAL PAGE IS
OF POOR QUALITY



(a) Continued.

Figure 5.- Continued.

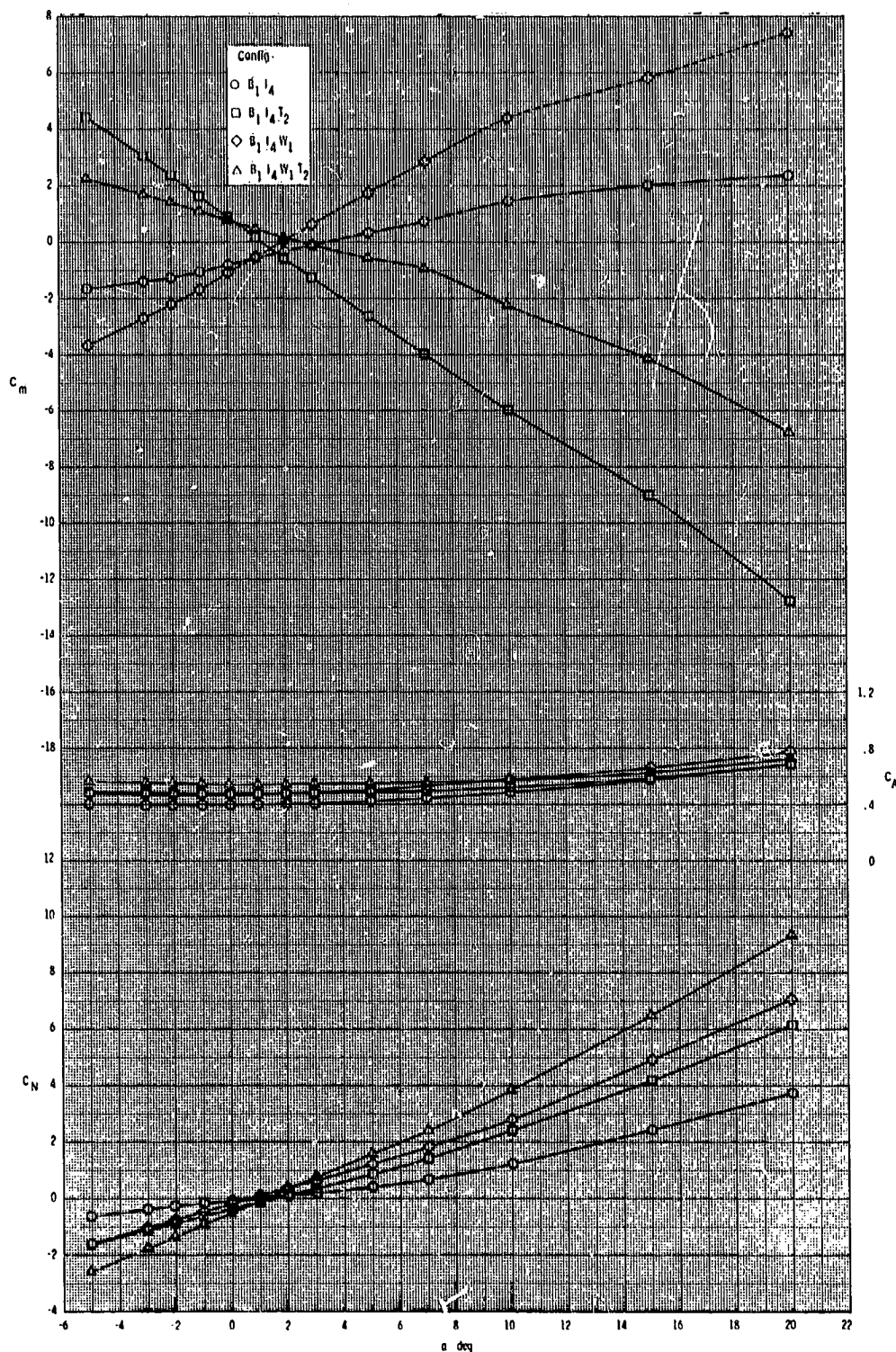
ORIGINAL PAGE IS
OF POOR QUALITY



(a) Concluded.

Figure 5.- Continued.

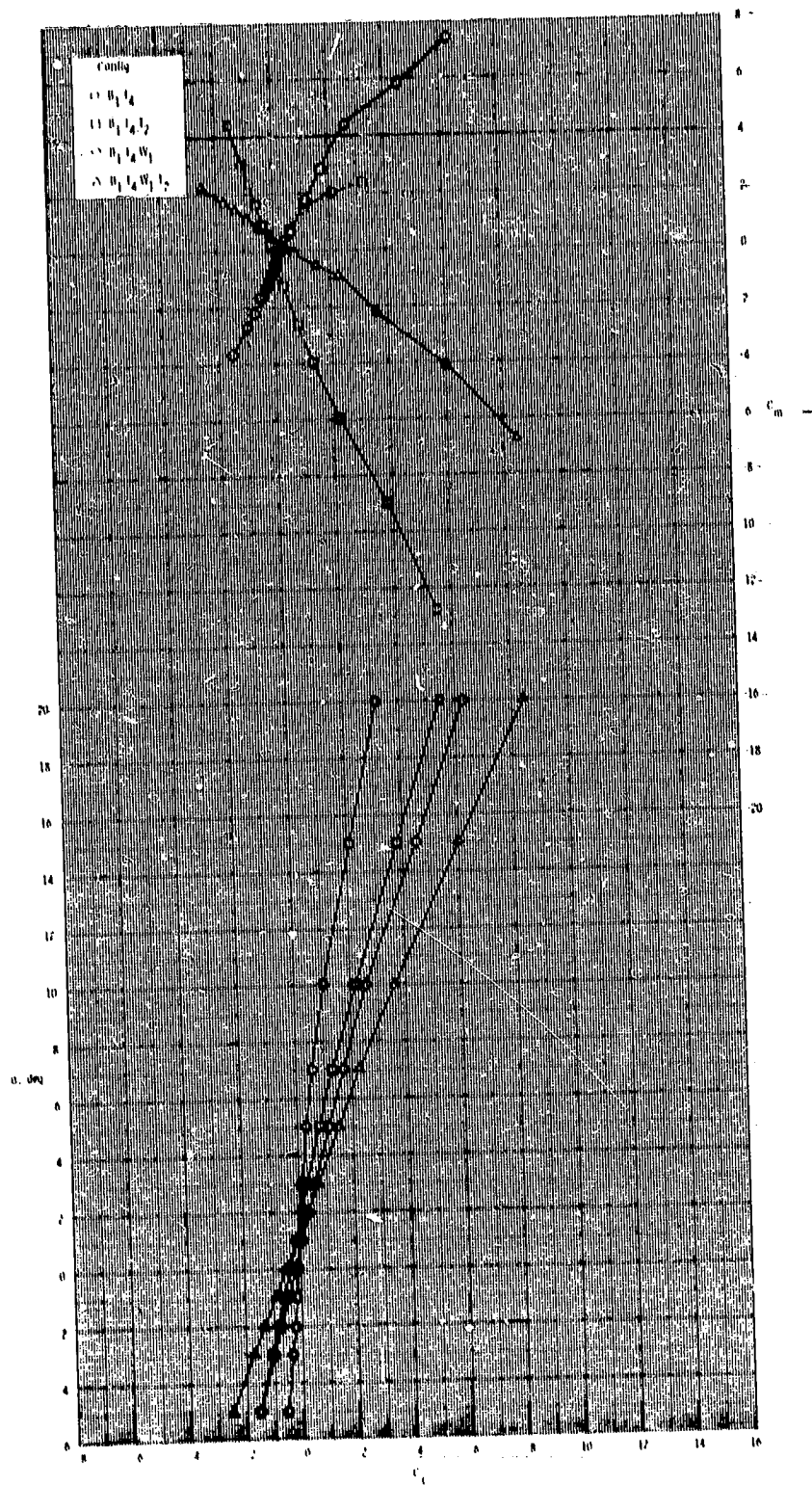
ORIGINAL PAGE IS
OF POOR QUALITY



(b) $M = 2.95$.

Figure 5.- Continued.

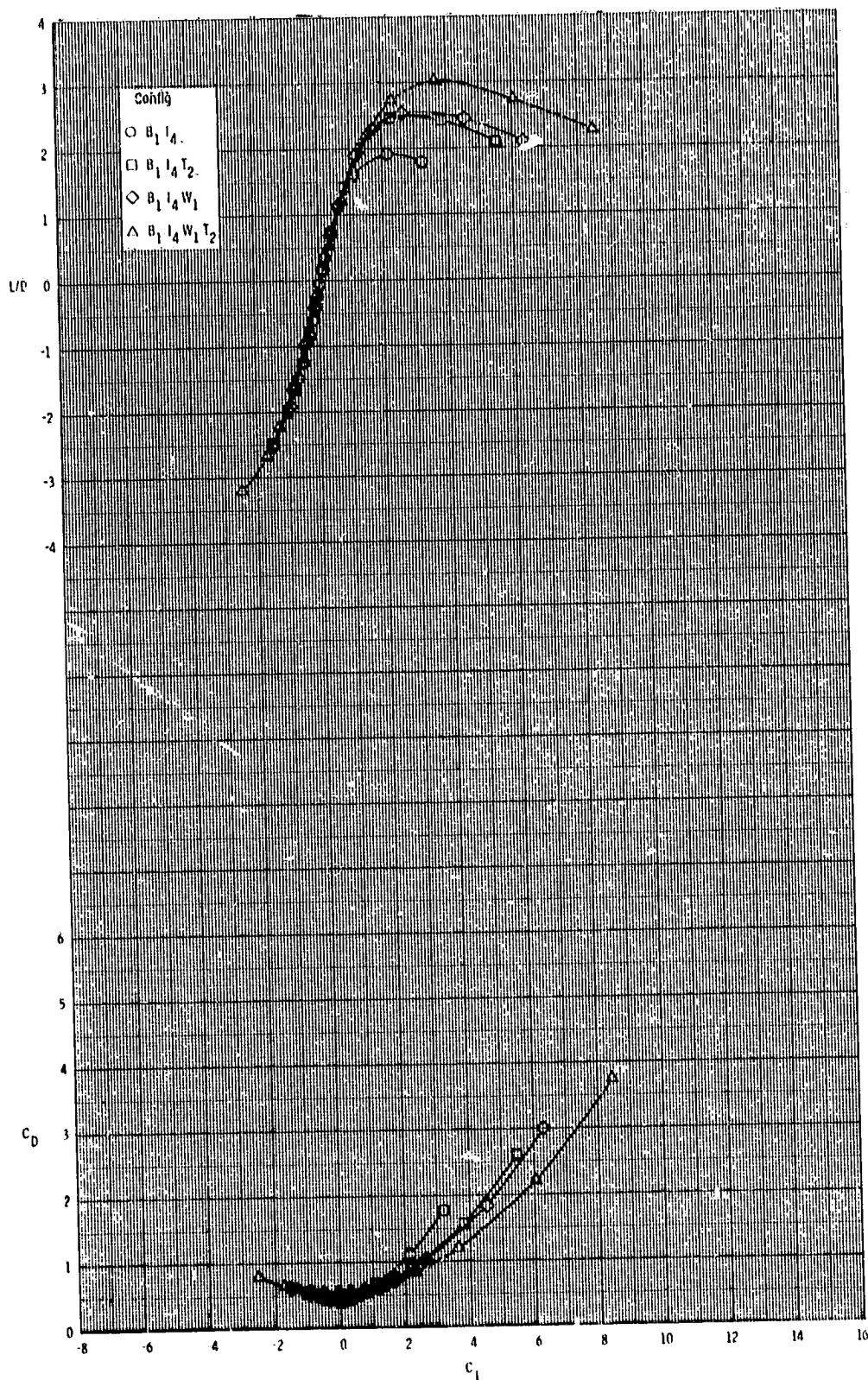
ORIGINAL PAGE IS
OF POOR QUALITY



(b) Continued.

Figure 5.- Continued.

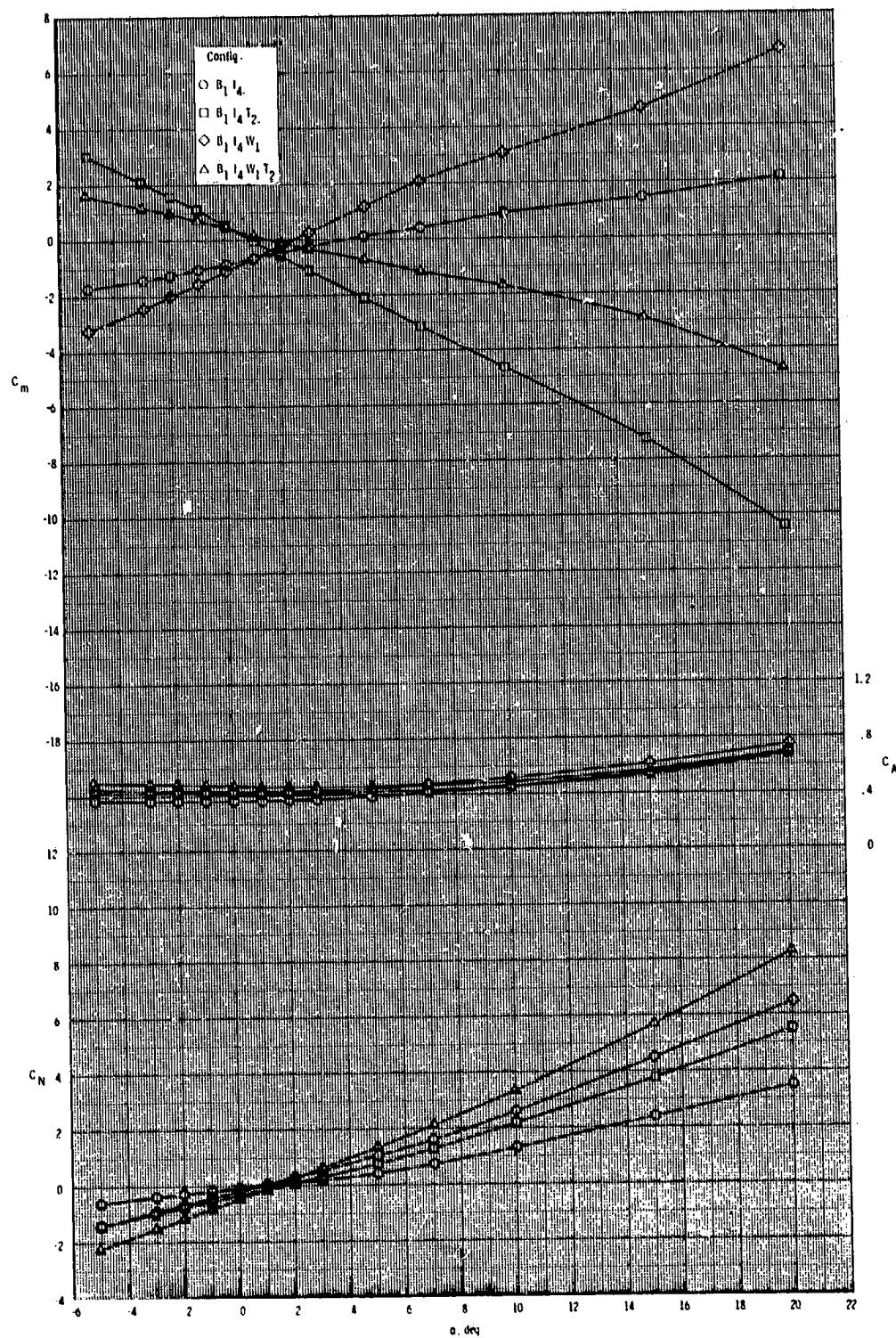
ORIGINAL PAGE IS
OF POOR QUALITY



(b) Concluded.

Figure 5.- Continued.

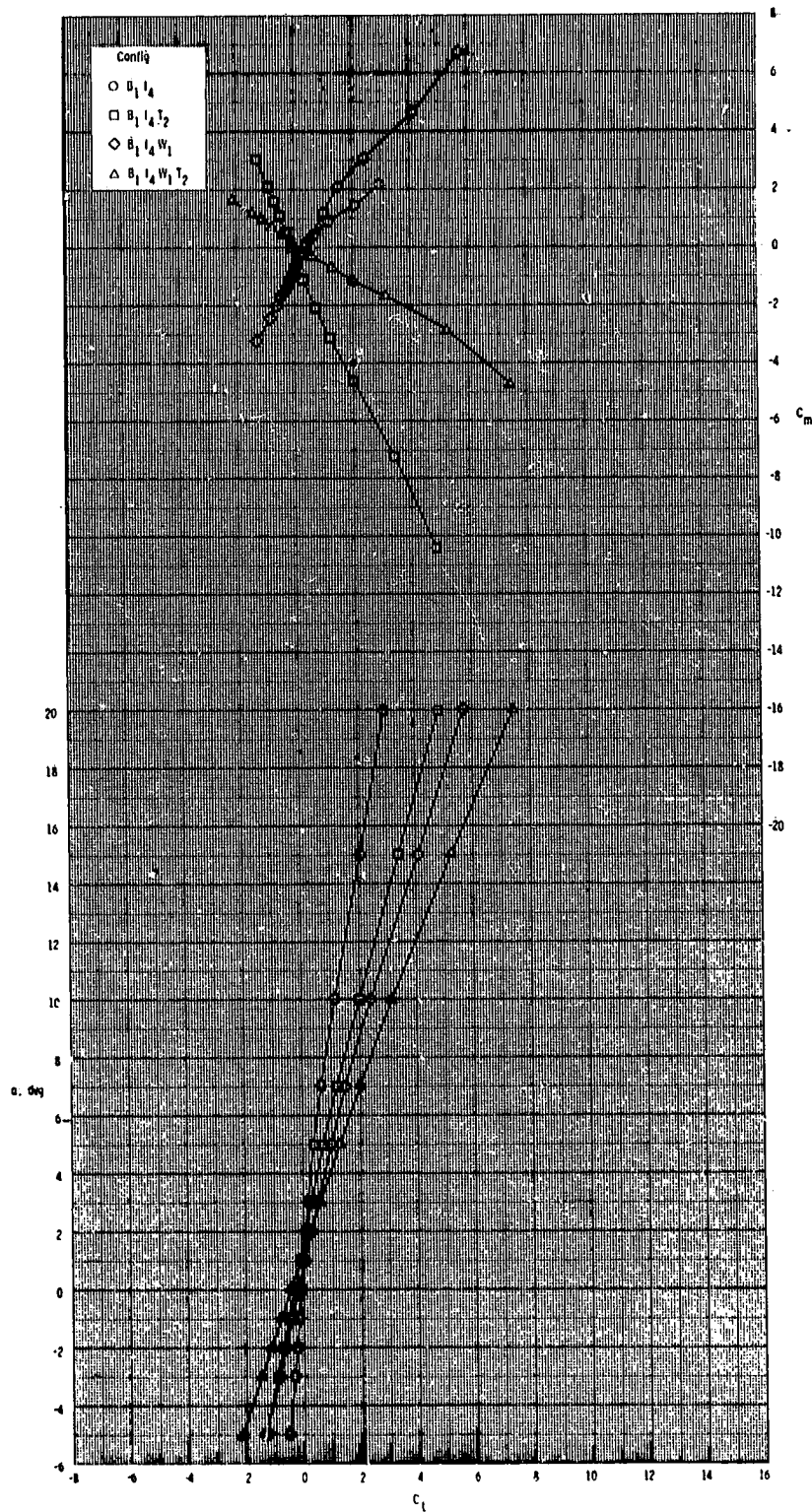
ORIGINAL PAGE IS
OF POOR QUALITY



(c) $M = 3.50$.

Figure 5.- Continued.

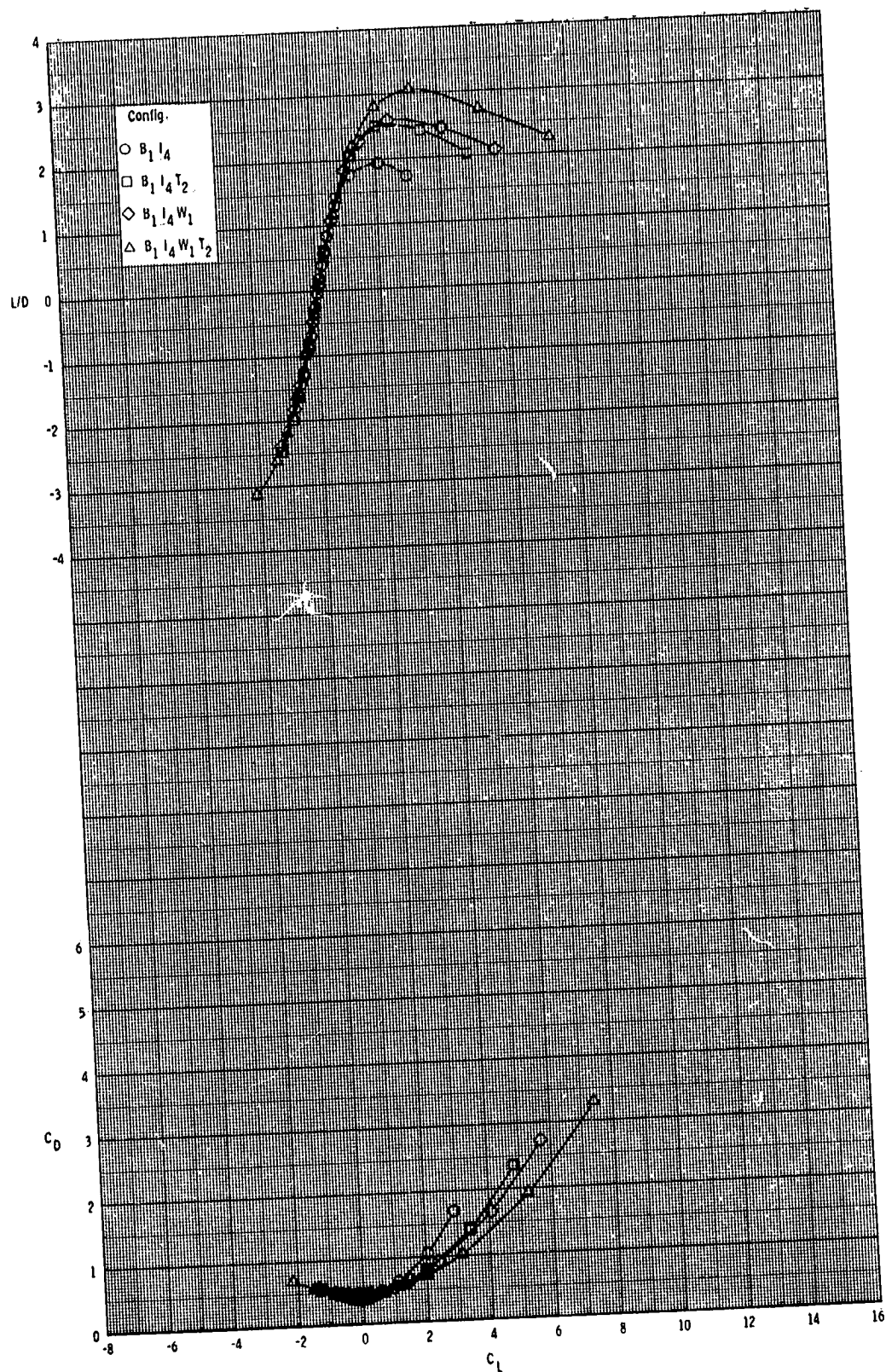
ORIGINAL PAGE IS
OF POOR QUALITY



(c) Continued.

Figure 5.- Continued.

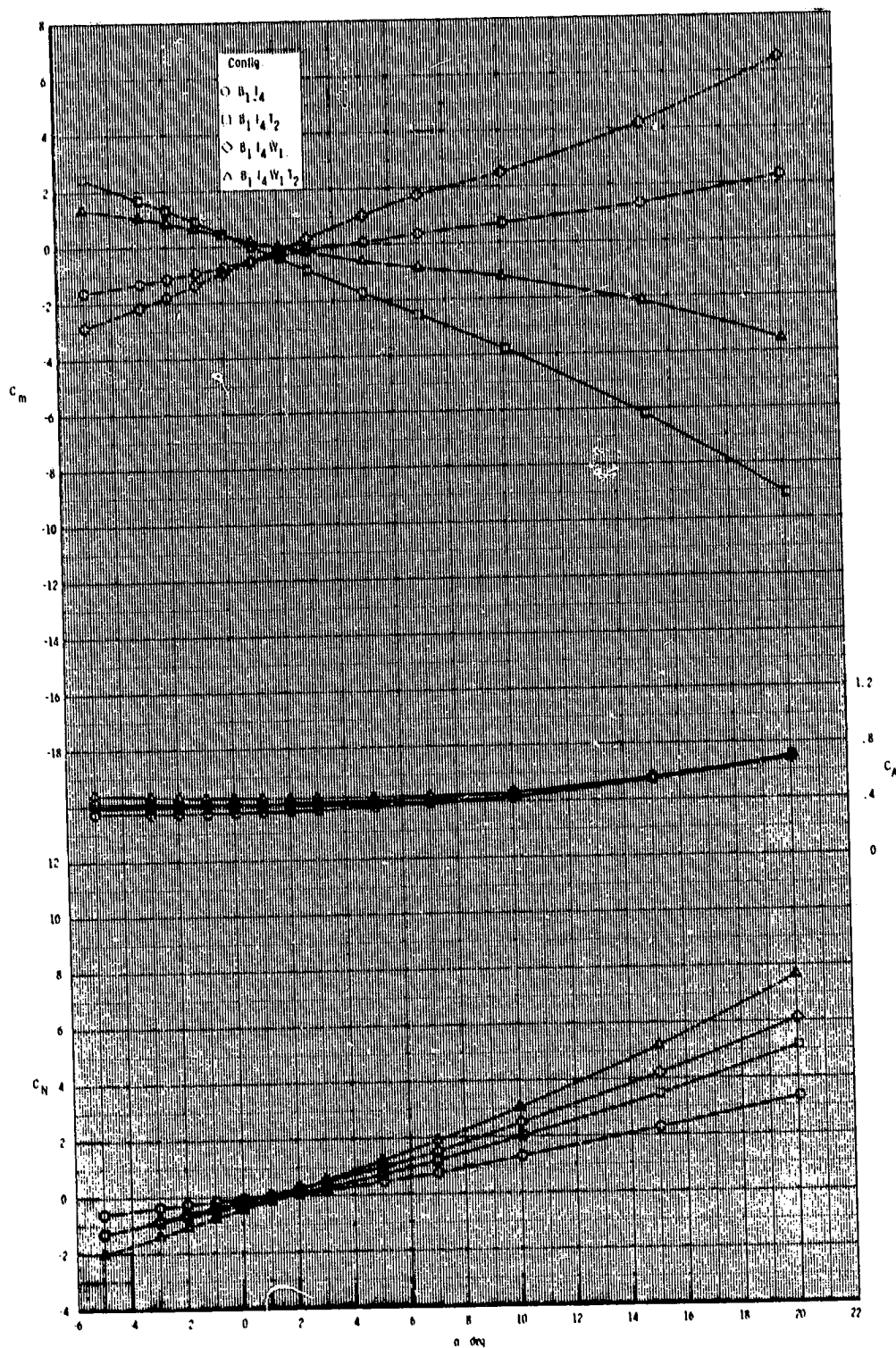
ORIGINAL PAGE IS
OF POOR QUALITY



(c) Concluded.

Figure 5.- Continued.

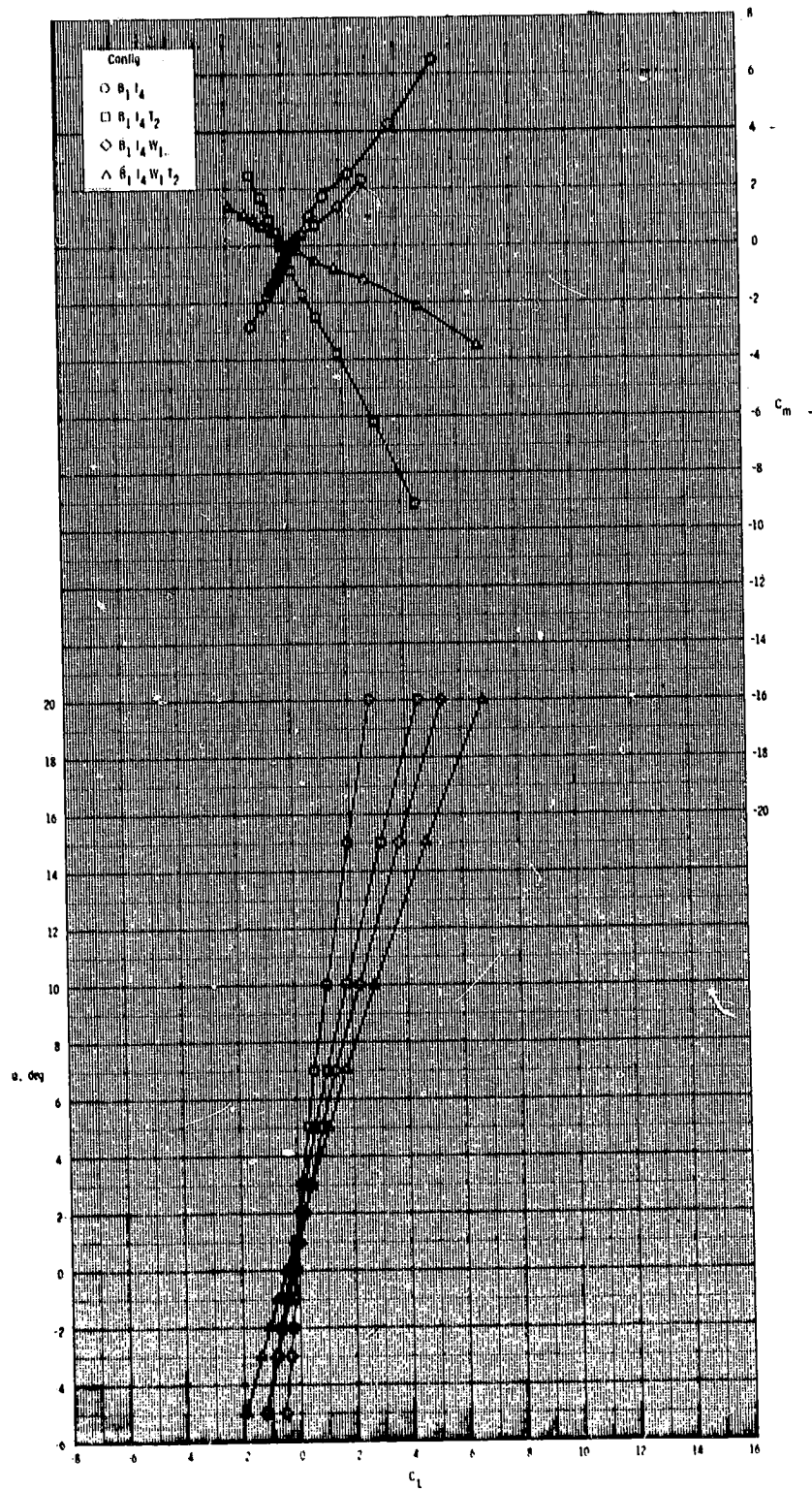
ORIGINAL PAGE IS
OF POOR QUALITY.



(d) $M = 3.95$.

Figure 5.- Continued.

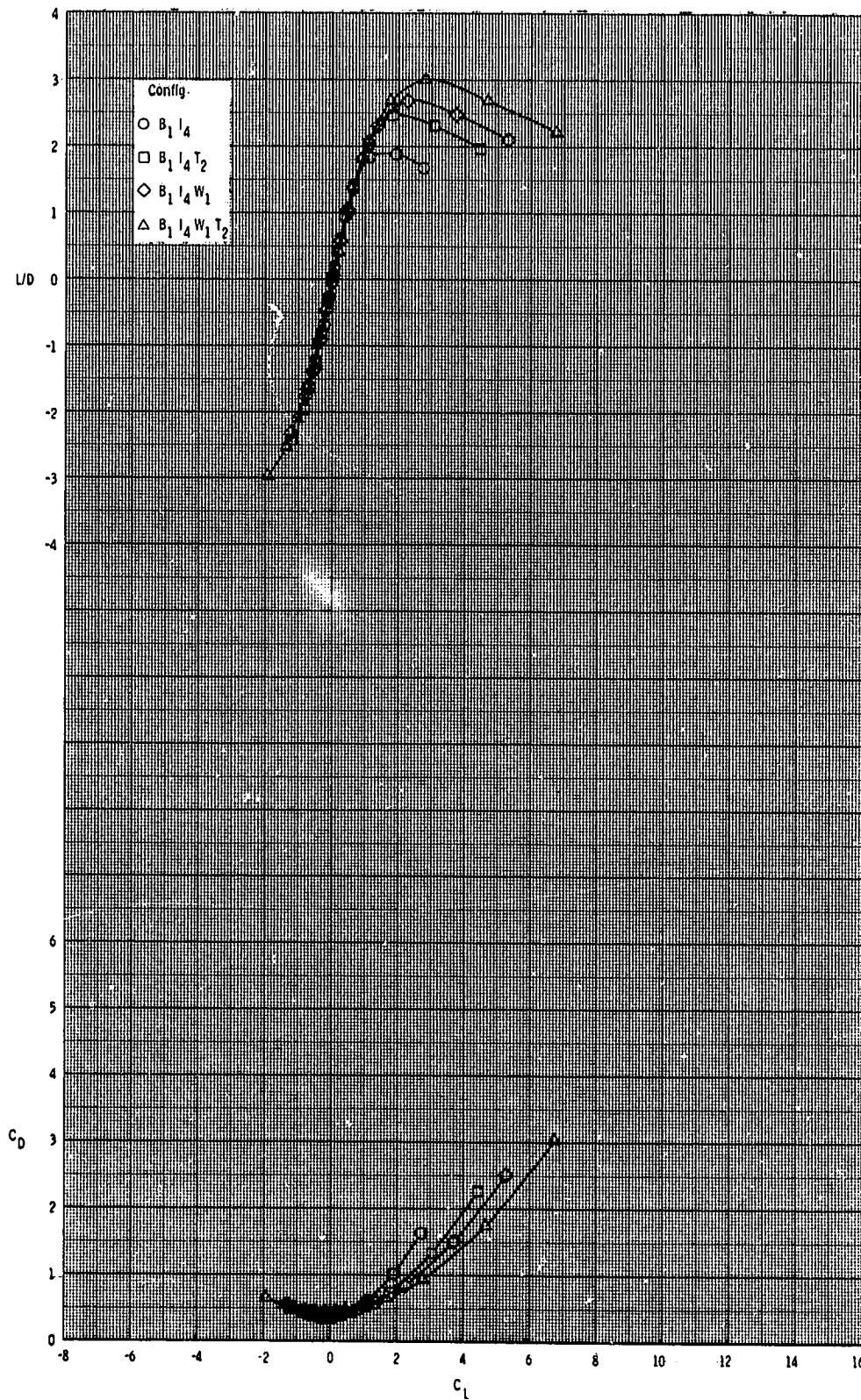
ORIGINAL PAGE IS
OF POOR QUALITY



(d) Continued.

Figure 5.- Continued.

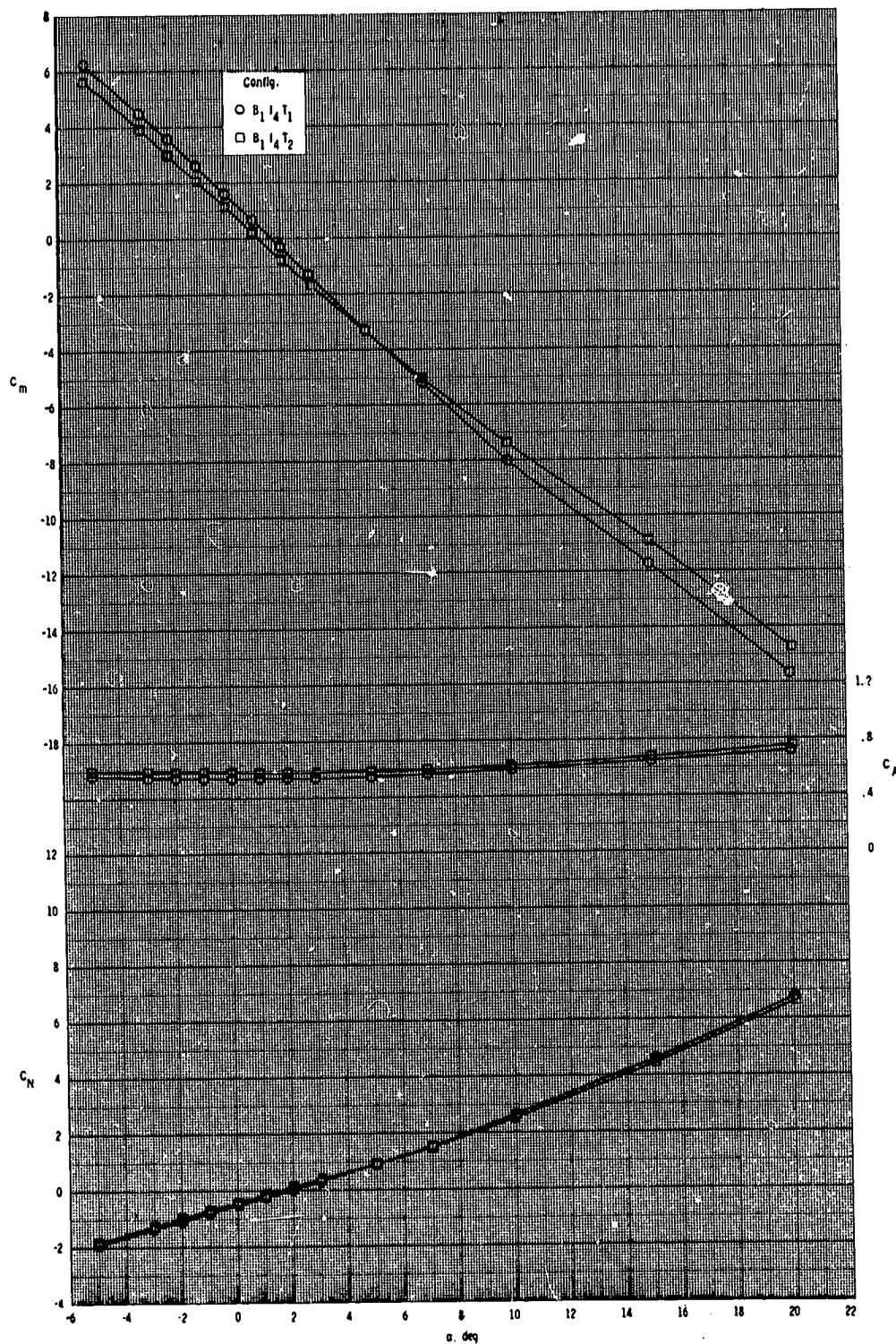
ORIGINAL PAGE IS
OF POOR QUALITY



(d) Concluded.

Figure 5.- Concluded.

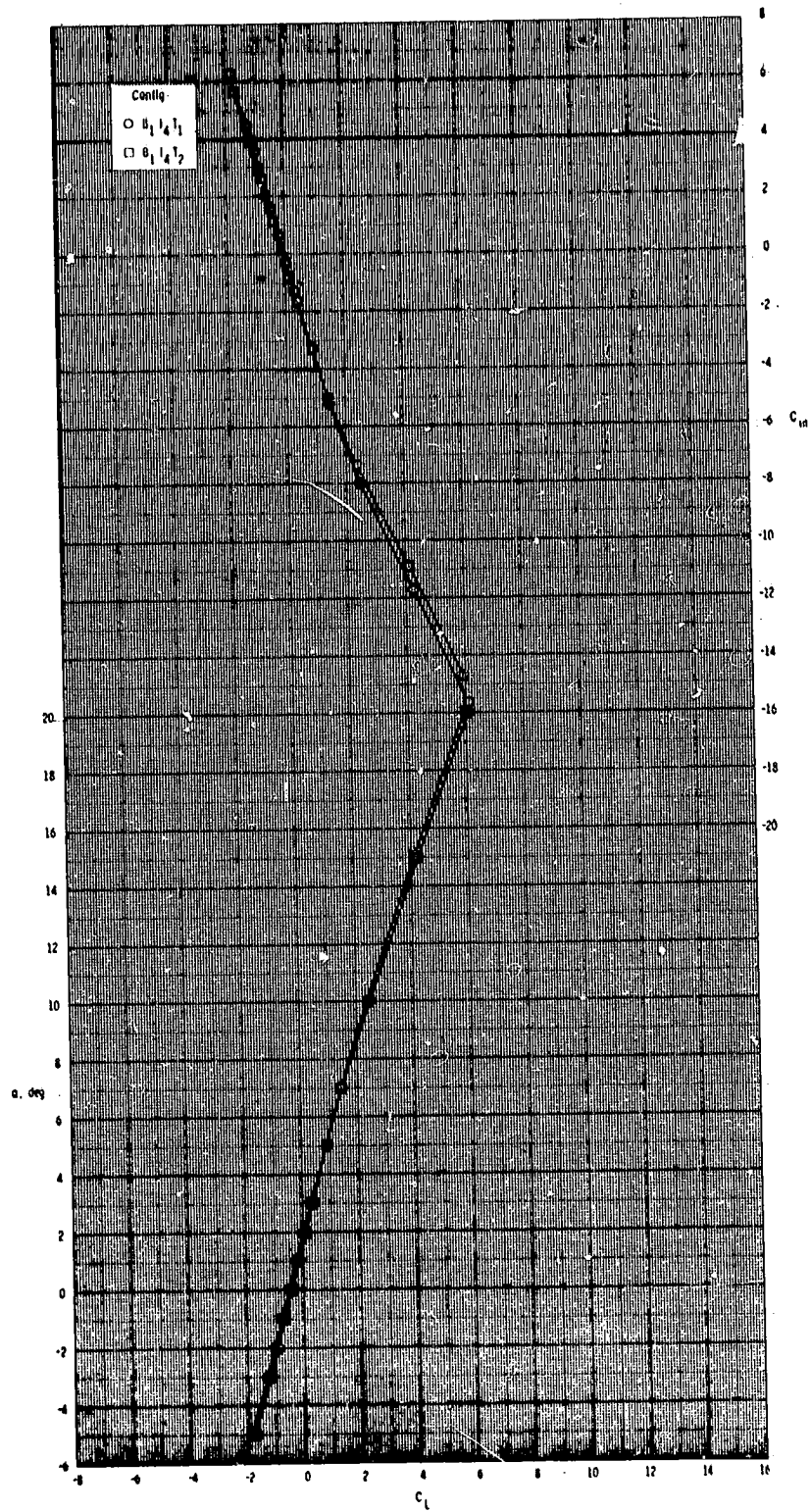
ORIGINAL PAGE IS
OF POOR QUALITY



(a) $M = 2.50$.

Figure 6.- Effect of tail configuration on longitudinal aerodynamic characteristics with wing off.

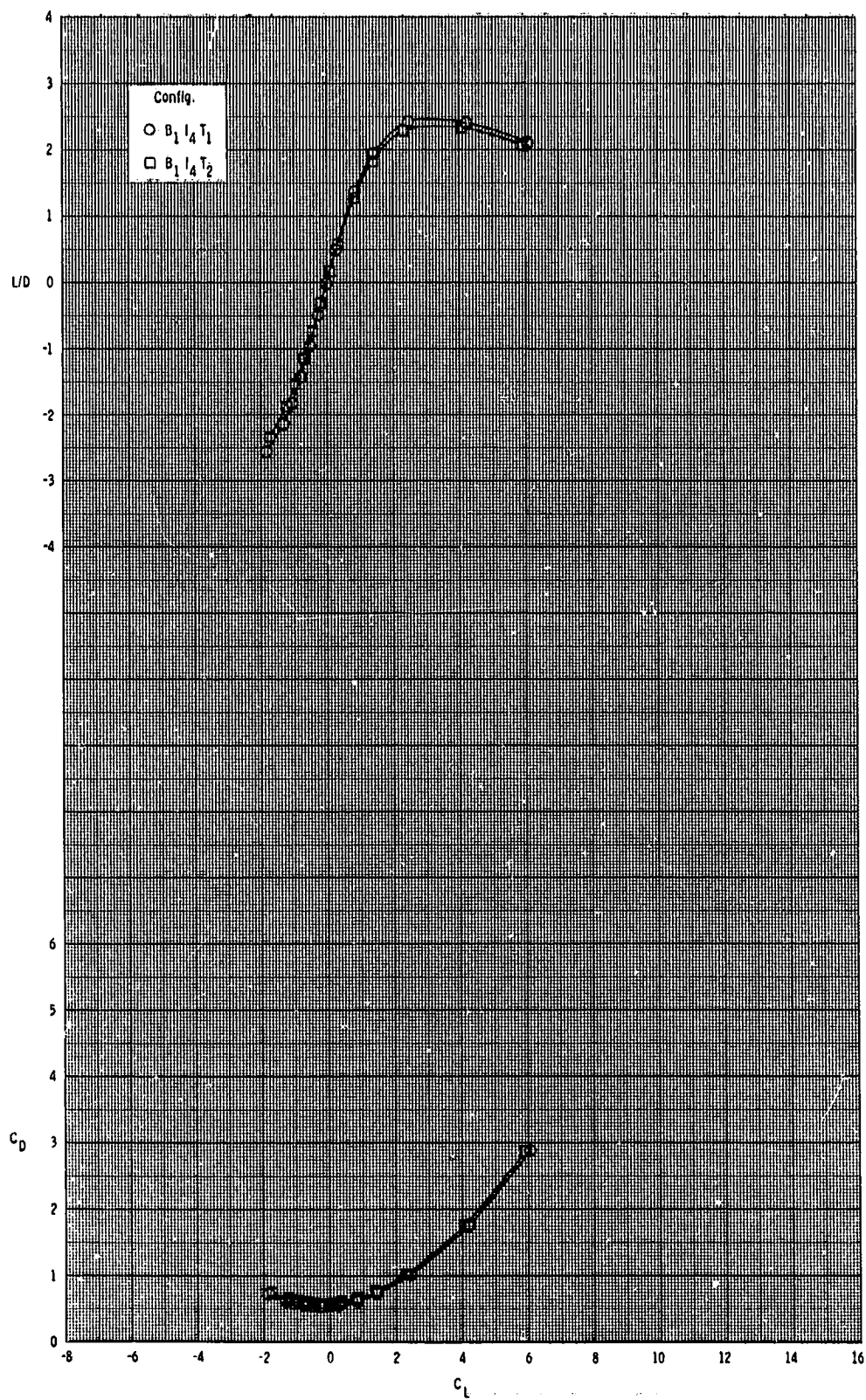
ORIGINAL PAGE IS
OF POOR QUALITY



(a) Continued.

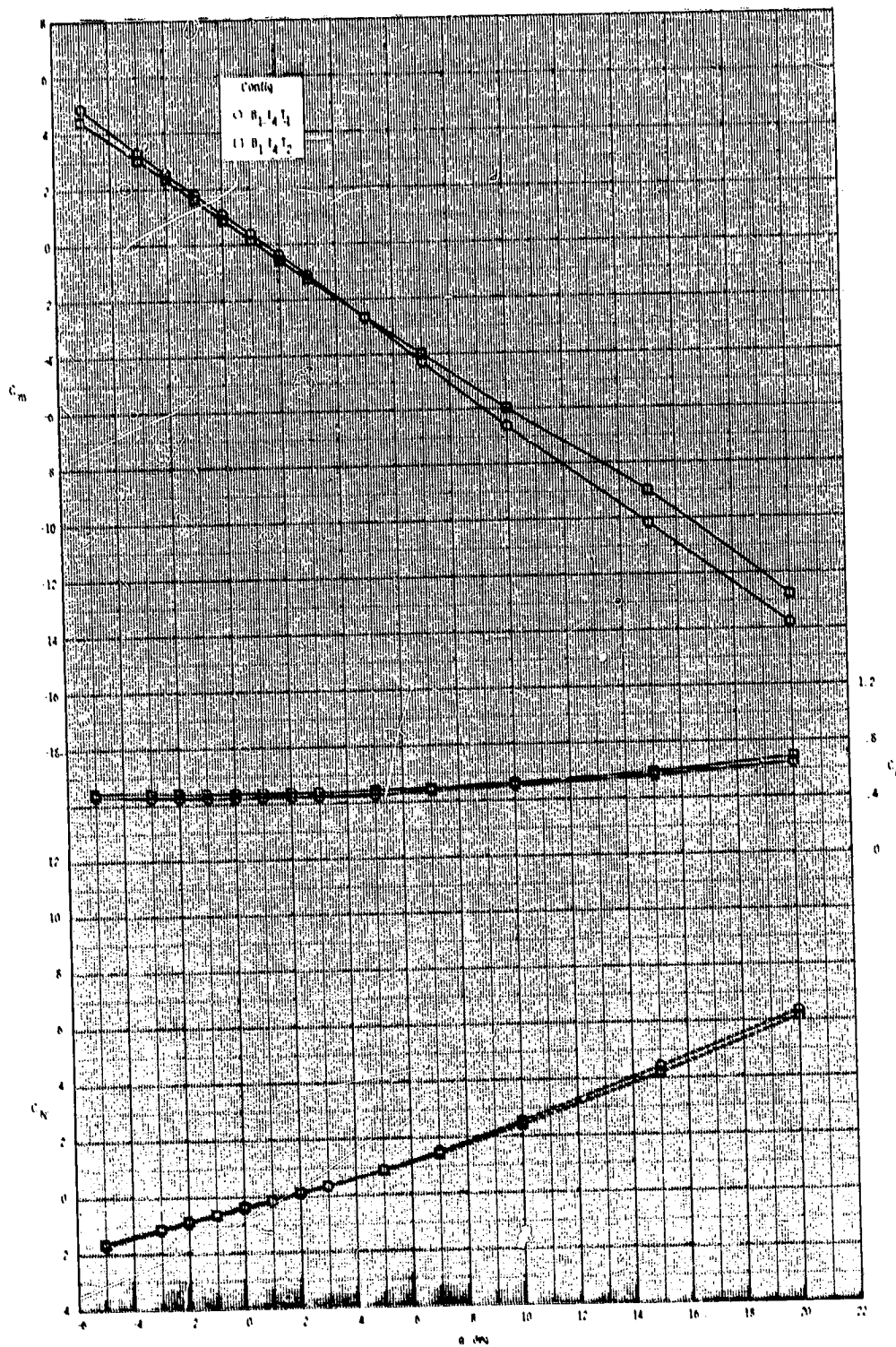
Figure 6.- Continued.

ORIGINAL PAGE IS
OF POOR QUALITY



(a) Concluded.

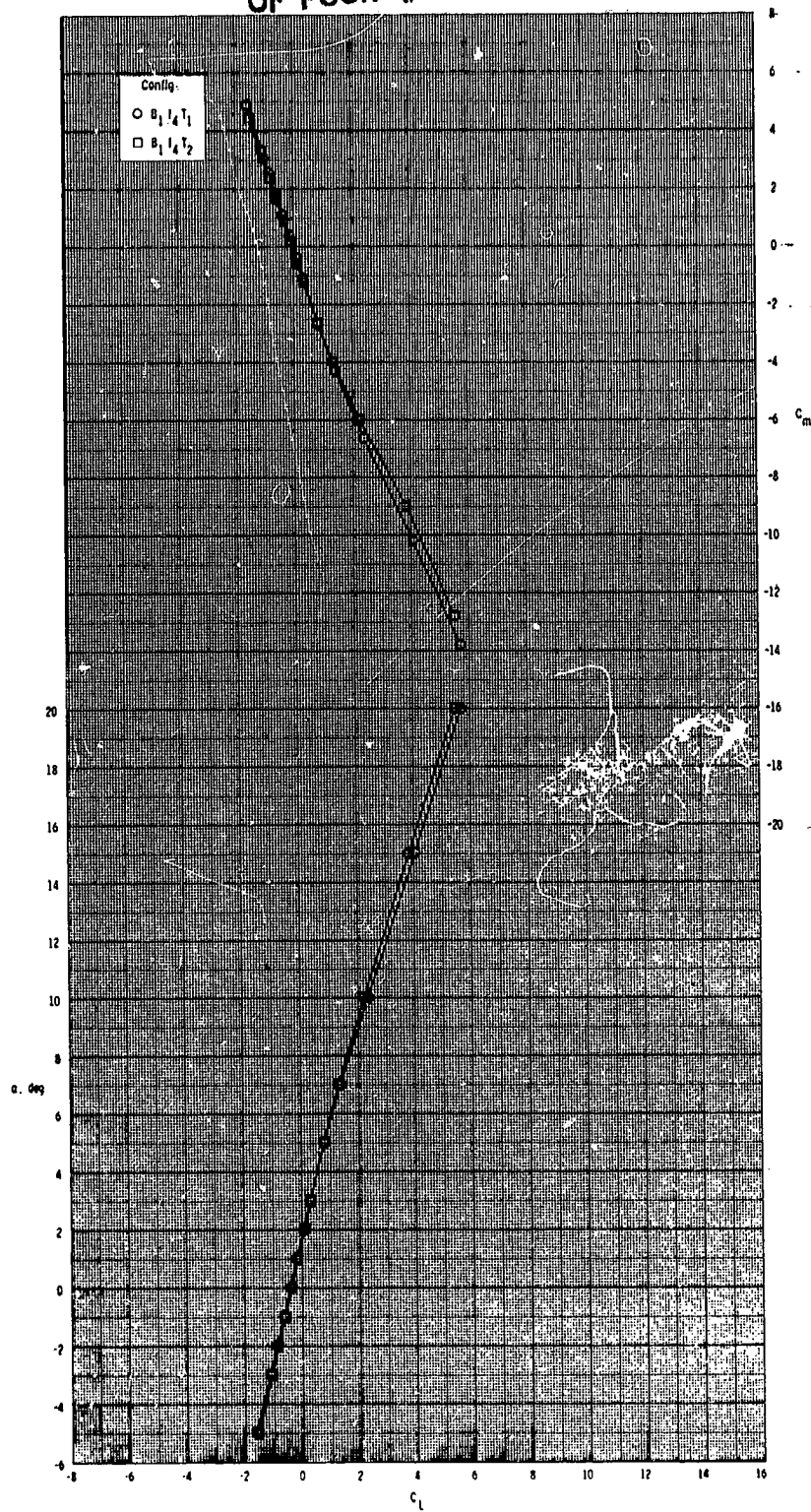
Figure 6.- Continued.



(b) $M = 2.95$.

Figure 6.- Continued.

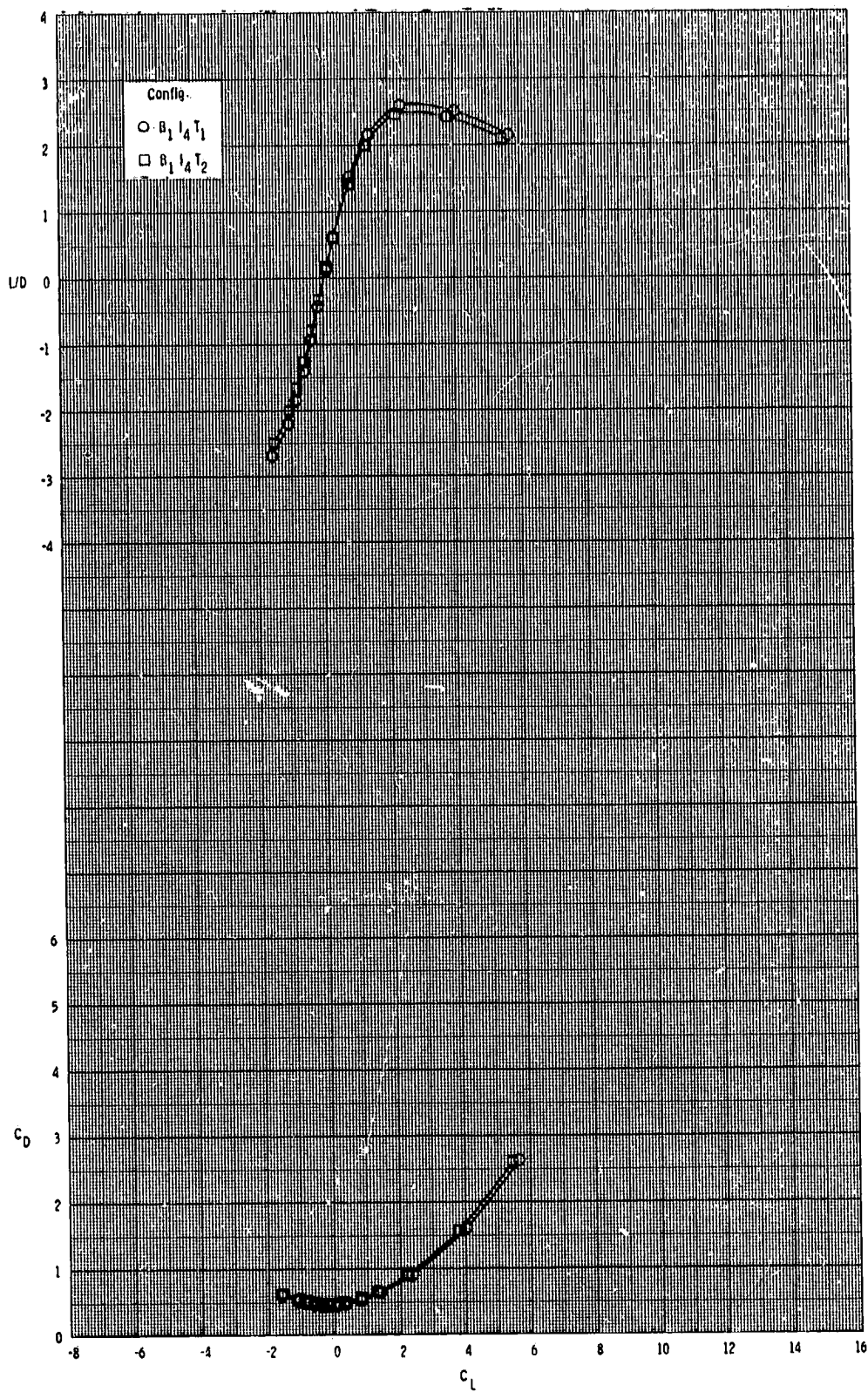
ORIGINAL PAGE IS
OF POOR QUALITY



(b) Continued.

Figure 6.- Continued.

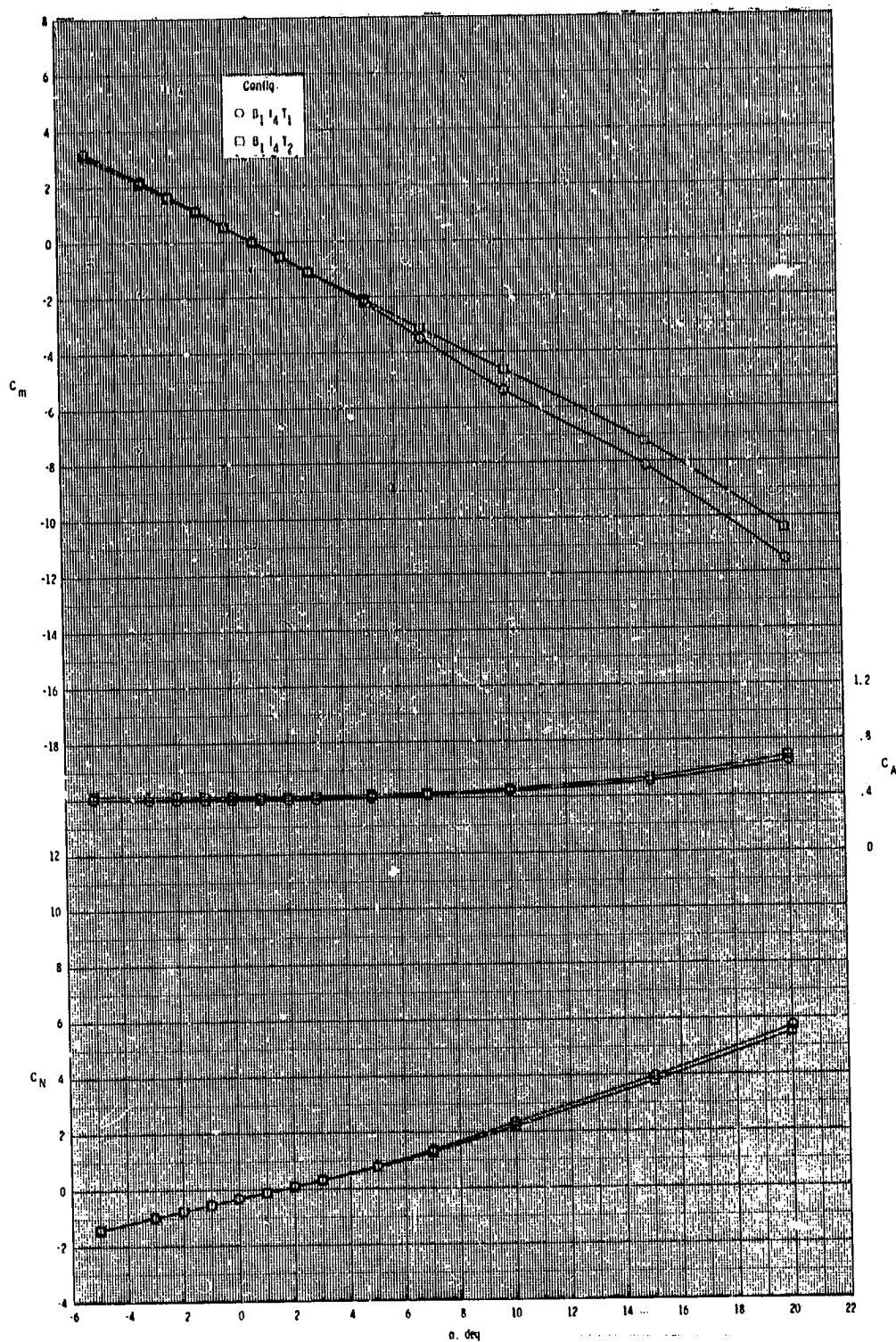
ORIGINAL PAGE IS
OF POOR QUALITY



(b) Concluded.

Figure 6.- Continued.

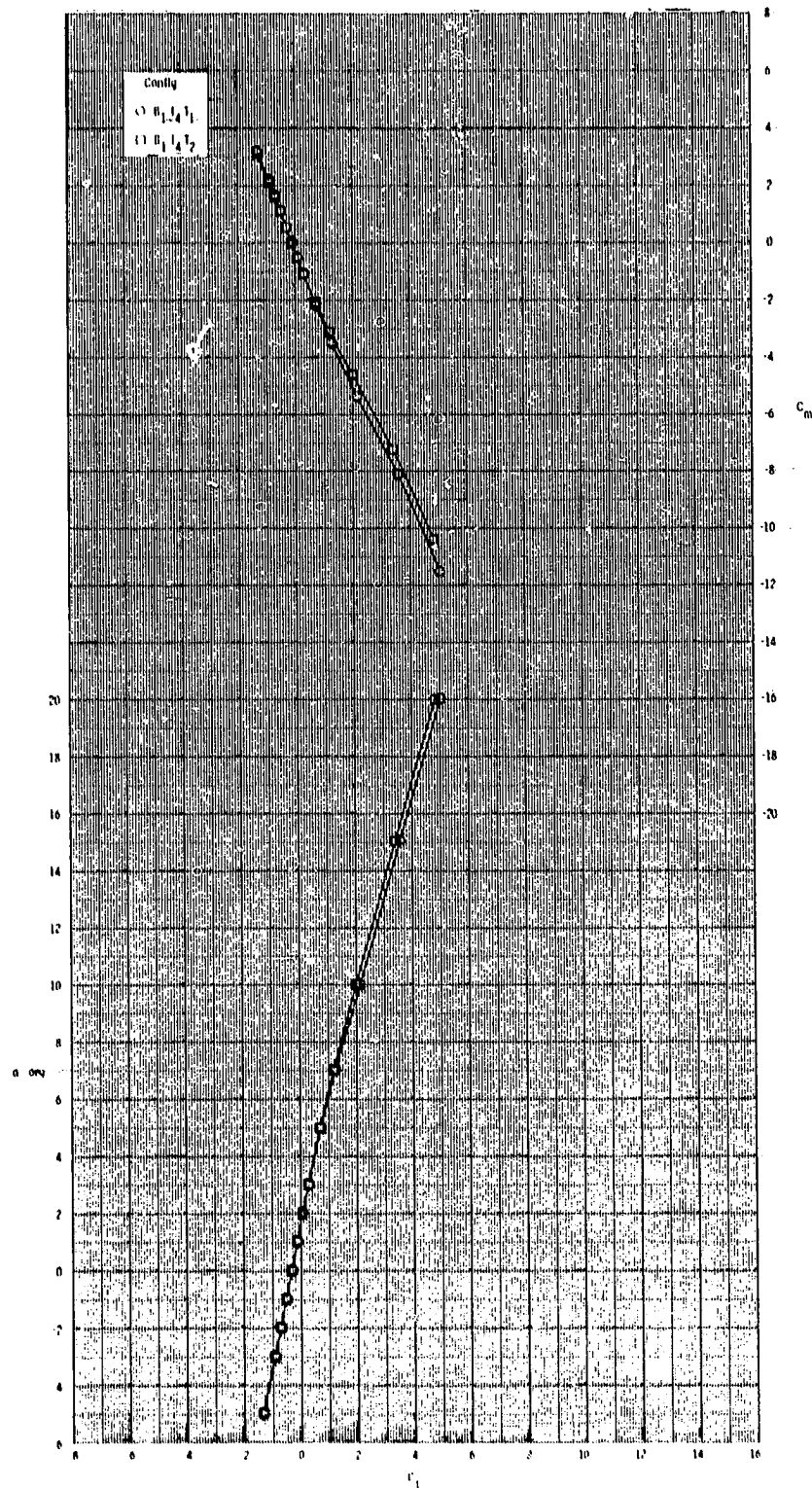
ORIGINAL PAGE IS
OF POOR QUALITY



(c) $M = 3.50$.

Figure 6.- Continued.

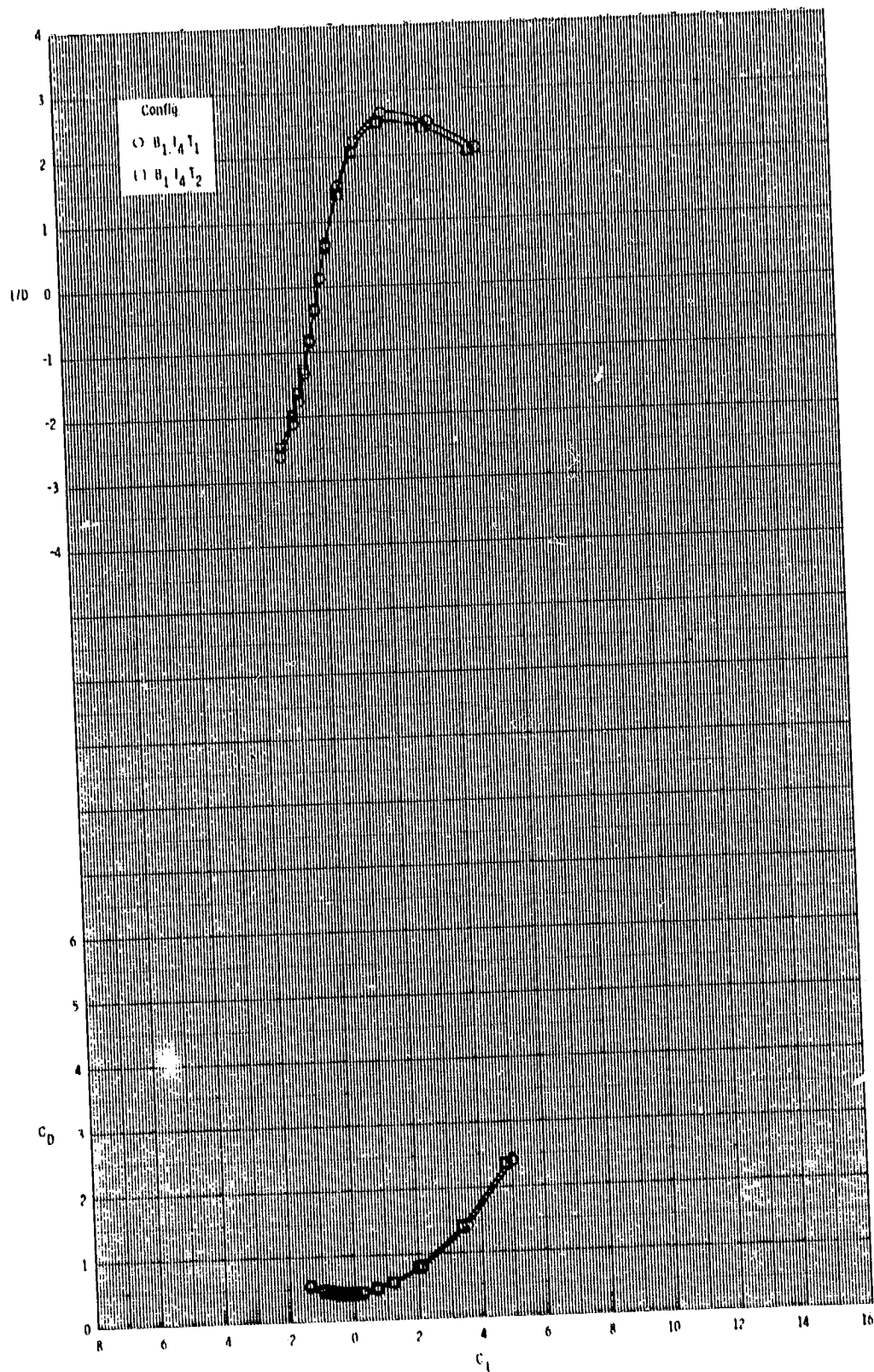
ORIGINAL PAGE IS
OF POOR QUALITY



(c) Continued.

Figure 6.- Continued.

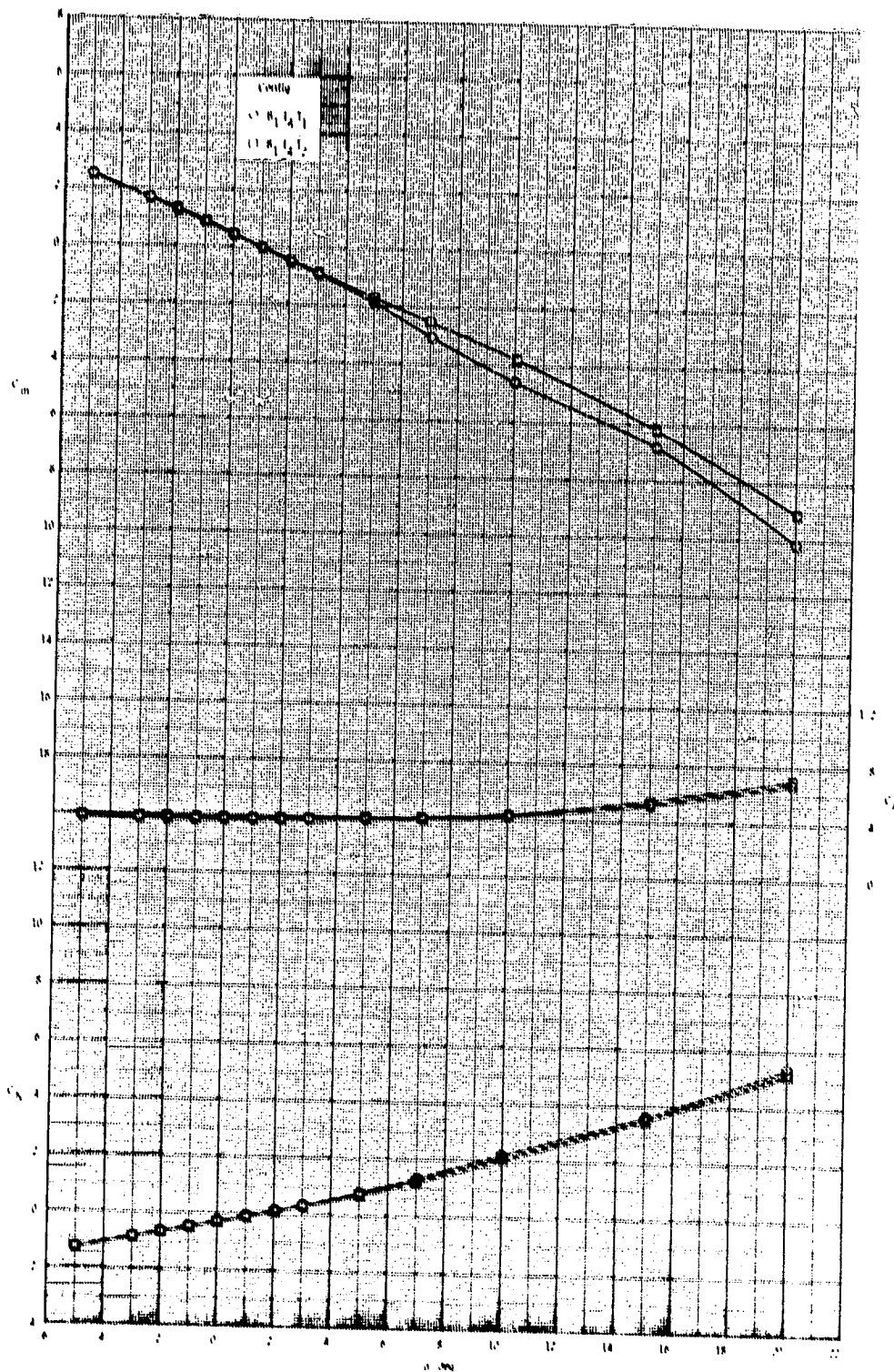
ORIGINAL PAGE IS
OF POOR QUALITY



(c) Concluded.

Figure 6.- Continued.

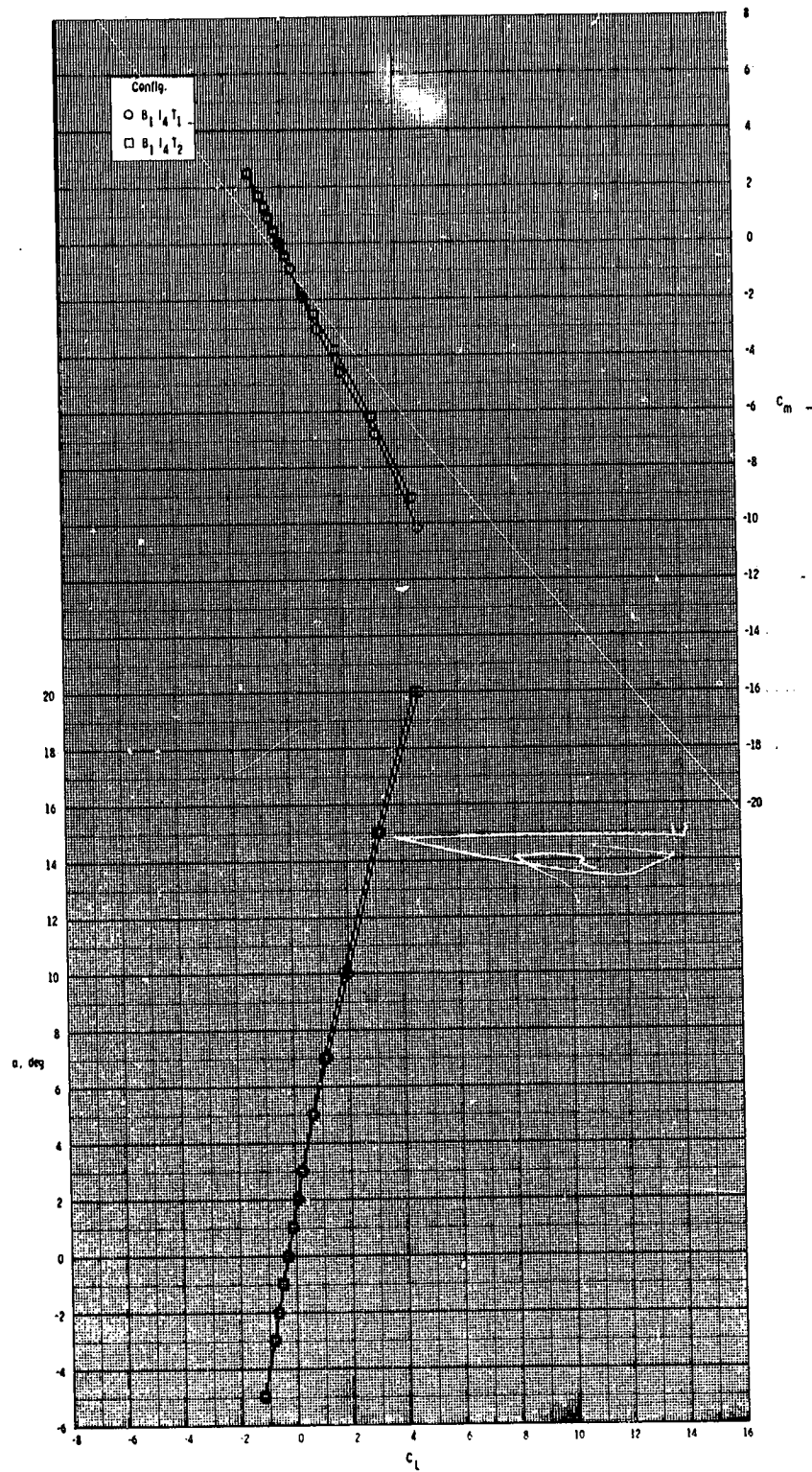
ORIGINAL PAGE IS
OF POOR QUALITY



(d) $M = 3.95$.

Figure 6.- Continued.

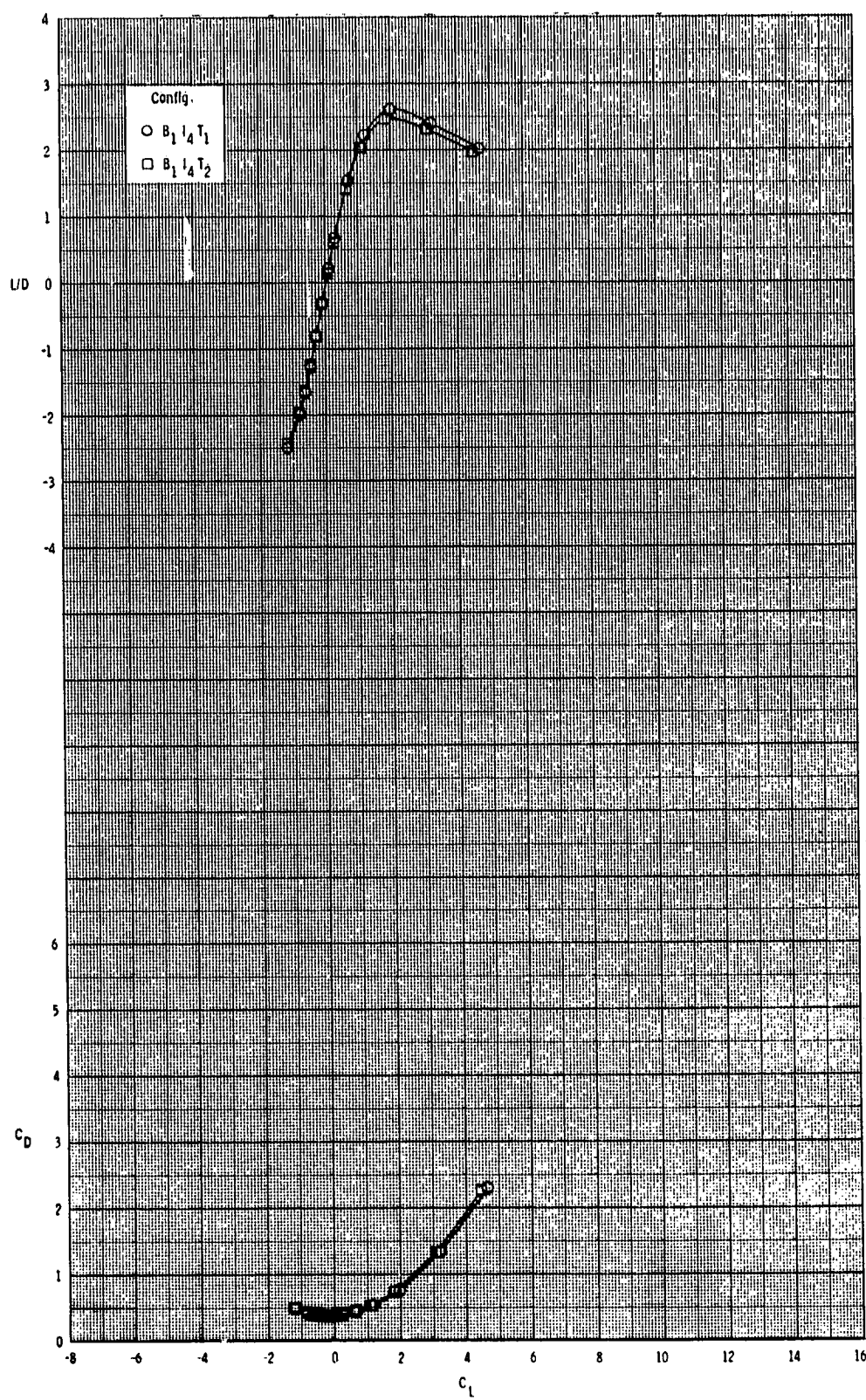
ORIGINAL PAGE IS
OF POOR QUALITY



(d) Continued.

Figure 6.- Continued.

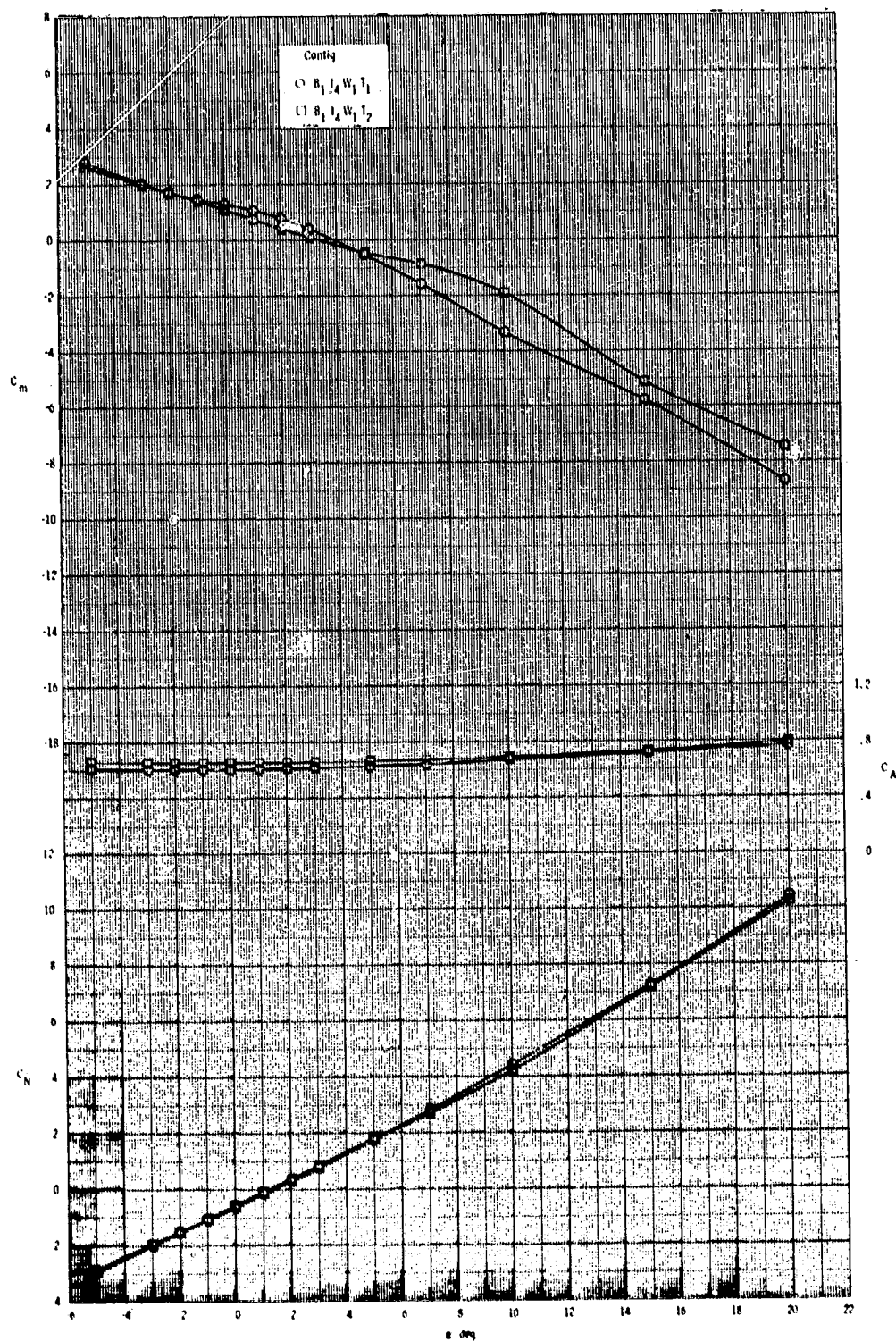
ORIGINAL PAGE IS
OF POOR QUALITY



(d) Concluded.

Figure 6.- Concluded.

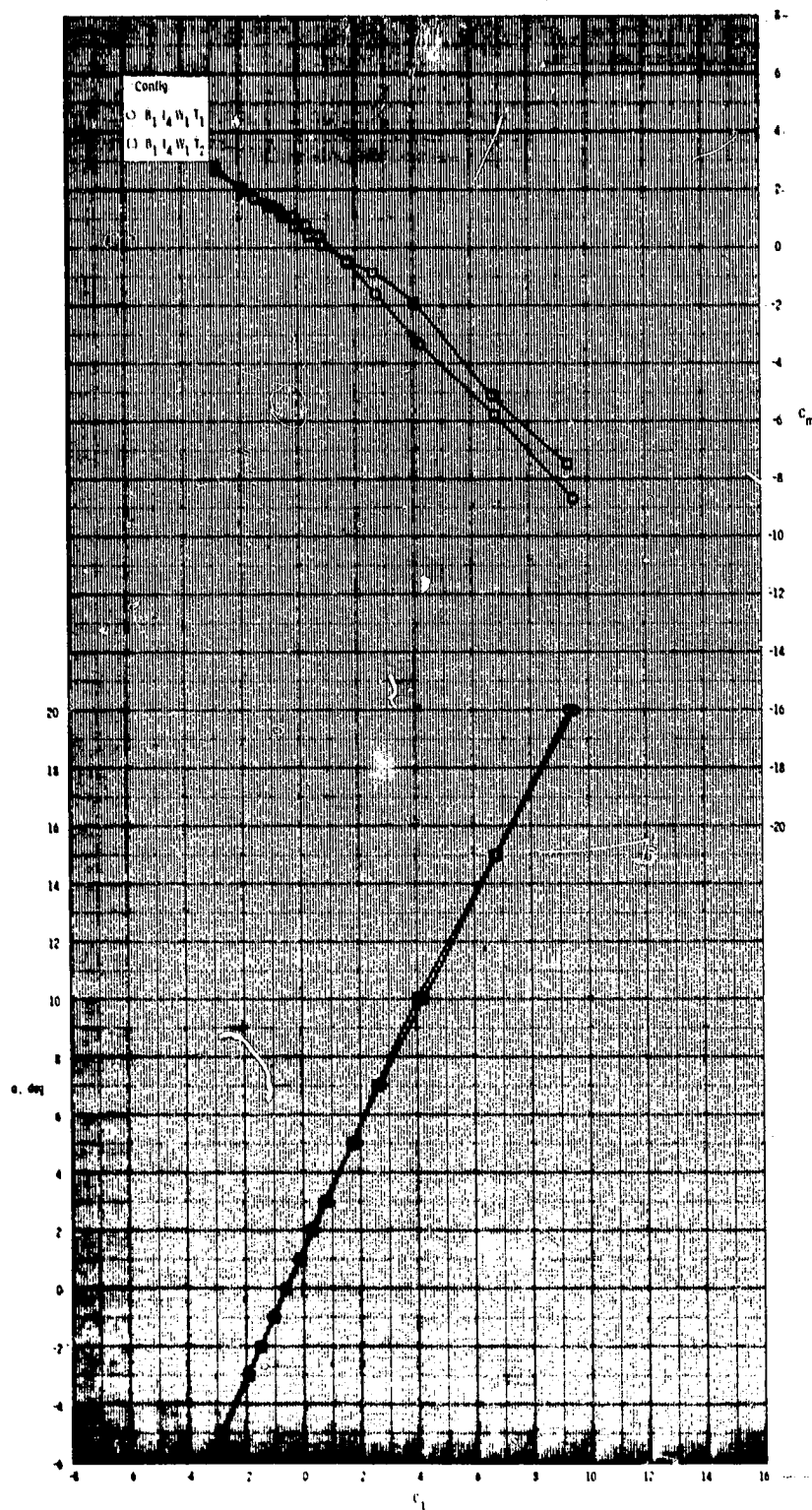
ORIGINAL PAGE IS
OF POOR QUALITY



(a) $M = 2.50$.

Figure 7.- Effect of tail configuration on longitudinal aerodynamic characteristics with wing on.

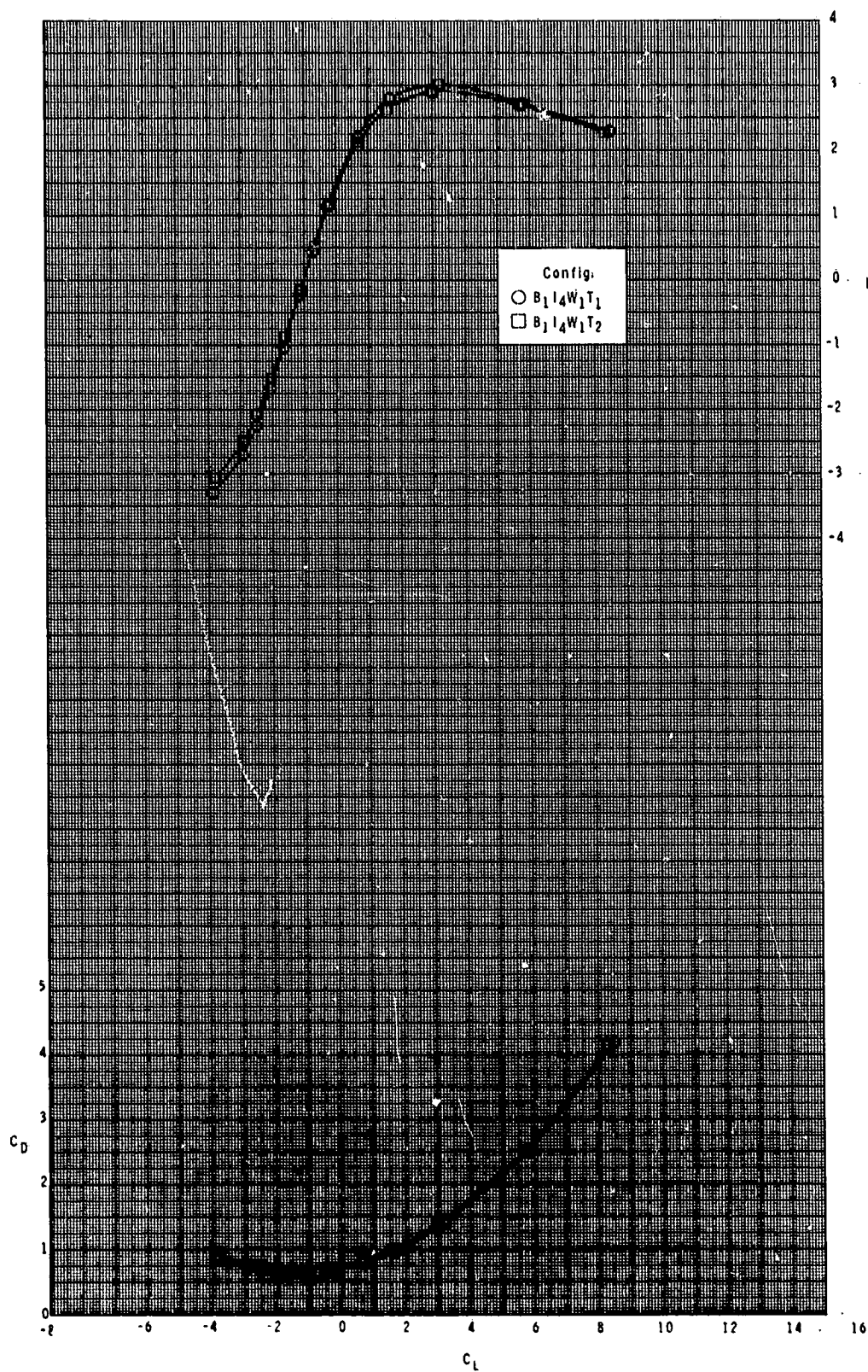
ORIGINAL PAGE IS
OF POOR QUALITY



(a) Continued.

Figure 7.- Continued.

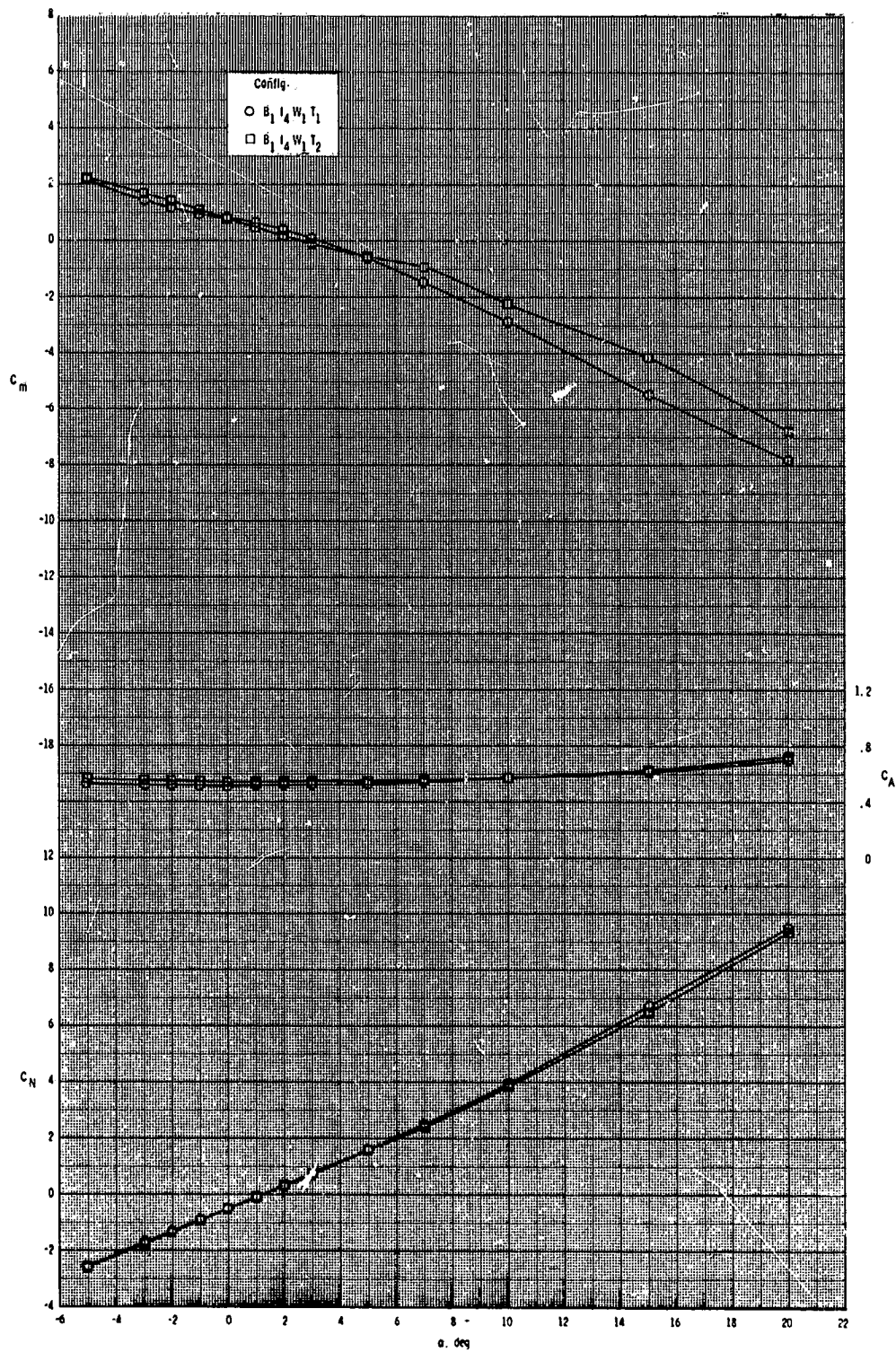
ORIGINAL PAGE IS
OF POOR QUALITY



(a) Concluded.

Figure 7.- Continued.

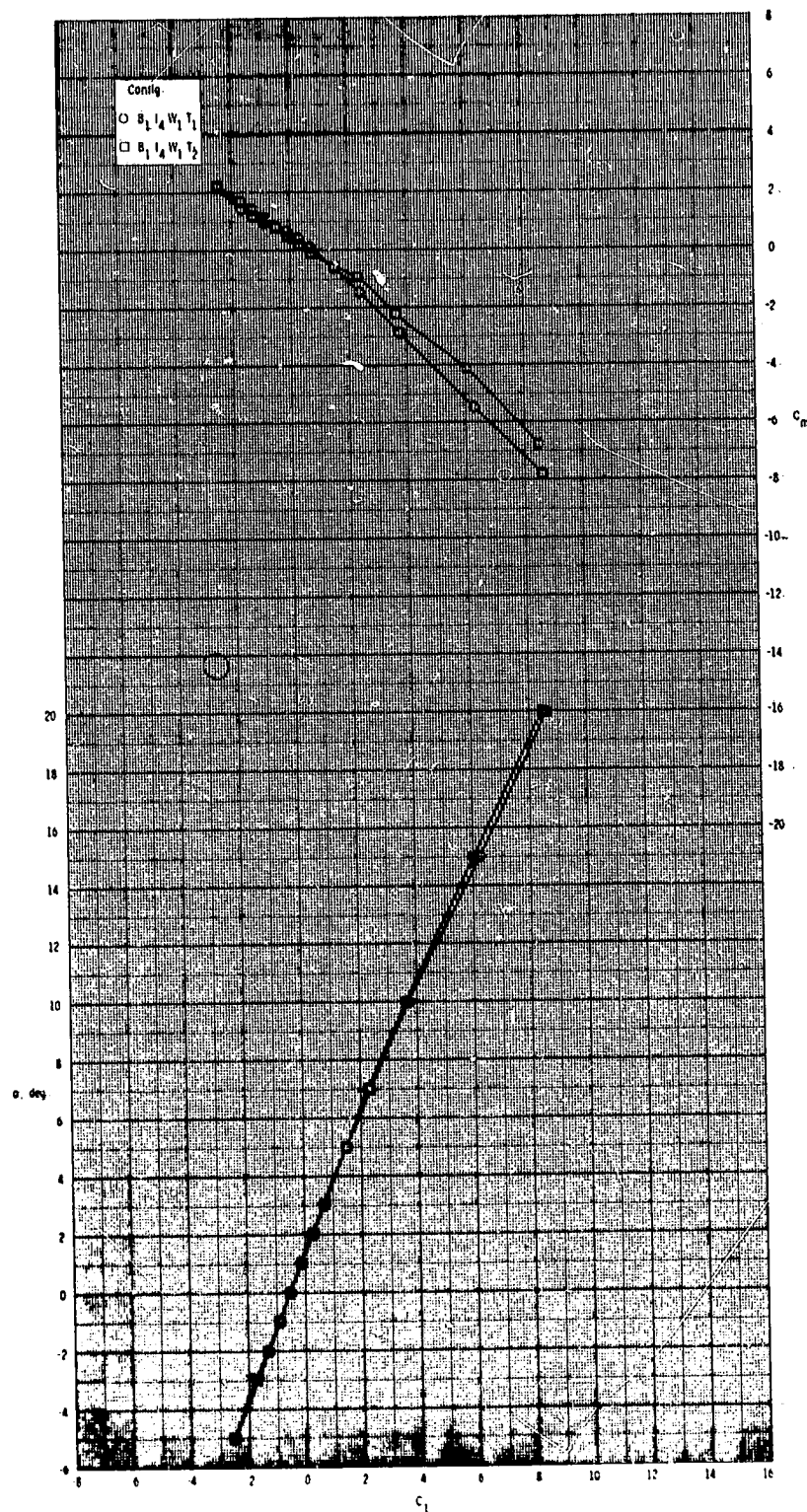
ORIGINAL PAGE IS
OF POOR QUALITY



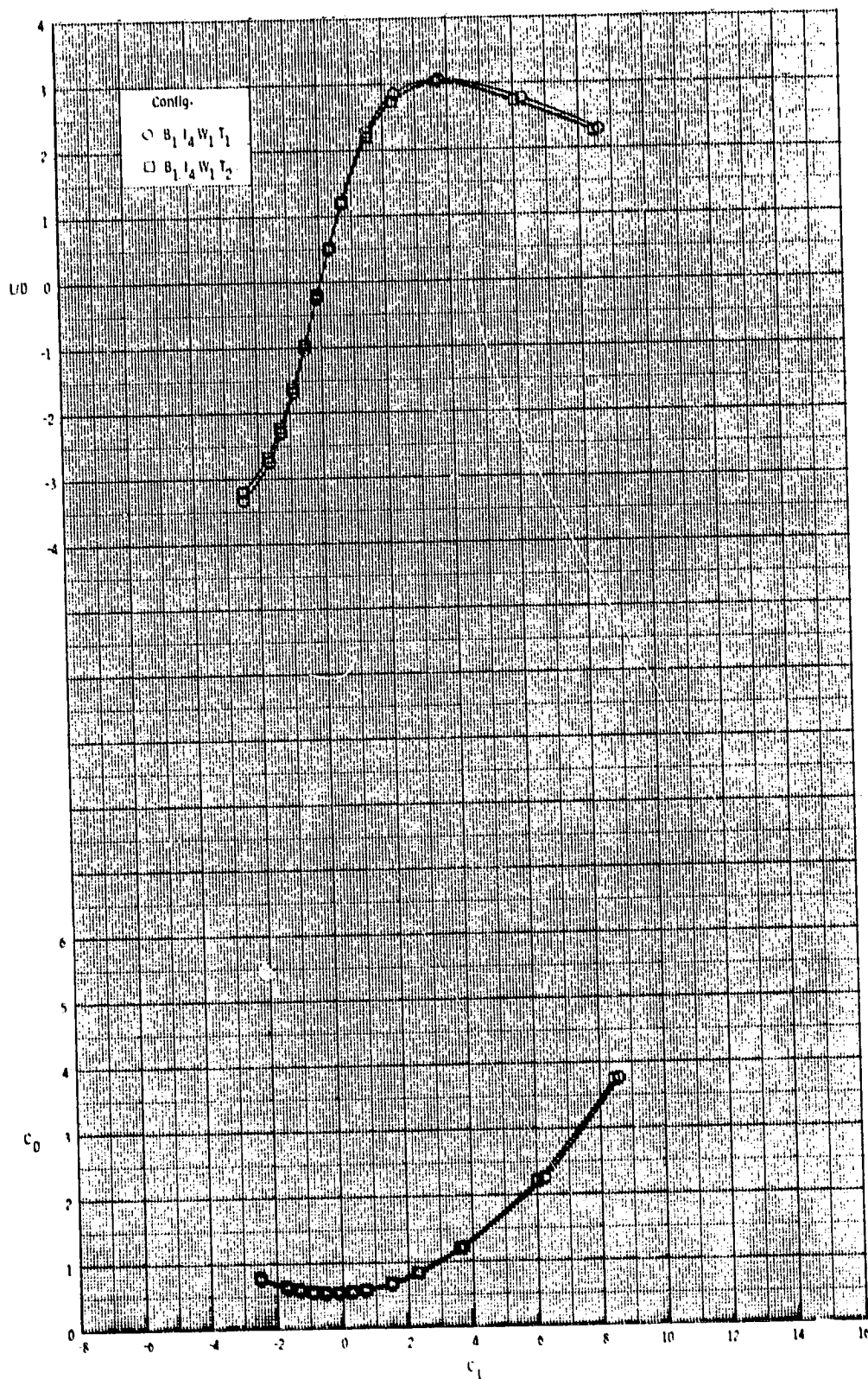
(b) $M = 2.95$.

Figure 7.- Continued.

ORIGINAL PAGE IS
OF POOR QUALITY



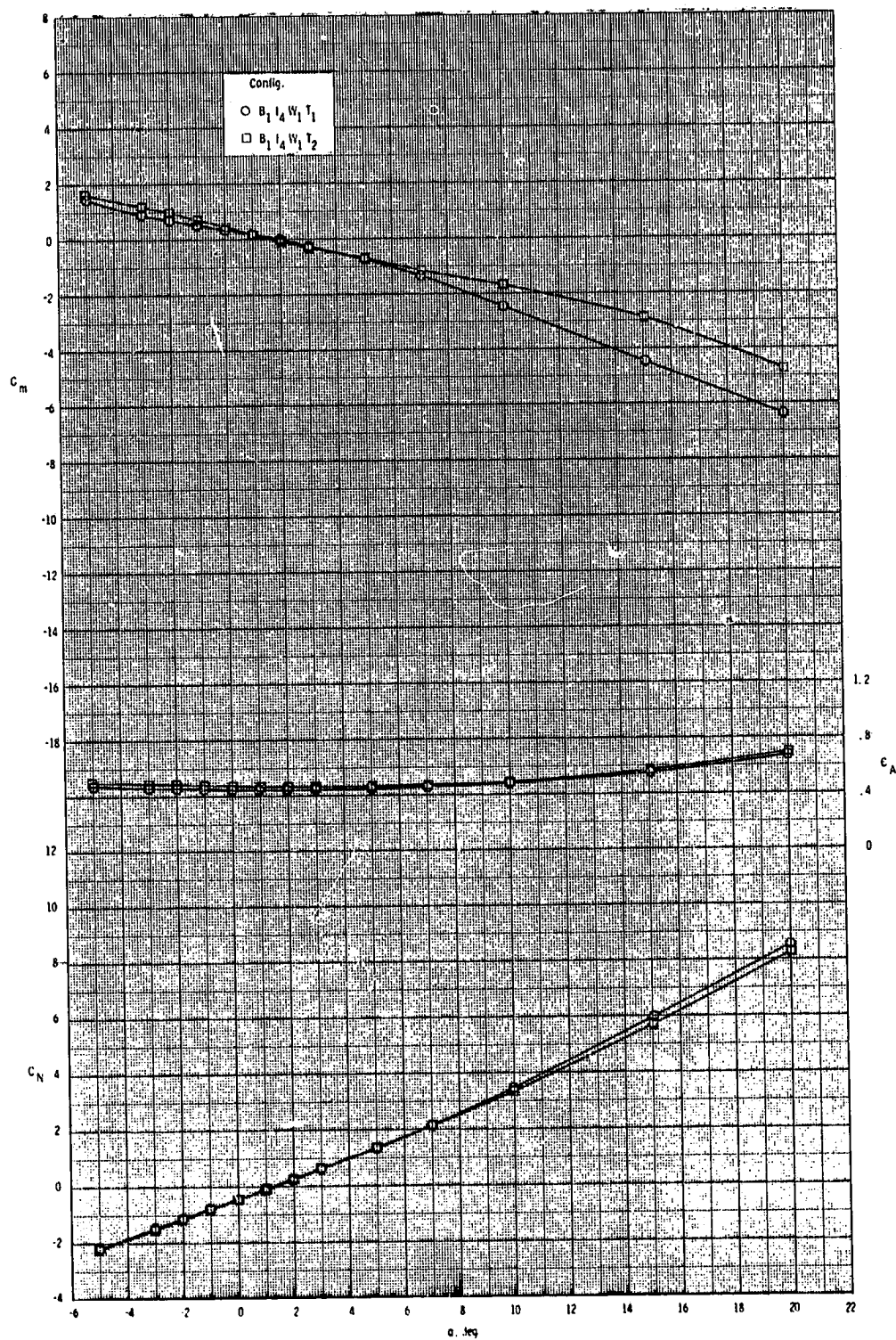
ORIGINAL PAGE IS
OF POOR QUALITY



(b) Concluded.

Figure 7.- Continued.

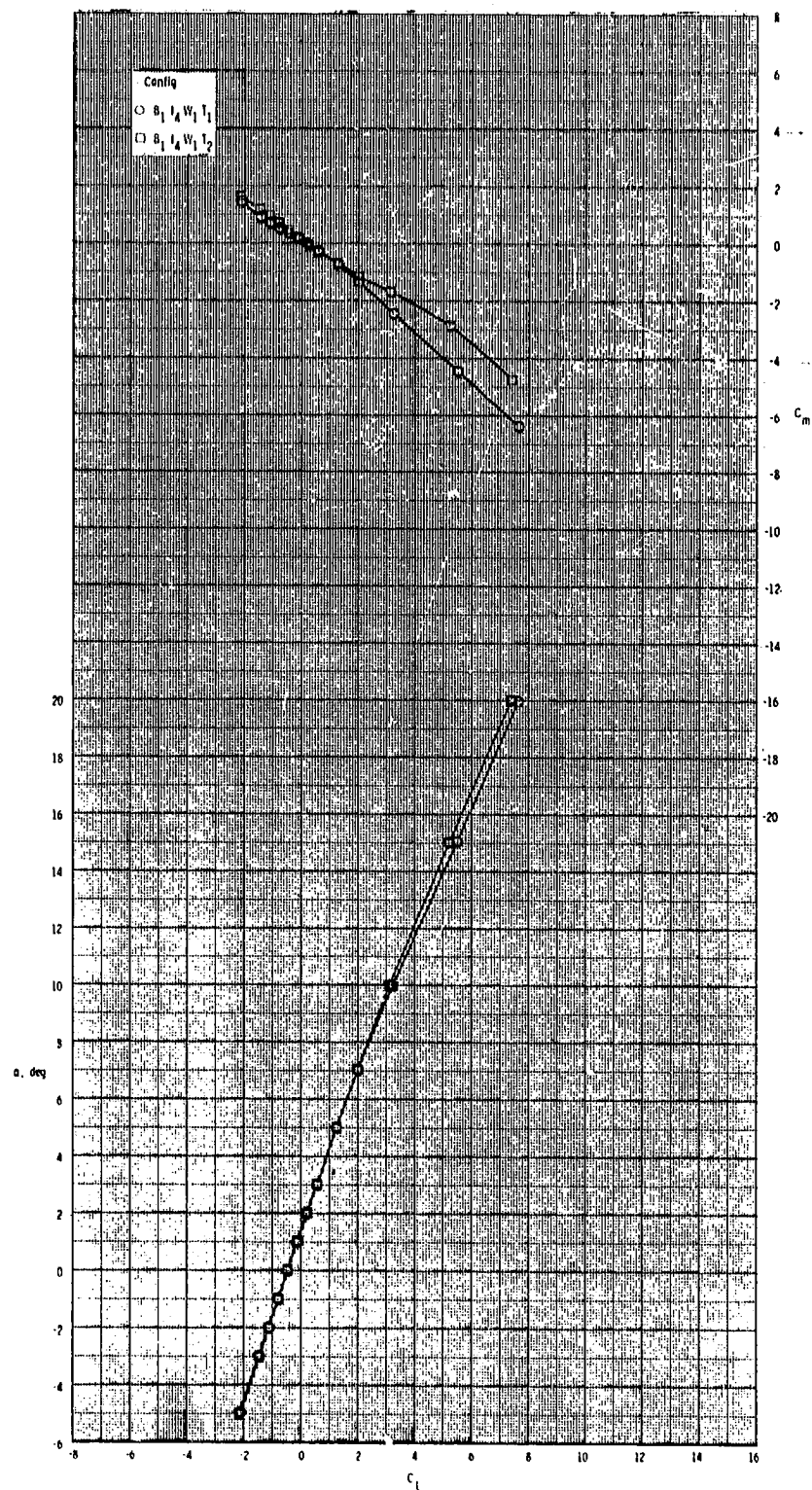
ORIGINAL PAGE IS
OF POOR QUALITY



(c) $M = 3.50$.

Figure 1.- Continued.

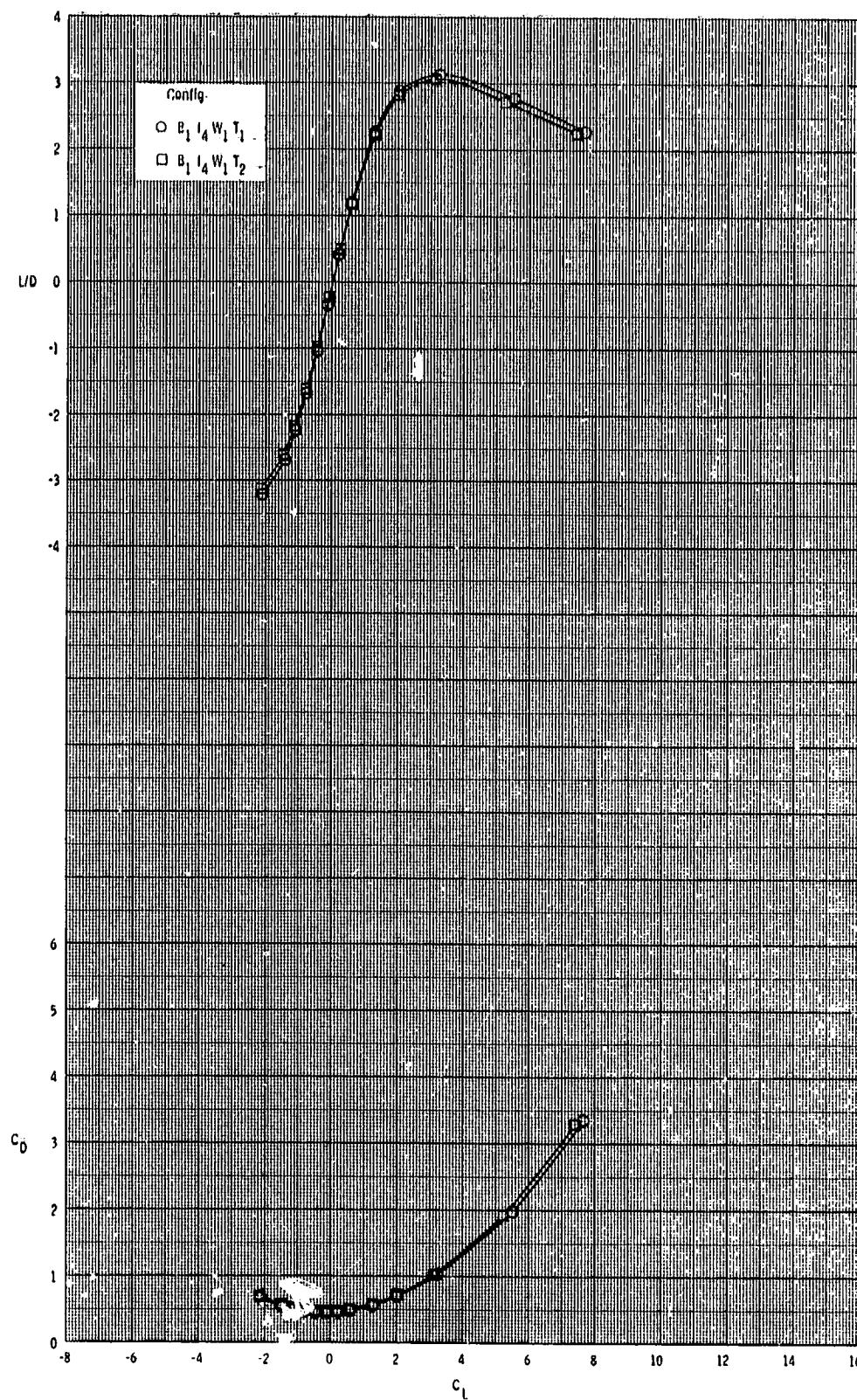
ORIGINAL PAGE IS
OF POOR QUALITY



(c) Continued.

Figure 7.- Continued.

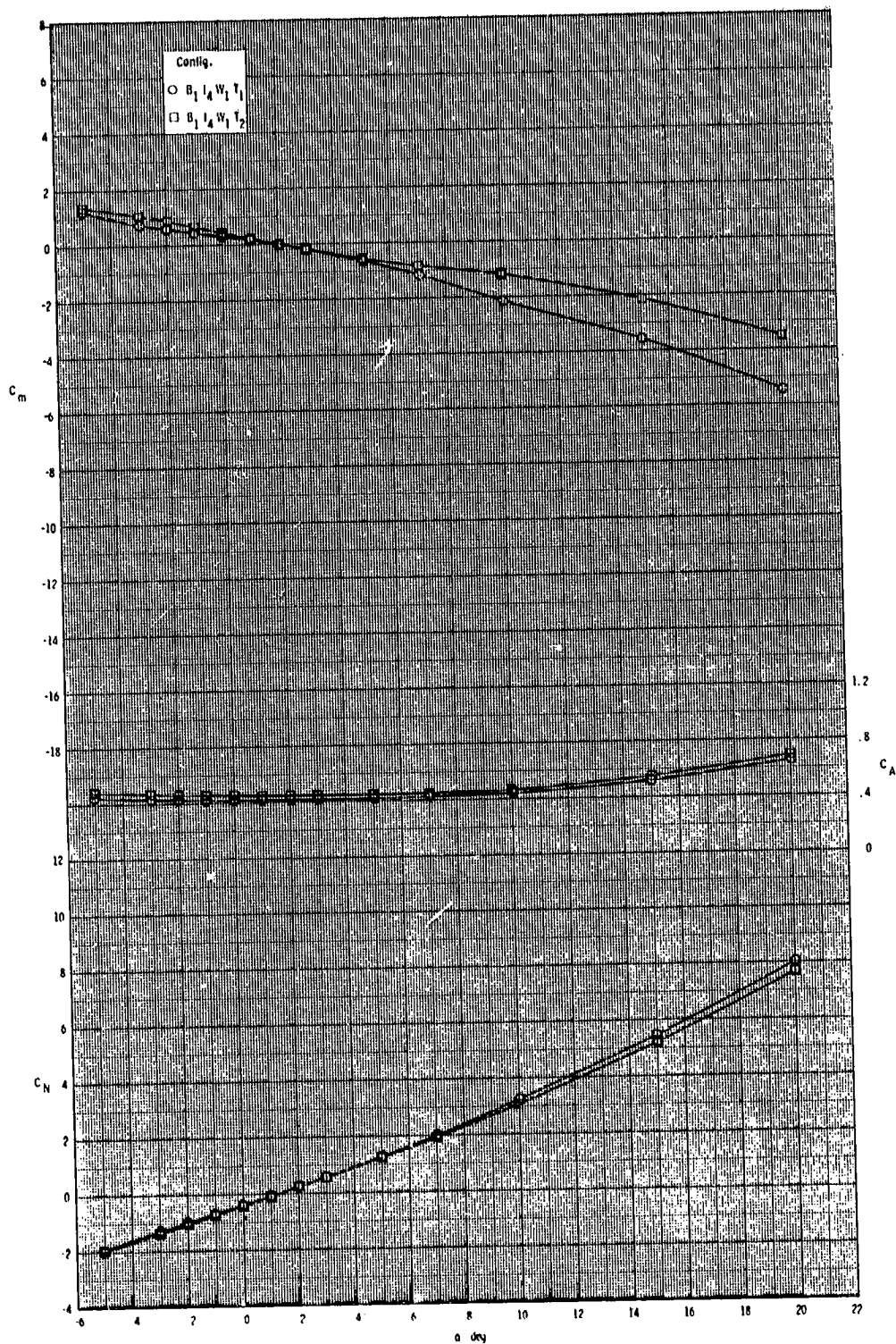
ORIGINAL PAGE IS
OF POOR QUALITY



(c) Concluded.

Figure 7.- Continued.

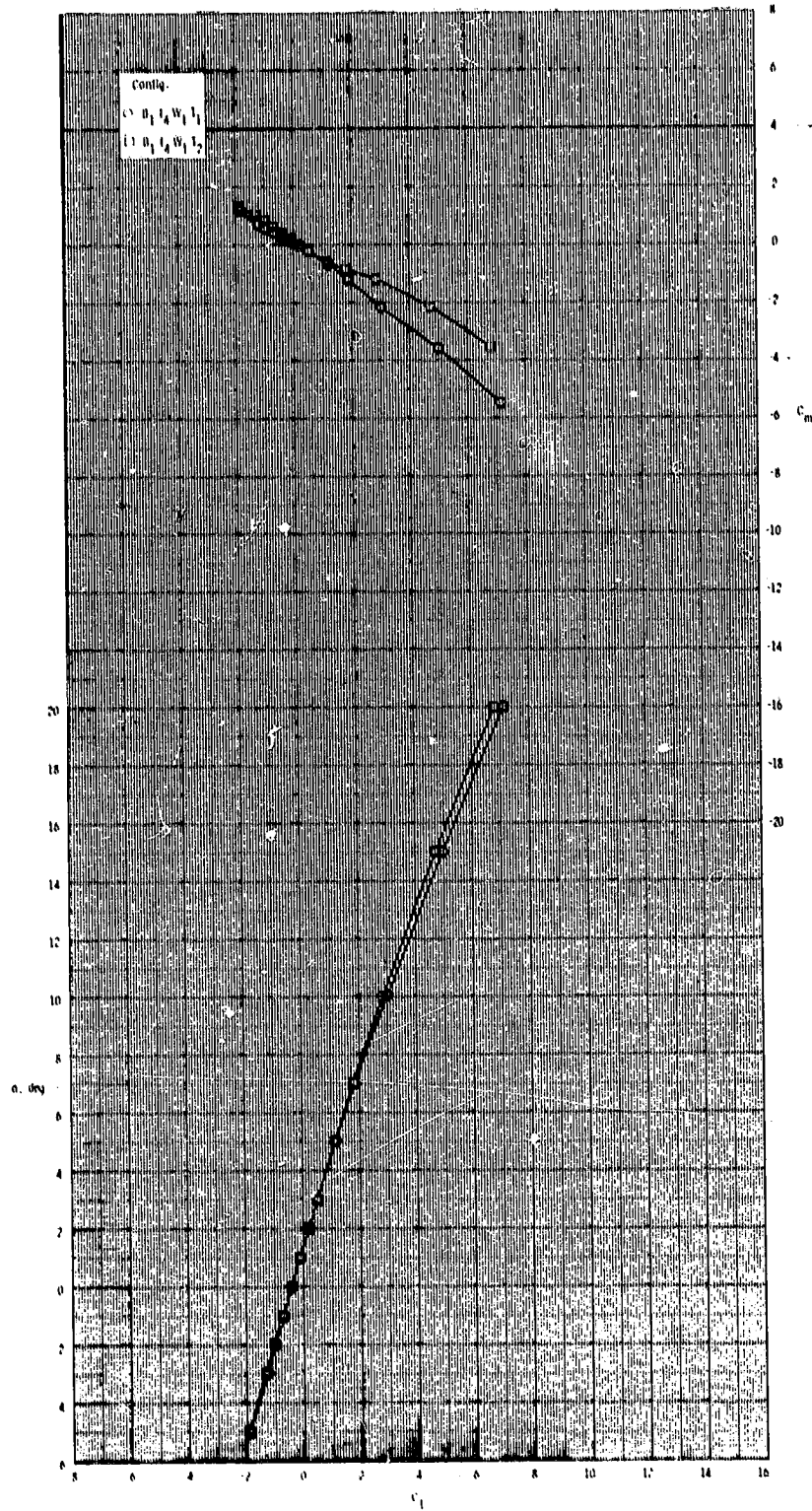
ORIGINAL PAGE IS
OF POOR QUALITY



(d) $M = 3.95$.

Figure 7.- Continued.

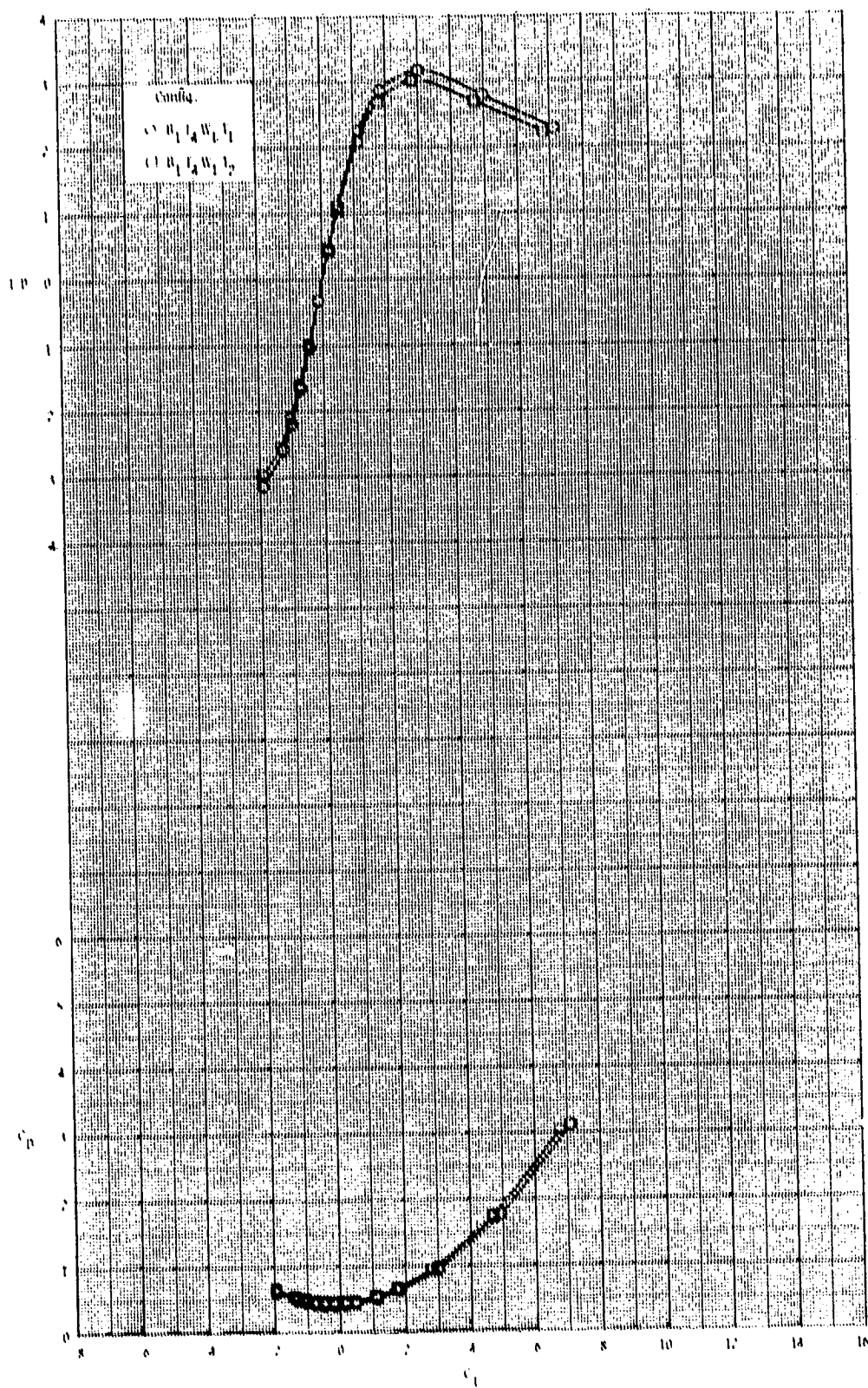
ORIGINAL PAGE IS
OF POOR QUALITY



(d) Continued.

Figure 7.- Continued.

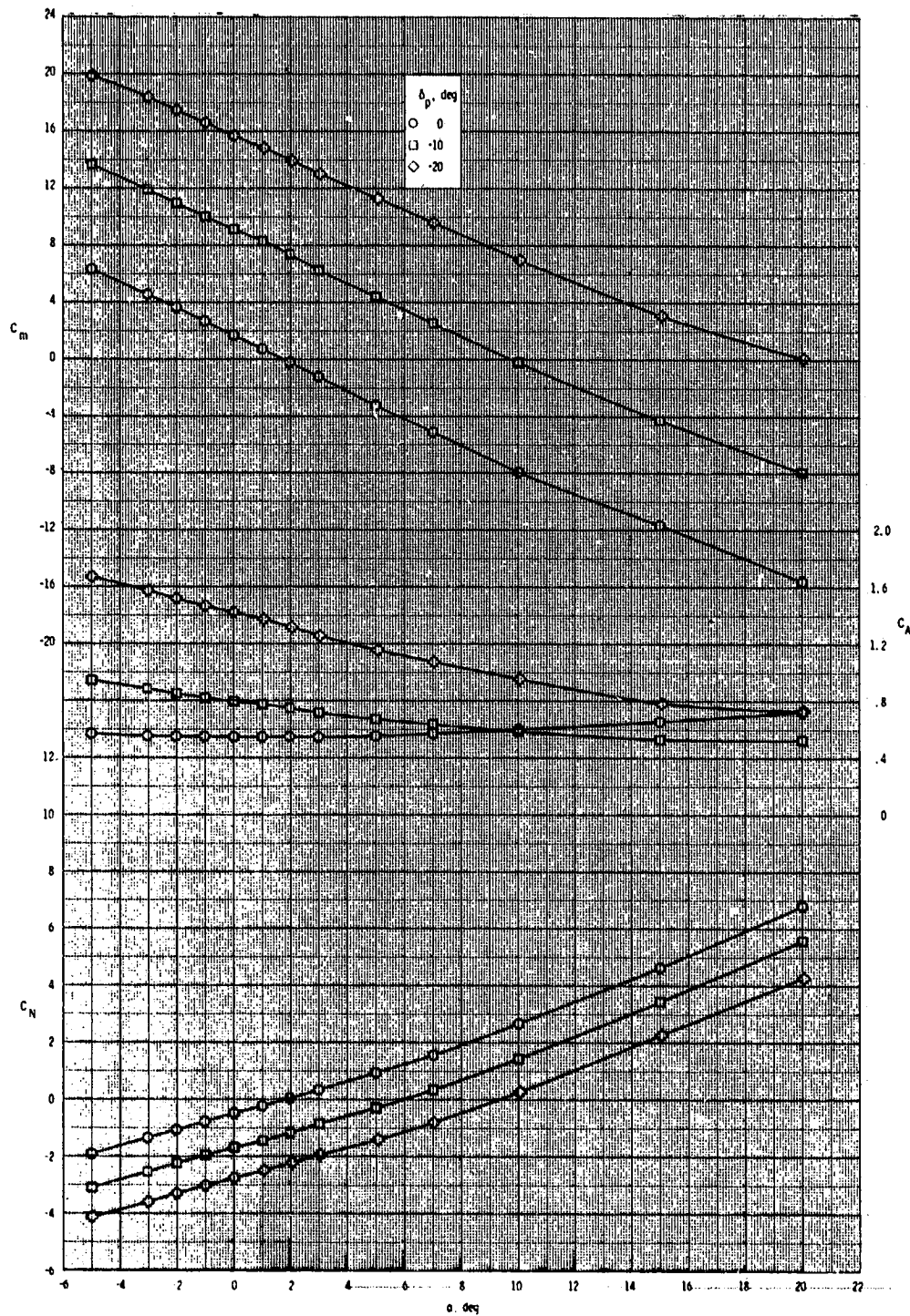
ORIGINAL PAGE IS
OF POOR QUALITY



(d) Concluded.

Figure 2. = Concluded.

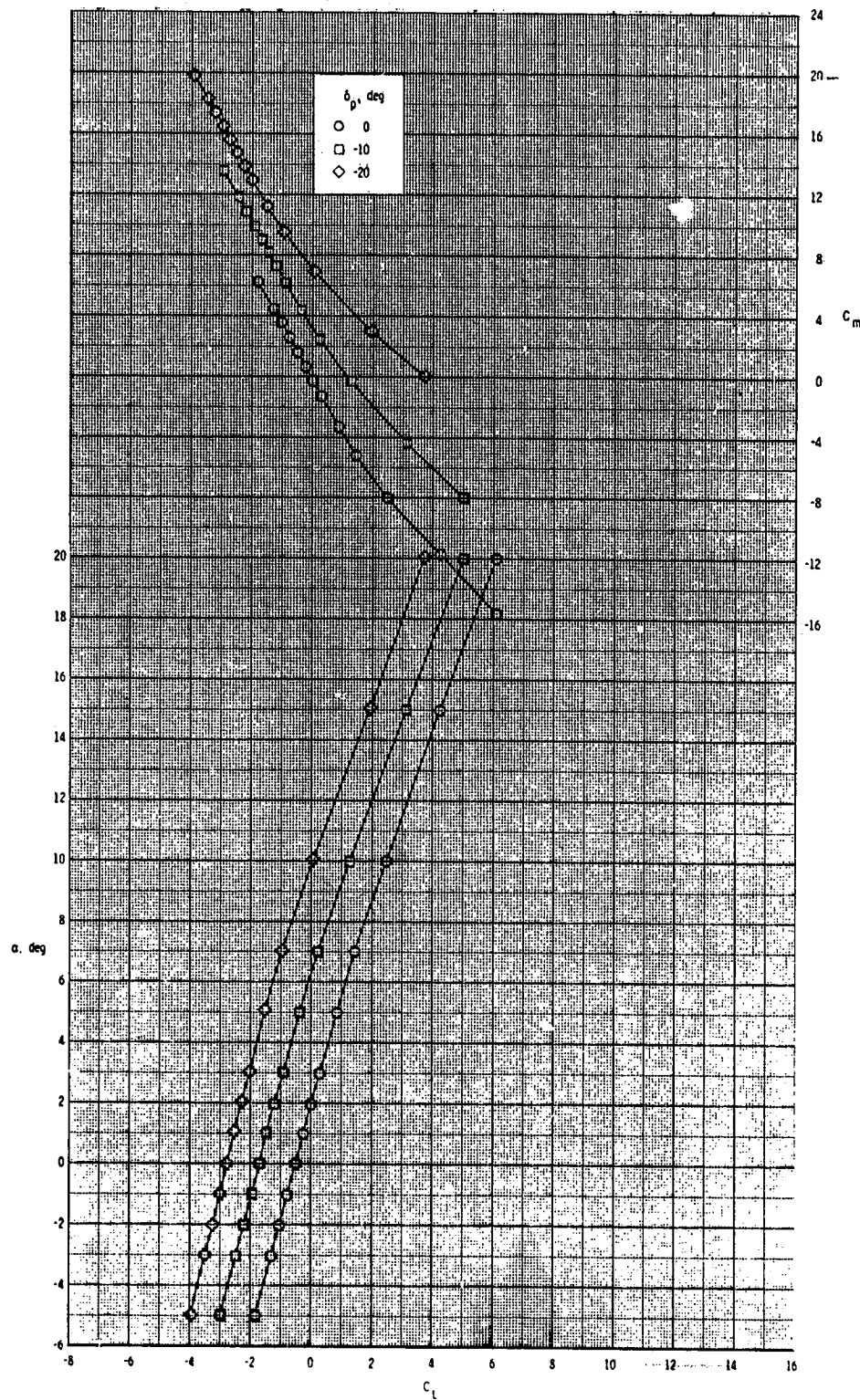
ORIGINAL PAGE IS
OF POOR QUALITY



(a) $M = 2.50$.

Figure 8.- Pitch-control effectiveness of configuration $B_1I_4T_1$.

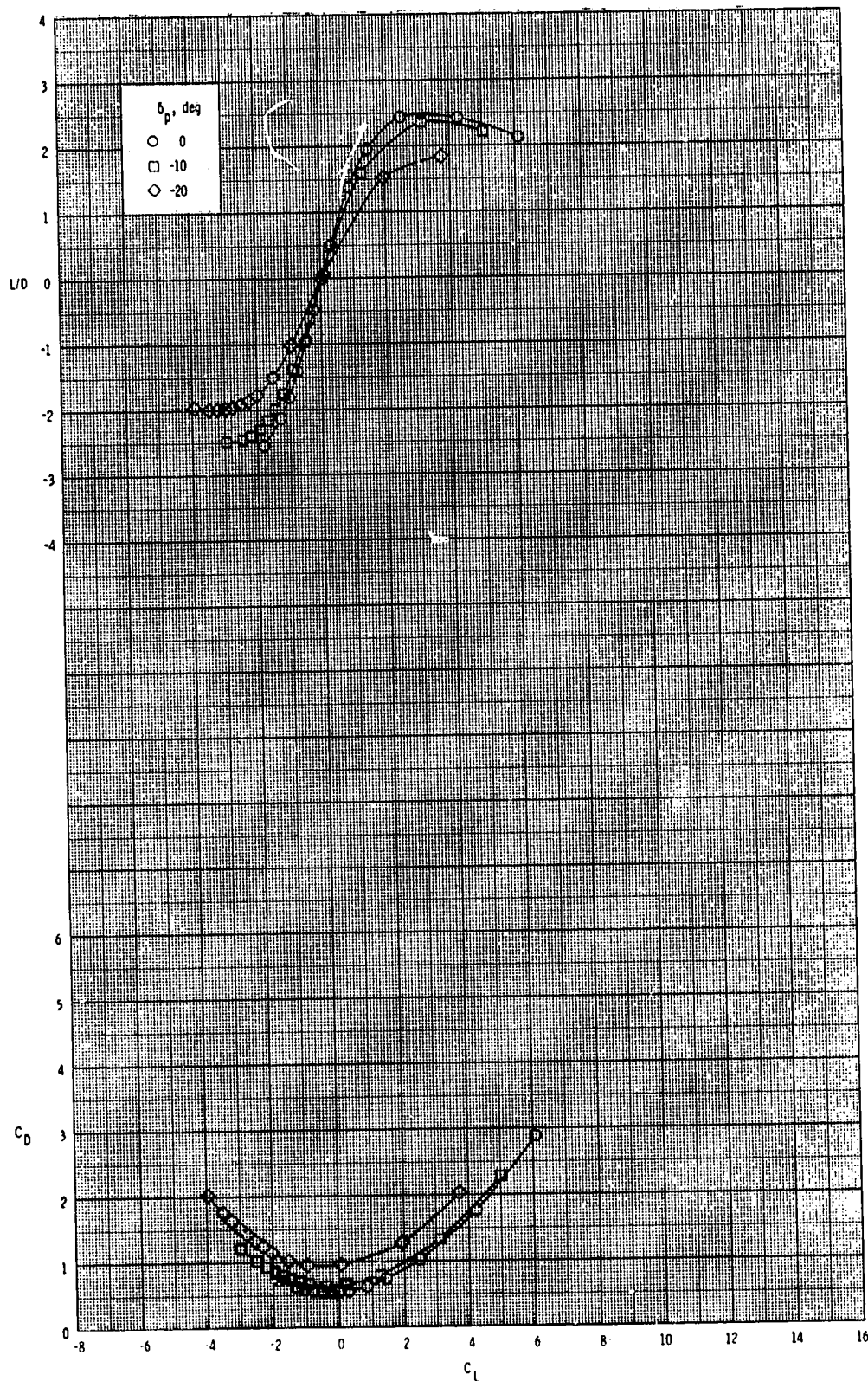
ORIGINAL PAGE IS
OF POOR QUALITY



(a) Continued.

Figure 8.- Continued.

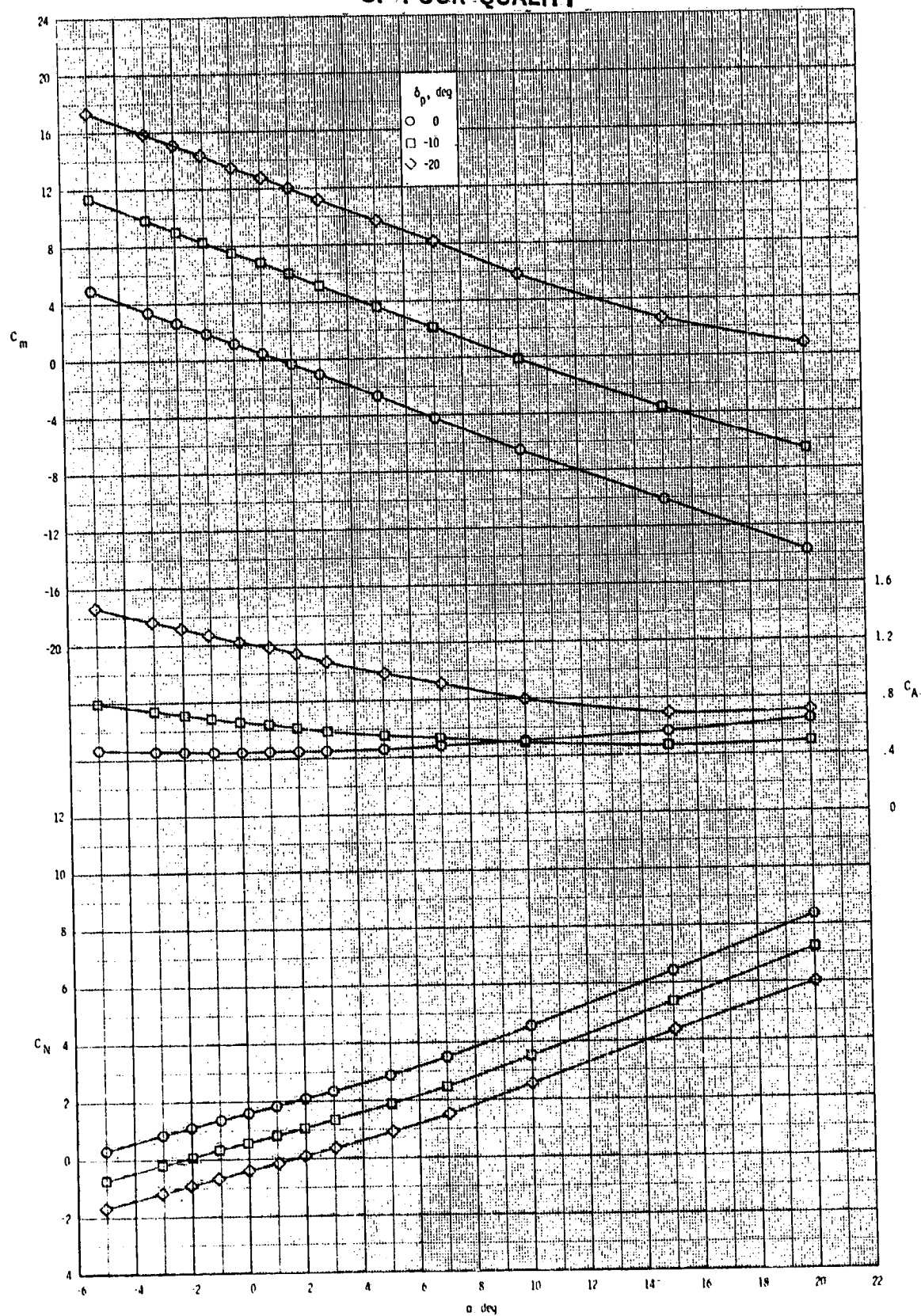
ORIGINAL PAGE IS
OF POOR QUALITY



(a) Concluded.

Figure 8.- Continued.

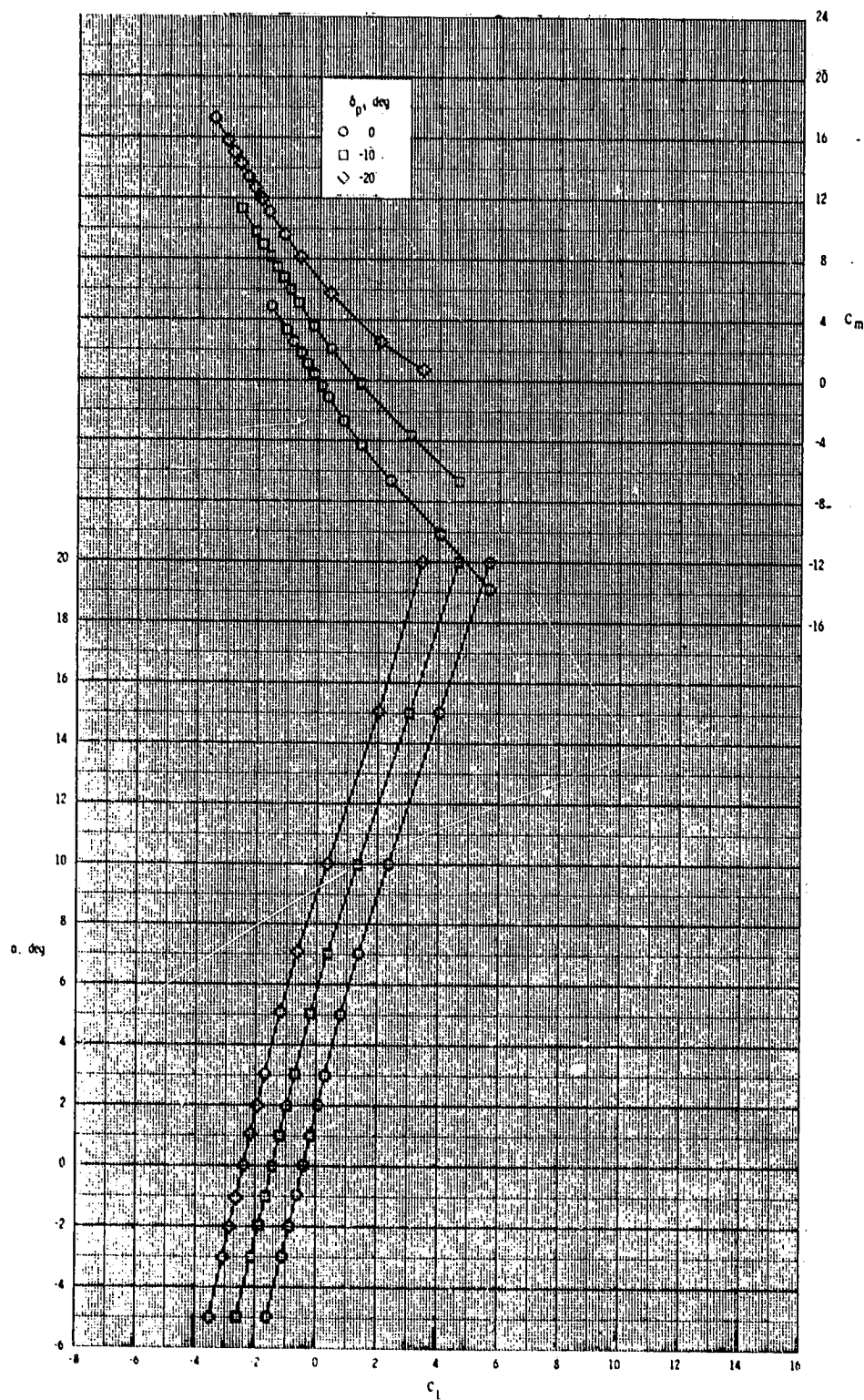
ORIGINAL PAGE IS
OF POOR QUALITY



(b) $M = 2.95$.

Figure 8.- Continued.

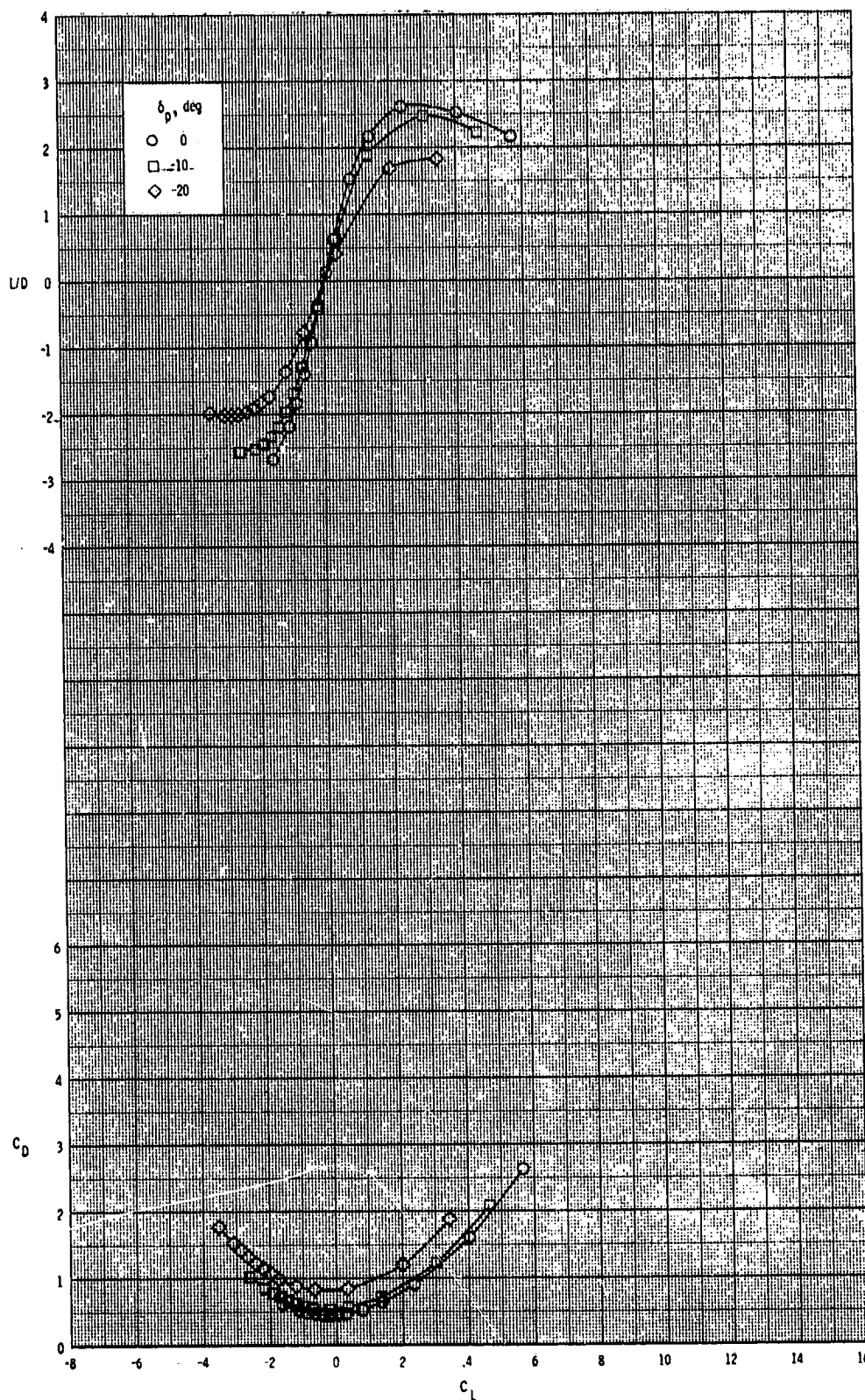
ORIGINAL PAGE IS
OF POOR QUALITY



(b) Continued.

Figure 8.- Continued.

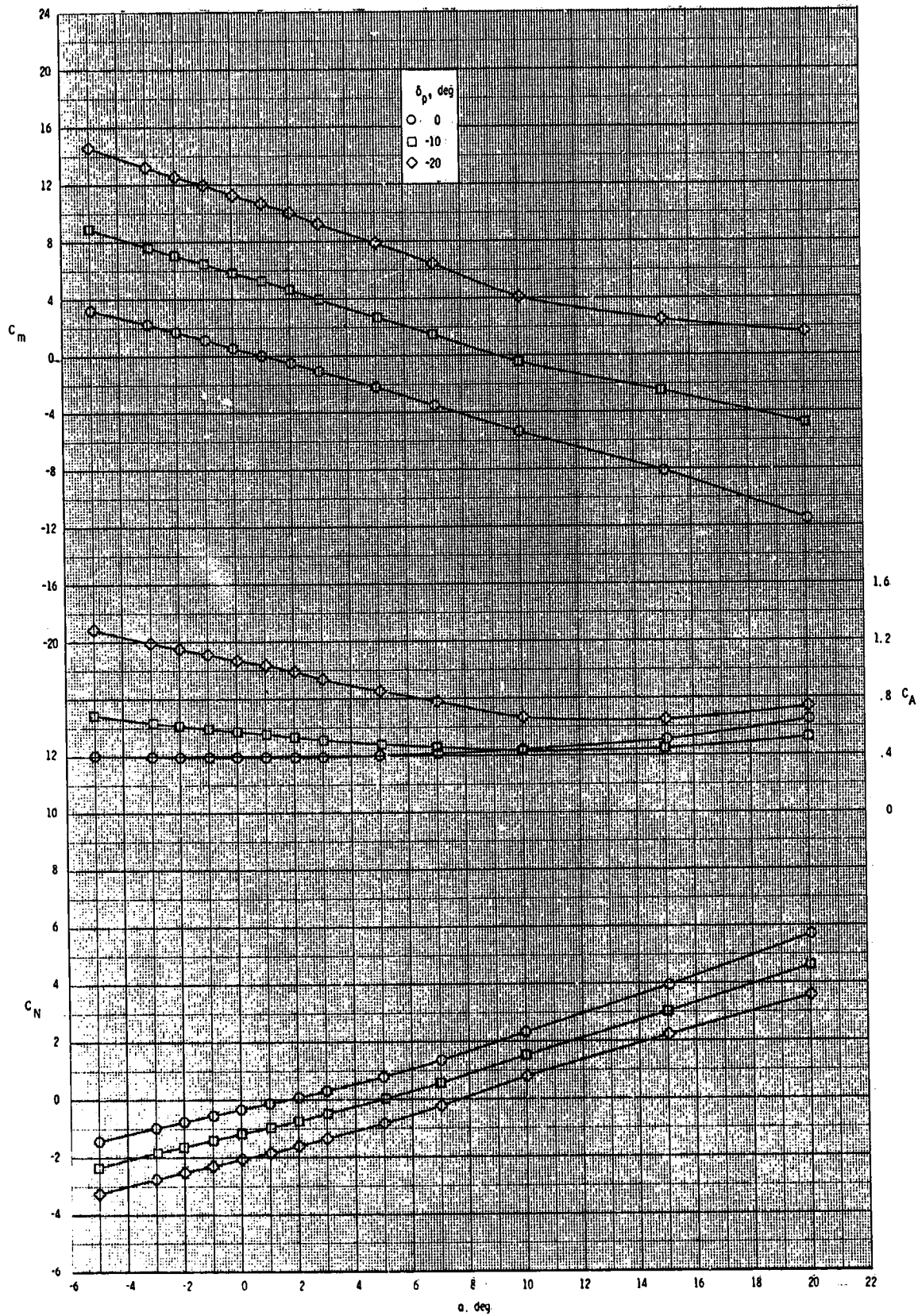
ORIGINAL PAGE IS
OF POOR QUALITY



(b) Concluded.

Figure 8.- Continued.

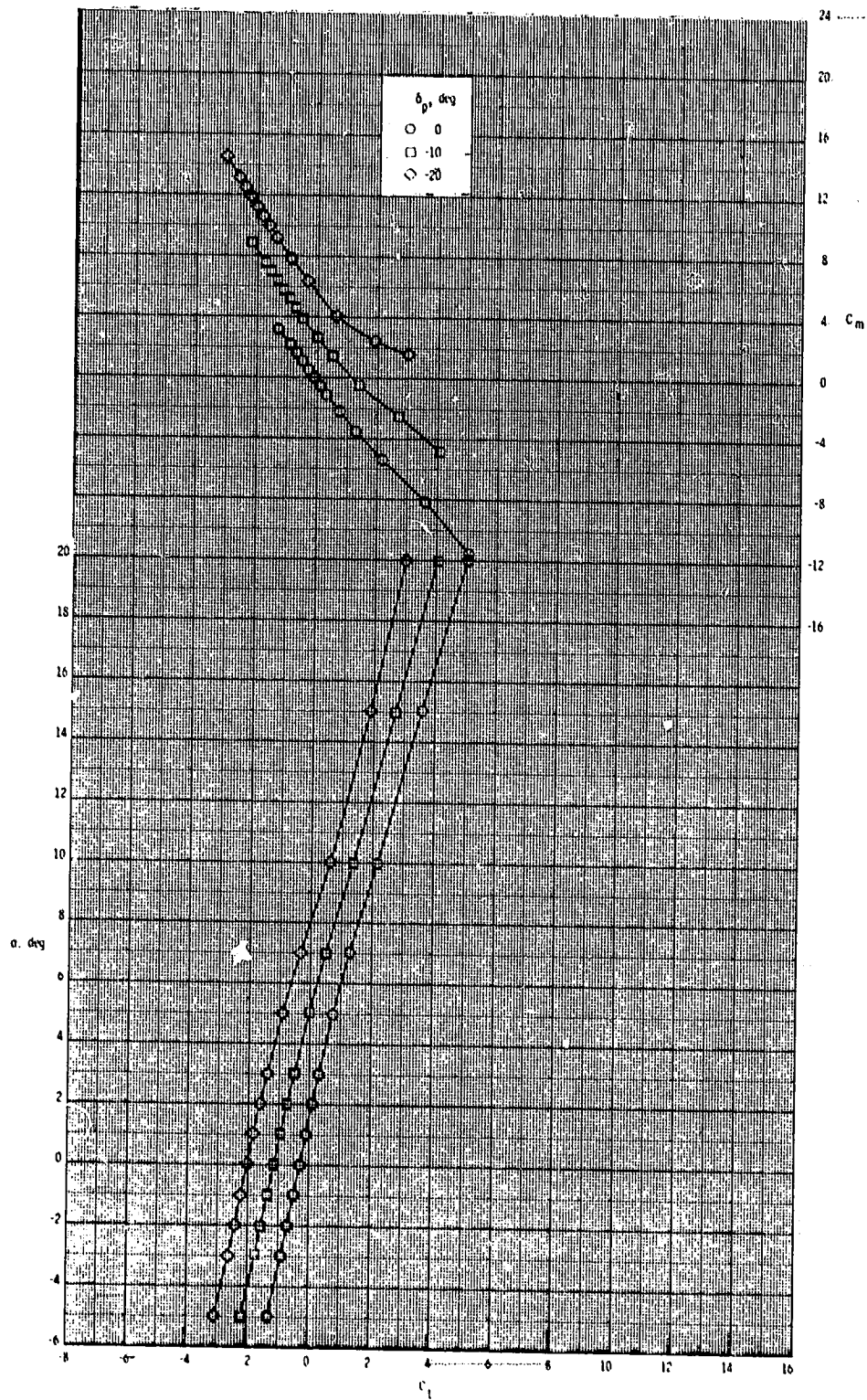
ORIGINAL PAGE IS
OF POOR QUALITY



(c) $M = 3.50$.

Figure 8.- Continued.

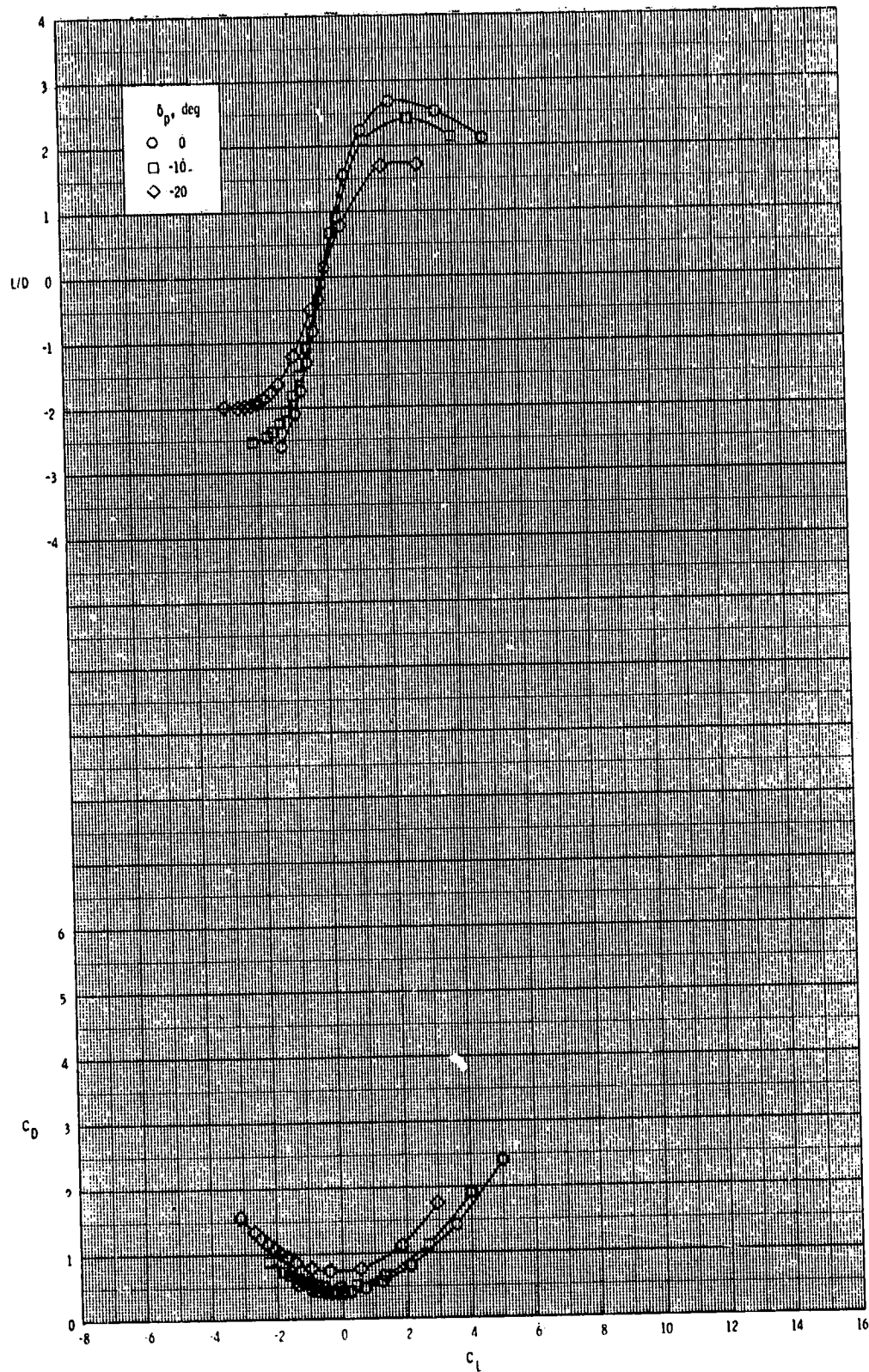
ORIGINAL PAGE
OF POOR QUALITY



(c) Continued.

Figure 8.- Continued.

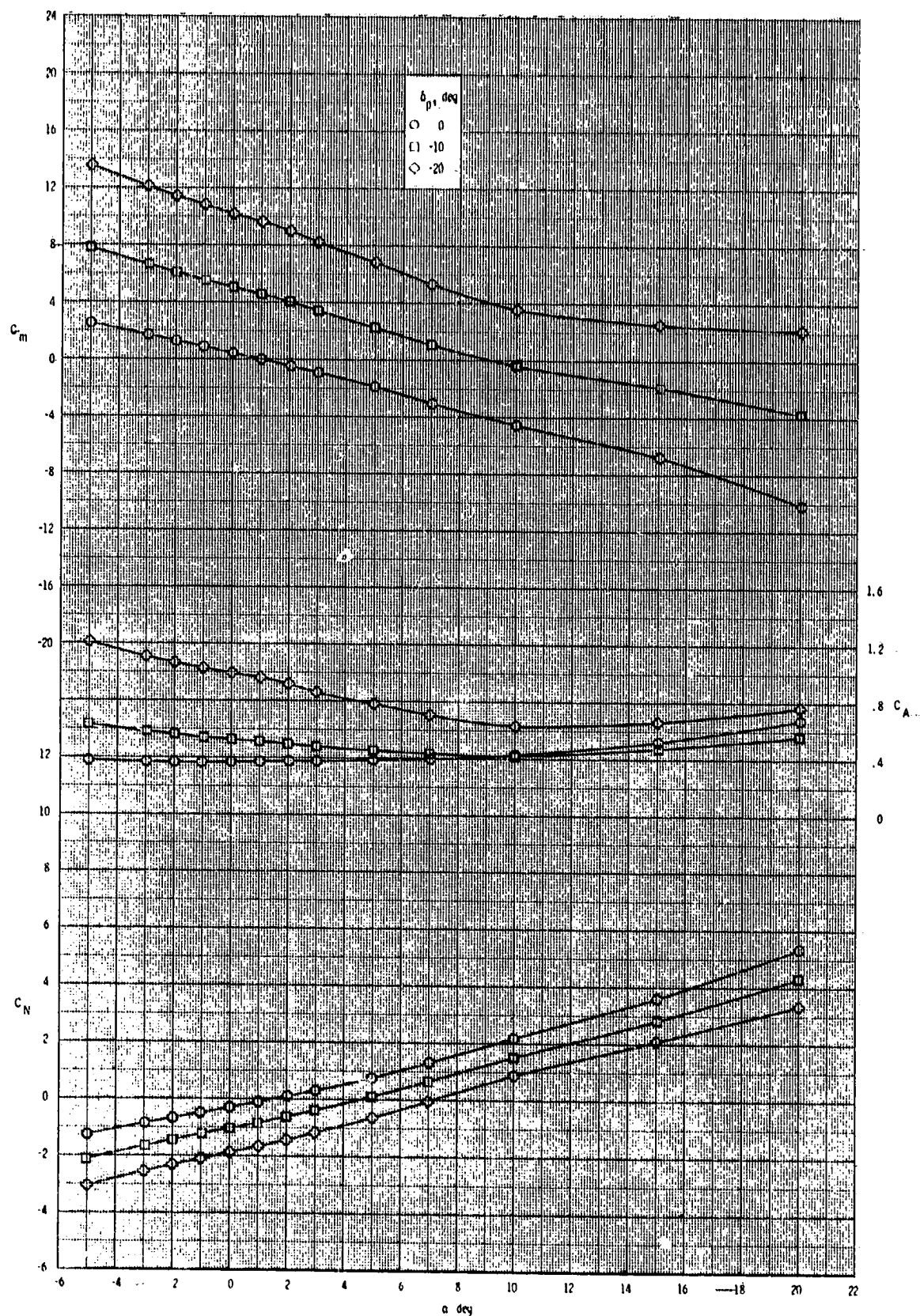
ORIGINAL PAGE IS
OF POOR QUALITY



(c) Concluded.

Figure 8.- Continued.

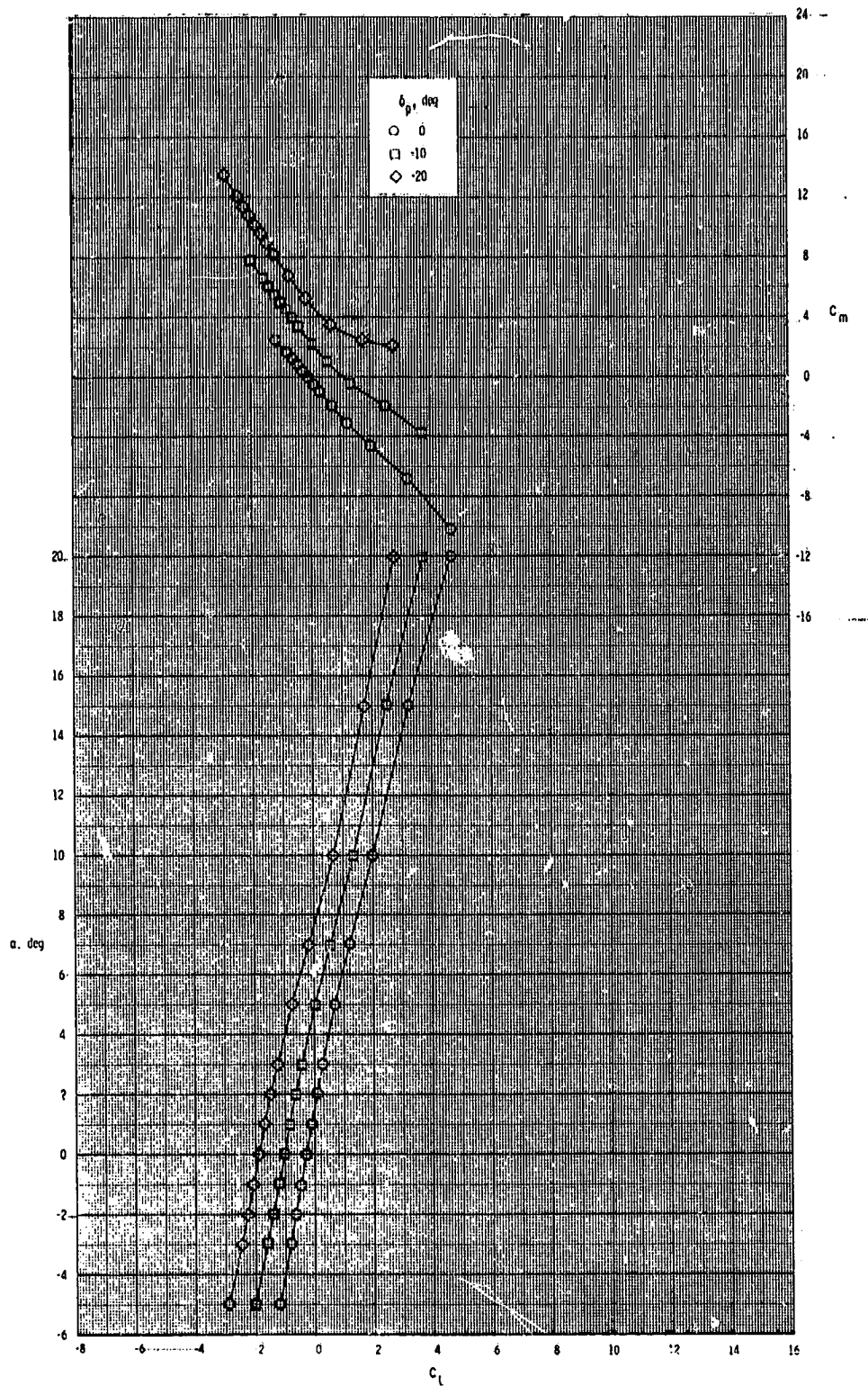
ORIGINAL PAGE IS
OF POOR QUALITY



(d) $M = 3.95$.

Figure 8.- Continued.

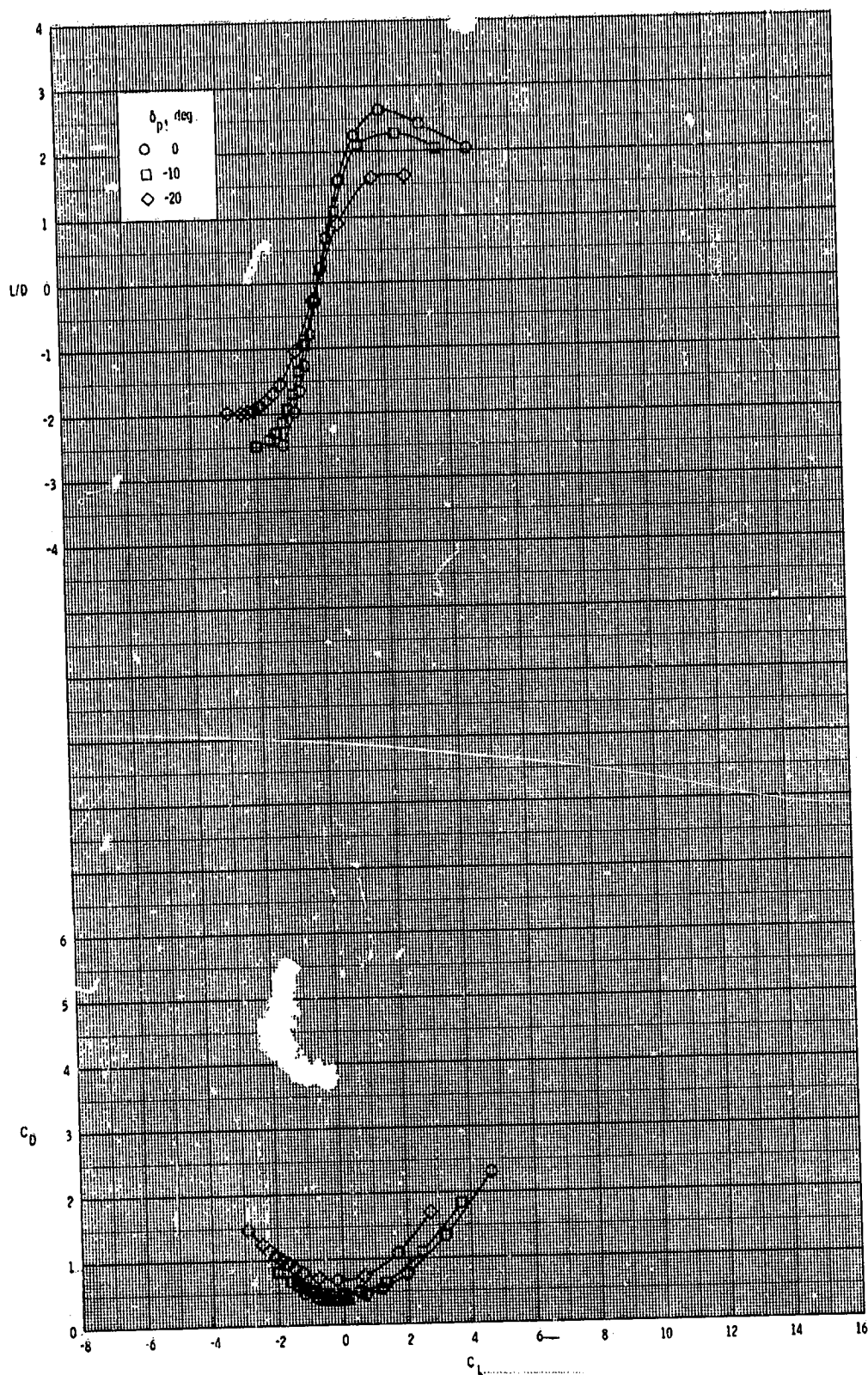
ORIGINAL PAGE IS
OF POOR QUALITY



(d) Continued.

Figure 8.- Continued.

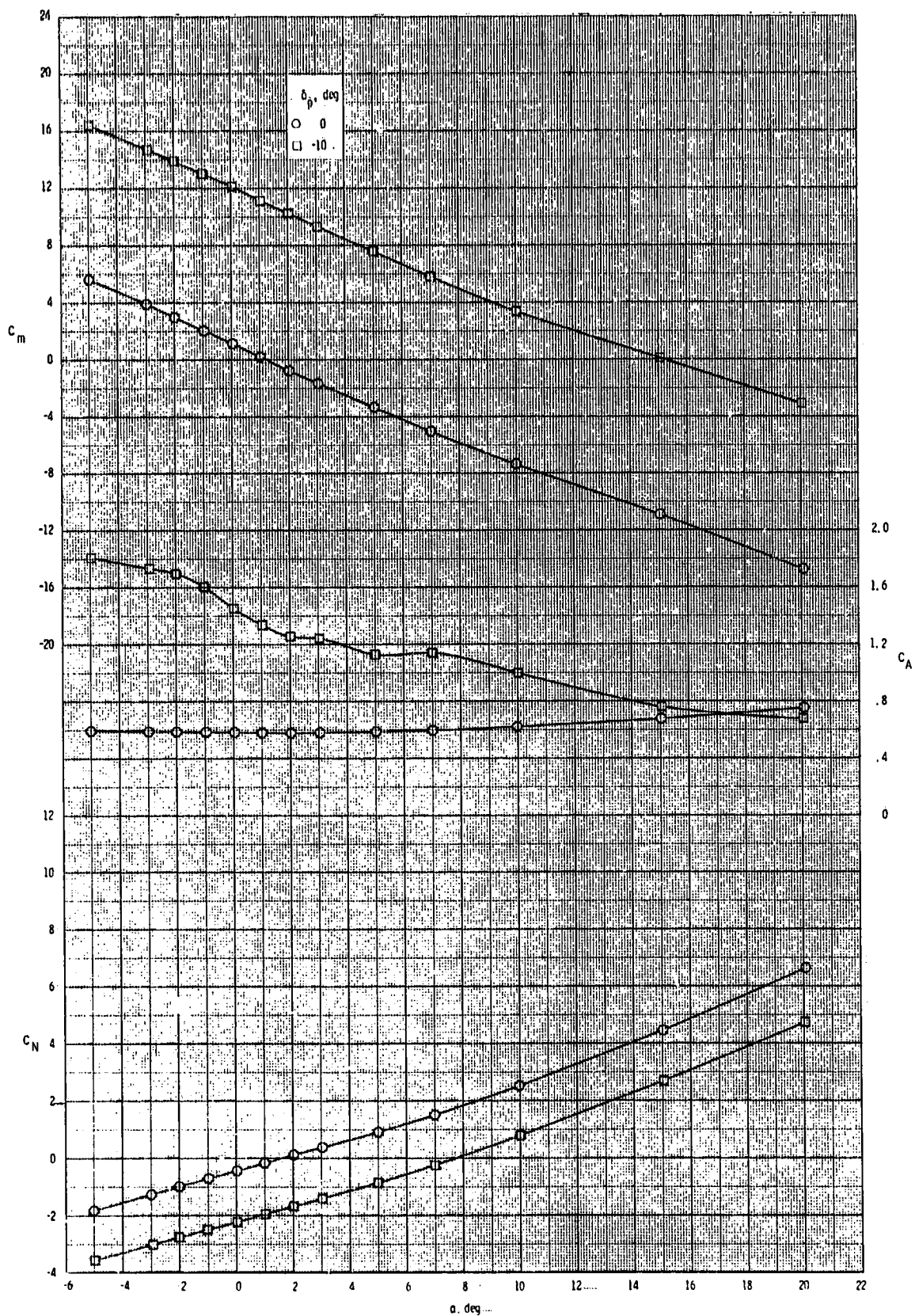
ORIGINAL PAGE IS
OF POOR QUALITY



(d) Concluded.

Figure 8.- Concluded.

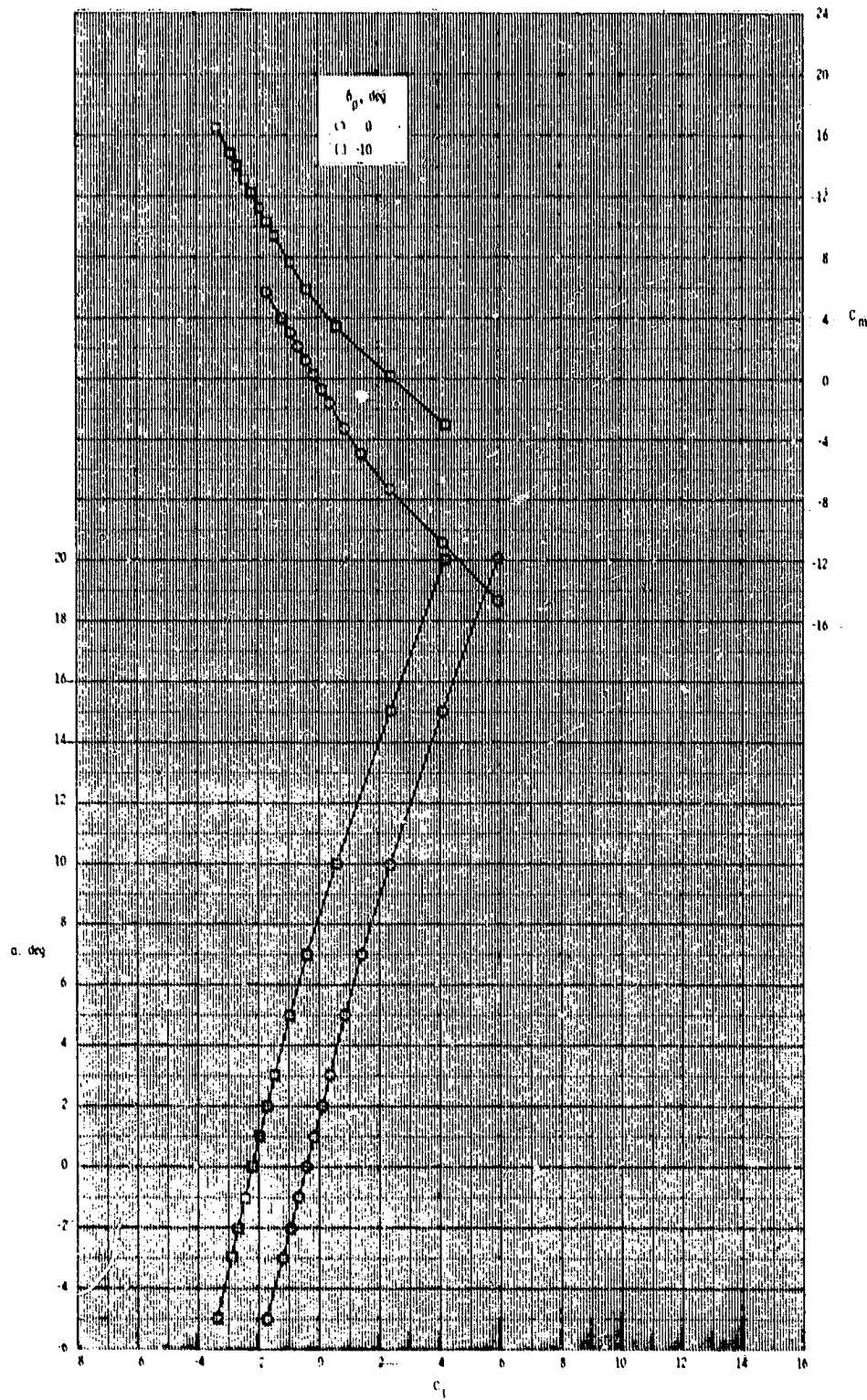
ORIGINAL PAGE IS
OF POOR QUALITY



(a) $M = 2.50$.

Figure 9.- Pitch-control effectiveness of configuration $B_1I_4T_2$.

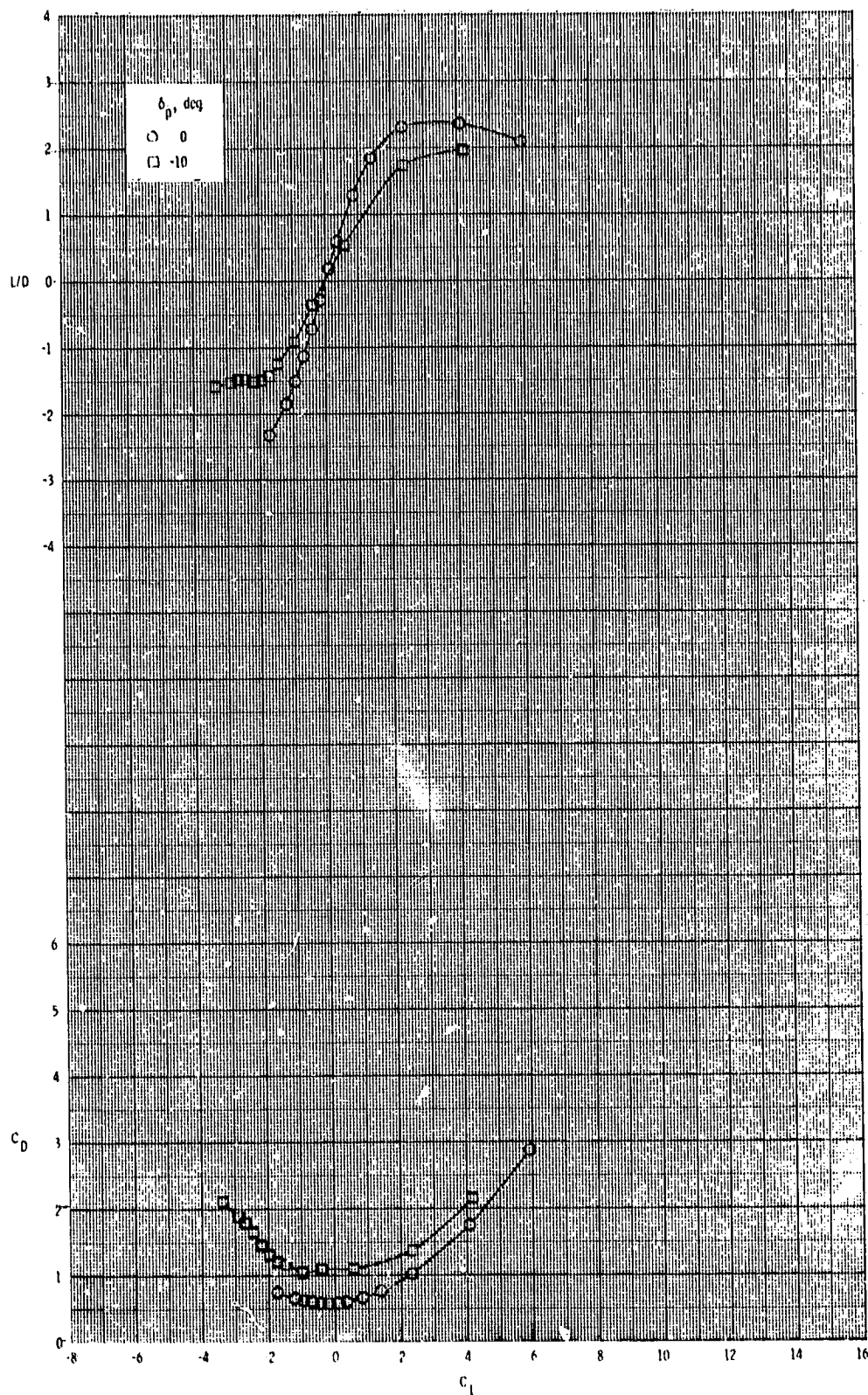
ORIGINAL PAGE IS
OF POOR QUALITY



(a) Continued.

Figure 9.- Continued.

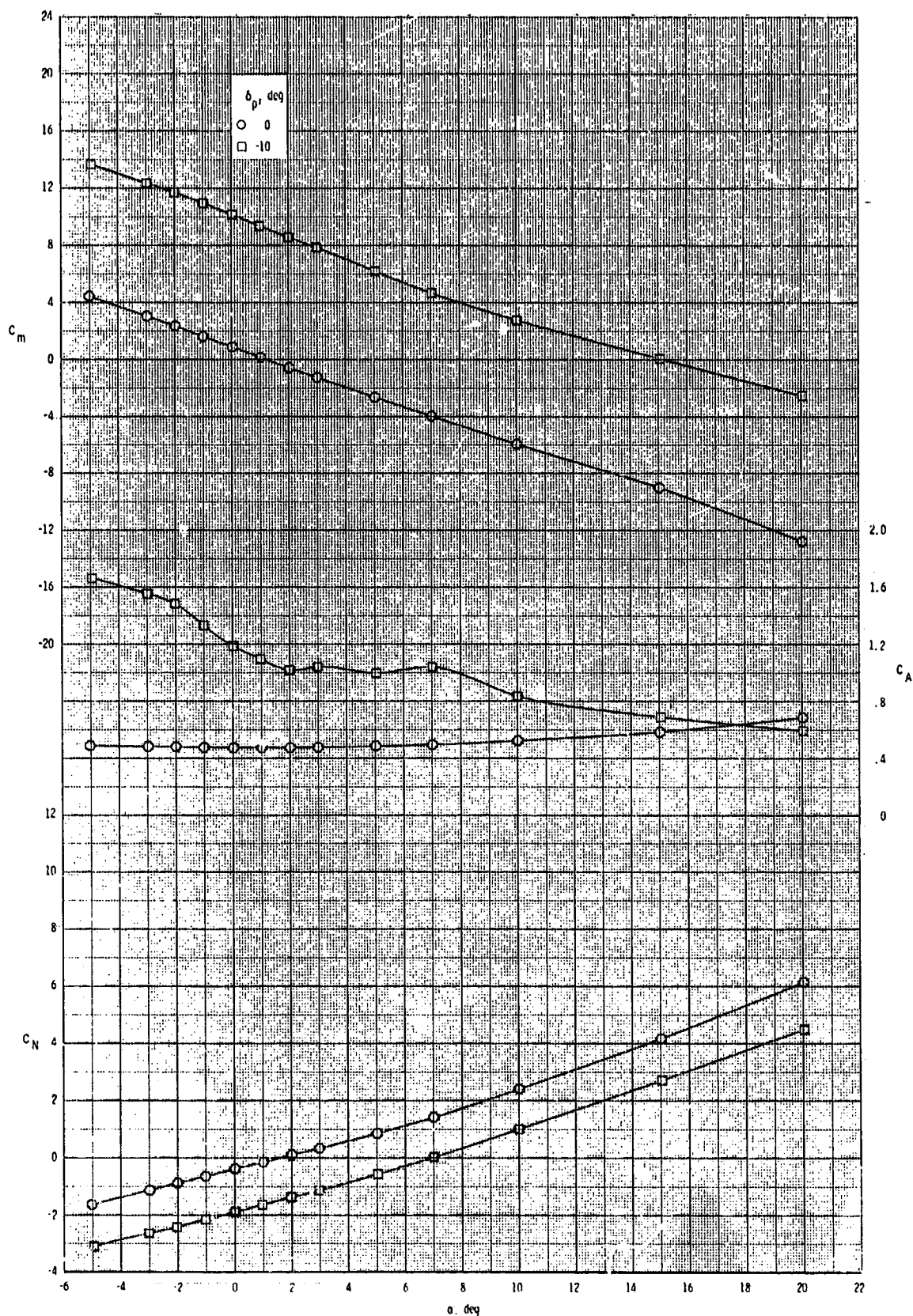
ORIGINAL PAGE IS
OF POOR QUALITY



(a) Concluded.

Figure 9.- Continued.

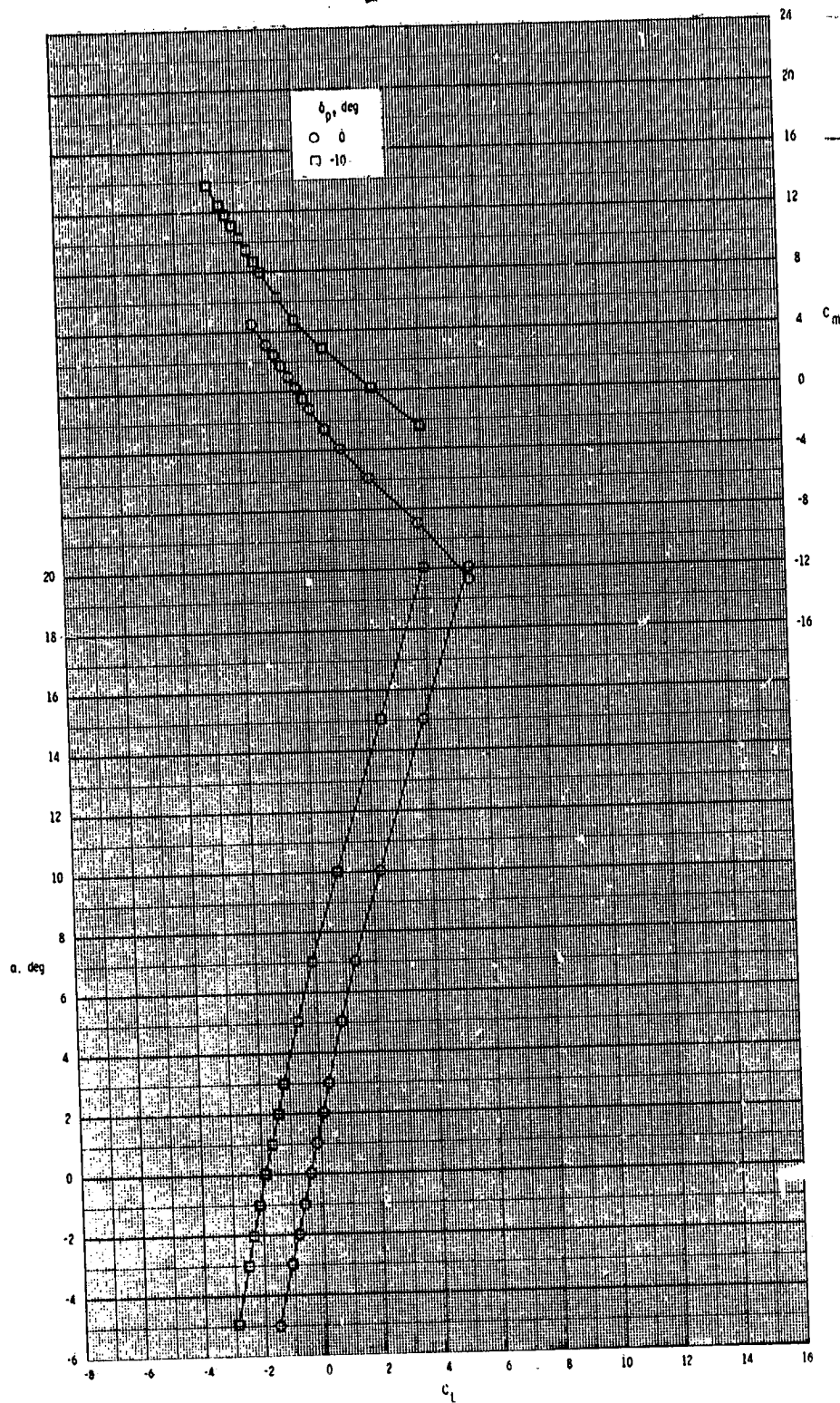
ORIGINAL PAGE IS
OF POOR QUALITY



(b) $M = 2.95$.

Figure 9.- Continued.

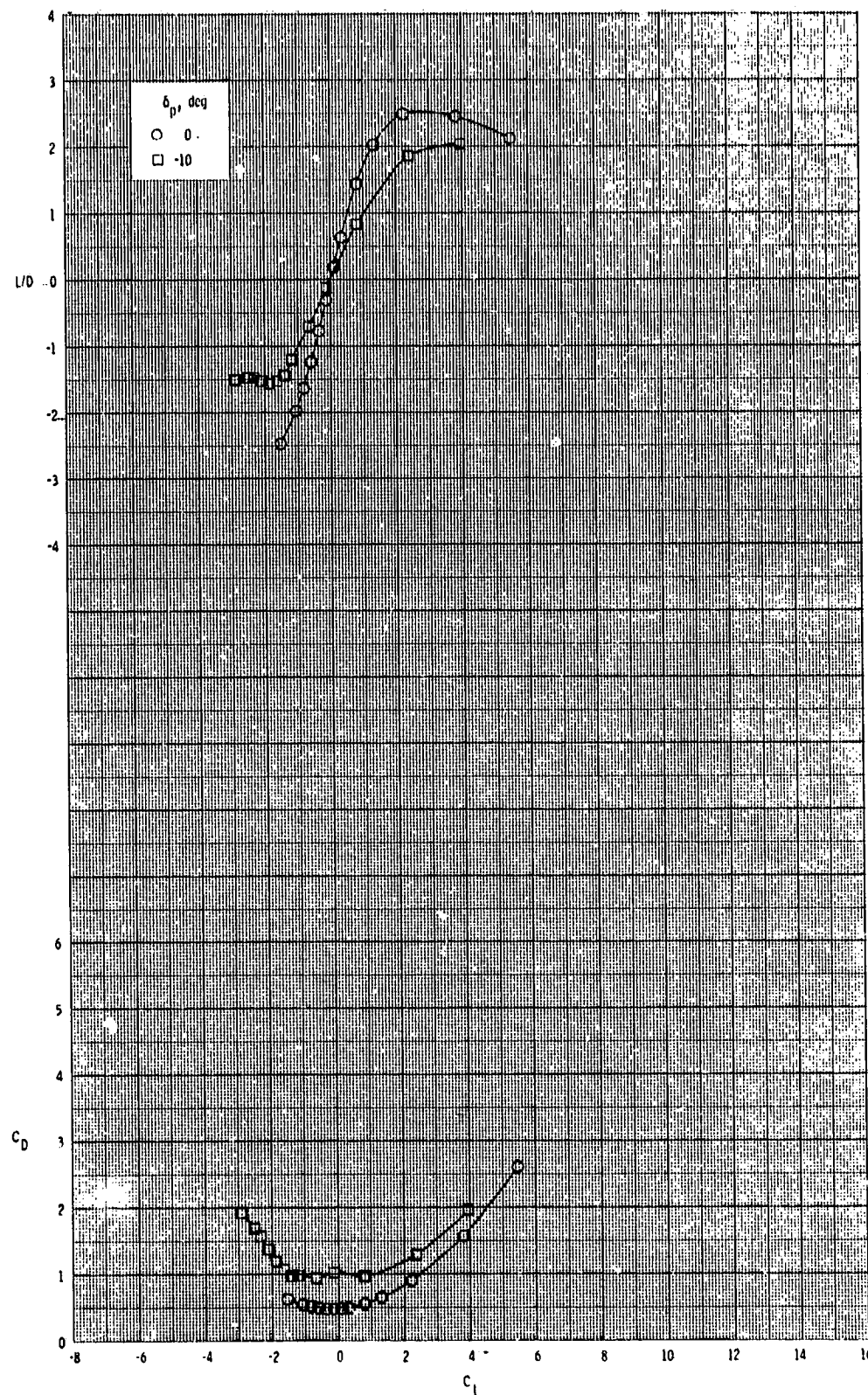
ORIGINAL PAGE IS
OF POOR QUALITY



(b) Continued.

Figure 9.- Continued.

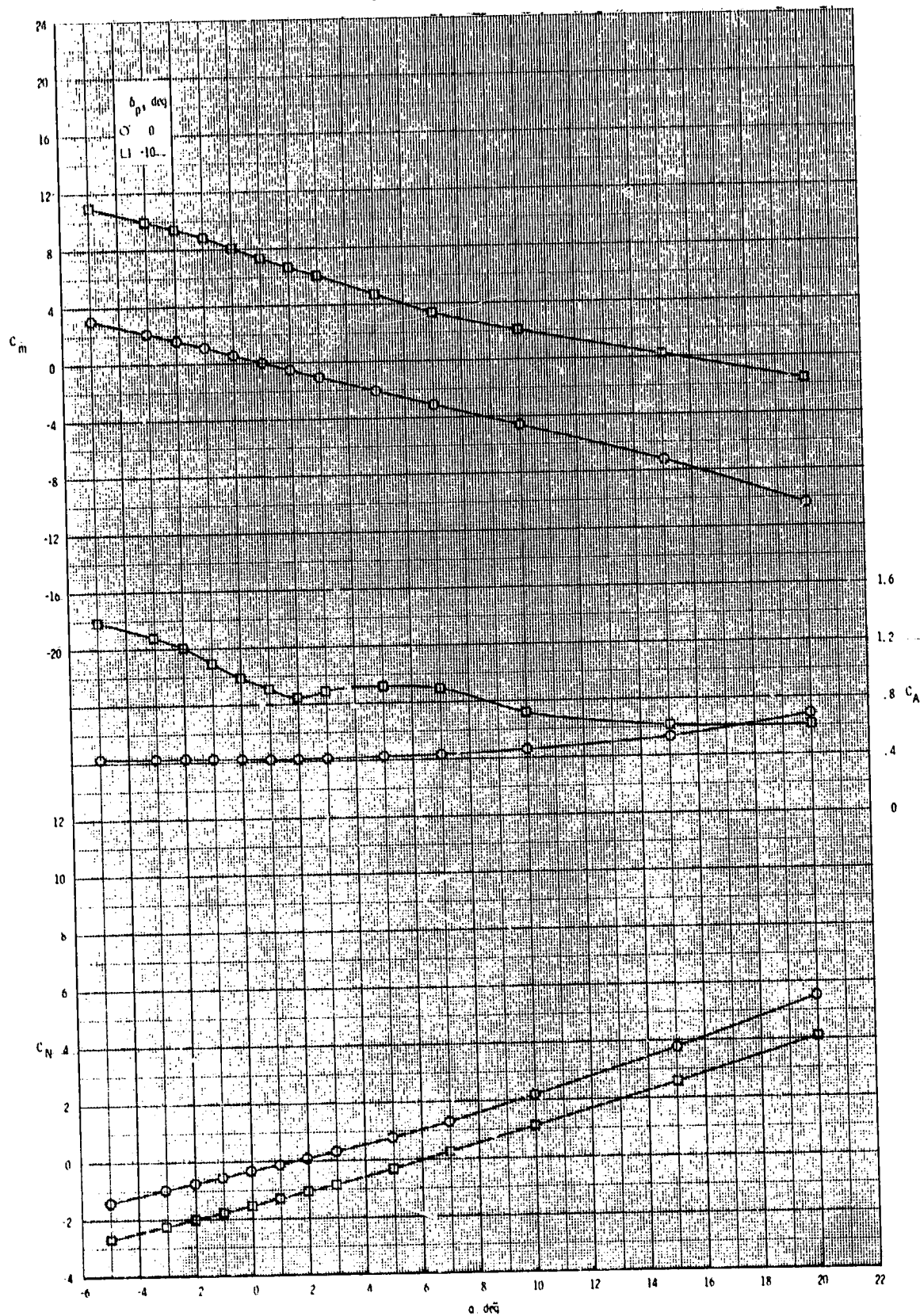
ORIGINAL PAGE IS
OF POOR QUALITY



(b) Concluded.

Figure 9.- Continued.

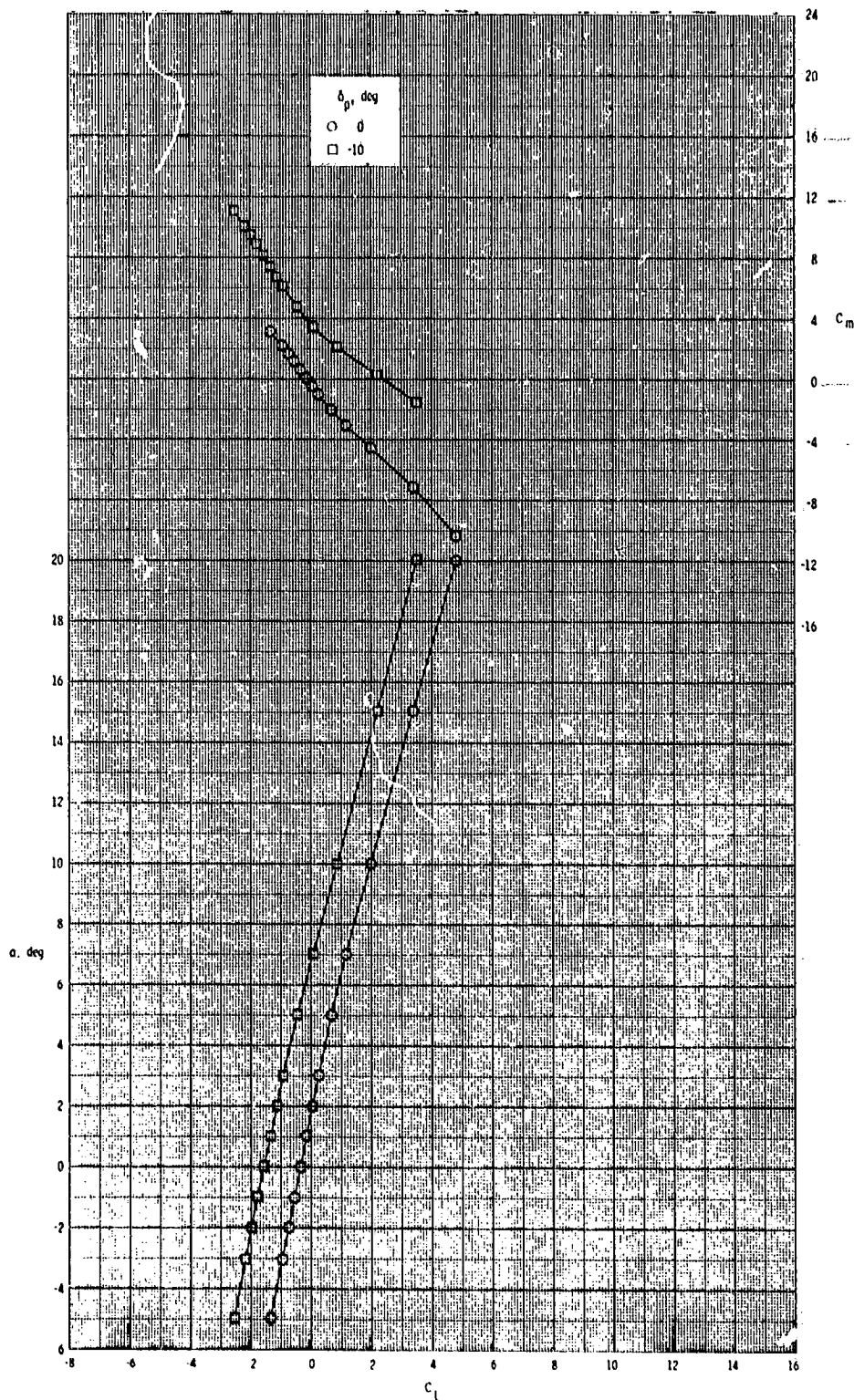
ORIGINAL PAGE IS
OF POOR QUALITY



(c) $M = 3.50$.

Figure 9.- Continued.

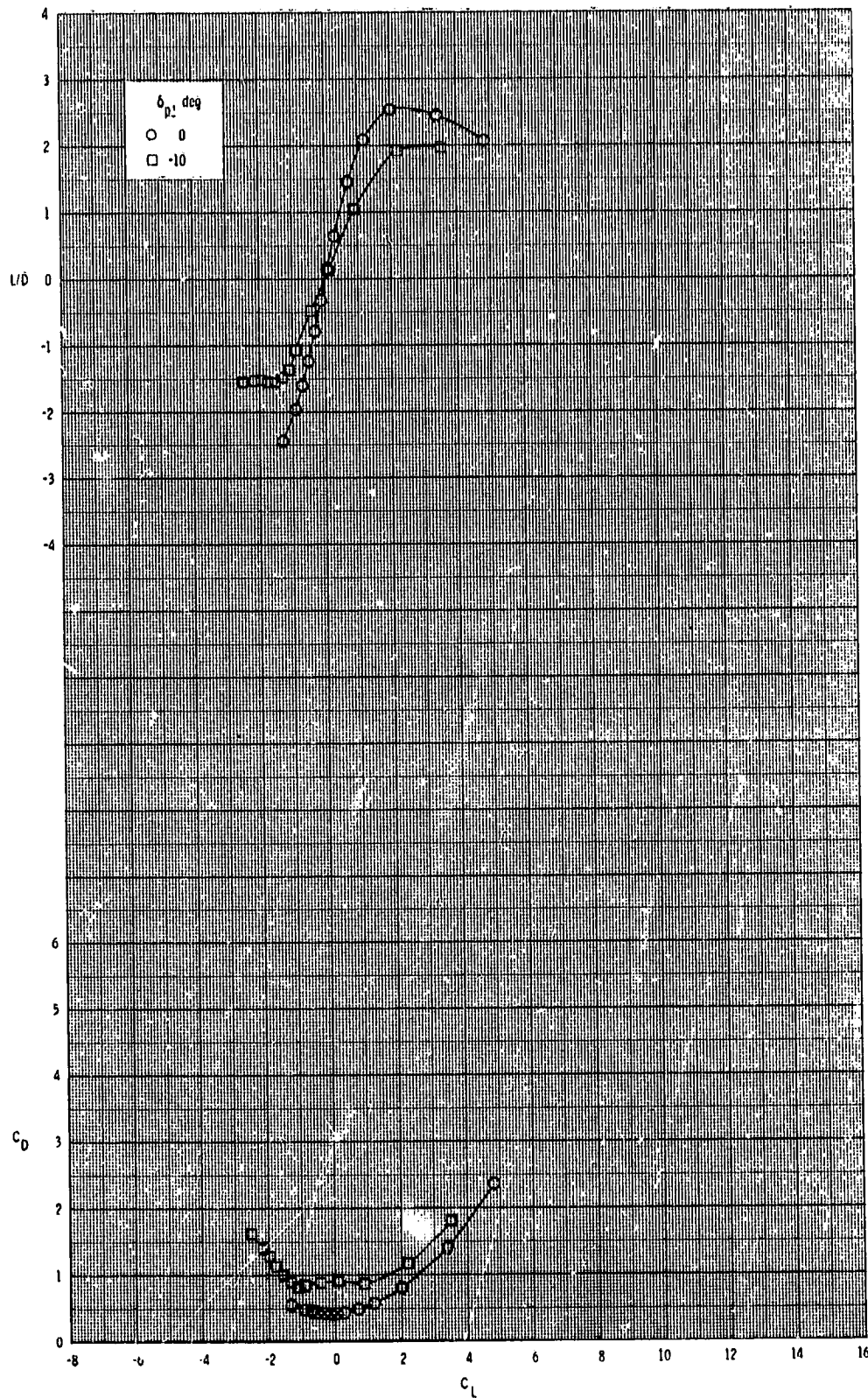
ORIGINAL PAGE IS
OF POOR QUALITY



(c) Continued.

Figure 9.- Continued.

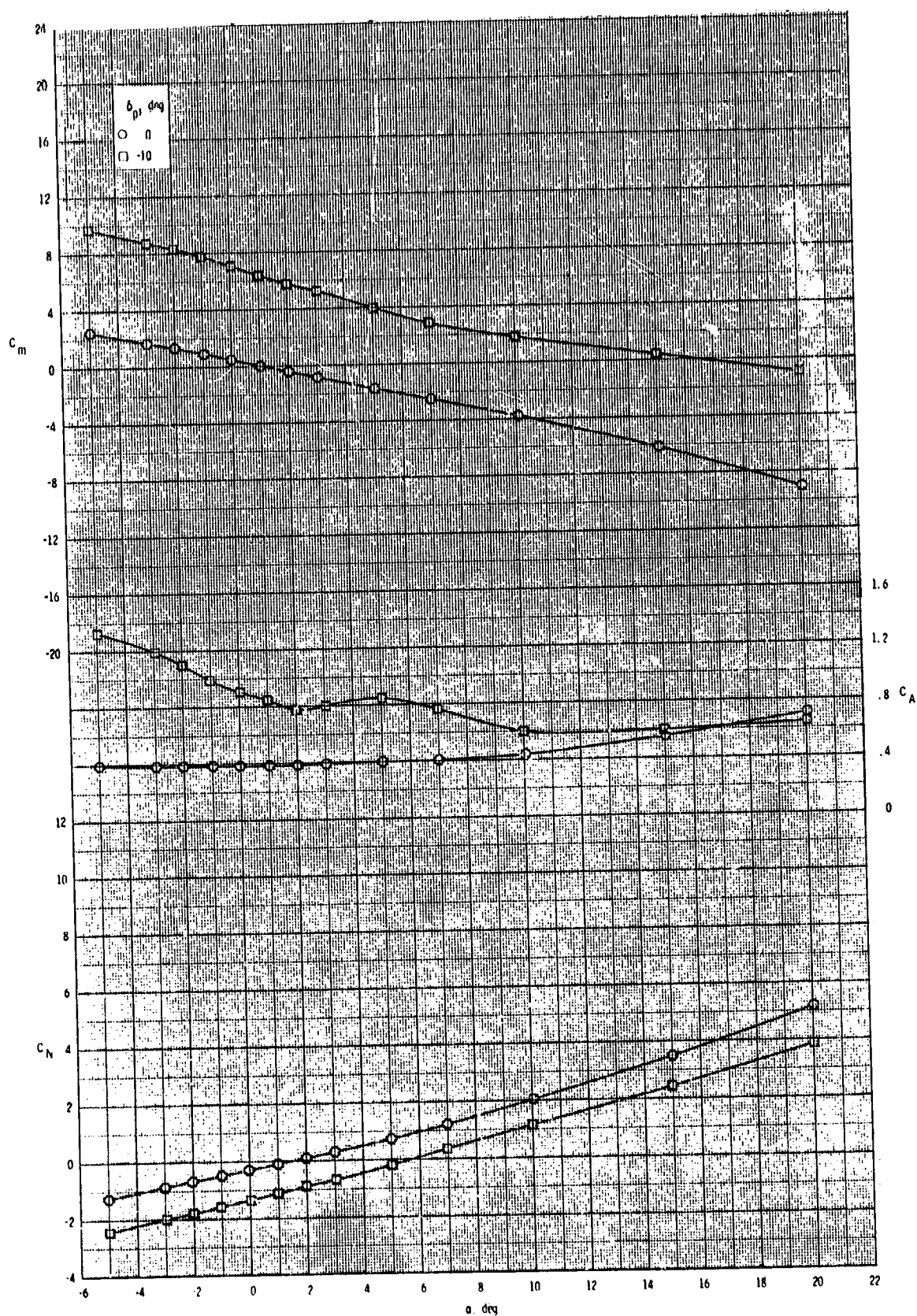
ORIGINAL PAGE 13
OF POOR QUALITY



(c) Concluded.

Figure 9.- Continued.

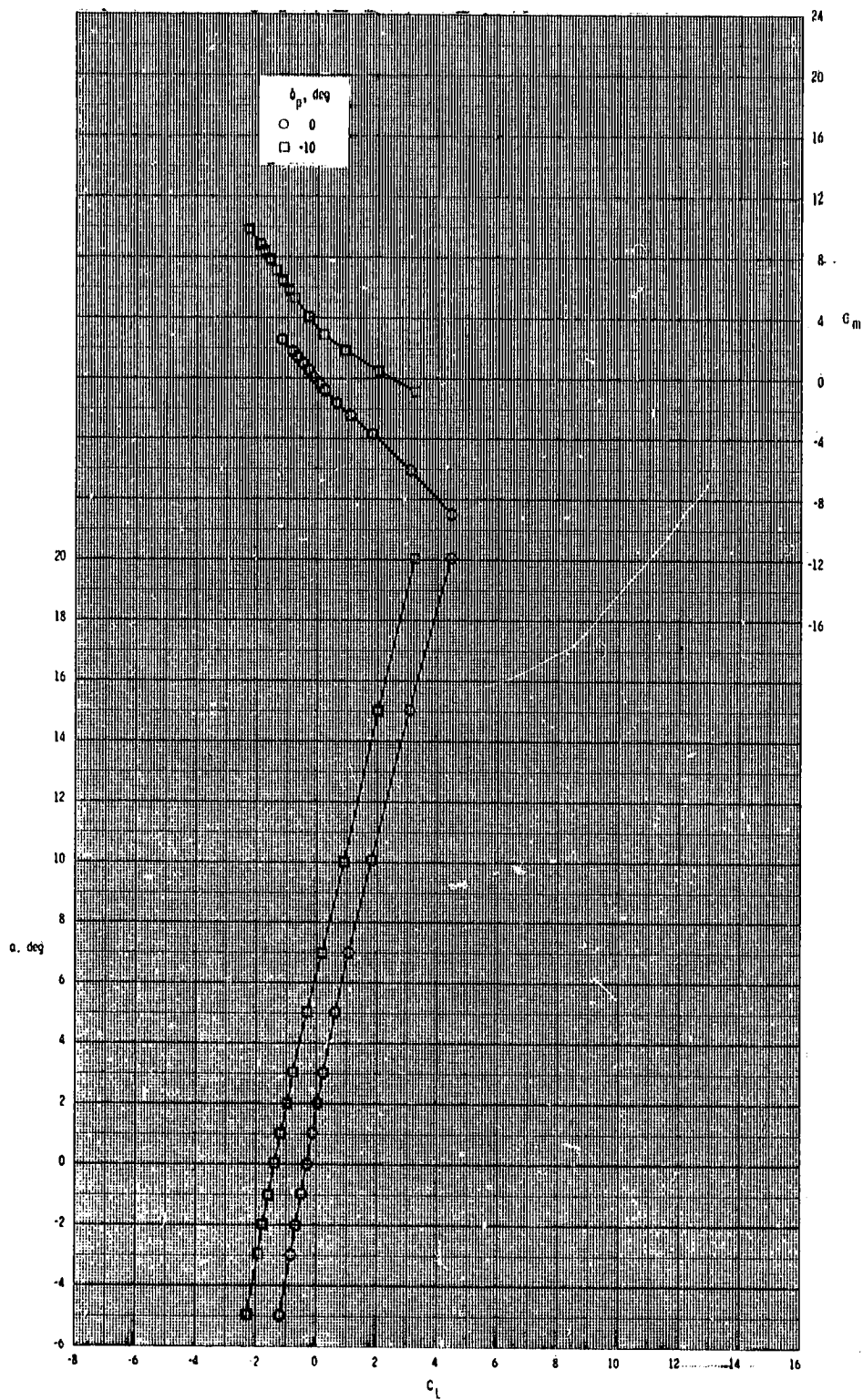
ORIGINAL TYPE IS
OF POOR QUALITY



(d) $M = 3.95$.

Figure 9.- Continued.

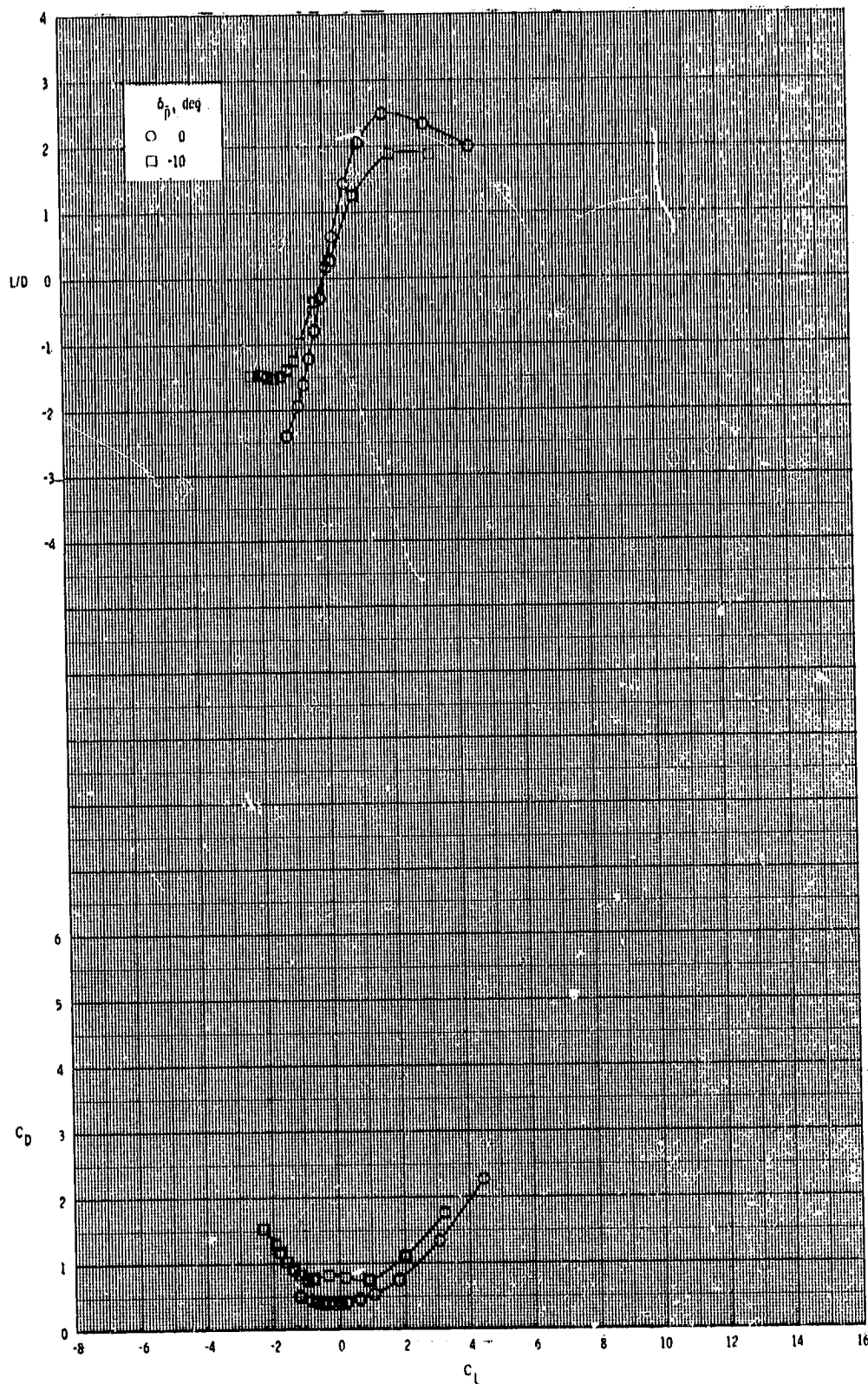
ORIGINAL PAGE IS
OF POOR QUALITY



(d) Continued.

Figure 9.- Continued.

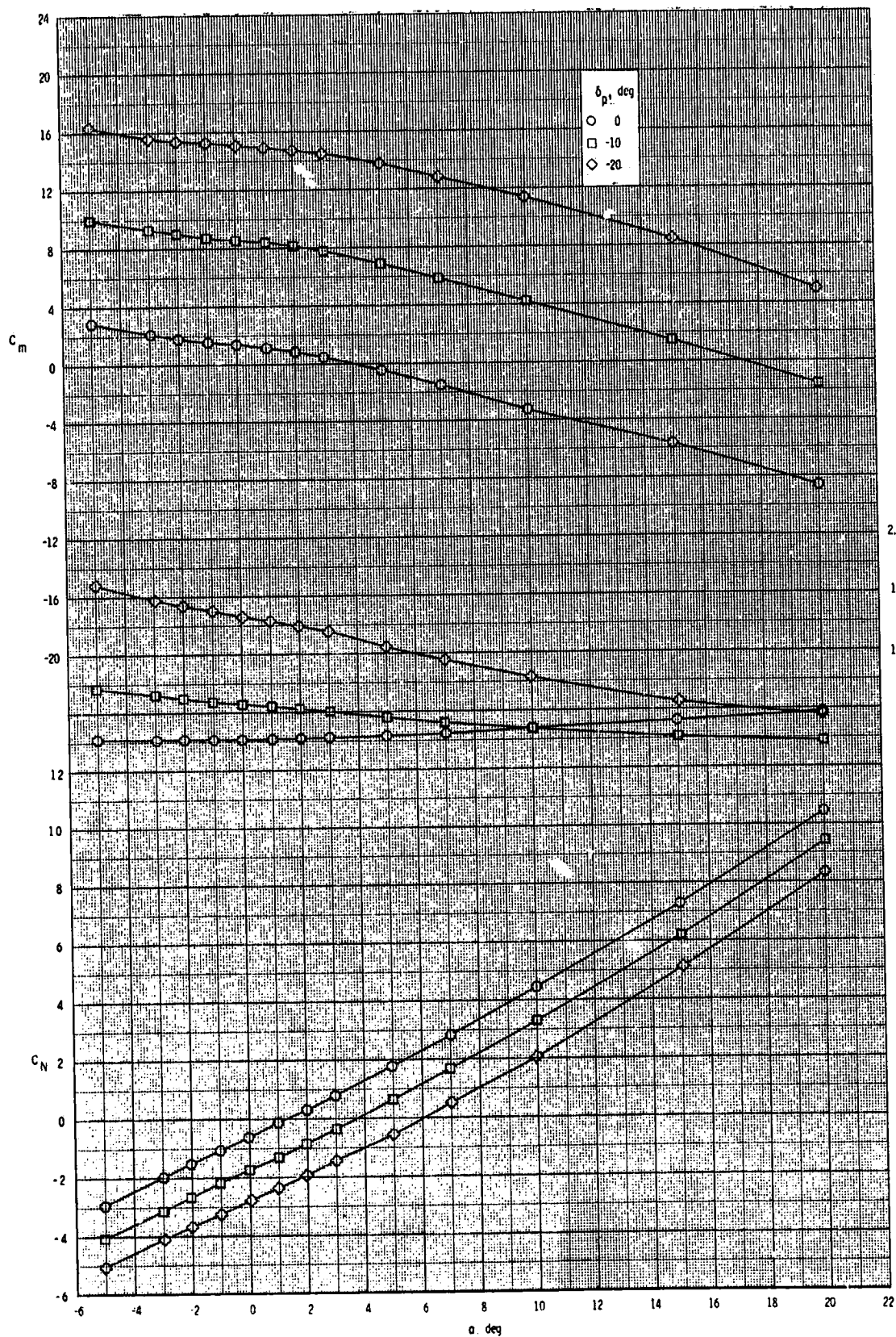
ORIGINAL PAGE IS
OF POOR QUALITY.



(d) Concluded.

Figure 9.- Concluded.

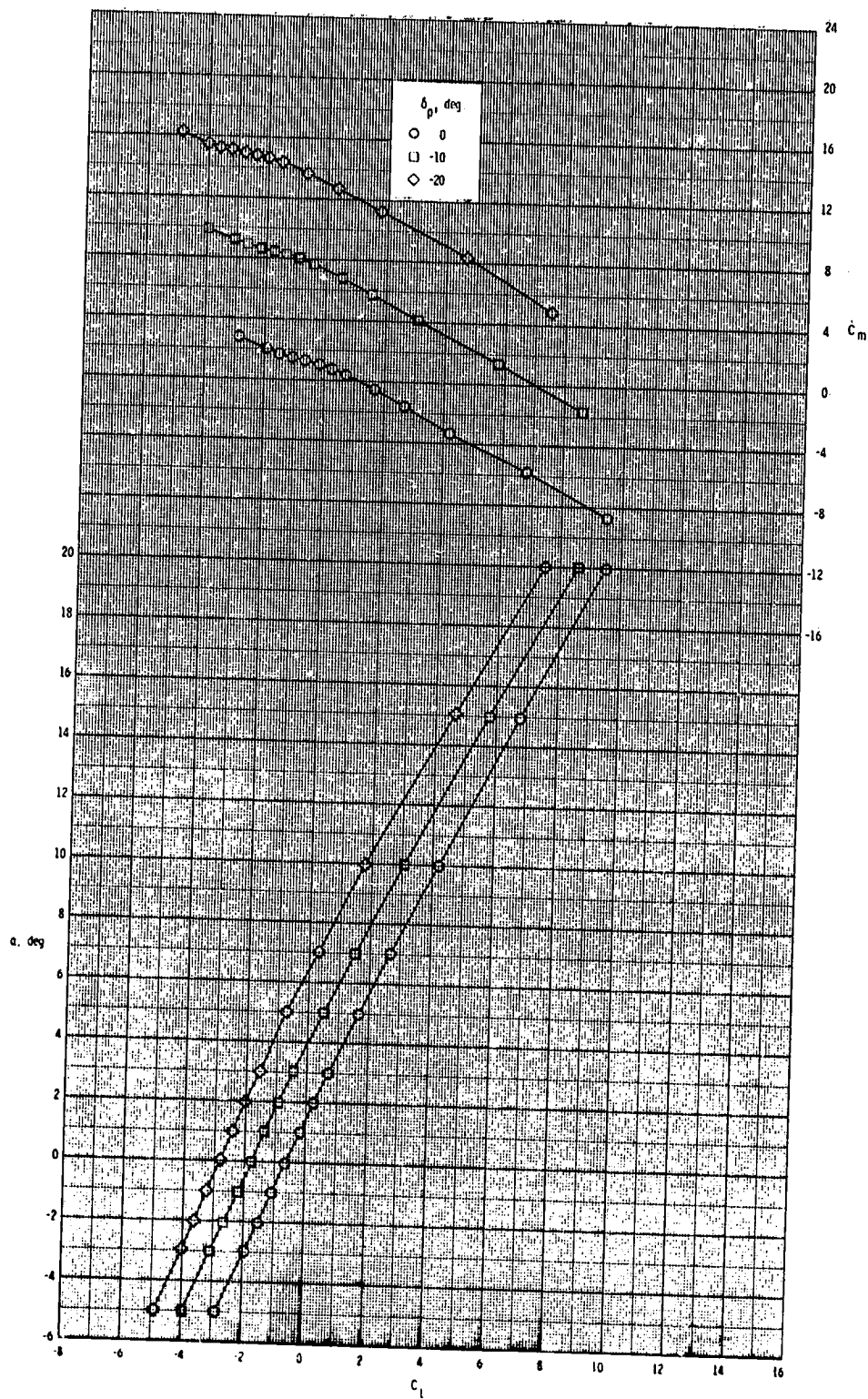
ORIGINAL PAGE IS
OF POOR QUALITY



(a) $M = 2.50$.

Figure 10.- Pitch-control effectiveness of configuration $B_1I_4W_1T_1$.

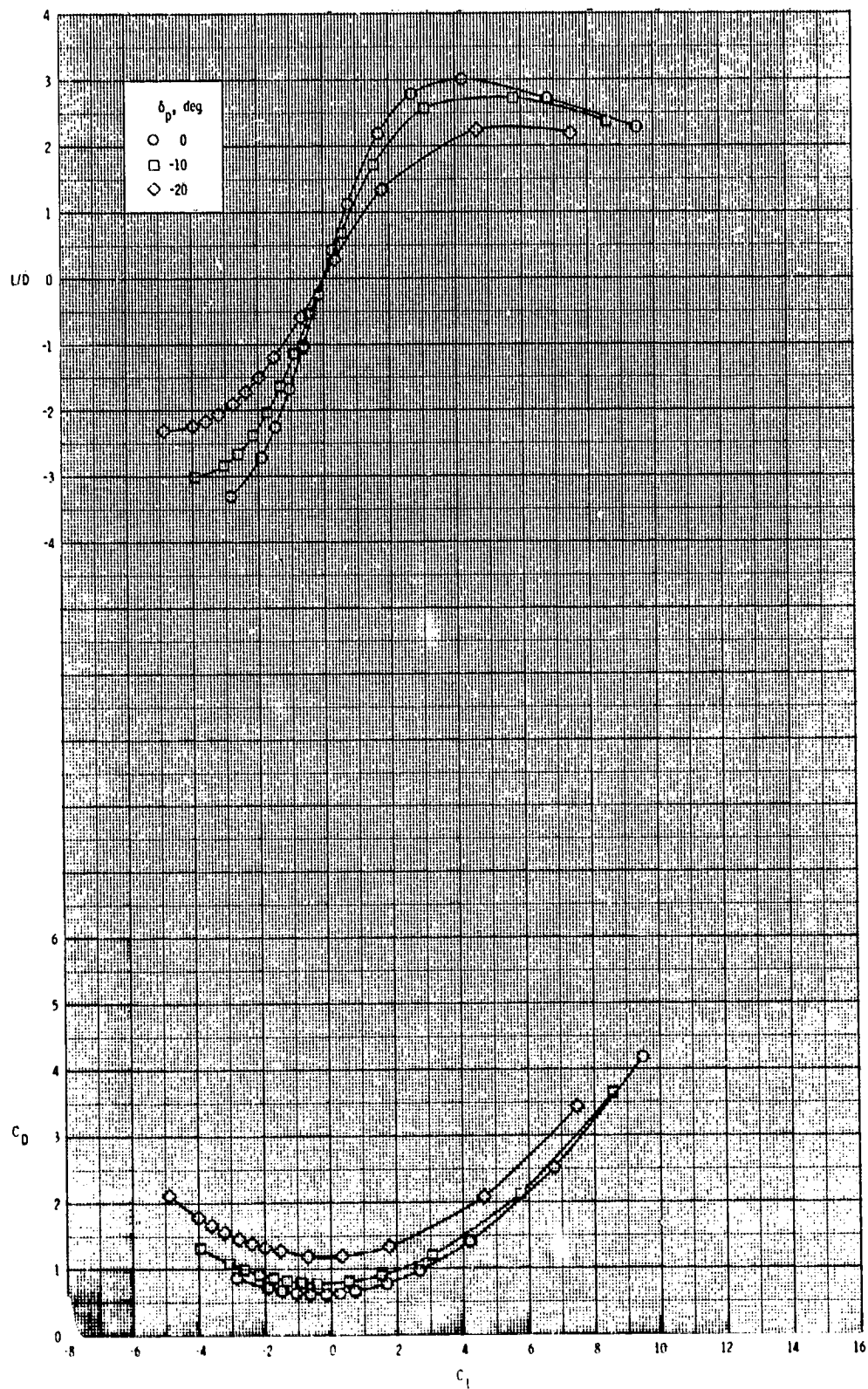
ORIGINAL PAGE IS
OF POOR QUALITY



(a) Continued.

Figure 10.- Continued.

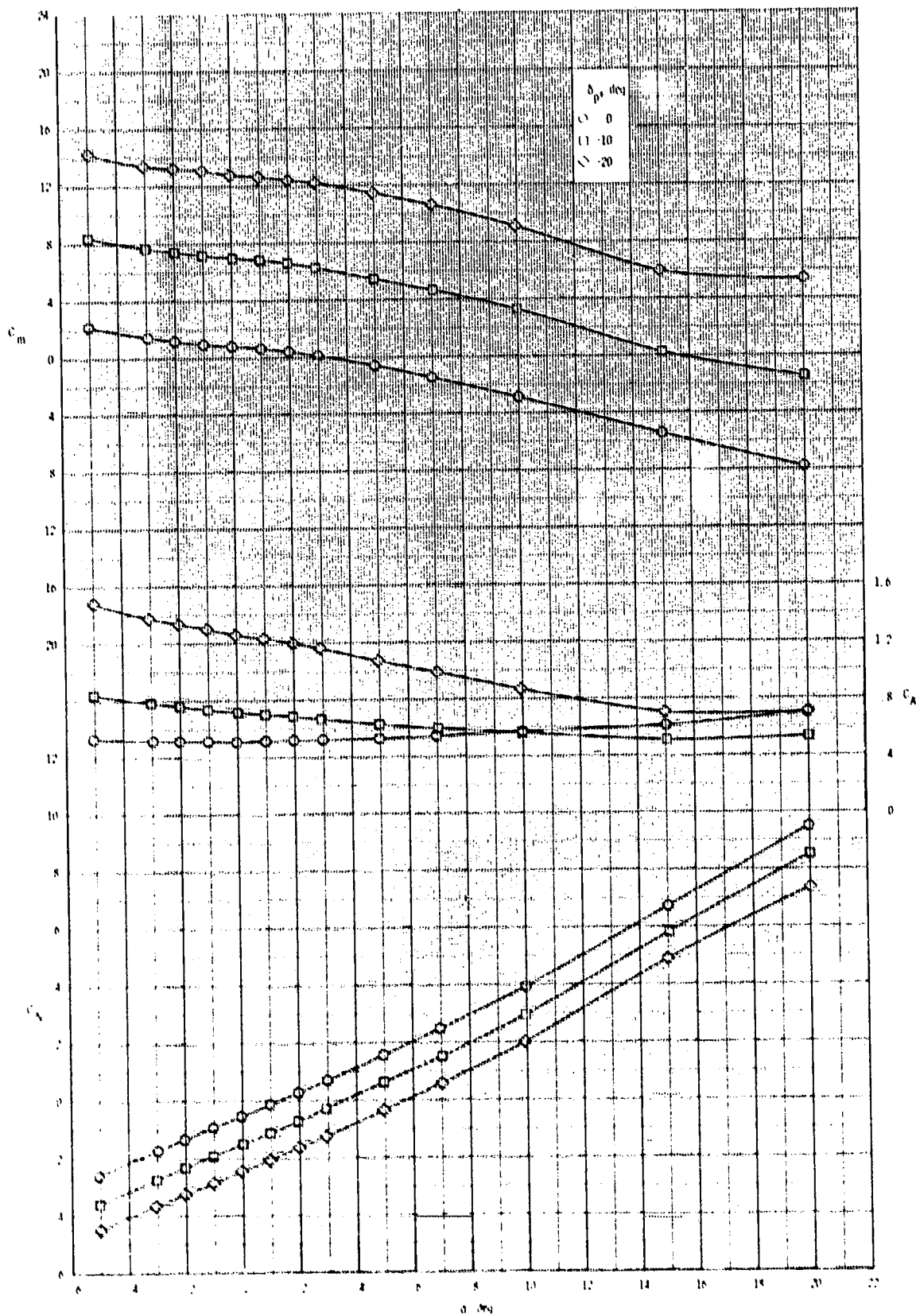
ORIGINAL PAGE IS
OF POOR QUALITY



(a) Concluded.

Figure 10.- Continued.

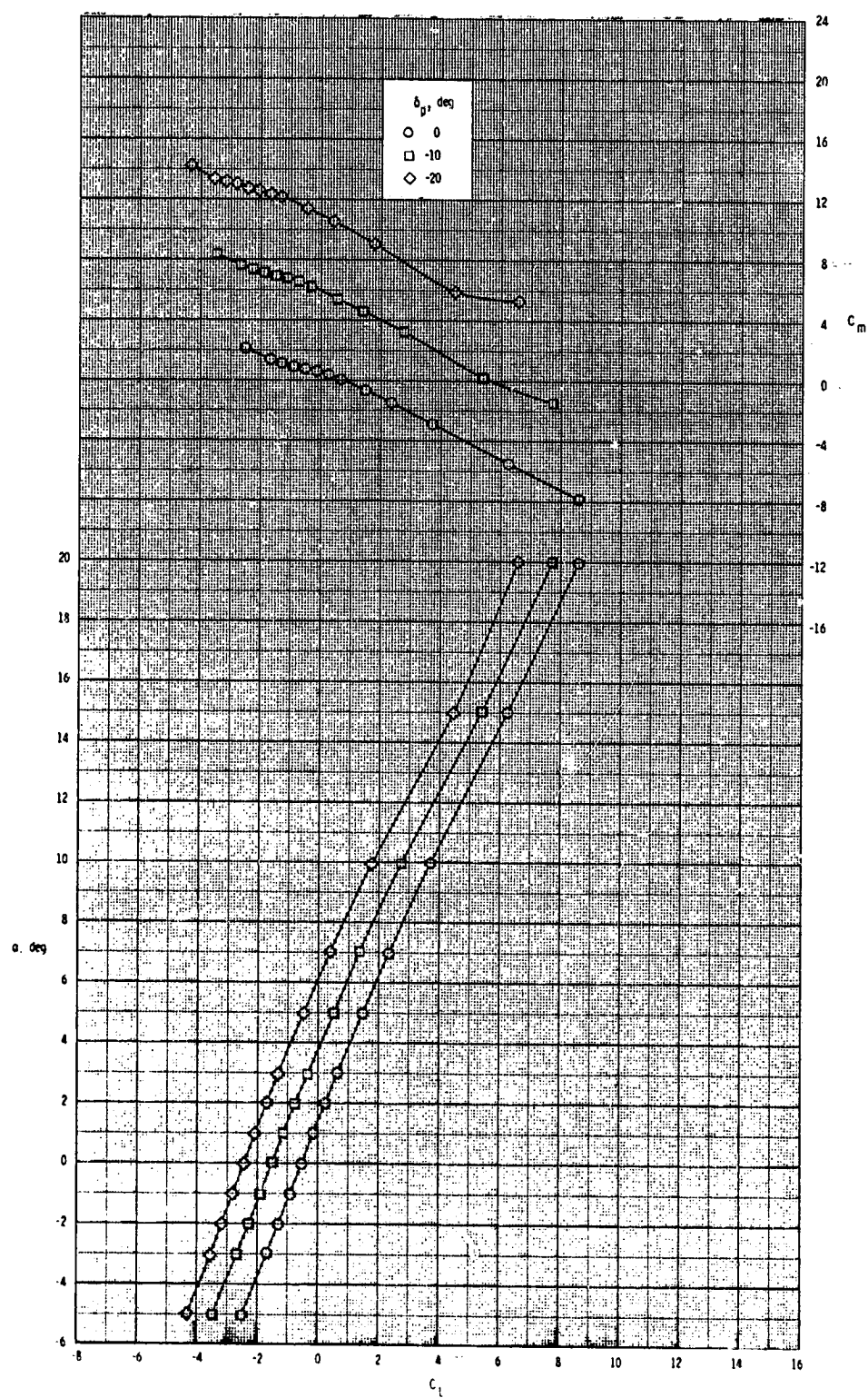
ORIGINAL PAGE IS
OF POOR QUALITY



(b) $M = 2.05$.

Figure 10.- Continued.

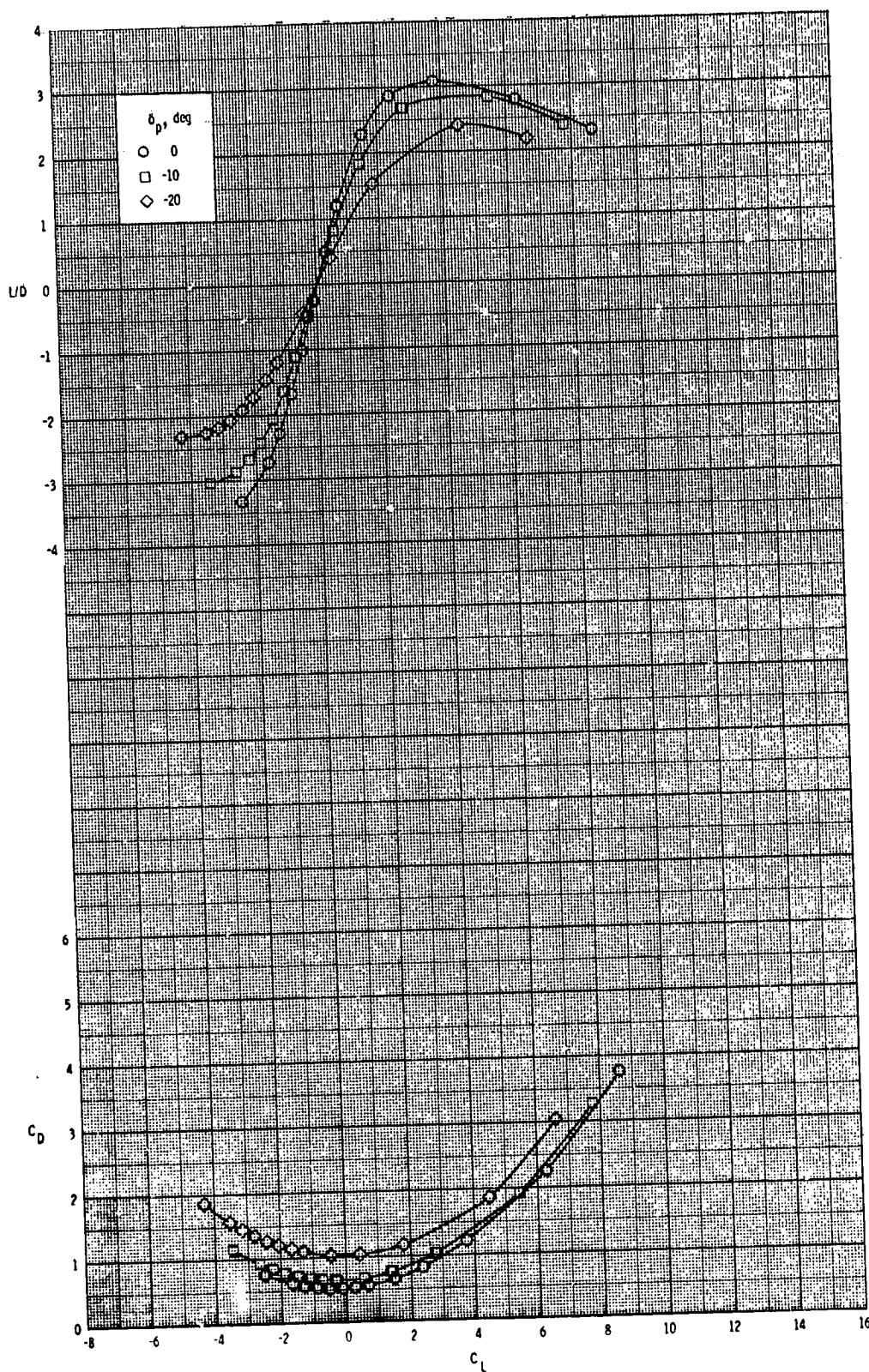
ORIGINAL PAGE IS
OF POOR QUALITY



(b) Continued.

Figure 10.- Continued.

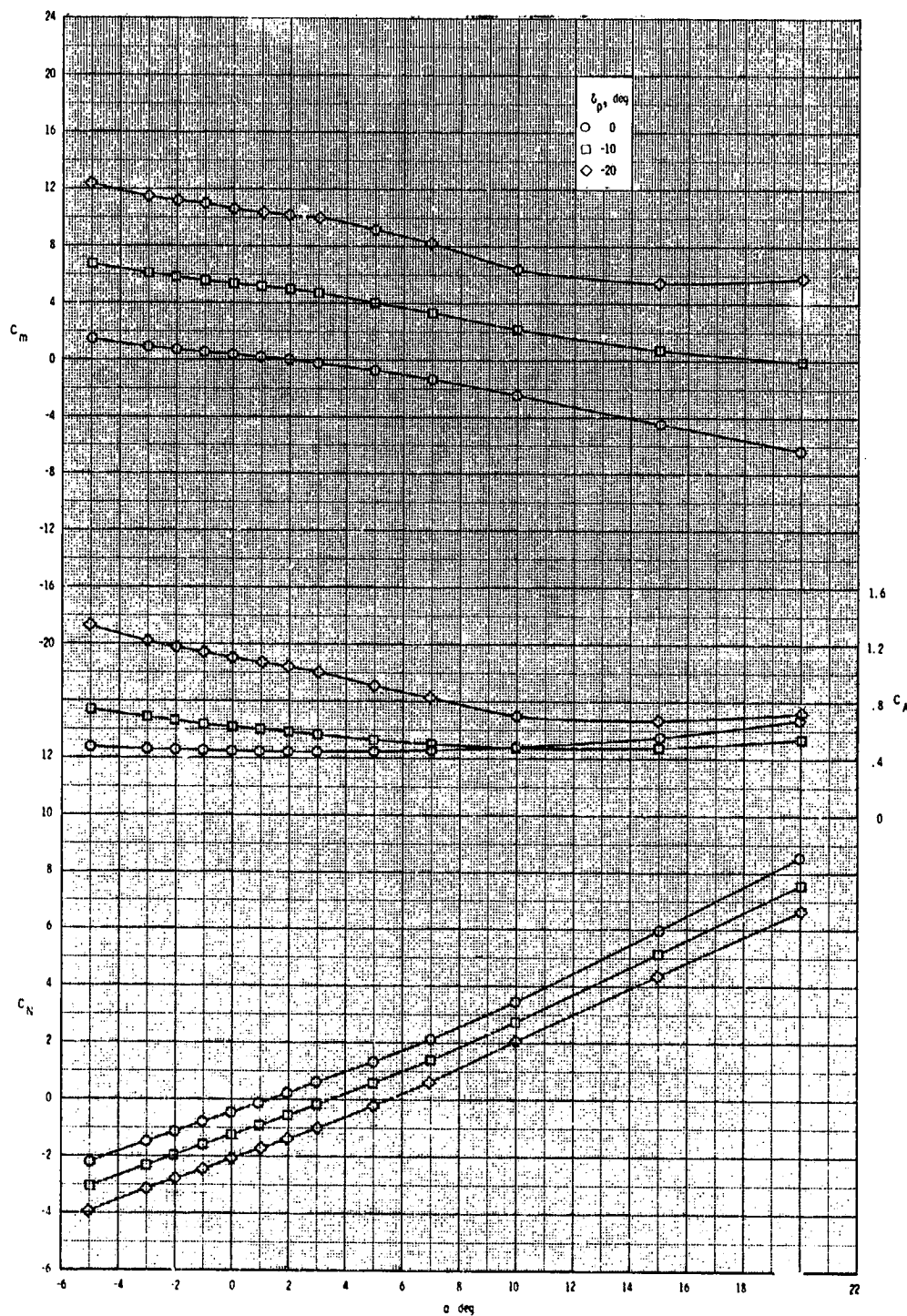
OROWEN, E. H. 10 OF POOR QUALITY



(b) Concluded.

Figure 10.- Continued.

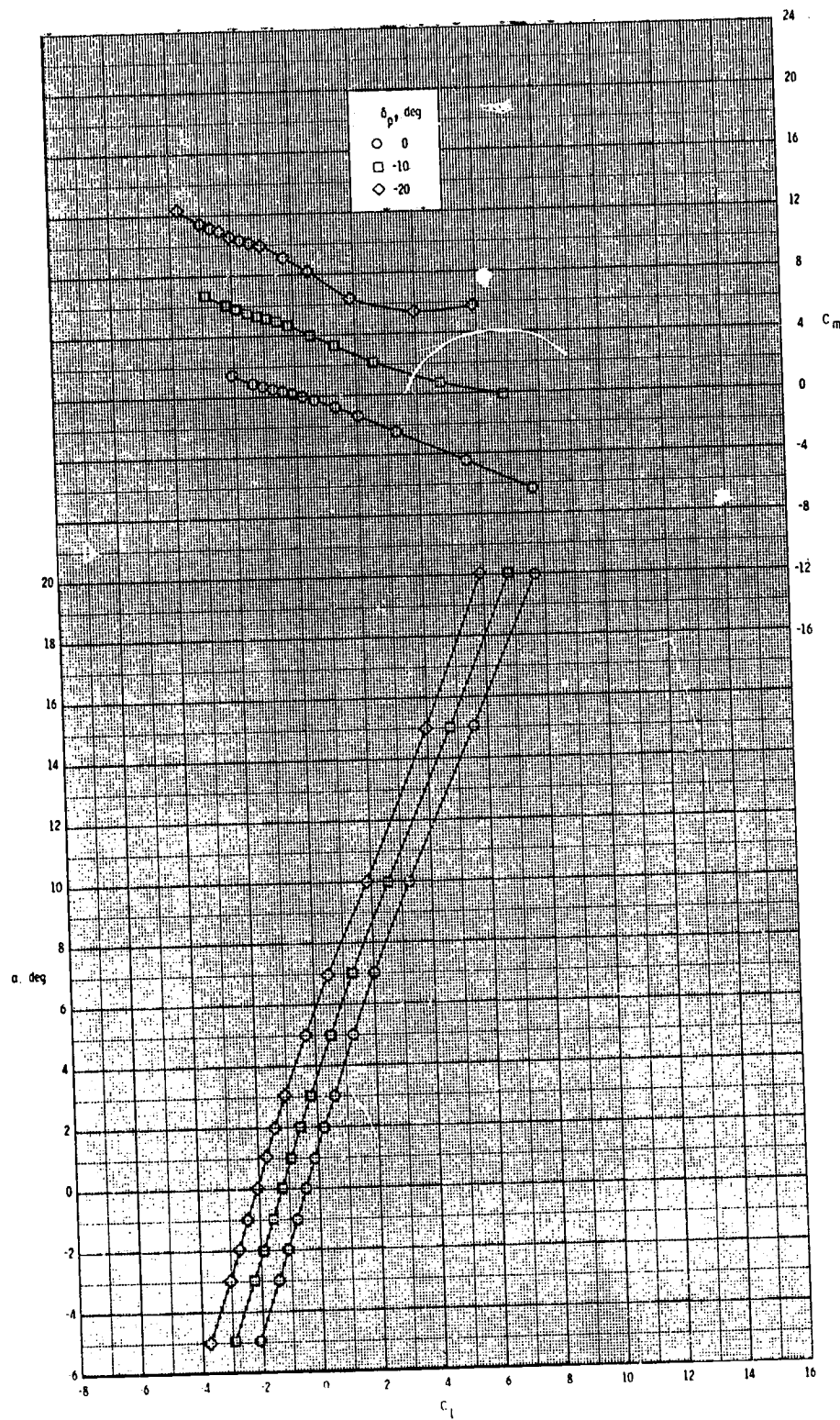
ORIGINAL PAGE IS
OF POOR QUALITY



(c) $M = 3.50$.

Figure 10.- Continued.

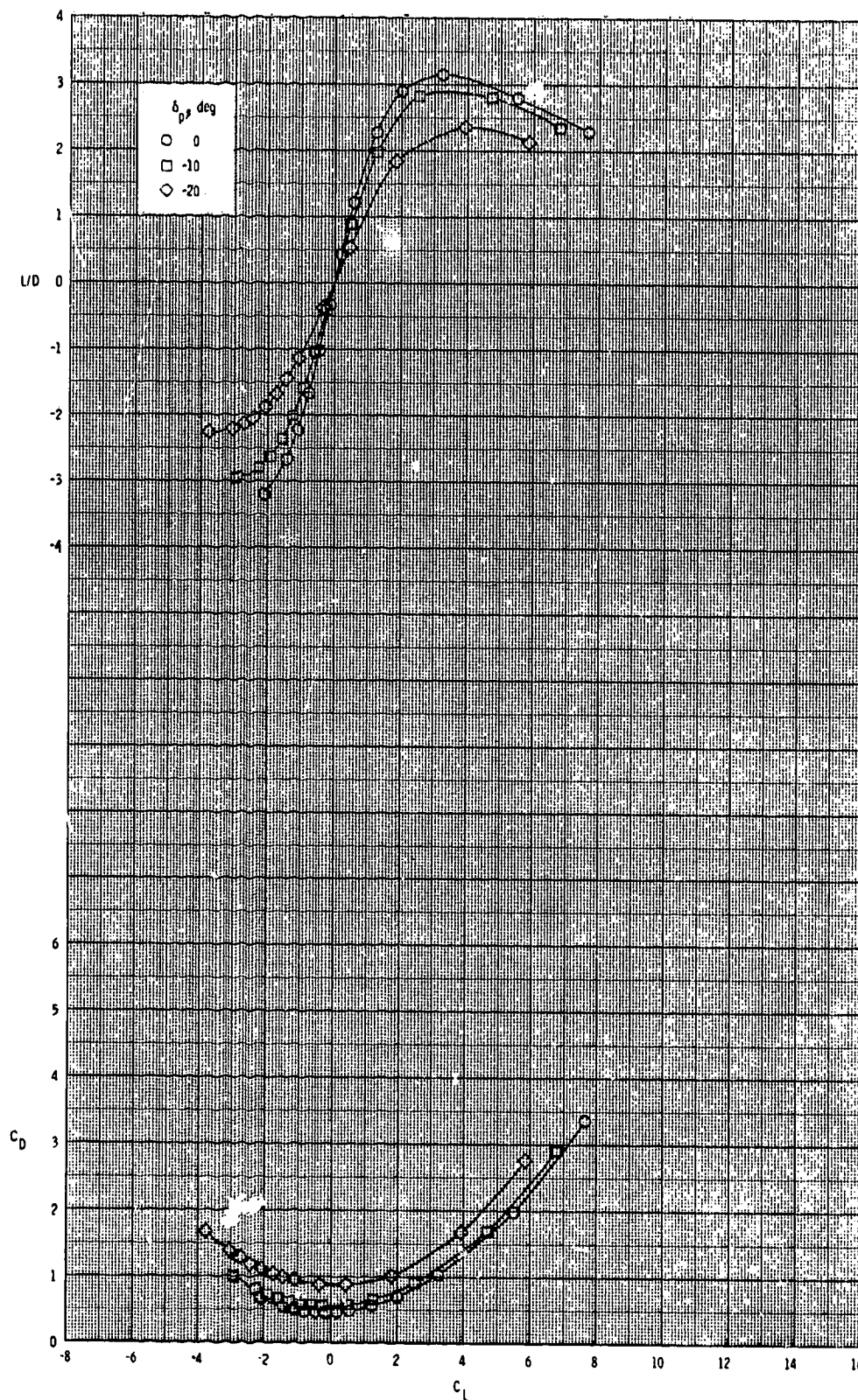
ORIGINAL PAGE IS
OF POOR QUALITY



(c) Continued.

Figure 10.- Continued.

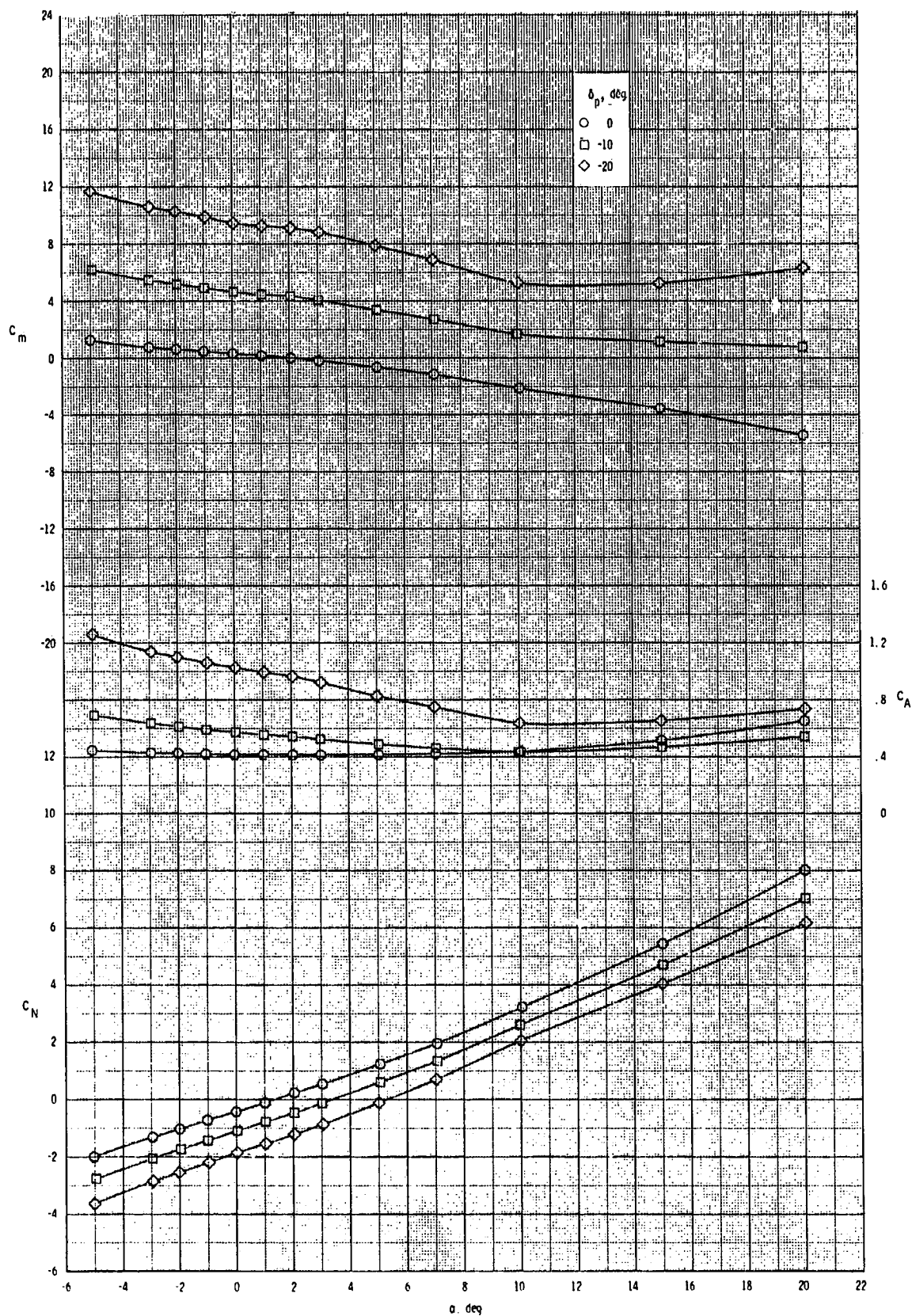
ORIGINAL PAGE IS
OF POOR QUALITY



(c) Concluded.

Figure 10.- Continued.

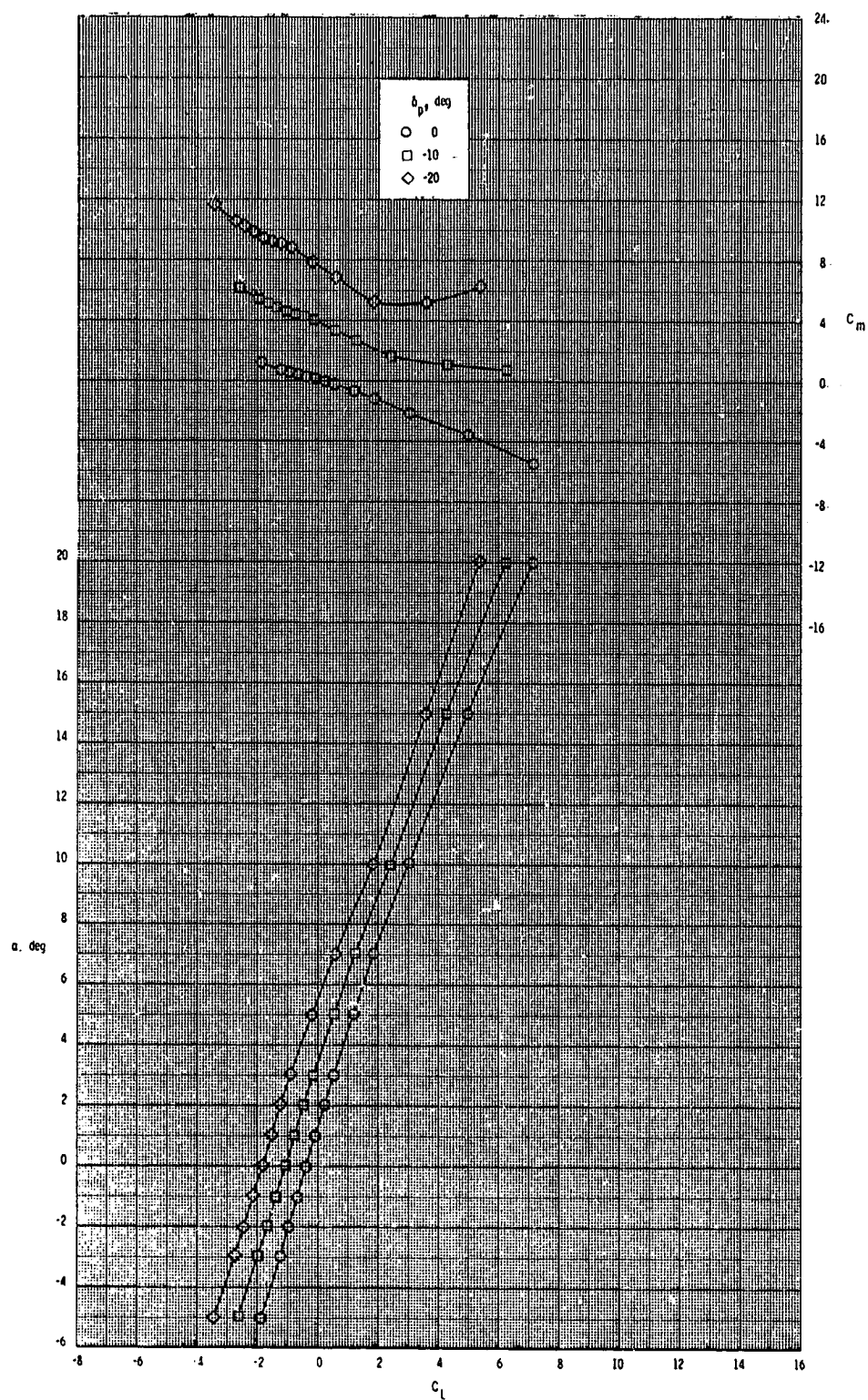
ORIGINAL PAGE IS
OF POOR QUALITY



(d) $M = 3.95$.

Figure 10.- Continued.

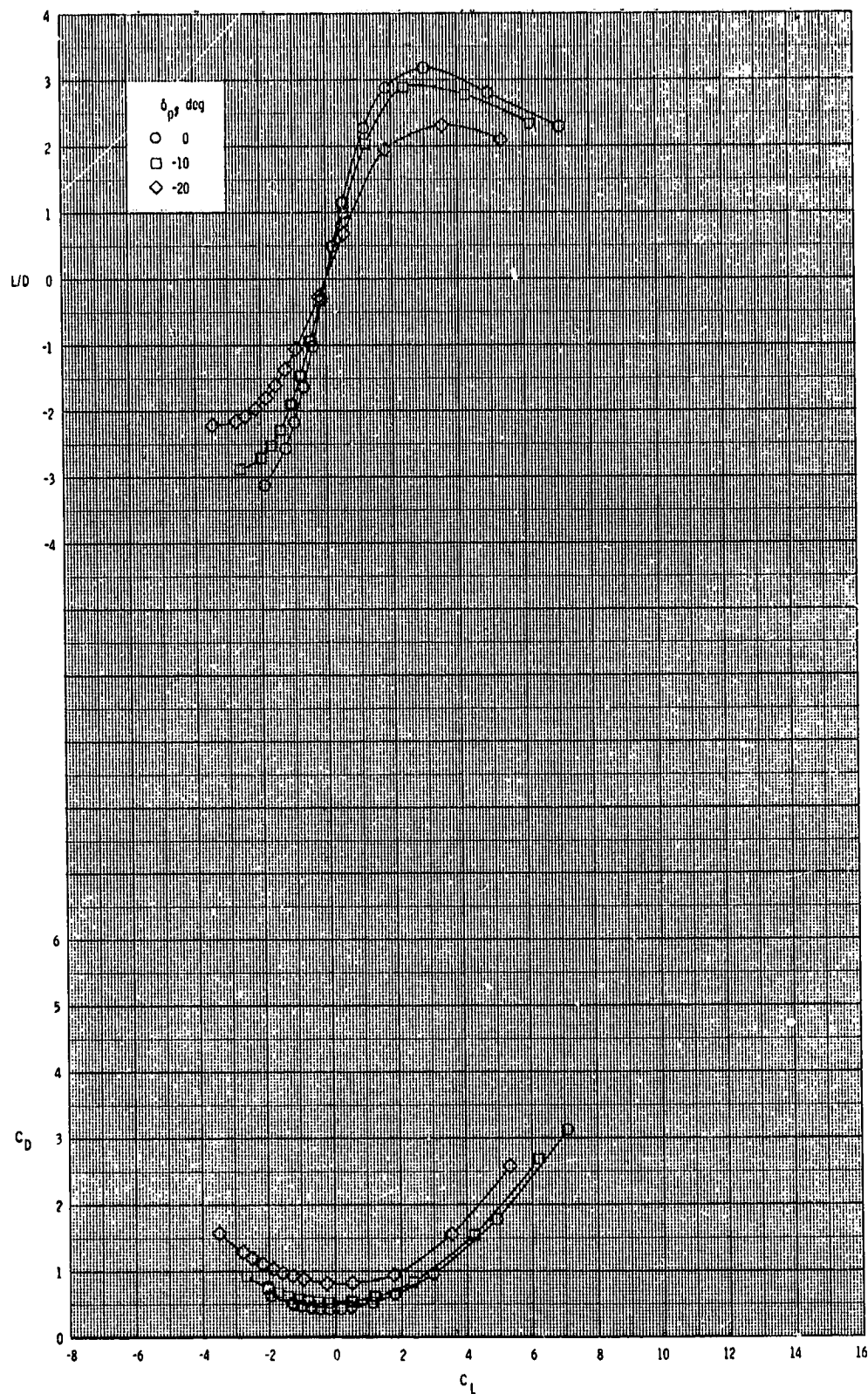
ORIGINAL PAGE 15
OF POOR QUALITY



(d) Continued.

Figure 10.- Continued.

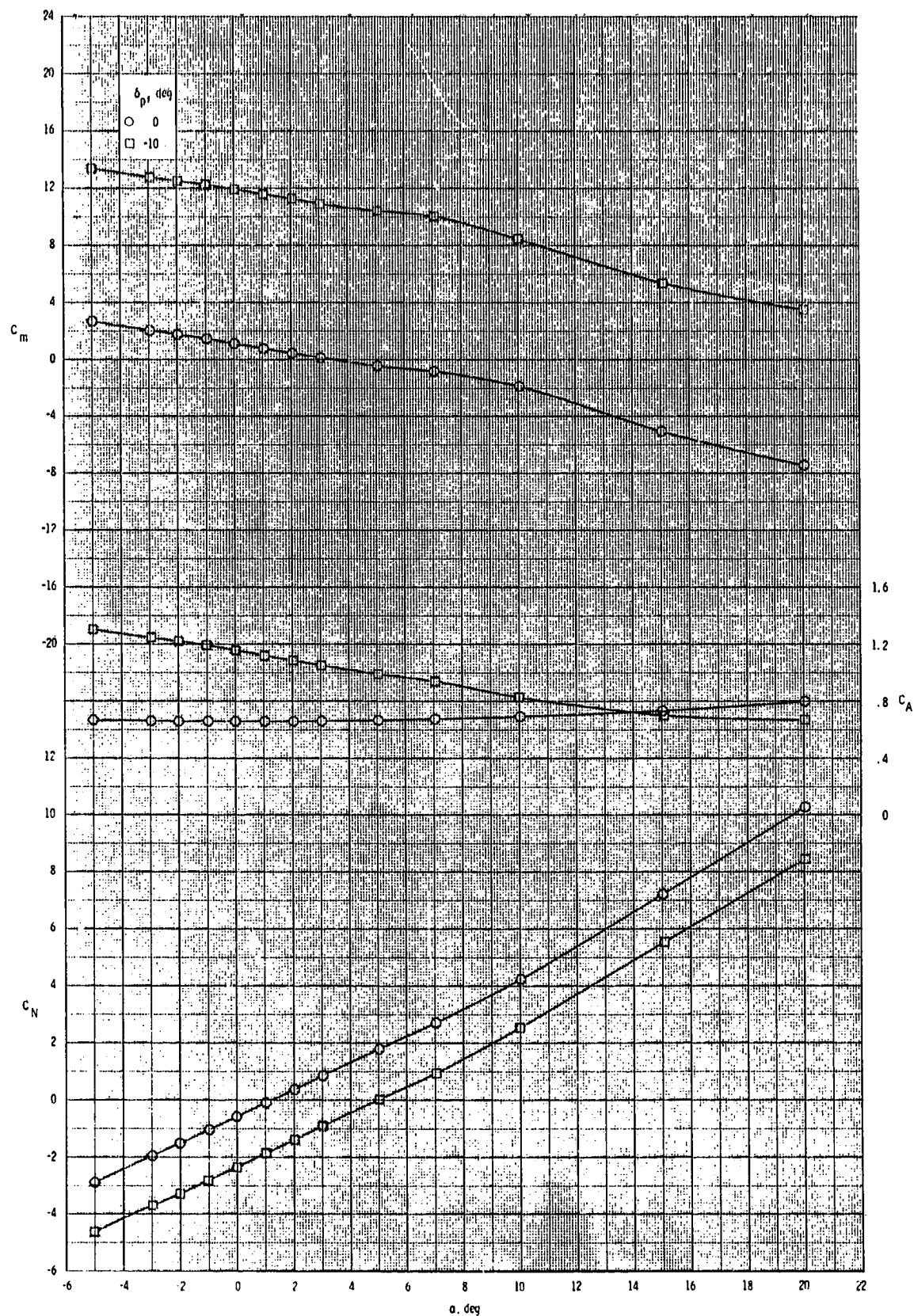
ORIGINAL PAGE IS
OF POOR QUALITY



(d) Concluded.

Figure 10.- Concluded.

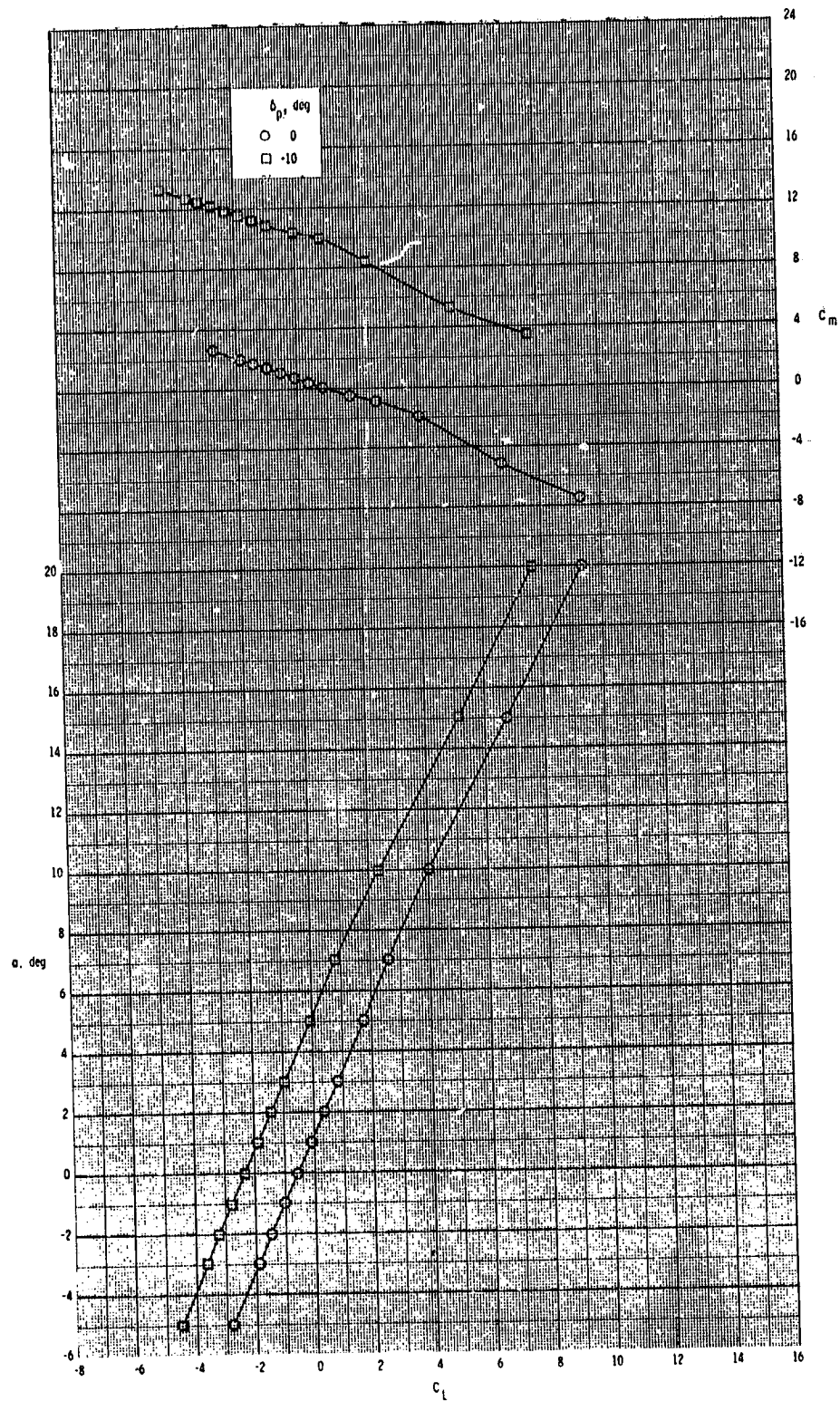
ORIGINAL PAGE IS
OF POOR QUALITY



(a) $M = 2.50$.

Figure 11.- Pitch-control effectiveness of configuration $B_1I_4W_1T_2$.

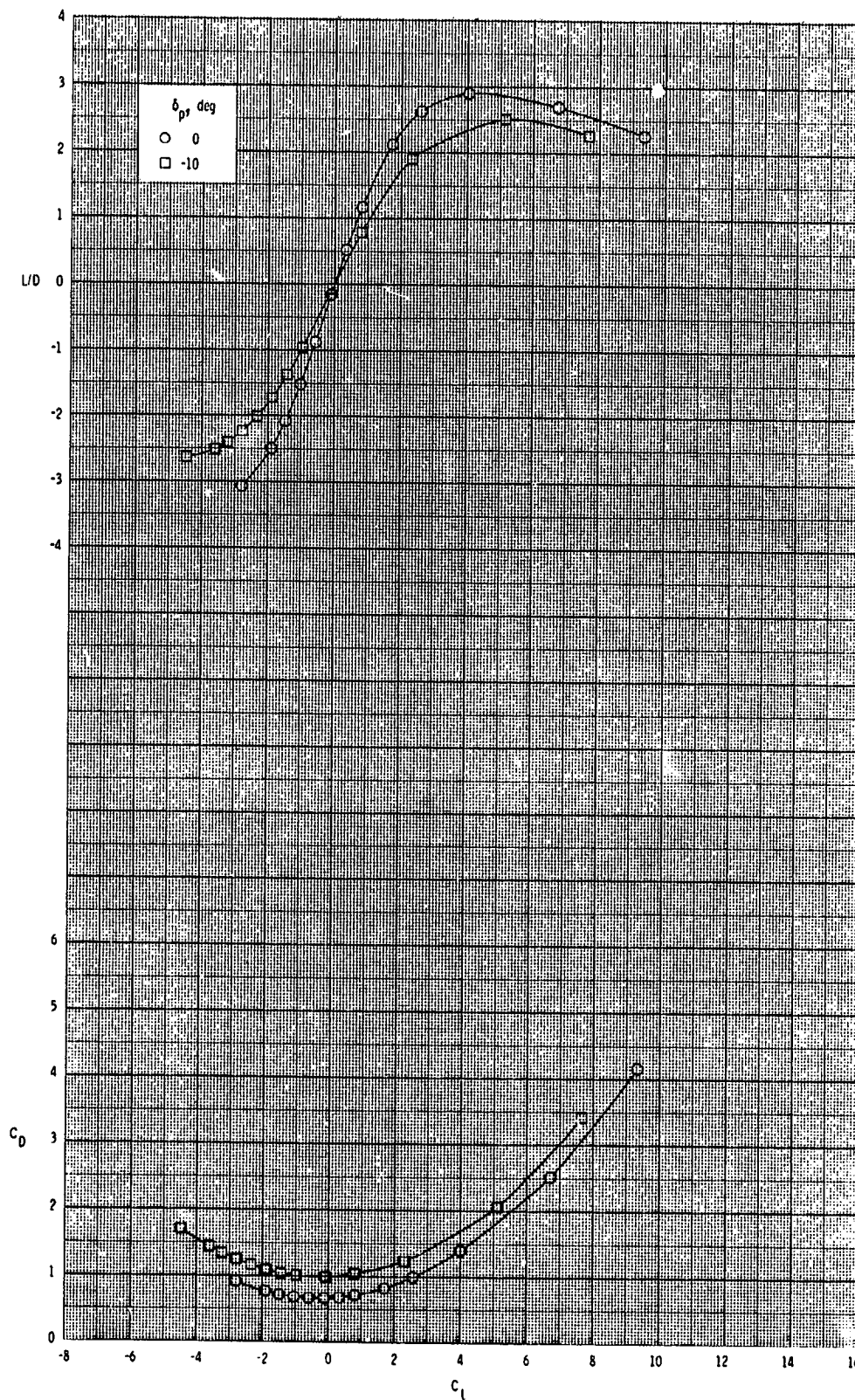
ORIGINAL PAGE IS
OF POOR QUALITY



(a) Continued.

Figure 11.- Continued.

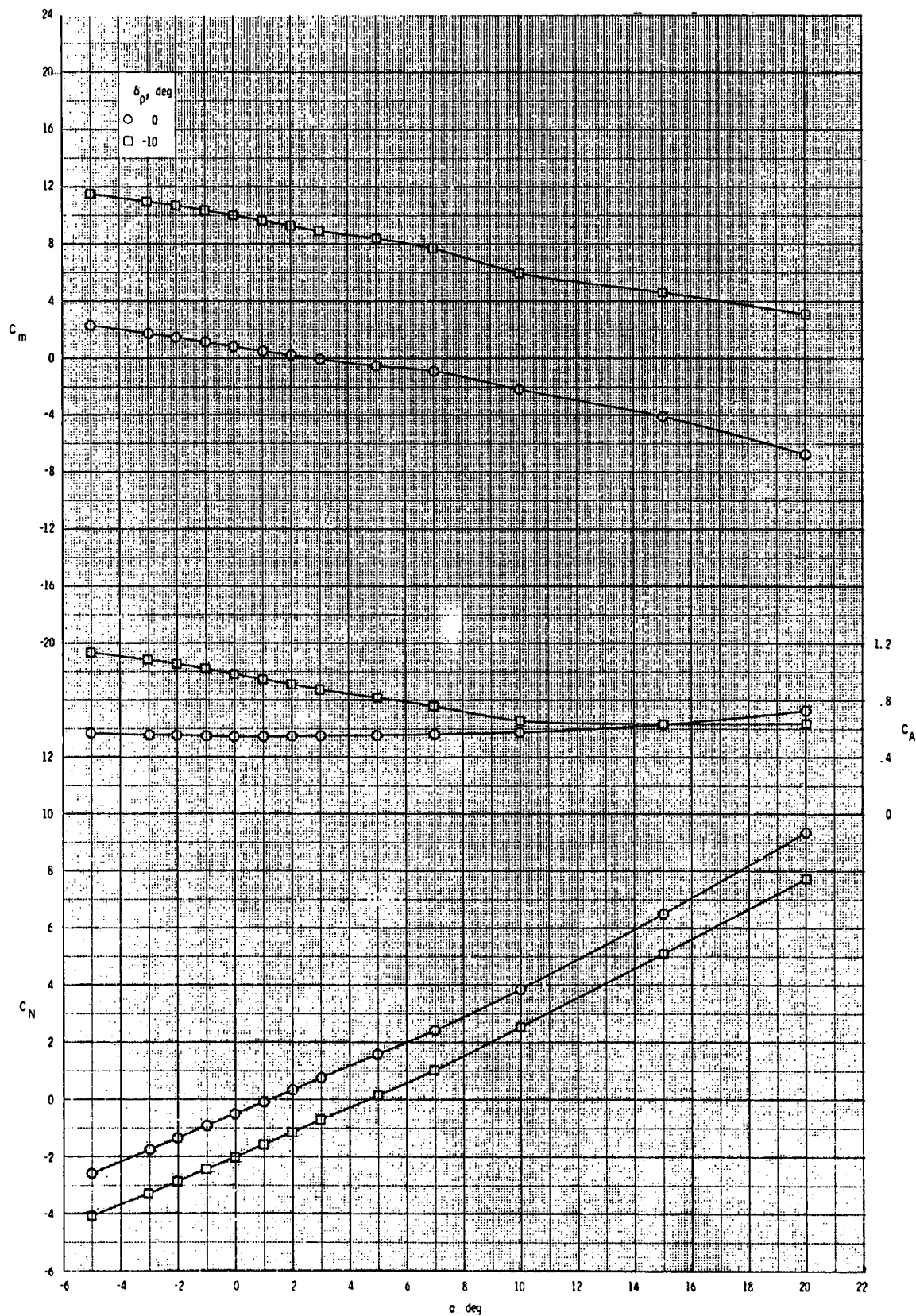
ORIGINAL PAGE IS
OF POOR QUALITY



(a) Concluded.

Figure 11.- Continued.

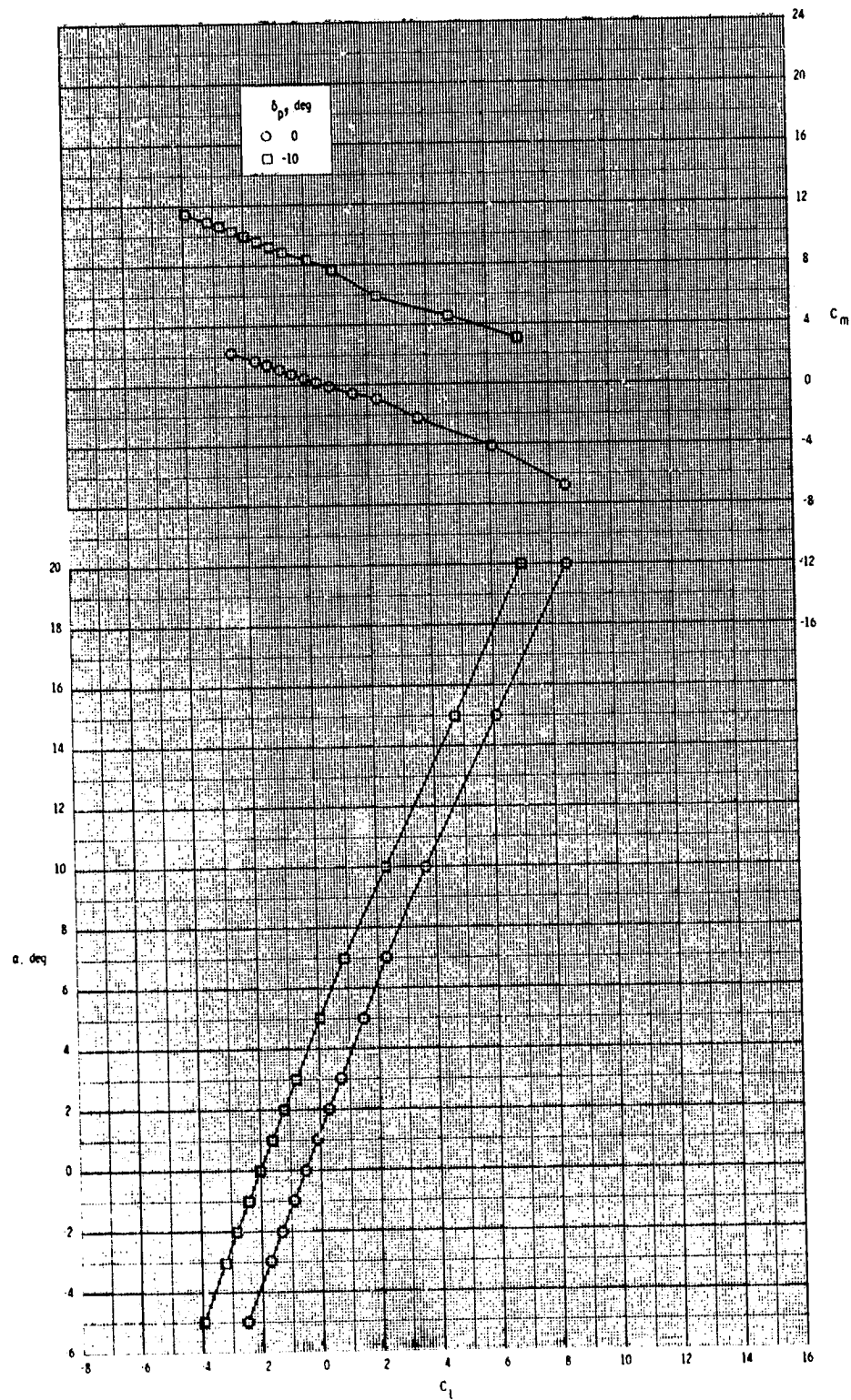
ORIGINAL PAGE IS
OF POOR QUALITY



(b) $M = 2.95$.

Figure 11.- Continued.

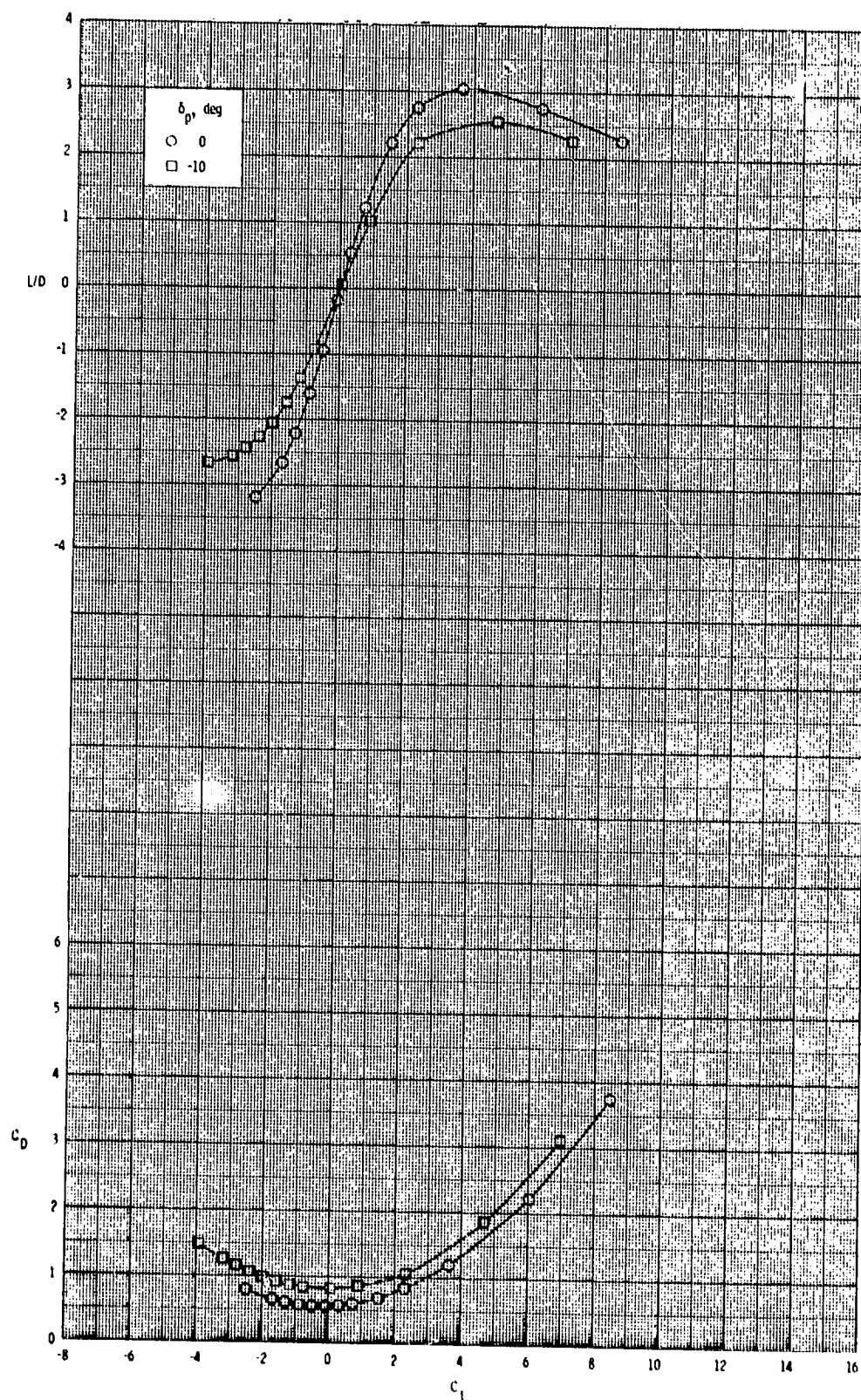
ORIGINAL PAGE IS
OF POOR QUALITY



(b) Continued.

Figure 11.- Continued.

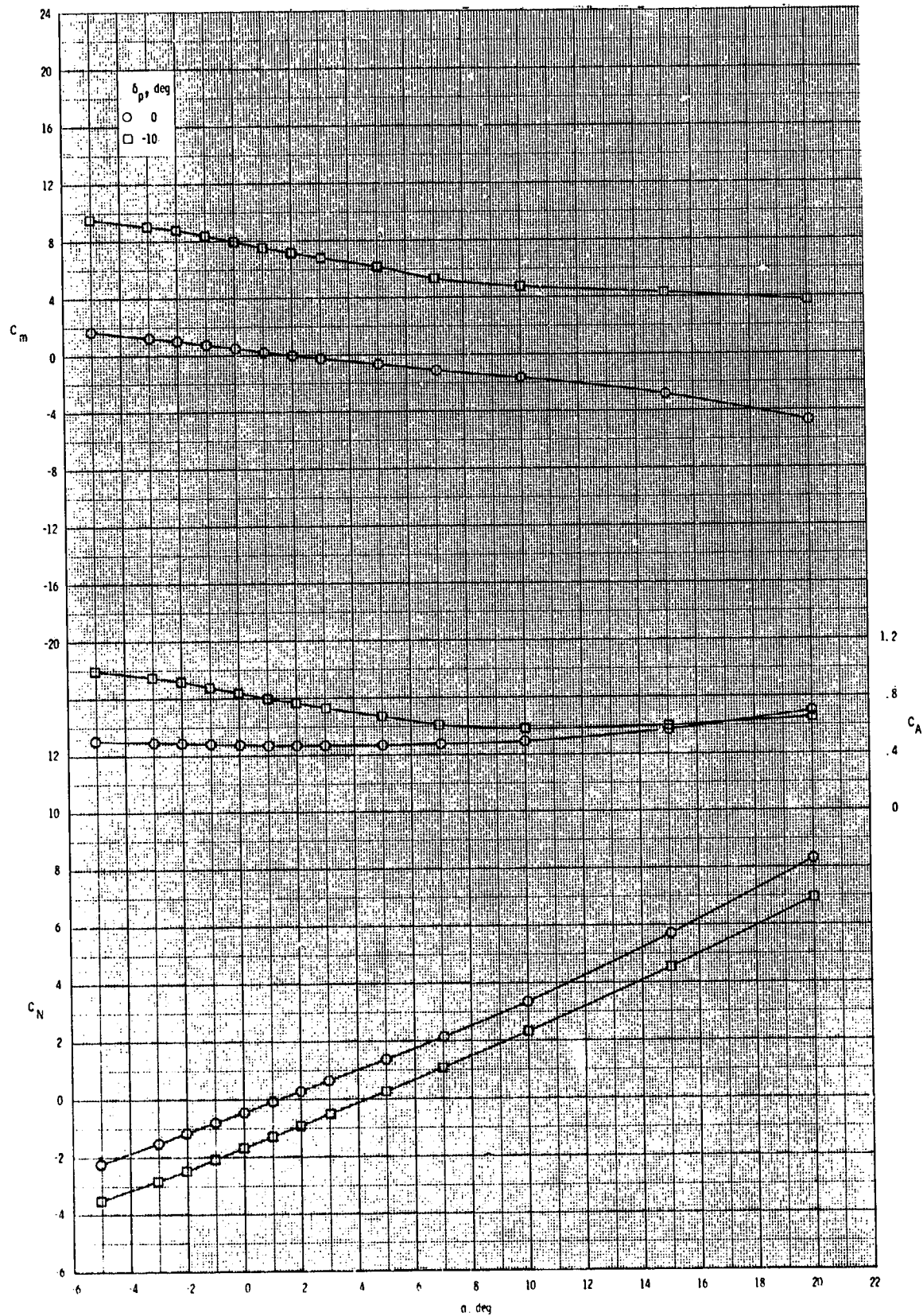
ORIGINAL PAGE IS
OF POOR QUALITY



(b) Concluded.

Figure 11.- Continued.

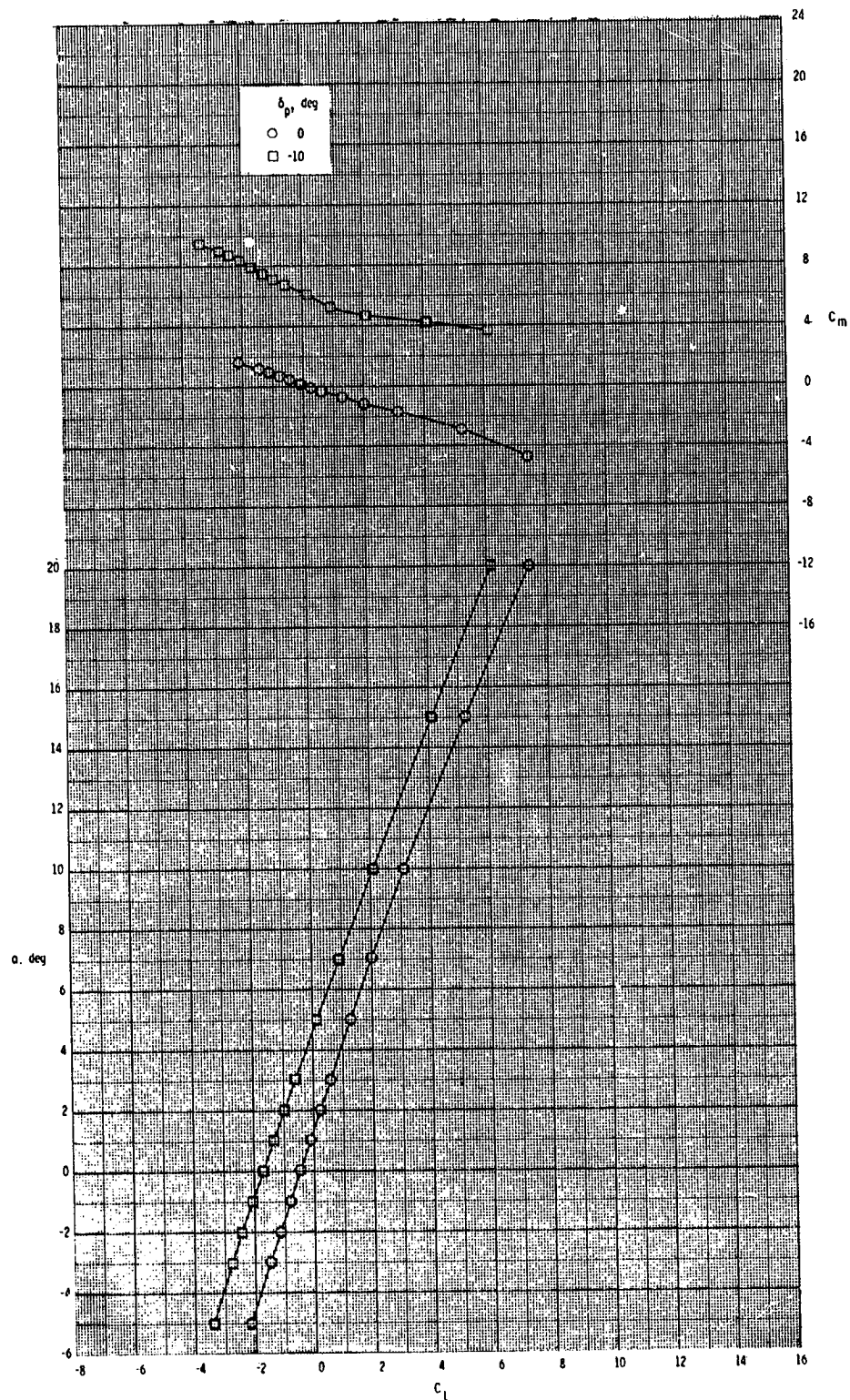
ORIGINAL PAGE 15
OF POOR QUALITY



(c) $M = 3.50$.

Figure 11.- Continued.

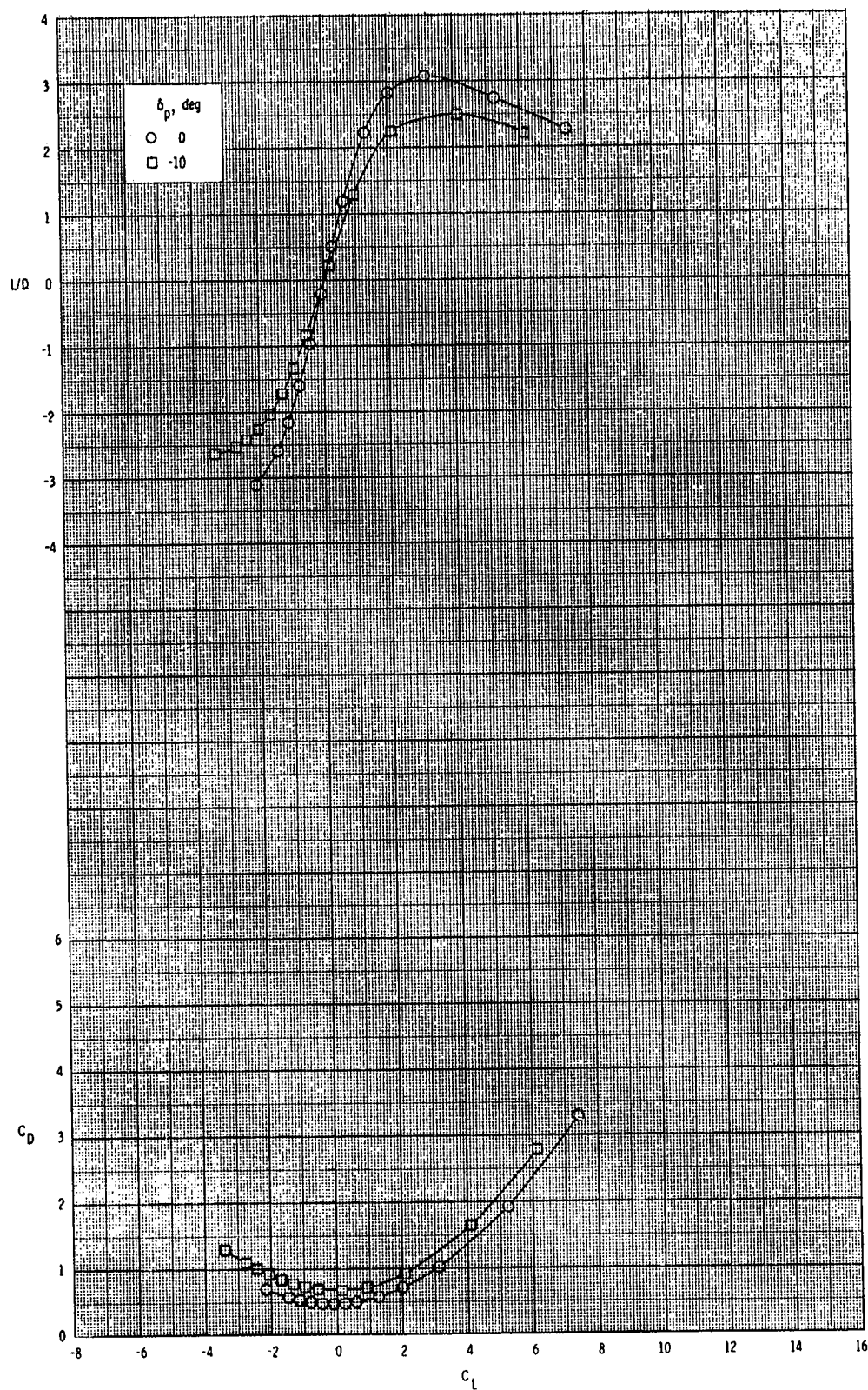
ORIGINAL PAGE IS
OF POOR QUALITY



(c) Continued.

Figure 11.- Continued.

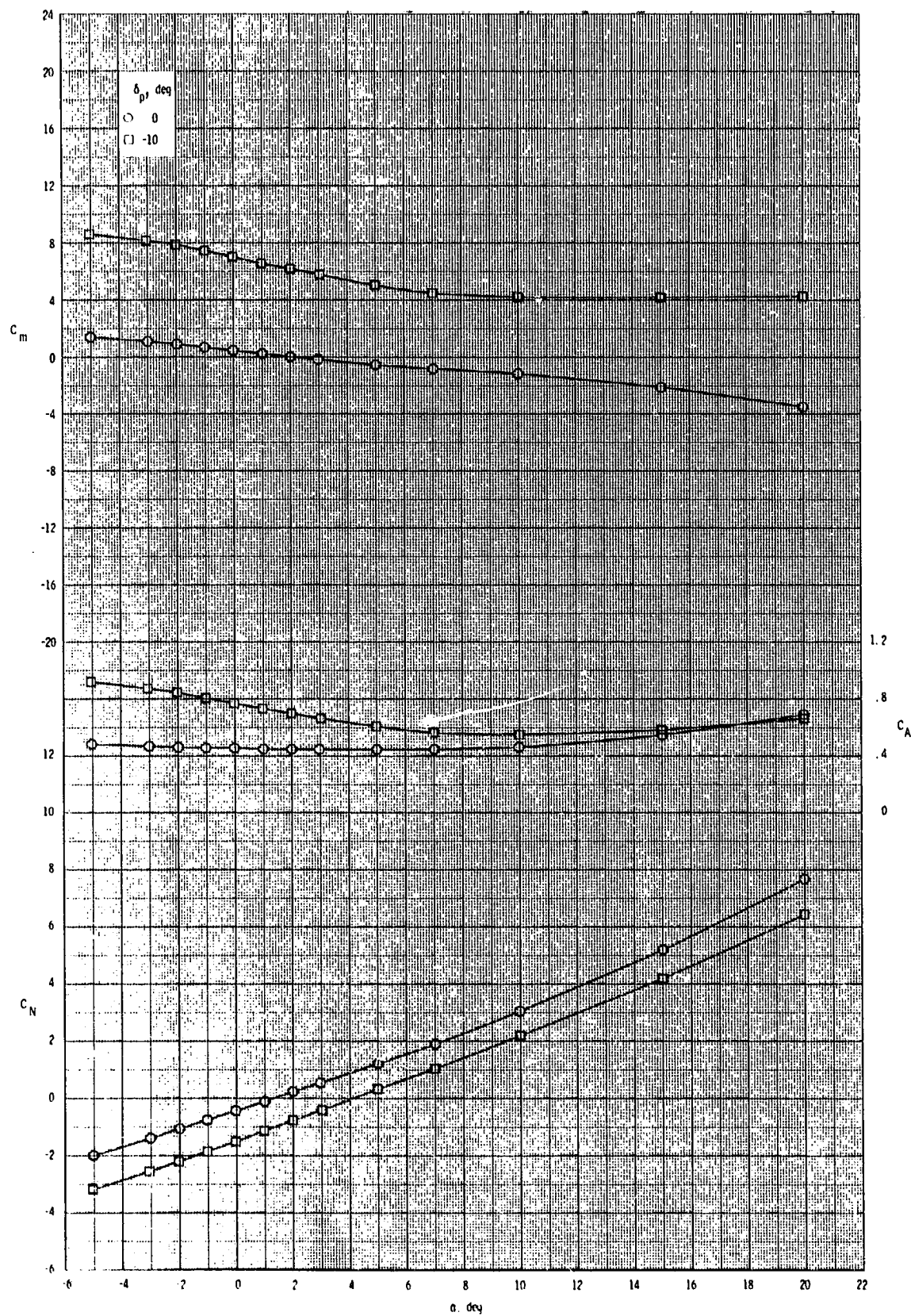
ORIGINAL PAGE IS
OF POOR QUALITY



(c) Concluded.

Figure 11.- Continued.

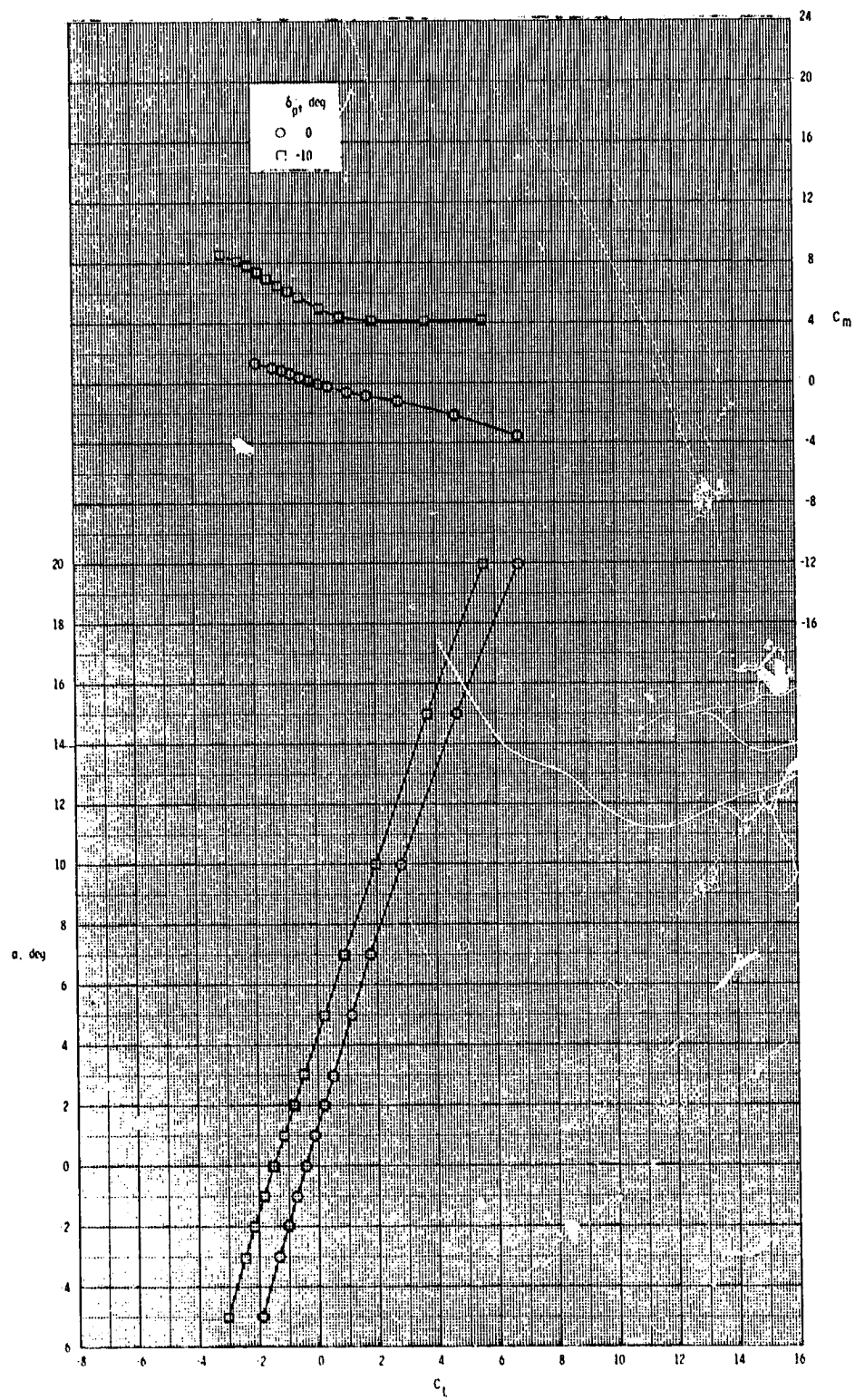
ORIGINAL PAGE IS
OF POOR QUALITY



(d) $M = 3.95$.

Figure 11.- Continued.

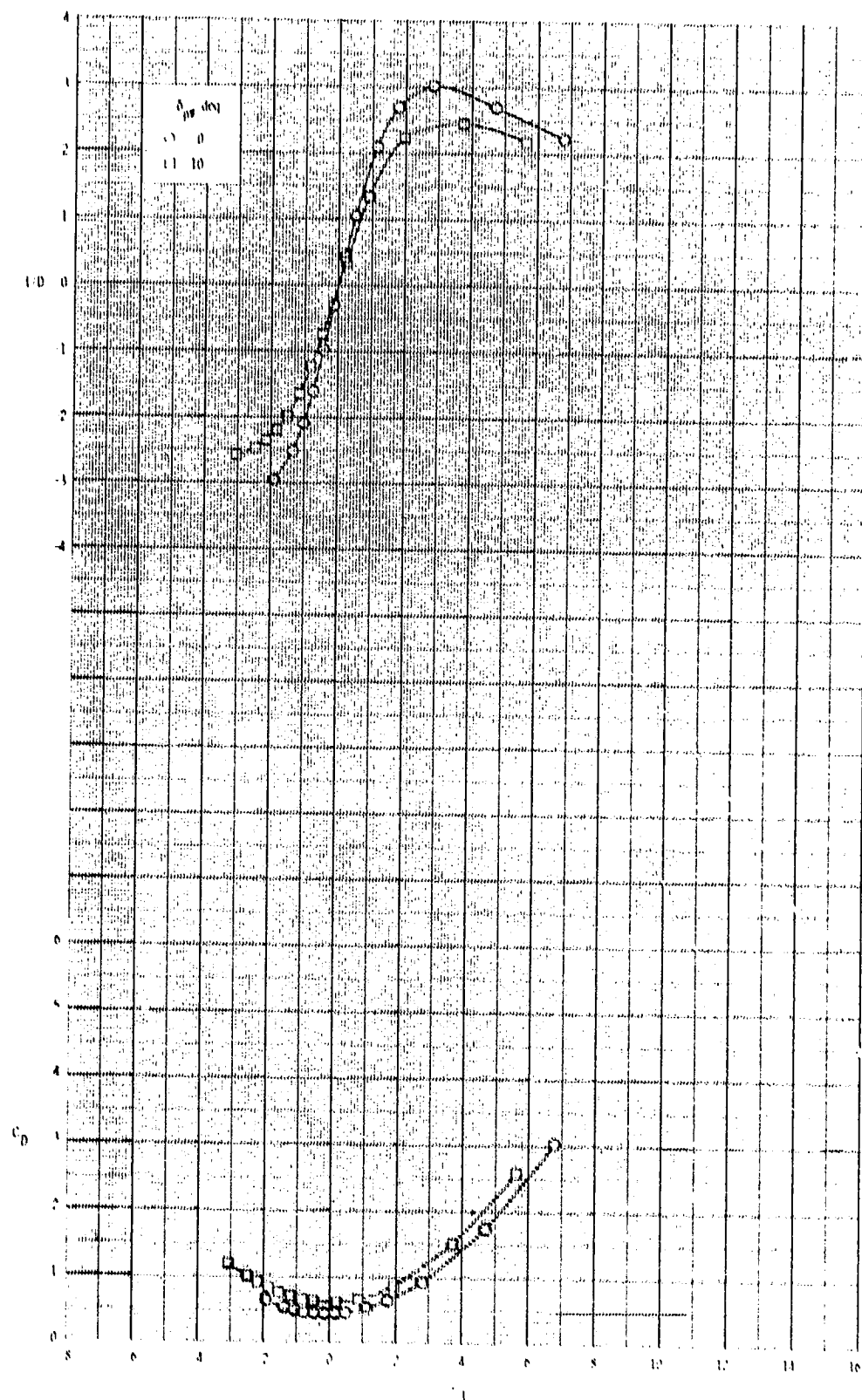
ORIGINAL PAGE IS
OF POOR QUALITY



(d) Continued.

Figure 11.- Continued.

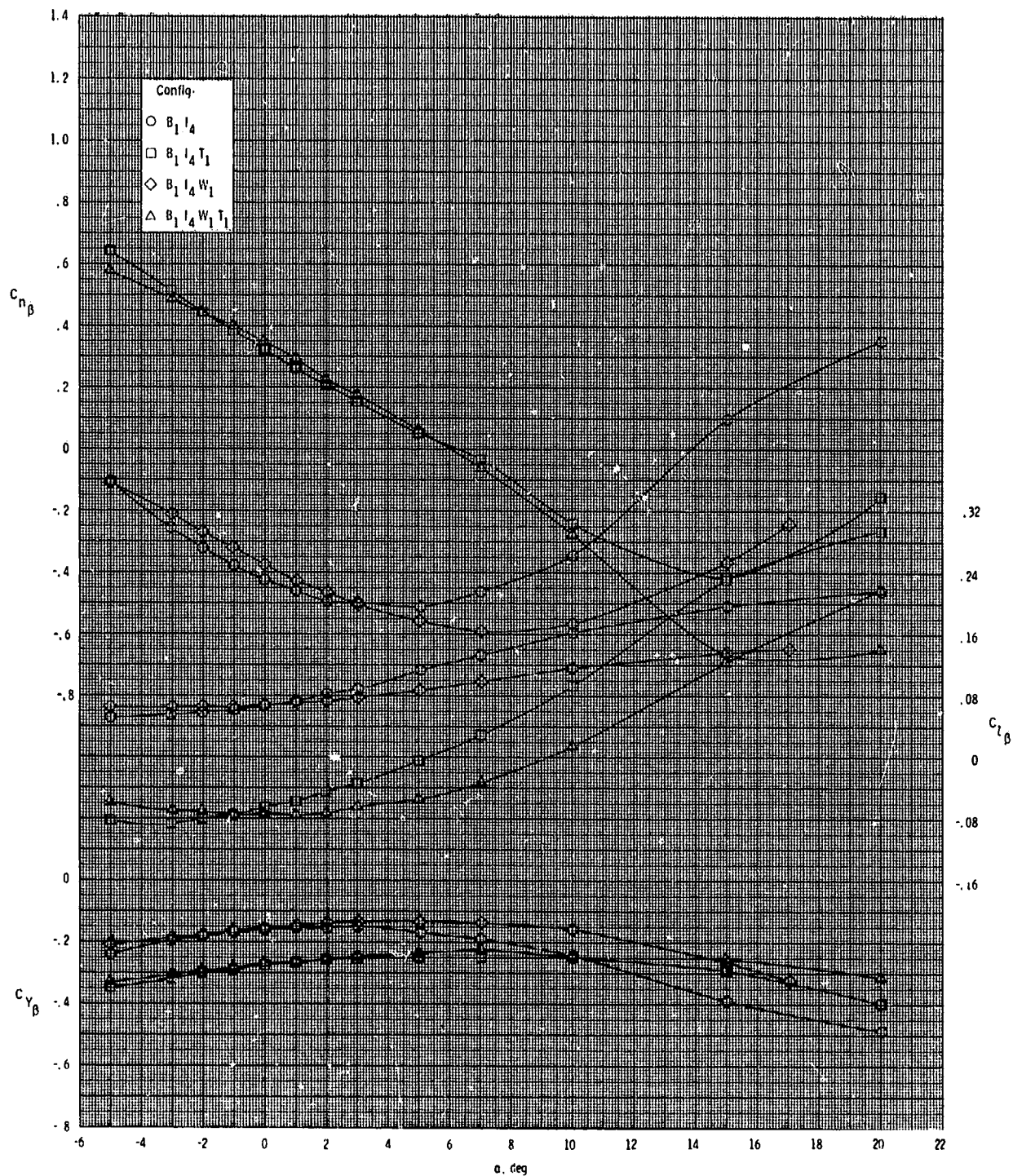
ORIGINAL PAGE IS
OF POOR QUALITY



(d) Concluded.

Figure 11.- Concluded.

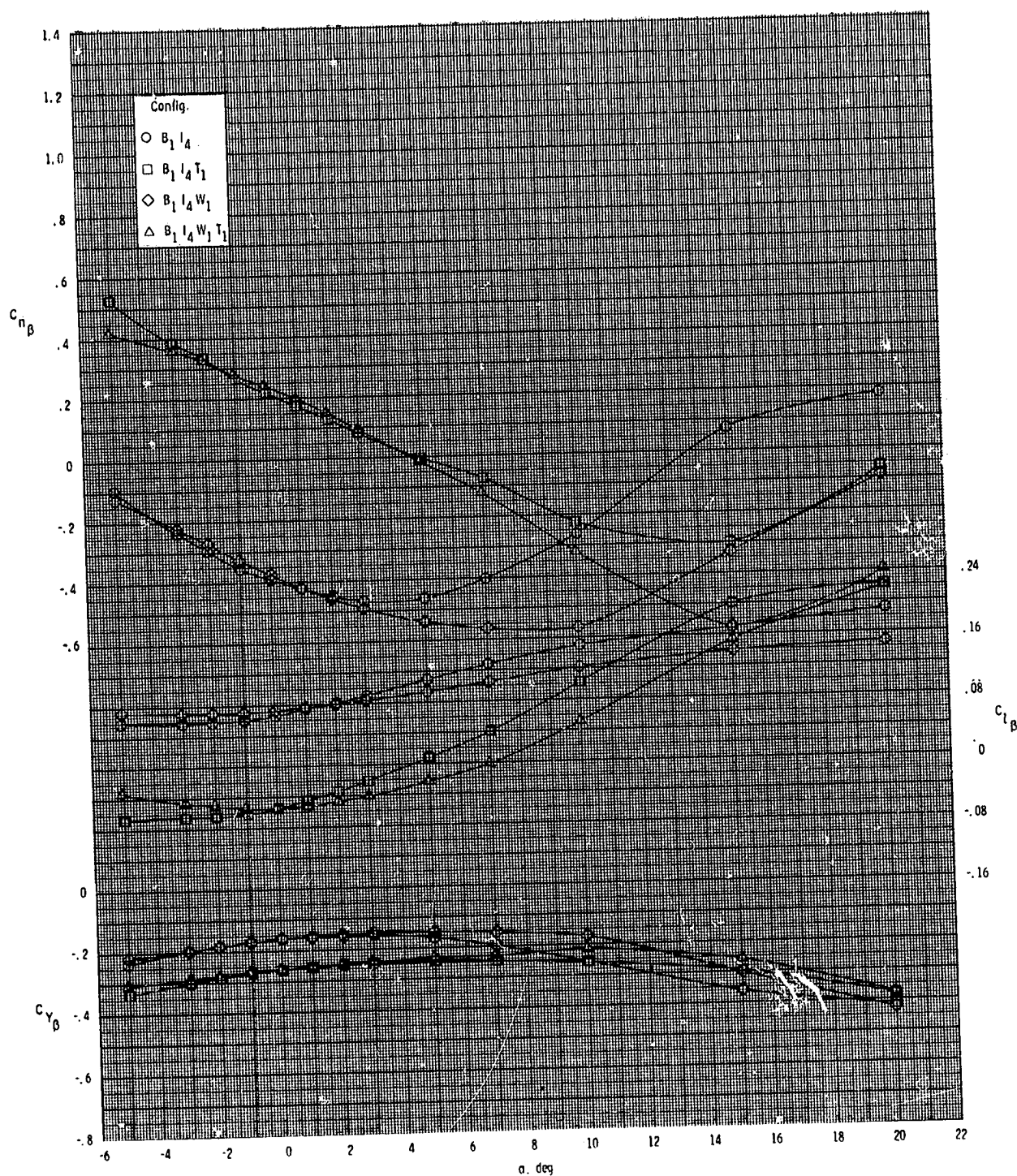
ORIGINAL PAGE IS
OF POOR QUALITY



(a) $M = 2.50$.

Figure 12.- Effect of various model components on lateral-directional stability for axisymmetric inlet with T_1 .

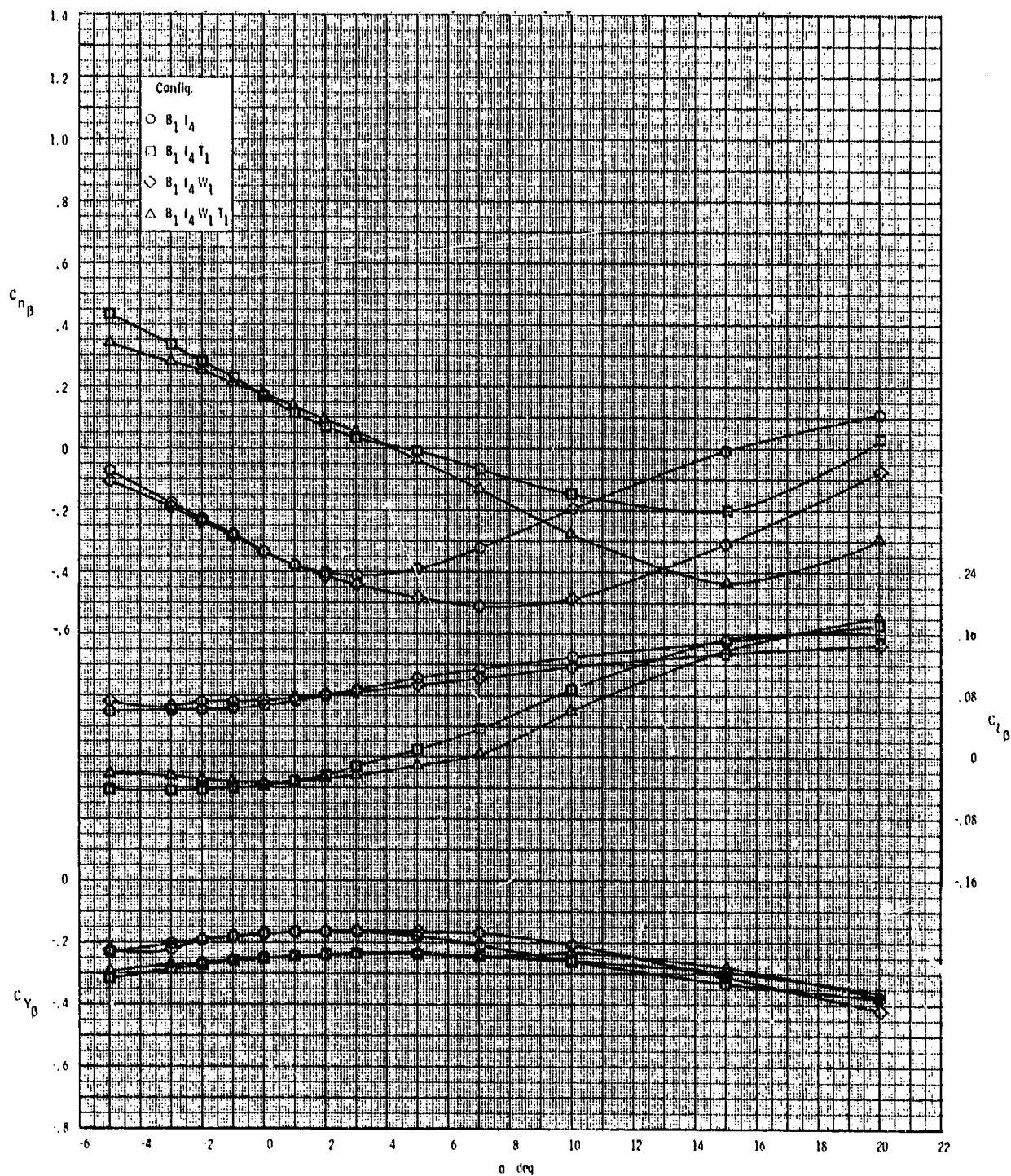
ORIGINAL PAGE IS
OF POOR QUALITY



(b) $M = 2.95$.

Figure 12.- Continued.

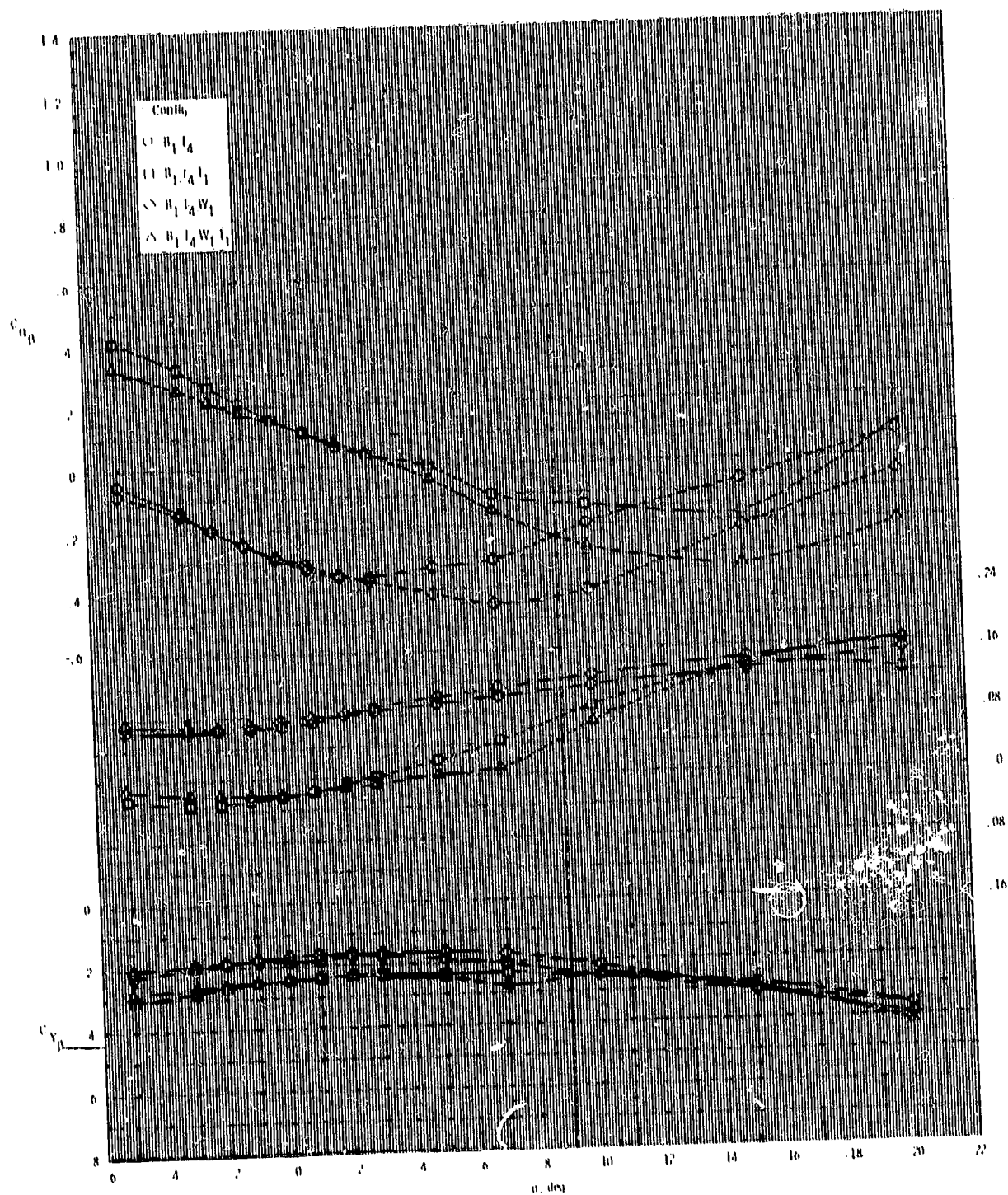
ORIGINAL PAGE IS
OF POOR QUALITY



(c) $M = 3.50$.

Figure 12.- Continued.

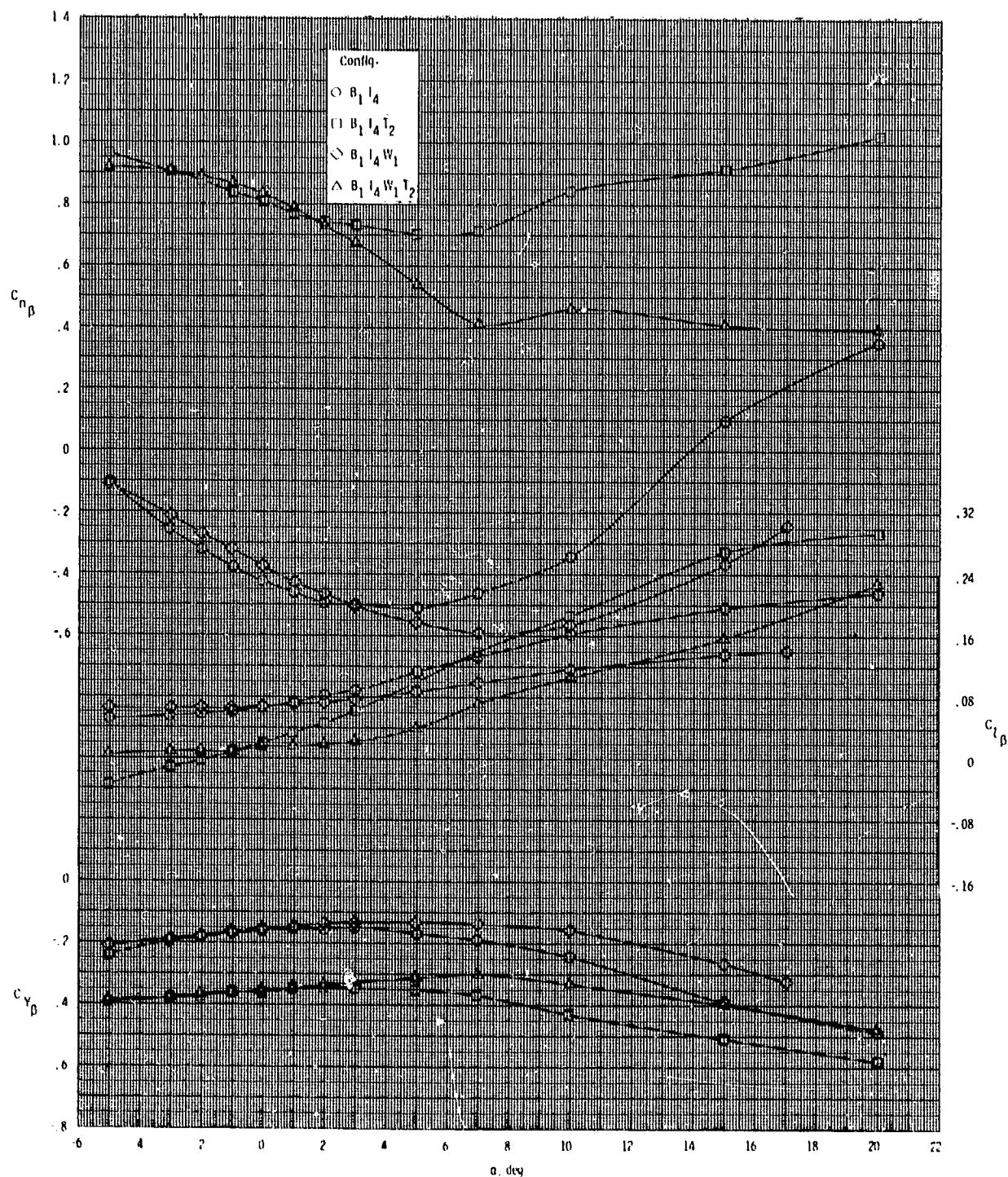
ORIGINAL PAGE 12
OF POOR QUALITY.



(d) $M = 3.95$.

Figure 12.- Concluded.

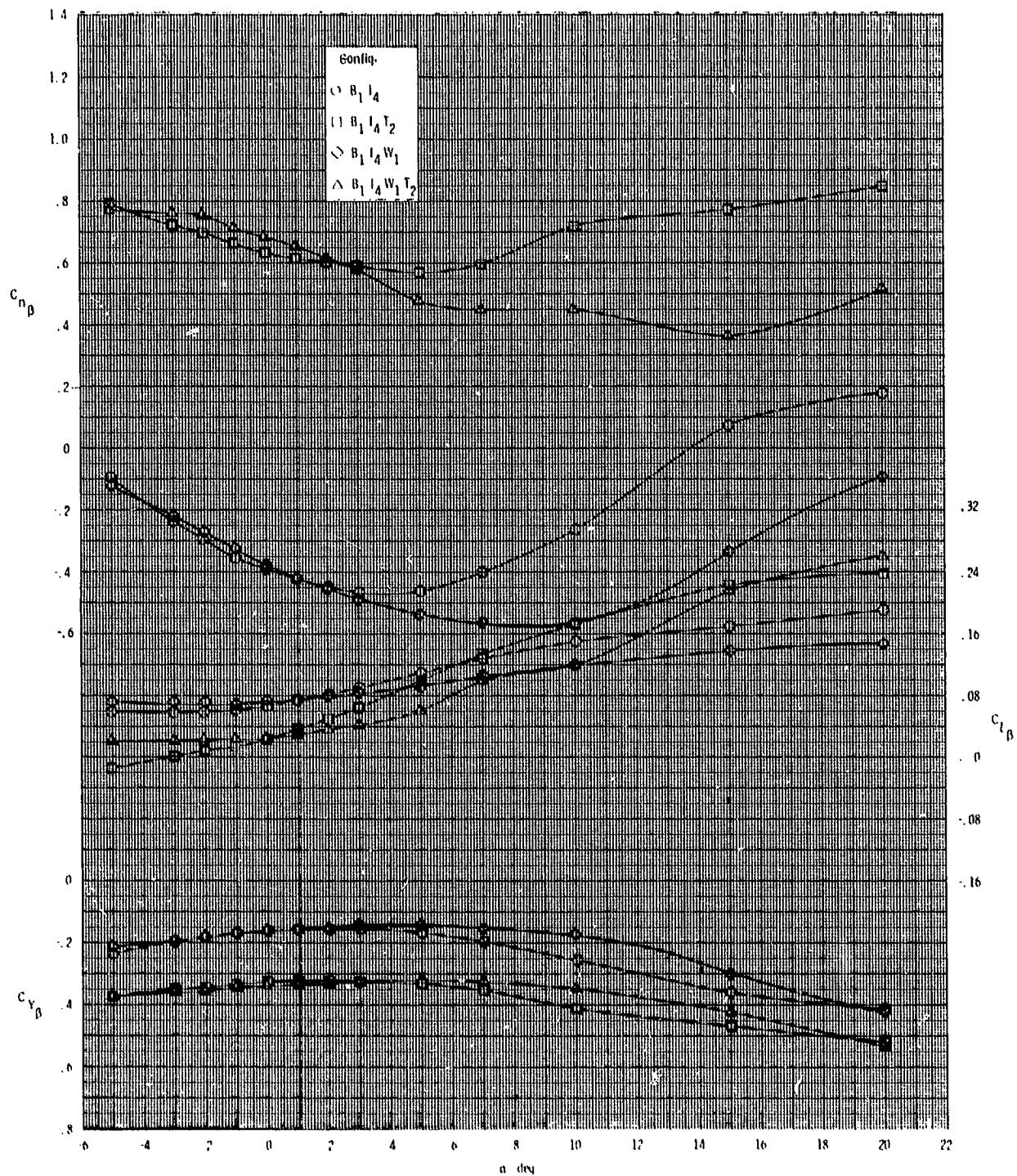
ORIGINAL PAGE IS
OF POOR QUALITY



(a) $M = 2.50$.

Figure 13.- Effect of various model components on lateral-directional stability for axisymmetric inlets with T_2 .

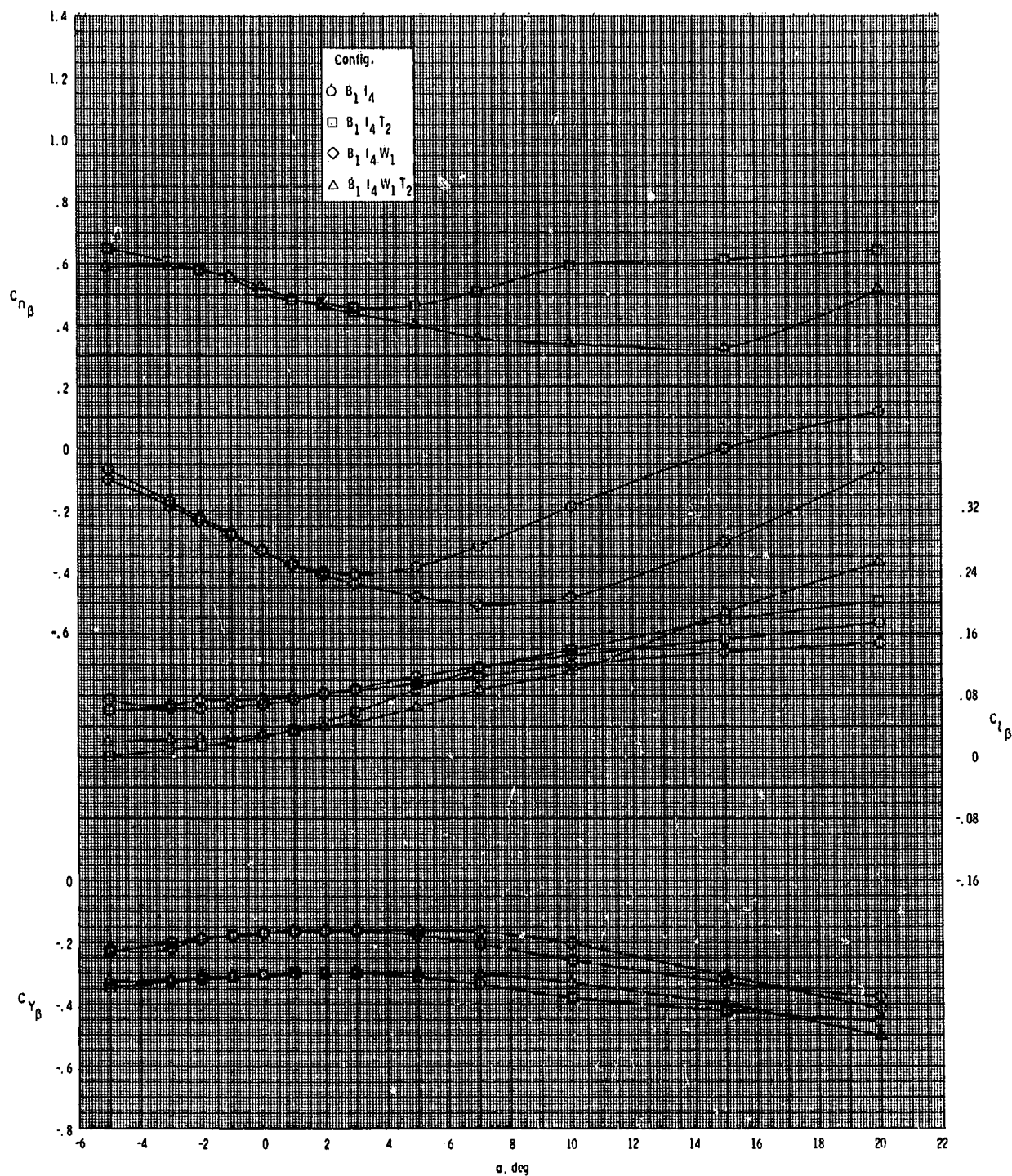
ORIGINAL PAGE IS
OF POOR QUALITY



(b) $M = 2.95$.

Figure 13.- Continued.

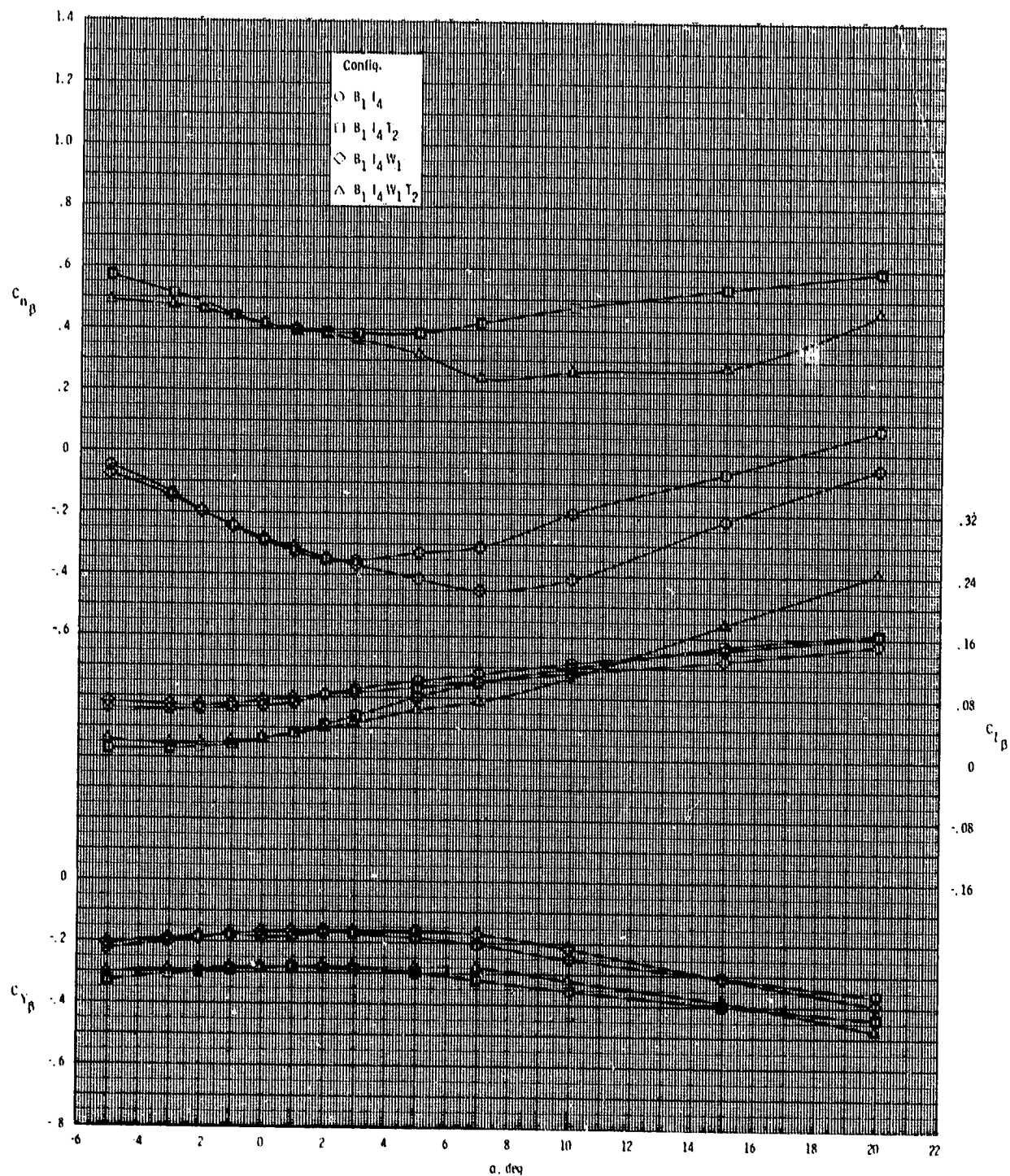
ORIGINAL PAGE IS
OF POOR QUALITY



(c) $M = 3.50$.

Figure 13.- Continued.

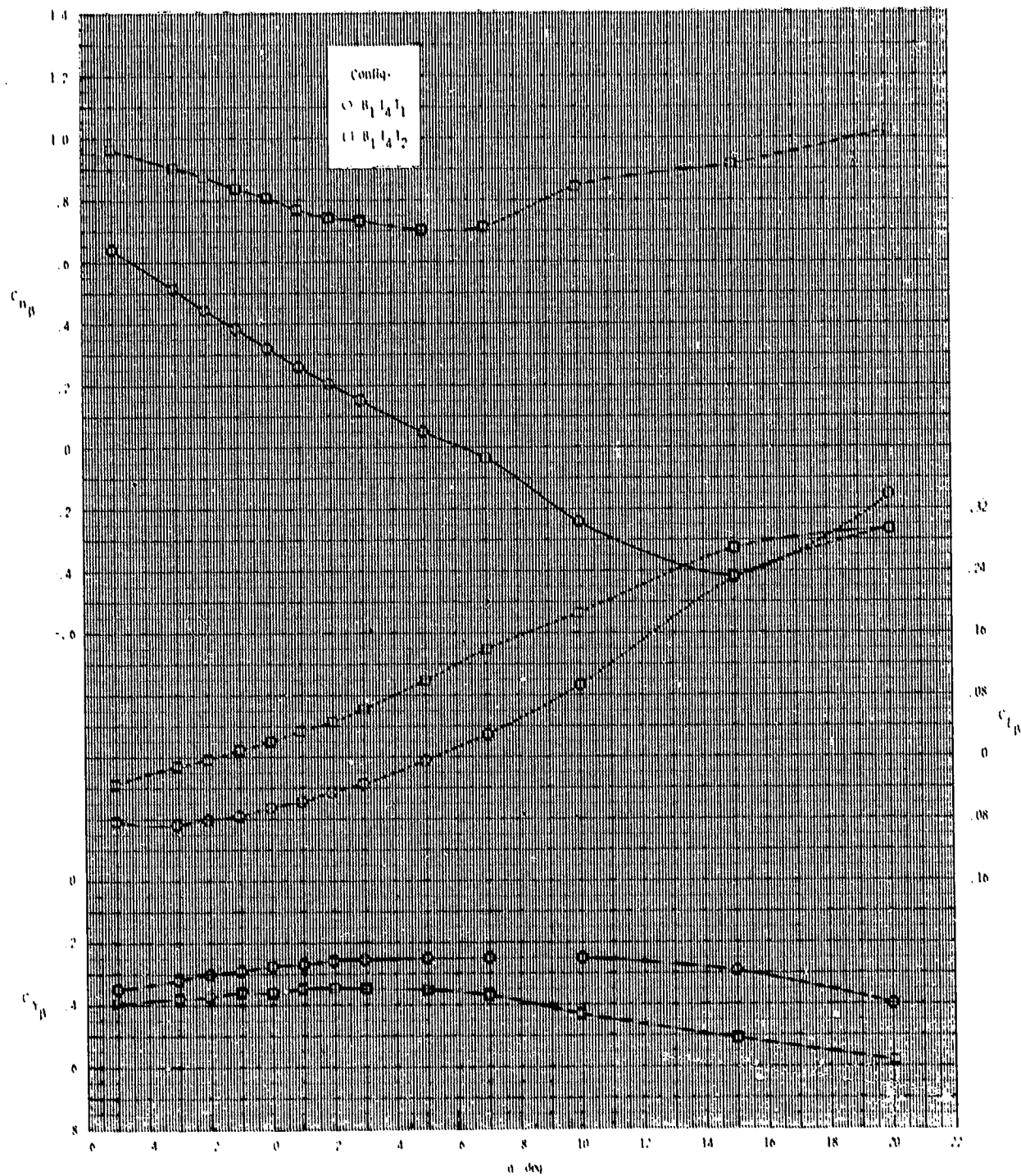
ORIGINAL PAGE IS
OF POOR QUALITY



(d) $M = 3.95$.

Figure 13.- Concluded.

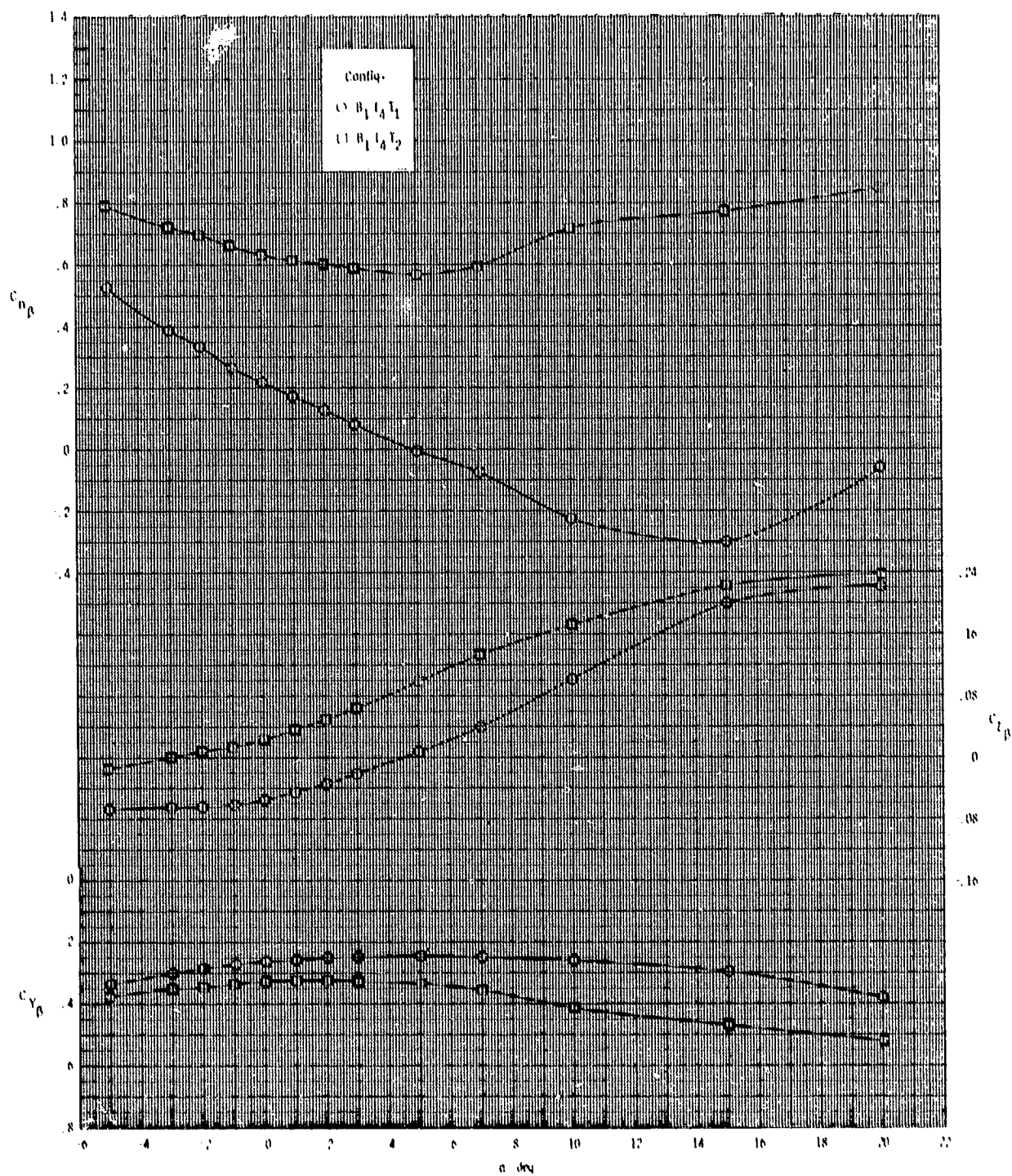
ORIGINAL PAGE IS
OF POOR QUALITY



(a) $M = 2.50$.

Figure 14.- Effect of tail configuration on lateral-directional stability for axisymmetric inlet with wing off.

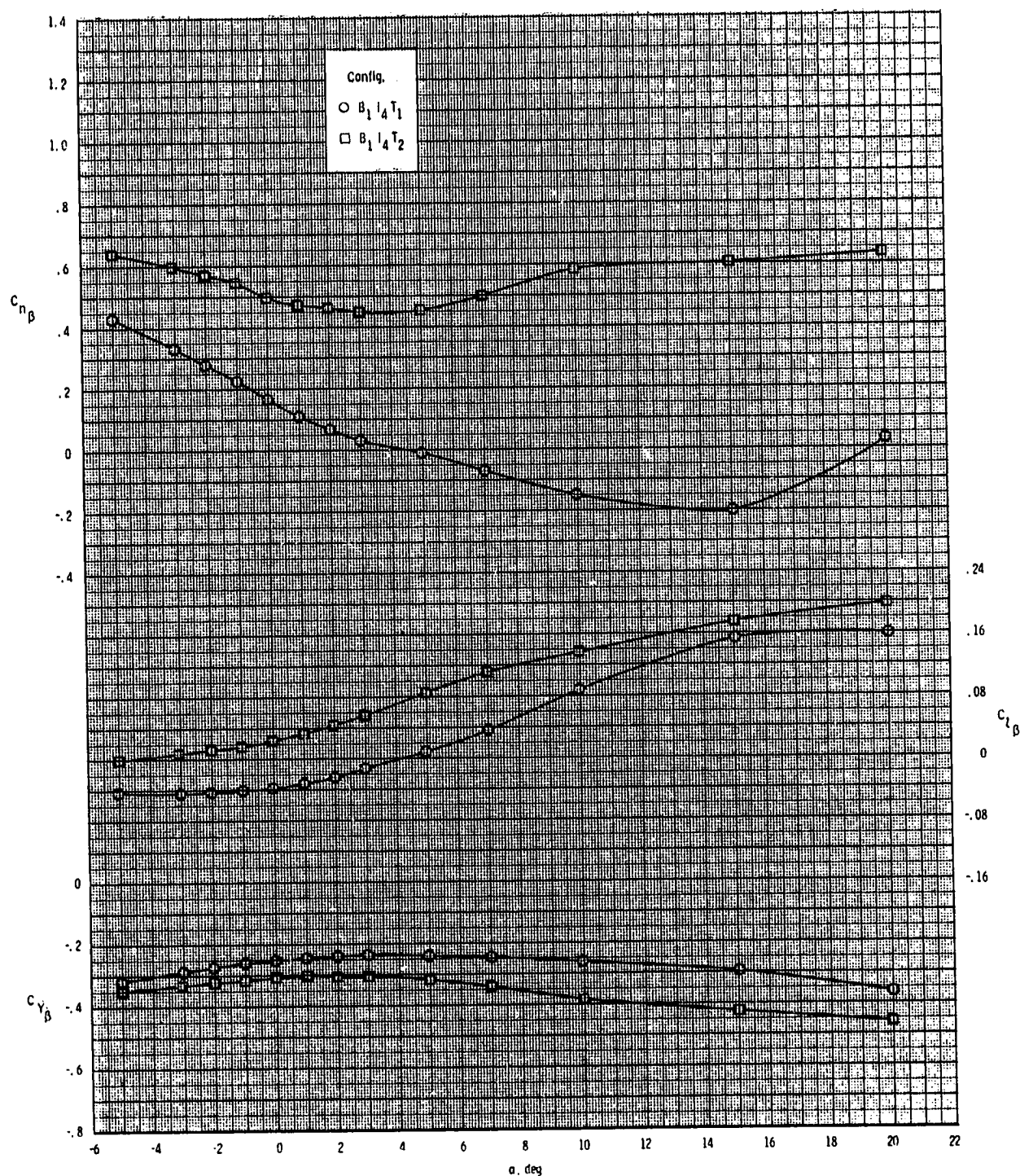
ORIGINAL PAGE IS
OF POOR QUALITY



(b) $M = 2.95$.

Figure 14.- Continued.

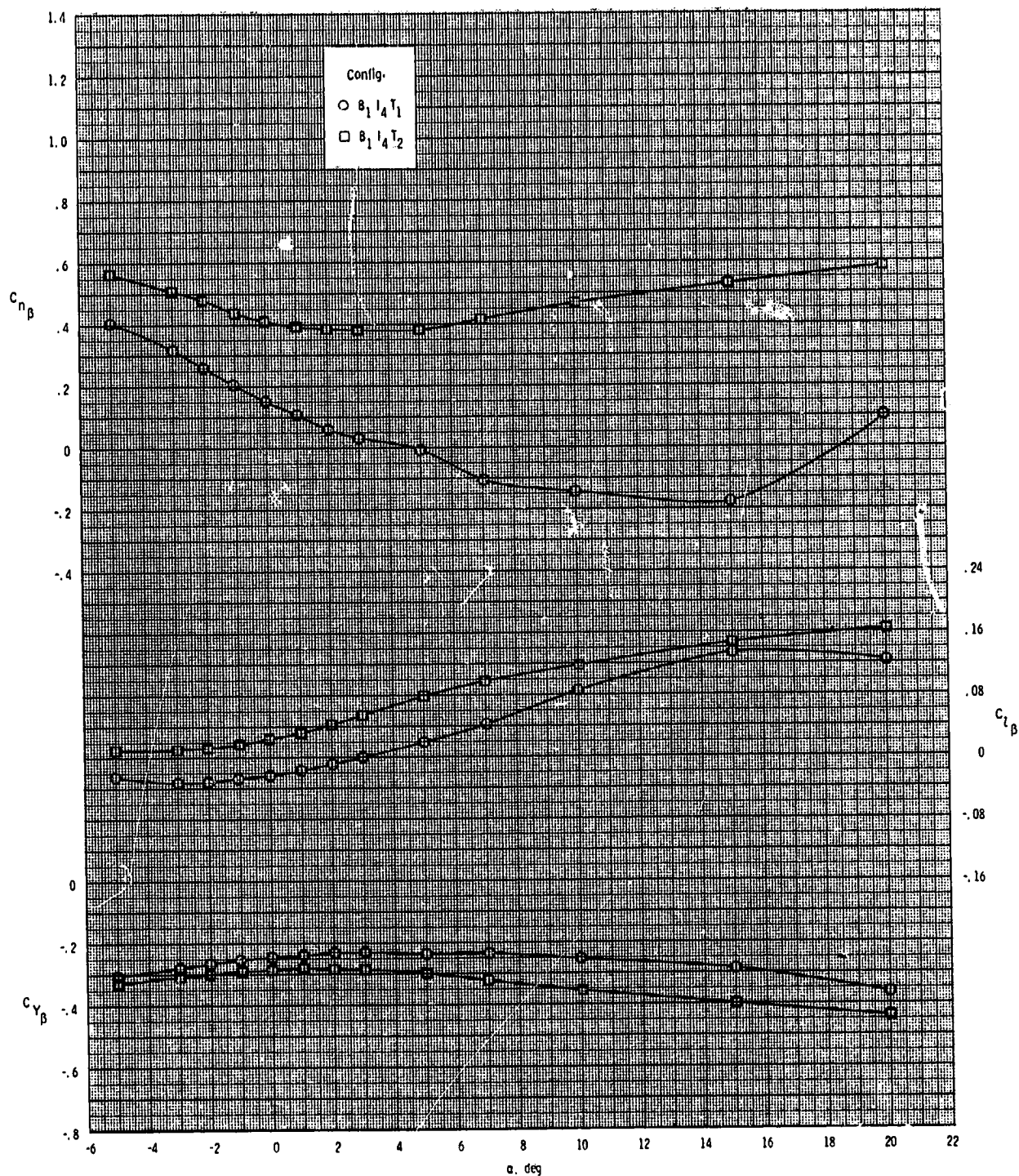
ORIGINAL PAGE IS
OF POOR QUALITY



(c) $M = 3.50$.

Figure 14.- Continued.

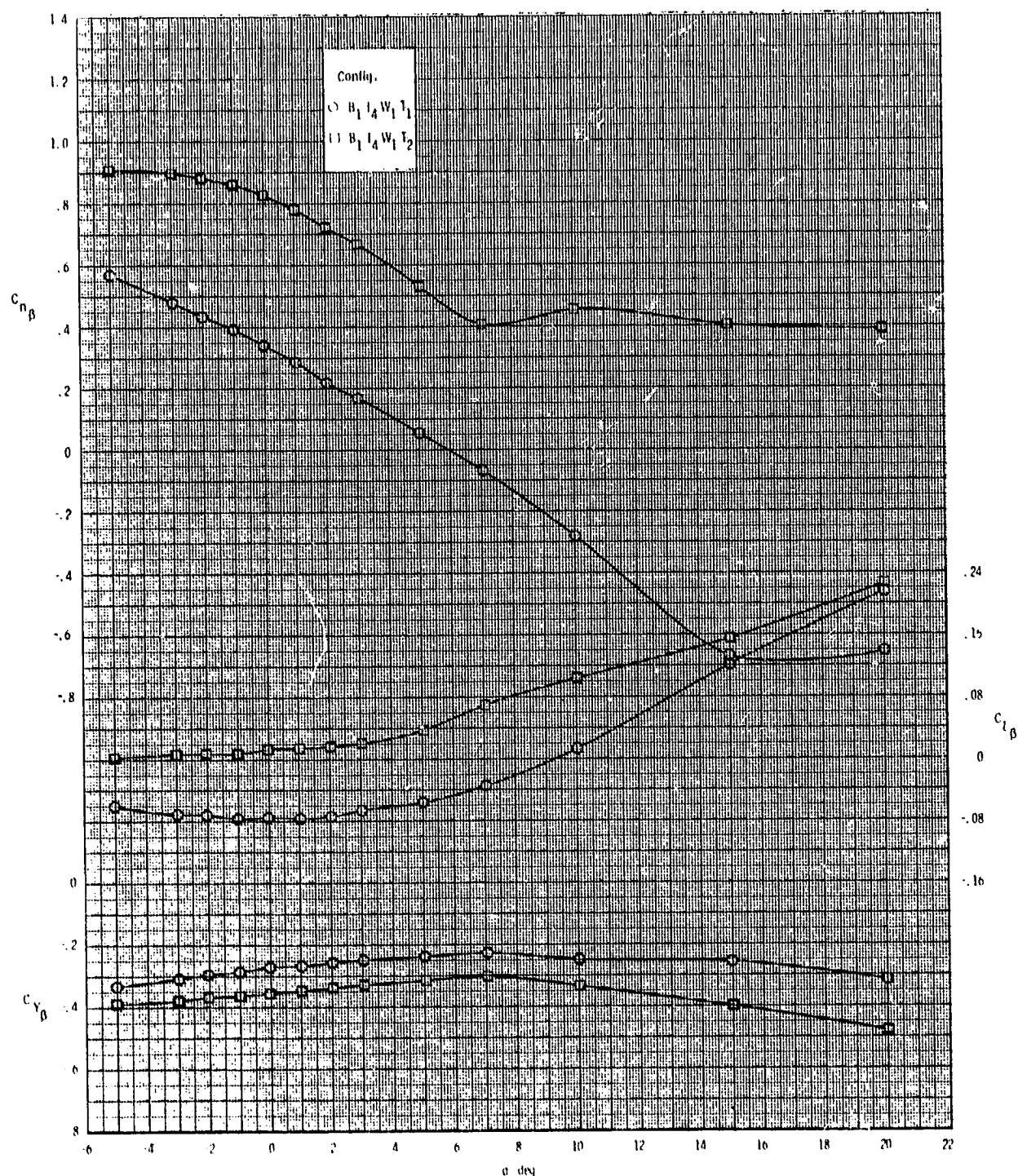
ORIGINAL PAGE IS
OF POOR QUALITY



(d) $M = 3.95$.

Figure 14.- Concluded.

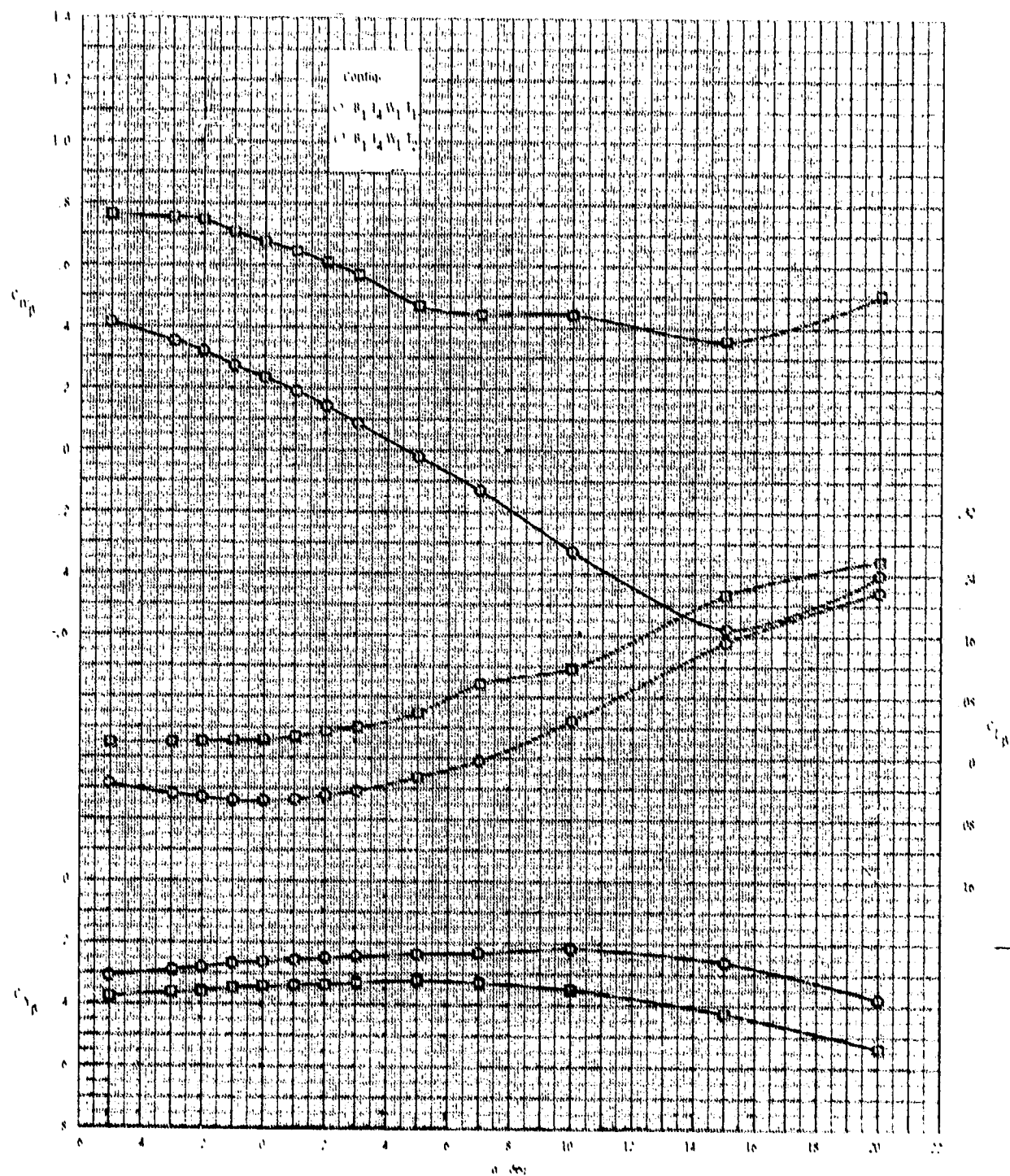
ORIGINAL PAGE IS
OF POOR QUALITY



(a) $M = 2.50$.

Figure 15.- Effect of tail configuration on lateral-directional stability for axisymmetric inlet with wing on.

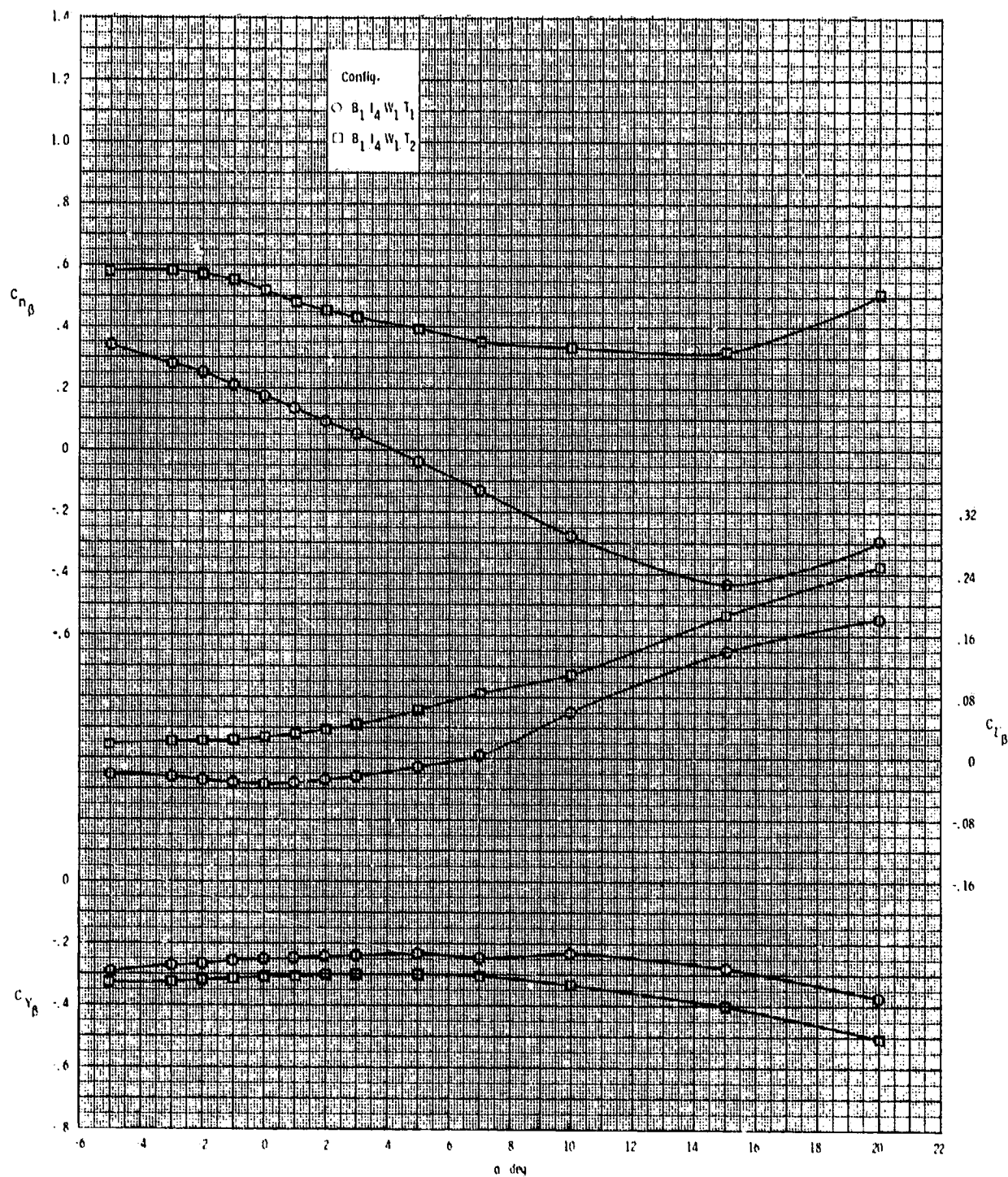
ORIGINAL PAGE IS
OF POOR QUALITY



(b) $M = 2.95$.

Figure 15.- Continued.

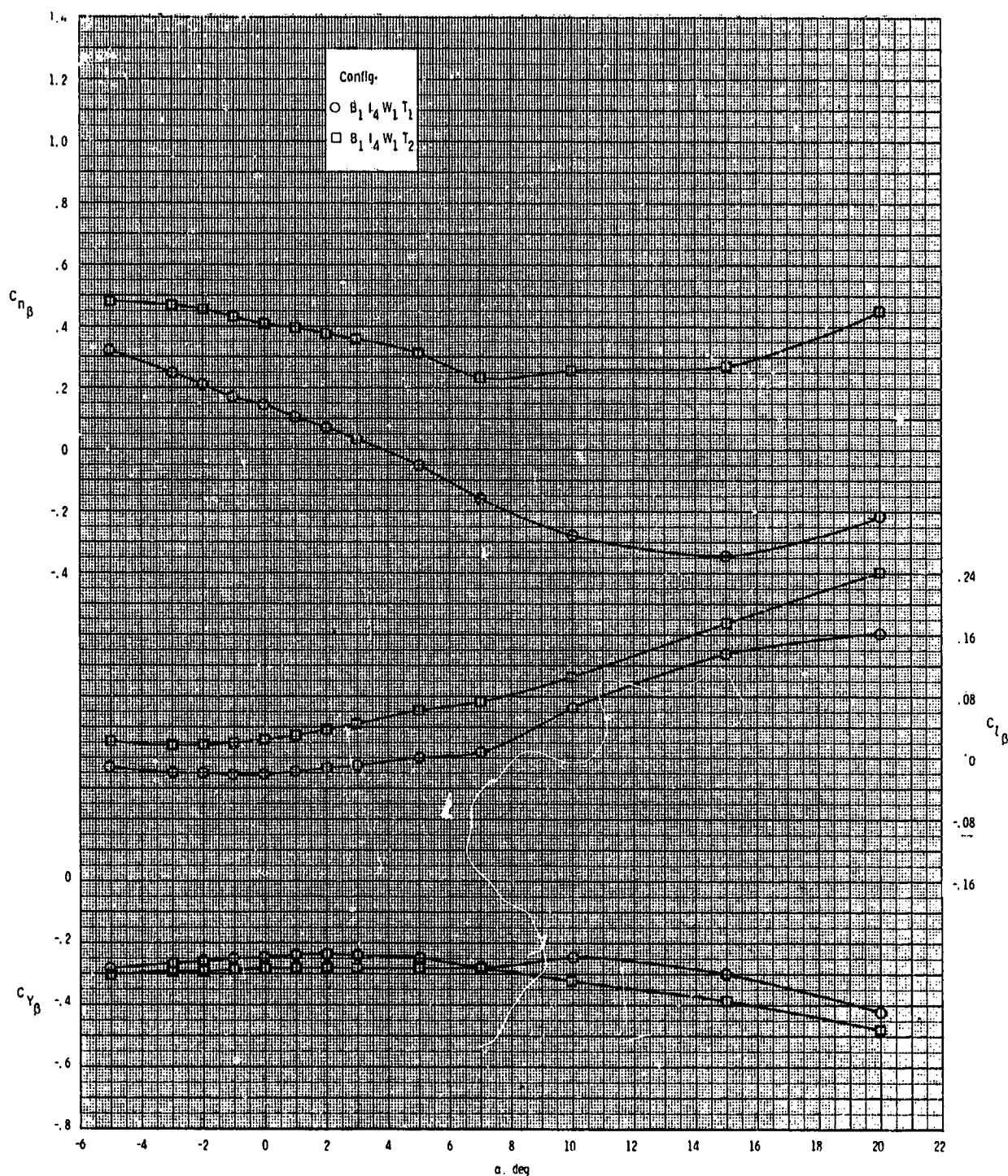
ORIGINAL PAGE IS
OF POOR QUALITY



(c) $M = 3.50$.

Figure 15.- Continued.

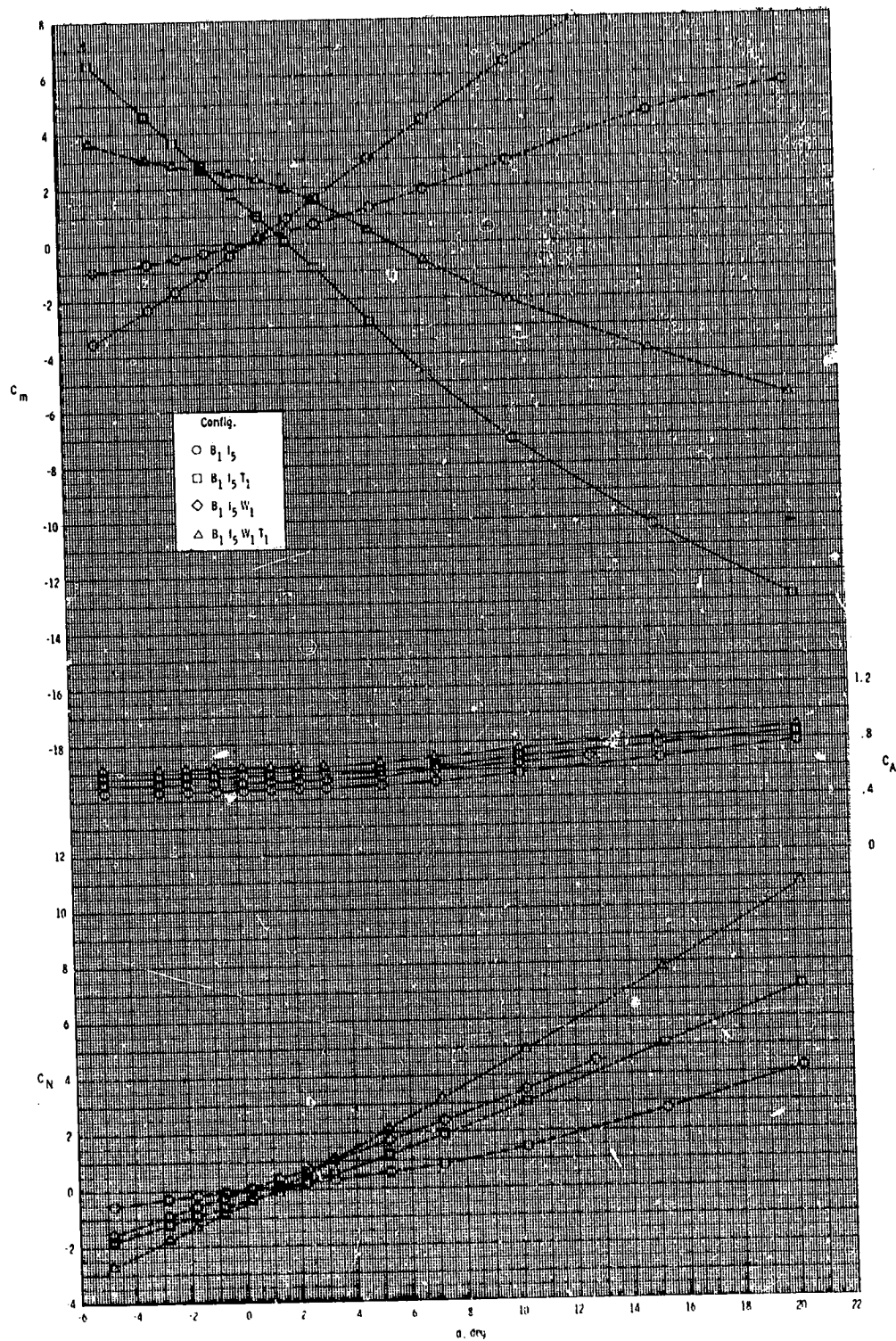
ORIGINAL PAGE IS
OF POOR QUALITY



(d) $M = 3.95$.

Figure 15.- Concluded.

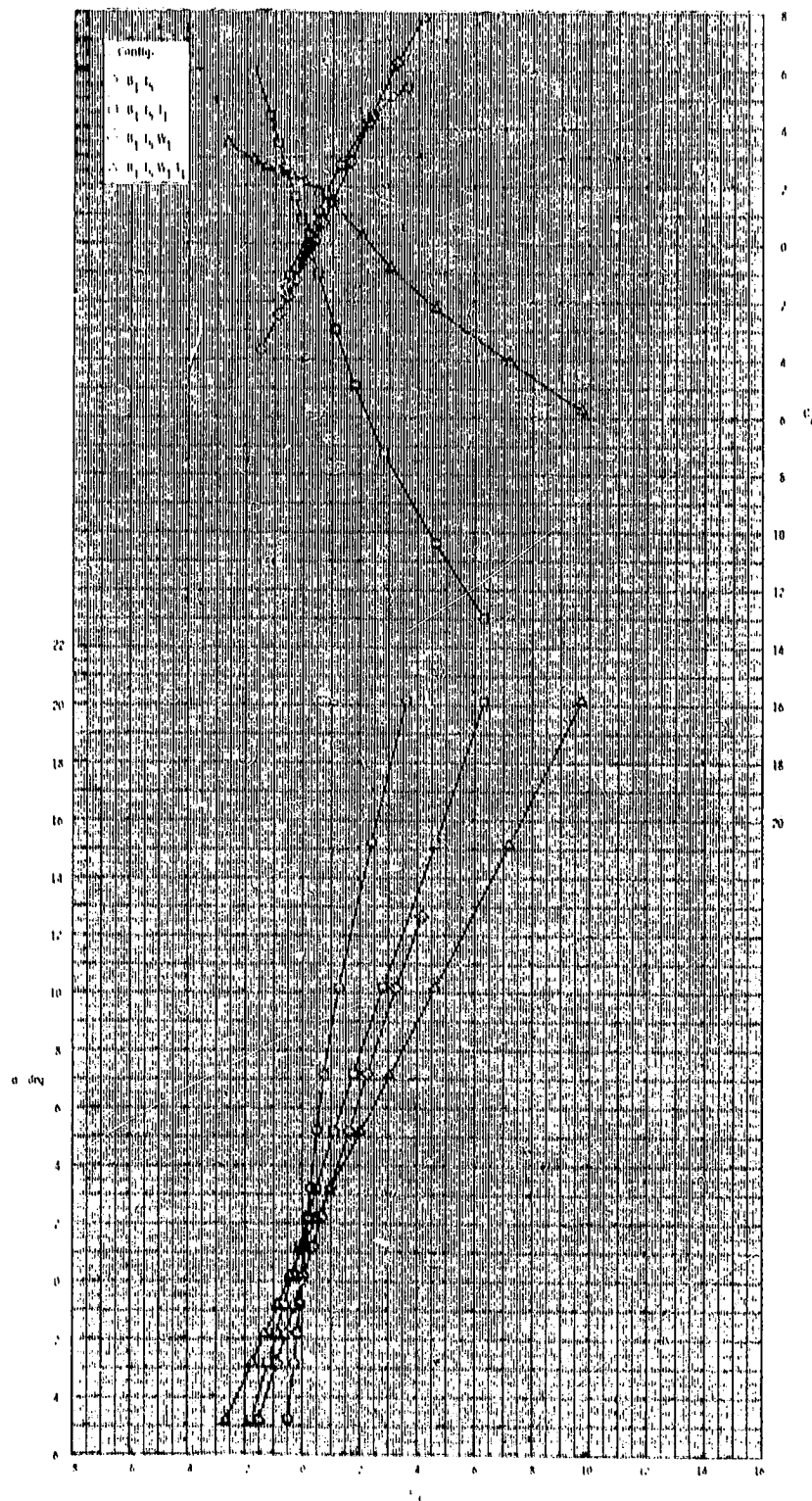
ORIGINAL PAGE IS
OF POOR QUALITY



(a) $M = 2.50$.

Figure 16.- Effect of various model components on longitudinal aerodynamic characteristics for 2-D inlet with T_1 .

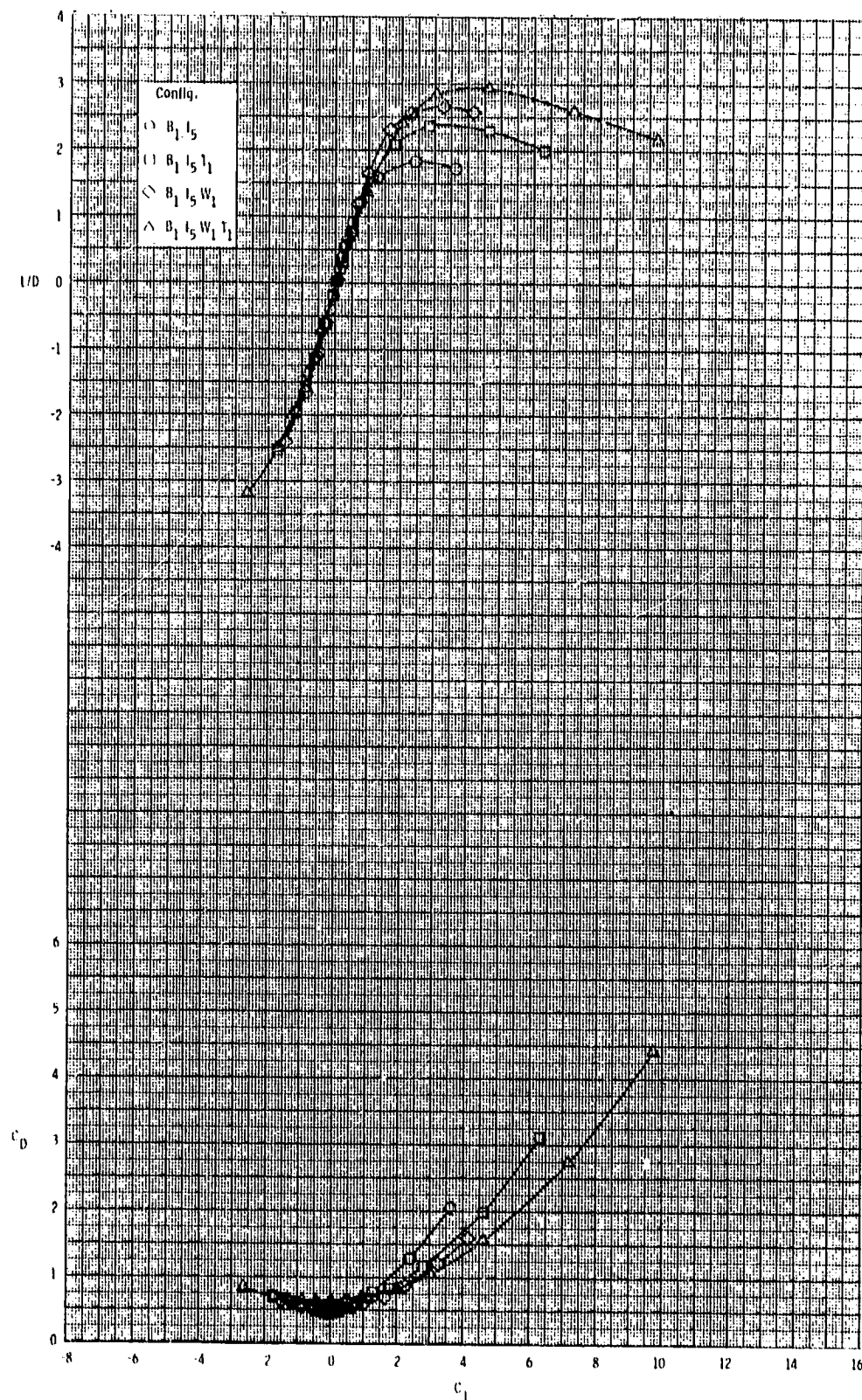
ORIGINAL PAGE IS
OF POOR QUALITY



(a) Continued.

Figure 16.- Continued.

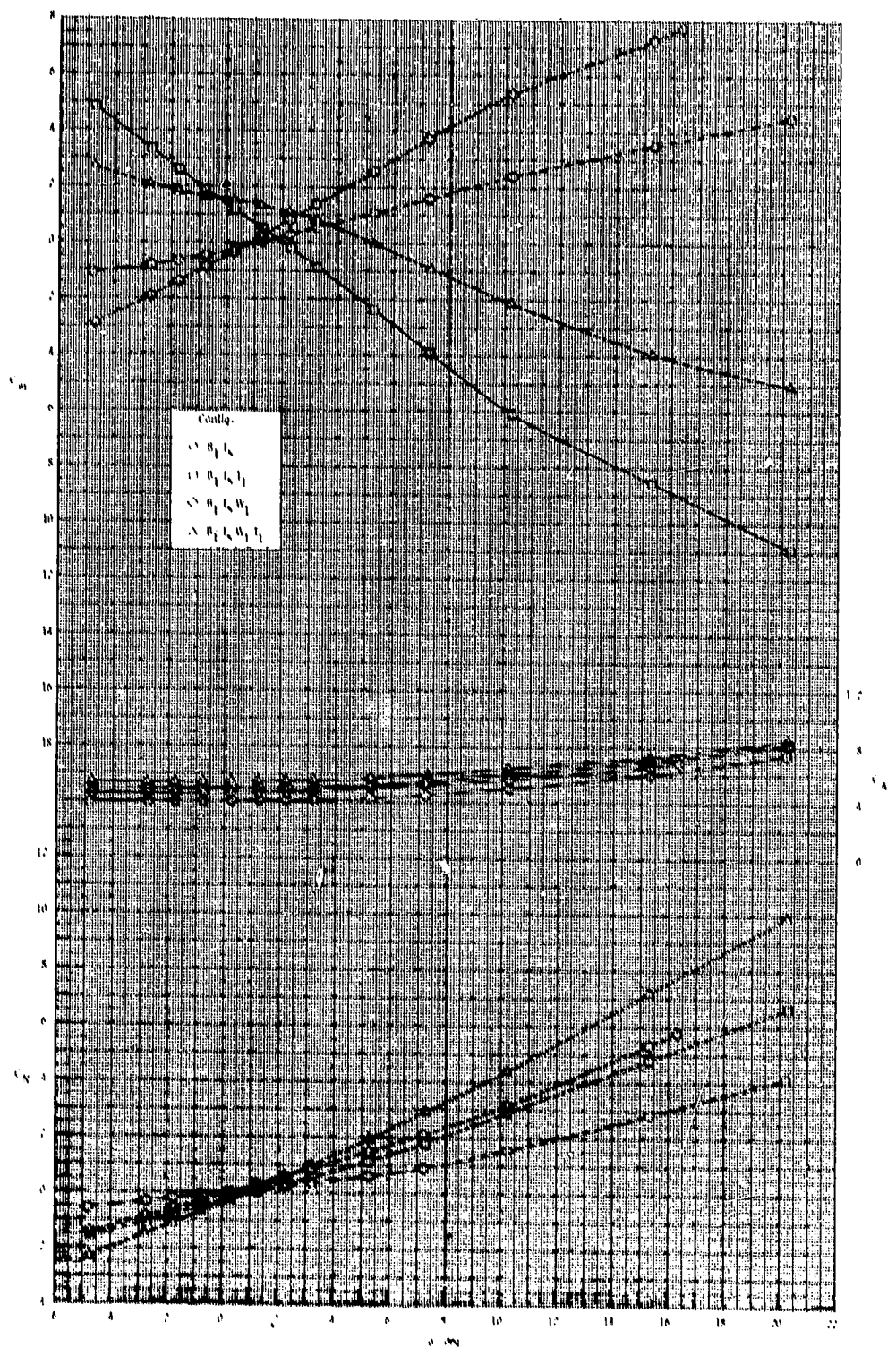
ORIGINAL PAGE IS
OF POOR QUALITY



(a) Concluded.

Figure 16.- Continued.

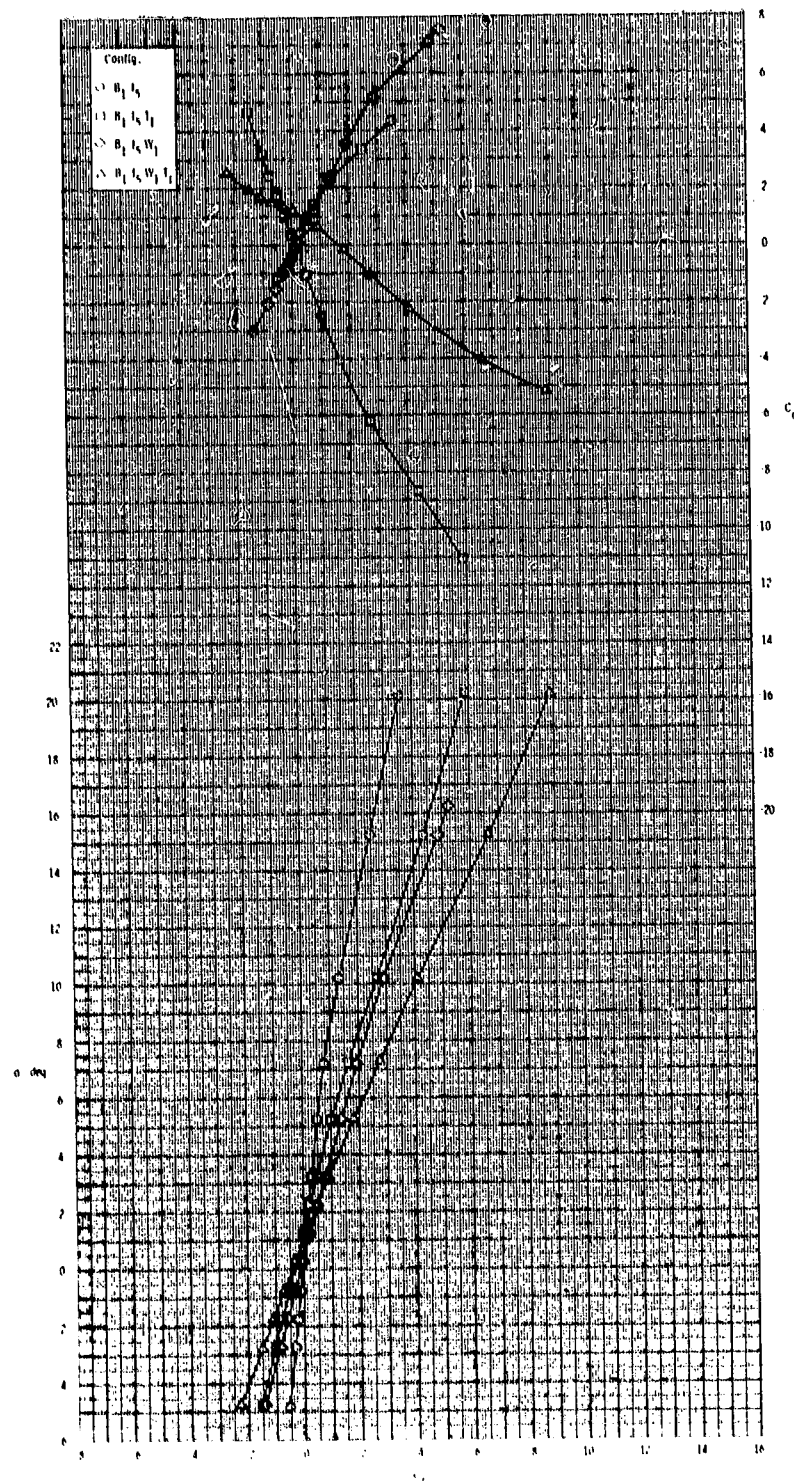
ORIGINAL PAGE IS
OF POOR QUALITY



(b) $M = 2.95$.

Figure 16.- Continued.

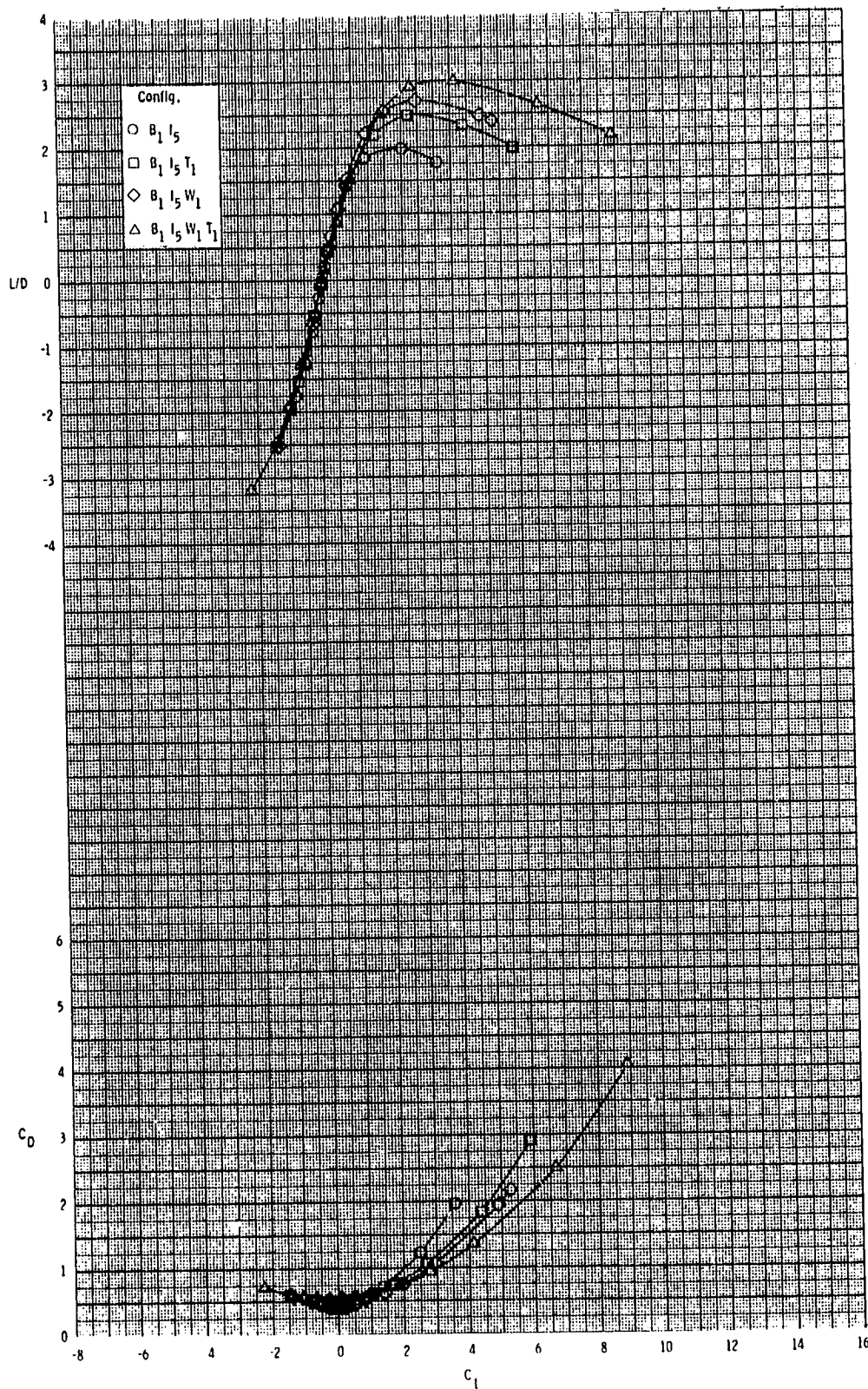
ORIGINAL PAGE IS
OF POOR QUALITY



(b) Continued.

Figure 16.- Continued.

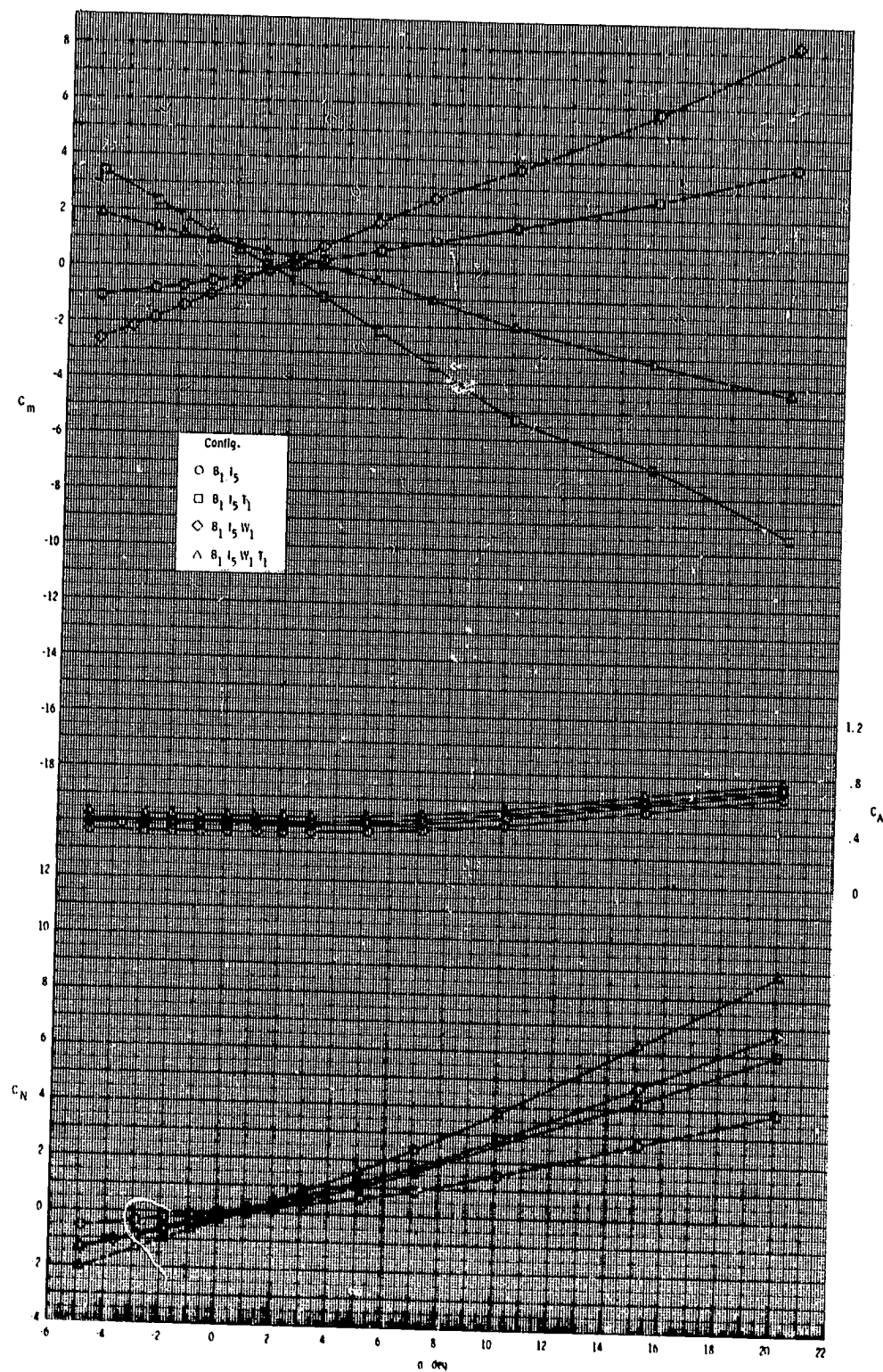
ORIGINAL RESULTS
OF POOR QUALITY



(b) Concluded.

Figure 16.- Continued.

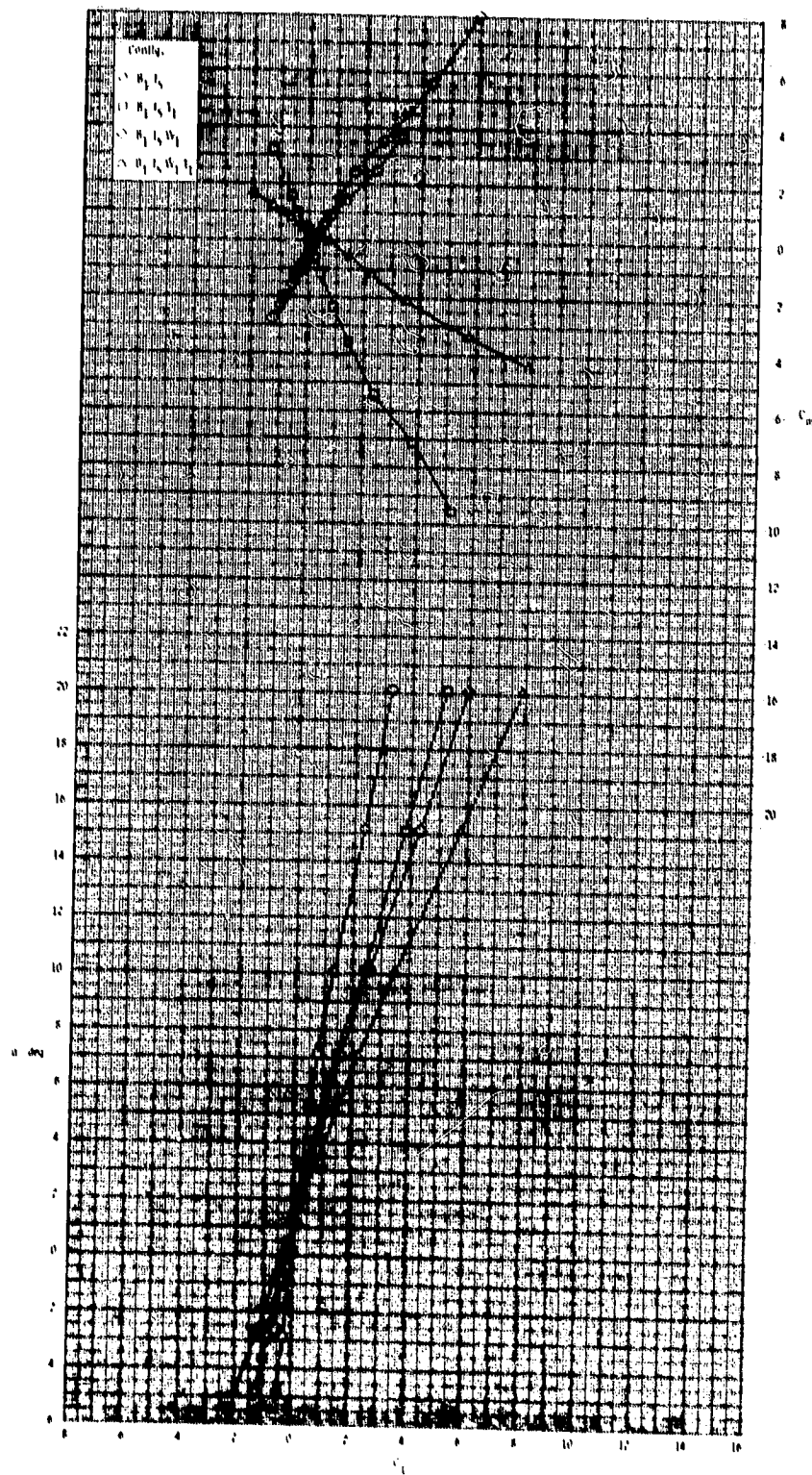
ORIGINAL PAGE IS
OF POOR QUALITY



(c) $M = 3.50$.

Figure 16.- Continued.

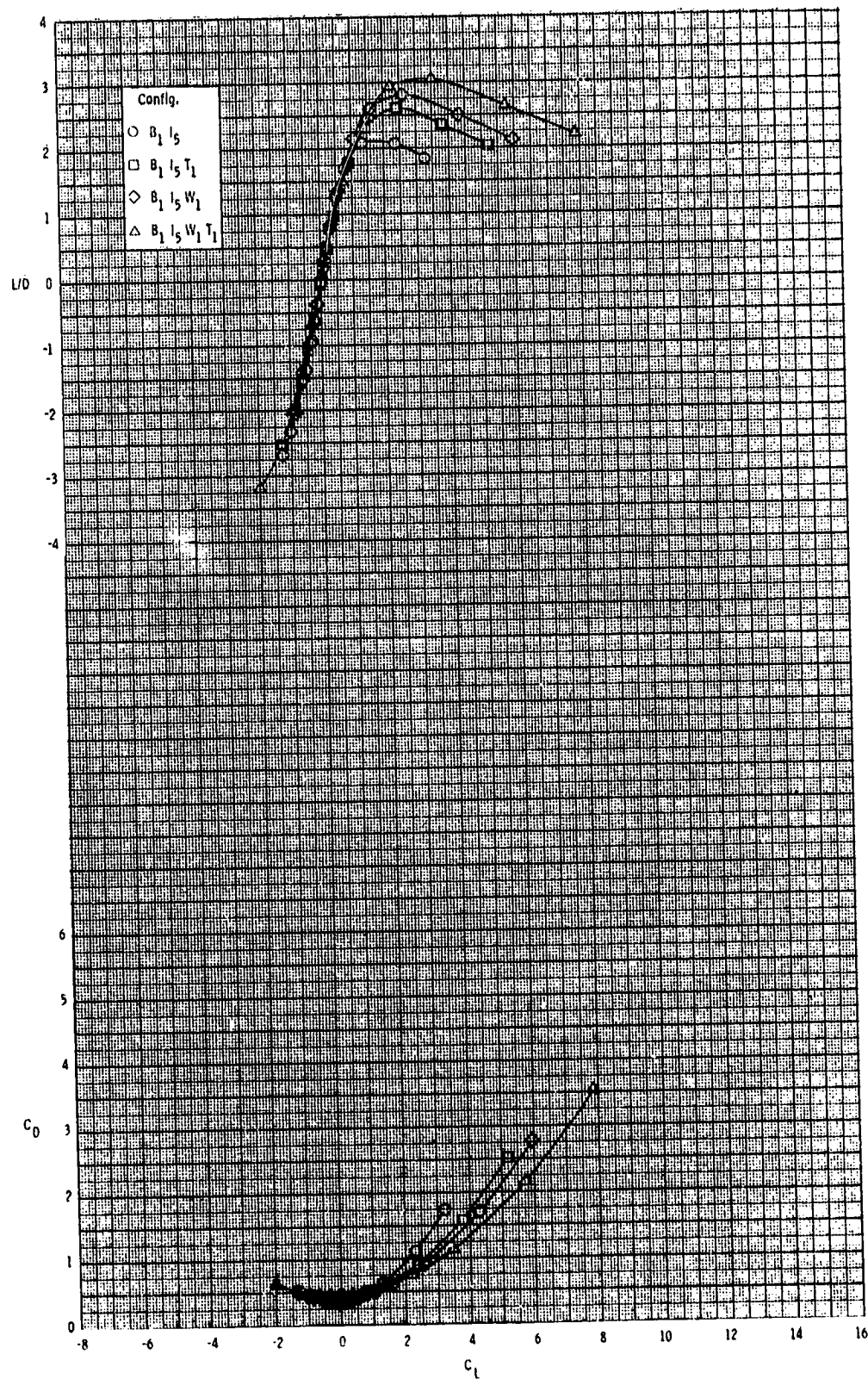
ORIGINAL PAGE IS
OF POOR QUALITY



(c) Continued.

Figure 16.- Continued.

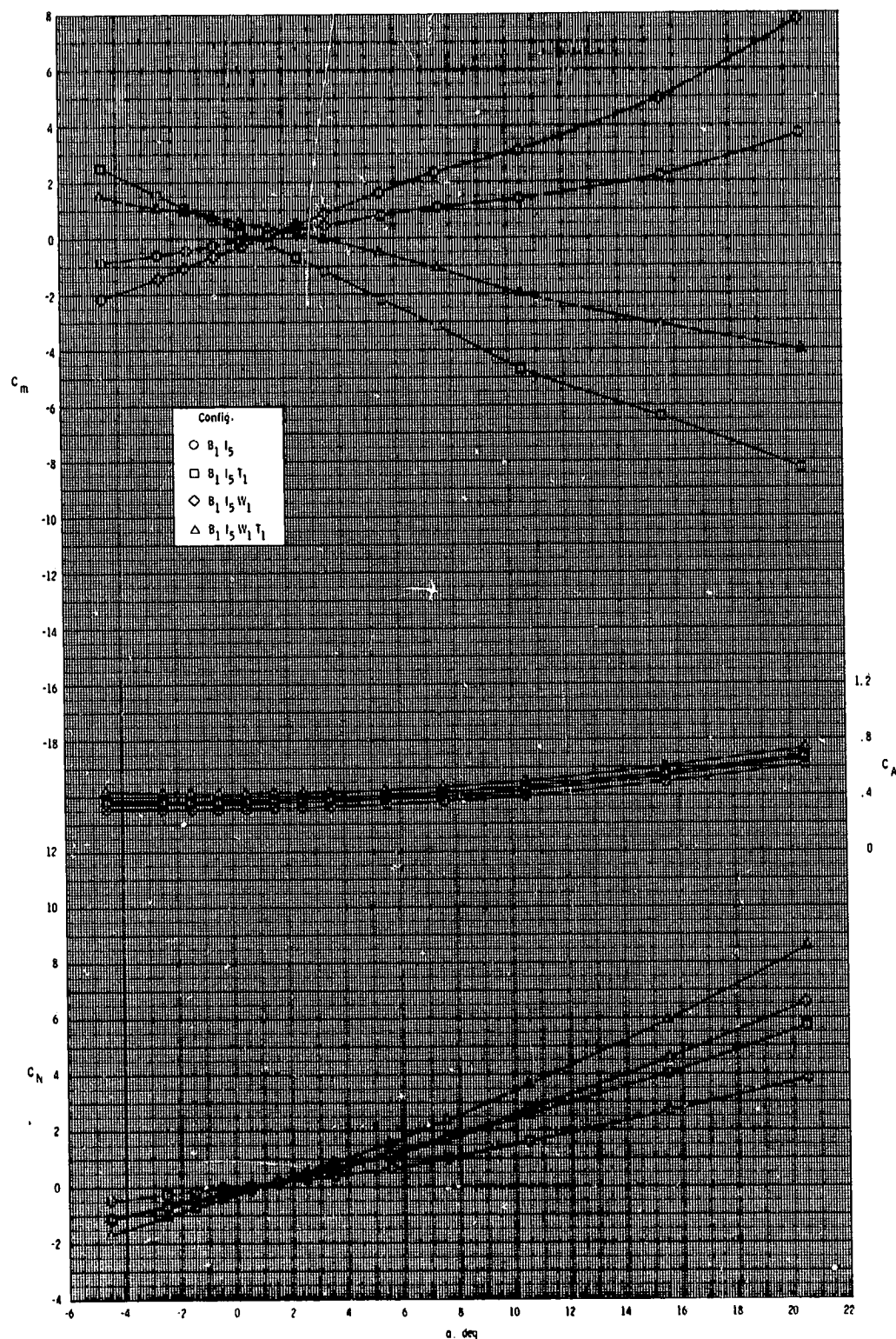
ORIGINAL PAGE IS
OF POOR QUALITY



(c) Concluded.

Figure 16.- Continued.

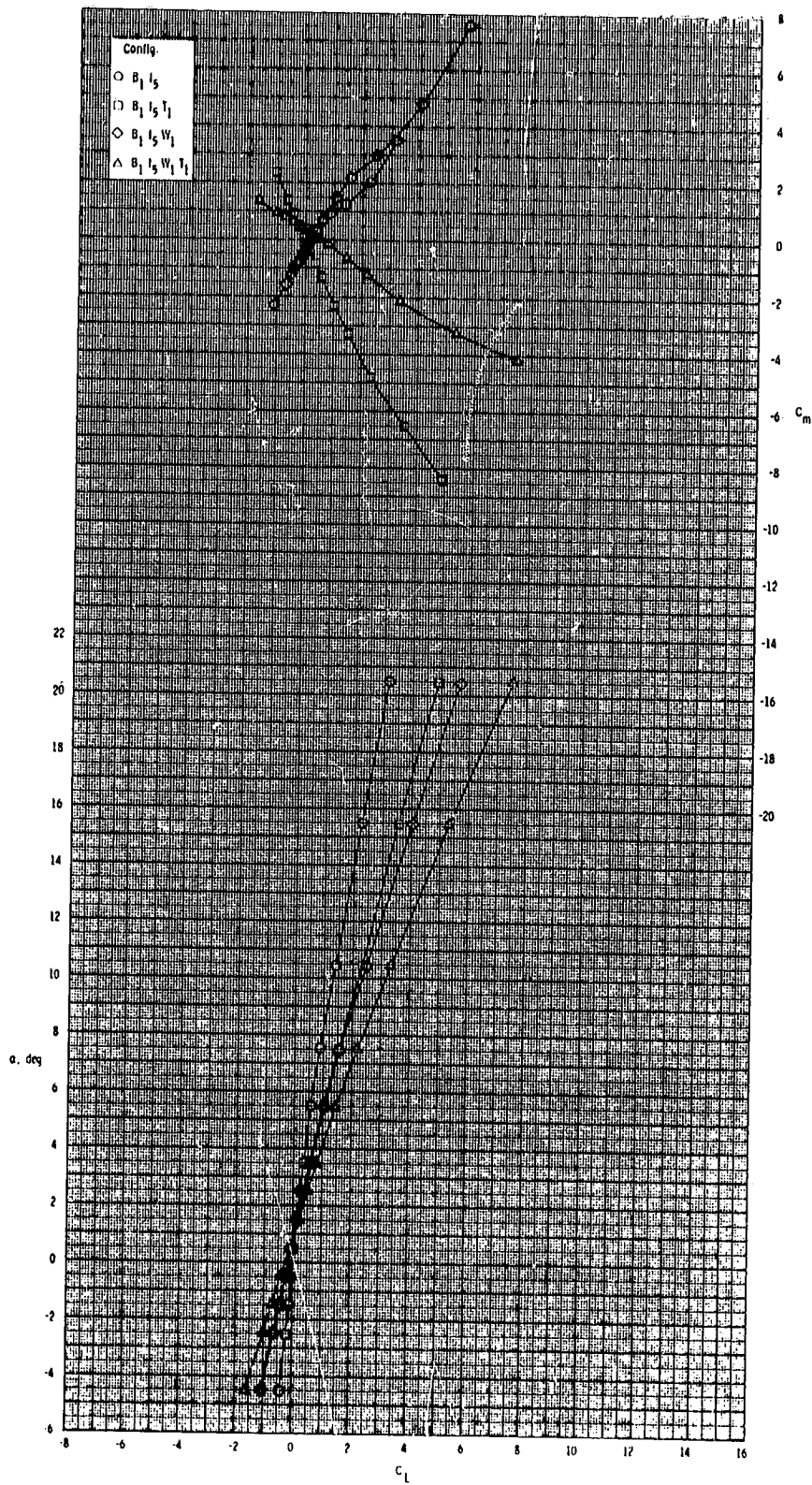
ORIGINAL PAGE 13
OF POOR QUALITY



(d) $M = 3.95$.

Figure 16.- Continued.

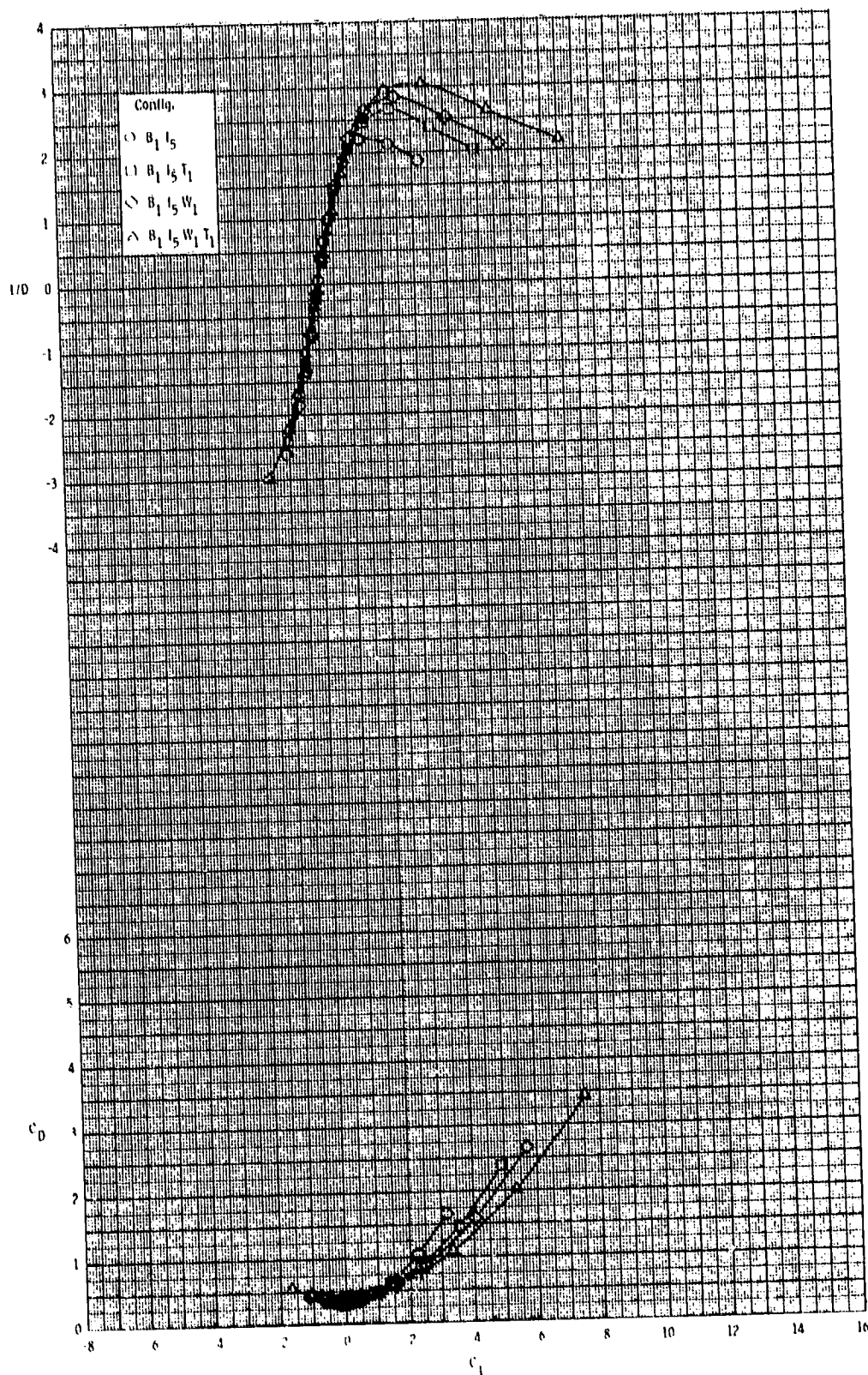
ORIGINAL PAGE IS
OF POOR QUALITY



(d) Continued.

Figure 16.- Continued.

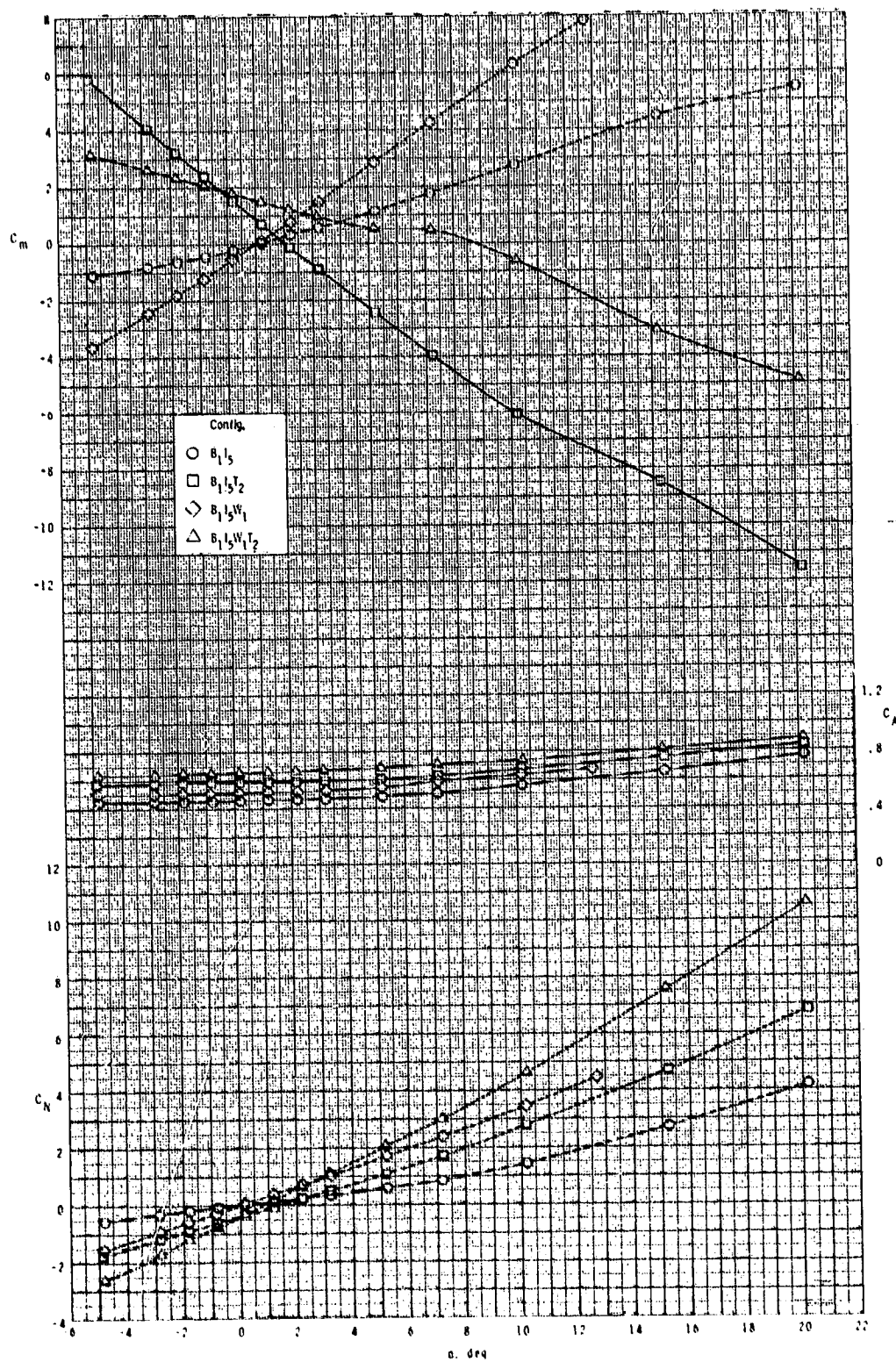
ORIGINAL PAGE IS
OF POOR QUALITY



(d) Concluded.

Figure 16.- Concluded.

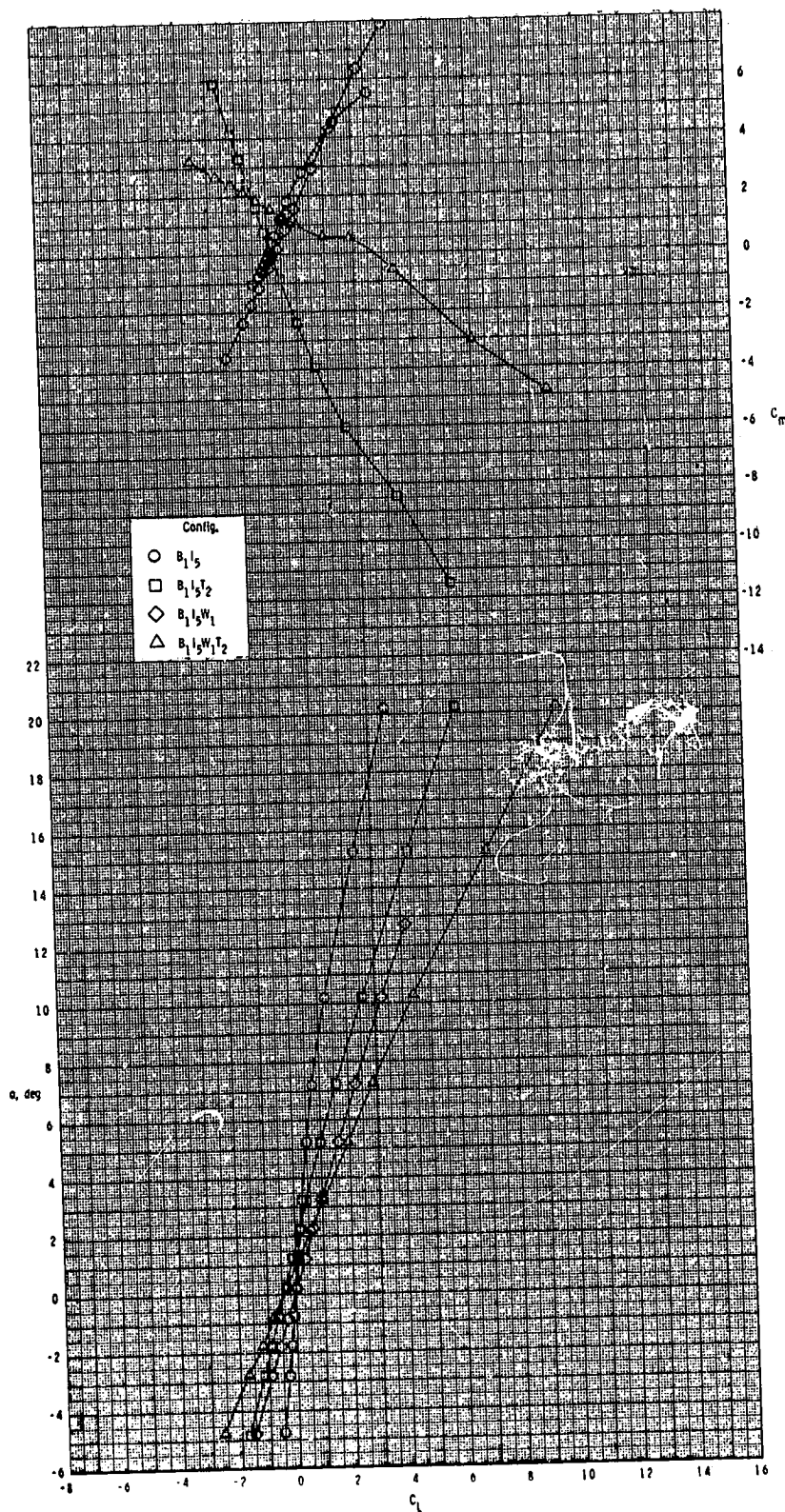
ORIGINAL PAGE IS
OF POOR QUALITY



(a) $M = 2.50$.

Figure 17.- Effect of various model components on longitudinal aerodynamic characteristics for 2-D inlet with T_2 .

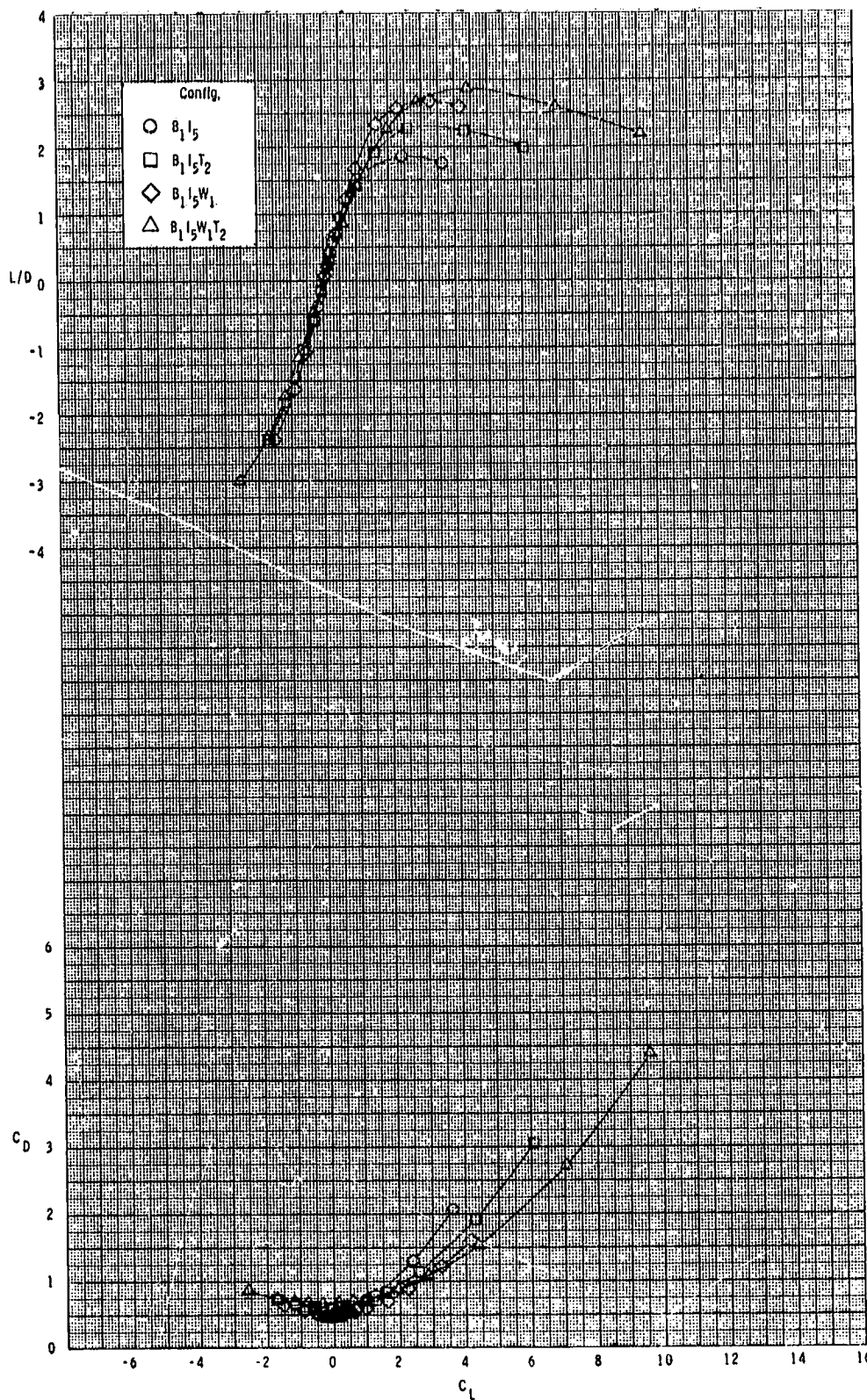
ORIGINAL PAGE IS
OF POOR QUALITY



(a) Continued.

Figure 17.- Continued.

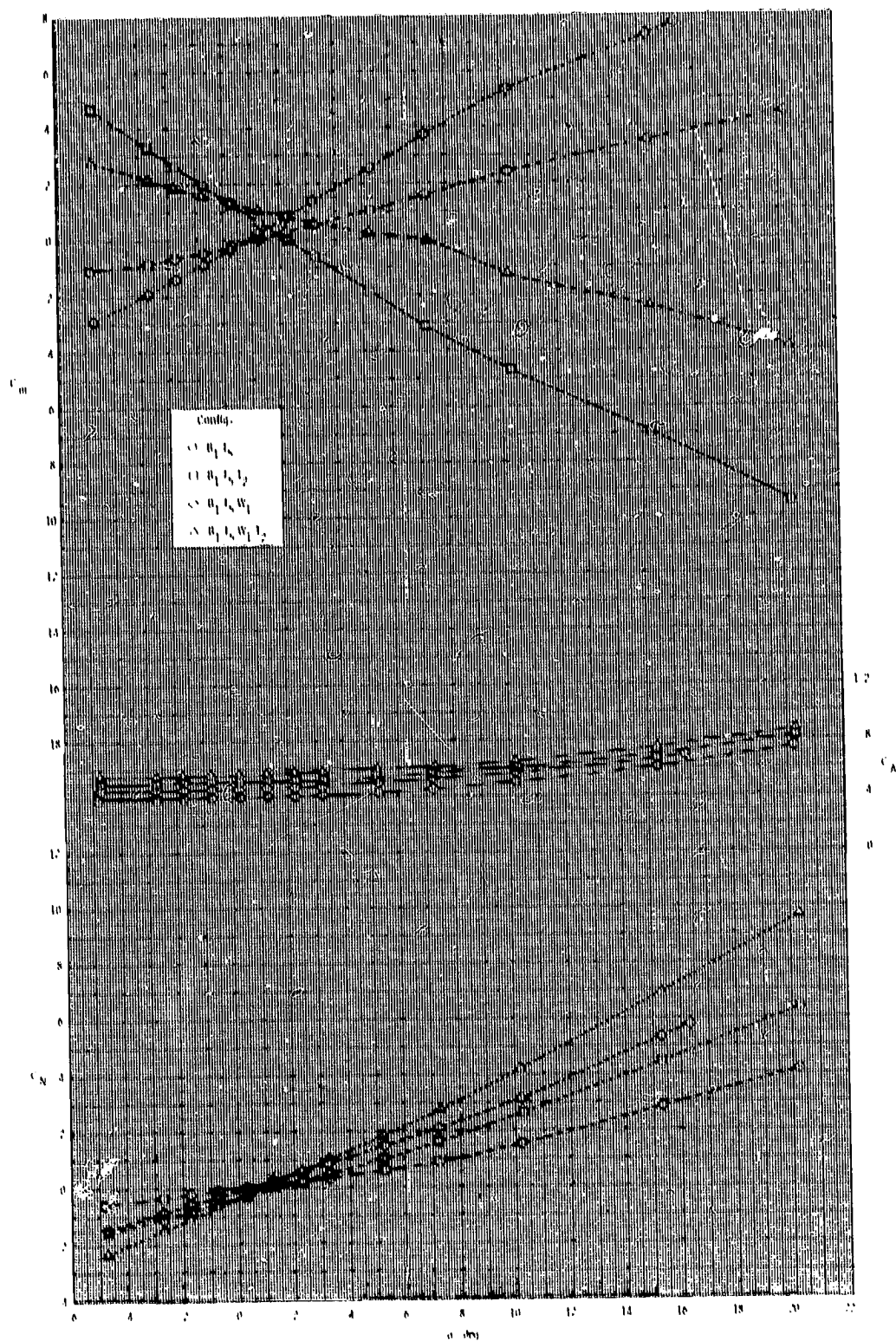
ORIGINAL PAGE IS
OF POOR QUALITY



(a) Concluded.

Figure 17.- Continued.

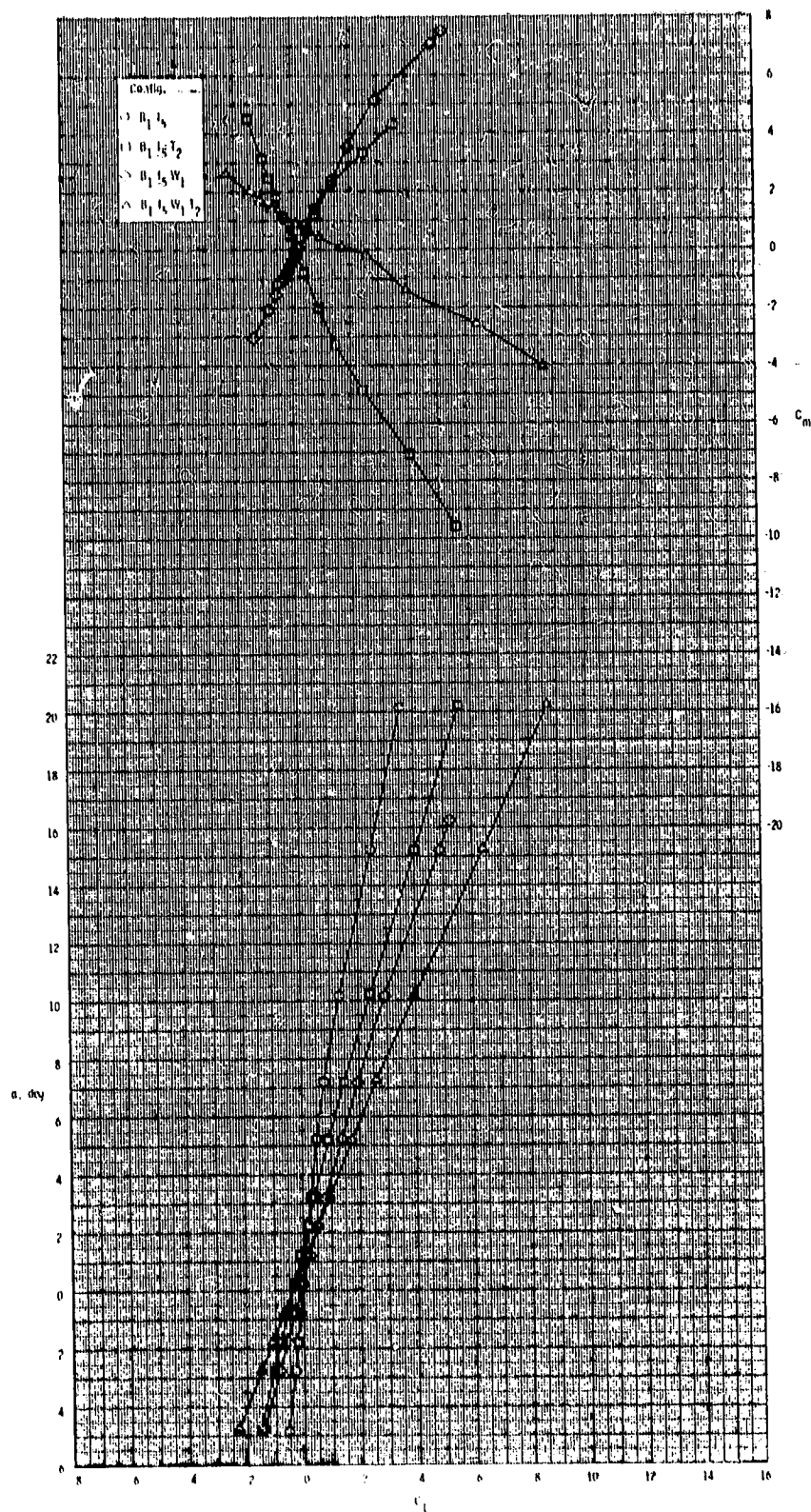
ORIGINAL PAGE 19
OF POOR QUALITY



(b) $M = 2.05$.

Figure 17.- Continued.

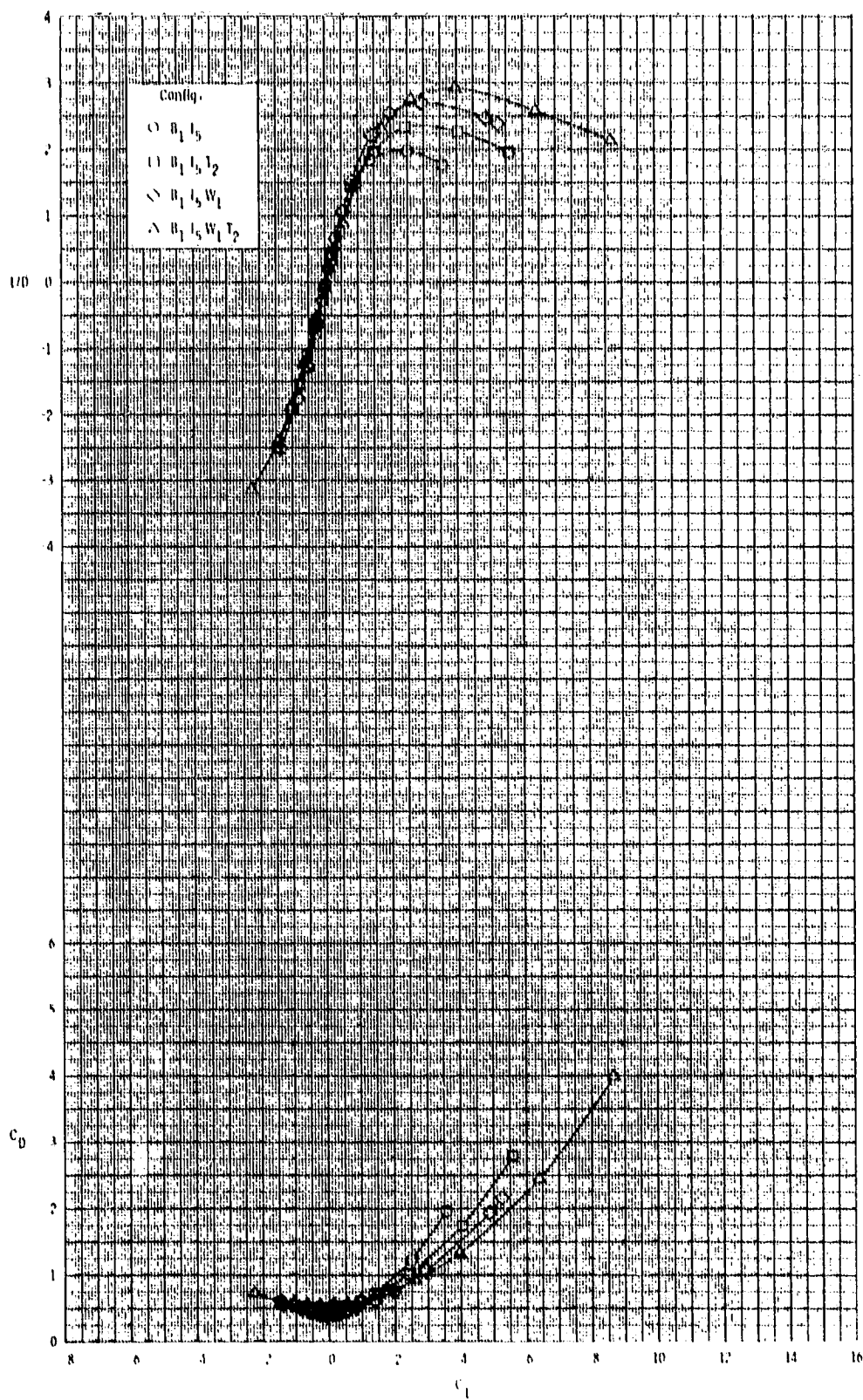
ORIGINAL PAGE IS
OF POOR QUALITY



(b) Continued.

Figure 17.- Continued.

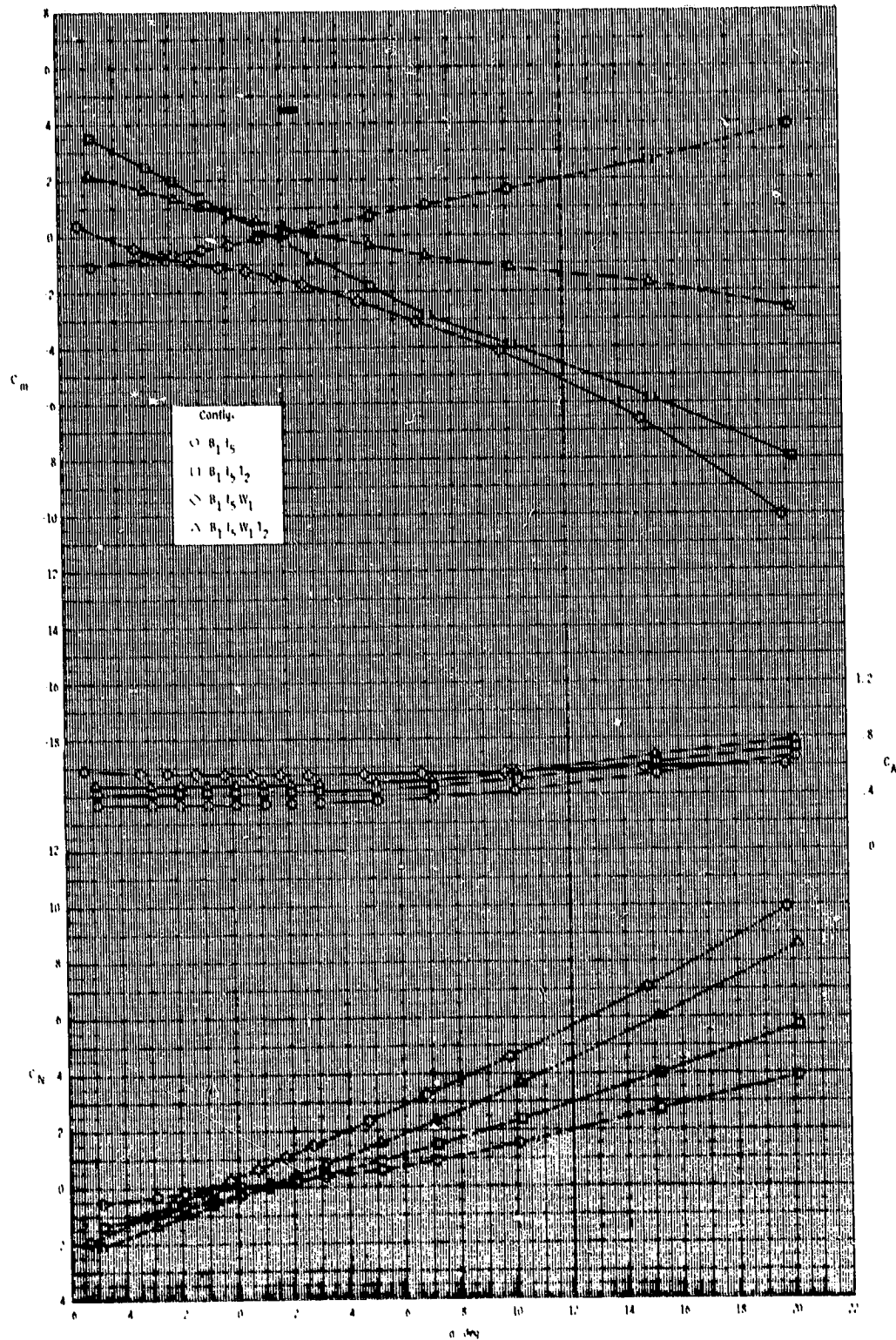
ORIGINAL PAGE IS
OF POOR QUALITY



(b) Concluded.

Figure 17.- Continued.

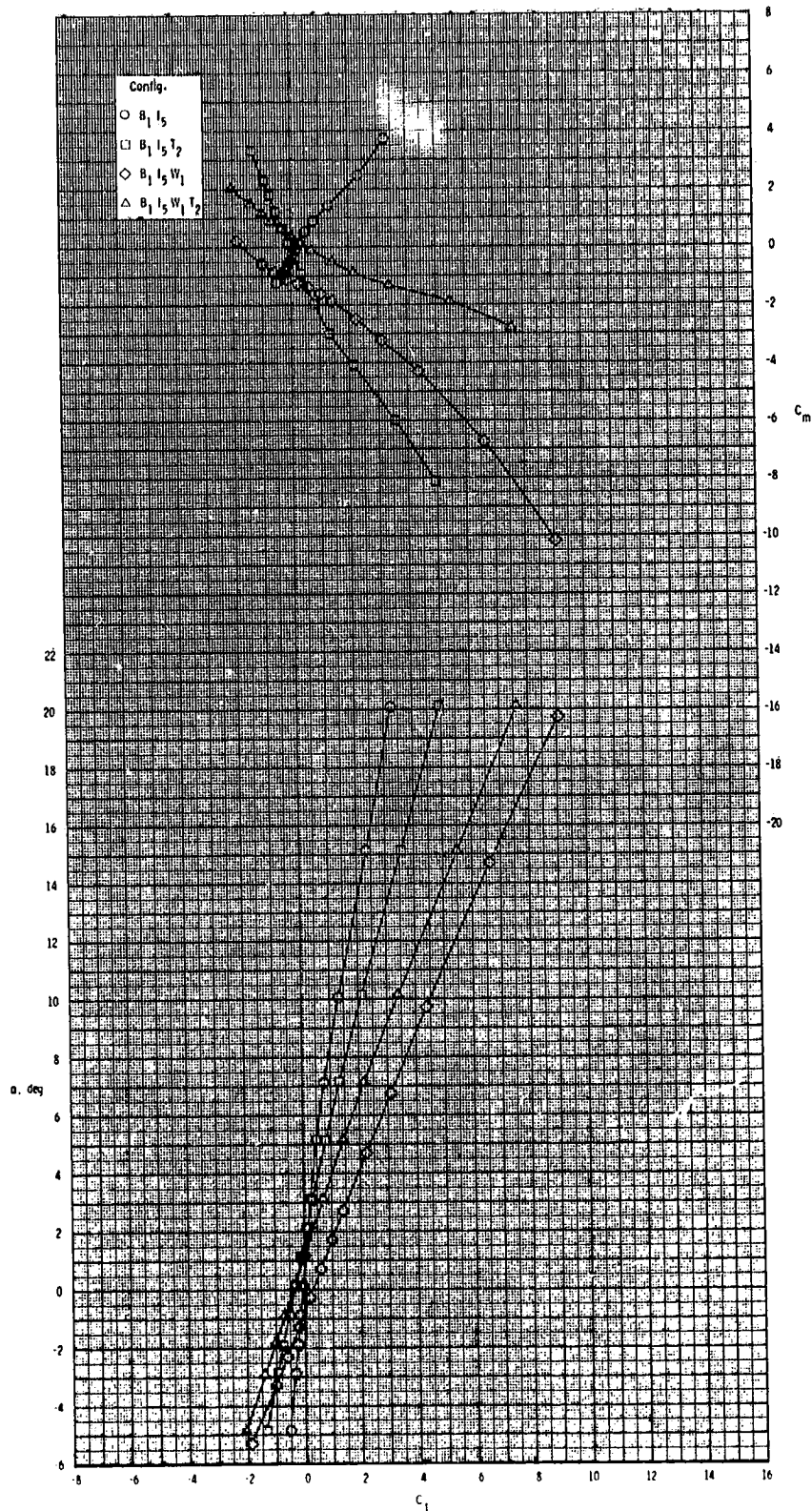
ORIGINAL PAGE IS
OF POOR QUALITY



(c) $M = 3.50$.

Figure 17.- Continued.

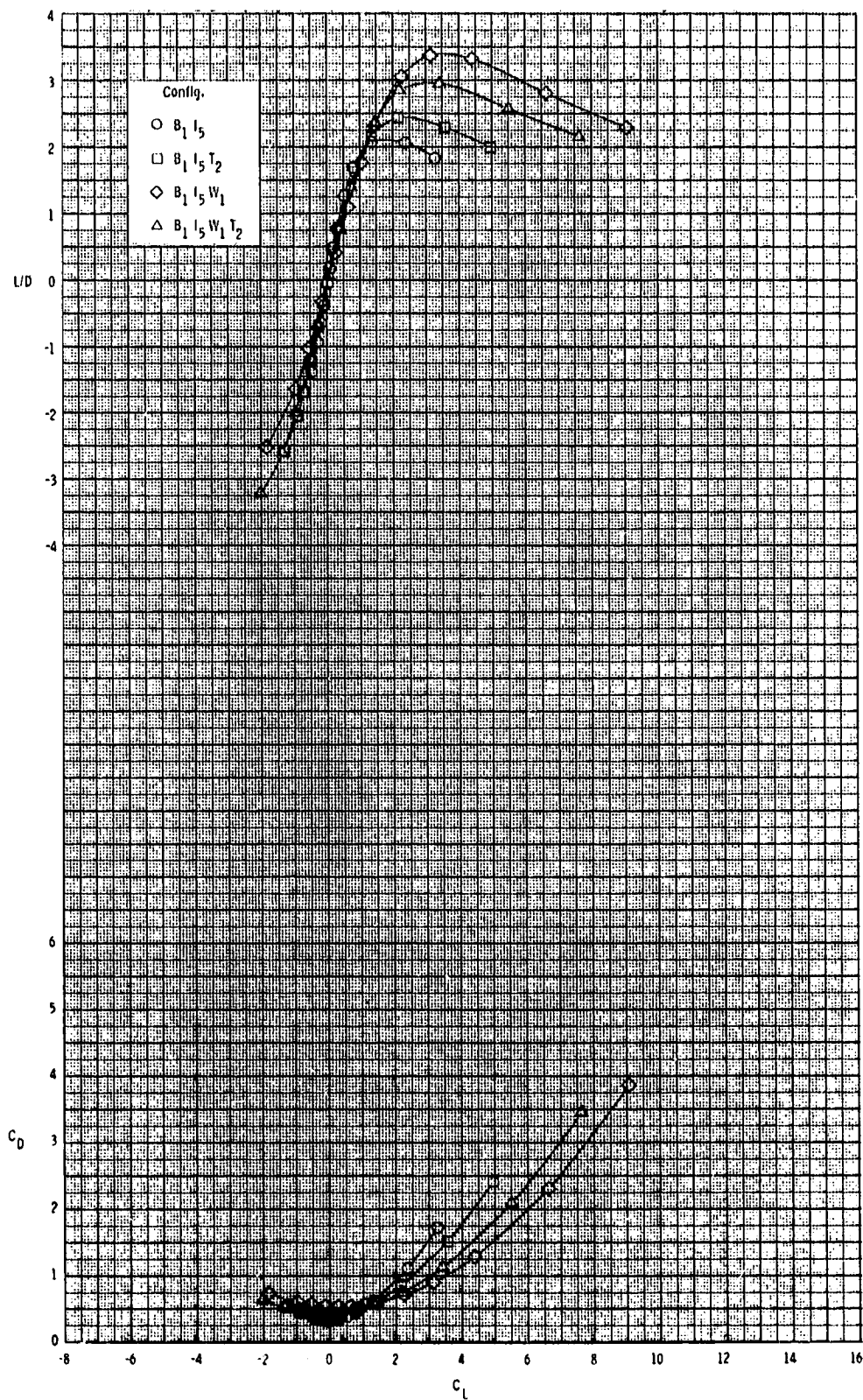
ORIGINAL PAGE IS
OF POOR QUALITY



(c) Continued.

Figure 17.- Continued.

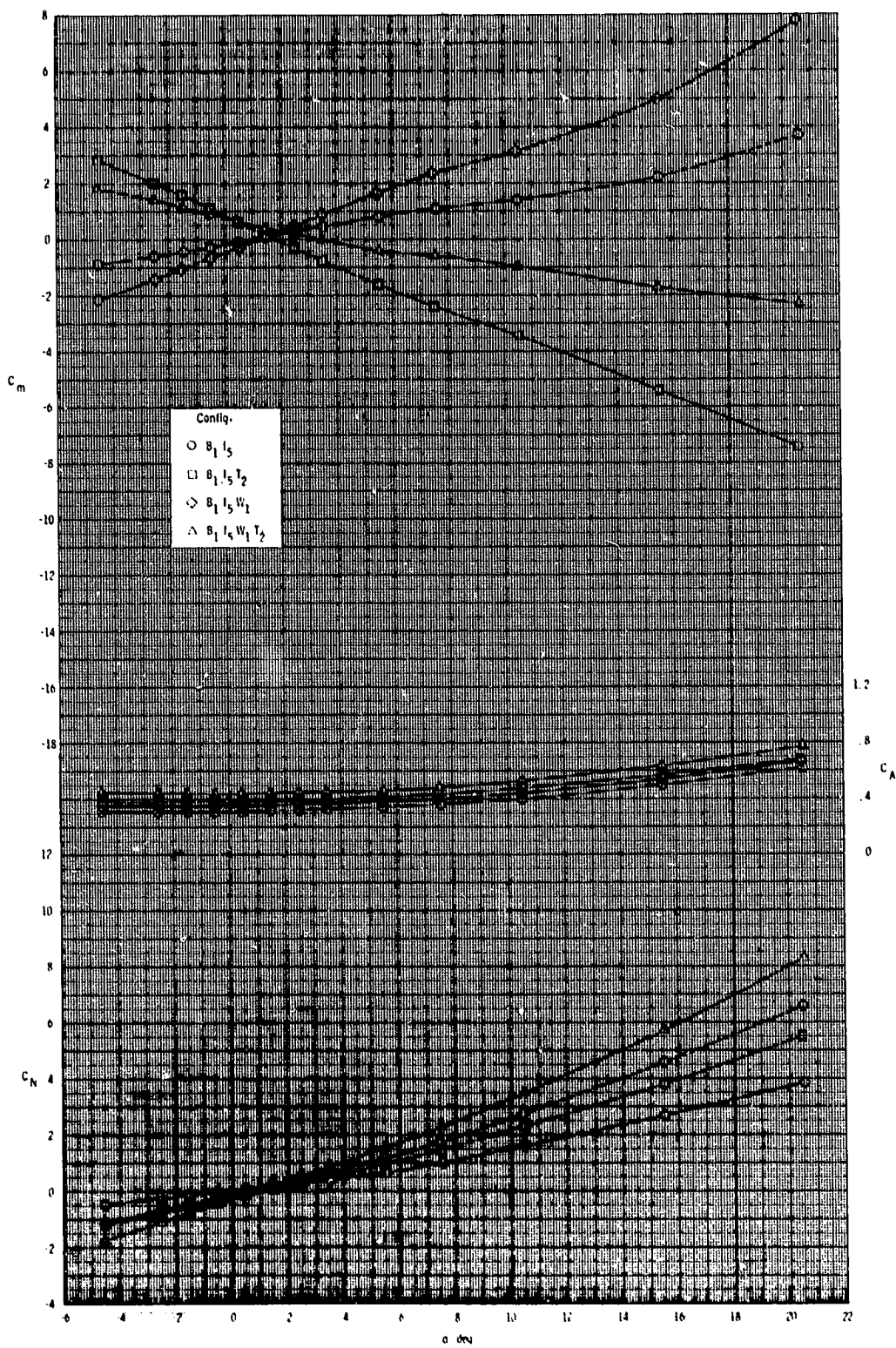
ORIGINAL PAGE IS
OF POOR QUALITY



(c) Concluded.

Figure 17.- Continued.

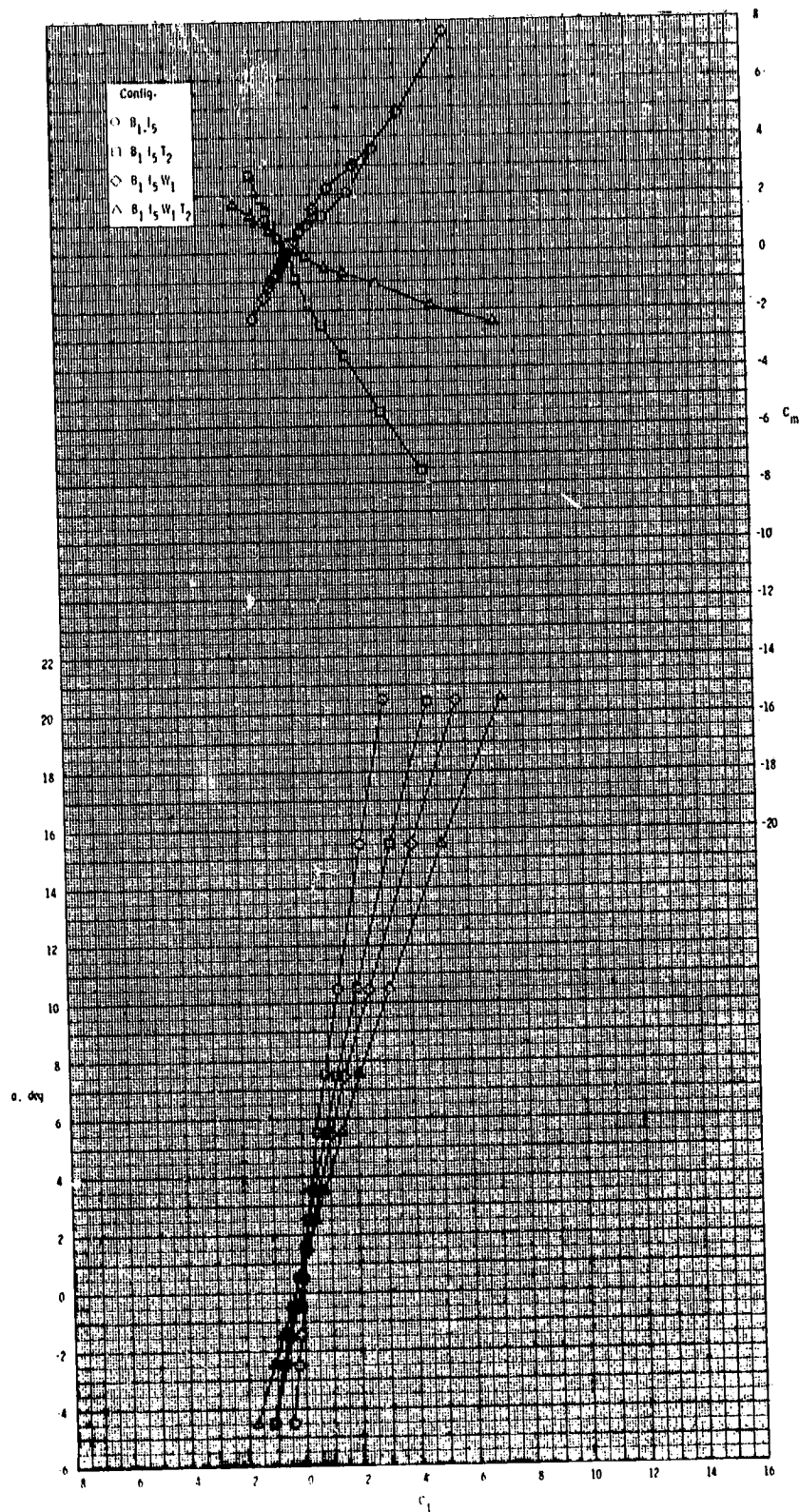
ORIGINAL PAGE IS
OF POOR QUALITY



(d) $M = 3.95$.

Figure 17.- Continued.

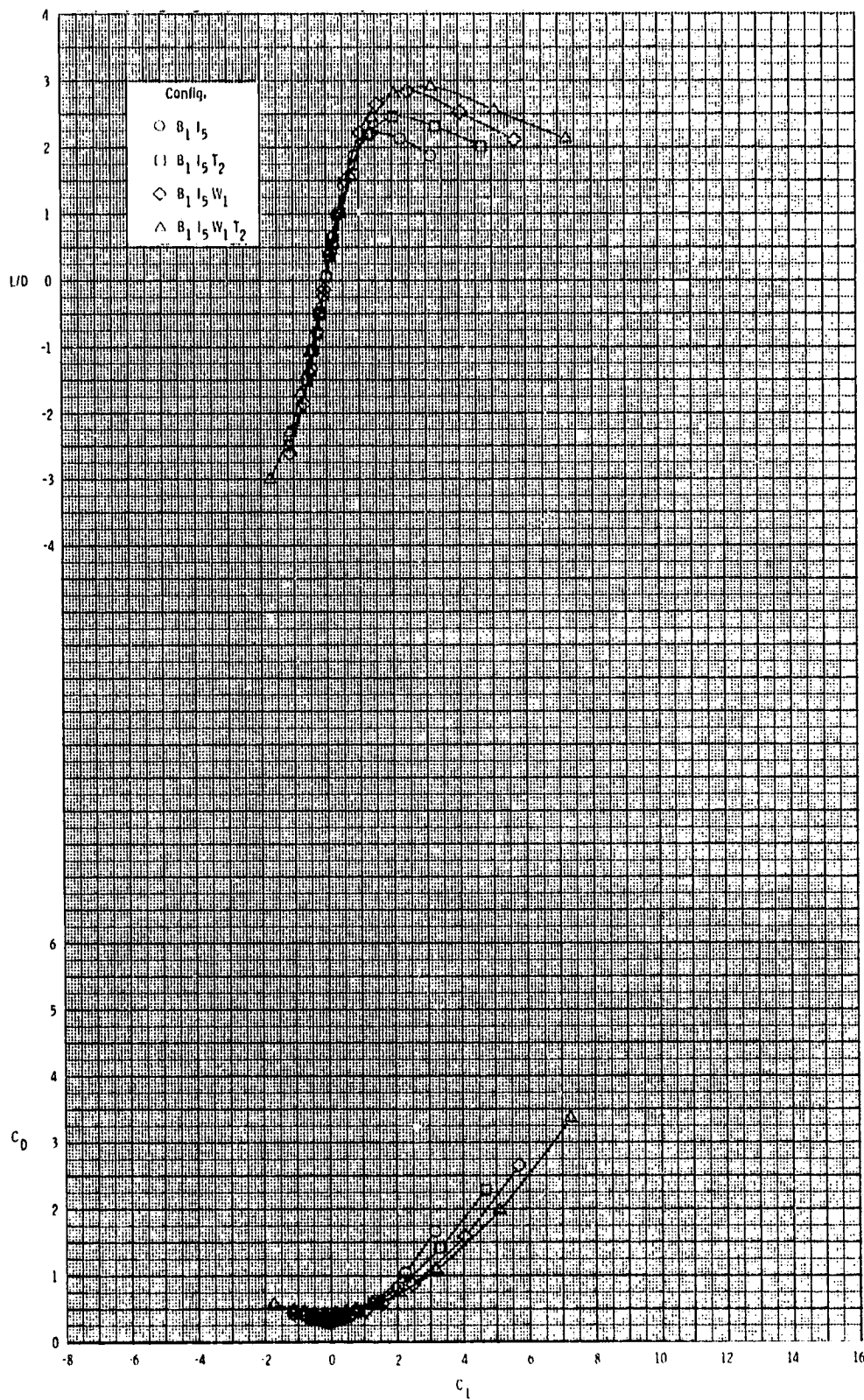
ORIGINAL PAGE IS
OF POOR QUALITY



(d) Continued.

Figure 17.- Continued.

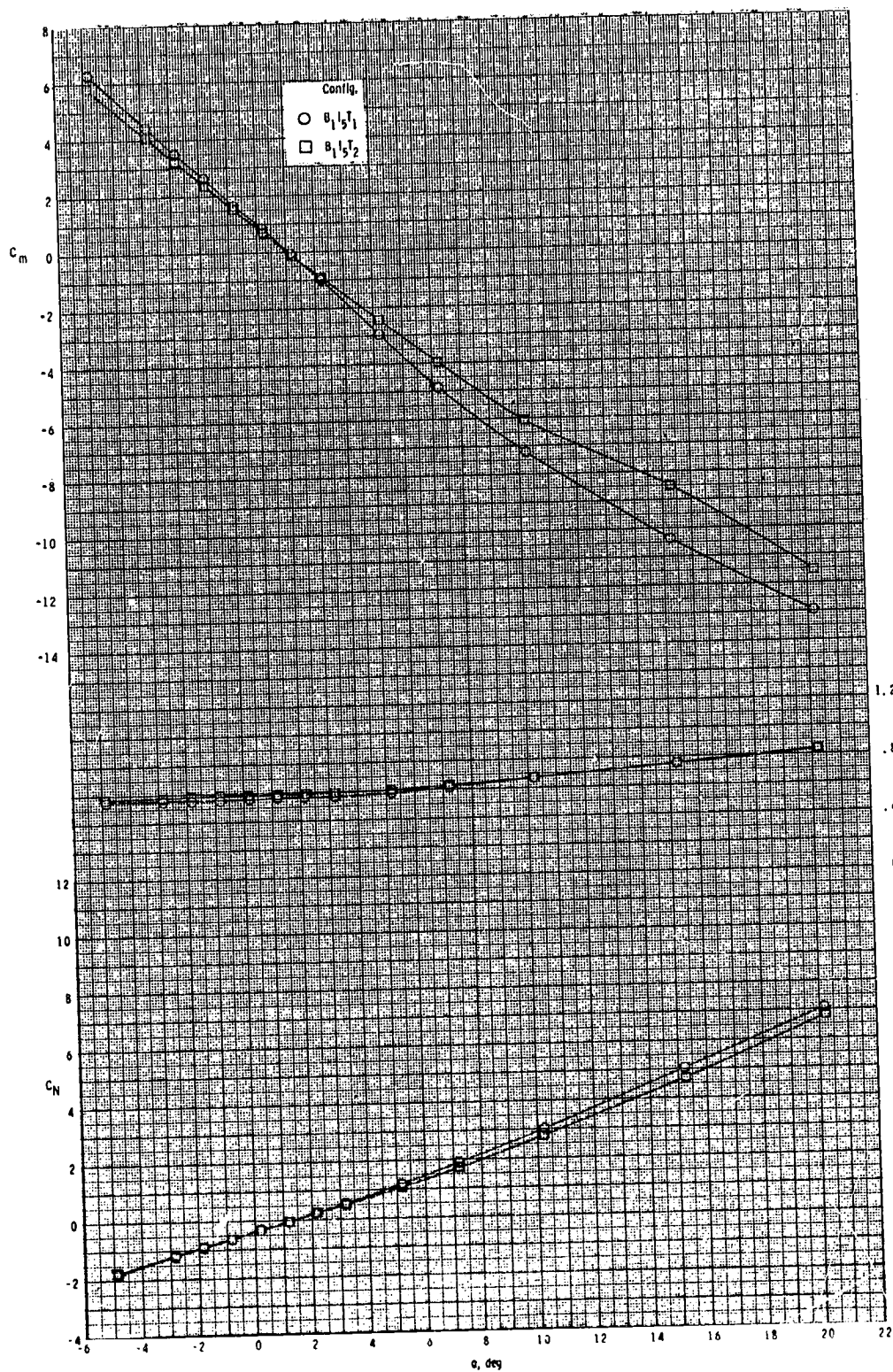
ORIGINAL PAGE IS
OF POOR QUALITY



(d) Concluded.

Figure 17.- Concluded.

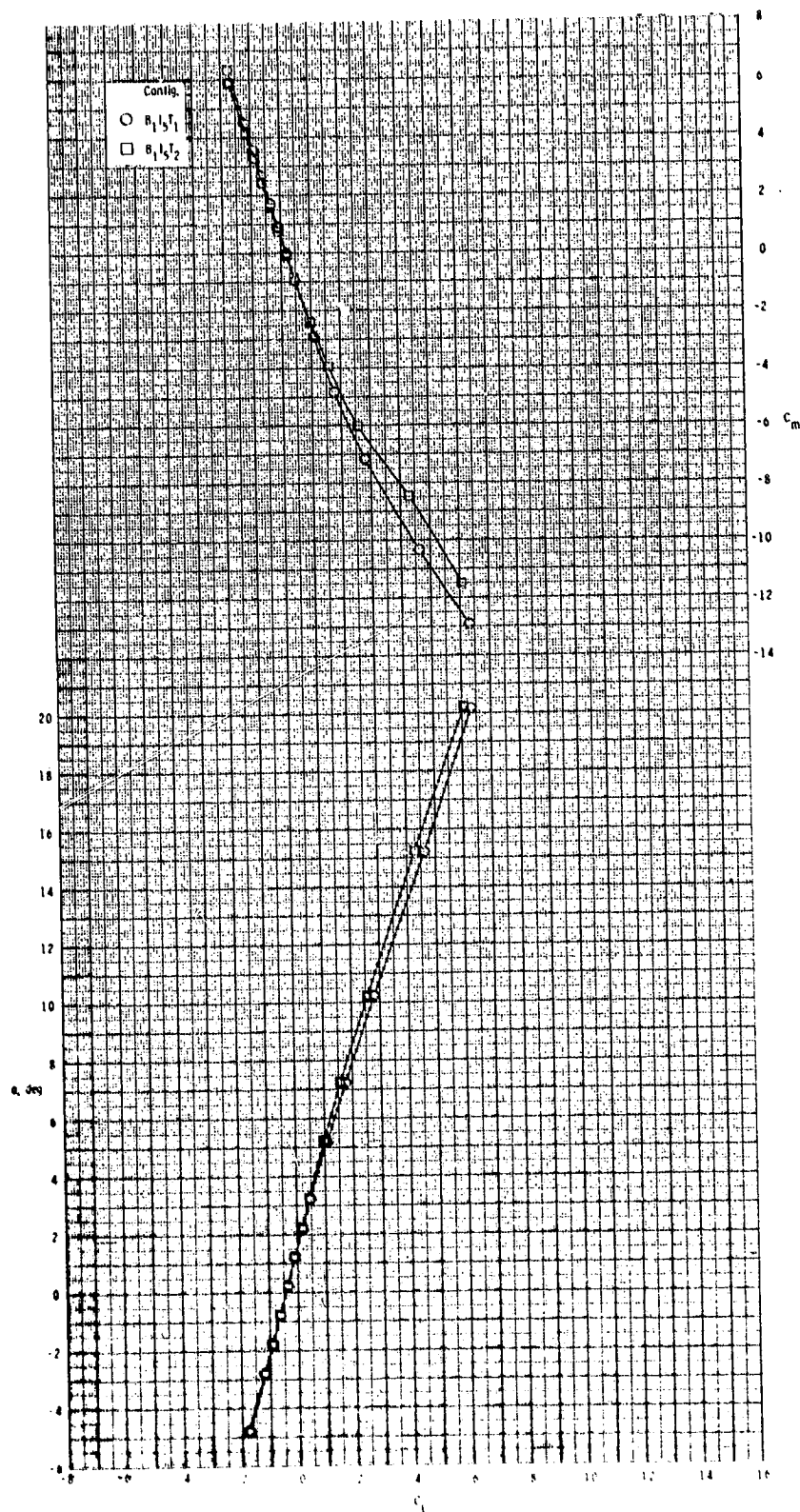
ORIGINAL PAGE IS
OF POOR QUALITY



(a) $M = 2.50$.

Figure 18.- Effect of tail configuration on longitudinal aerodynamic characteristics for 2-D inlets with wing off.

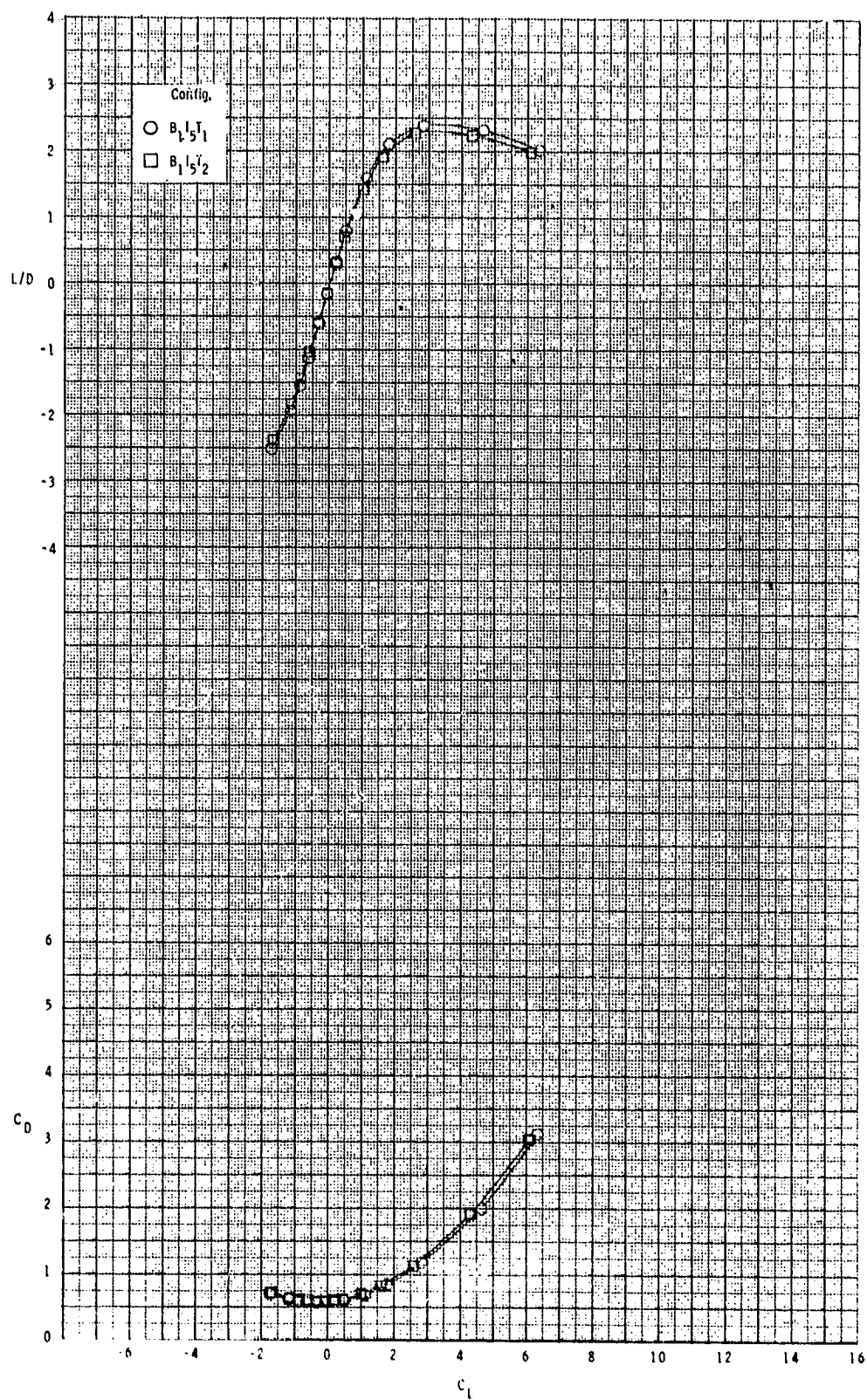
ORIGINAL PAGE IS
OF POOR QUALITY



(a) Continued.

Figure 18.- Continued.

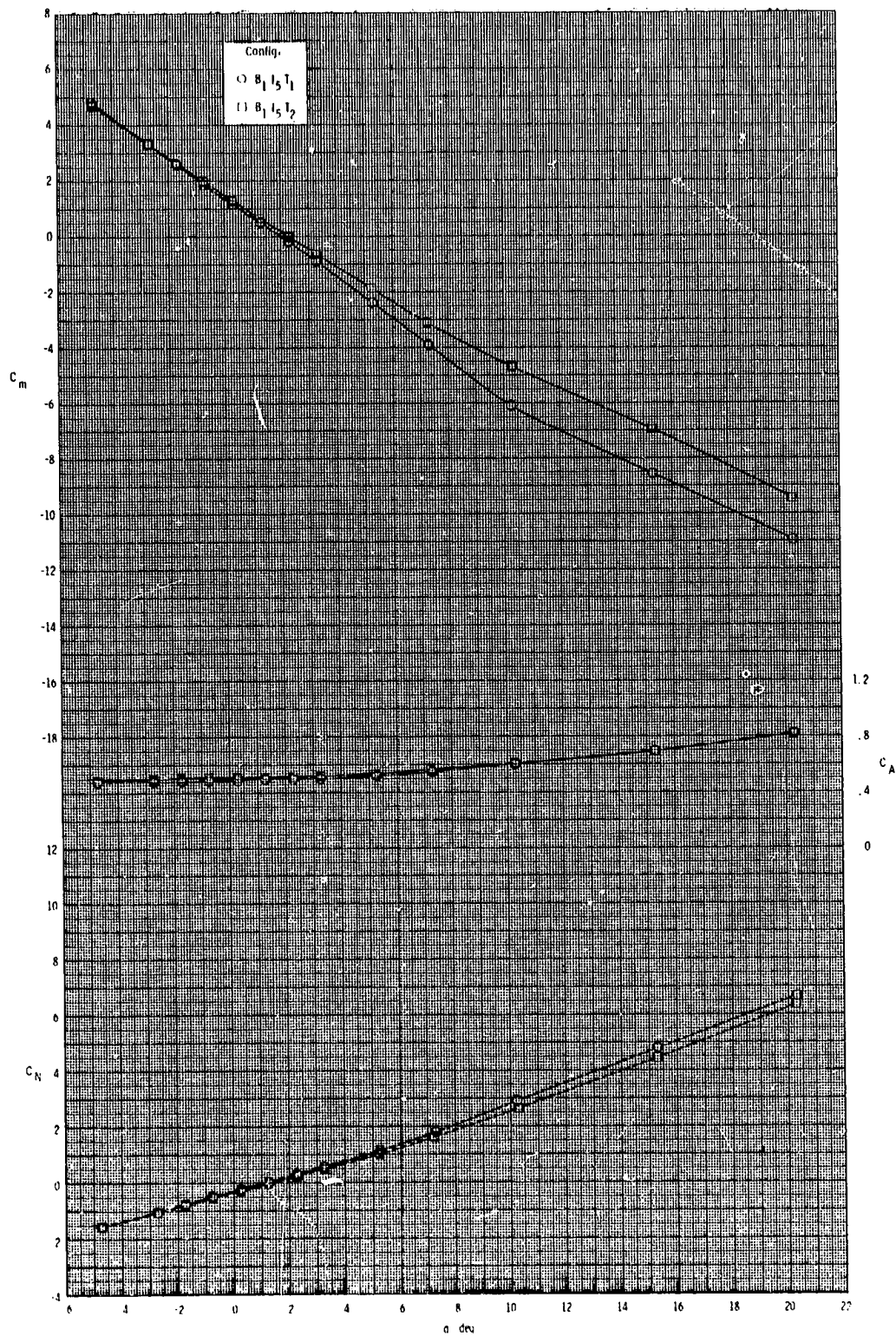
ORIGINAL PAGE 13
OF POOR QUALITY



(a) Concluded.

Figure 18.- Continued.

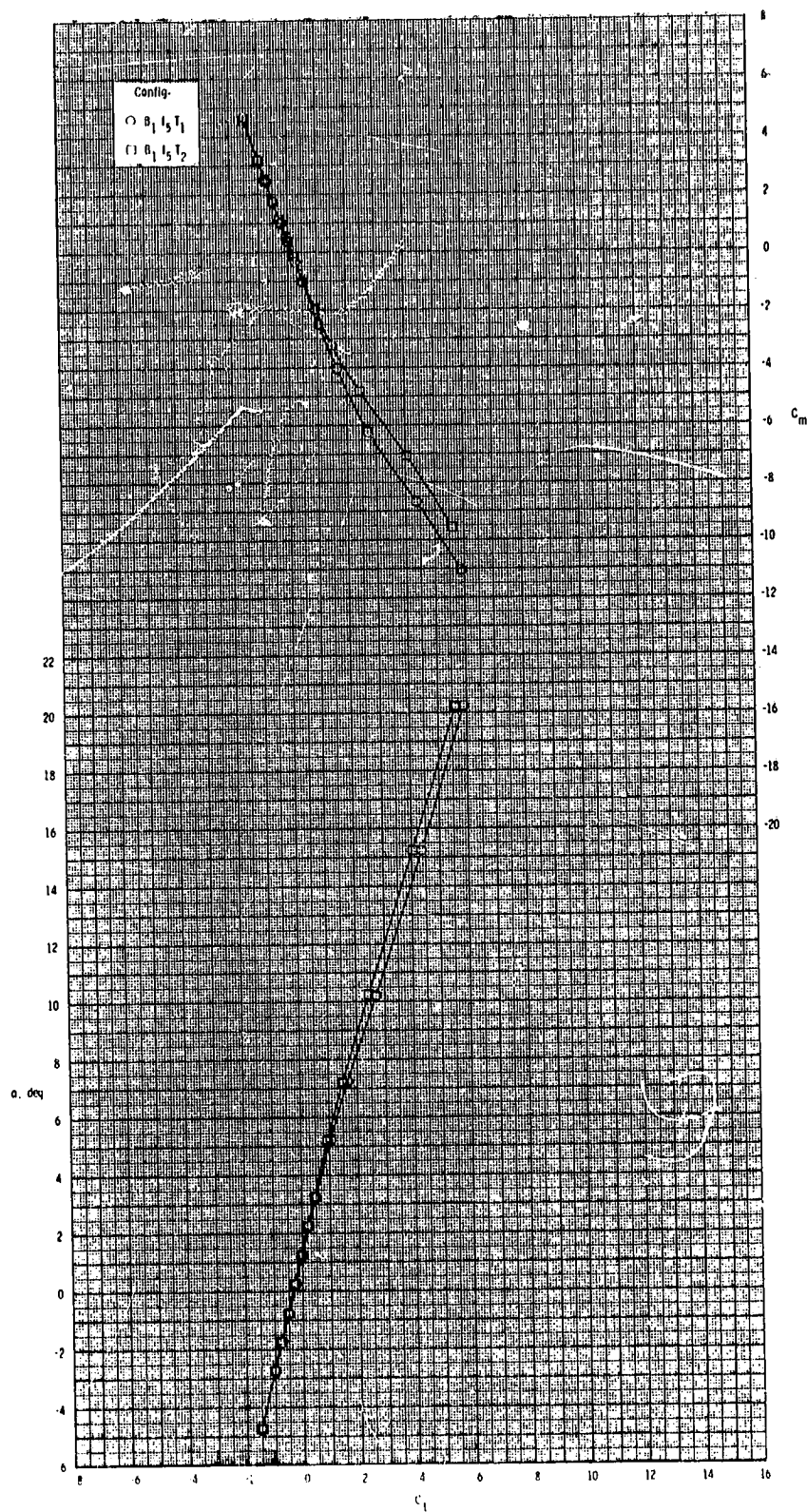
ORIGINAL PAGE IS
OF POOR QUALITY



(b) $M = 2.95$.

Figure 18.- Continued.

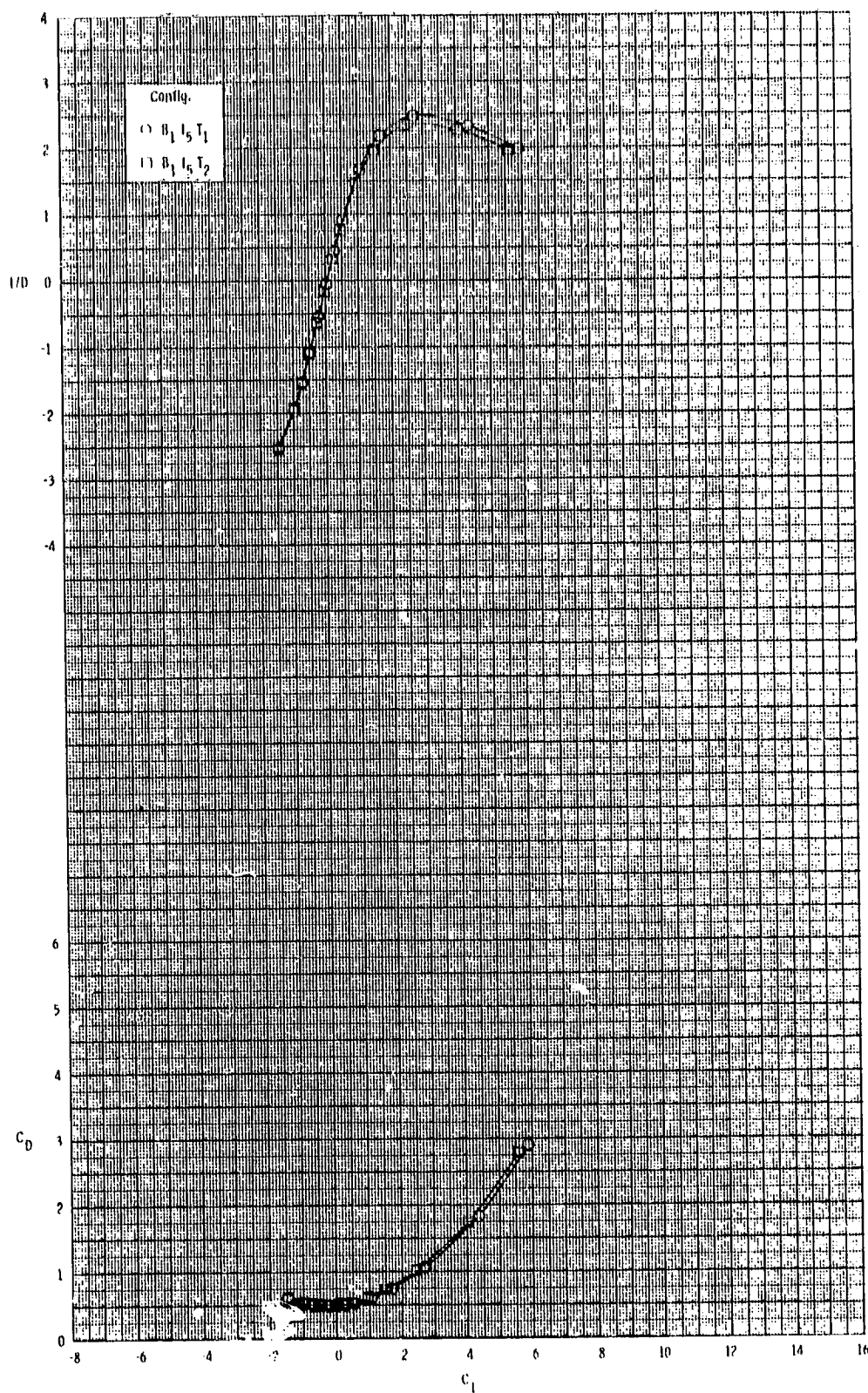
ORIGINAL PAGE IS
OF POOR QUALITY



(b) Continued.

Figure 18.- Continued.

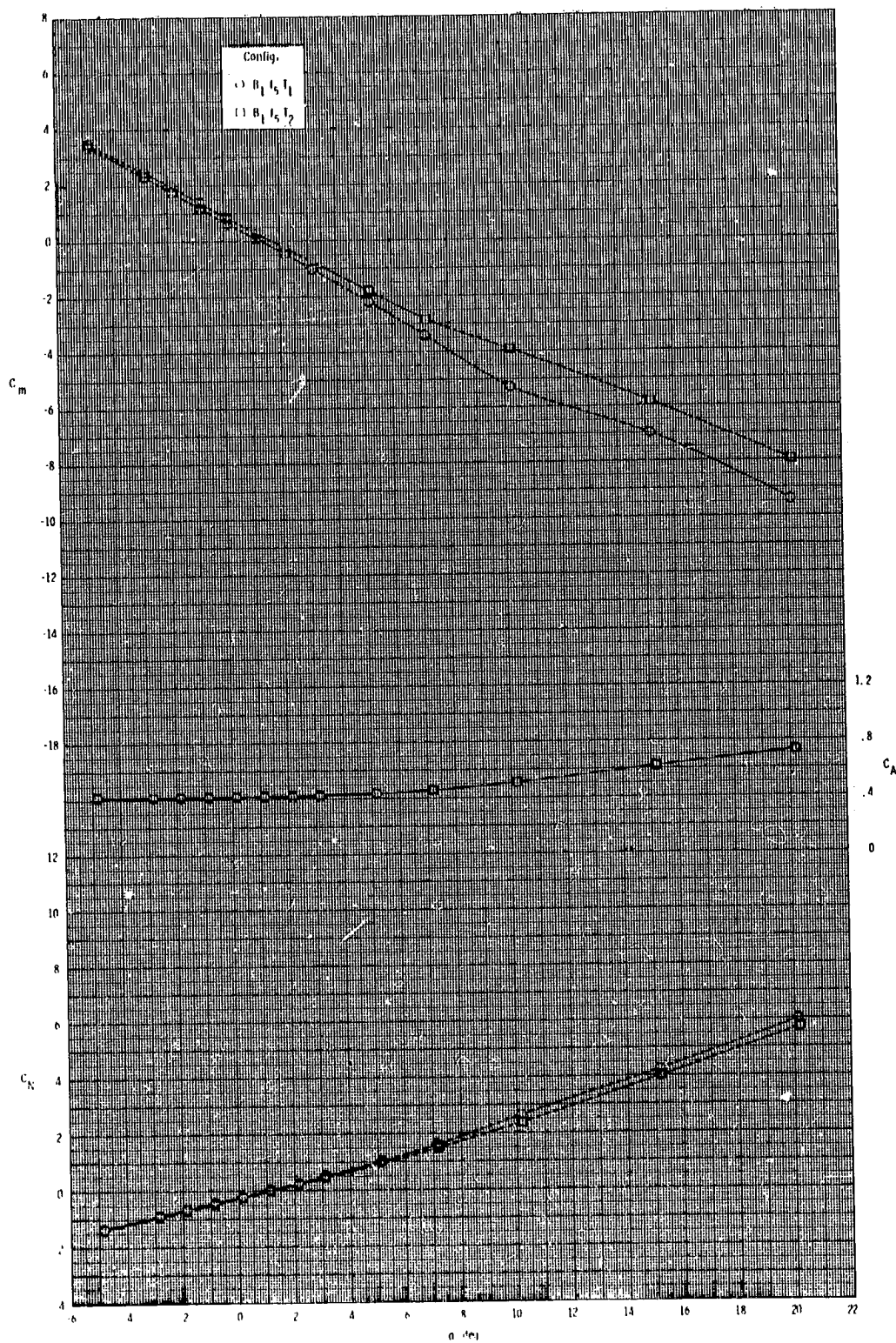
ORIGINAL PAGE IS
OF POOR QUALITY



(b) Concluded. _

Figure 18.- Continued.

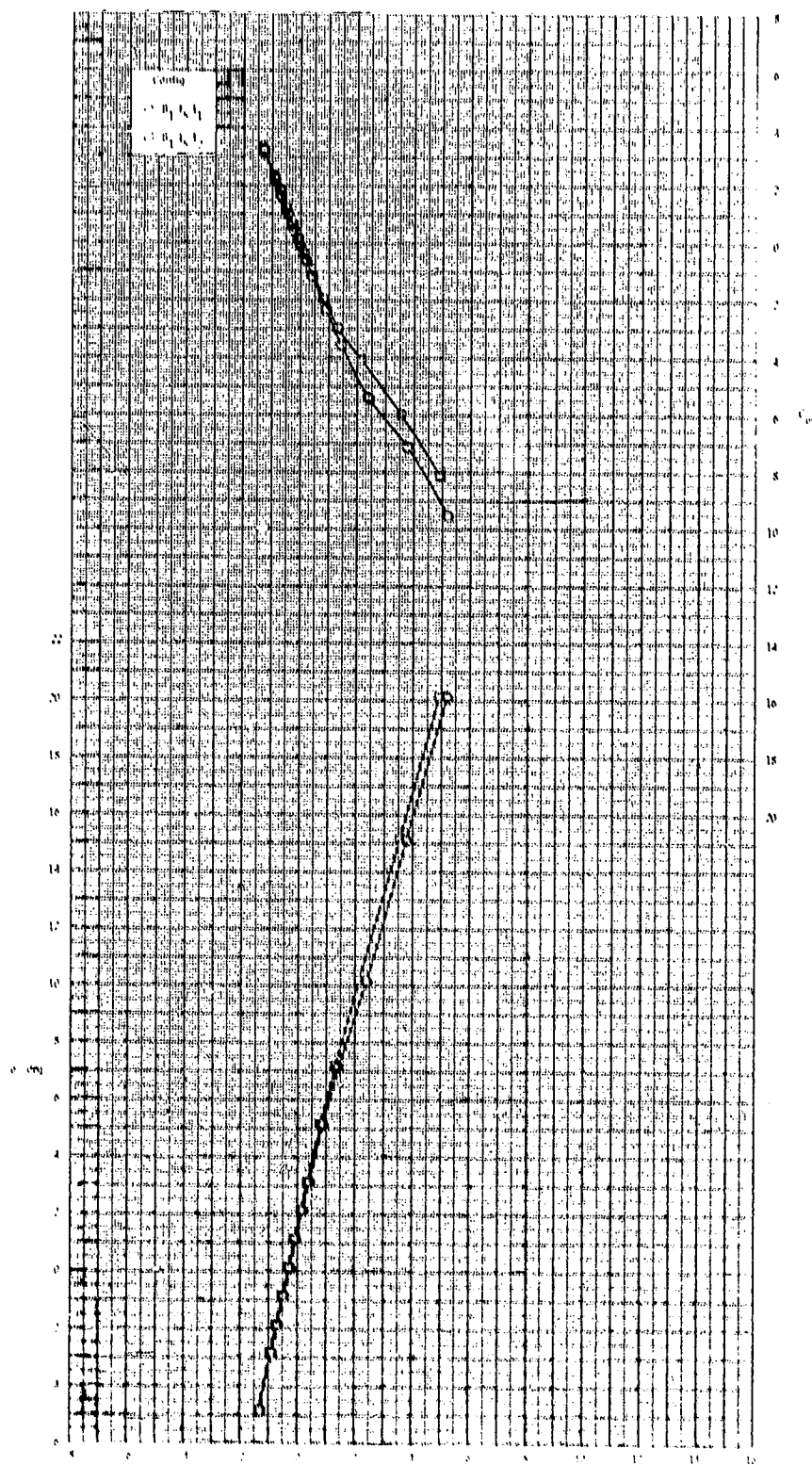
ORIGINAL PAGE IS
OF POOR QUALITY



(c) $M = 3.50$.

Figure 18.- Continued.

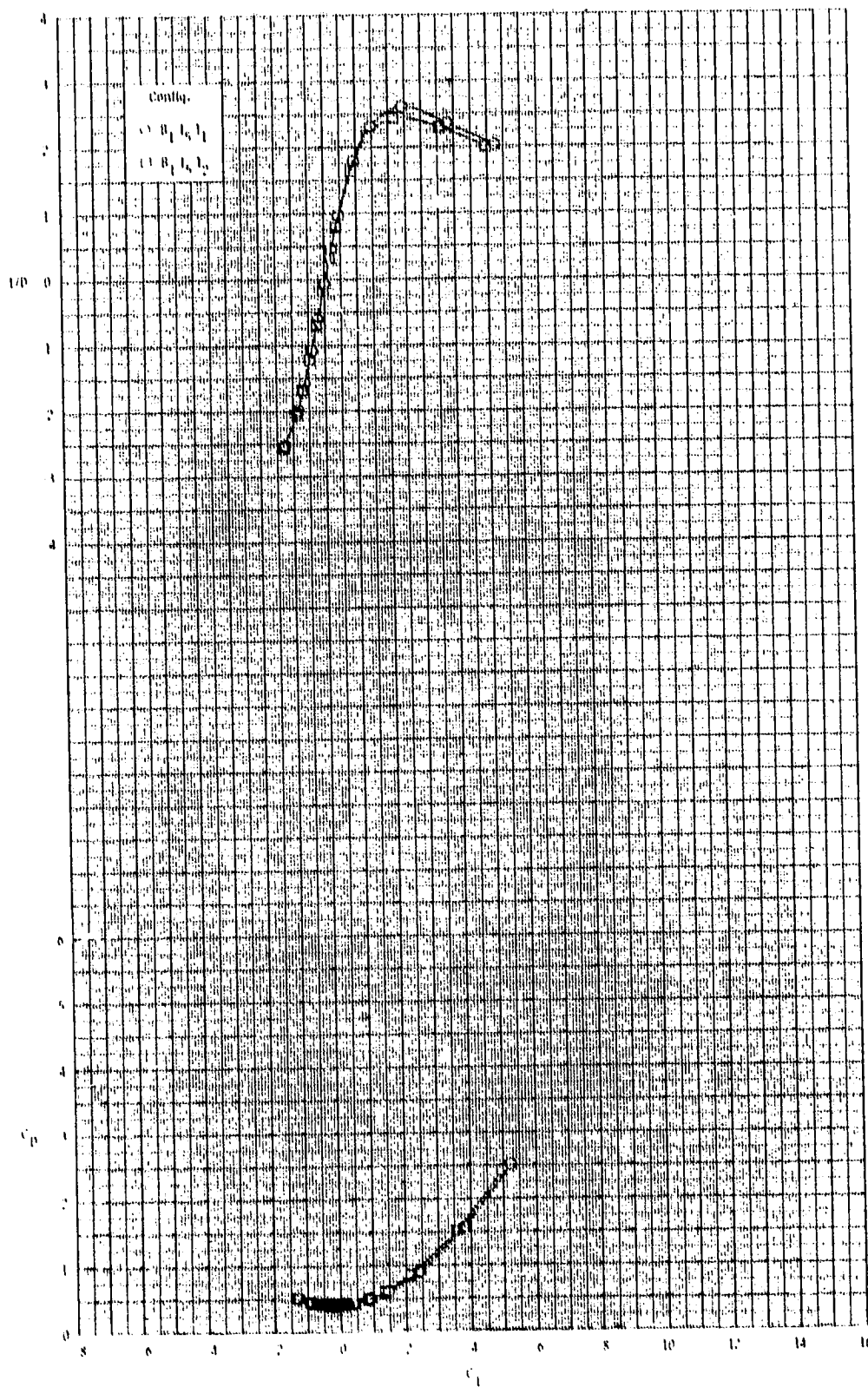
ORIGINAL PAGE IS
OF POOR QUALITY



(c) Continued.

Figure 18.- Continued.

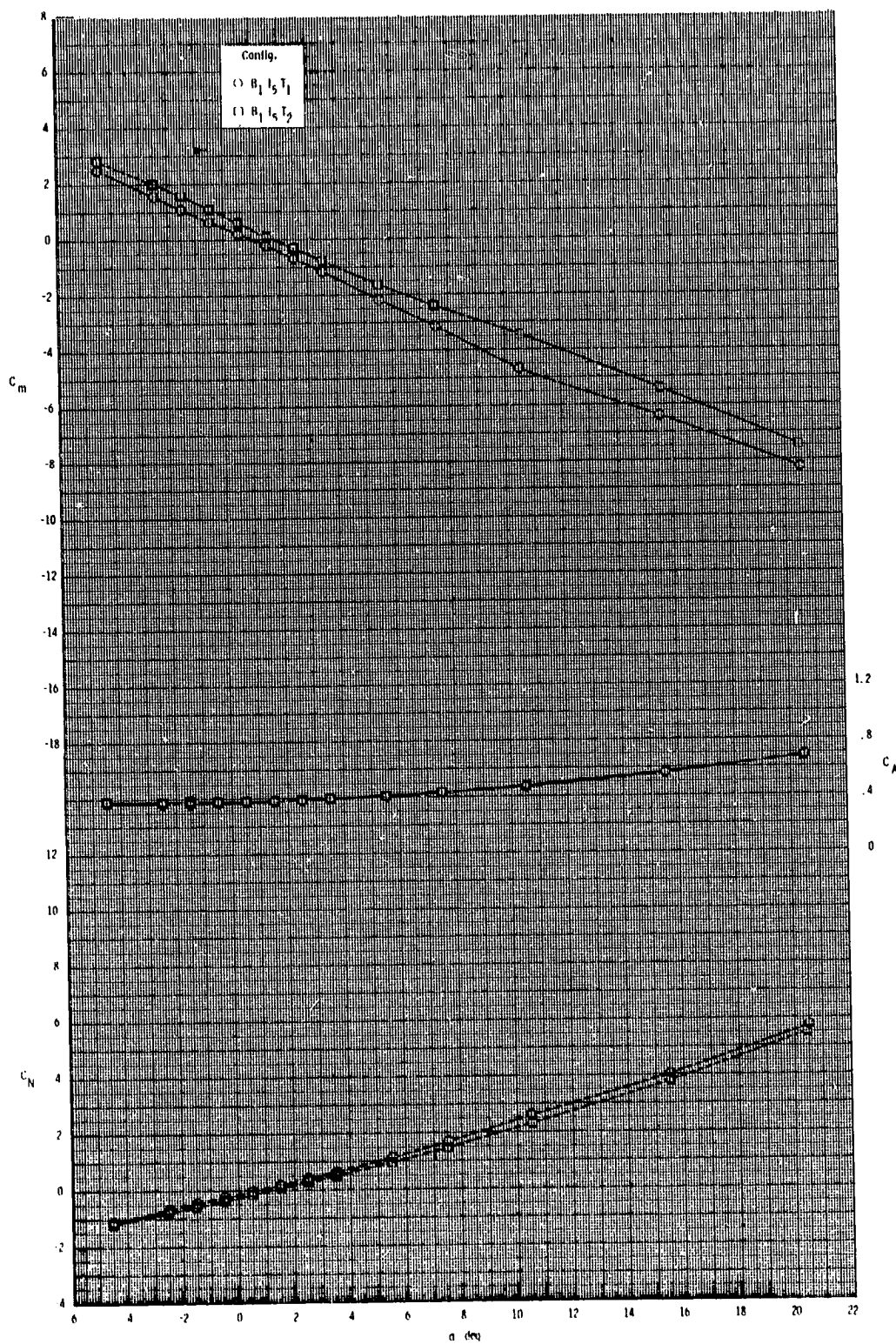
ORIGINAL PAGE IS
OF POOR QUALITY



(c) Concluded.

Figure 18. - Continued.

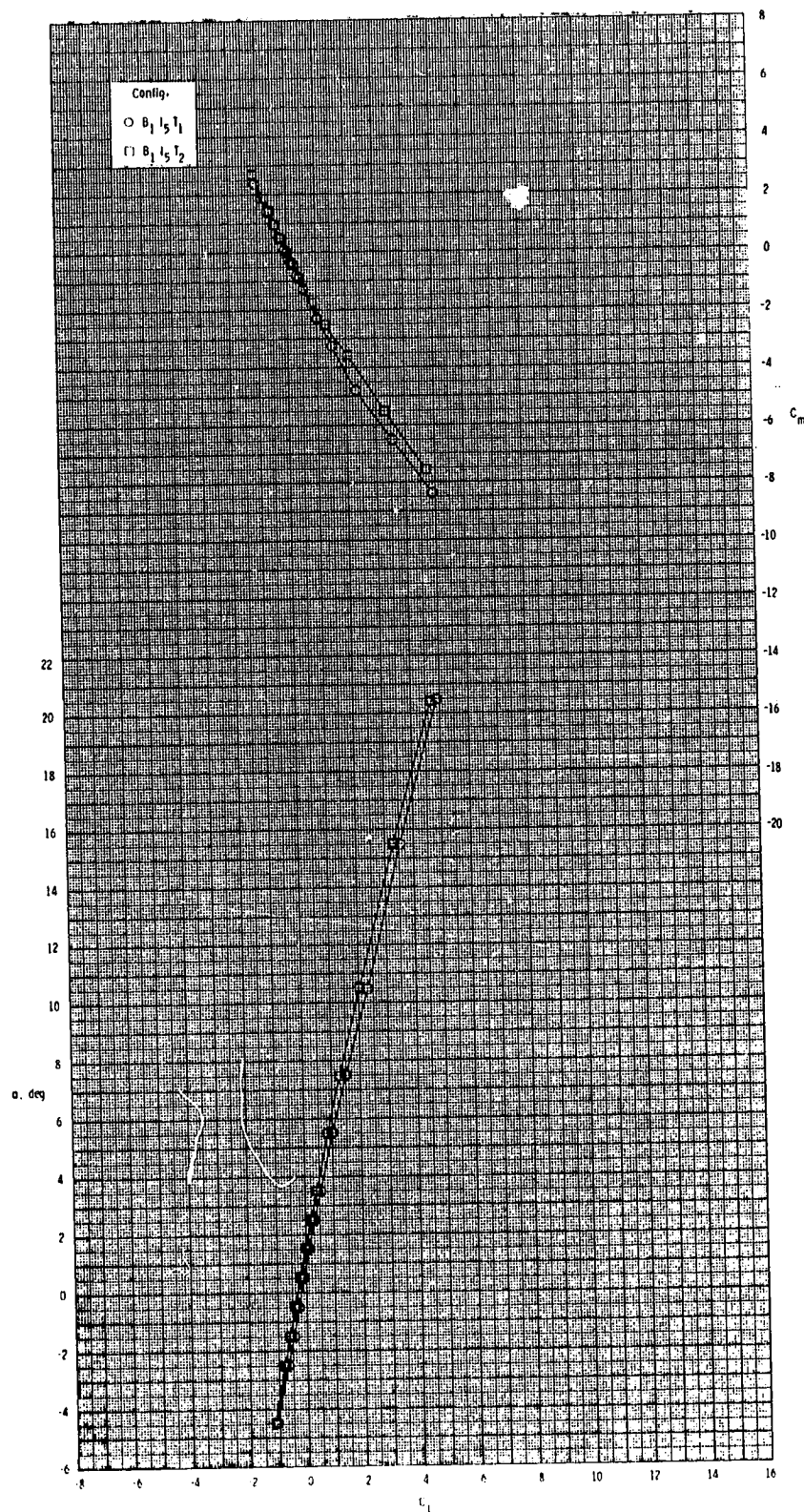
ORIGINAL PAGE IS
OF POOR QUALITY



(d) $M = 3.95$.

Figure 18.- Continued.

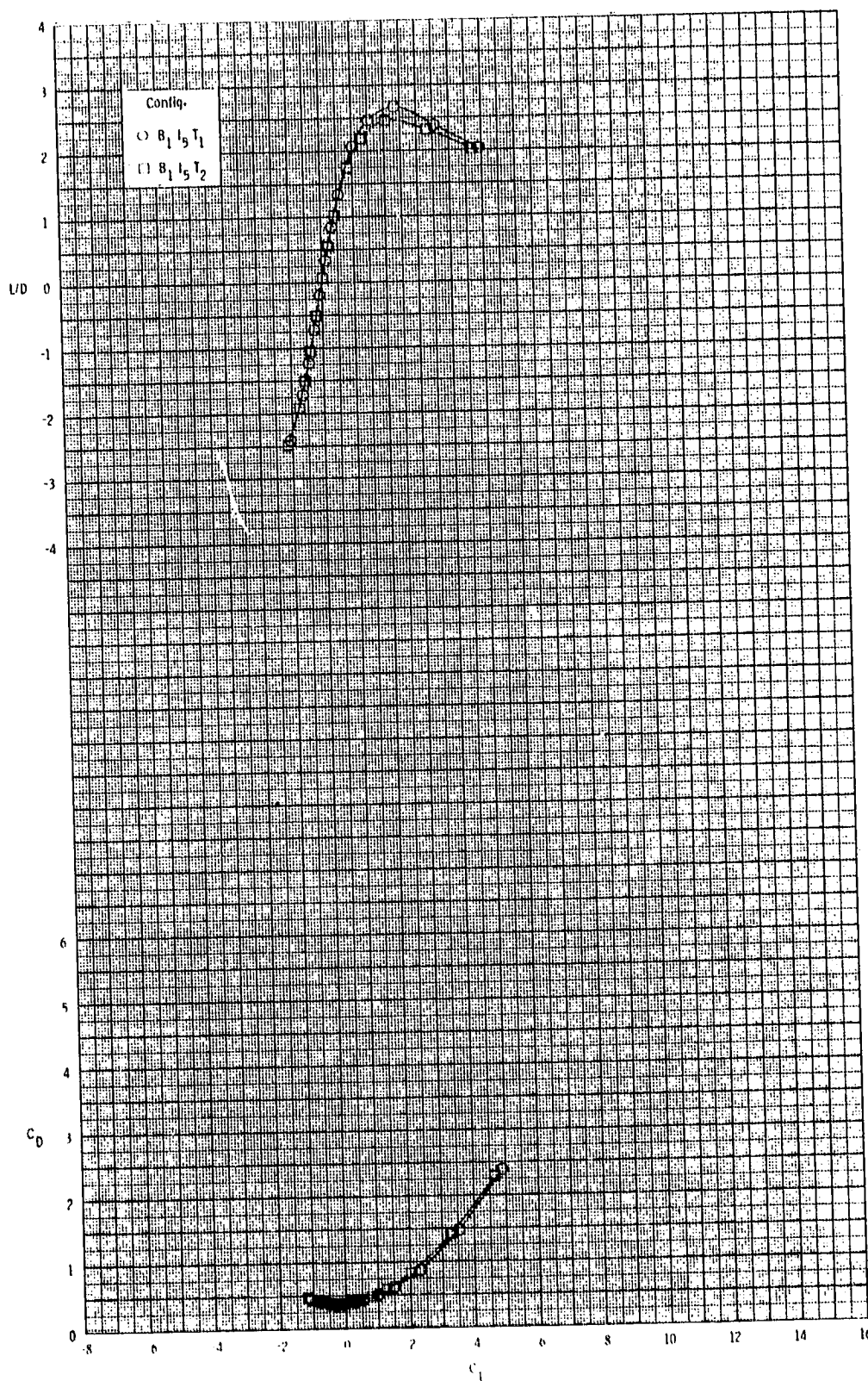
ORIGINAL PAGE IS
OF POOR QUALITY



(d) Continued.

Figure 18.- Continued.

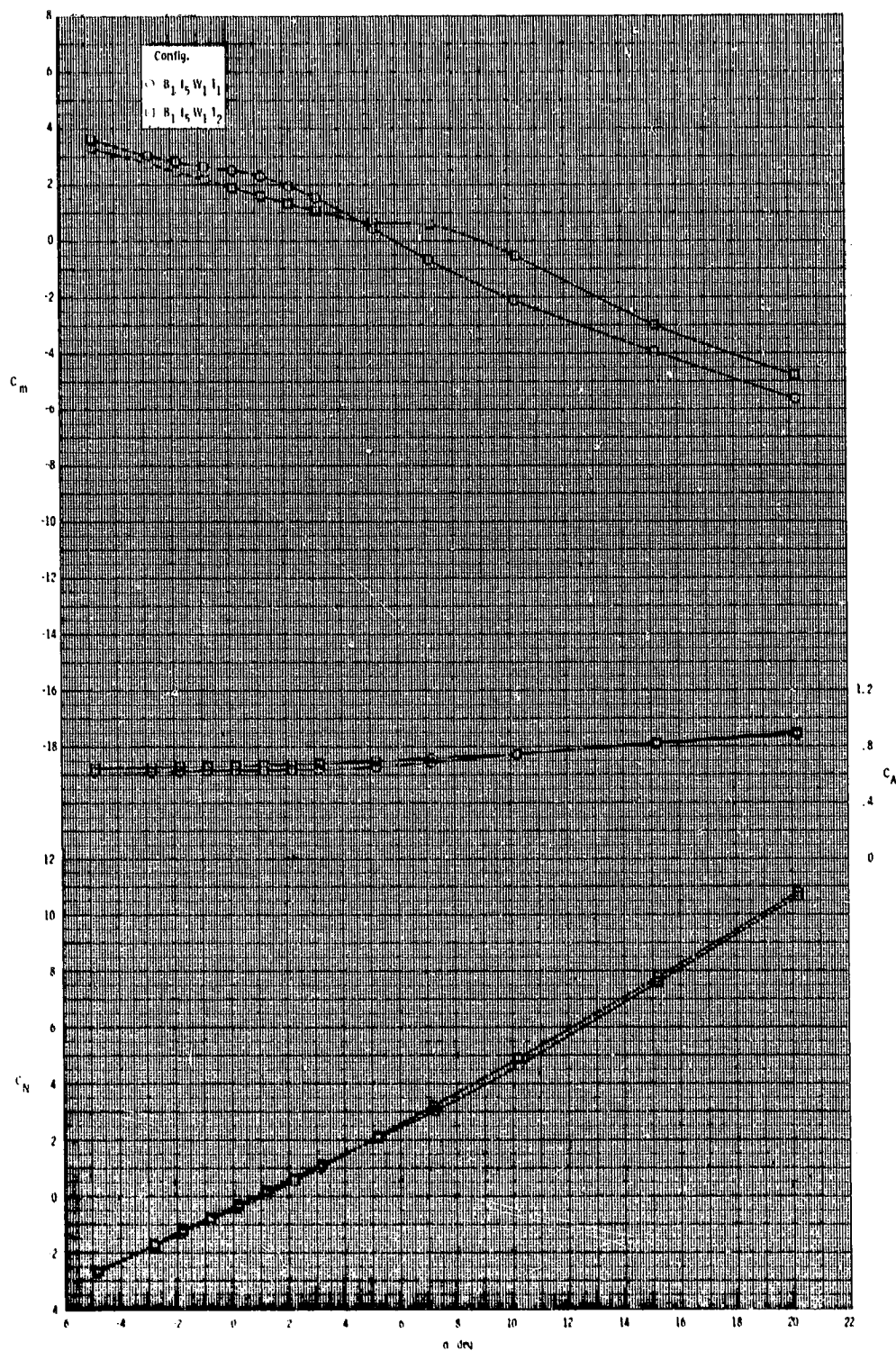
ORIGINAL PAGE IS
OF POOR QUALITY



(d) Concluded.

Figure 18.- Concluded.

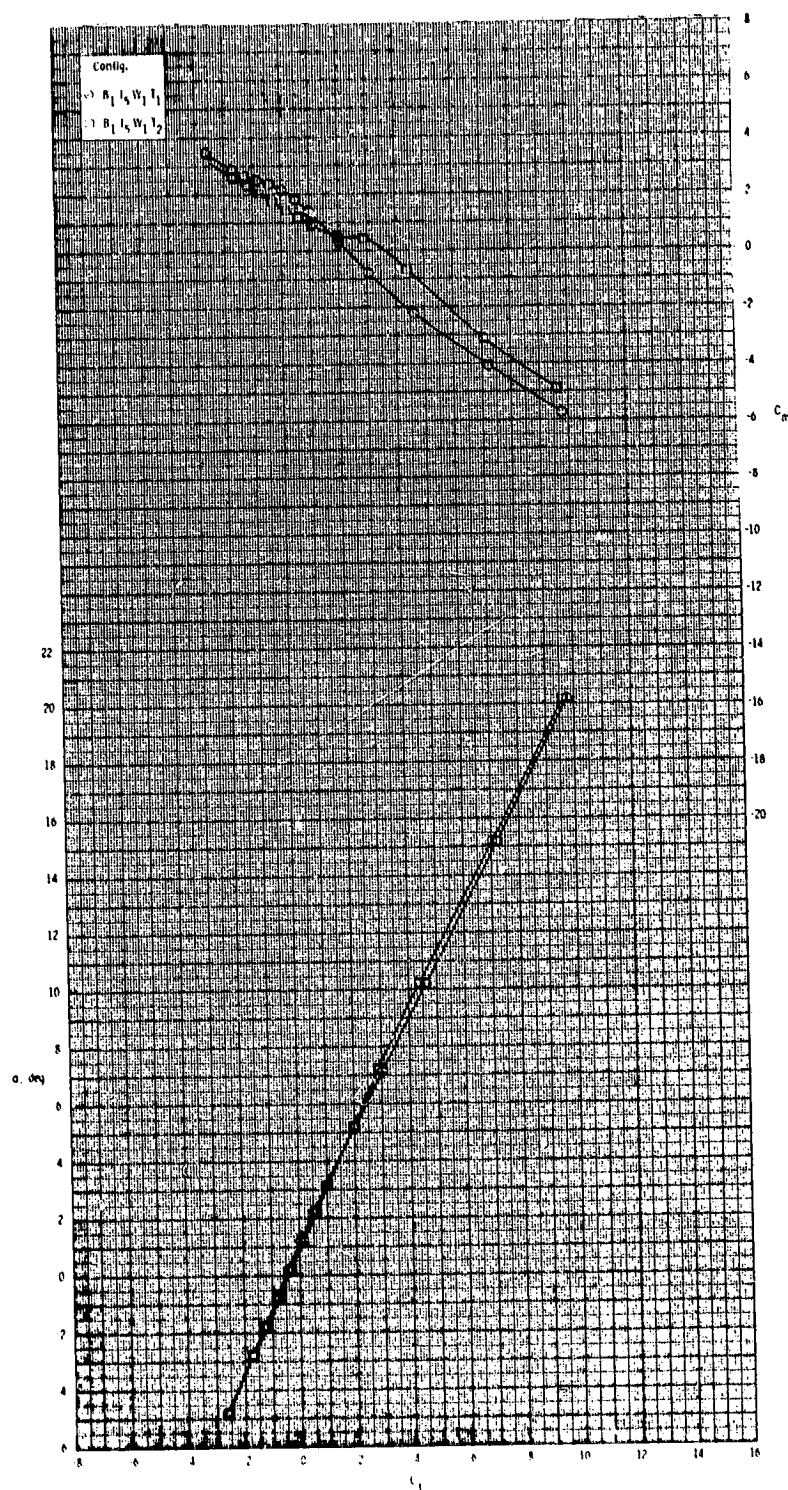
ORIGINAL PAGE 13
OF POOR QUALITY



(a) $M = 2.50$.

Figure 19.- Effect of tail configuration on longitudinal aerodynamic characteristics for 2-D inlets with wing on.

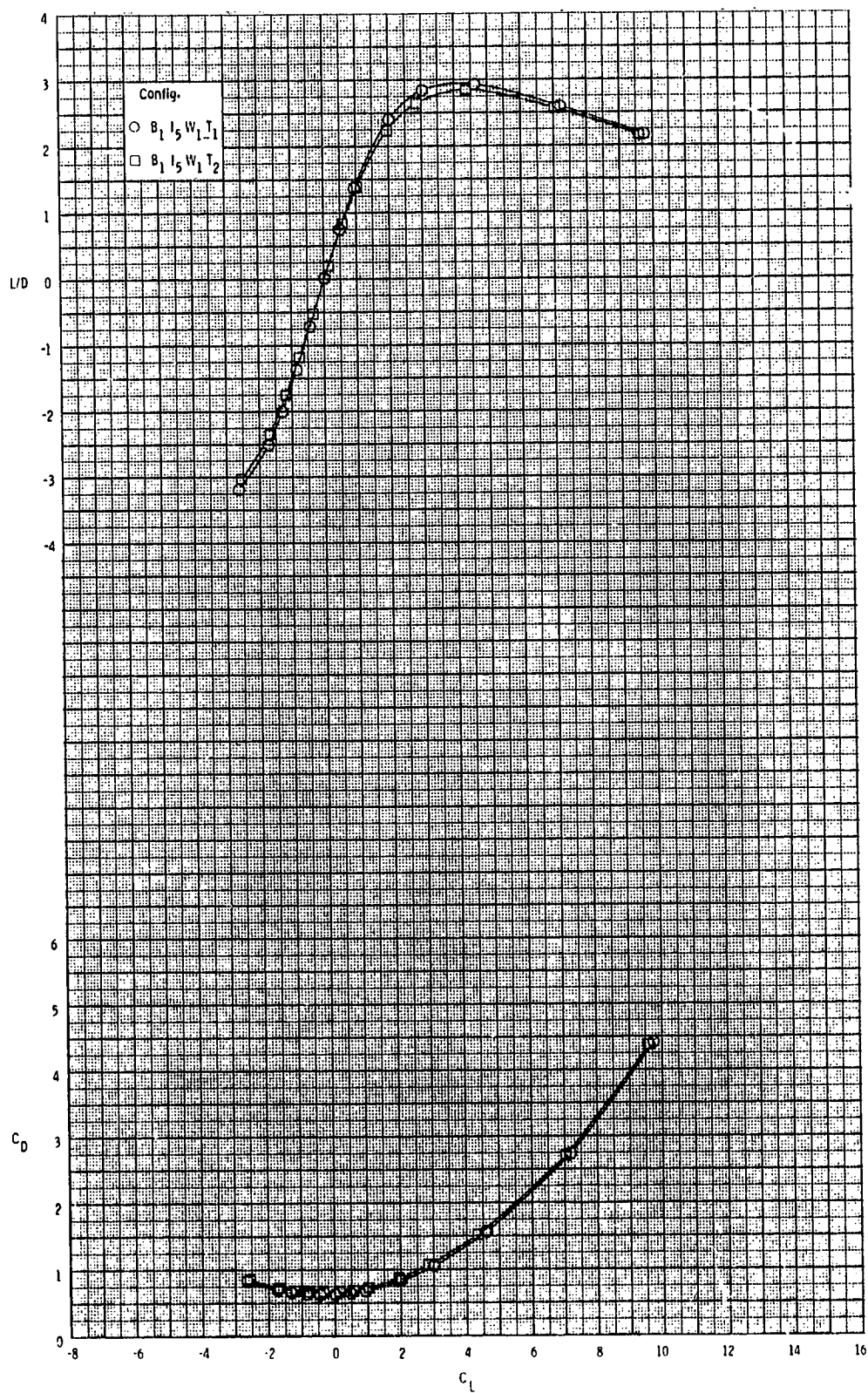
ORIGINAL PAGE IS
OF POOR QUALITY



(a) Continued.

Figure 19.- Continued.

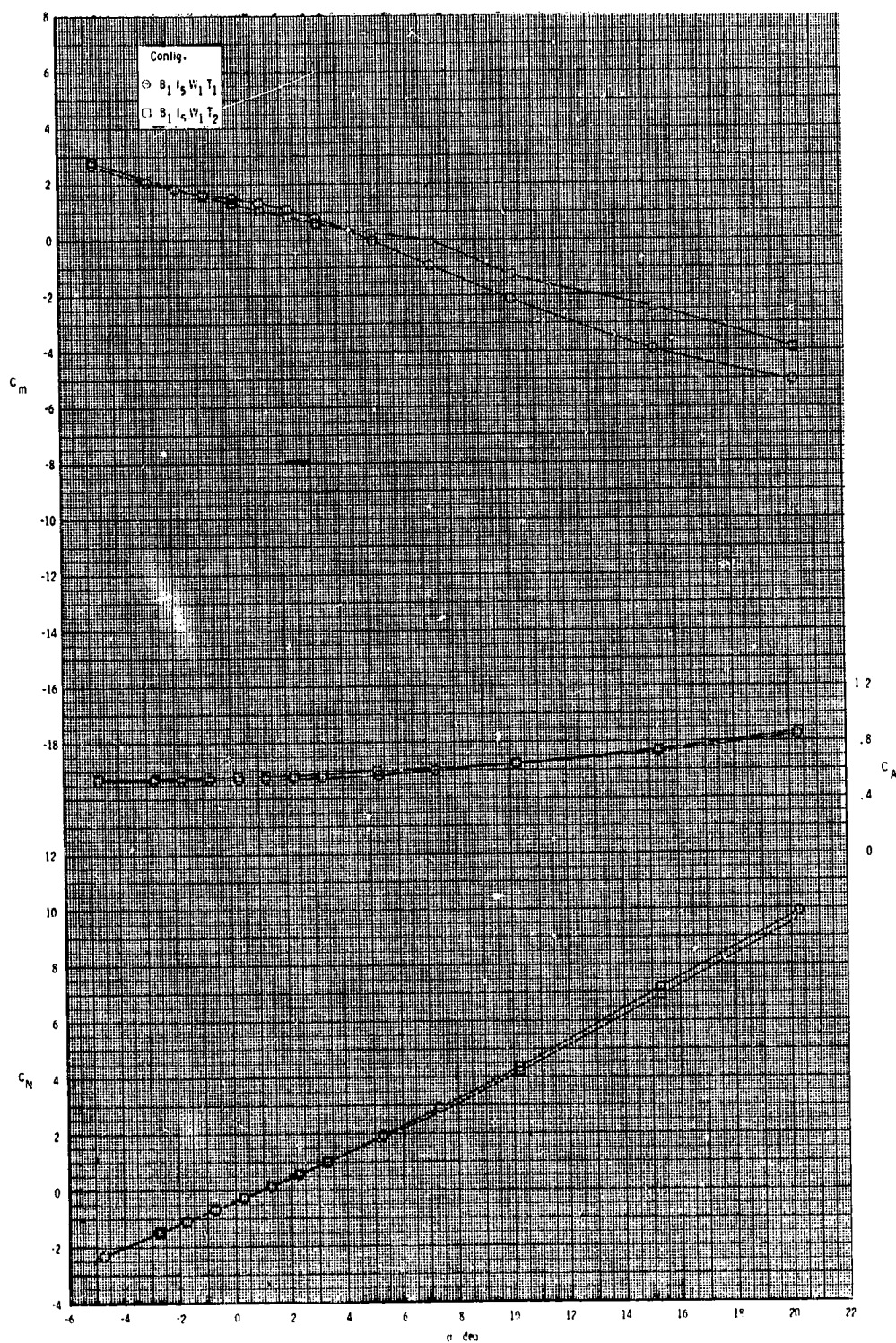
ORIGINAL PAGE IS
OF POOR QUALITY



(a) Concluded.

Figure 19.- Continued.

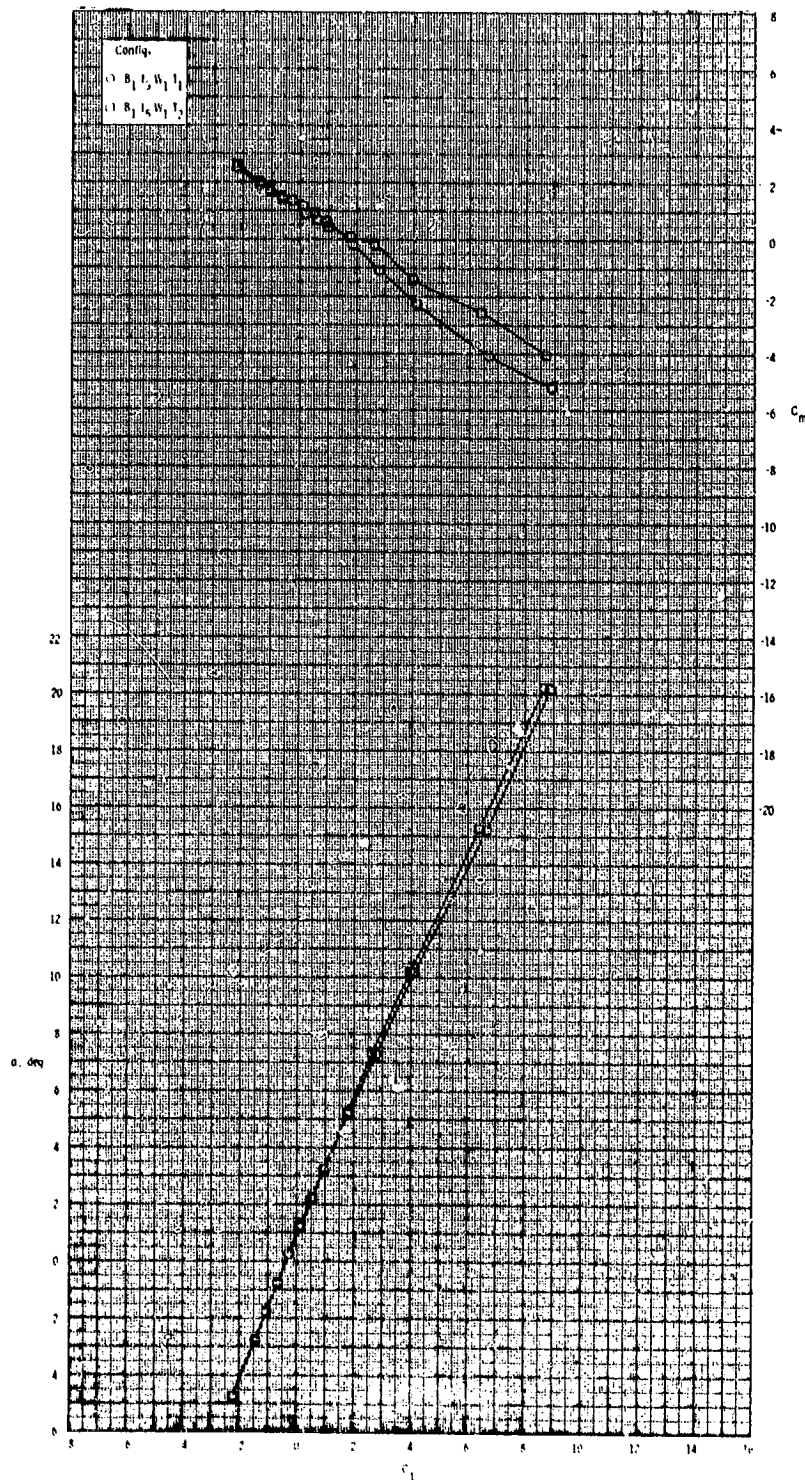
ORIGINAL PAGE IS
OF POOR QUALITY



(b) $M = 2.95$.

Figure 19.- Continued.

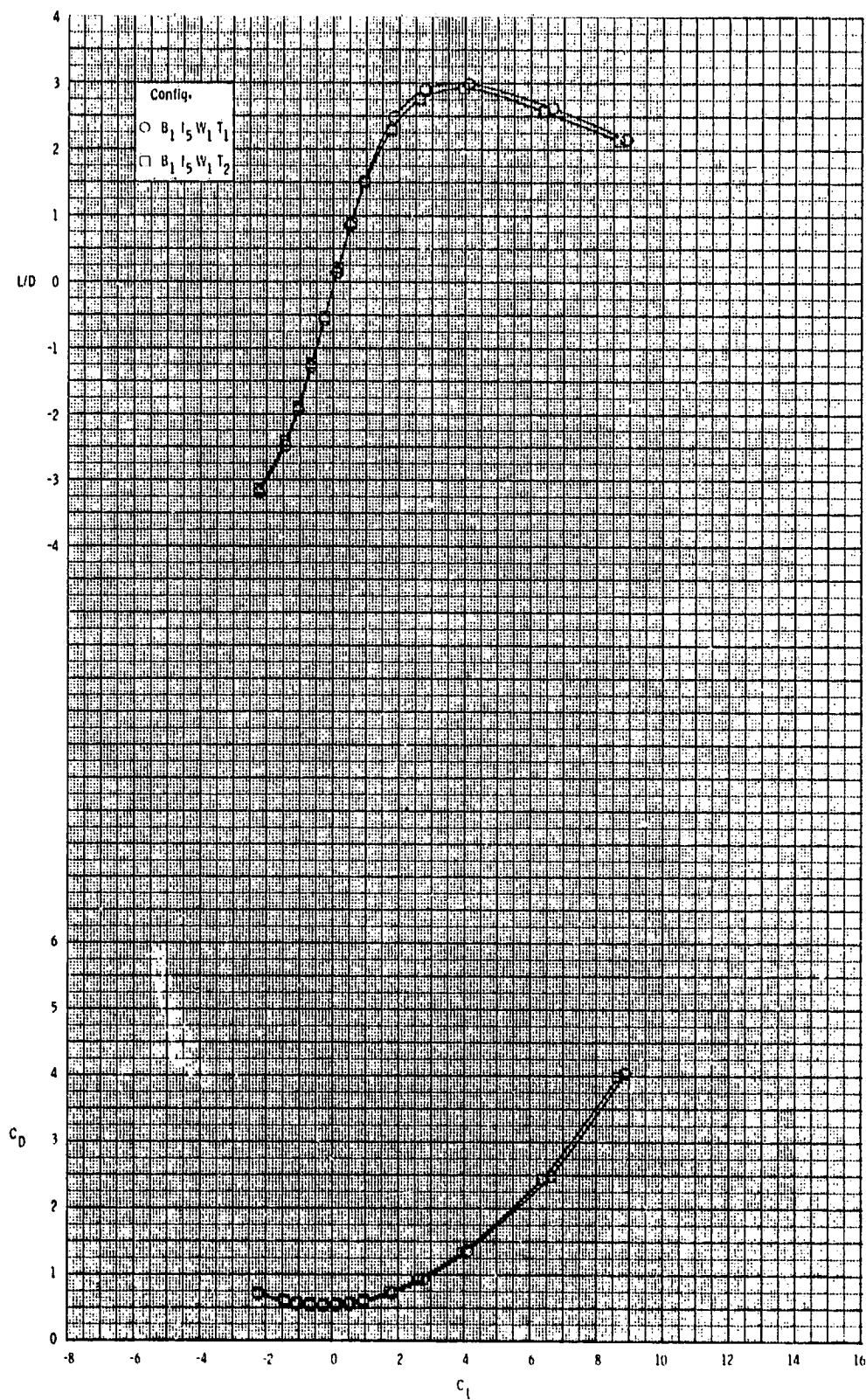
ORIGINAL PAGE 13
OF POOR QUALITY



(b) Continued.

Figure 19.- Continued.

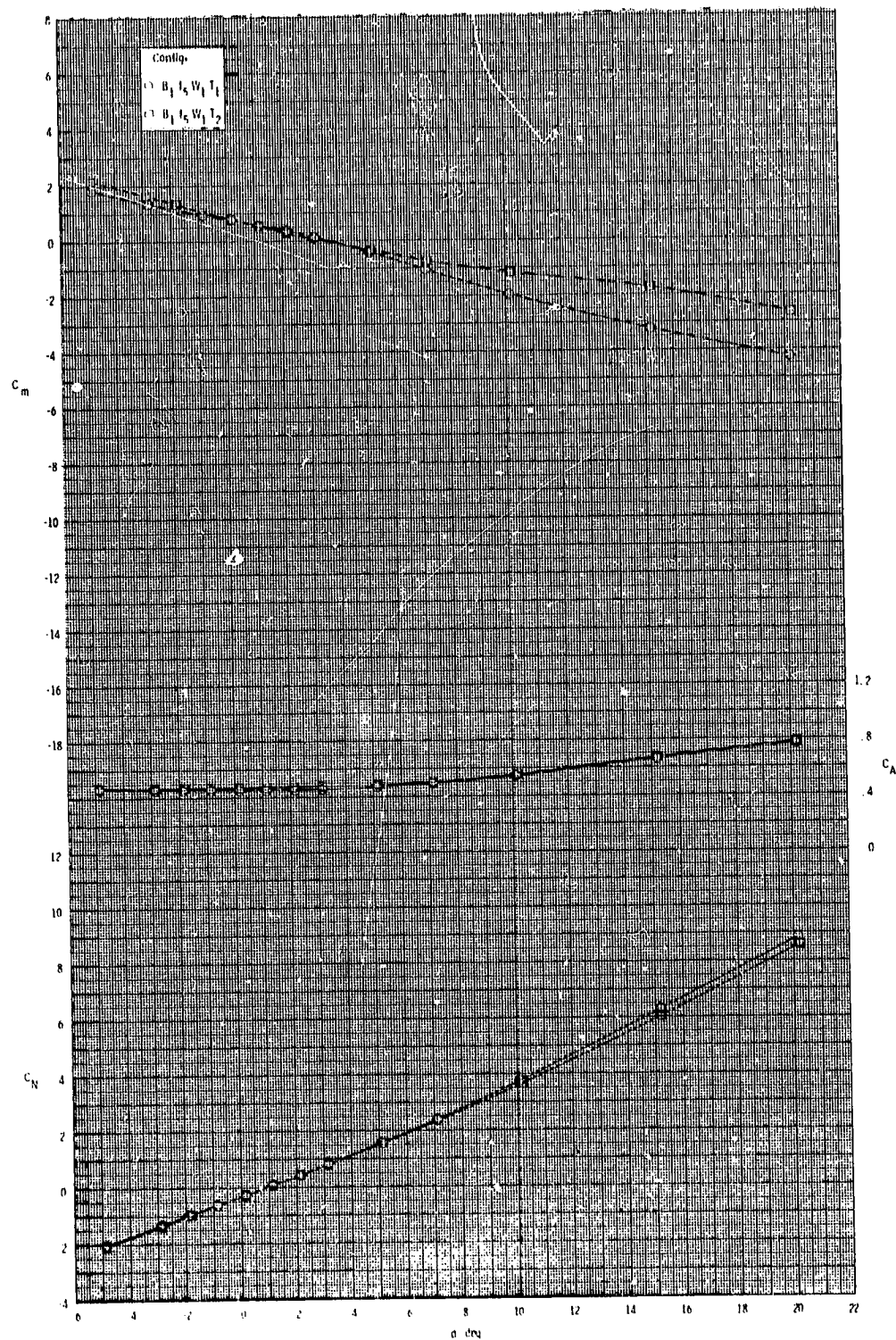
ORIGINAL PAGE IS
OF POOR QUALITY



(b) Concluded.

Figure 19.- Continued.

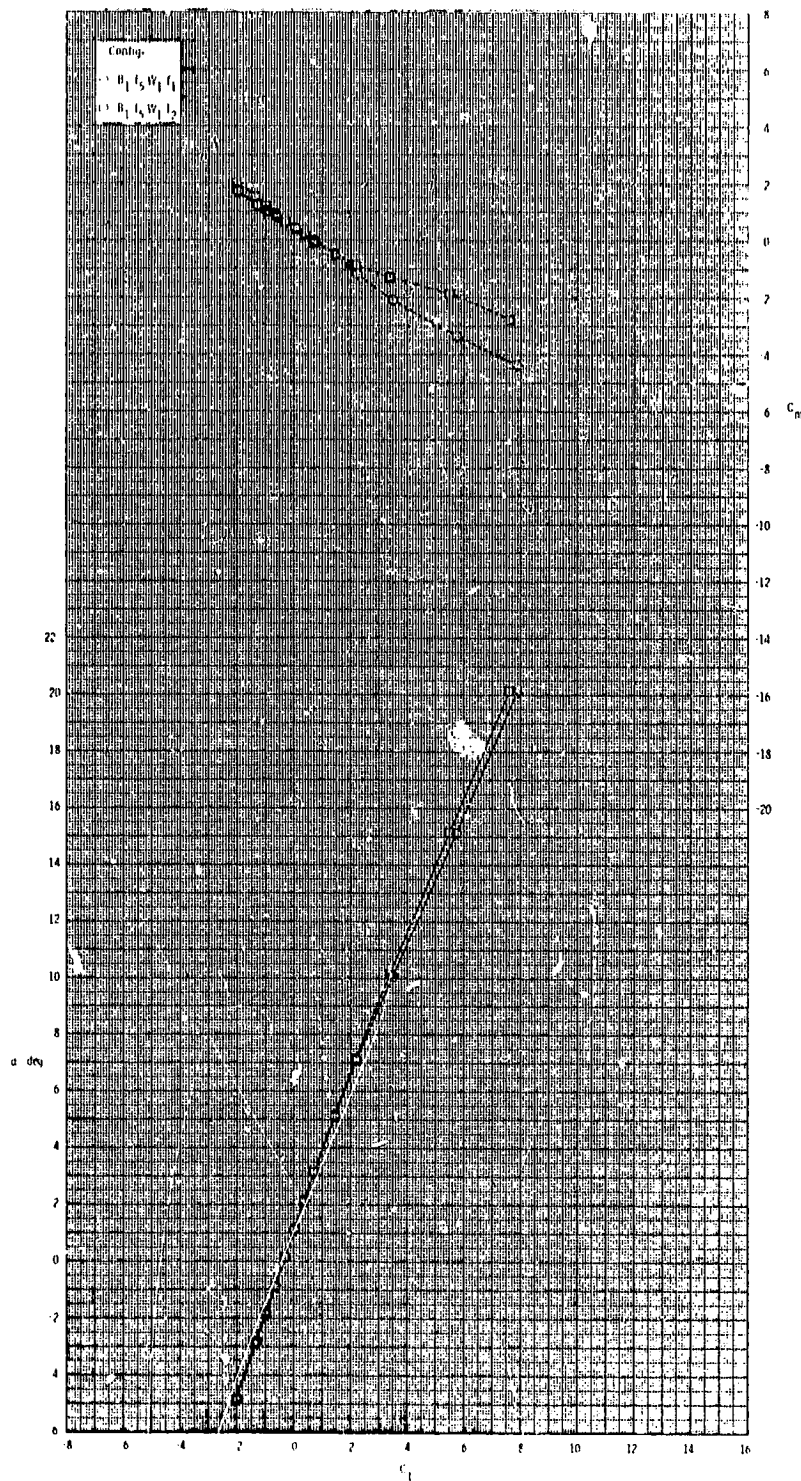
ORIGINAL PAGE IS
OF POOR QUALITY



(c) $M = 3.50$.

Figure 19.- Continued.

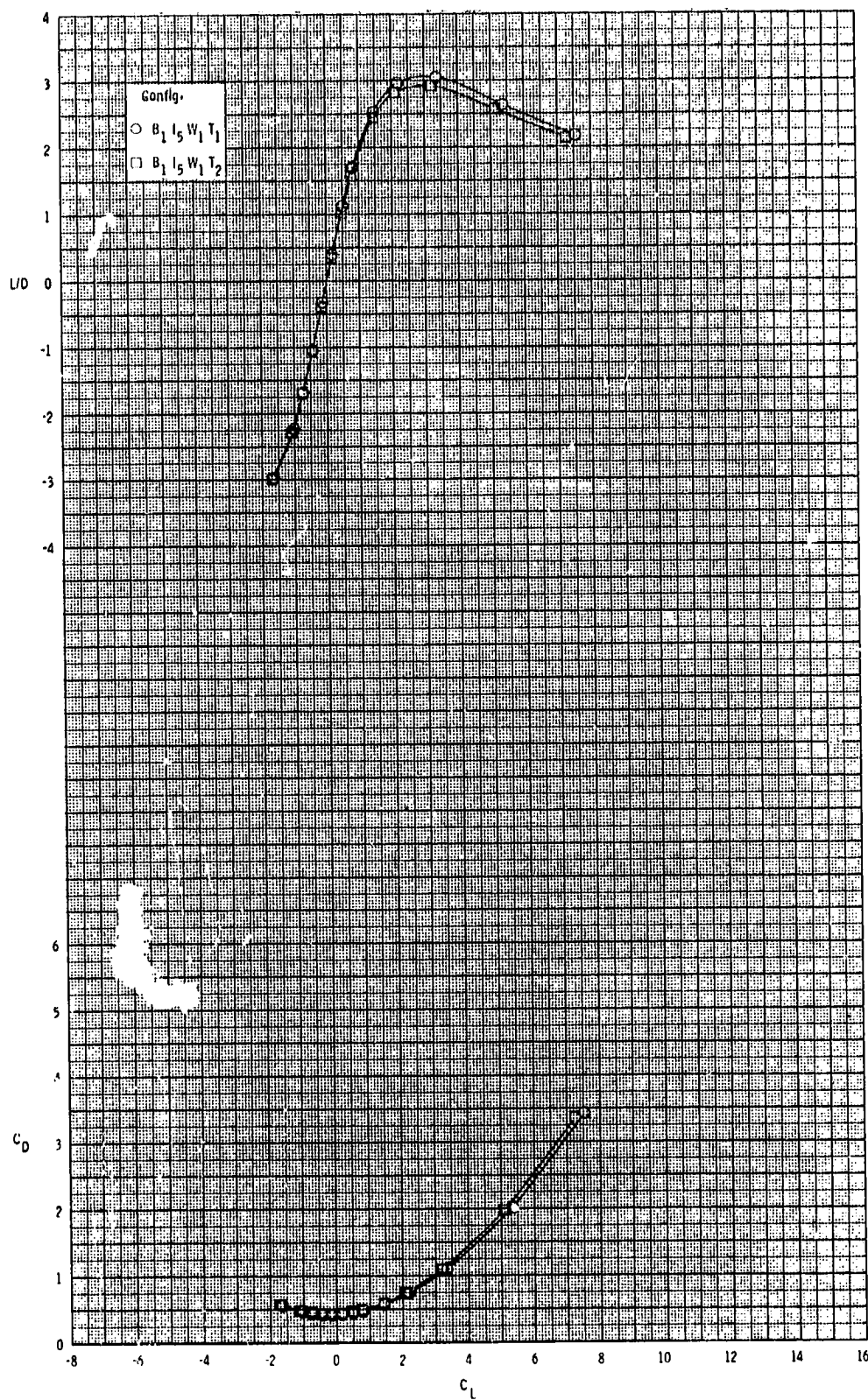
ORIGINAL PAGE IS
OF POOR QUALITY



(c) Continued.

Figure 19.- Continued.

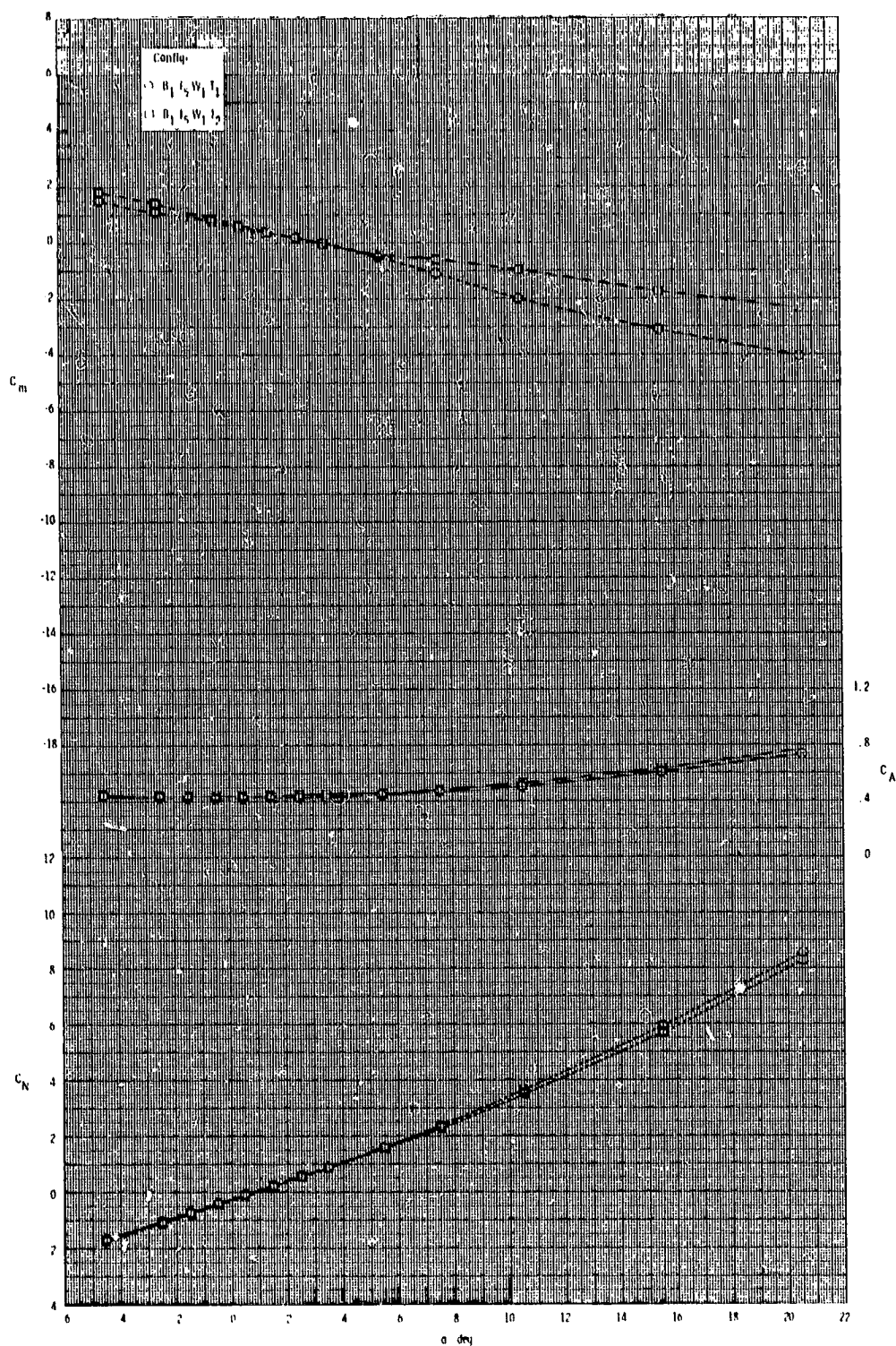
ORIGINAL PAGE IS
OF POOR QUALITY



(c) Concluded.

Figure 19.- Continued.

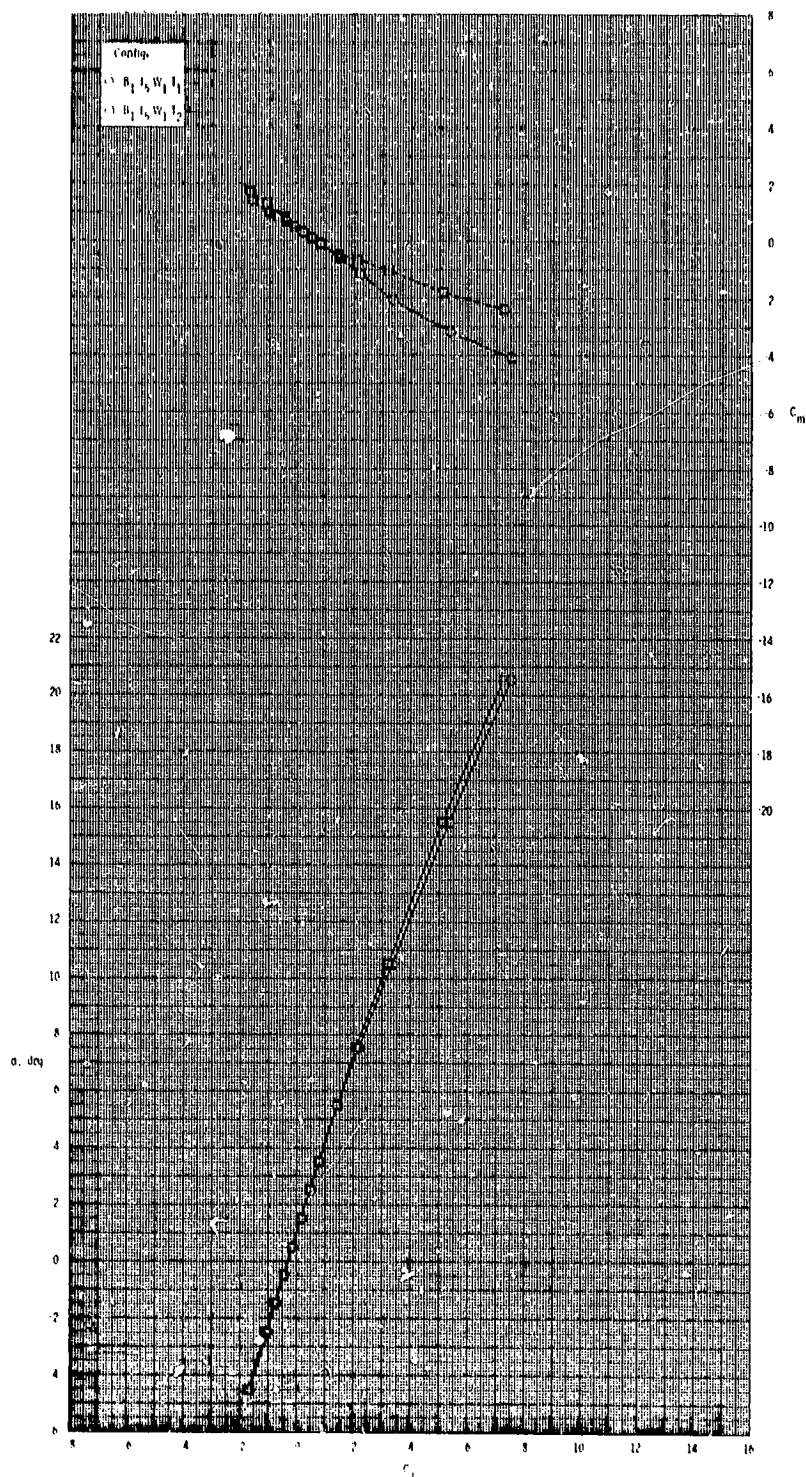
ORIGINAL PAGE IS
OF POOR QUALITY



(d) $M = 3.95$.

Figure 19.- Continued.

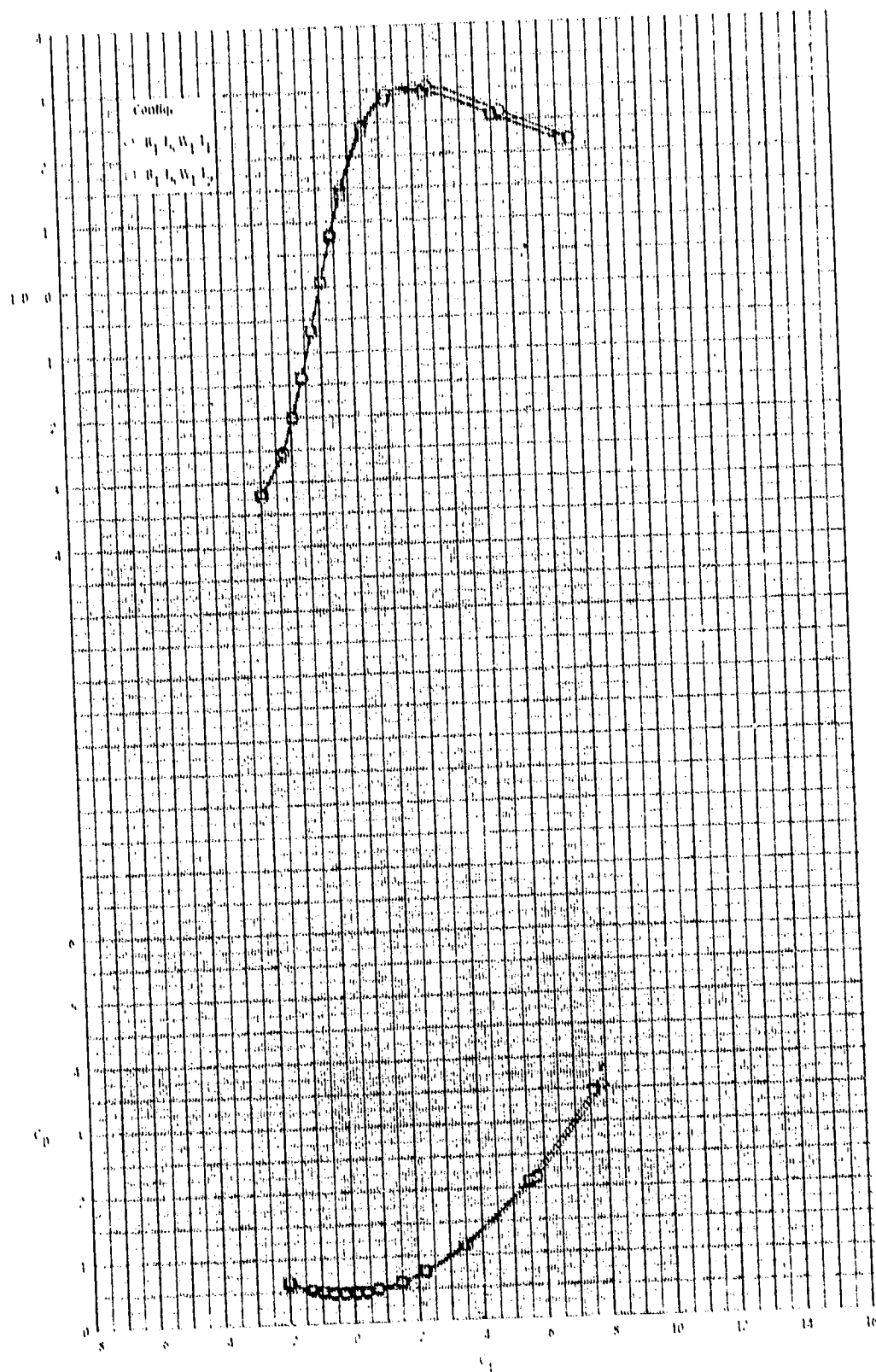
ORIGINAL PAGE IS
OF POOR QUALITY



(d) Continued.

Figure 19.- Continued.

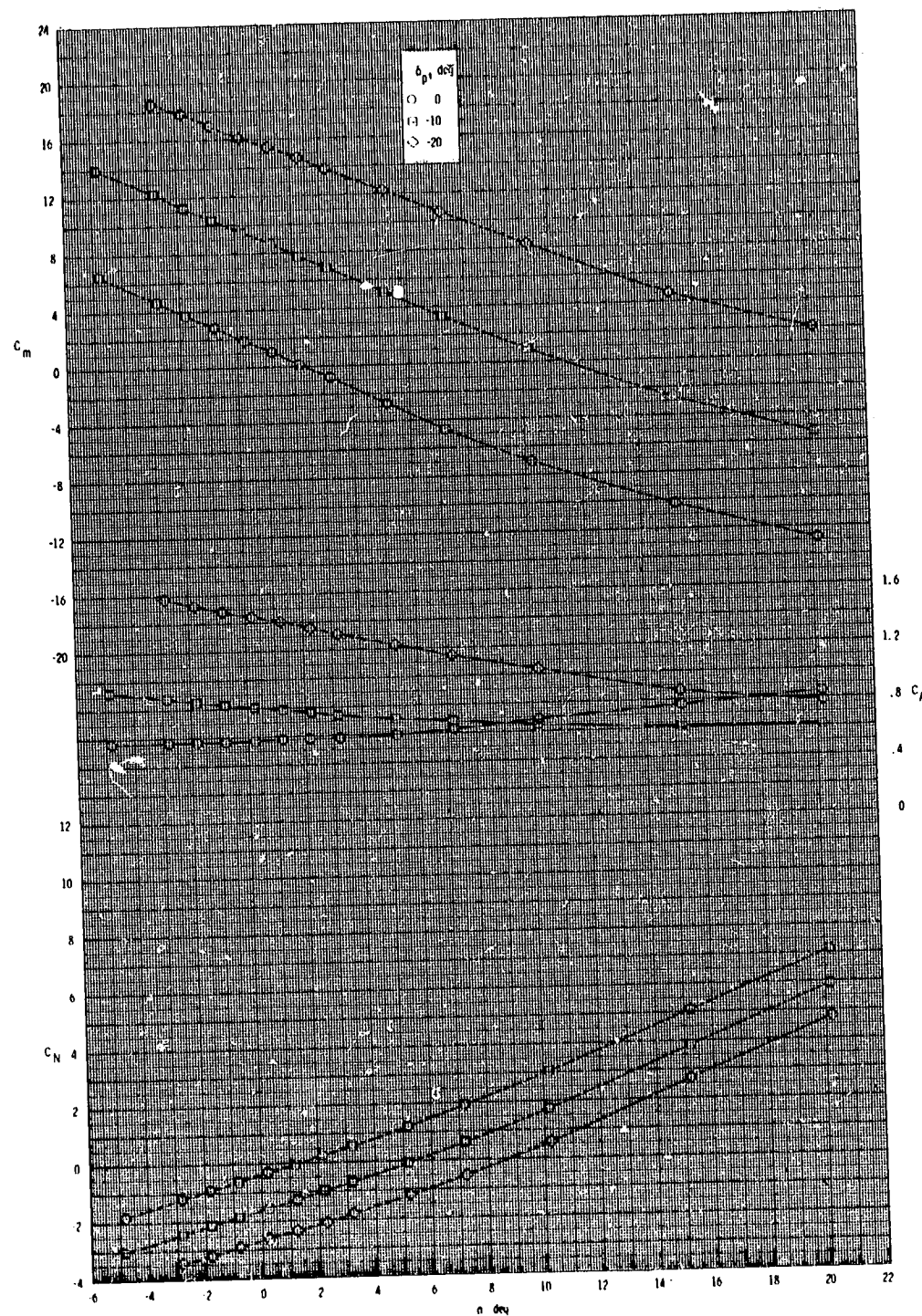
ORIGINAL PAGE IS
OF POOR QUALITY



(d) Concluded.

Figure 19.- Concluded.

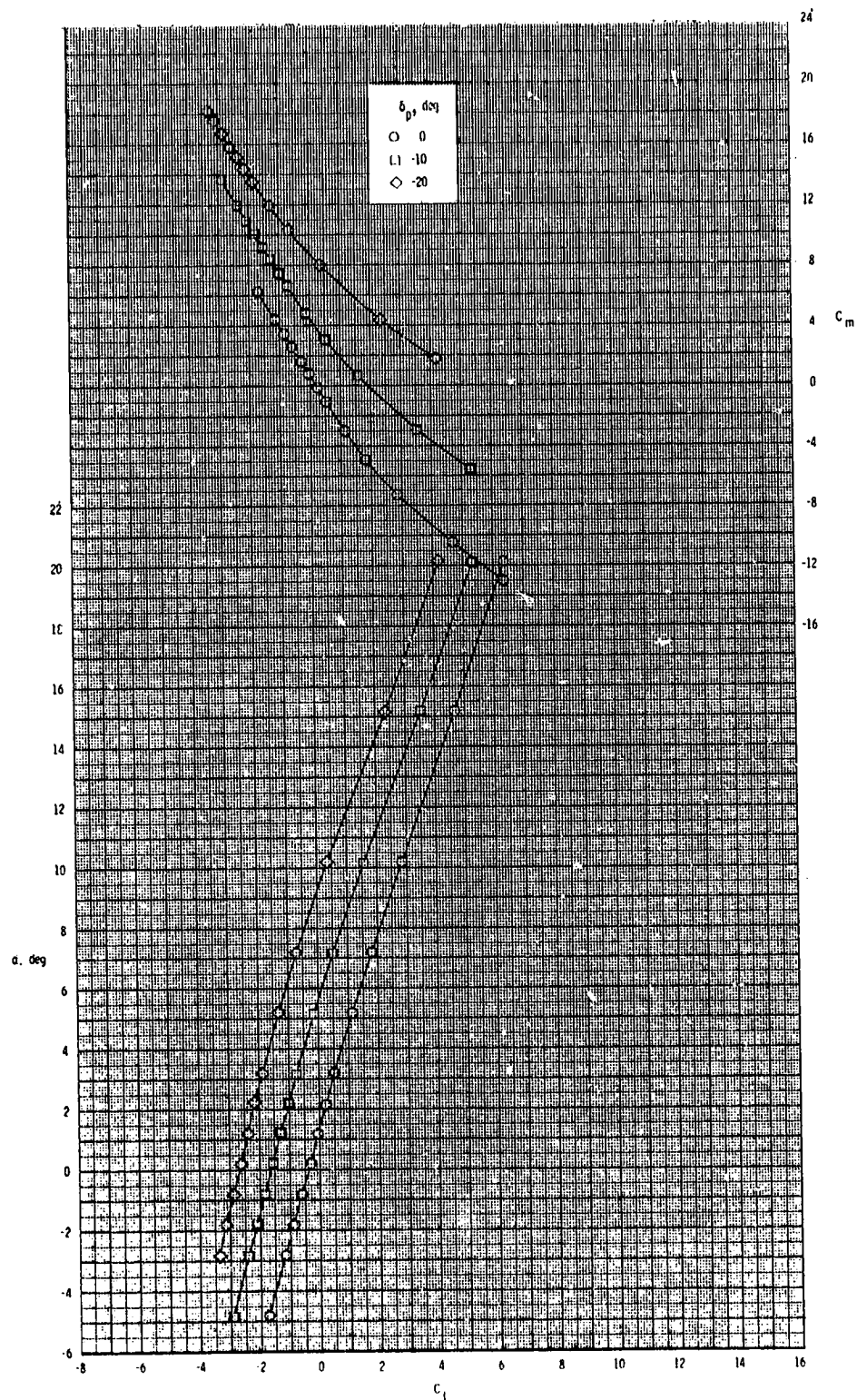
ORIGINAL PAGE IS
OF POOR QUALITY



(a) $M = 2.50$.

Figure 20.- Pitch-control effectiveness of configuration B₁I₅T₁.

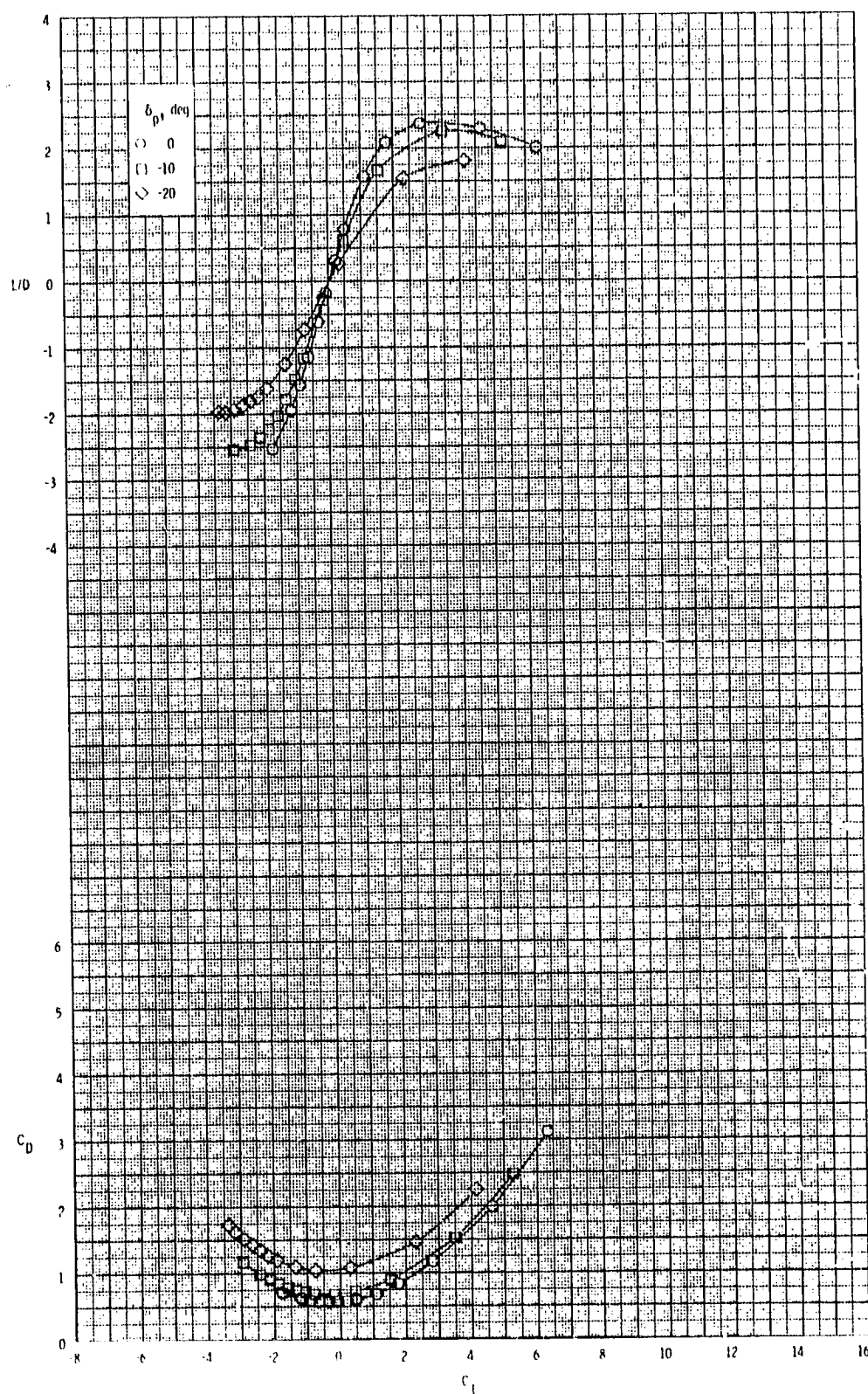
ORIGINAL PAGE IS
OF POOR QUALITY



(a) Continued.

Figure 20.- Continued.

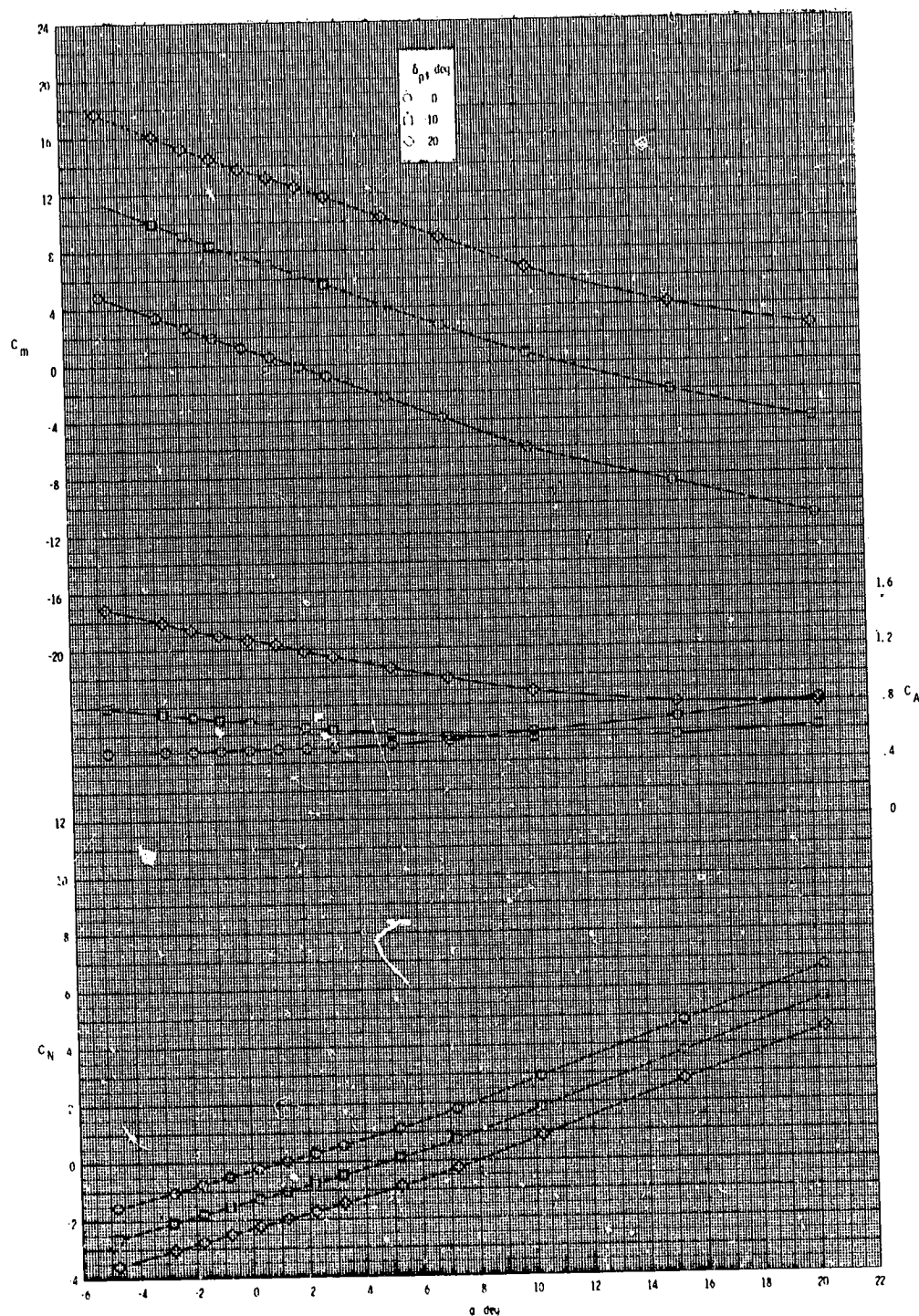
ORIGINAL PAGE IS
OF POOR QUALITY



(a) Concluded.

Figure 20.- Continued.

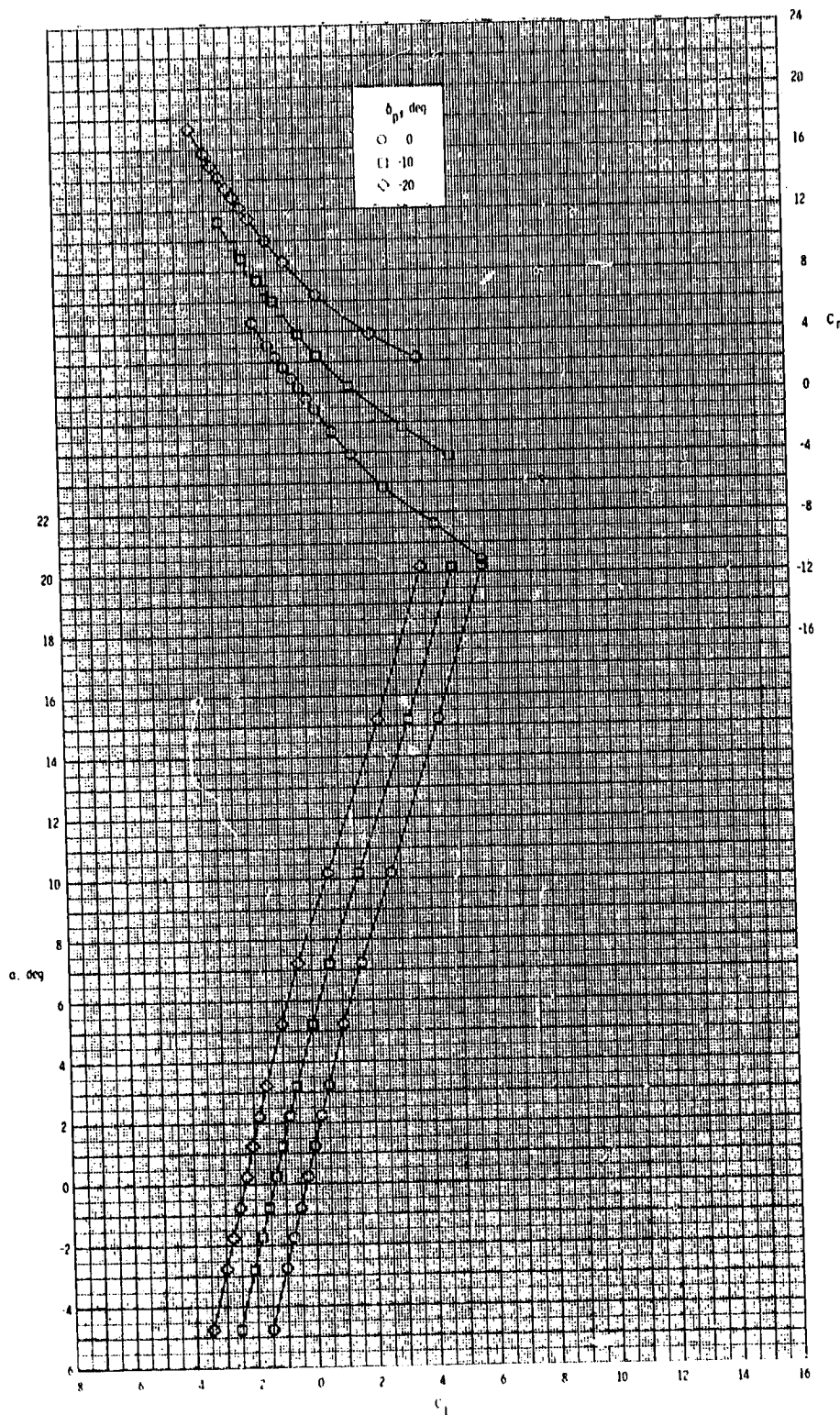
ORIGINAL PAGE IS
OF POOR QUALITY



(b) $M = 2.95$.

Figure 20.- Continued.

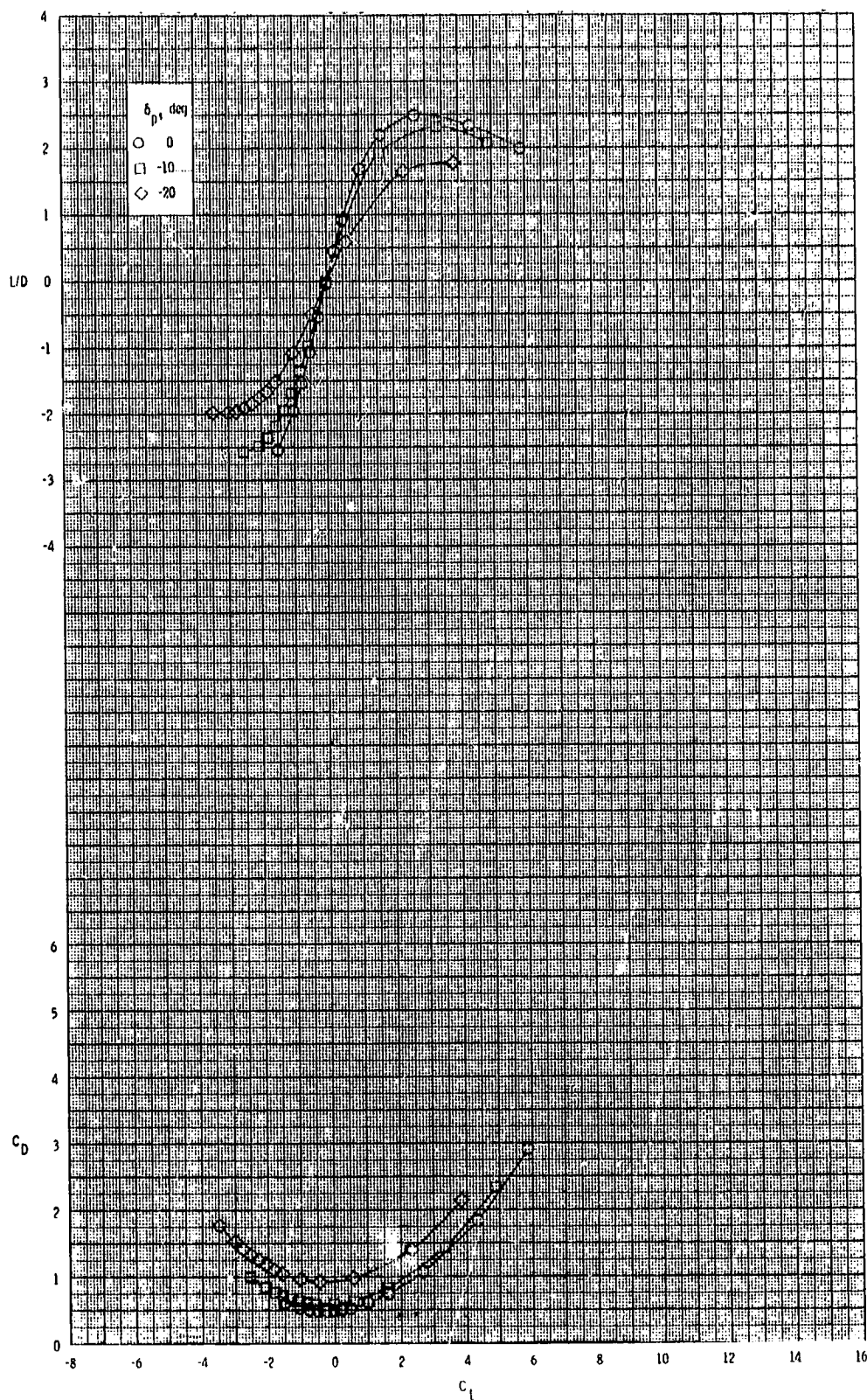
ORIGINAL PAGE IS
OF POOR QUALITY



(b) Continued.

Figure 20.- Continued.

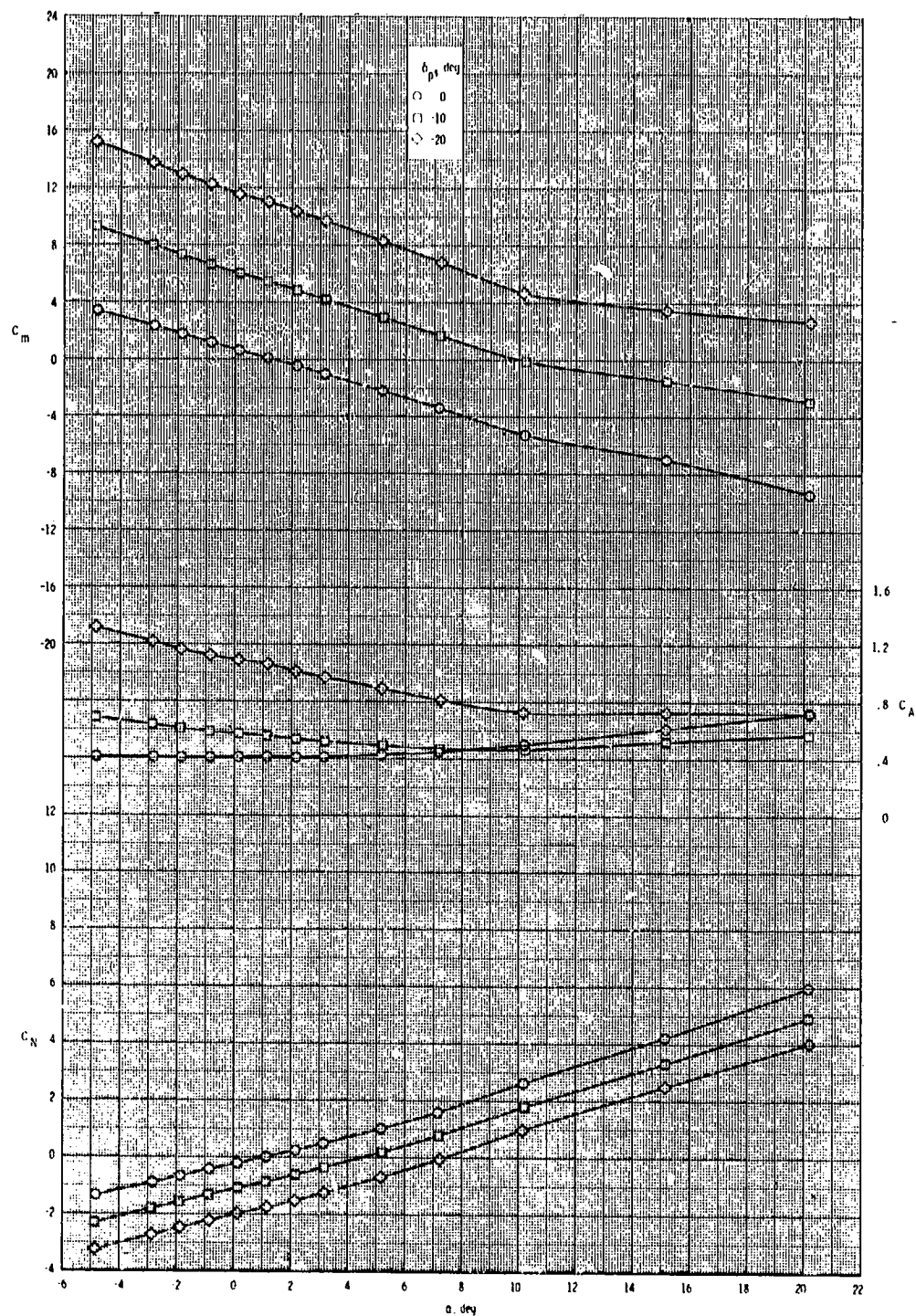
ORIGINAL PAGE IS
OF POOR QUALITY



(b) Concluded.

Figure 20.- Continued.

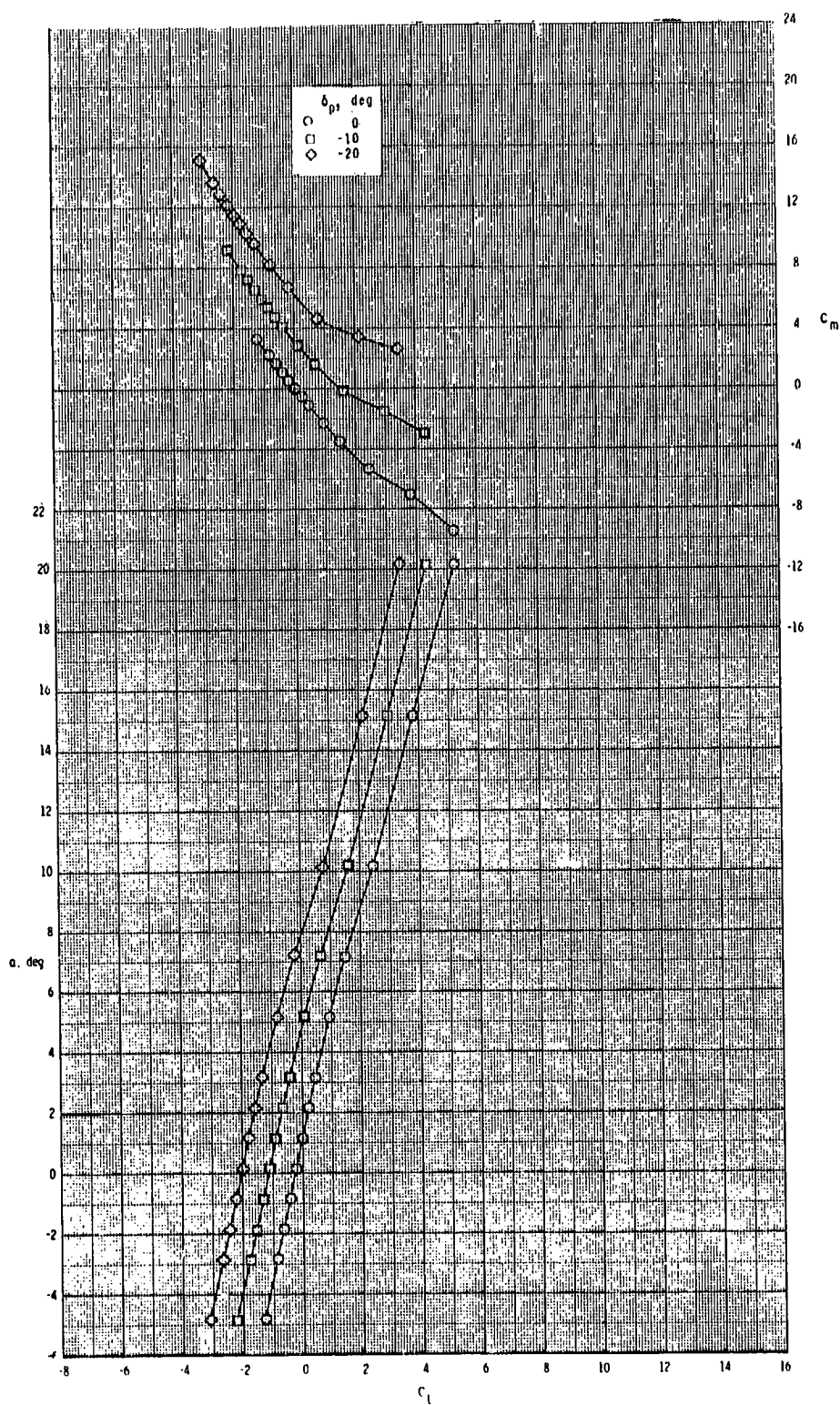
ORIGINAL PAGE IS
OF POOR QUALITY



(c) $M = 3.50$.

Figure 20.- Continued.

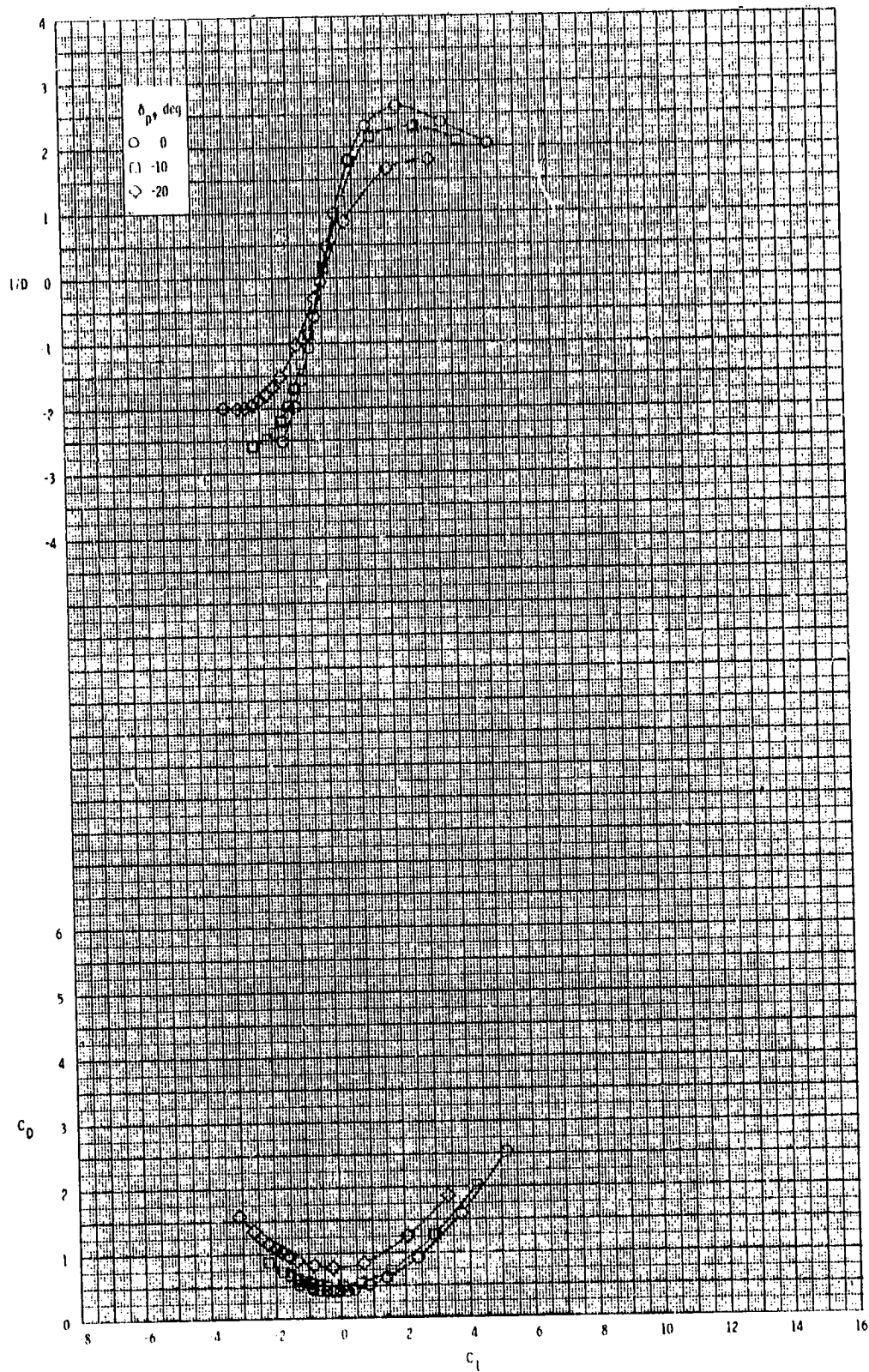
ORIGINAL PAGE IS
OF POOR QUALITY



(c) Continued.

Figure 20.- Continued.

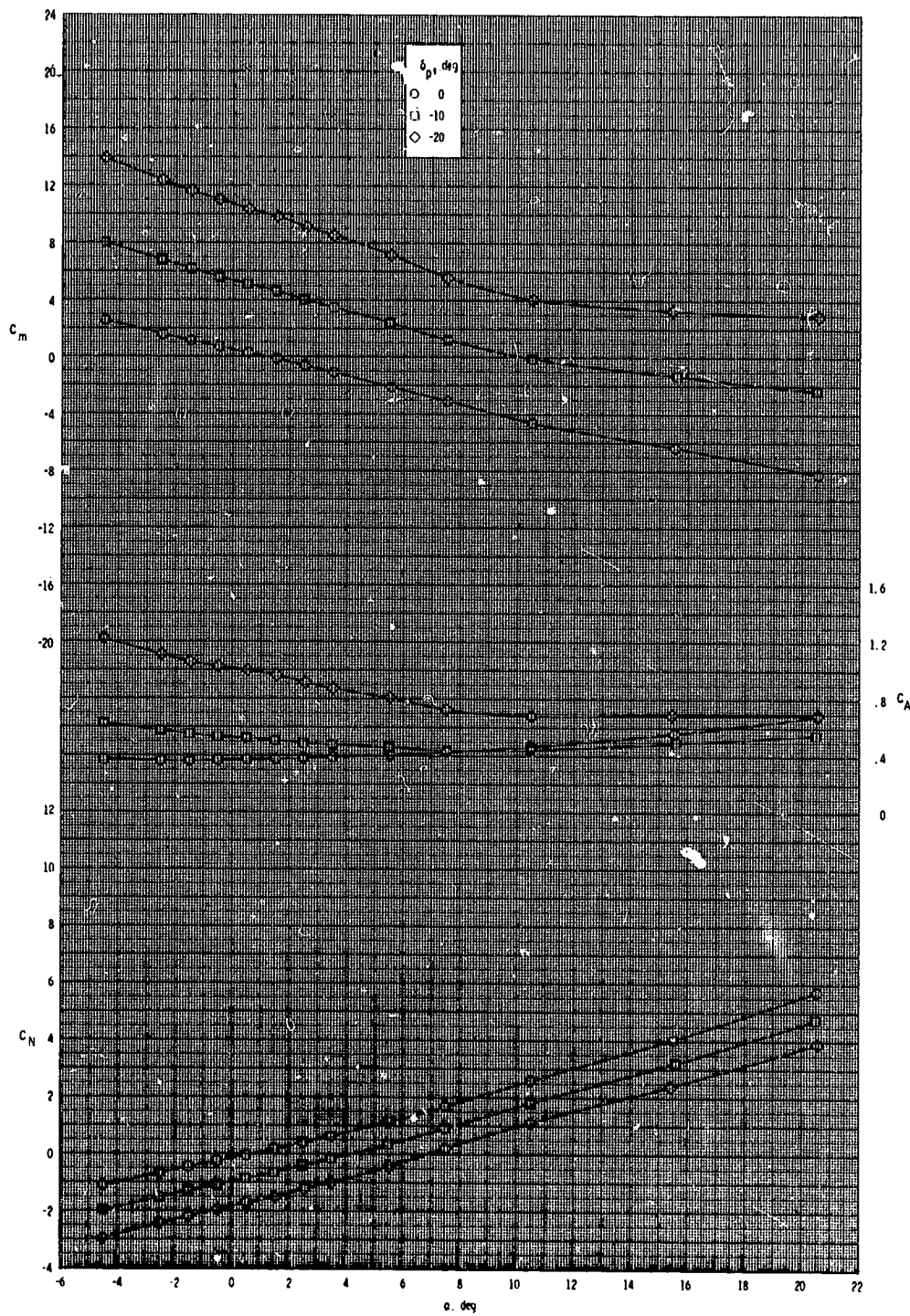
ORIGINAL PAGE IS
OF POOR QUALITY



(c) Concluded.

Figure 20.- Continued.

ORIGINAL PAGE IS
OF POOR QUALITY

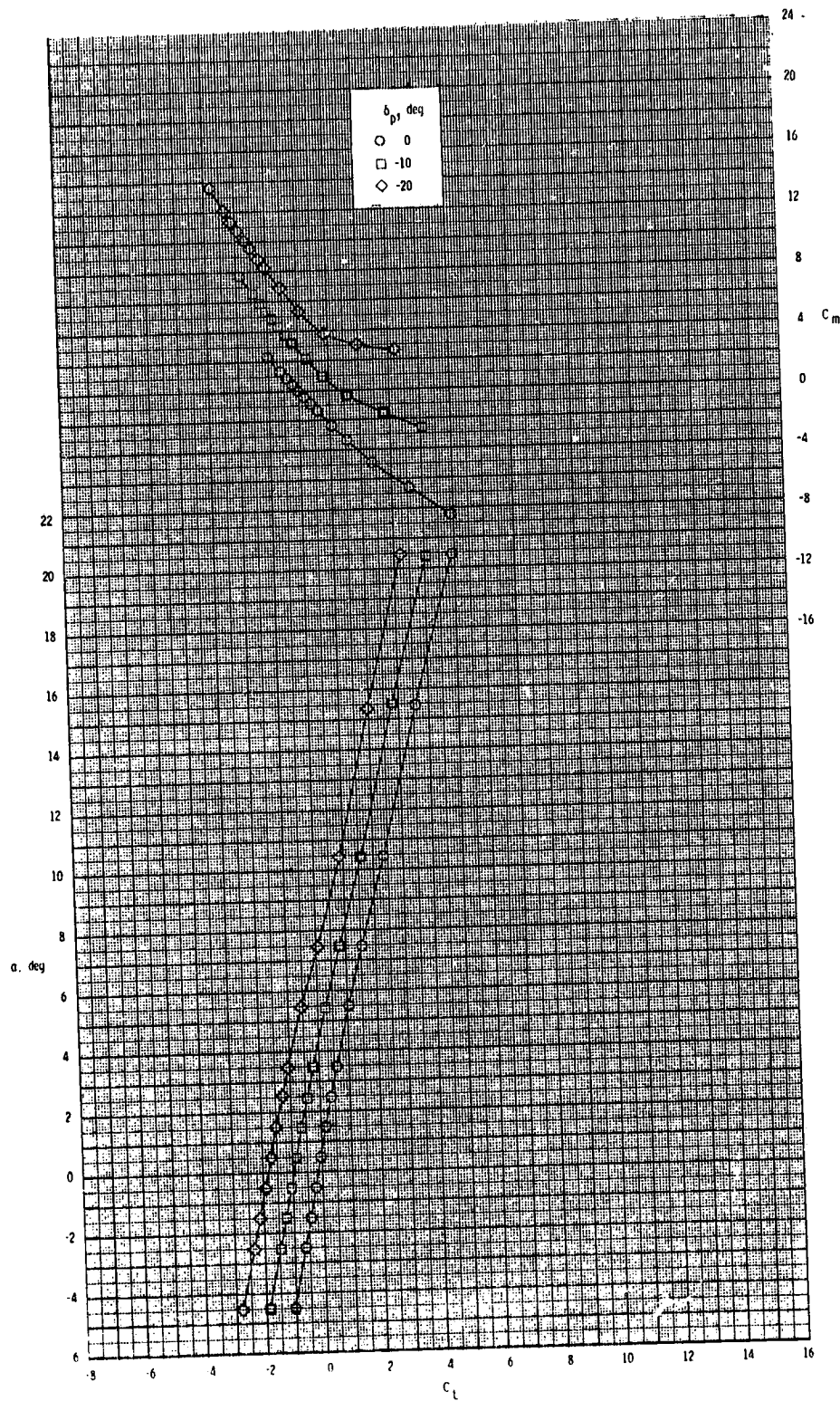


(d) $M = 3.95$.

Figure 20.- Continued.

C-3

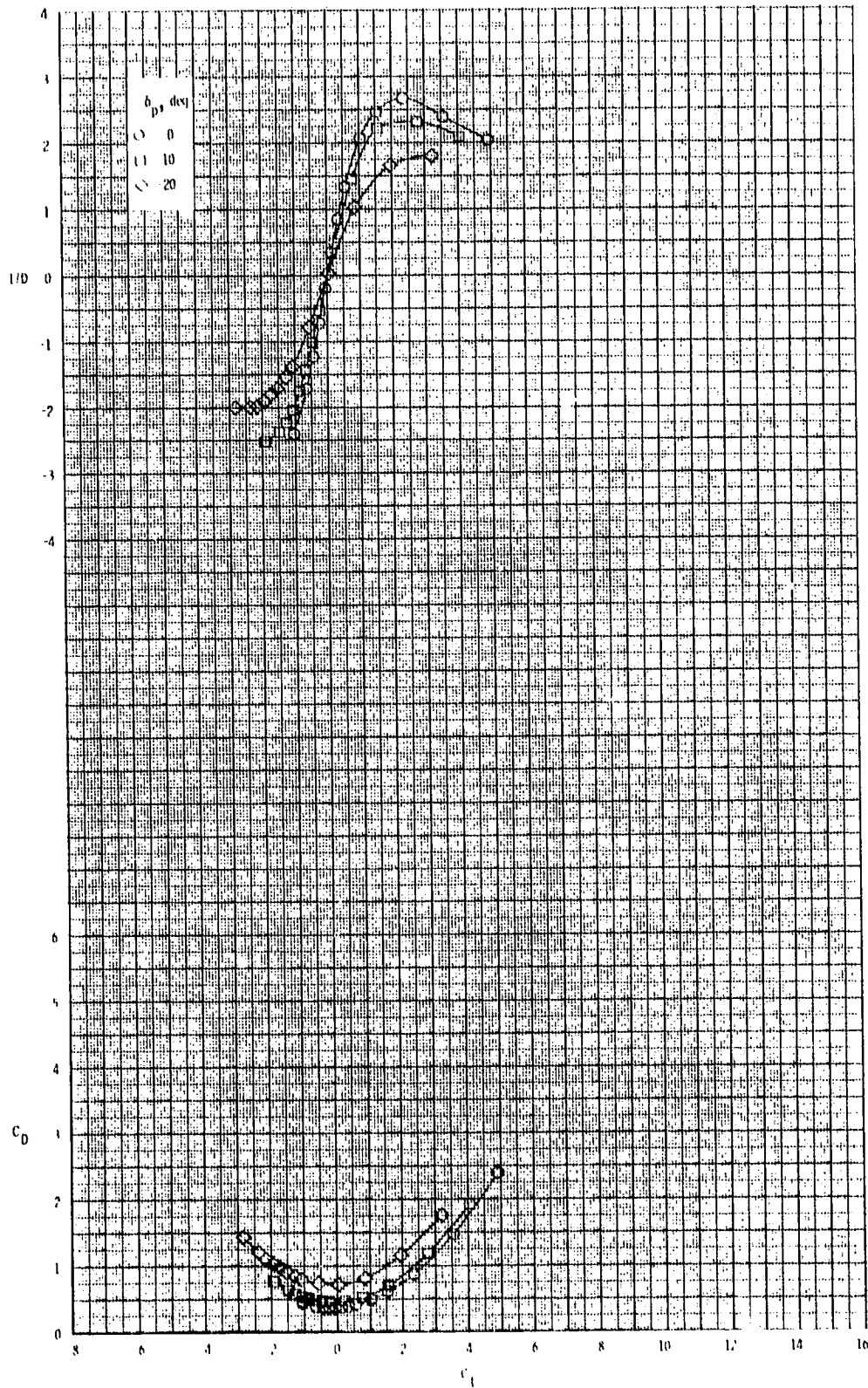
ORIGINAL PAGE IS
OF POOR QUALITY



(d) Continued.

Figure 20.- Continued.

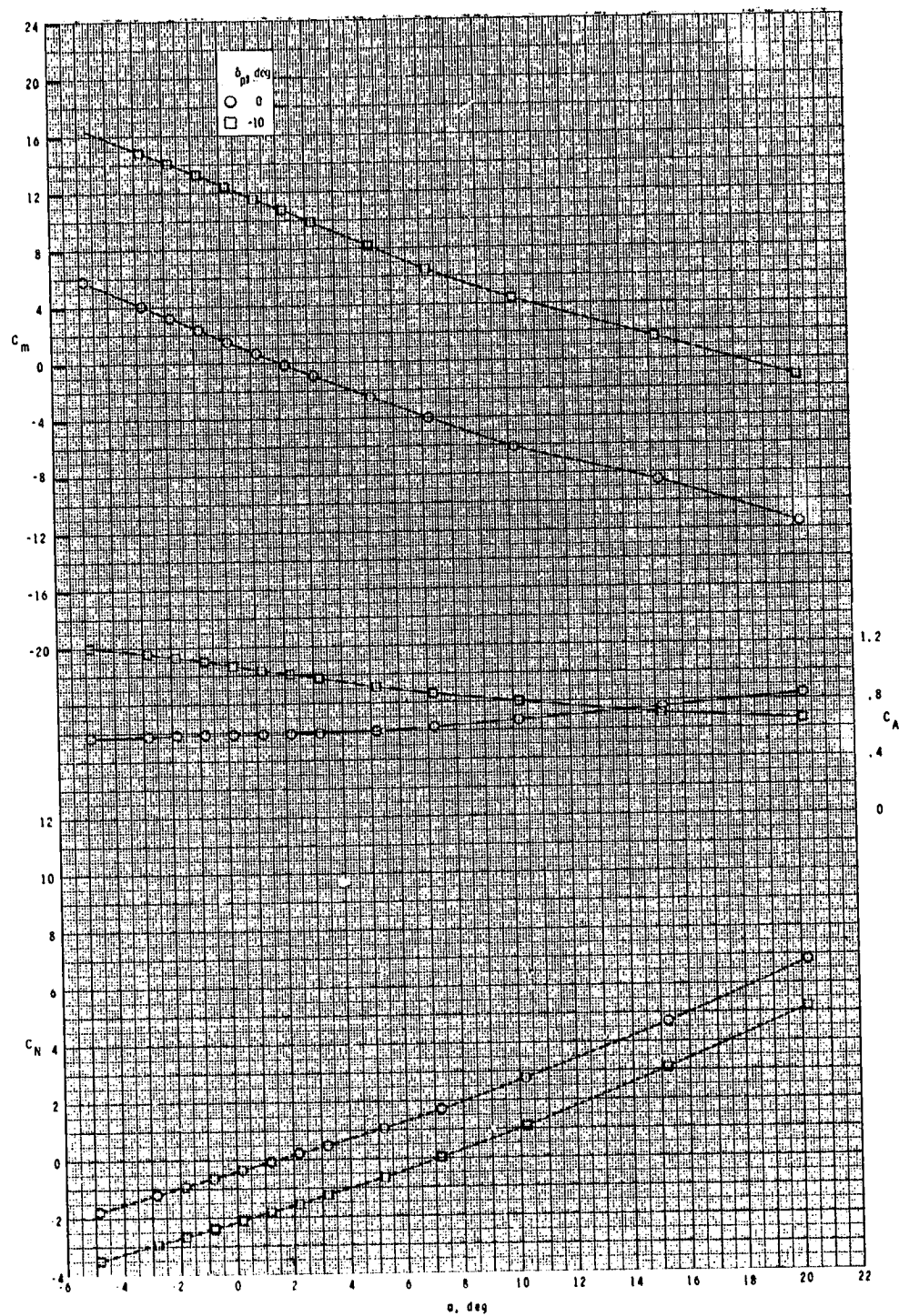
ORIGINAL PAGE IS
OF POOR QUALITY



(d) Concluded.

Figure 20.- Concluded.

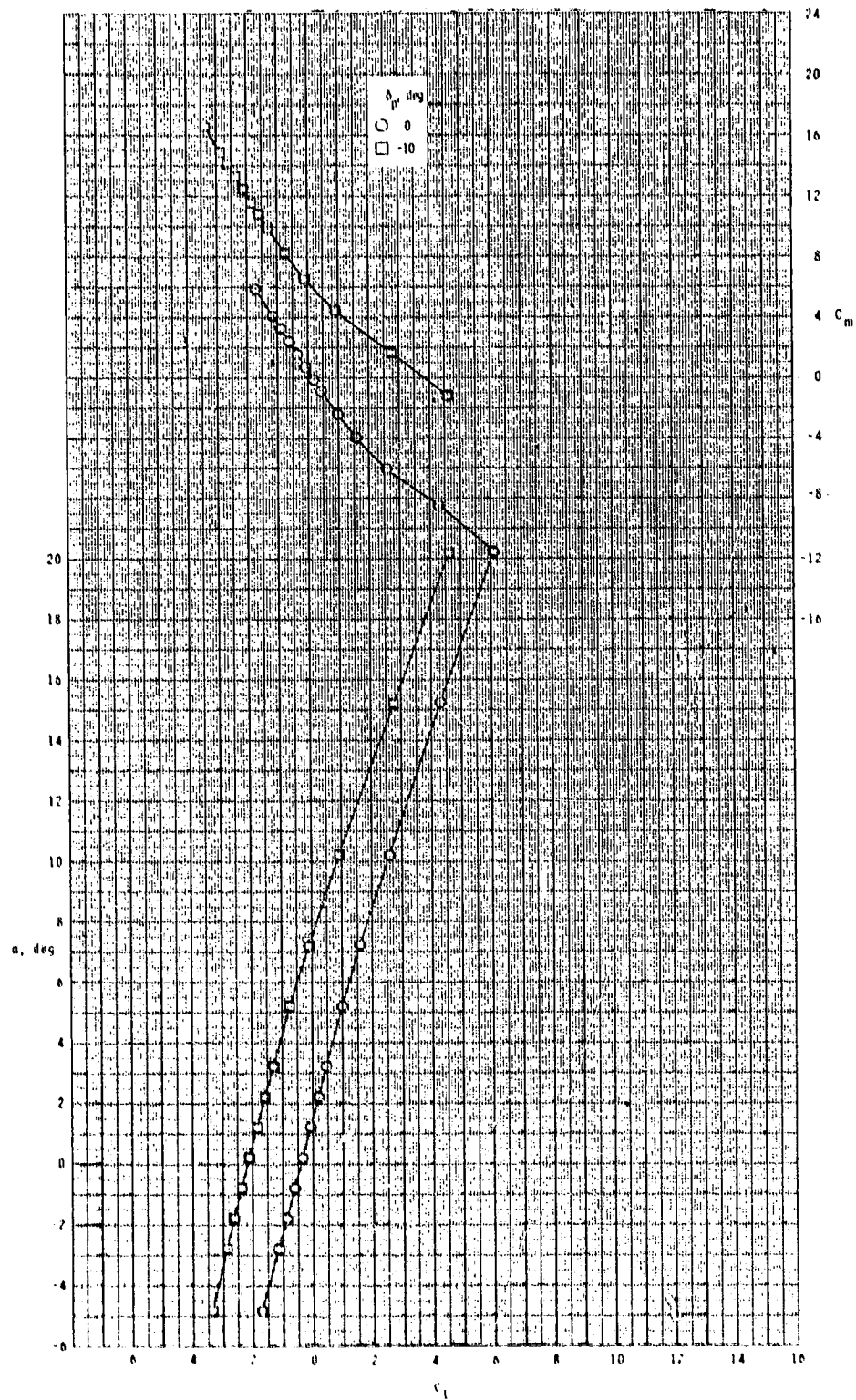
ORIGINAL PAGE IS
OF POOR QUALITY



(a) $M = 2.50$.

Figure 21.- Pitch-control effectiveness of configuration B₁I₅T₂.

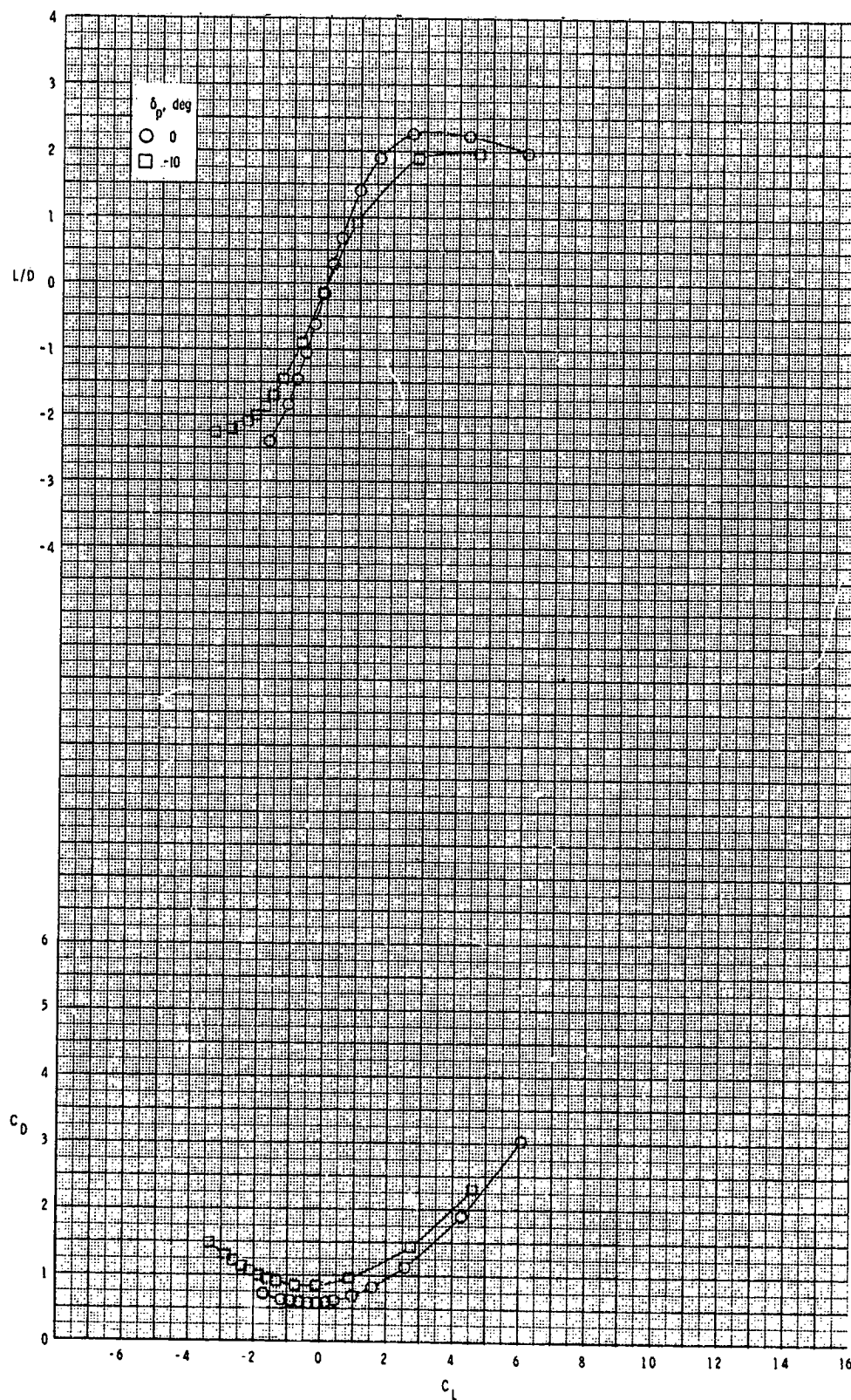
ORIGINAL PAGE IS
OF PGOR QUALITY



(a) Continued.

Figure 21.- Continued.

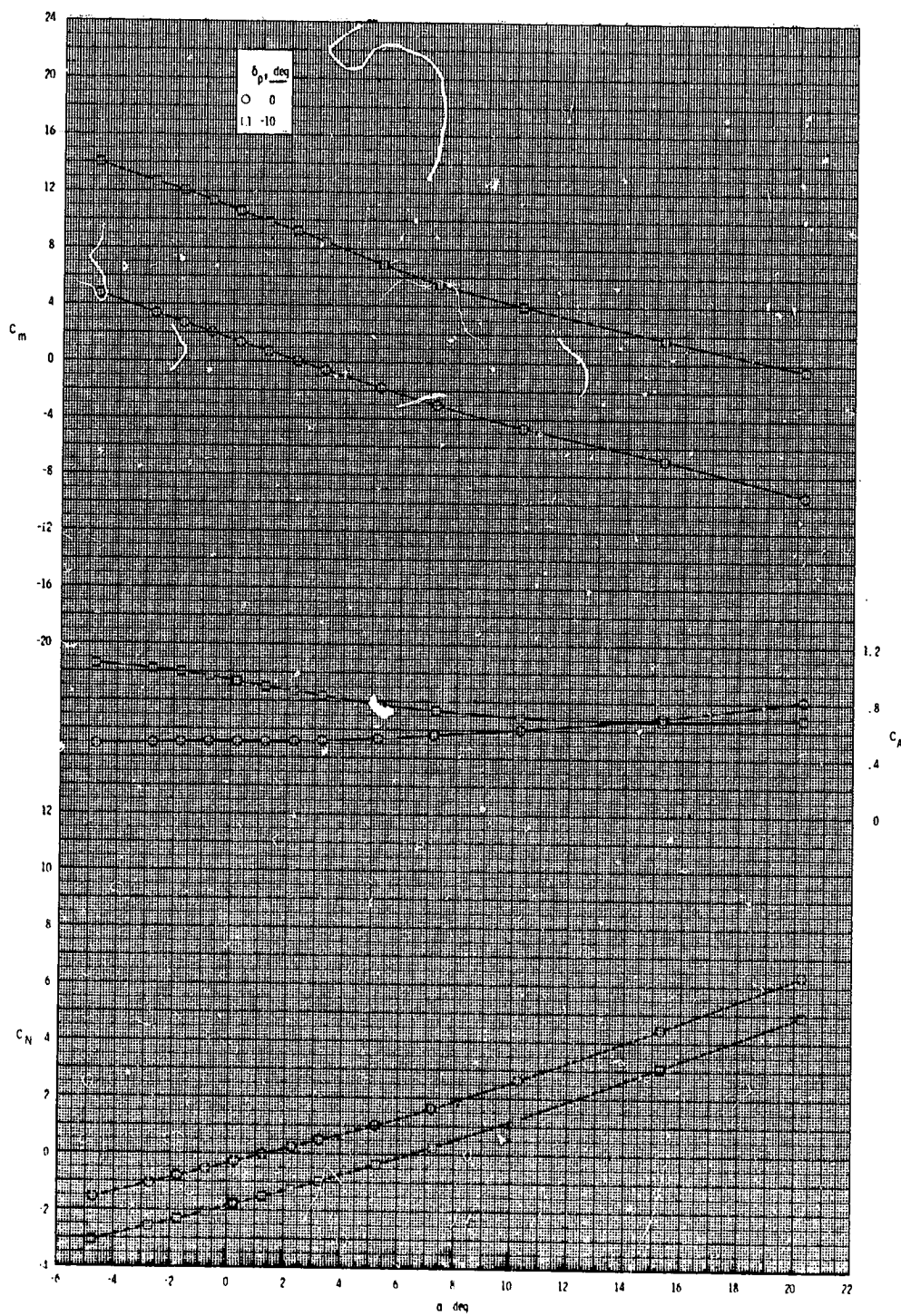
ORIGINAL PAGE IS
OF POOR QUALITY



(a) Concluded.

Figure 21.- Continued.

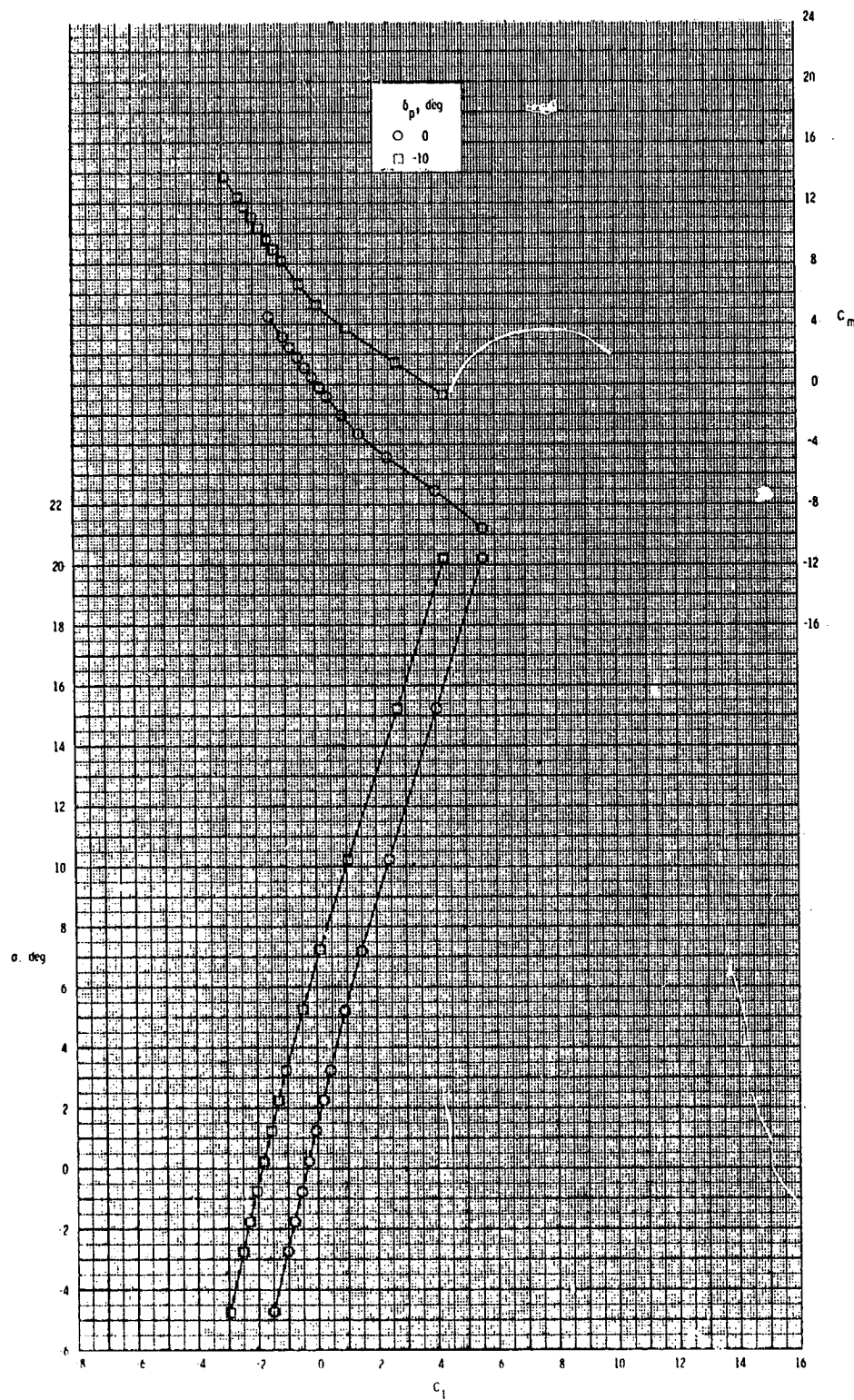
ORIGINAL PAGE IS
OF POOR QUALITY



(b) $M = 2.95$.

Figure 21.- Continued.

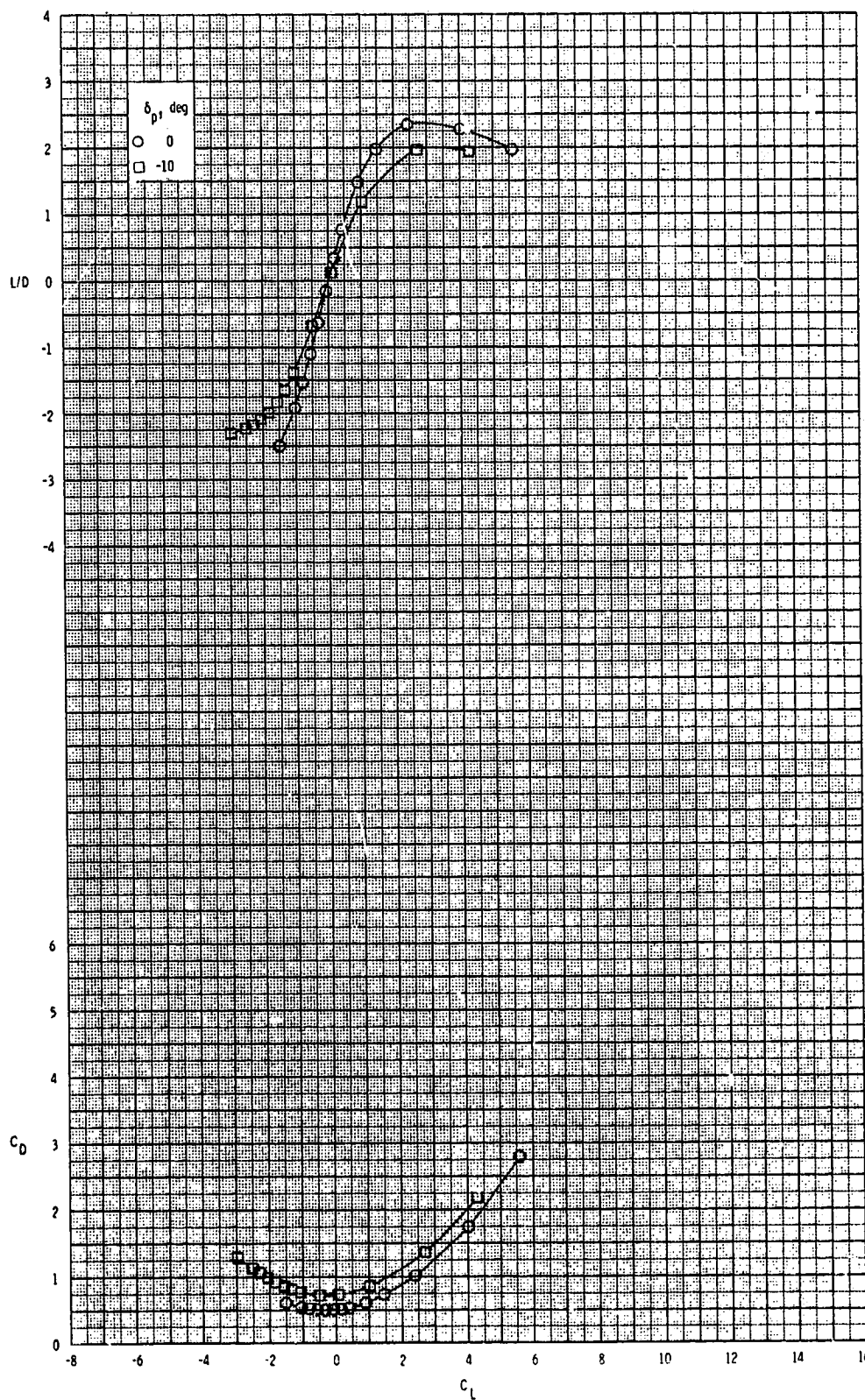
ORIGINAL PAGE IS
OF POOR QUALITY



(b) Continued.

Figure 21.- Continued.

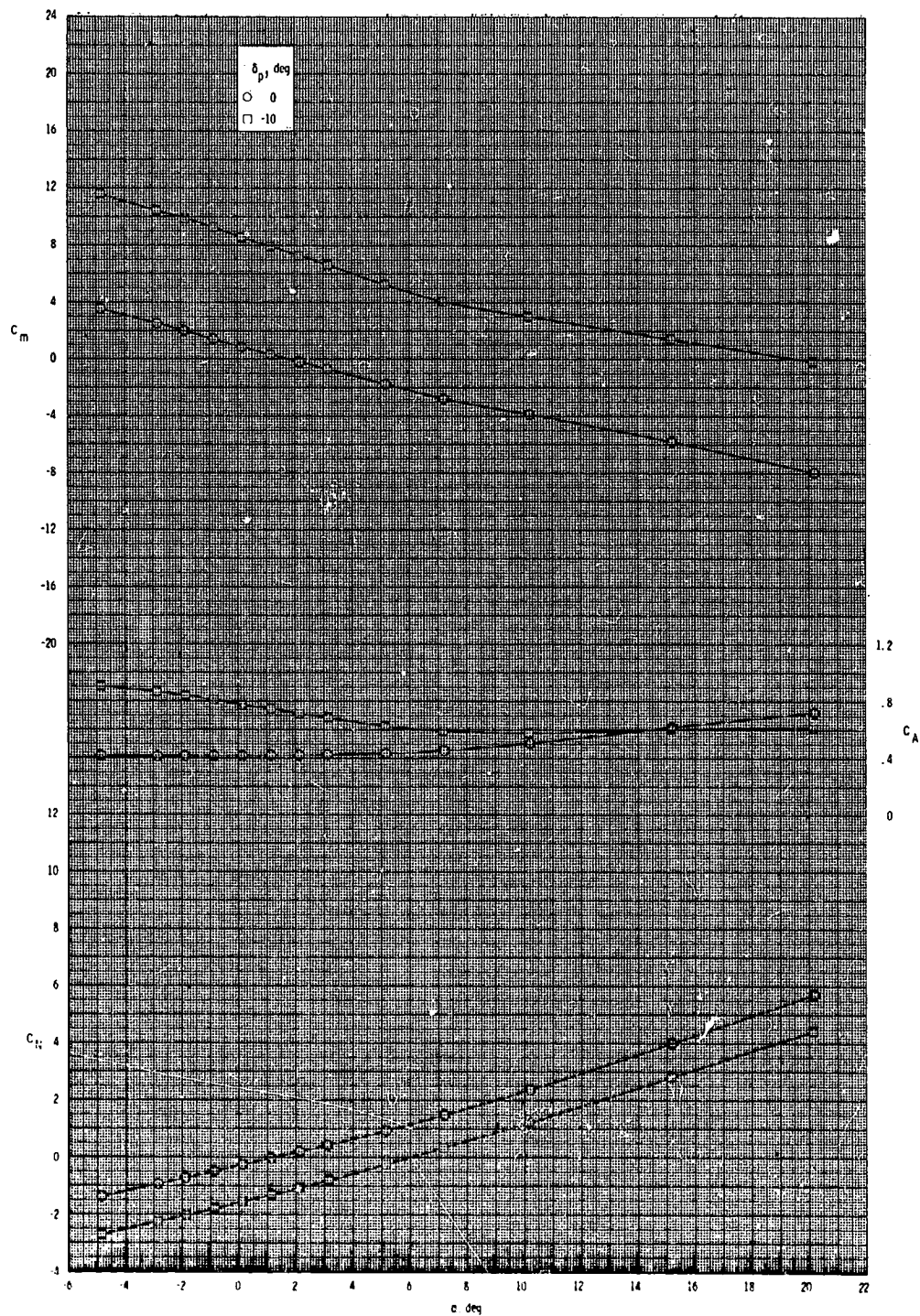
ORIGINAL PAGE IS
OF POOR QUALITY



(b) Concluded.

Figure 21.- Continued.

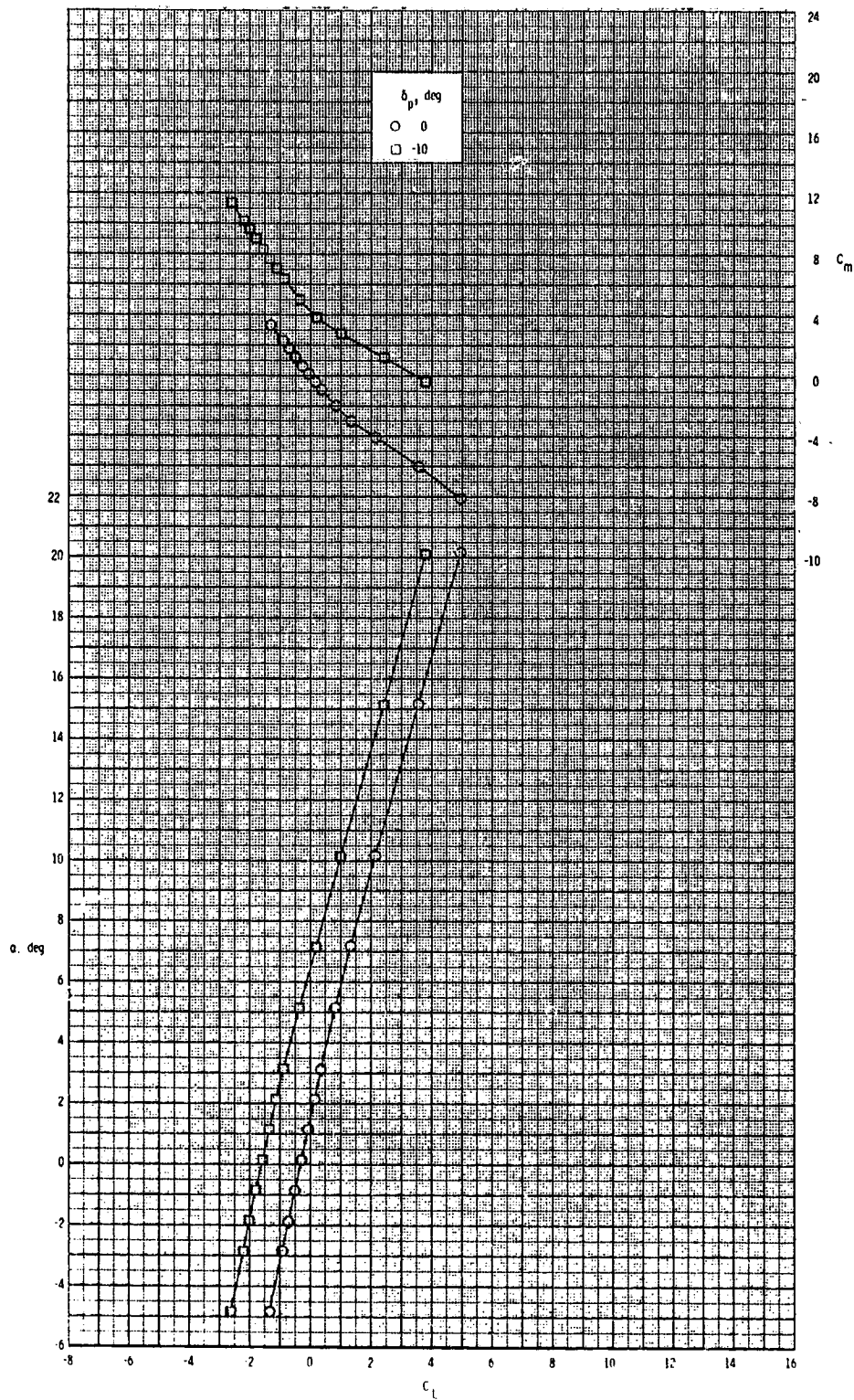
ORIGINAL PAGE IS
OF POOR QUALITY



(c) $M = 3.50$.

Figure 21.- Continued.

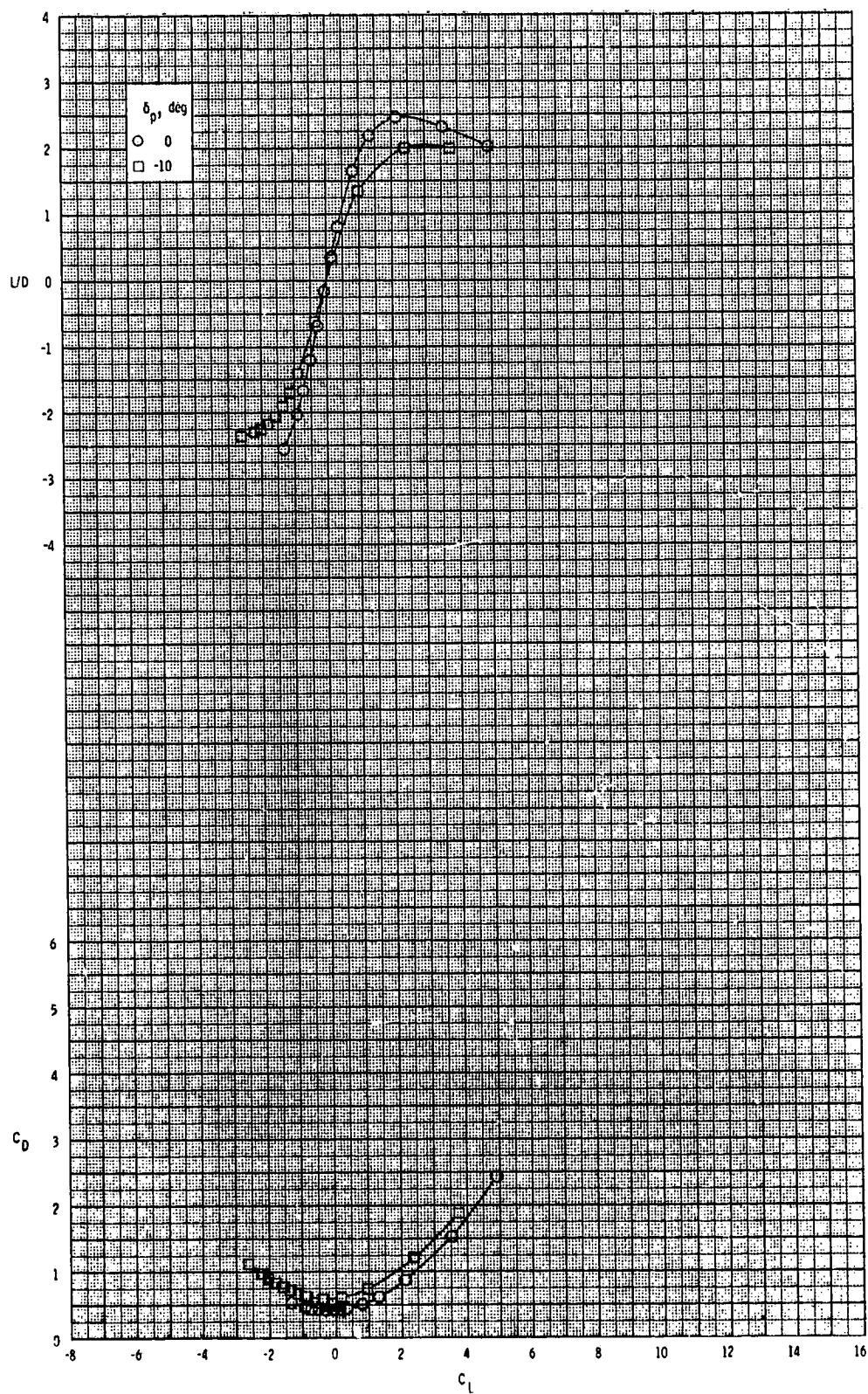
ORIGINAL PAGE IS
OF POOR QUALITY



(c) Continued.

Figure 21.- Continued.

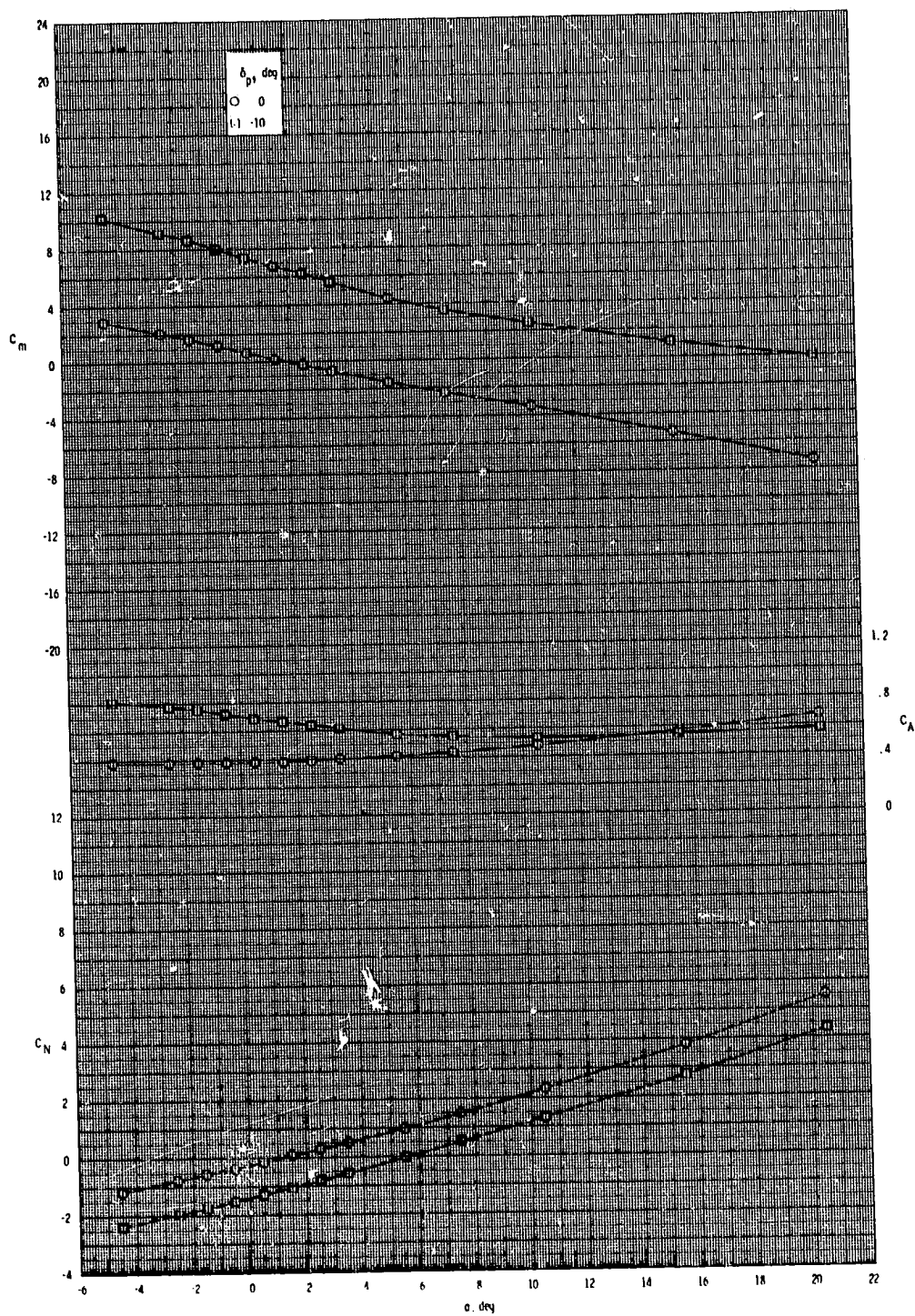
ORIGINAL PAGE 13
OF POOR QUALITY



(c) Concluded.

Figure 21.- Continued.

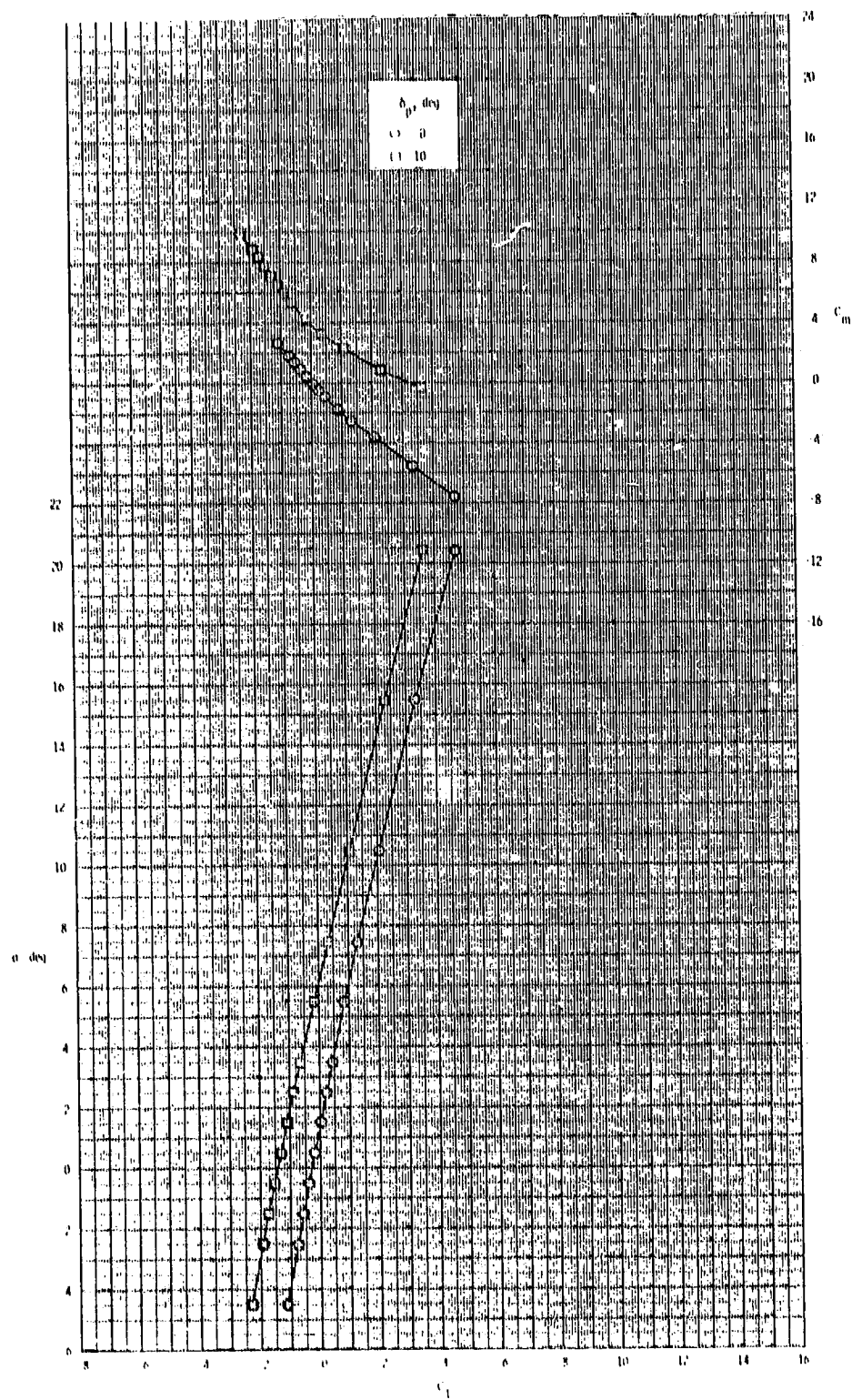
ORIGINAL PAGE IS
OF POOR QUALITY



(d) $M = 3.95$.

Figure 21.- Continued.

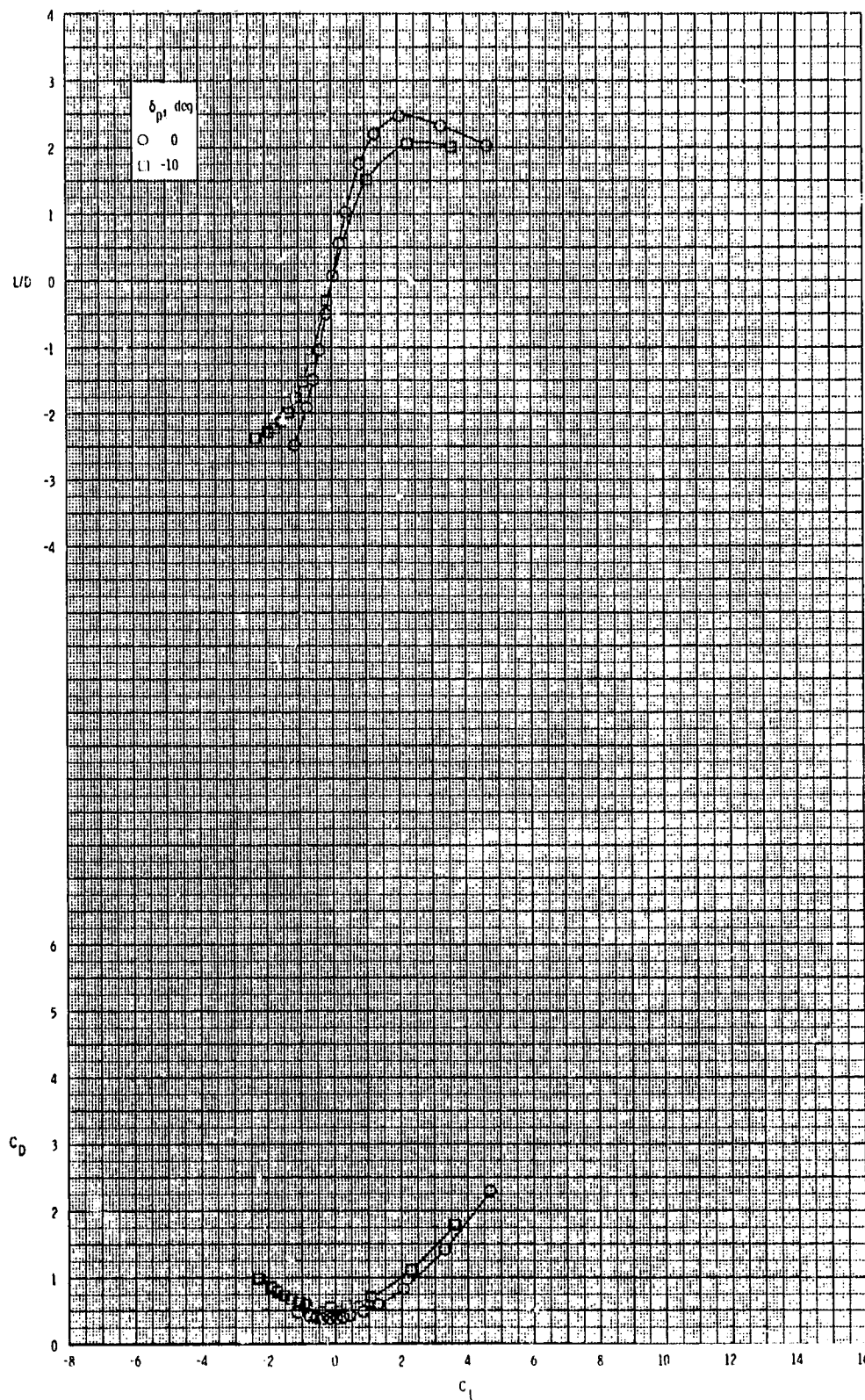
ORIGINAL PAGE IS
OF POOR QUALITY



(d) Continued.

Figure 21.- Continued.

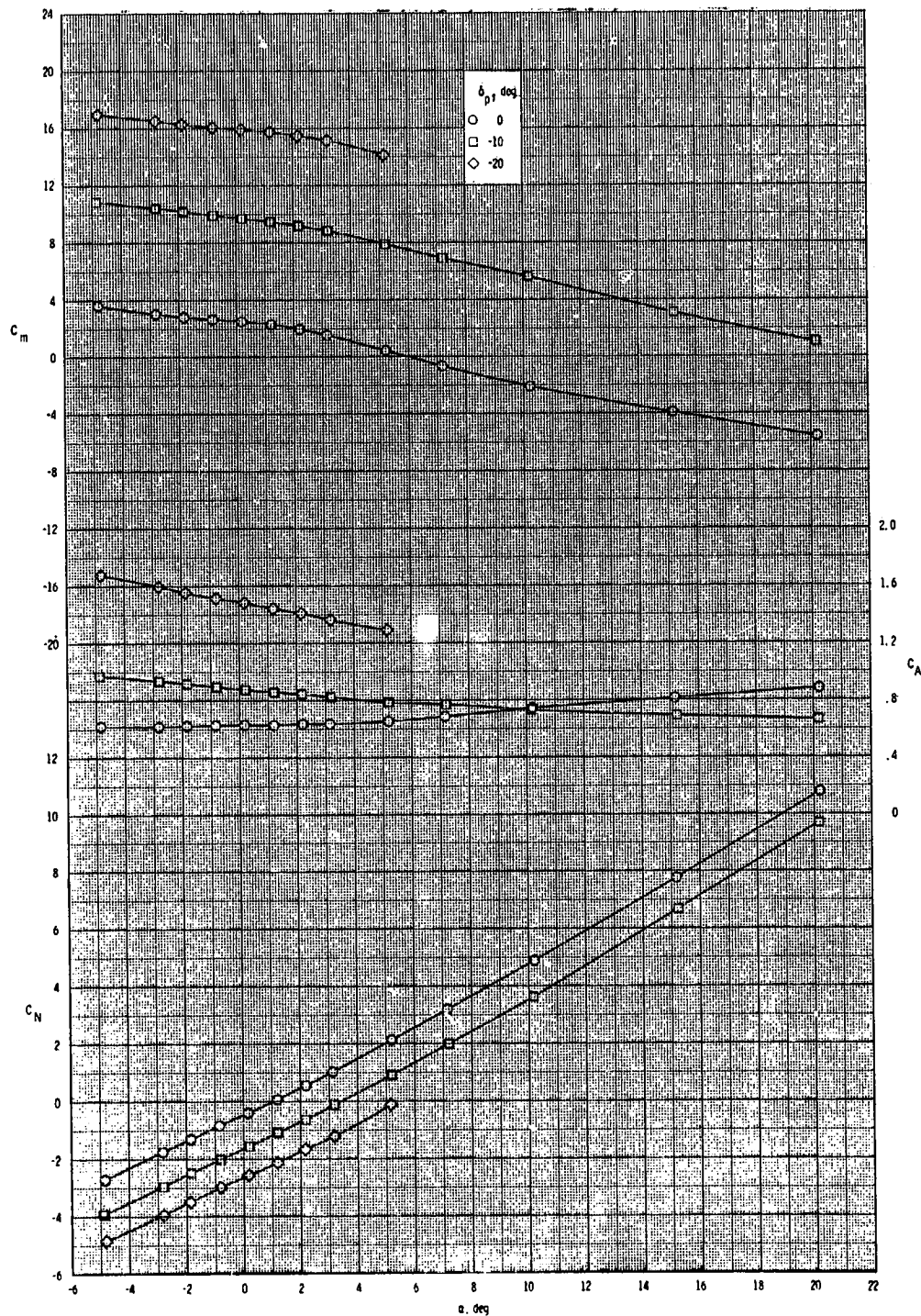
ORIGINAL PAGE IS
OF POOR QUALITY



(d) Concluded.

Figure 21.- Concluded.

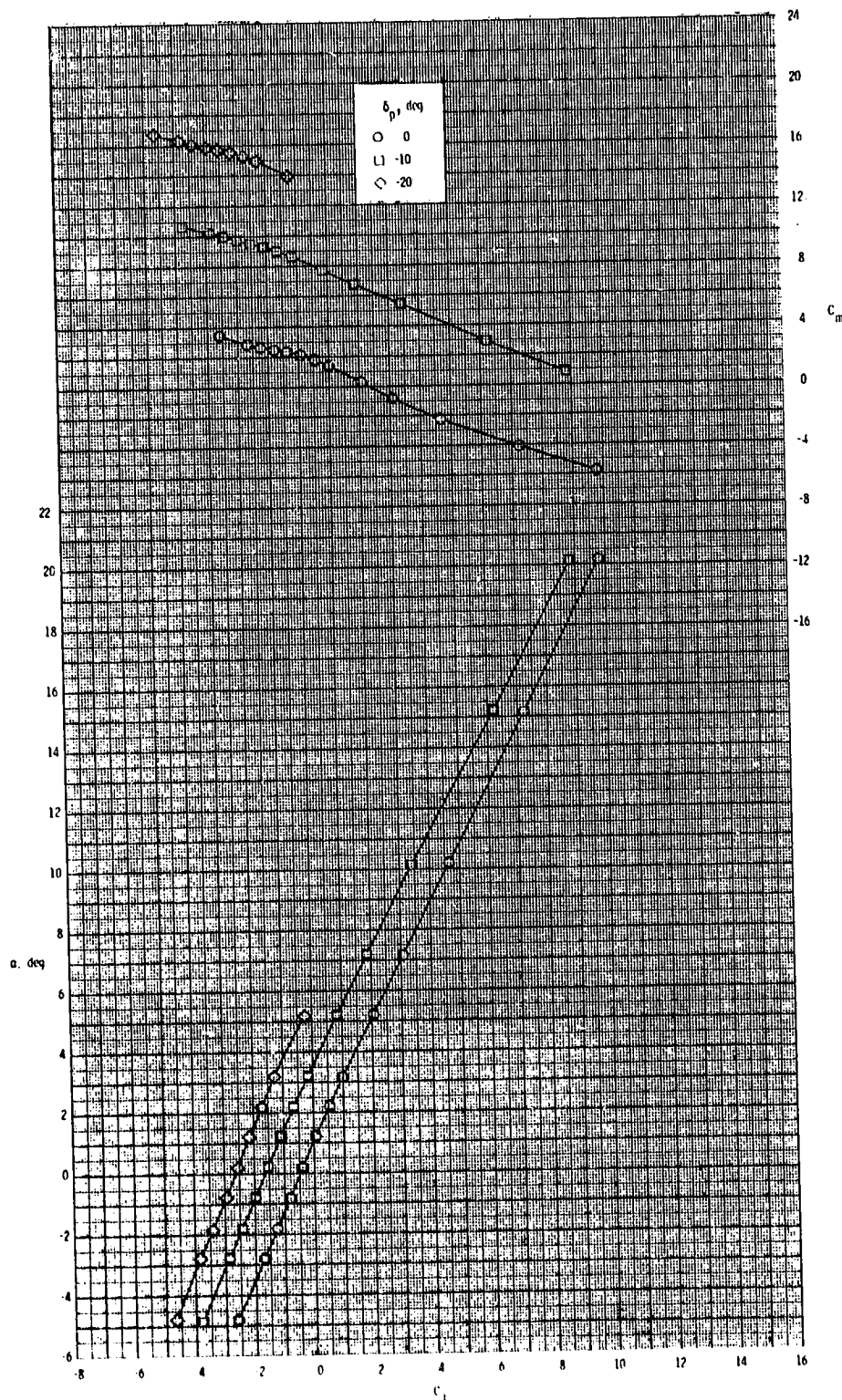
ORIGINAL PAGE IS
OF POOR QUALITY



(a) $M = 2.50$.

Figure 22.- Pitch-control effectiveness of configuration $B_1I_5W_1T_1$.

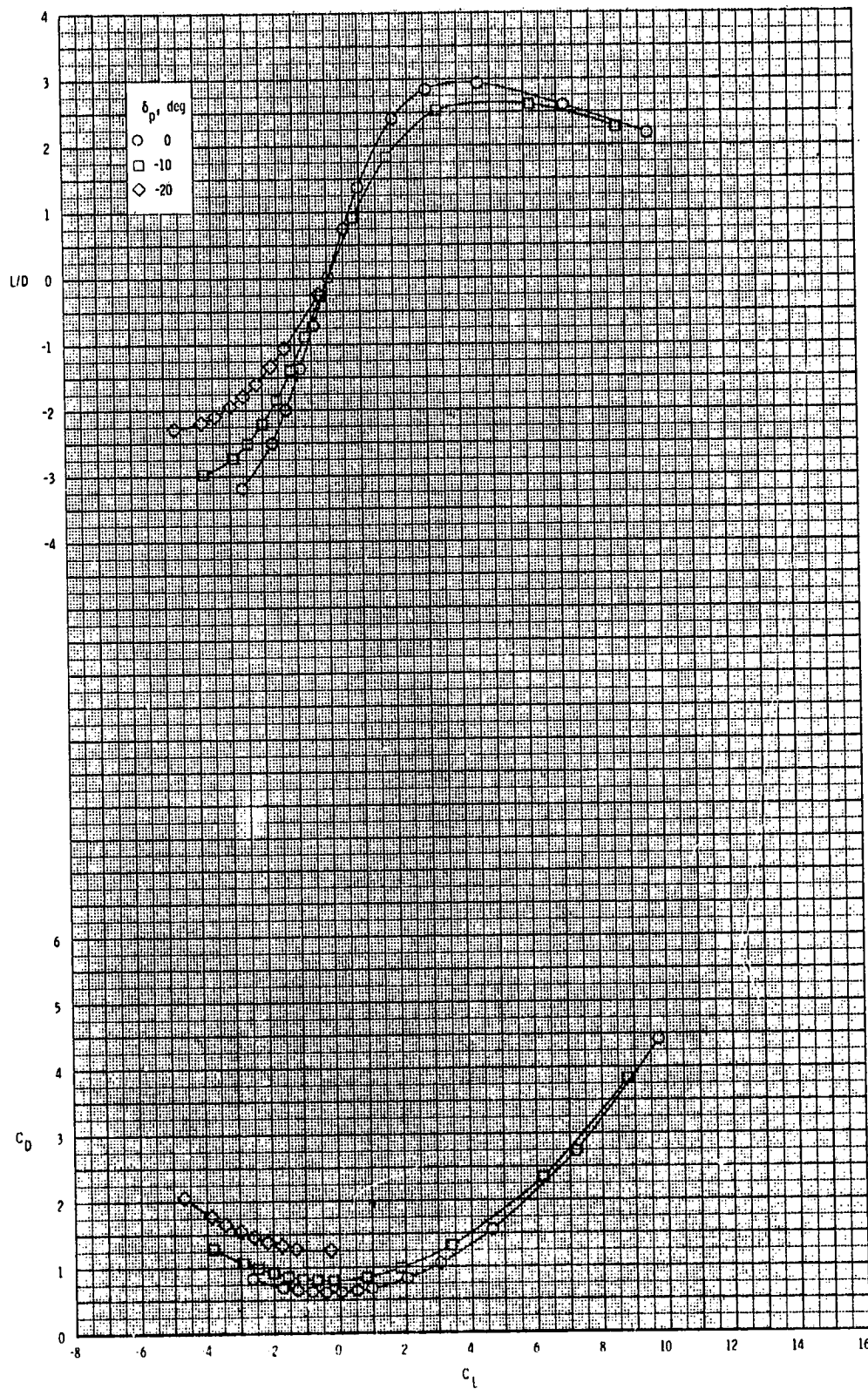
ORIGINAL PAGE IS
OF POOR QUALITY



(a) Continued.

Figure 22.- Continued.

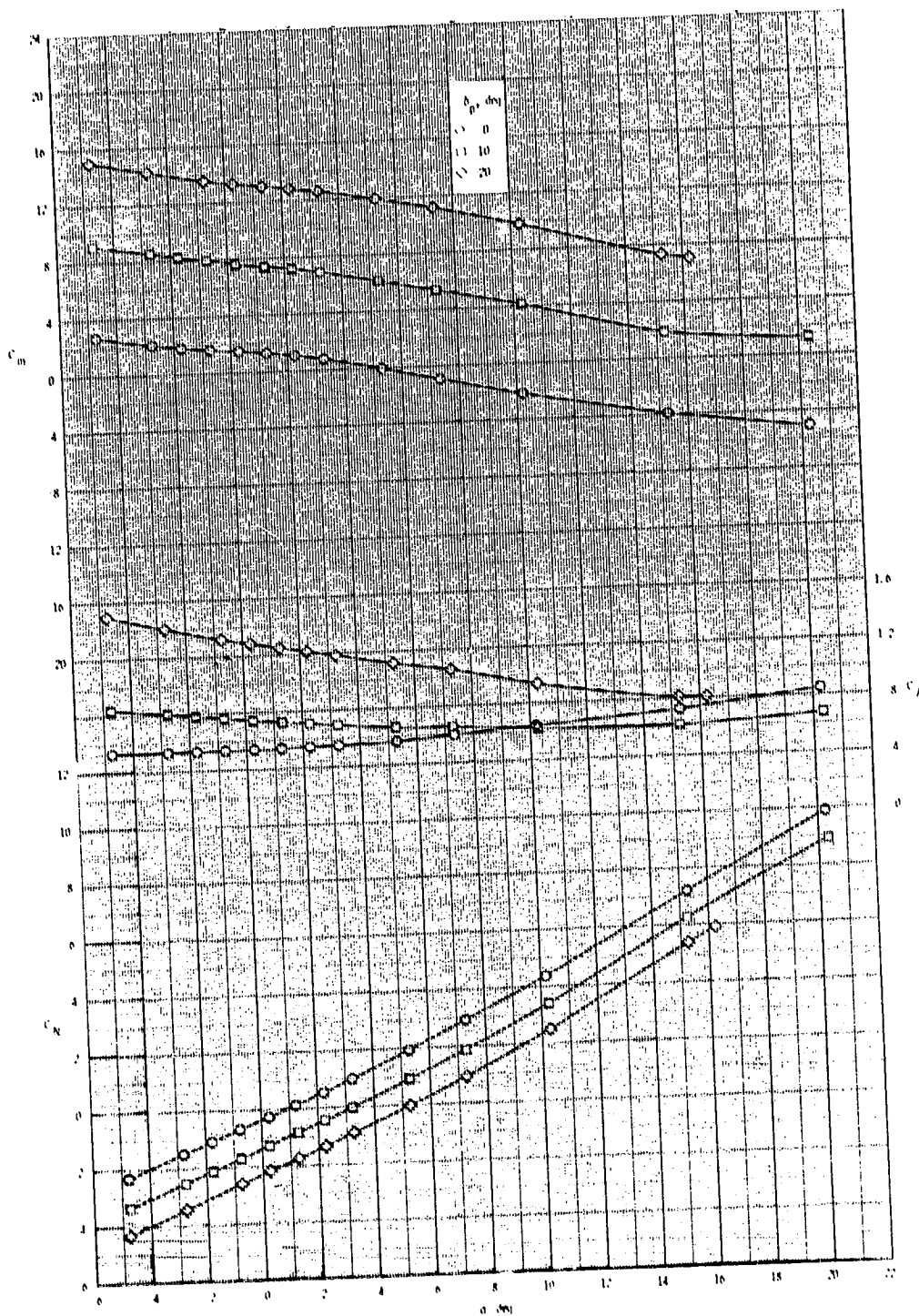
ORIGINAL PAGE IS
OF POOR QUALITY



(a) Concluded.

Figure 22.- Continued.

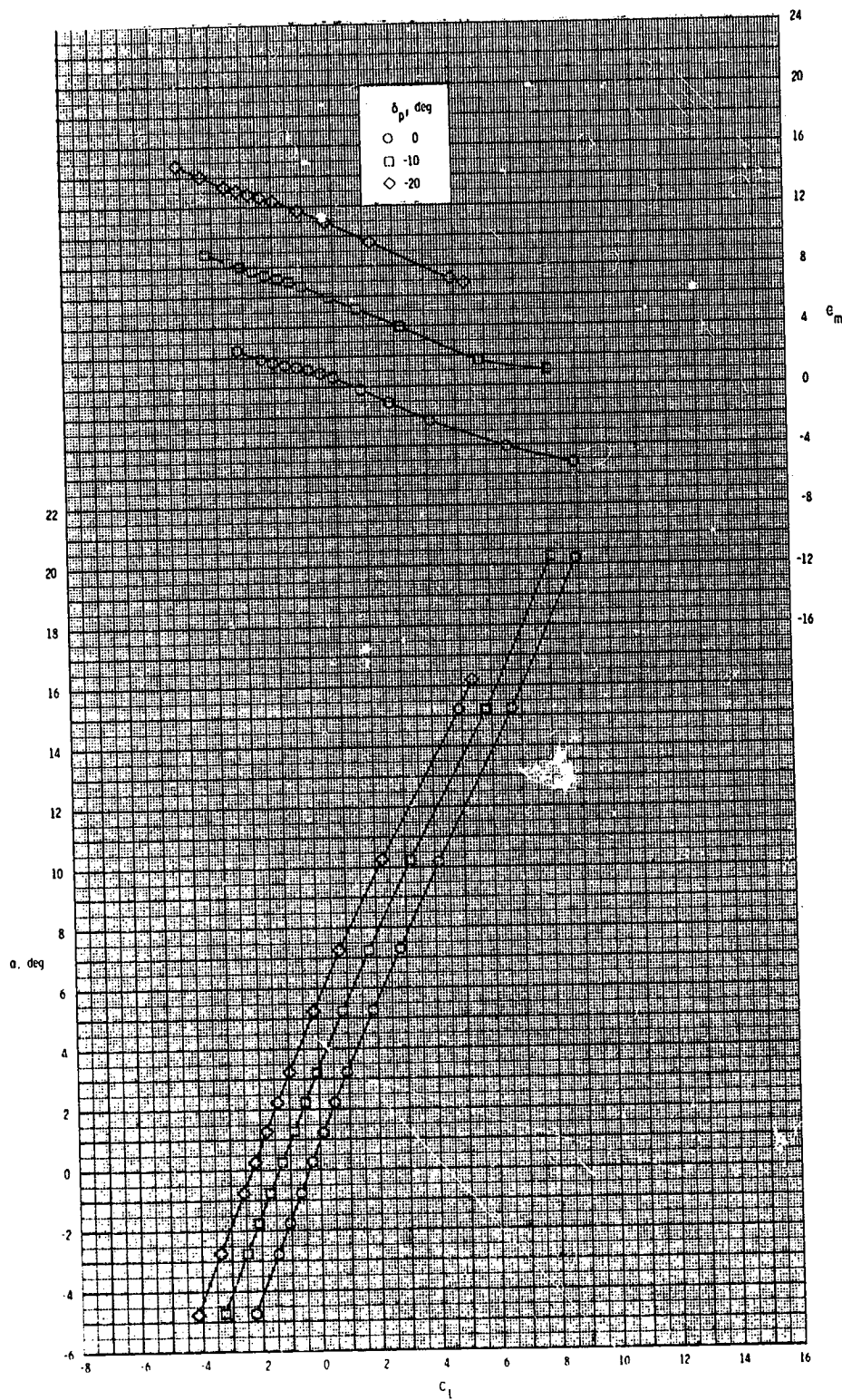
ORIGINAL PAGE IS
OF POOR QUALITY



(b) $M = 2.95$.

Figure 22.- Continued.

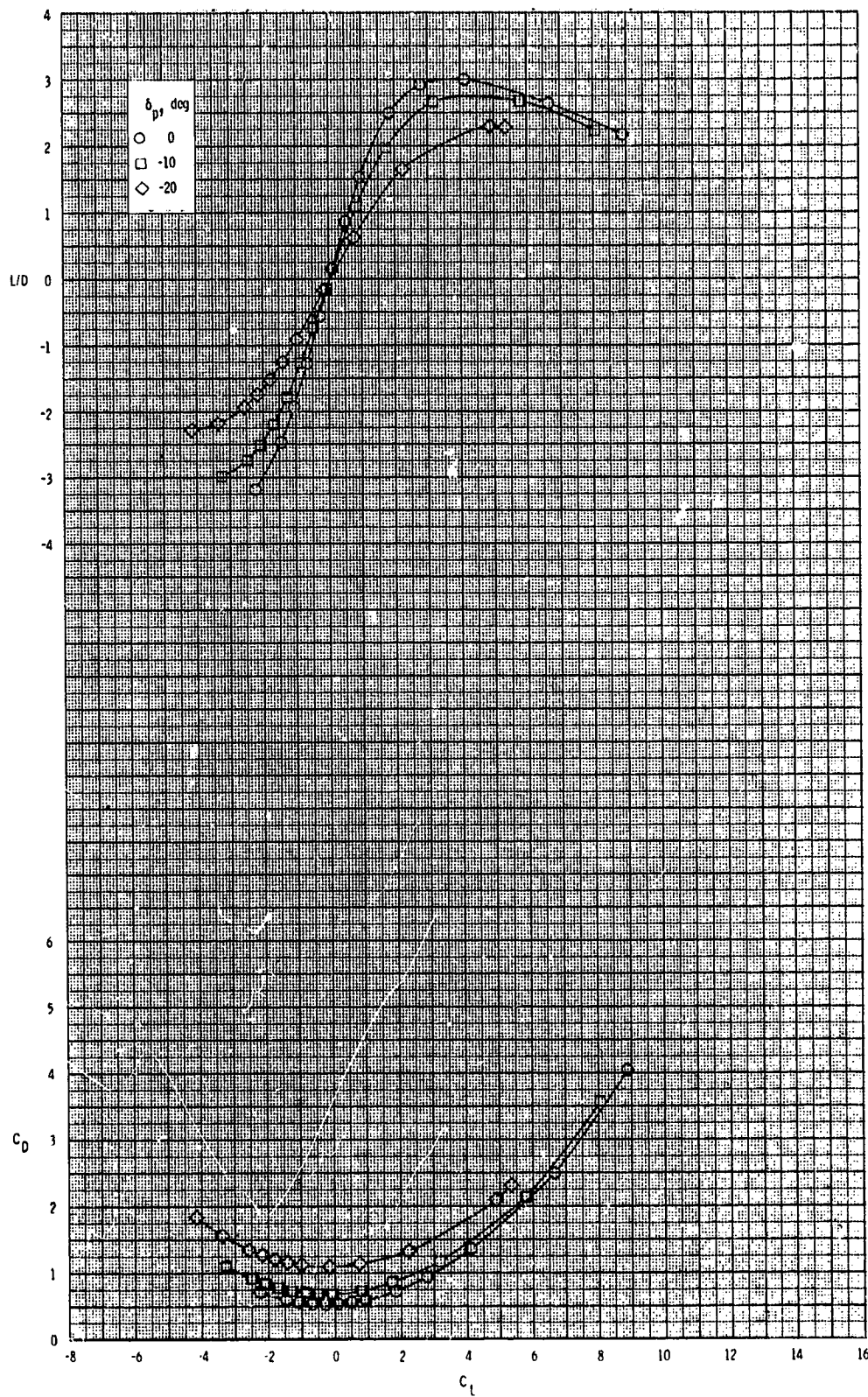
ORIGINAL PAGE IS
OF POOR QUALITY



(b) Continued.

Figure 22.- Continued.

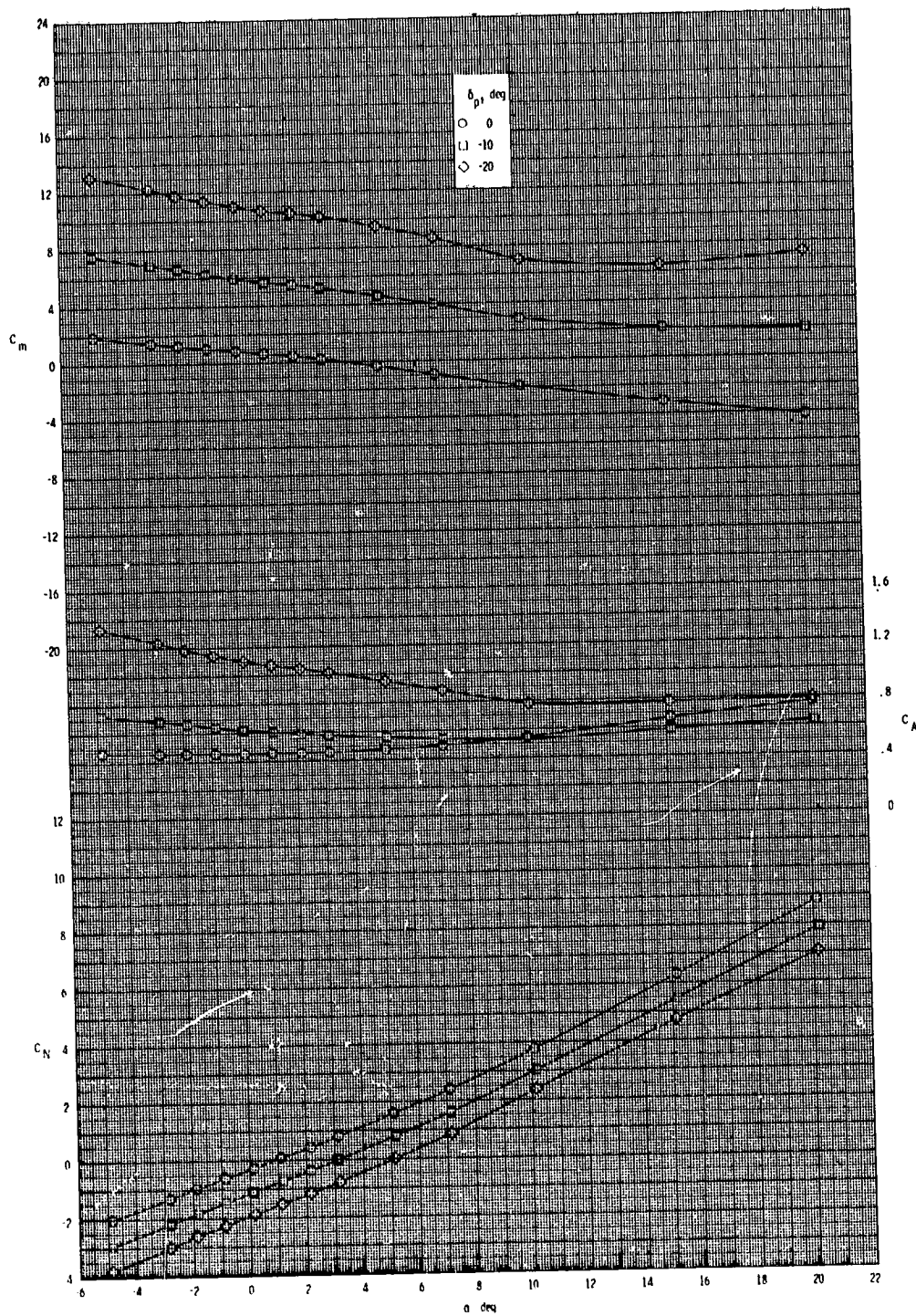
ORIGINAL FIGURE
OF POOR QUALITY



(b) Concluded.

Figure 22.- Continued.

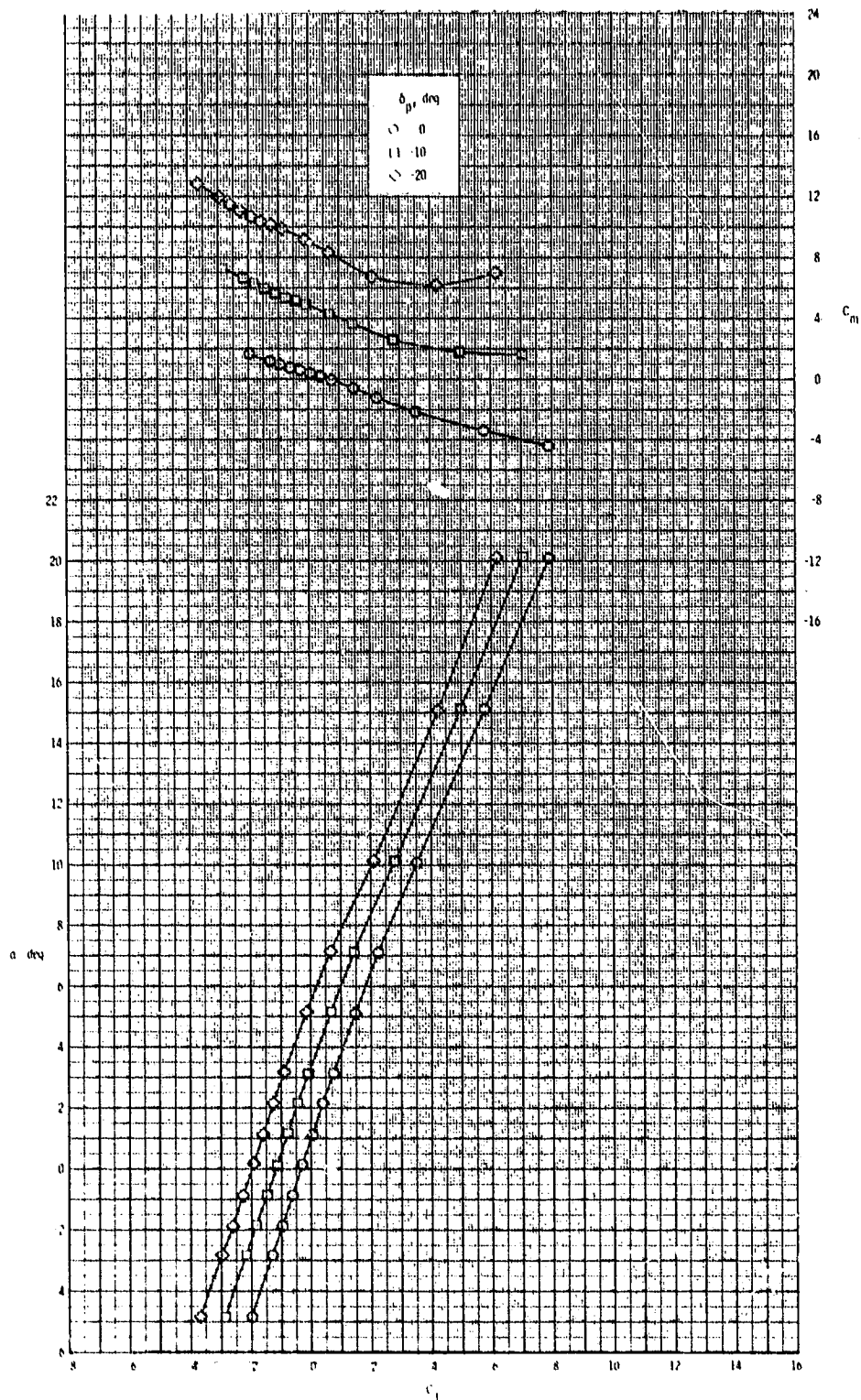
ORIGINAL PAGE 10
OF POOR QUALITY



(c) $M = 3.50$.

Figure 22.- Continued.

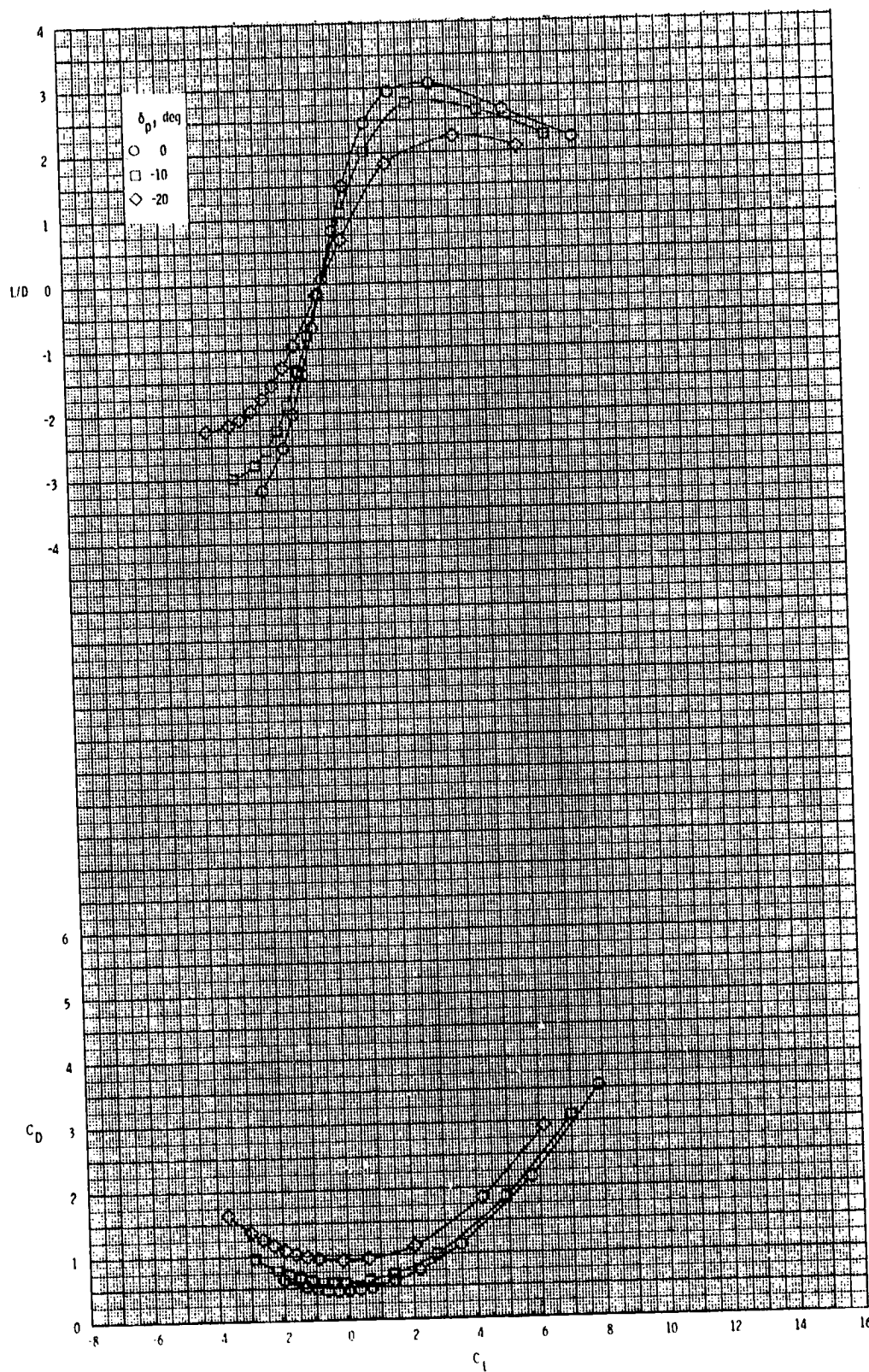
ORIGINAL PAGE IS
OF POOR QUALITY



(c) Continued.

Figure 22.- Continued.

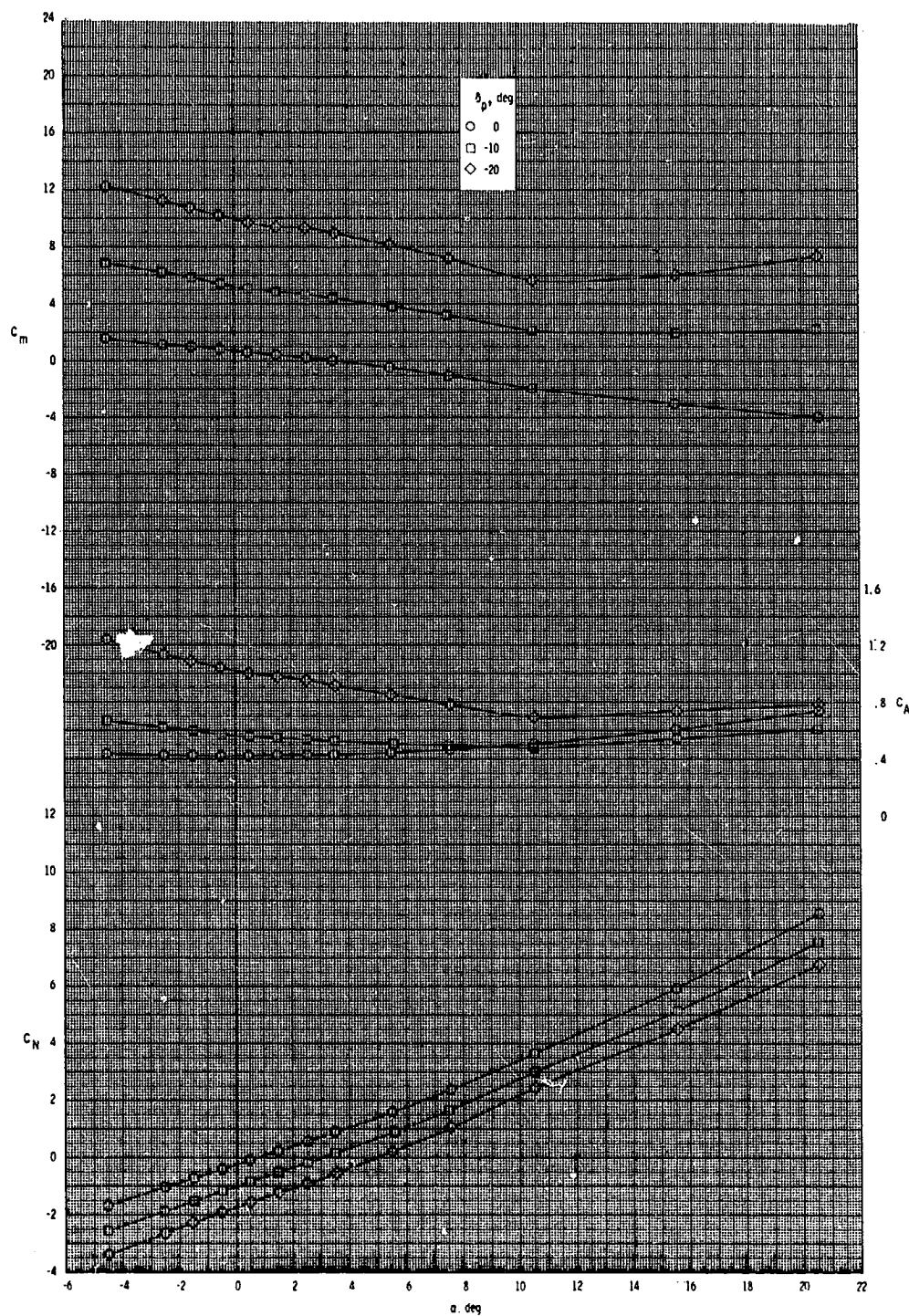
ORIGINAL PAGE IS
OF POOR QUALITY



(c) Concluded.

Figure 22.- Continued.

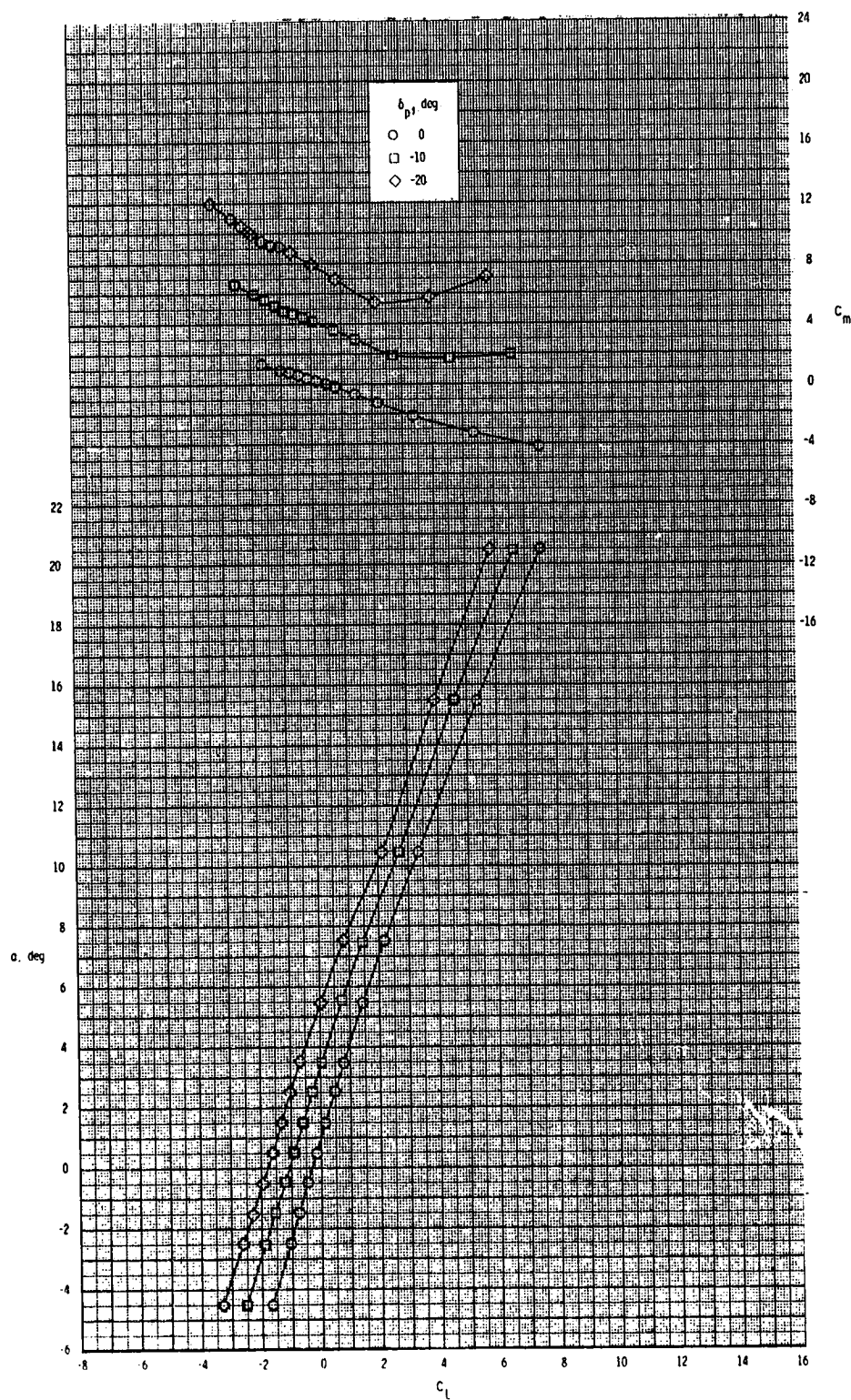
ORIGINAL PAGE IS
OF POOR QUALITY



(d) $M = 3.95$.

Figure 22.- Continued.

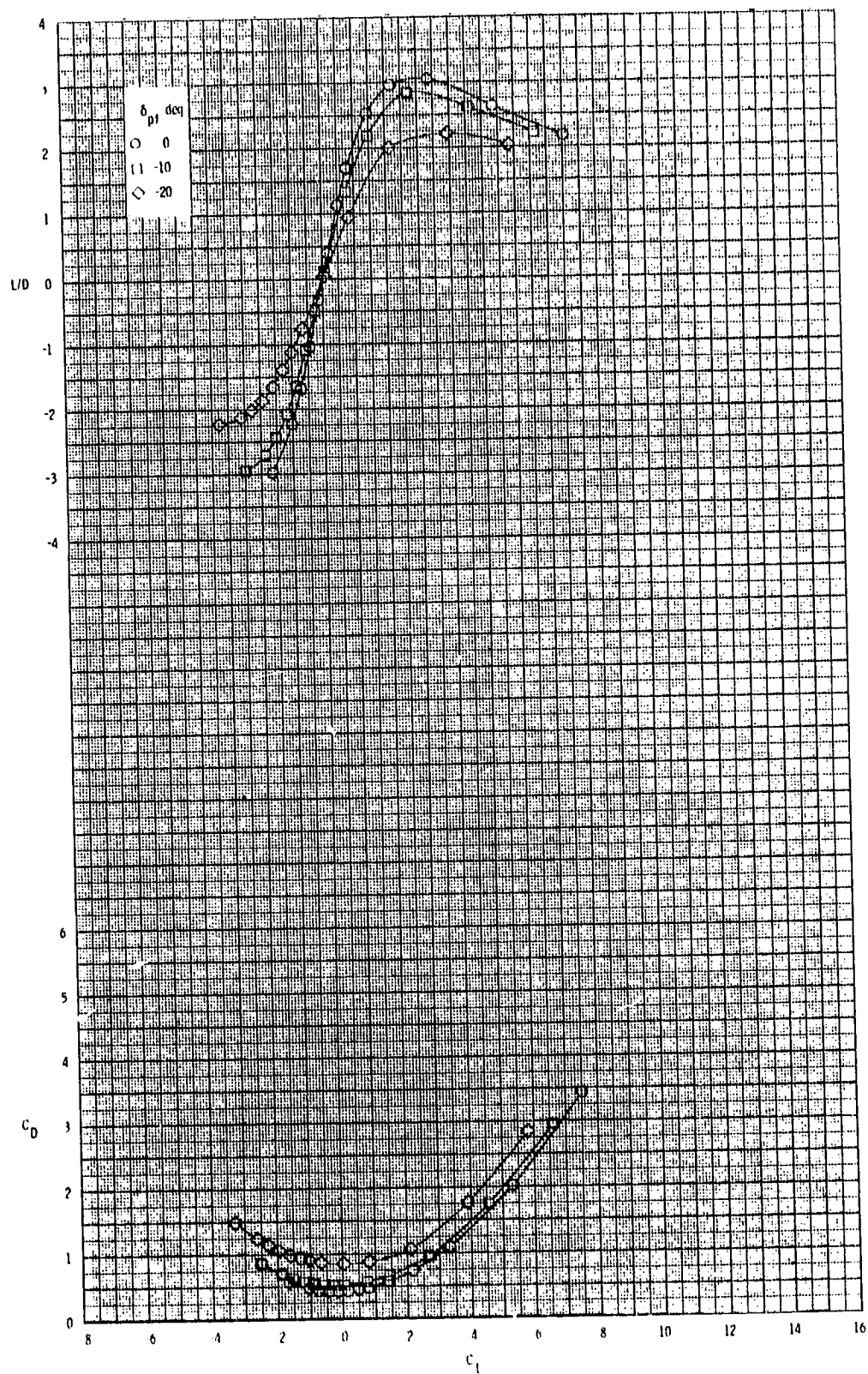
ORIGINAL PAGE IS
OF POOR QUALITY



(d) Continued.

Figure 22.- Continued.

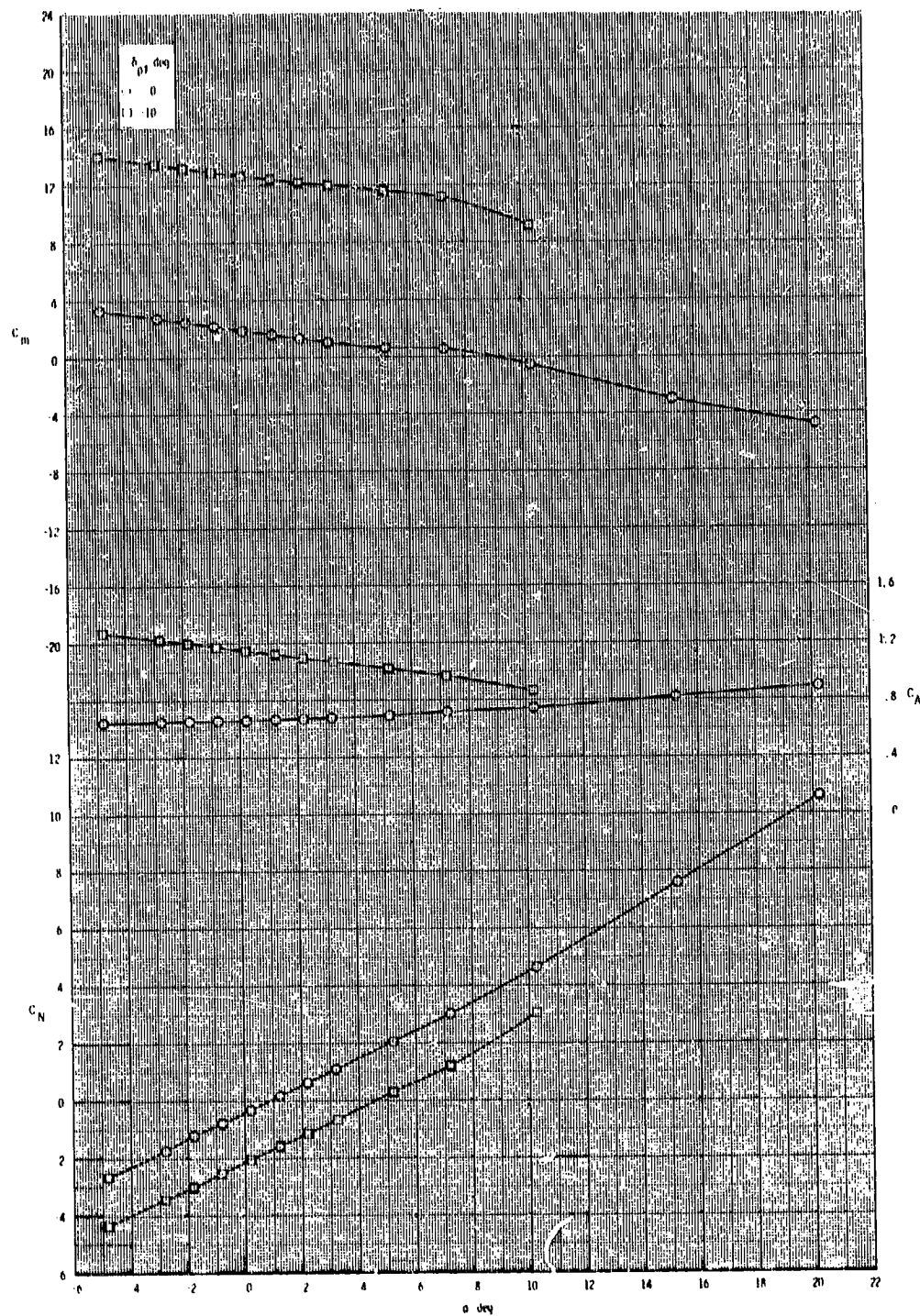
ORIGINAL PAGE IS
OF POOR QUALITY



(d) Concluded.

Figure 22.- Concluded.

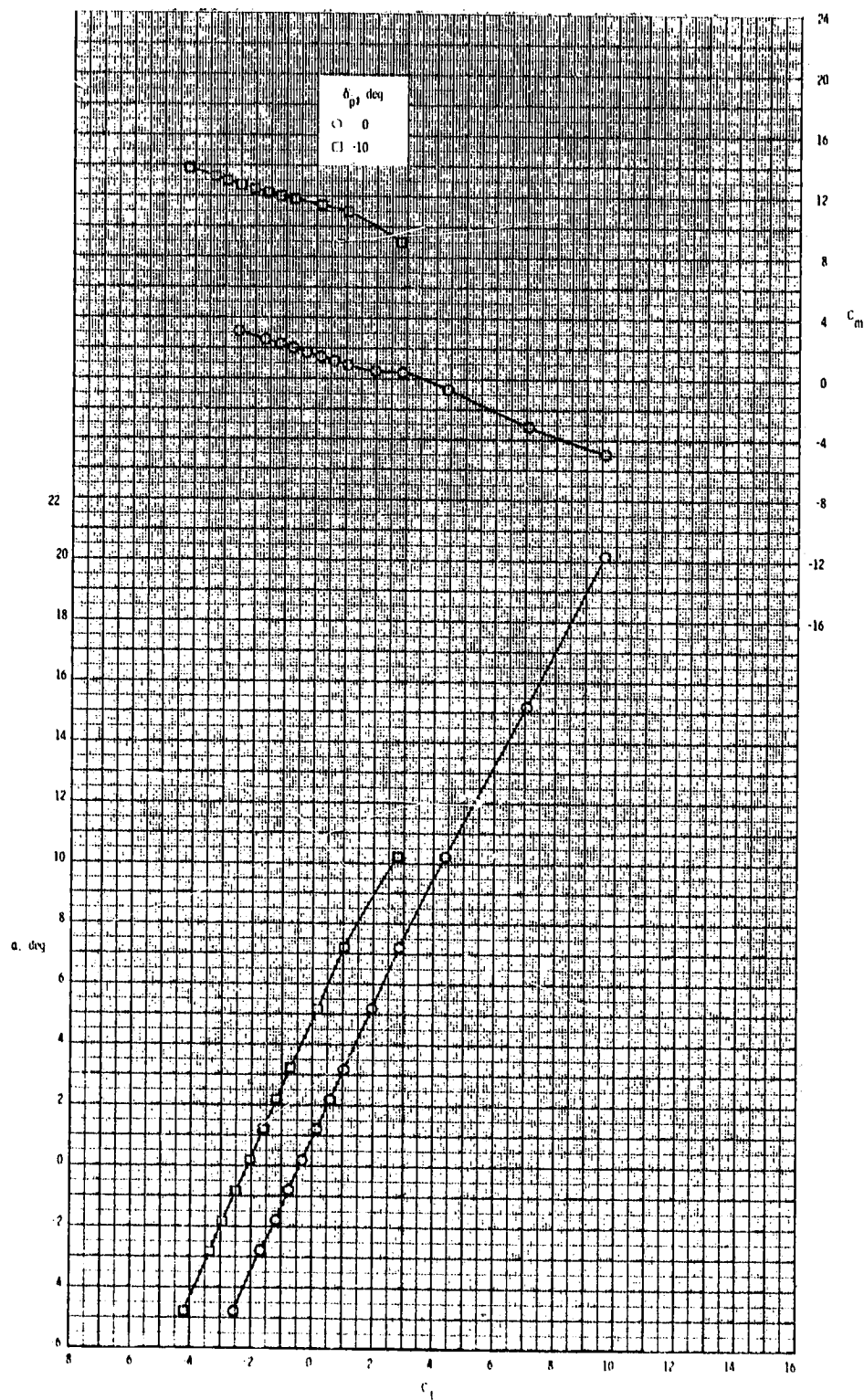
ORIGINAL PAGE IS
OF POOR QUALITY



(a) $M = 2.50$.

Figure 23.- Pitch-control effectiveness of configuration $B_{1I5W1T2}$.

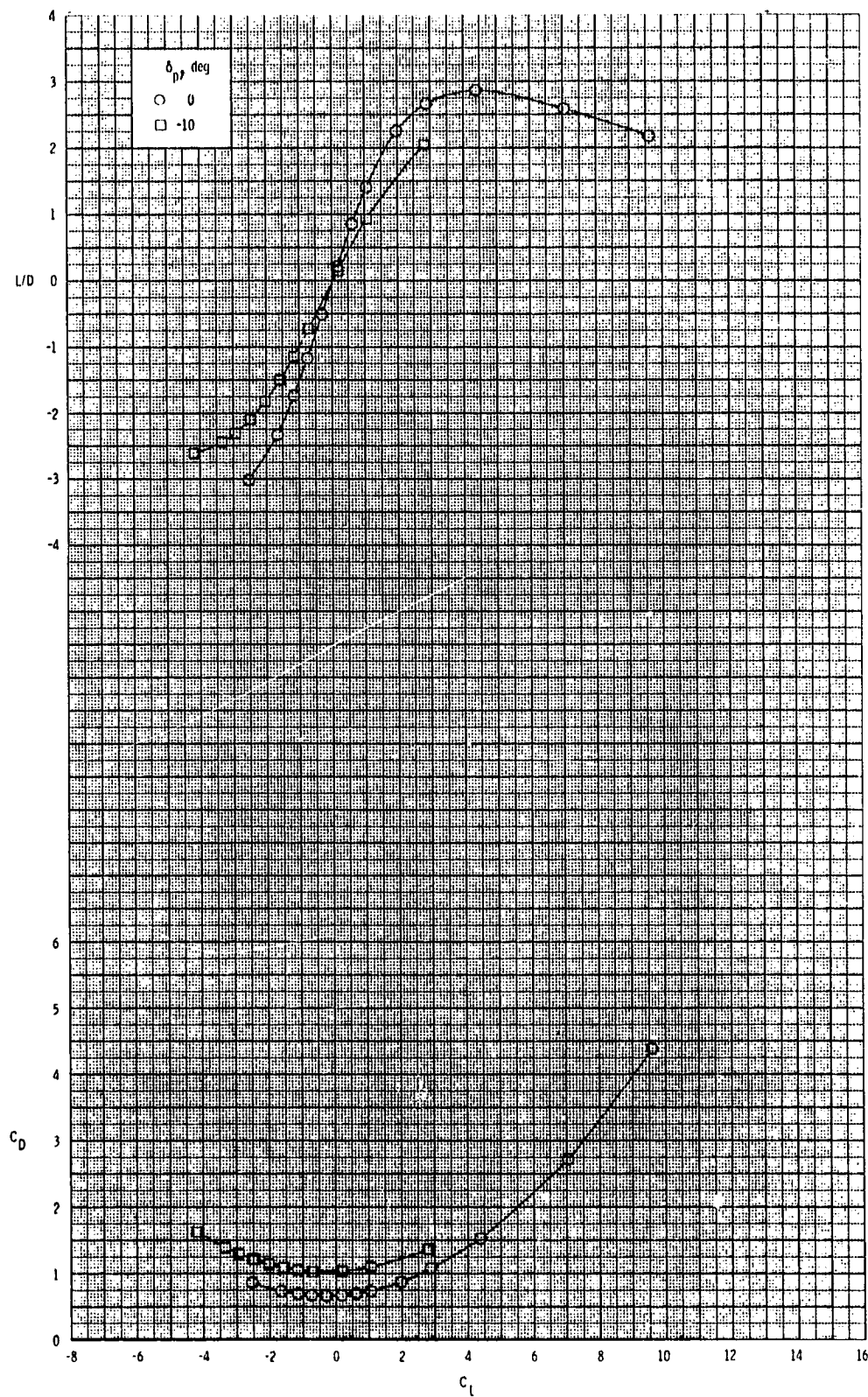
ORIGINAL PAGE IS
OF POOR QUALITY



(a) Continued.

Figure 23.- Continued.

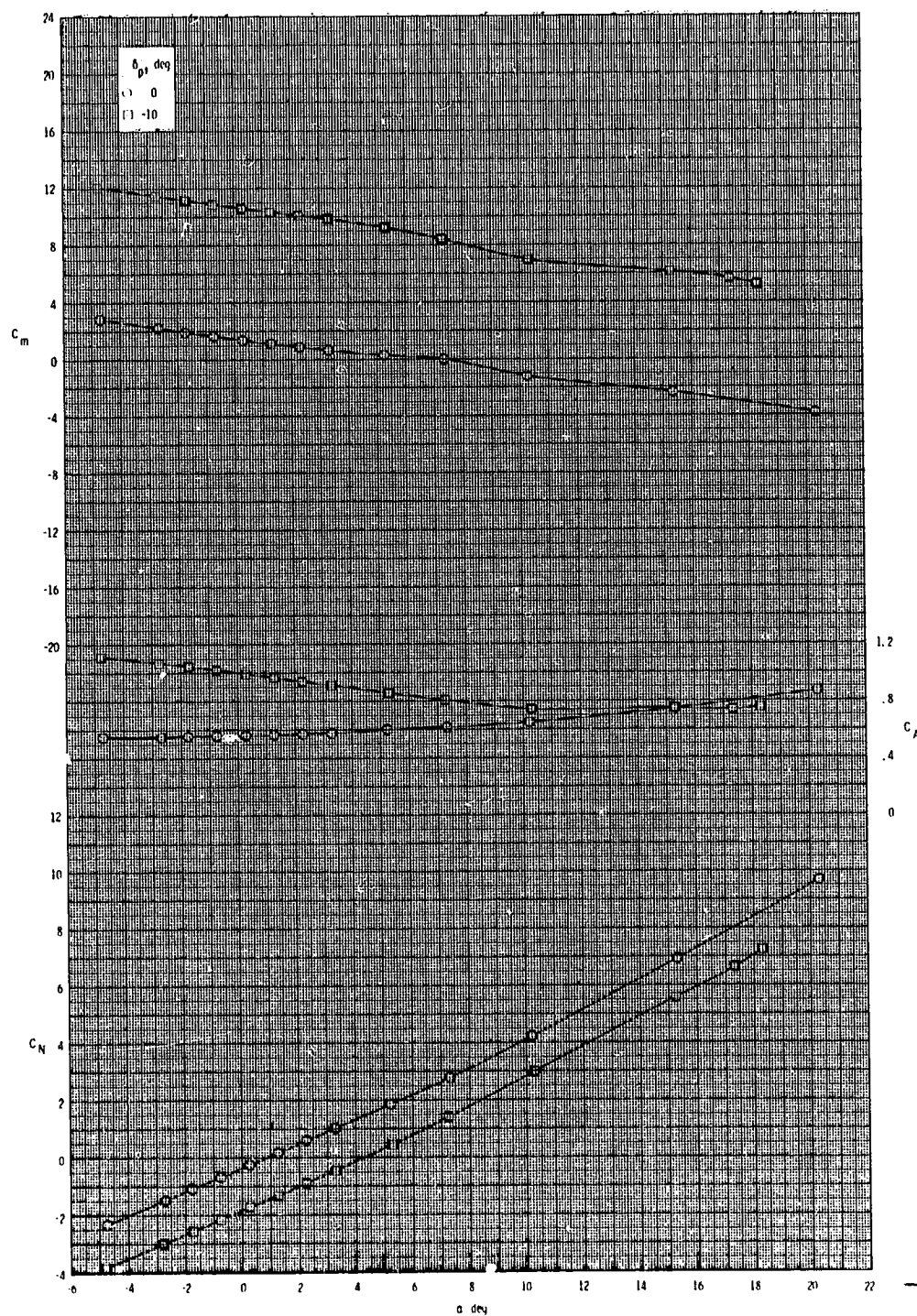
ORIGINAL PAGE IS
OF POOR QUALITY



(a) Concluded.

Figure 23.- Continued.

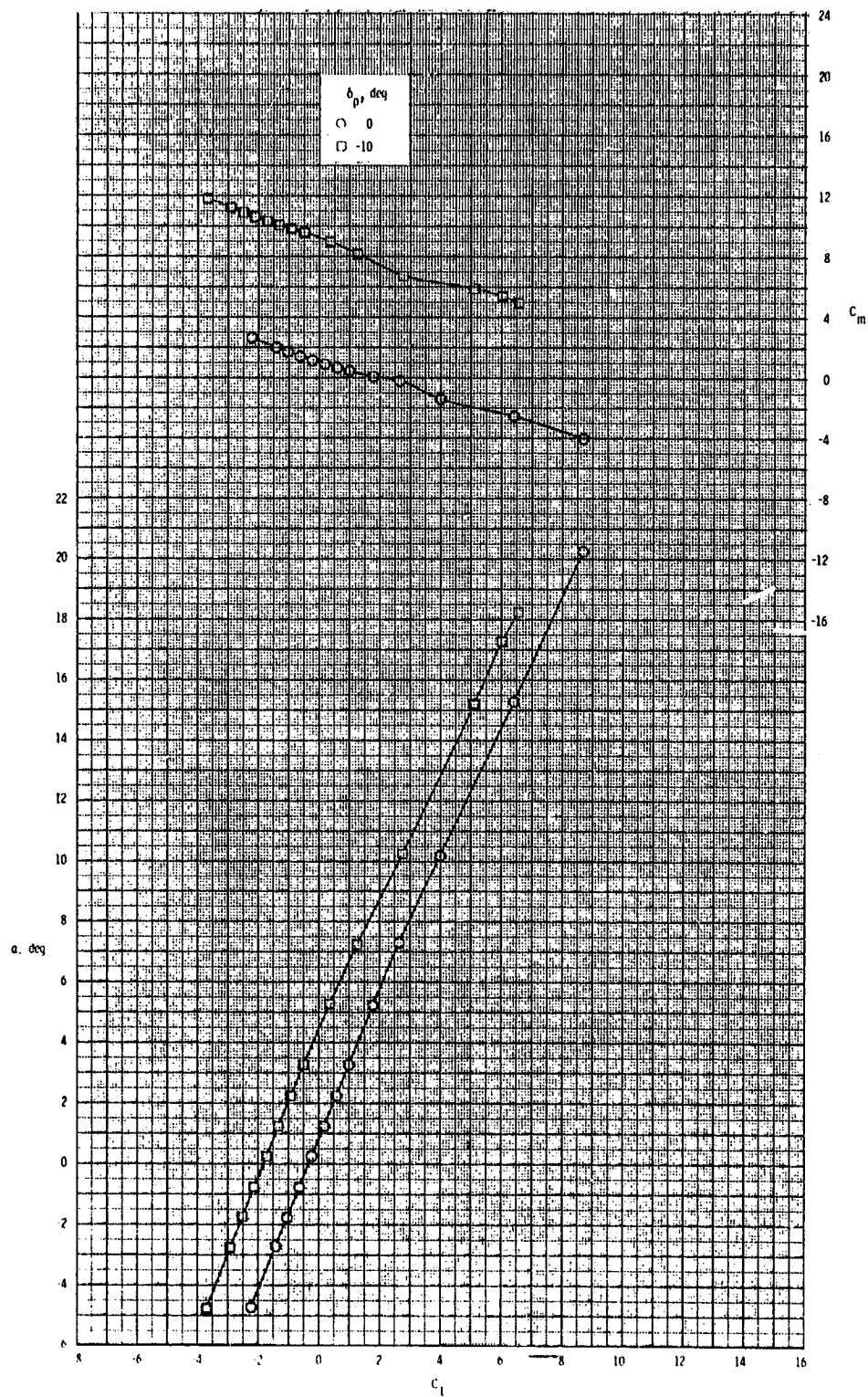
ORIGINAL PAGE IS
OF POOR QUALITY



(b) $M = 2.95$.

Figure 23.- Continued.

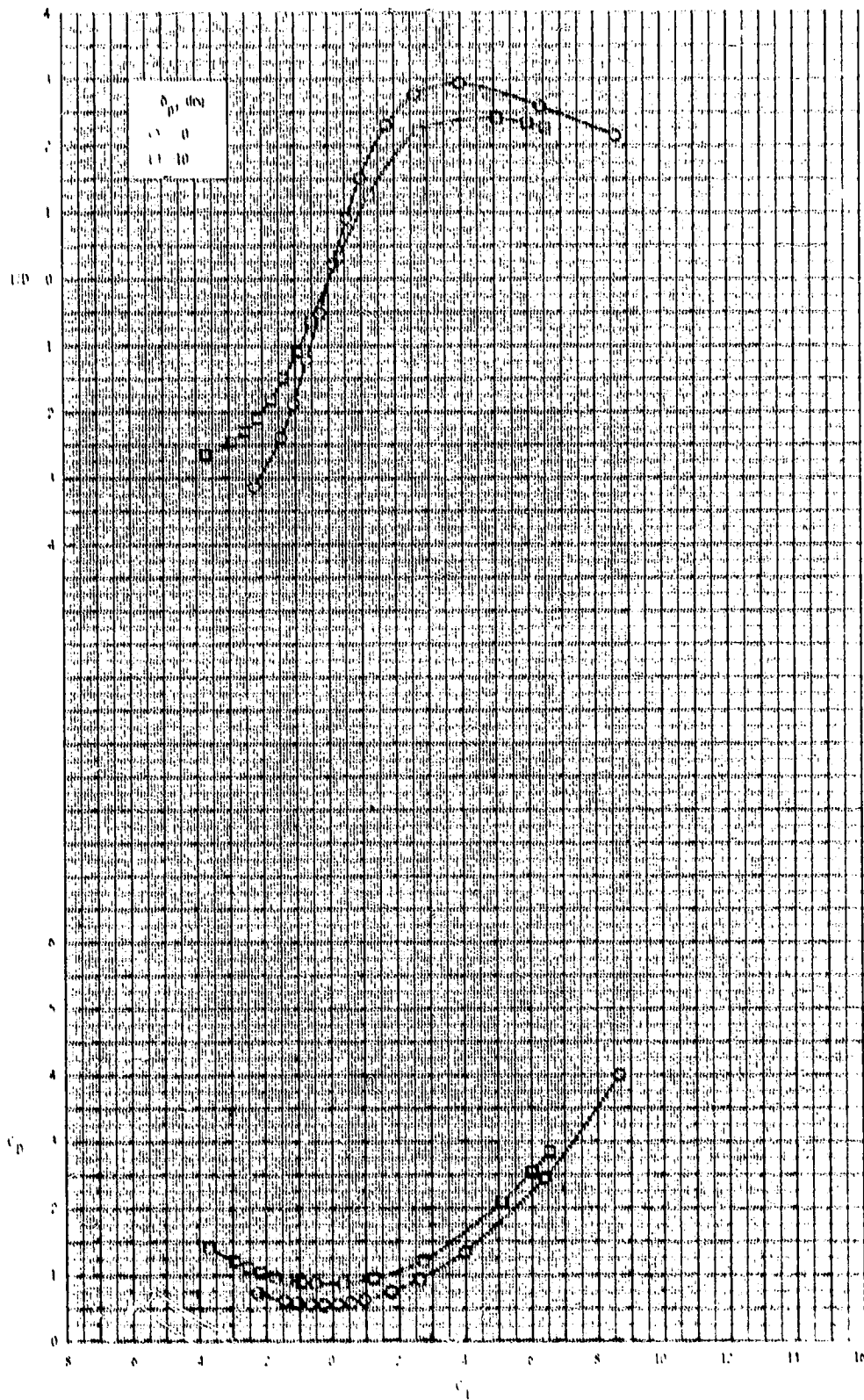
ORIGINAL PAGE IS
OF POOR QUALITY



(b) Continued.

Figure 23.- Continued.

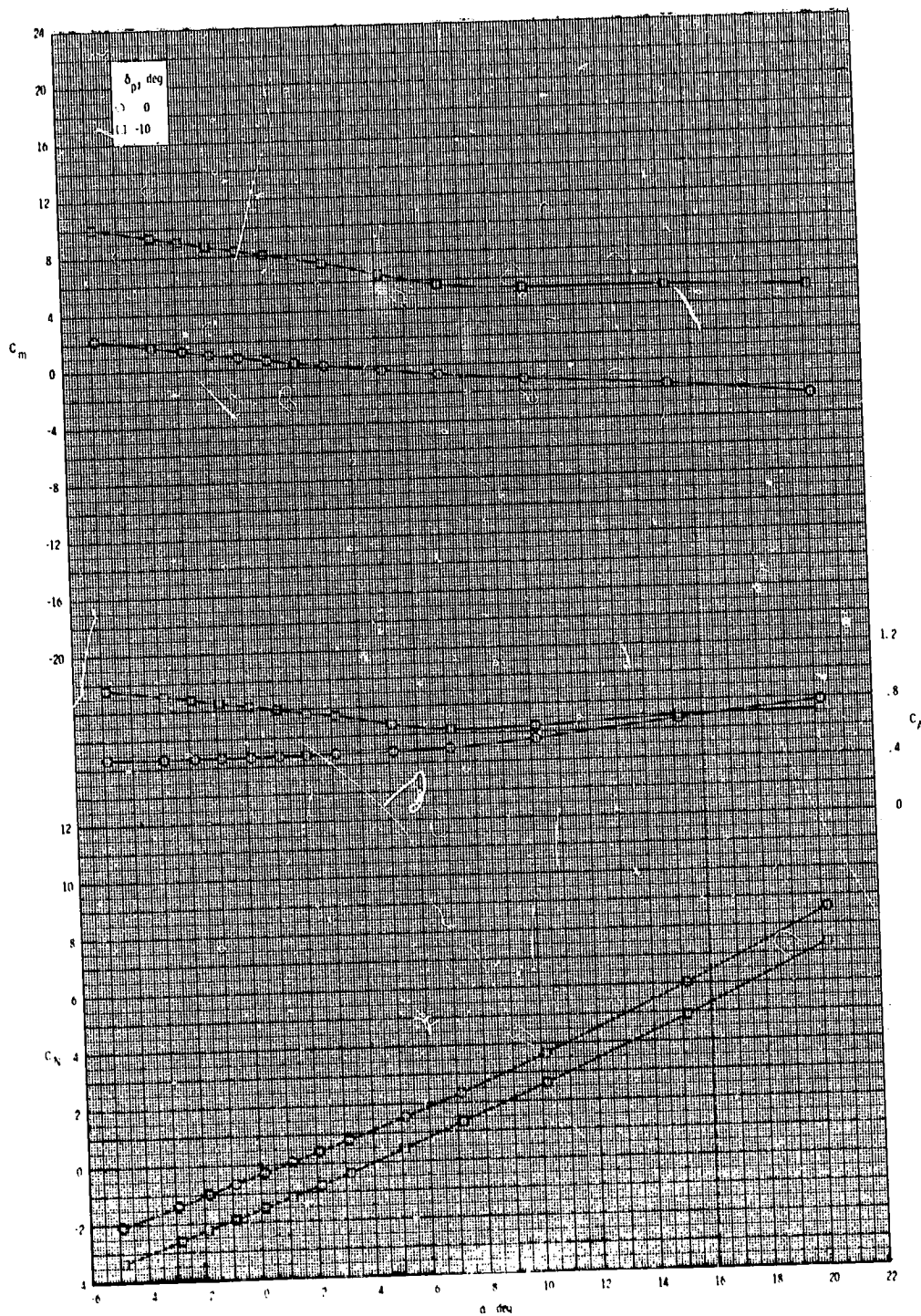
ORIGINAL PAGE IS
OF POOR QUALITY



(b) Concluded.

Figure 23.- Continued.

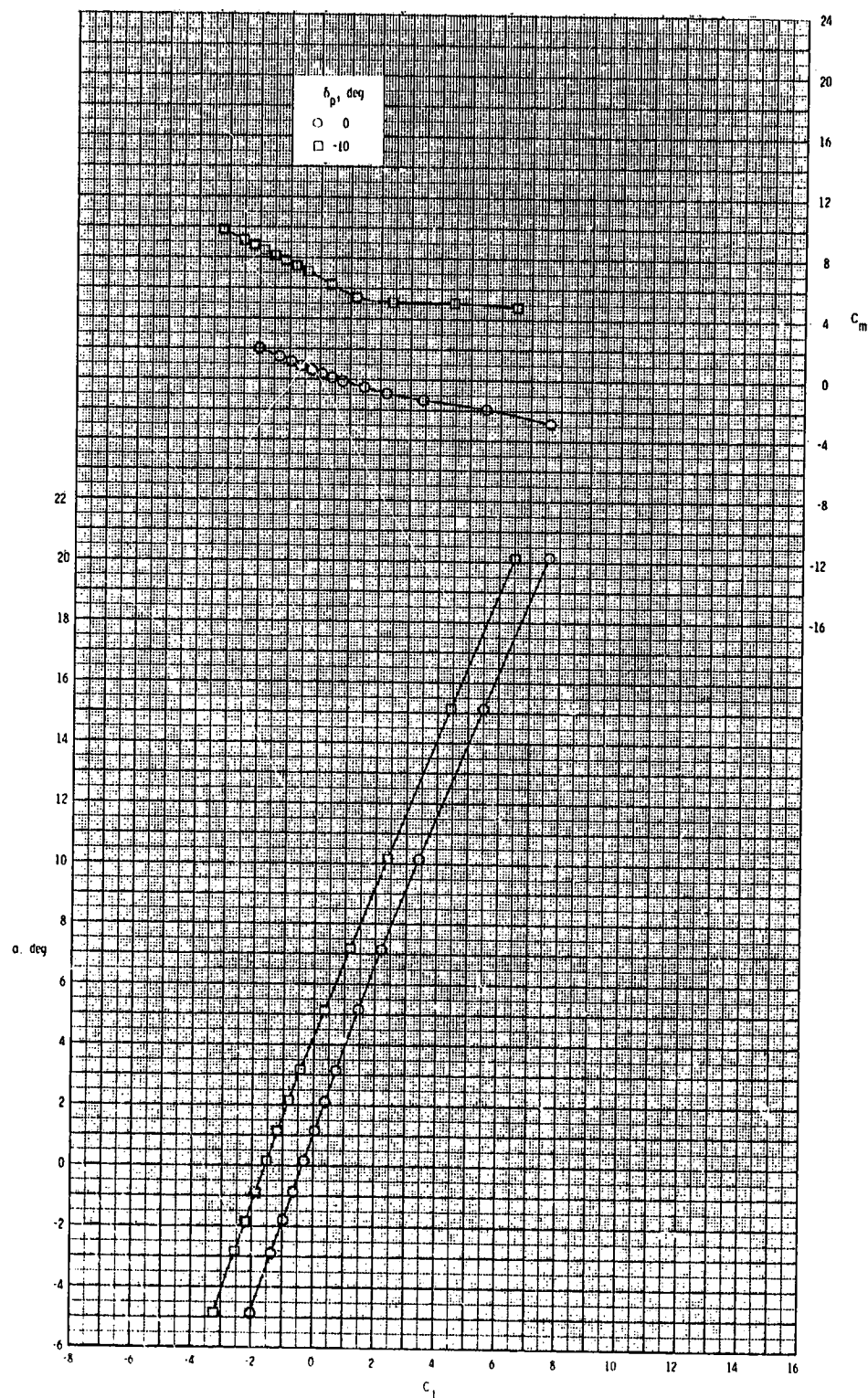
ORIGINAL PAGE IS
OF POOR QUALITY



(c) $M = 3.50$.

Figure 23.- Continued.

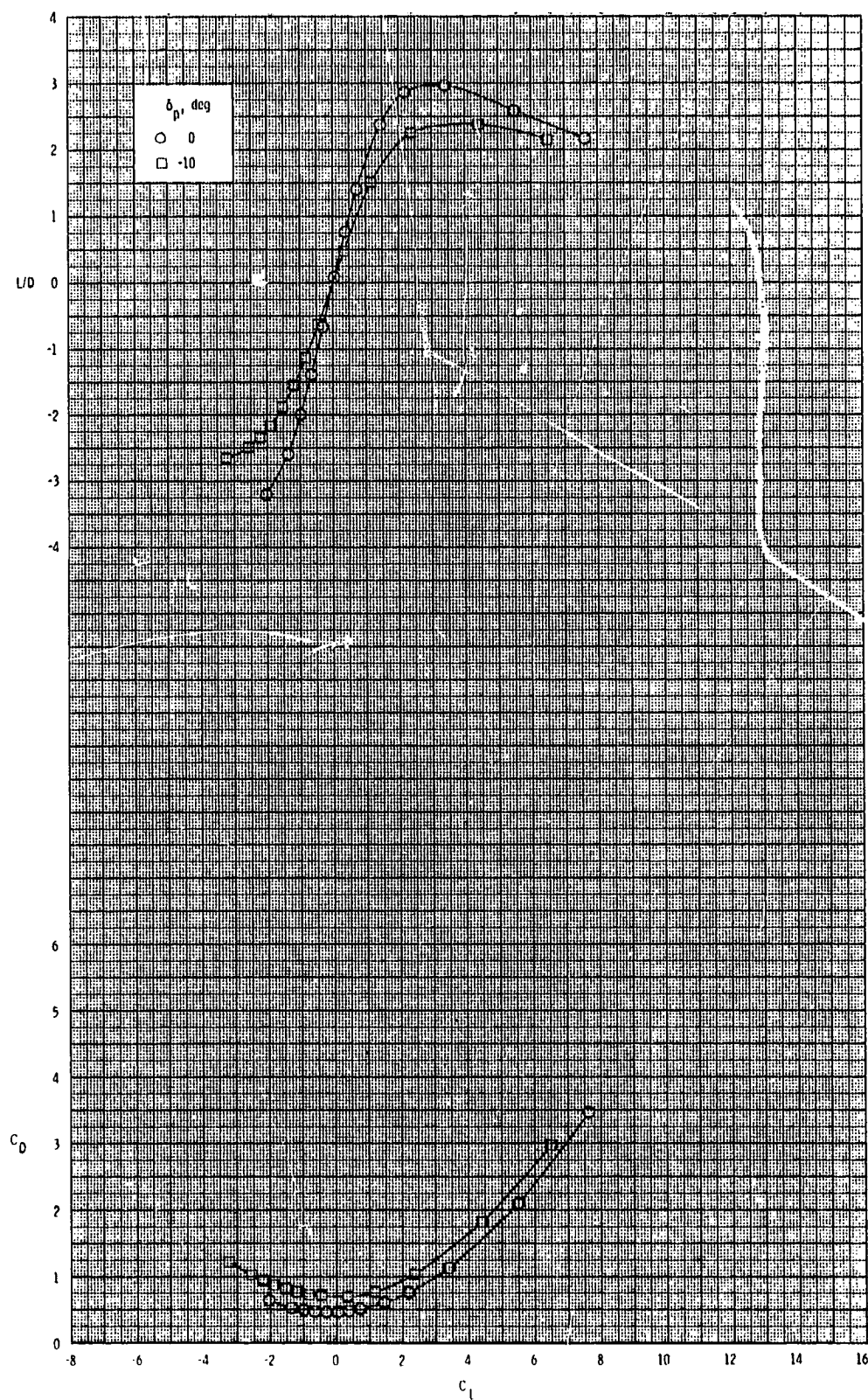
ORIGINAL PAGE IS
OF POOR QUALITY



(c) Continued.

Figure 23.- Continued.

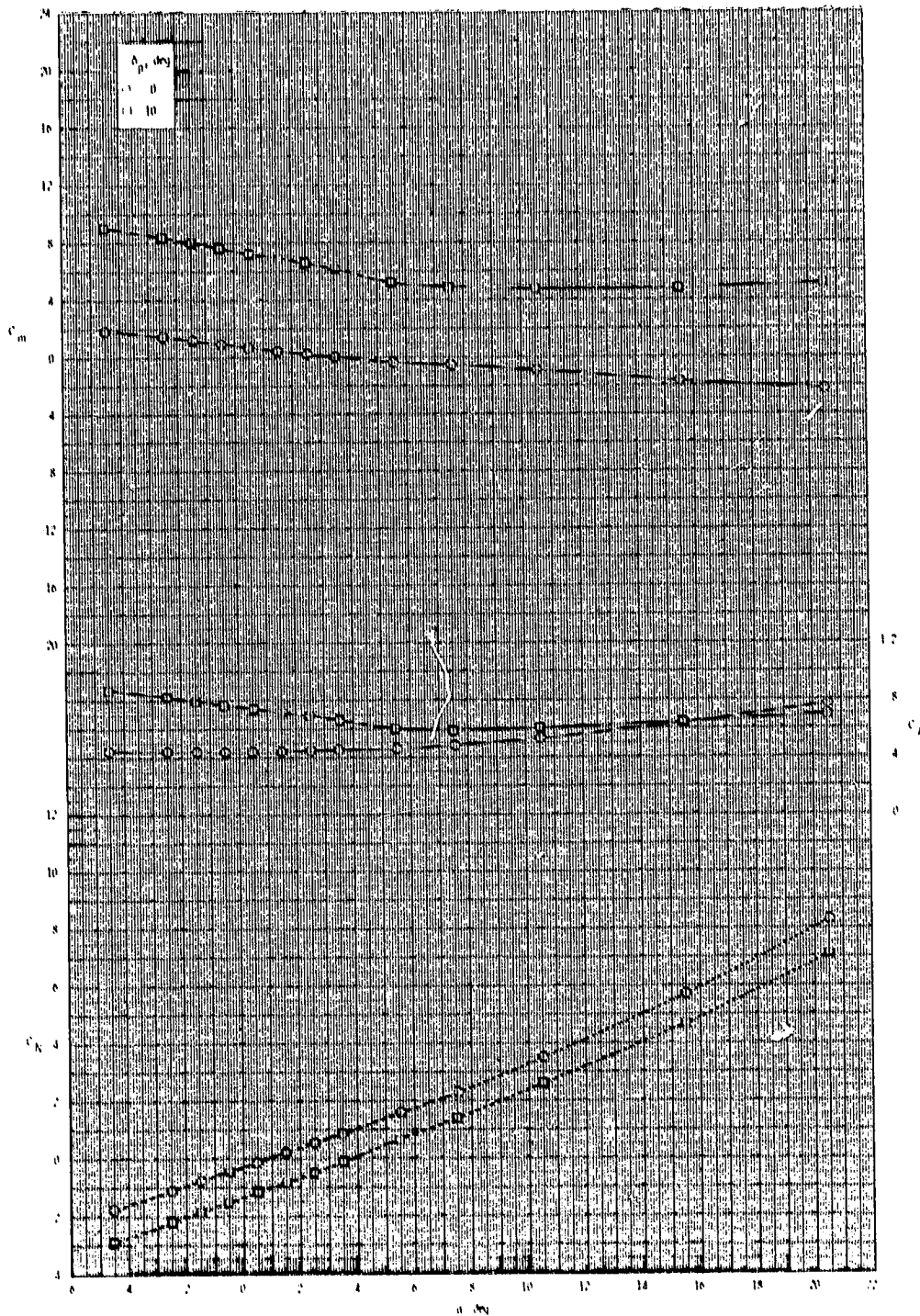
ORIGINAL PAGE IS
OF POOR QUALITY



(c) Concluded.

Figure 23.- Continued.

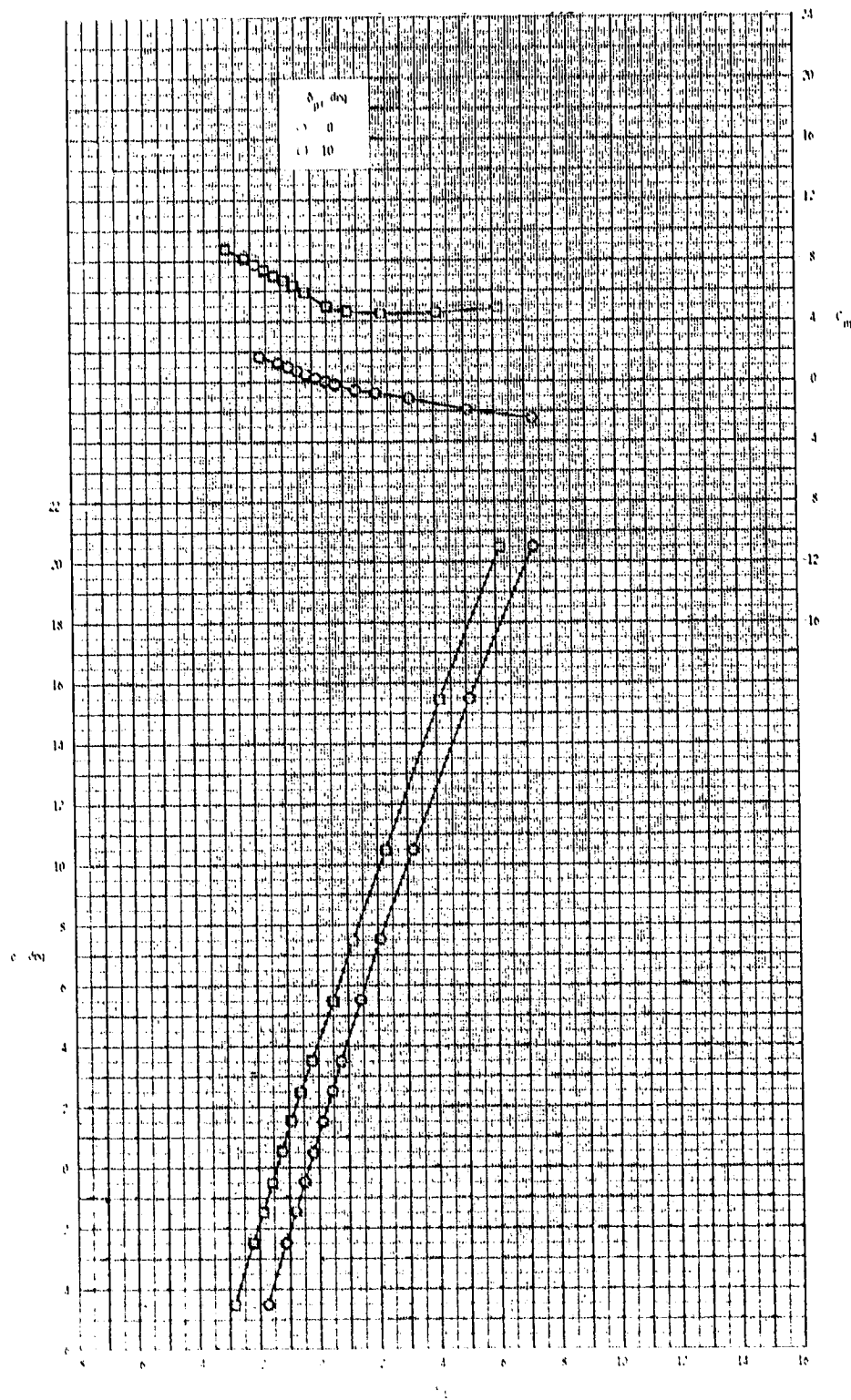
ORIGINAL PAGE IS
OF POOR QUALITY



(d) $M = 3.95$.

Figure 23.- Continued.

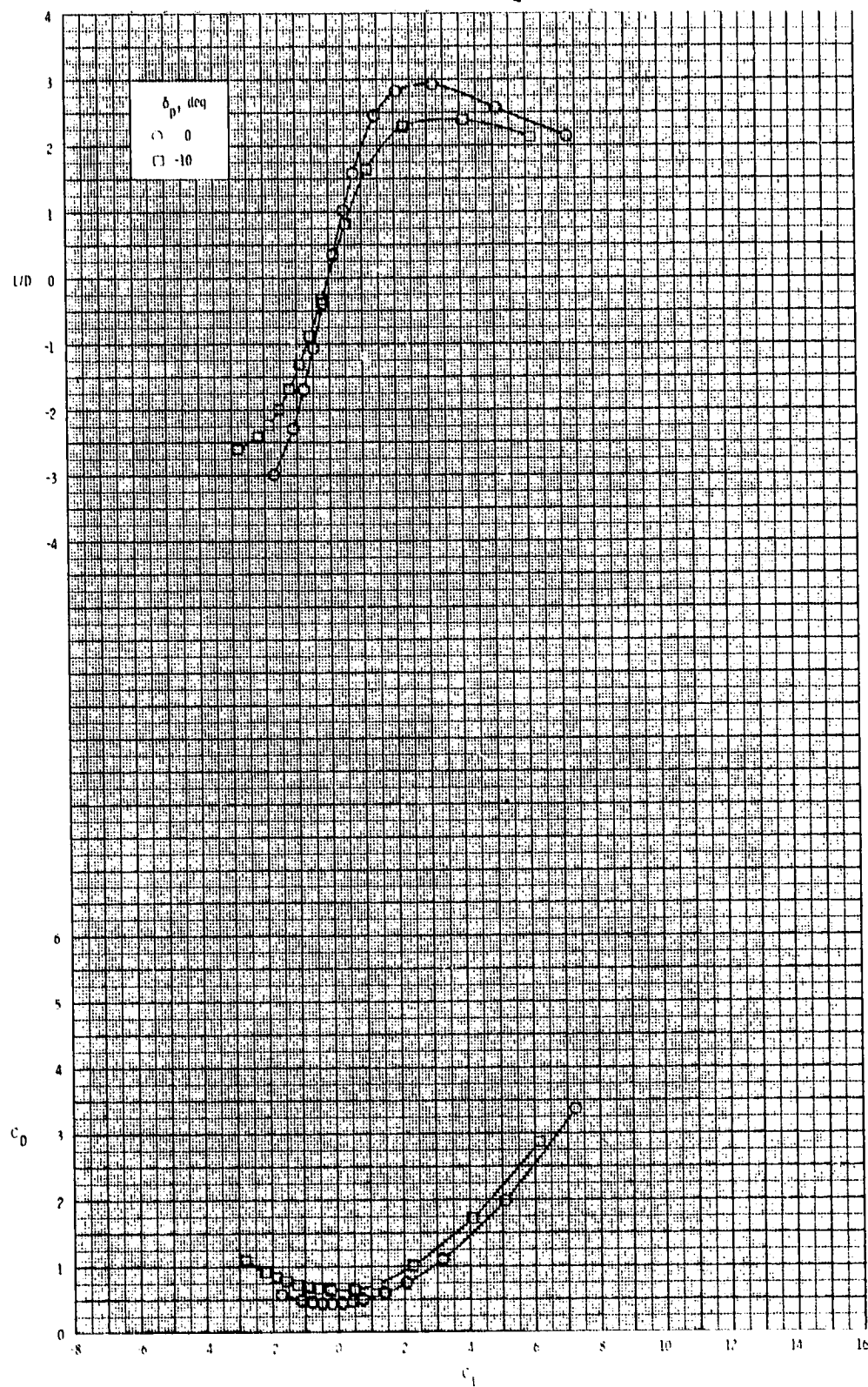
ORIGINAL PAGE IS
OF POOR QUALITY



(d) Continued.

Figure 23.- Continued.

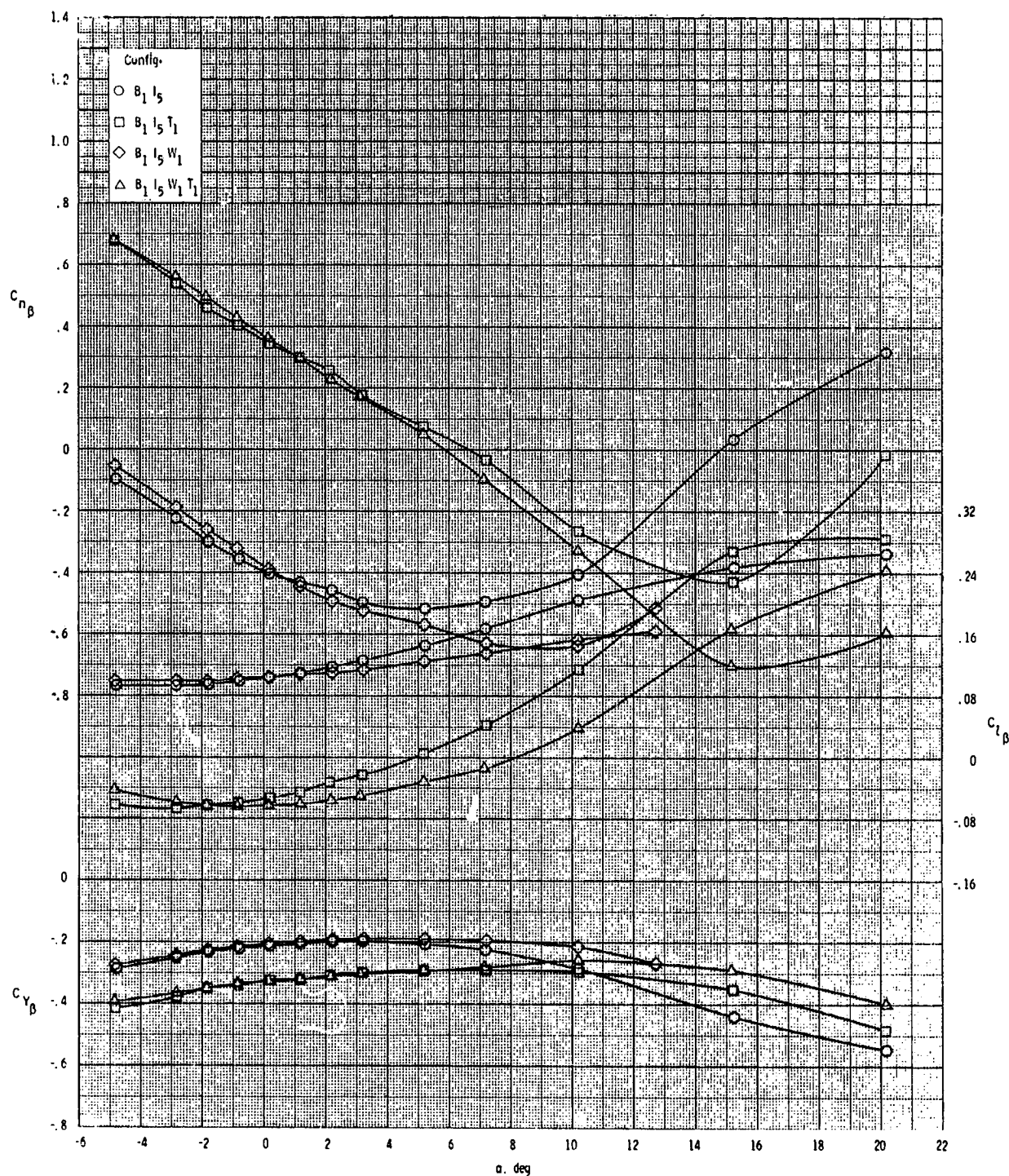
ORIGINAL PAGE IS
OF POOR QUALITY



(d) Concluded.

Figure 23.- Concluded.

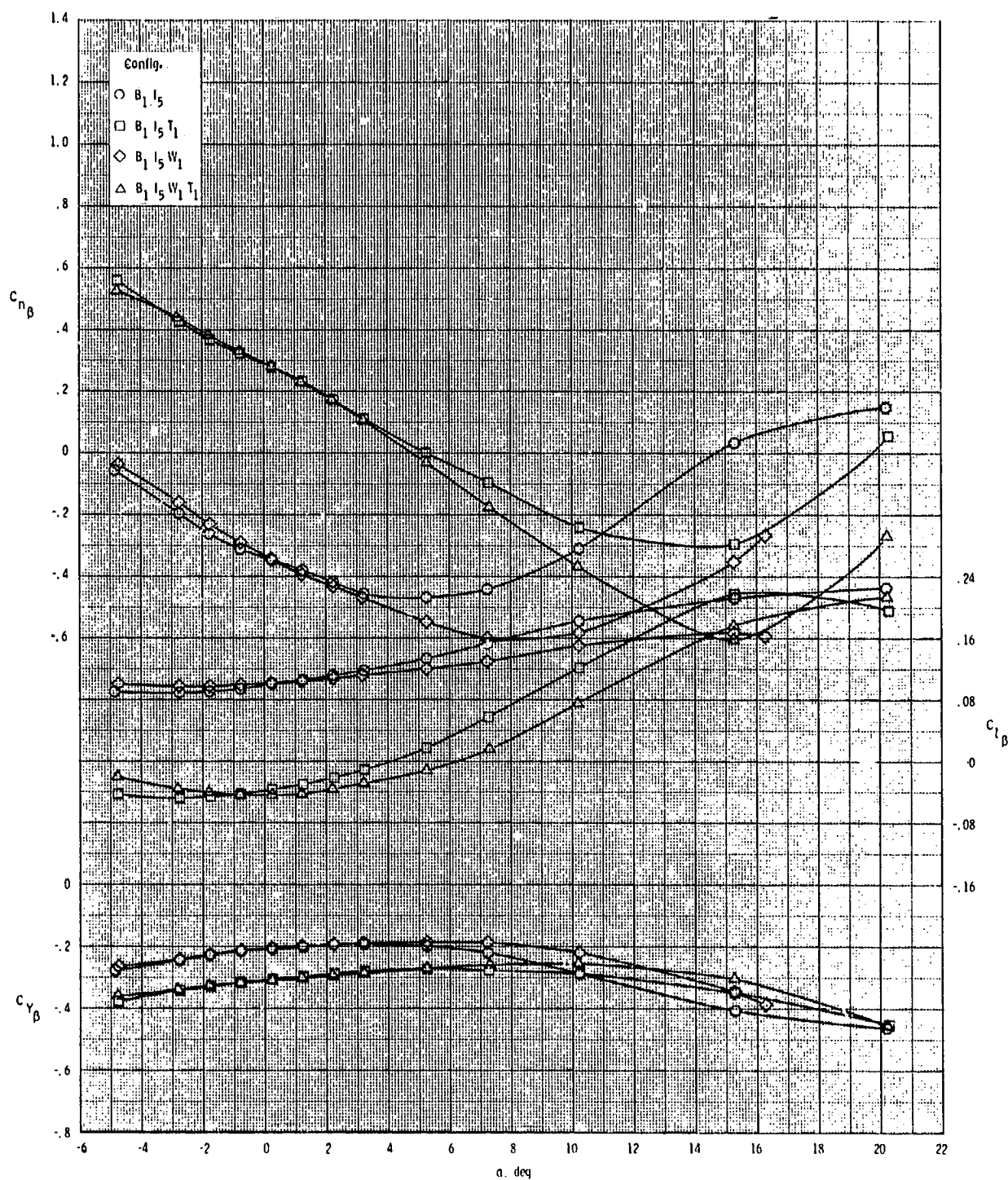
ORIGINAL PAGE 19
OF POOR QUALITY



(a) $M = 2.50$.

Figure 24.- Effect of various model components on lateral-directional stability for 2-D inlet with T_1 .

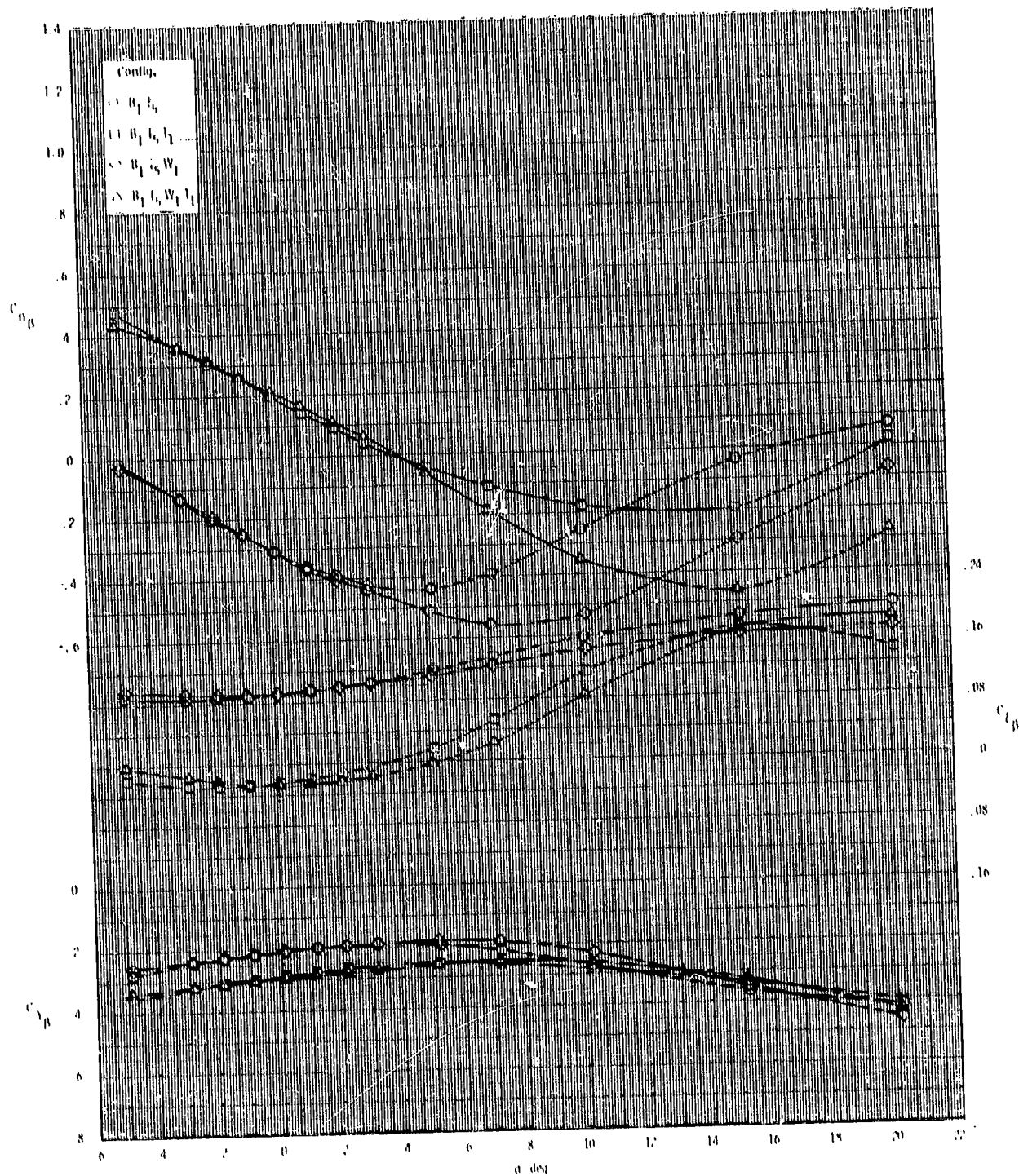
ORIGINAL PAGE IS
OF POOR QUALITY



(b) $M = 2.95$.

Figure 24.- Continued.

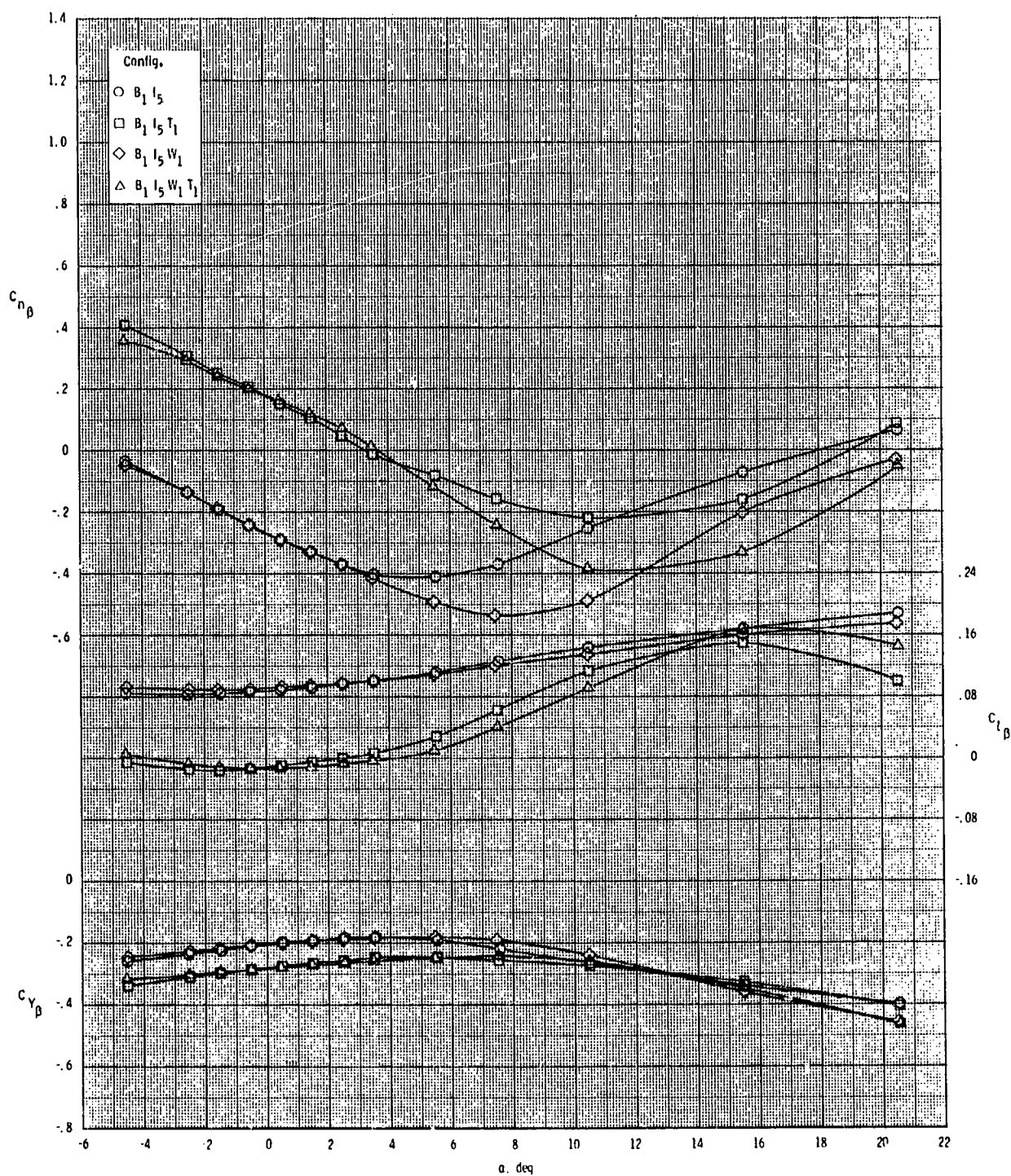
ORIGINAL PAGE IS
OF POOR QUALITY



(c) $M = 3.50$.

Figure 24.- Continued.

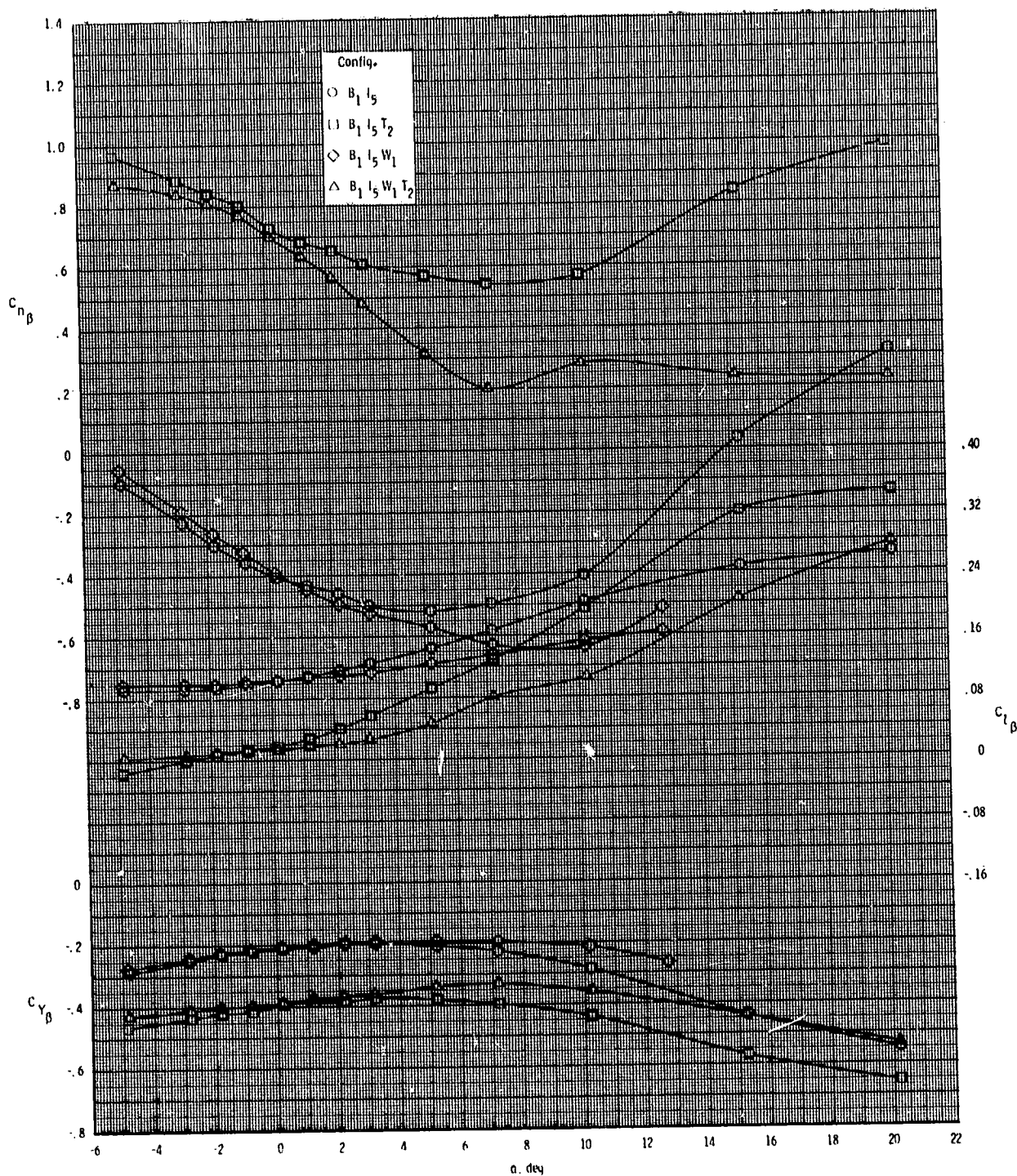
ORIGINAL PAGE IS
OF POOR QUALITY



(d) $M = 3.95$.

Figure 24.- Concluded.

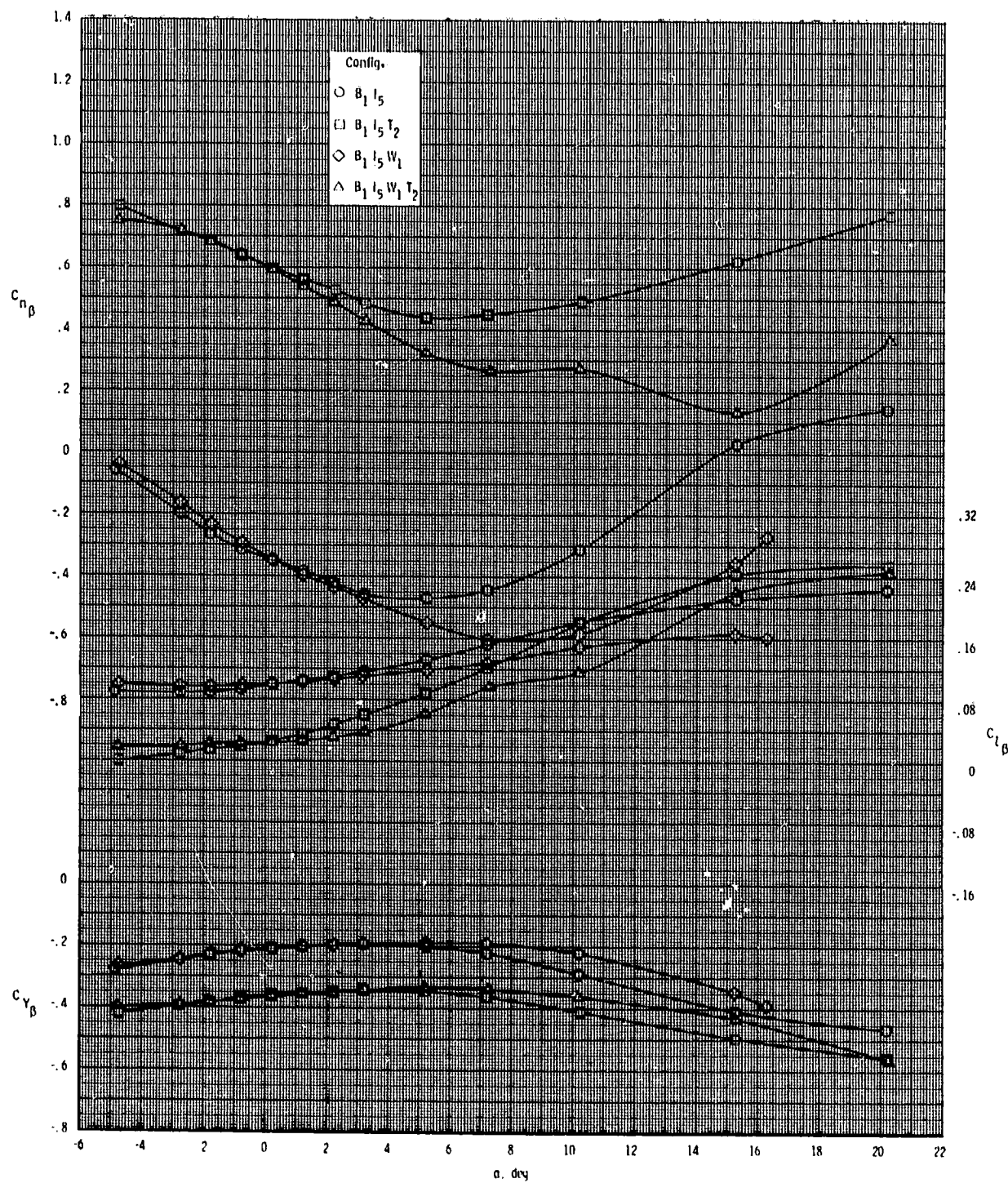
ORIGINAL PAGE IS
OF POOR QUALITY



(a) $M = 2.50$.

Figure 25.- Effect of various model components on lateral-directional stability for 2-D inlet with T_2 .

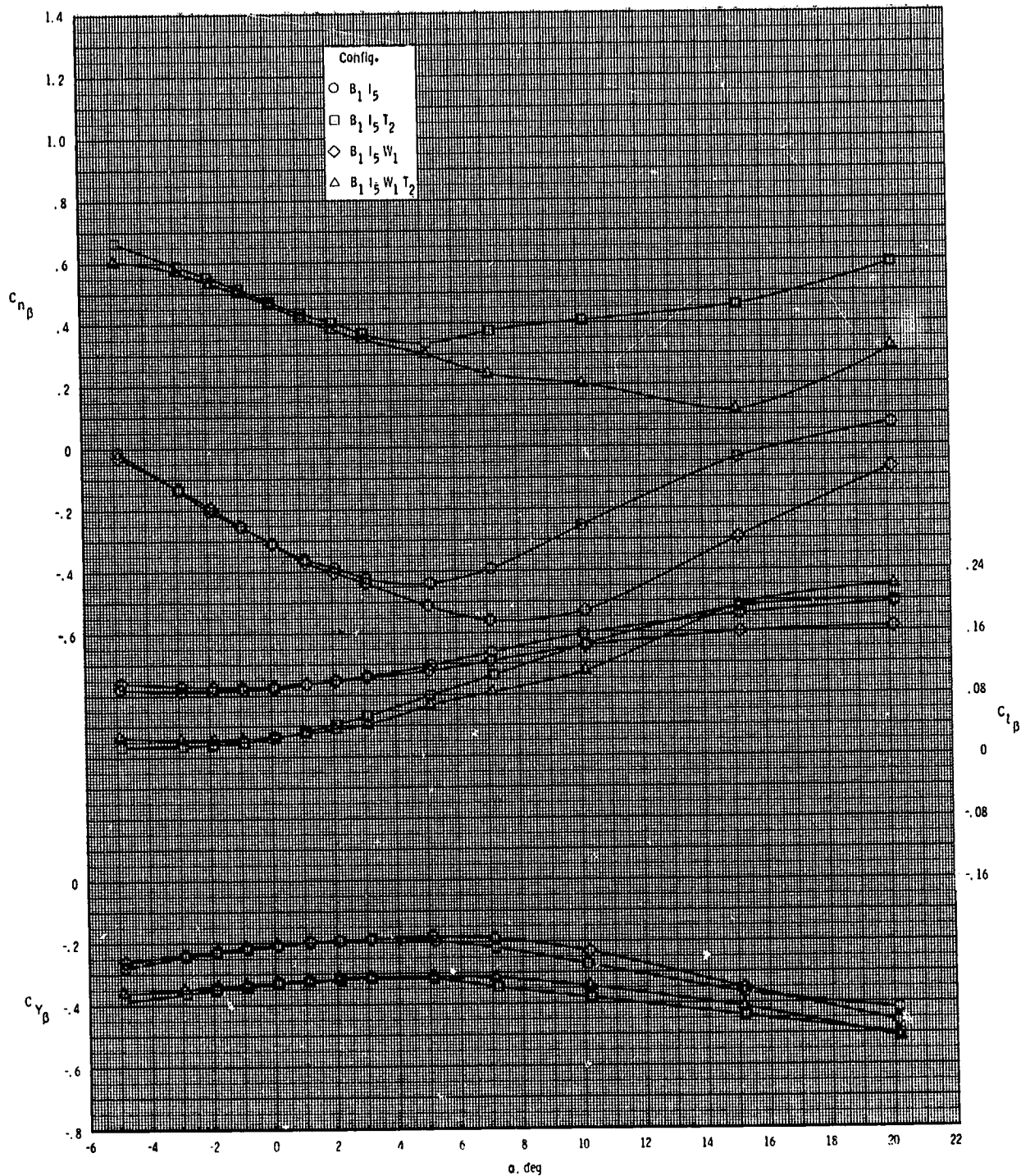
ORIGINAL PAGE IS
OF POOR QUALITY



(b) $M = 2.95$.

Figure 25.- Continued.

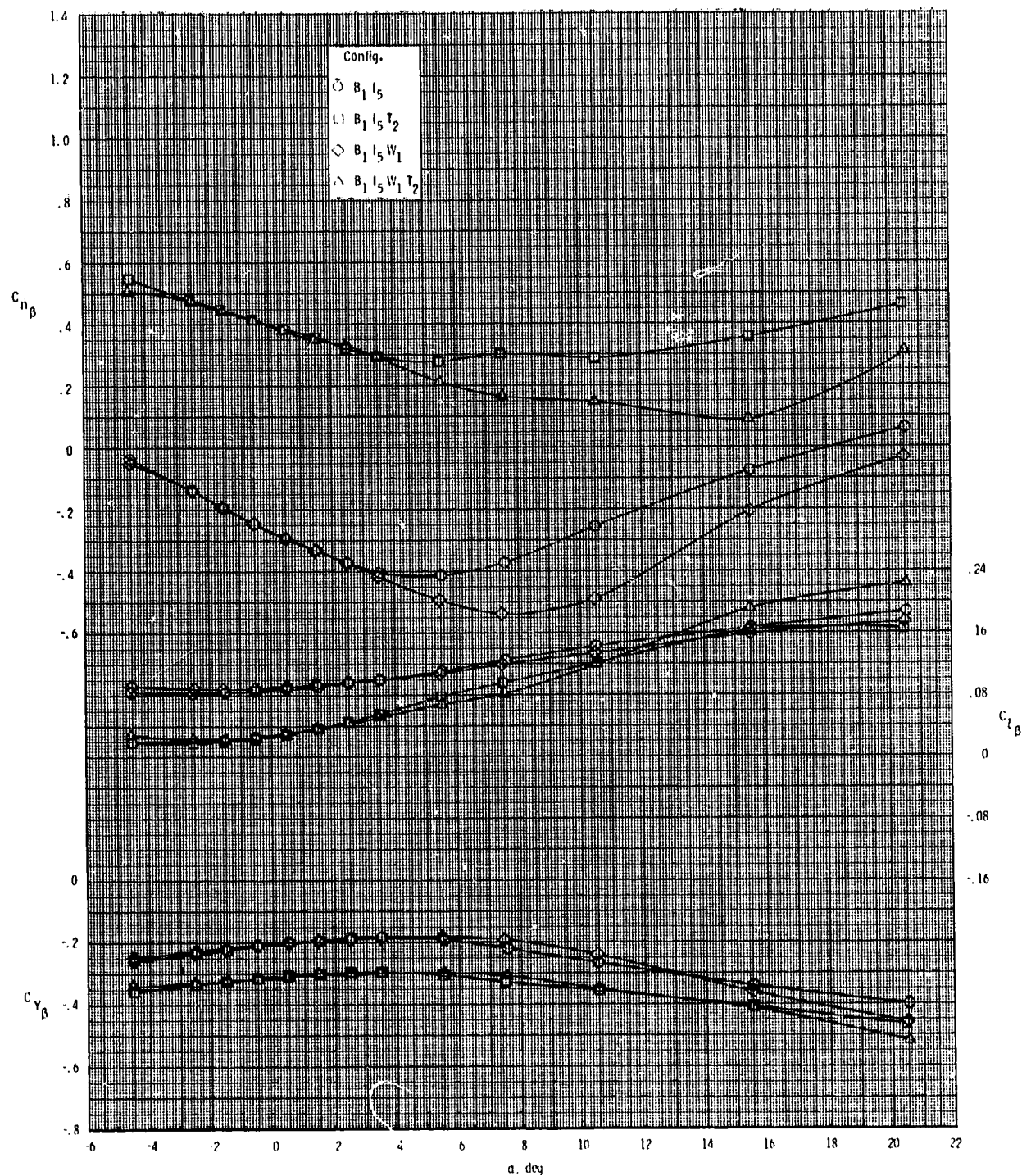
ORIGINAL PAGE IS
OF POOR QUALITY



(c) $M = 3.50$.

Figure 25.- Continued.

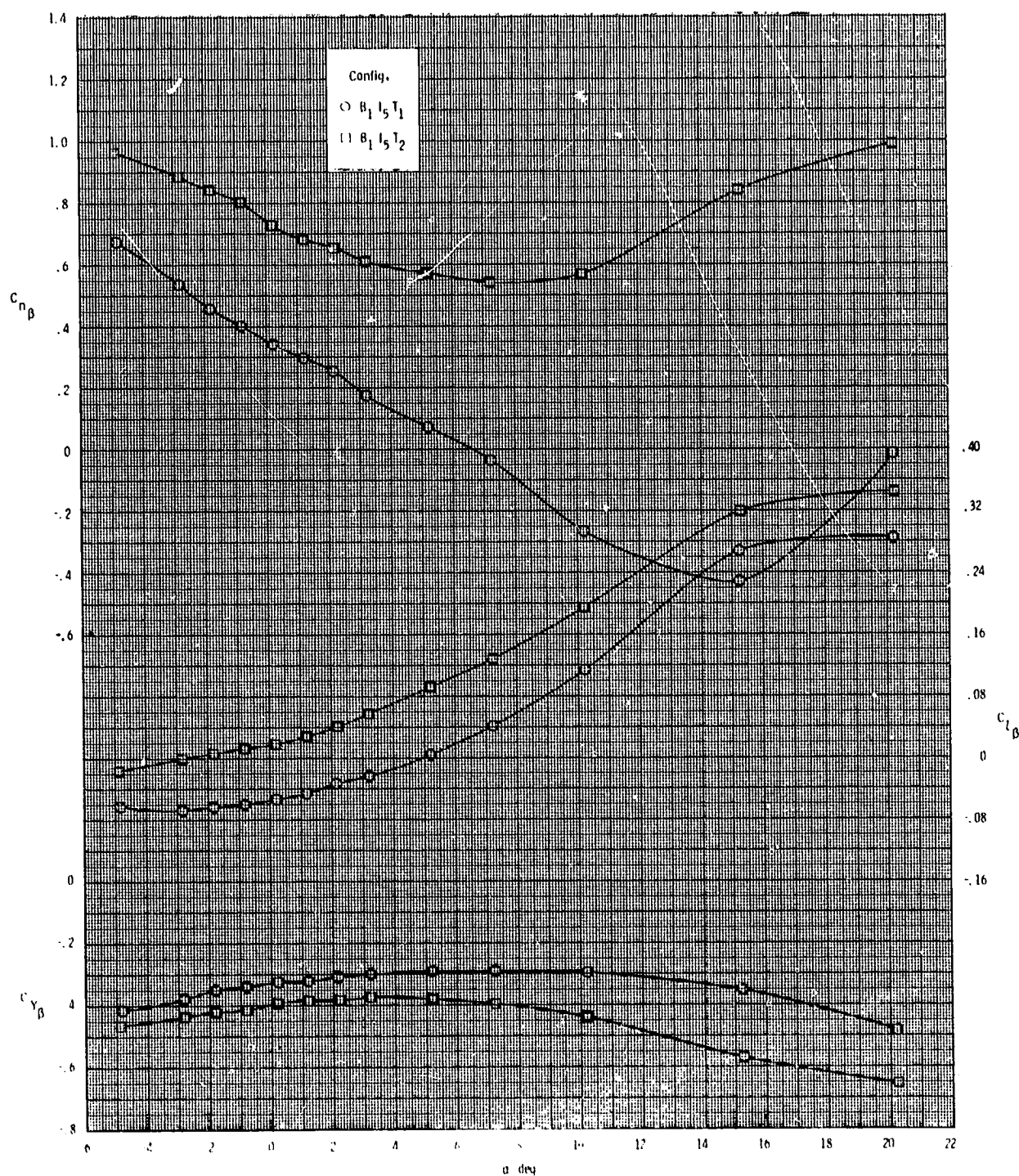
ORIGINAL PAGE IS
OF POOR QUALITY



(d) $M = 3.95$.

Figure 25.- Concluded.

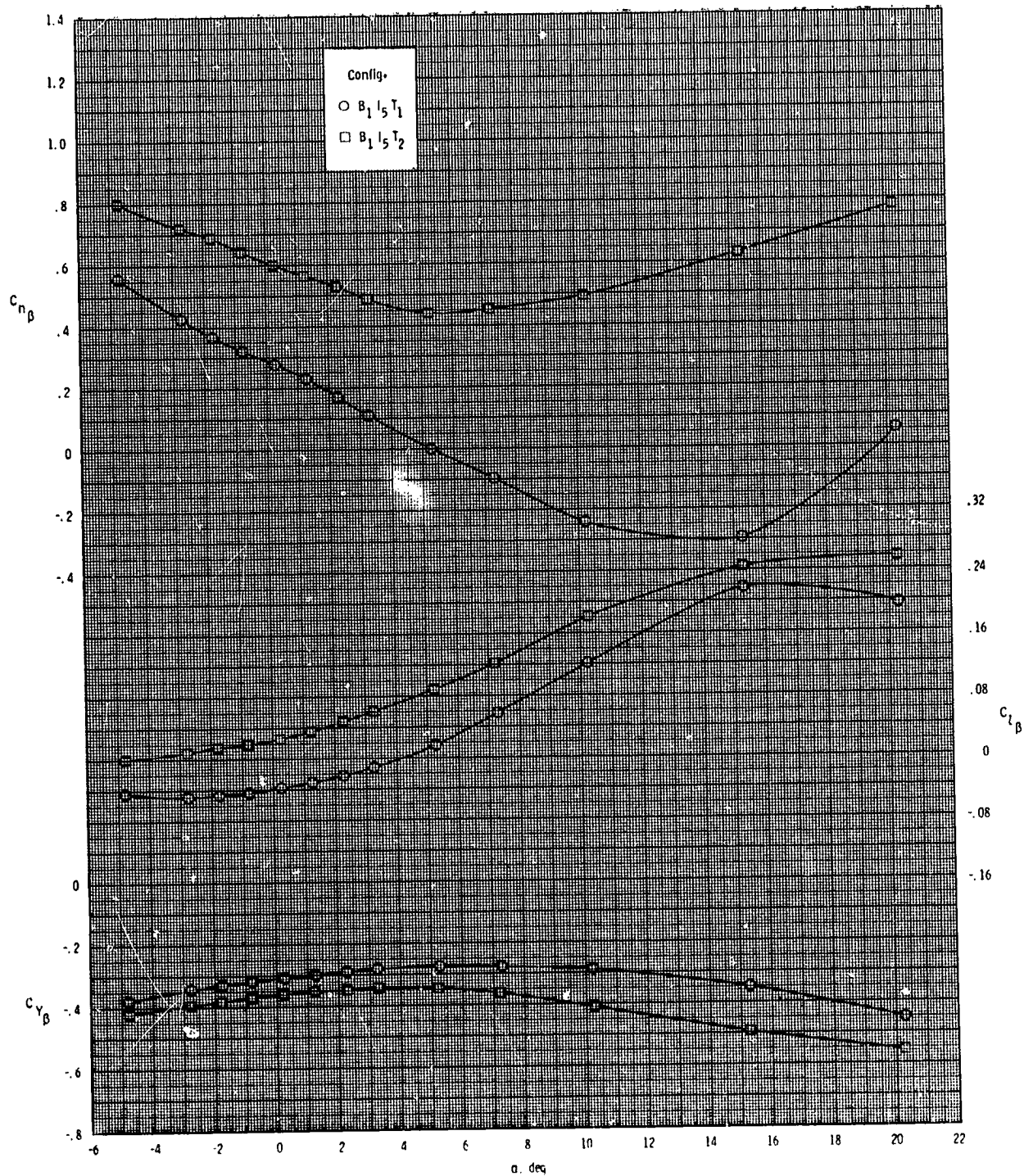
ORIGINAL PAGE IS
OF POOR QUALITY



(a) $M = 2.50$.

Figure 26.- Effect of tail configuration on lateral-directional stability for 2-D inlet with wing off.

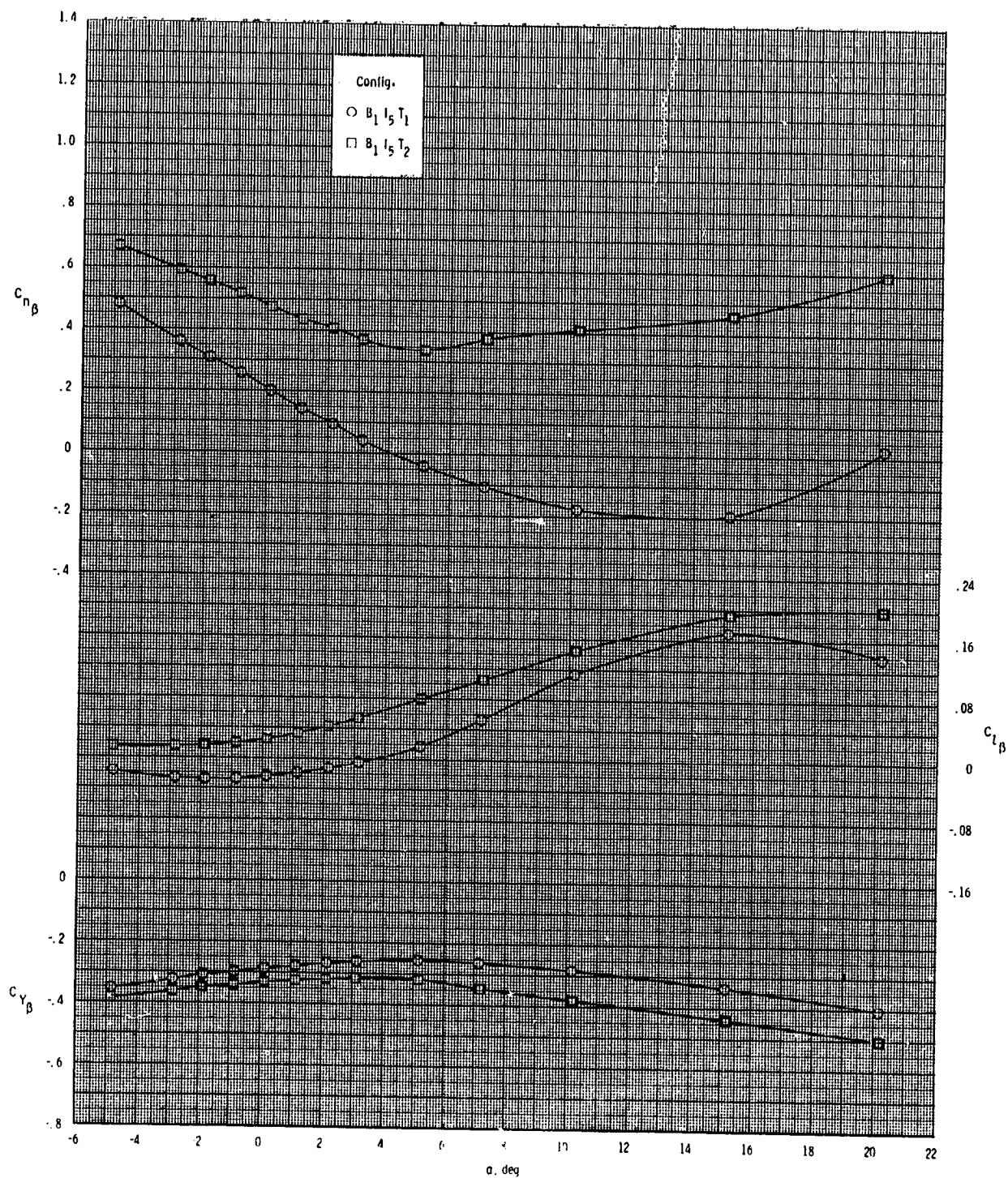
ORIGINAL PAGE IS
OF POOR QUALITY



(b) $M = 2.95$.

Figure 26.- Continued.

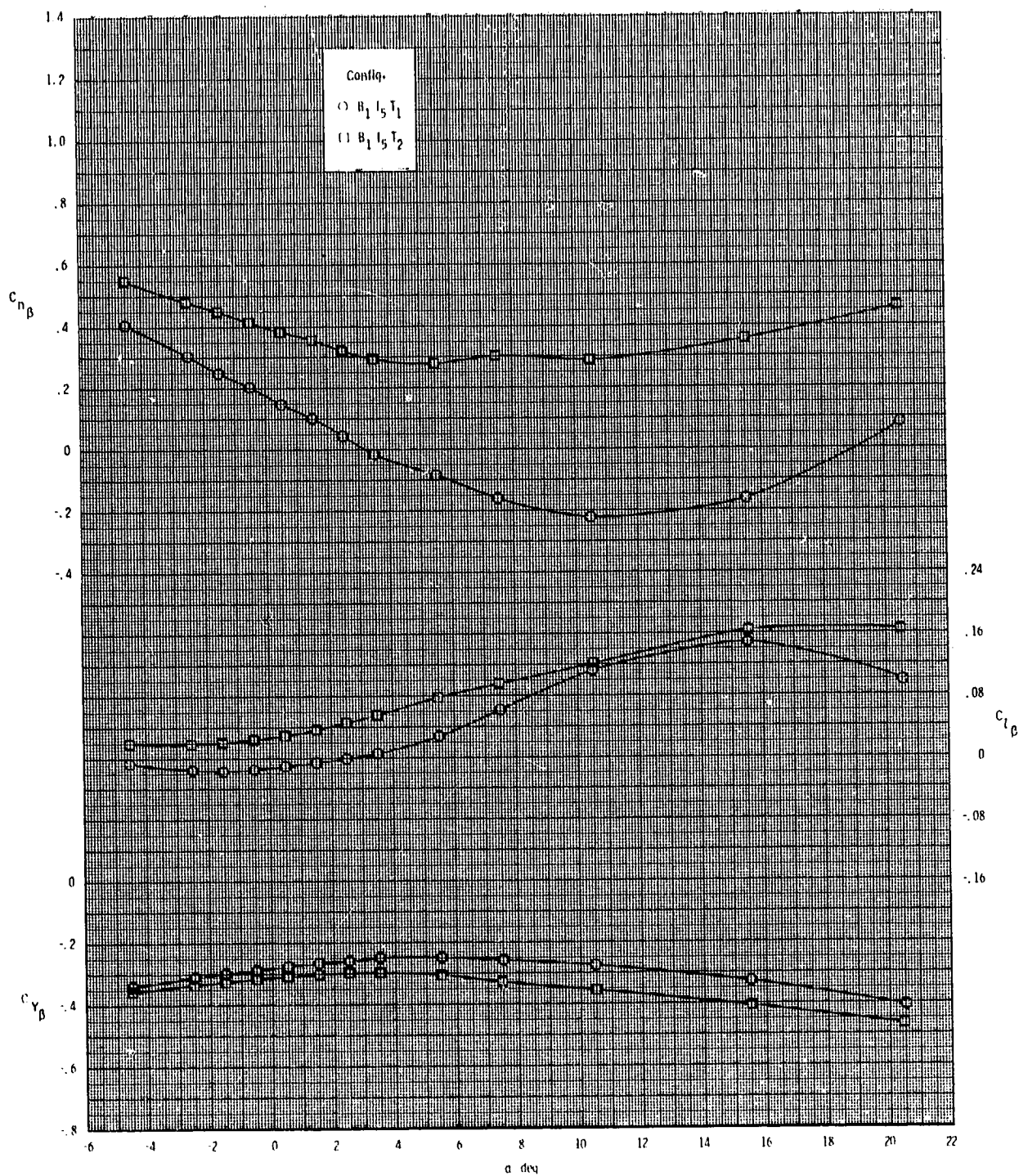
ORIGINAL PAGE IS
OF POOR QUALITY



(c) $M = 3.50$.

Figure 26.- Continued.

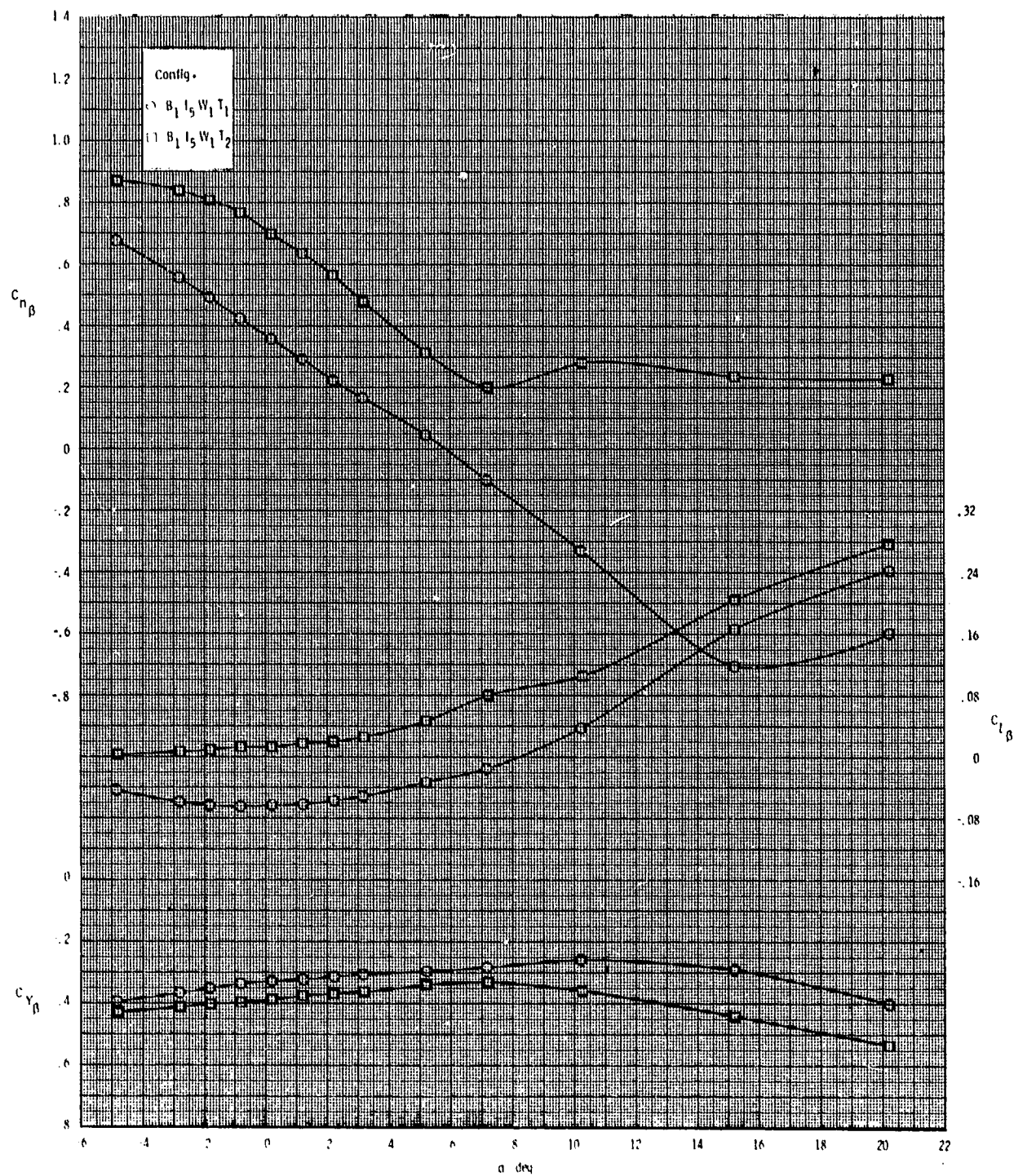
ORIGINAL PAGE IS
OF POOR QUALITY



(d) $M = 3.95$.

Figure 26.- Concluded.

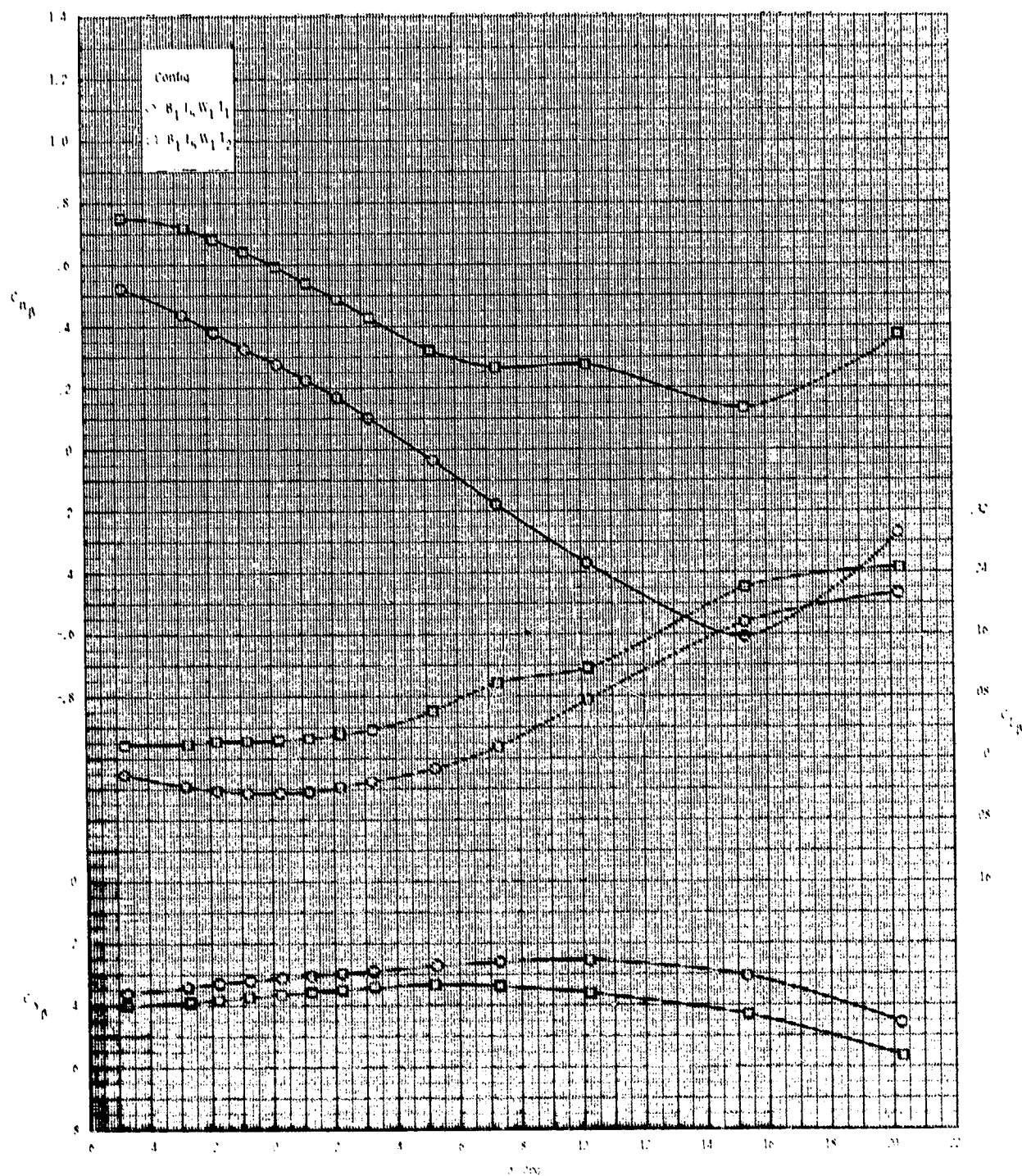
ORIGINAL PAGE IS
OF POOR QUALITY



(a) $M = 2.50$.

Figure 27.- Effect of tail configuration on lateral-directional stability for 2-D inlet with wing on.

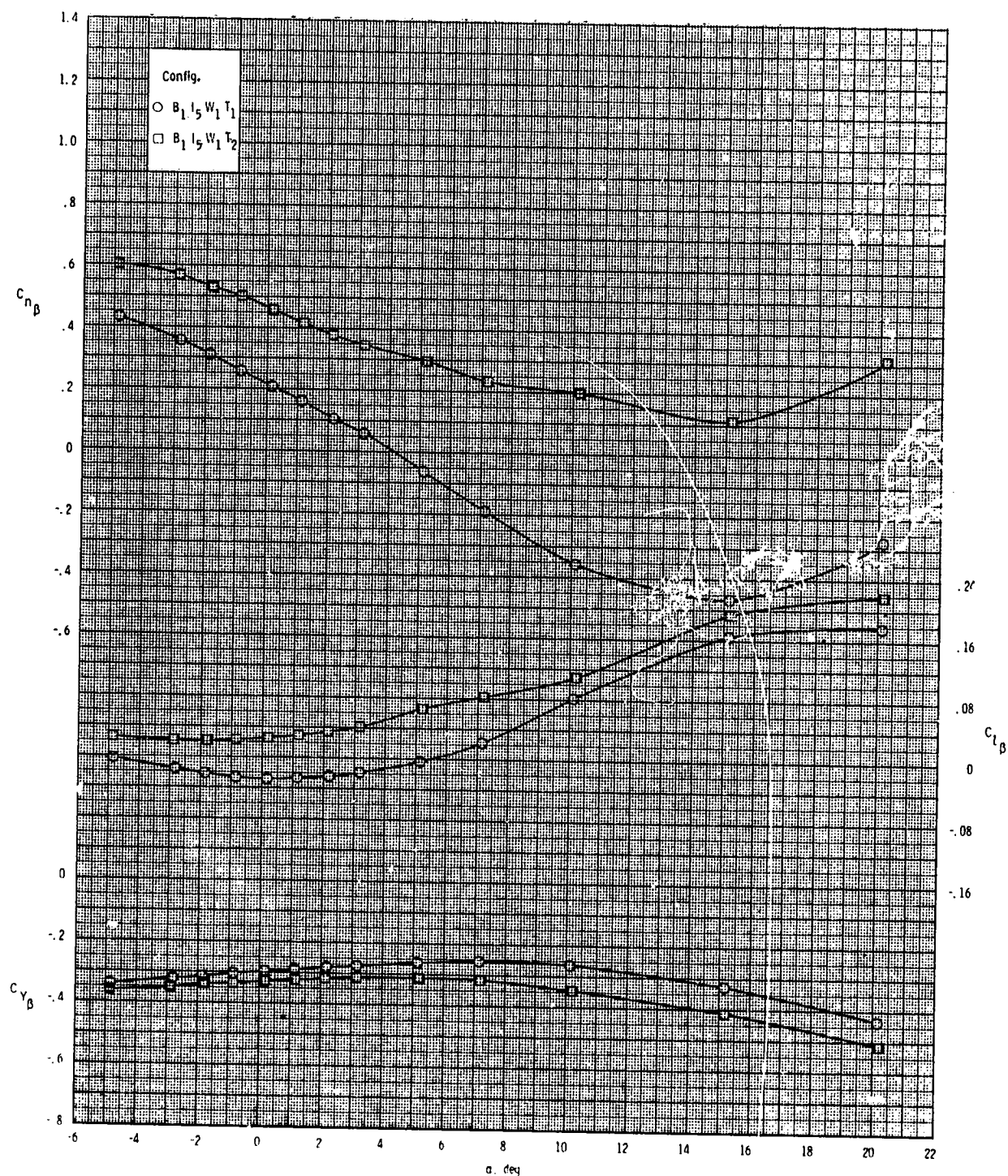
ORIGINAL PAGE 15
OF POOR QUALITY



(b) $M = 2.95$.

Figure 27.- Continued.

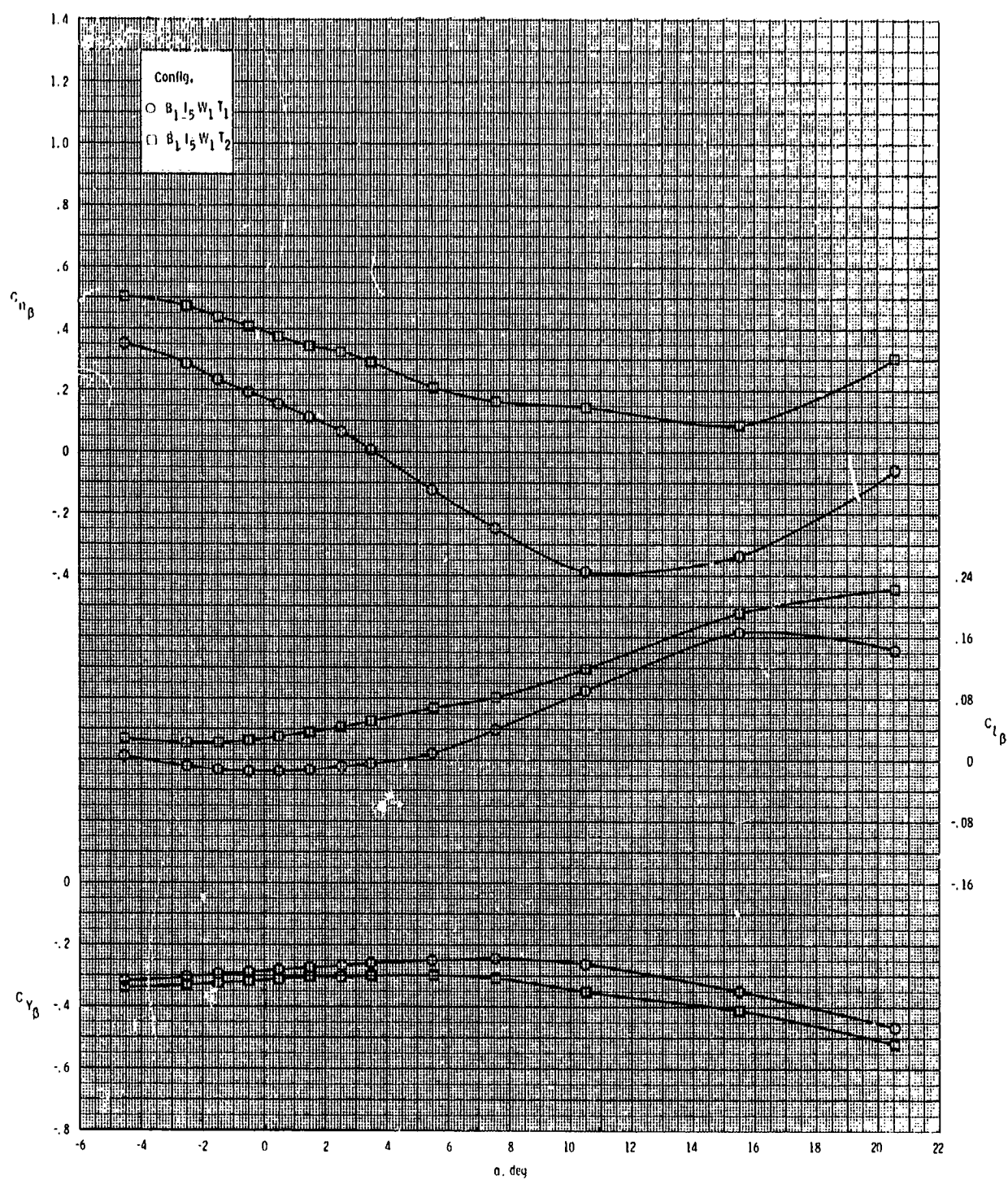
ORIGINAL PAGE IS
OF POOR QUALITY



(c) $M = 3.50$.

Figure 27.- Continued.

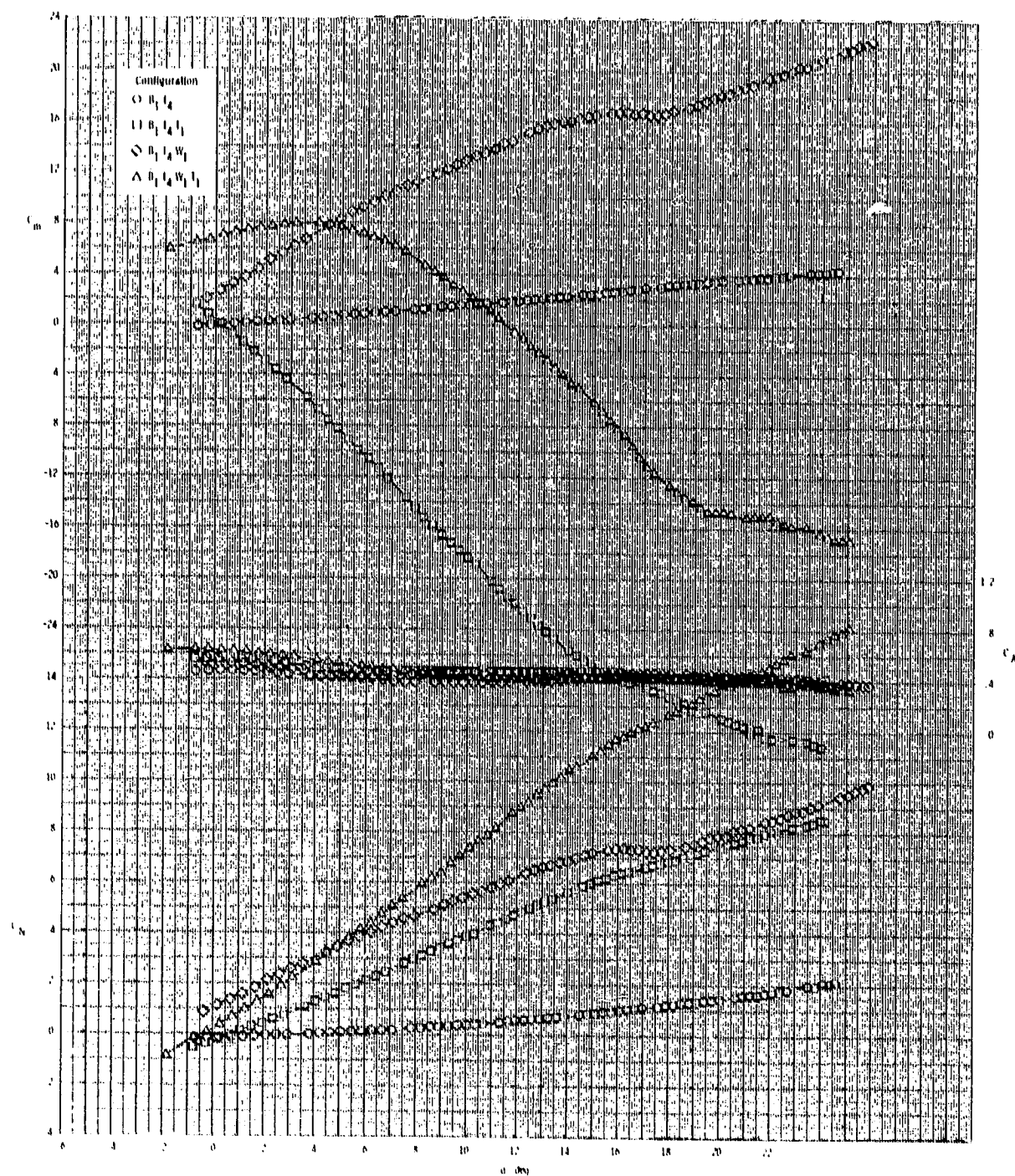
ORIGINAL PAGE IS
OF POOR QUALITY



(d) $M = 3.95$.

Figure 27.- Concluded.

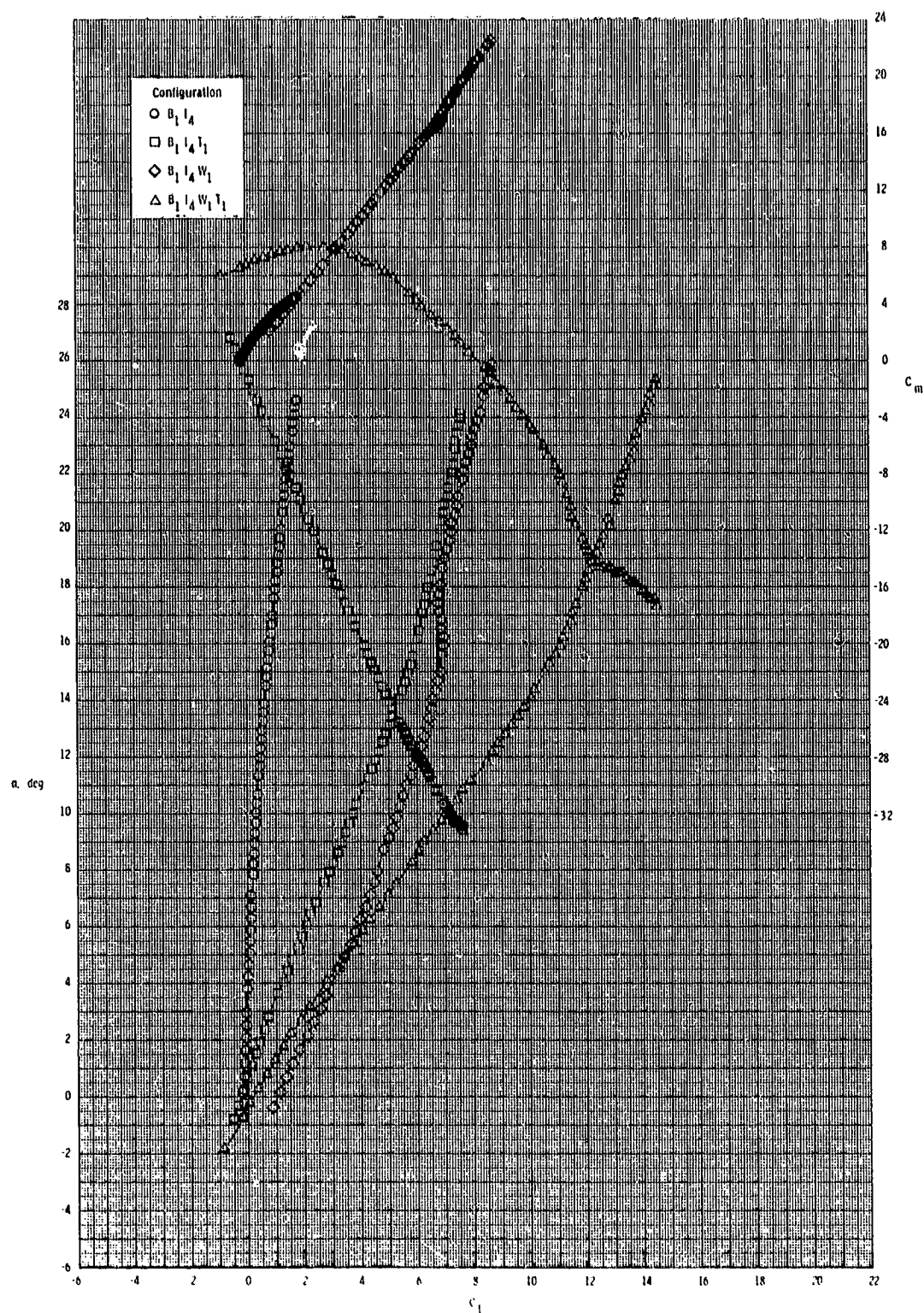
ORIGINAL PAGE IS
OF POOR QUALITY



(a) $M = 0.60$.

Figure 28.- Effect of various model components on longitudinal aerodynamic characteristics for axisymmetric inlet with T_1 and internal duct closed.

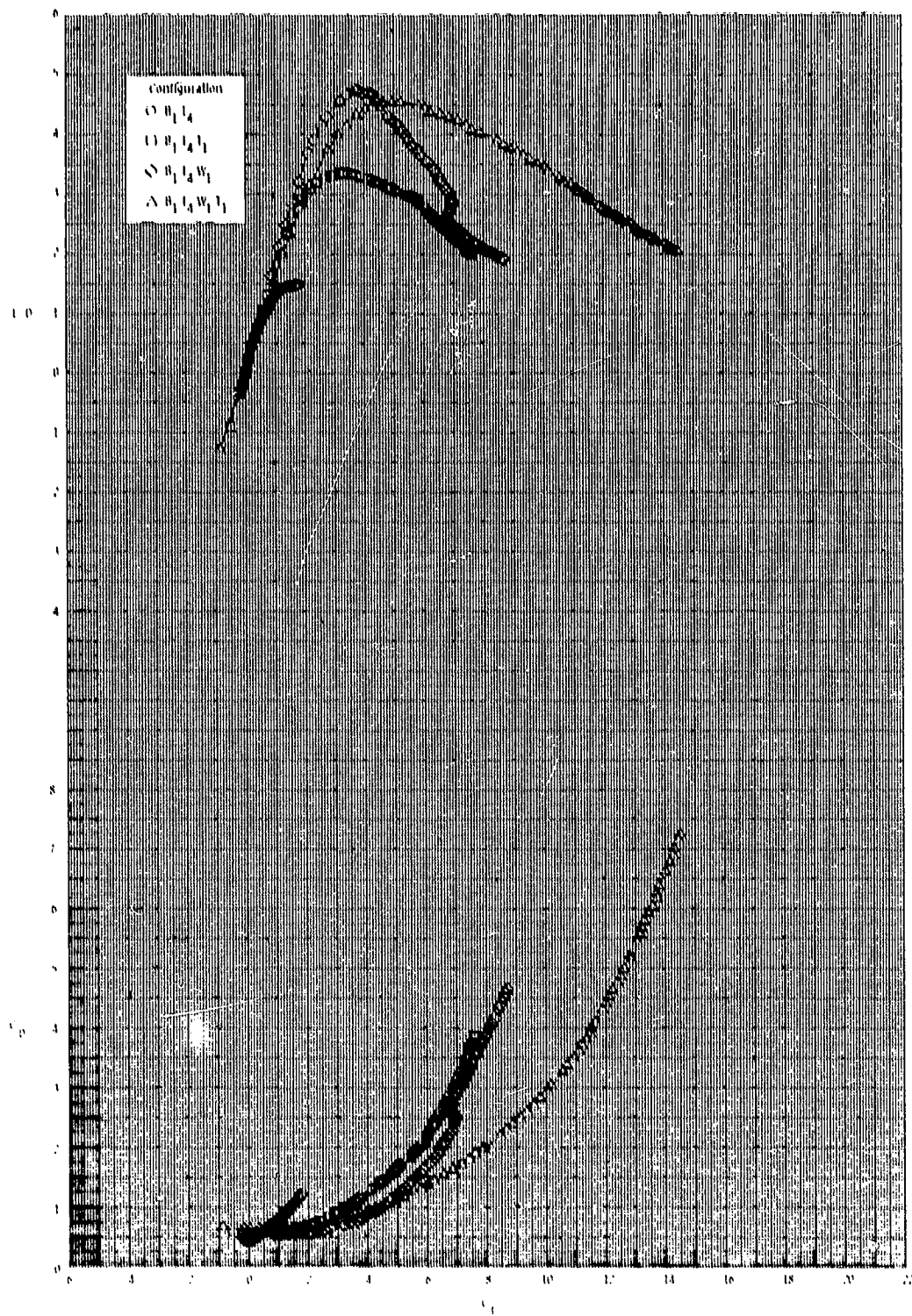
ORIGINAL PAGE IS
OF POOR QUALITY



(a) Continued.

Figure 28.- Continued.

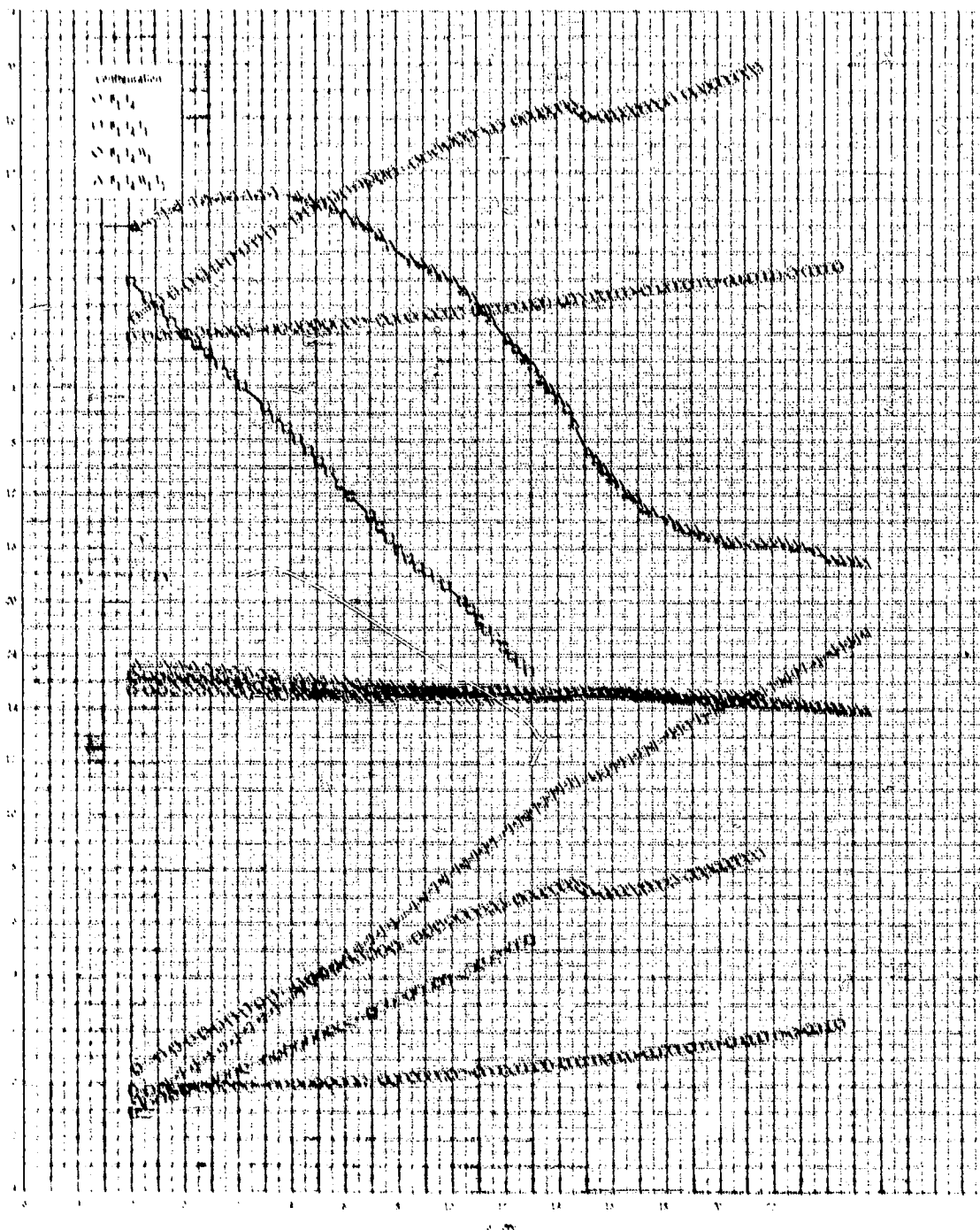
ORIGINAL PAGE IS
OF POOR QUALITY



(a) Concluded.

Figure 28.- Continued.

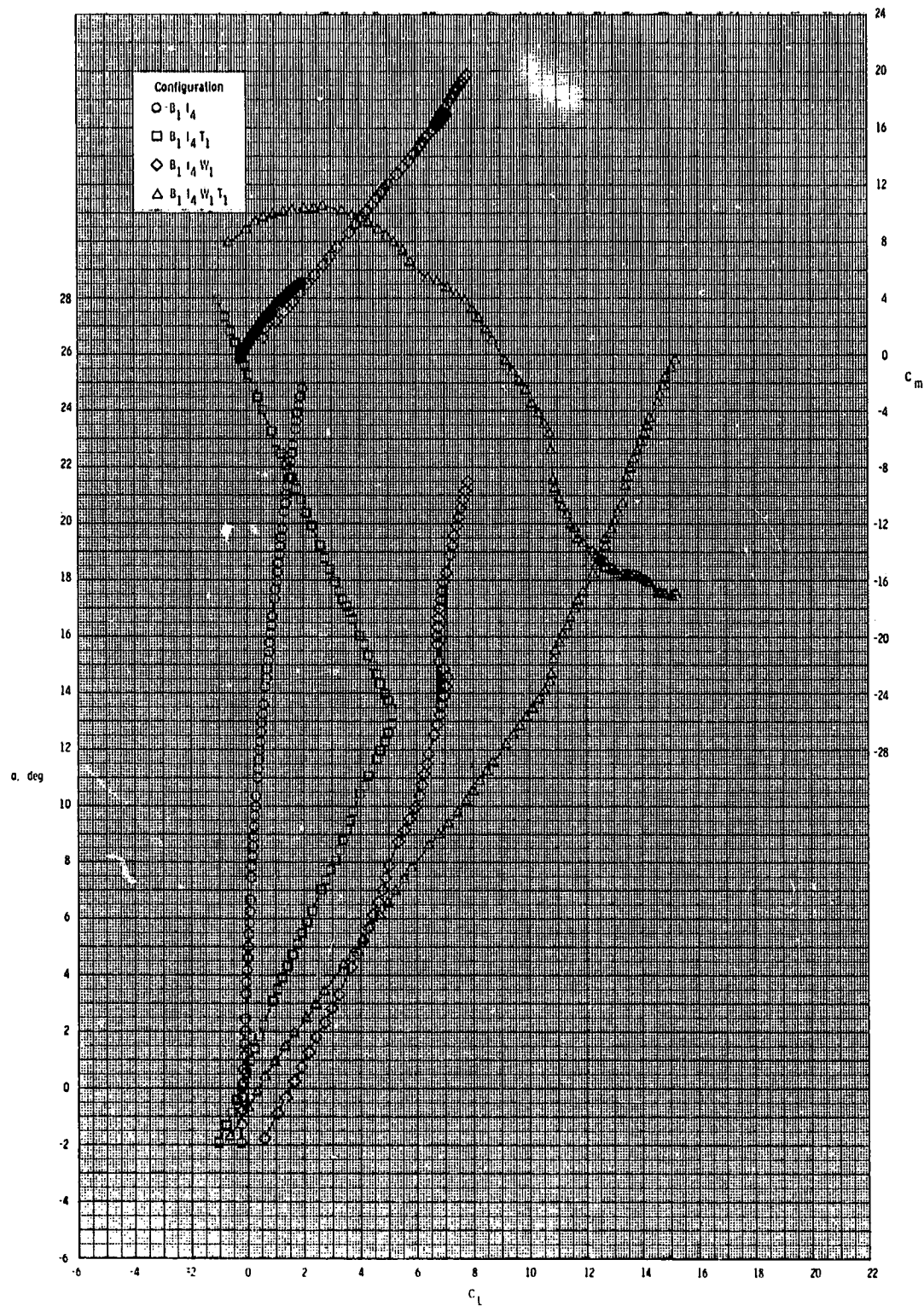
ORIGINAL PAGE IS
OF POOR QUALITY



(11) At 0.30.

Figure A3. continued.

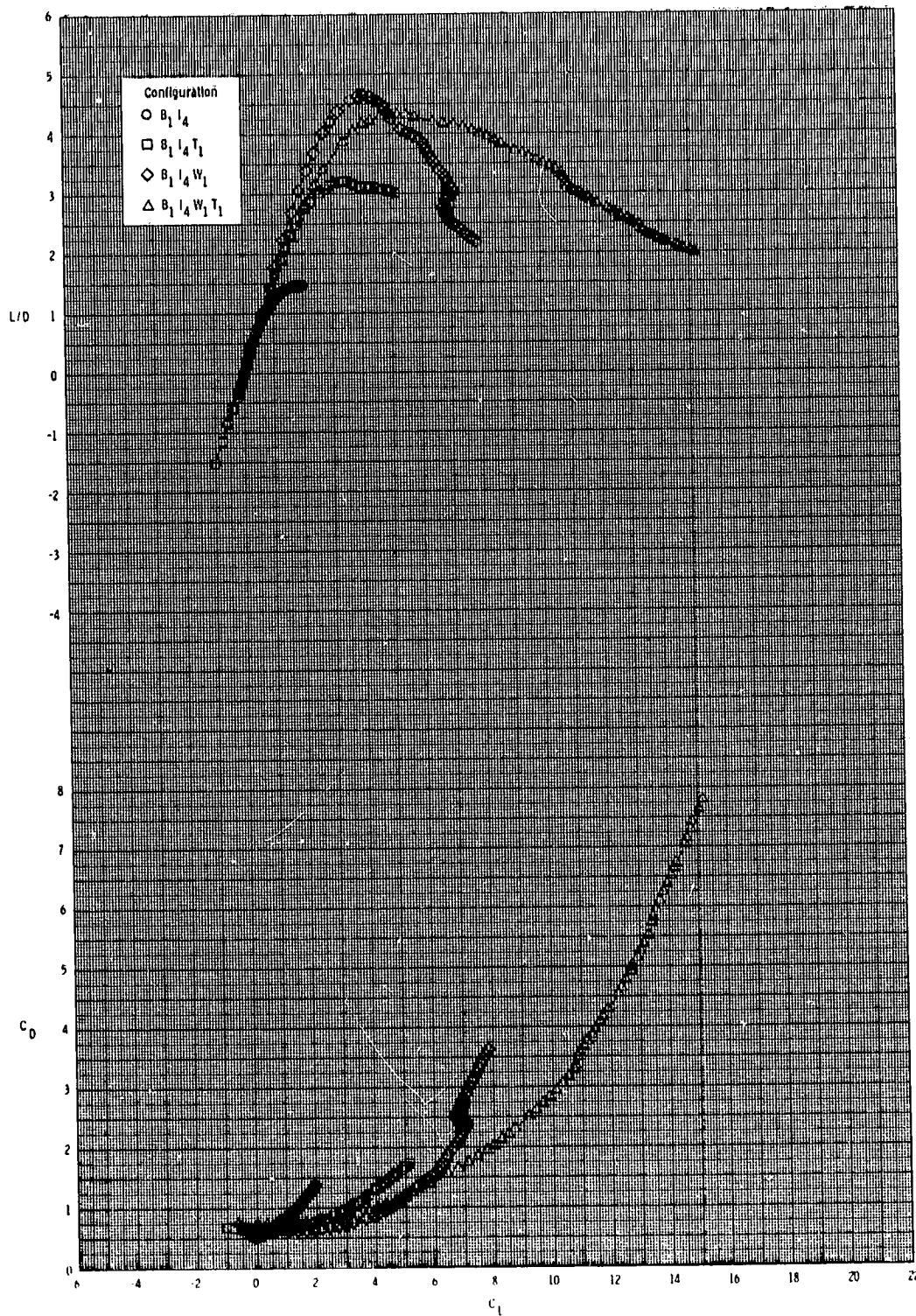
ORIGINAL PAGE IS
OF POOR QUALITY



(b) Continued.

Figure 28.- Continued.

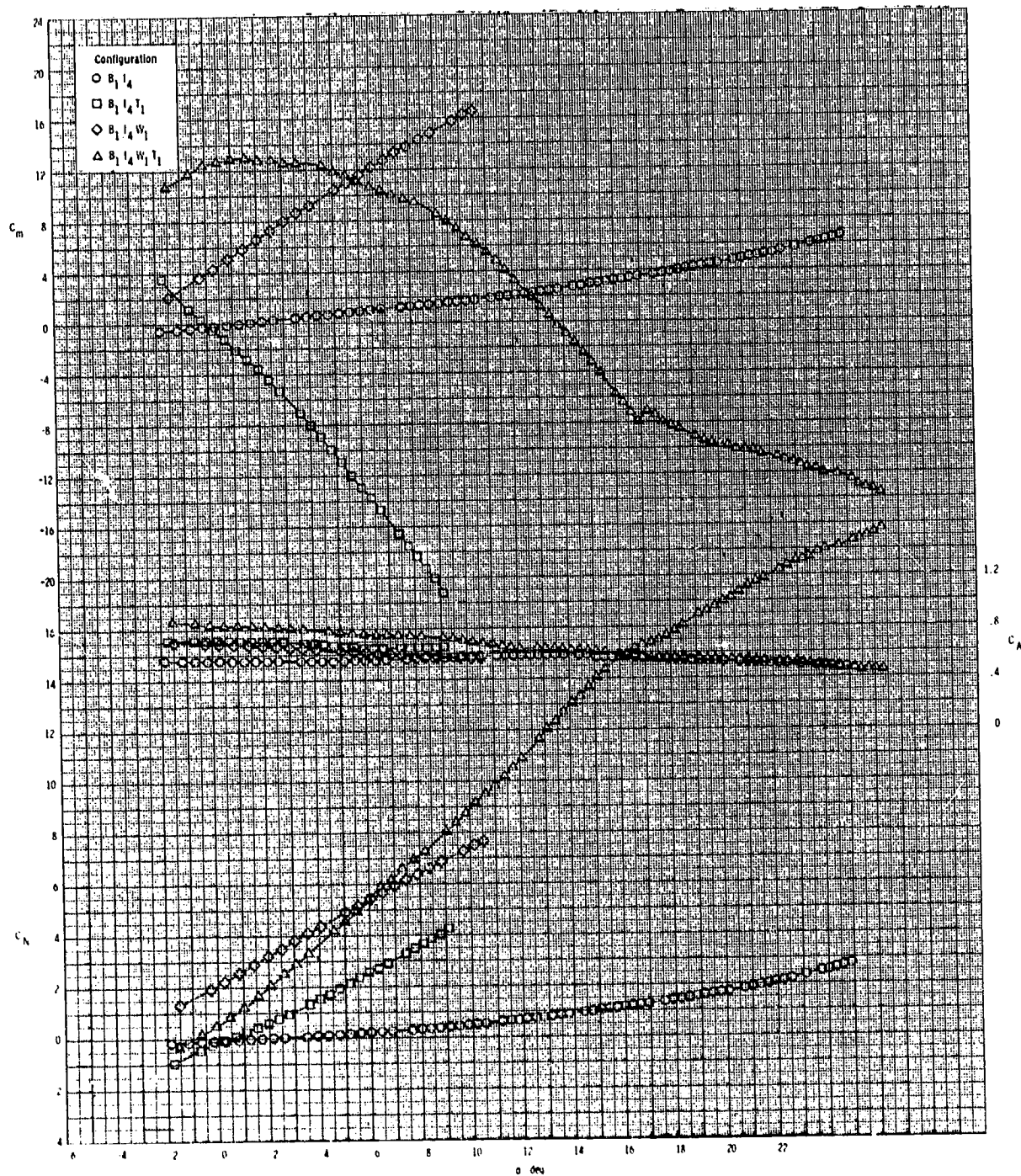
ORIGINAL PAGE IS
OF POOR QUALITY



(b) Concluded.

Figure 28.- Continued.

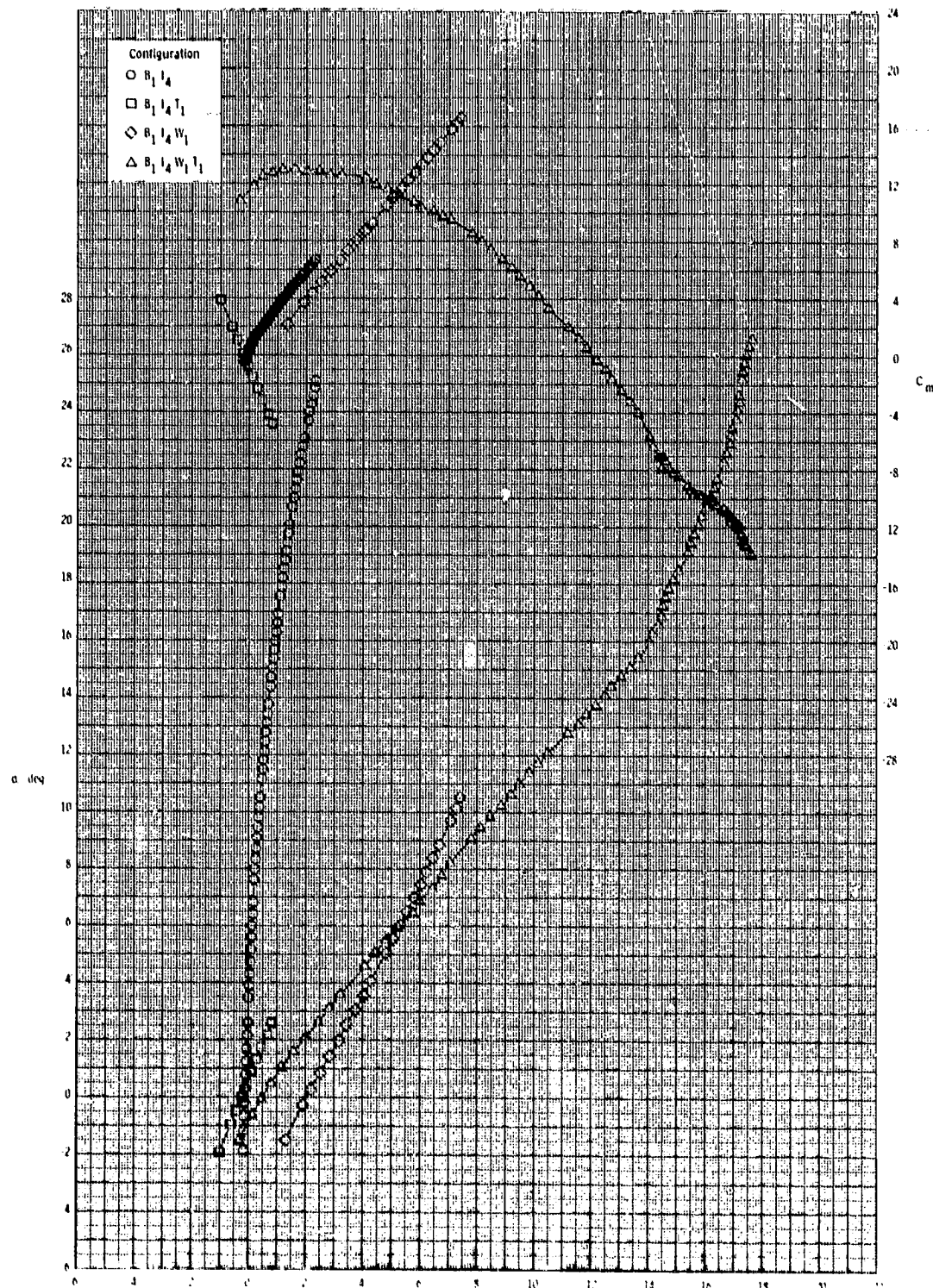
ORIGINAL PAGE IS
OF POOR QUALITY



(c) $M = 0.95$.

Figure 28.- Continued.

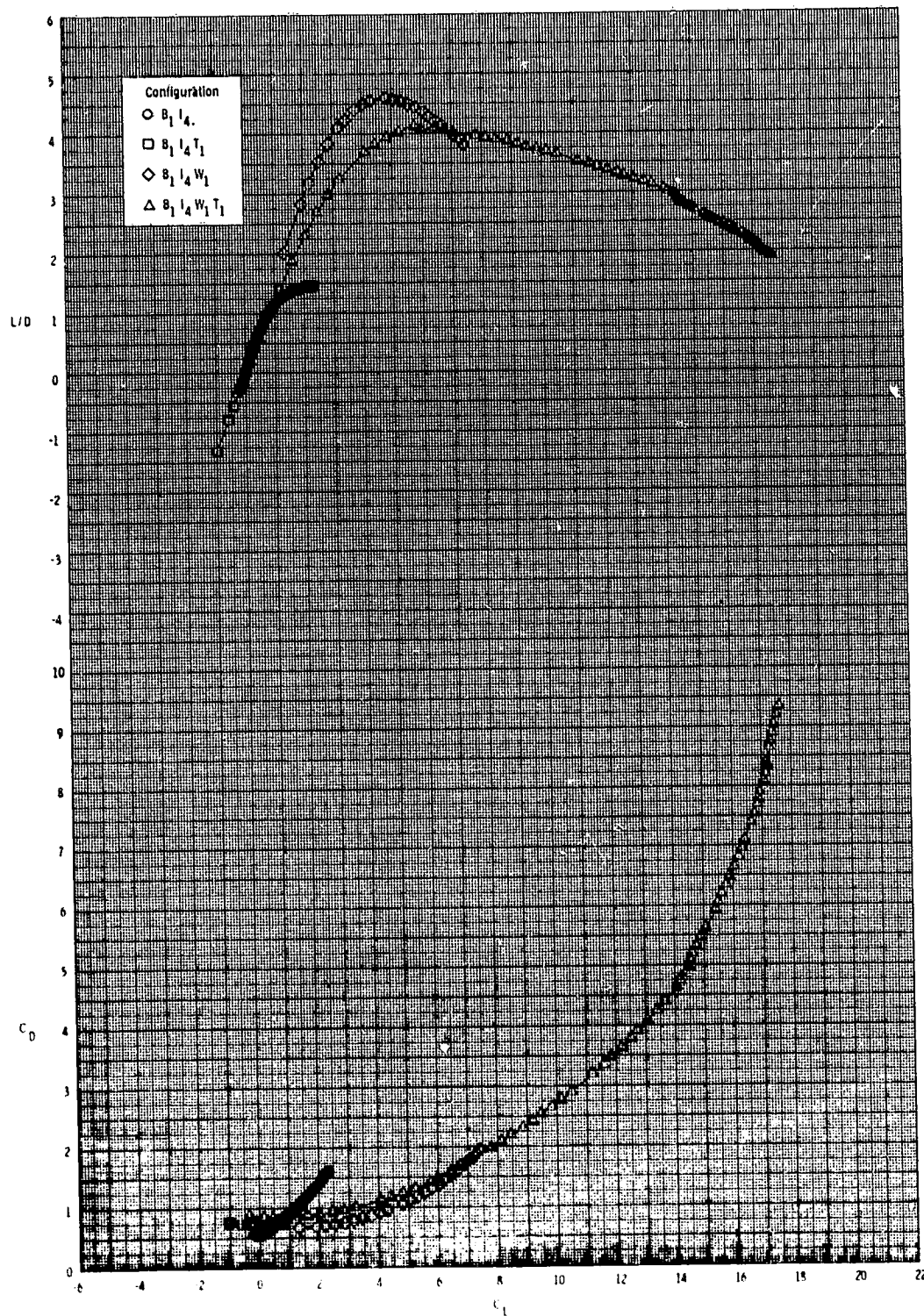
ORIGINAL PAGE IS
OF POOR QUALITY.



(c) Continued.

Figure 28.- Continued.

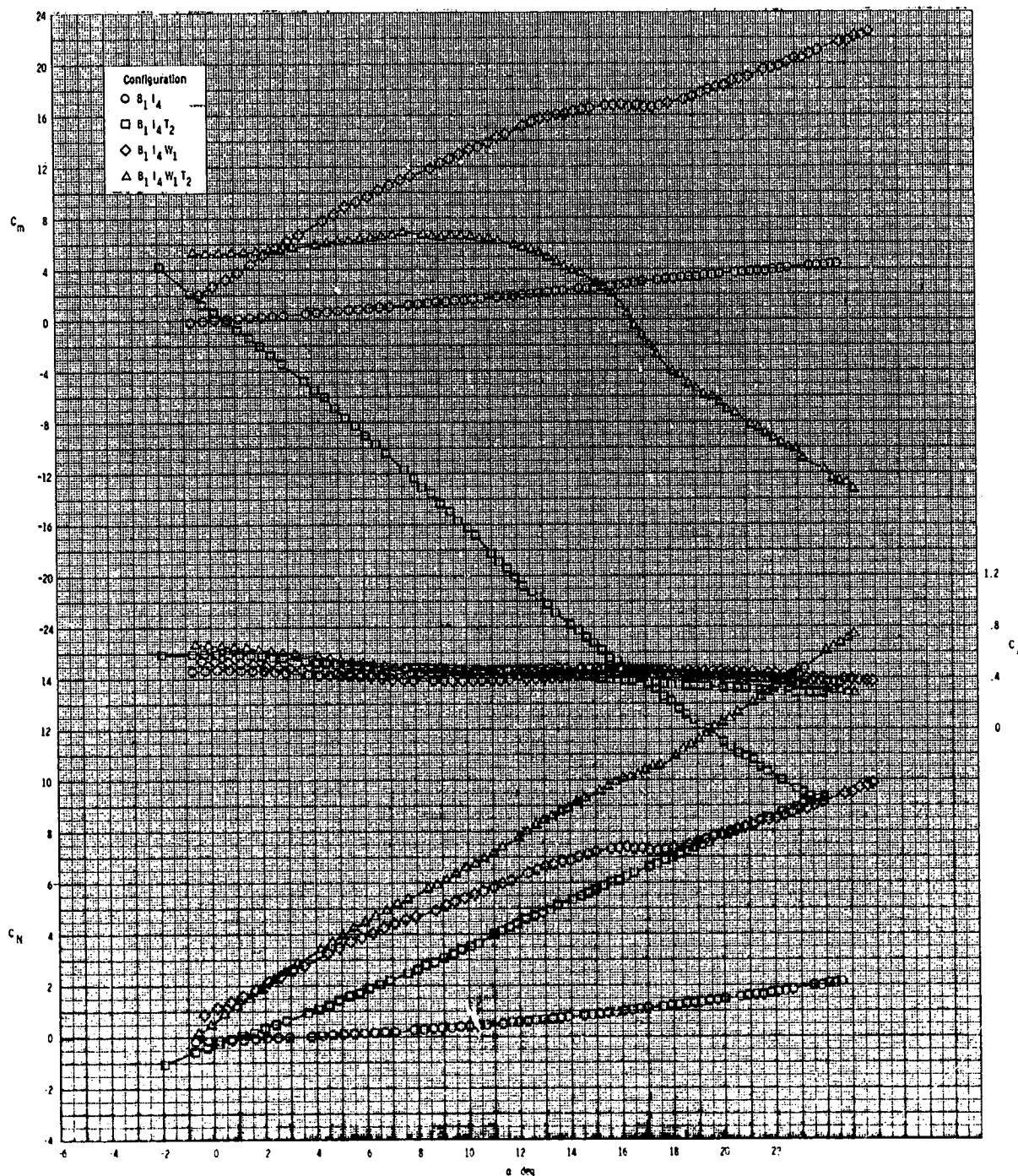
ORIGINAL PAGE IS
OF POOR QUALITY



(c) Concluded.

Figure 28.- Concluded.

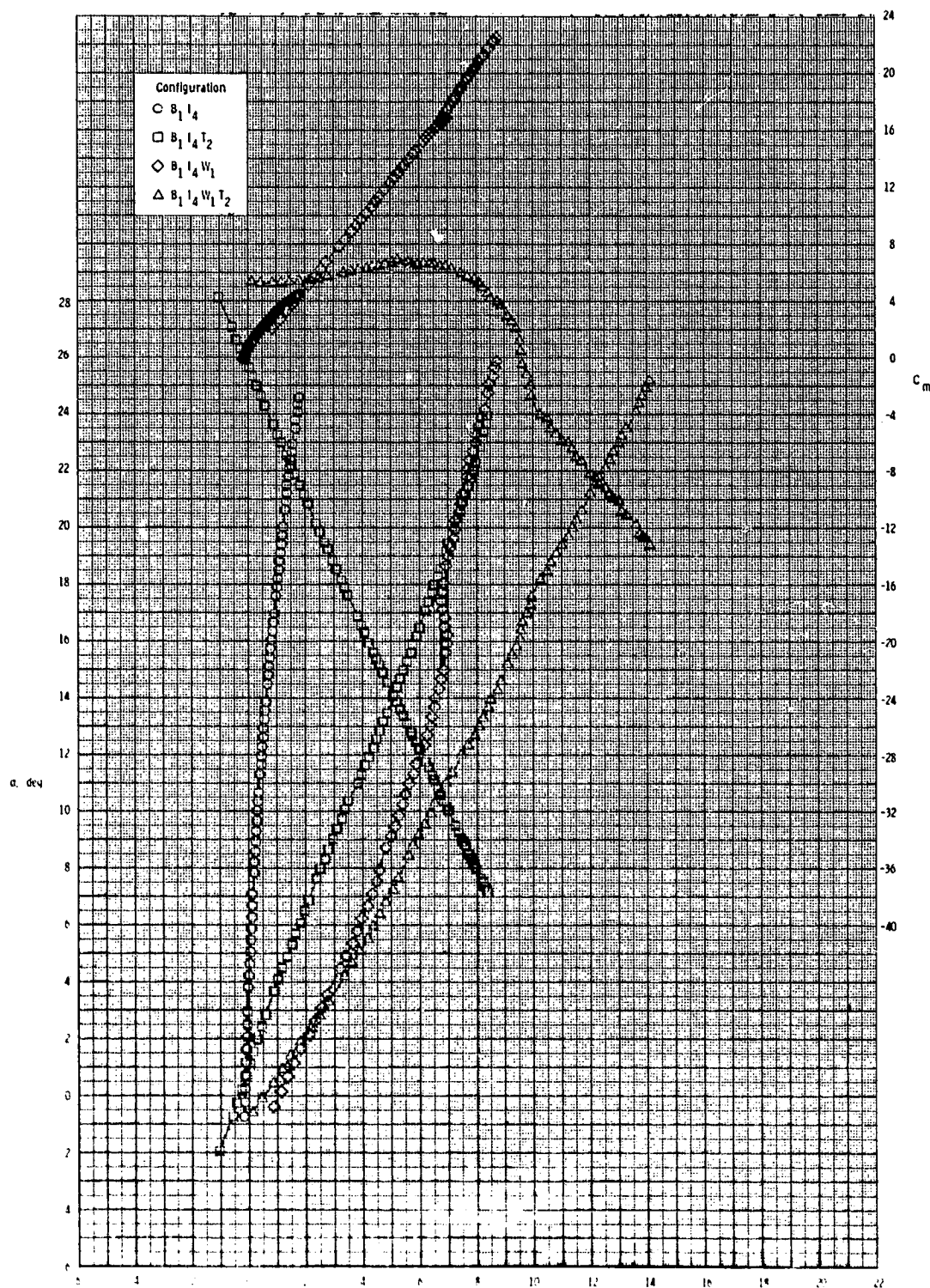
ORIGINAL PAGE IS
OF POOR QUALITY



(a) $M = 0.60$.

Figure 29.- Effect of various model components on longitudinal aerodynamic characteristics for axisymmetric inlet with T_2 and internal duct closed.

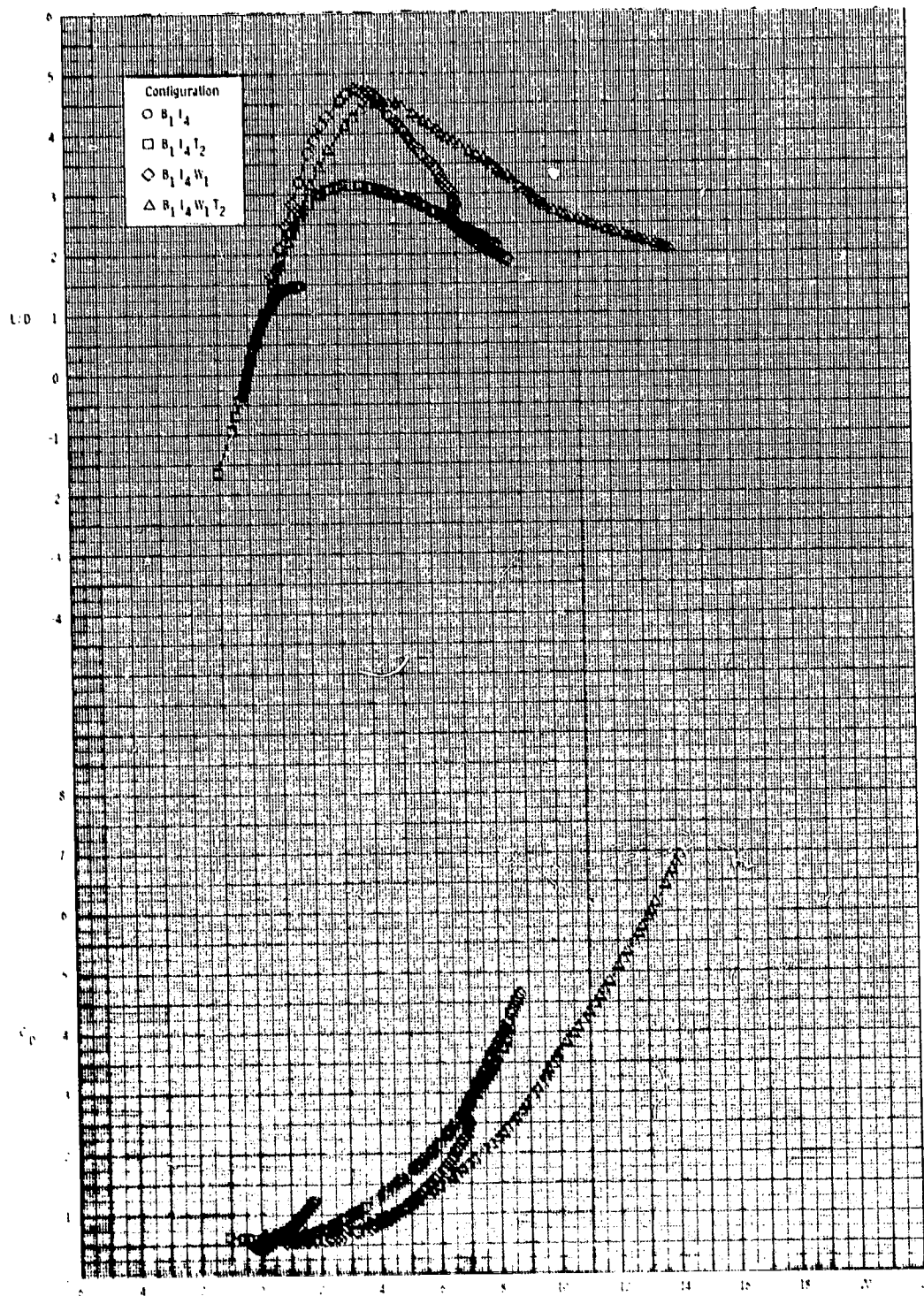
ORIGINAL PAGE IS
OF POOR QUALITY



(a) Continued.

Figure 29.- Continued.

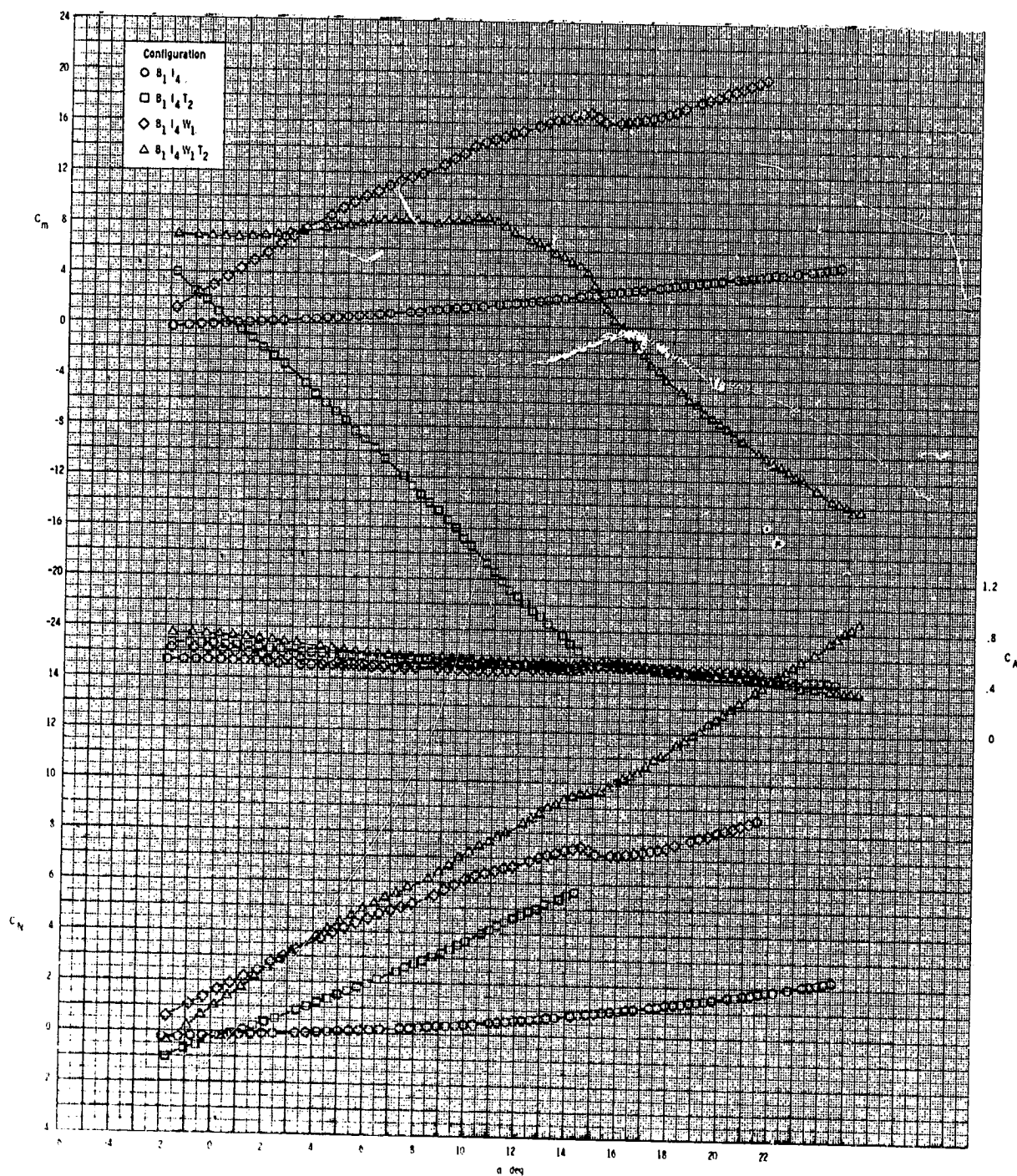
ORIGINAL PAGE IS
OF POOR QUALITY



(a) Concluded.

Figure 29.- Continued.

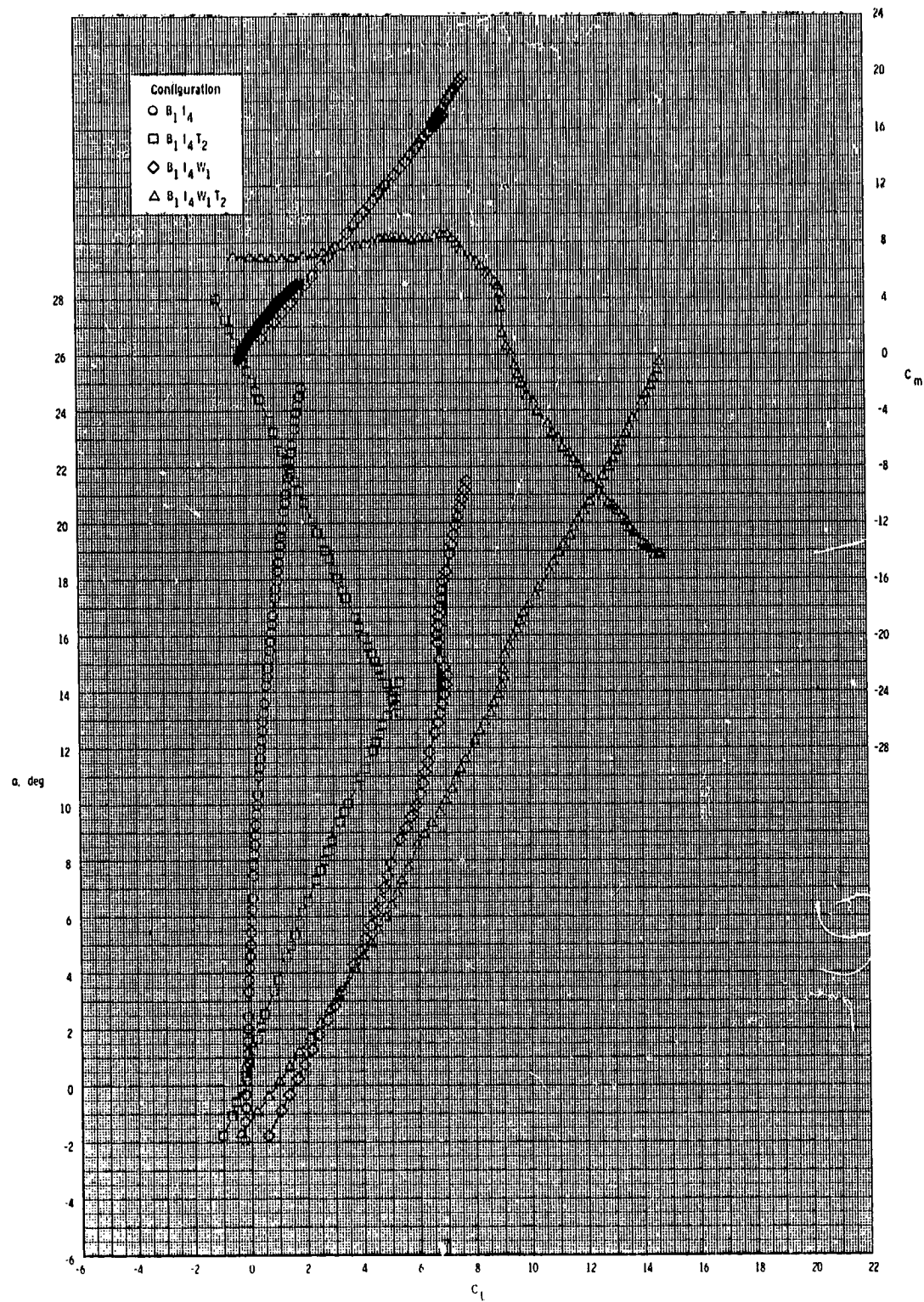
ORIGINAL PAGE IS
OF POOR QUALITY



(b) $M = 0.80$.

Figure 29.- Continued.

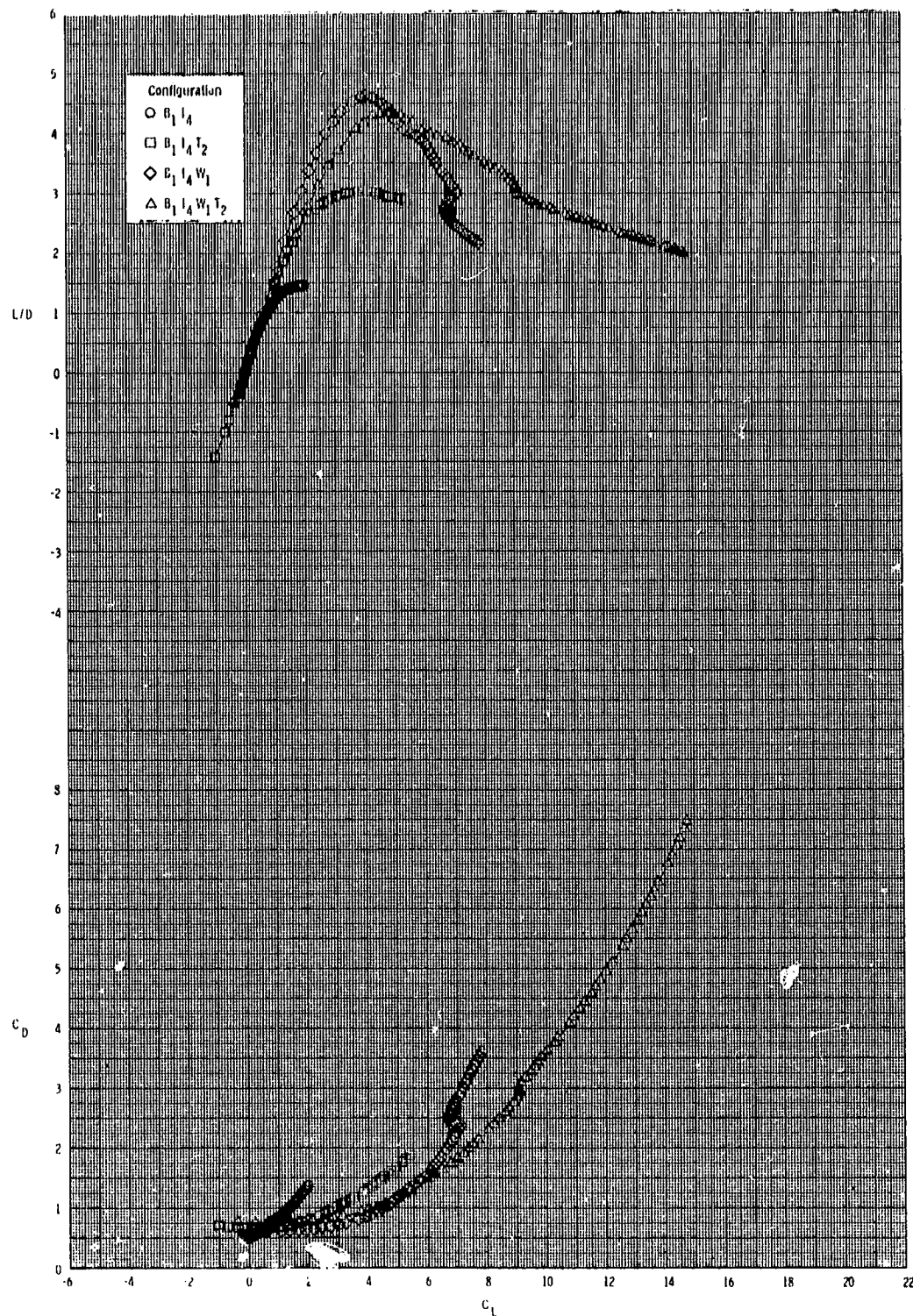
ORIGINAL PAGE IS
OF POOR QUALITY



(b) Continued.

Figure 29.- Continued.

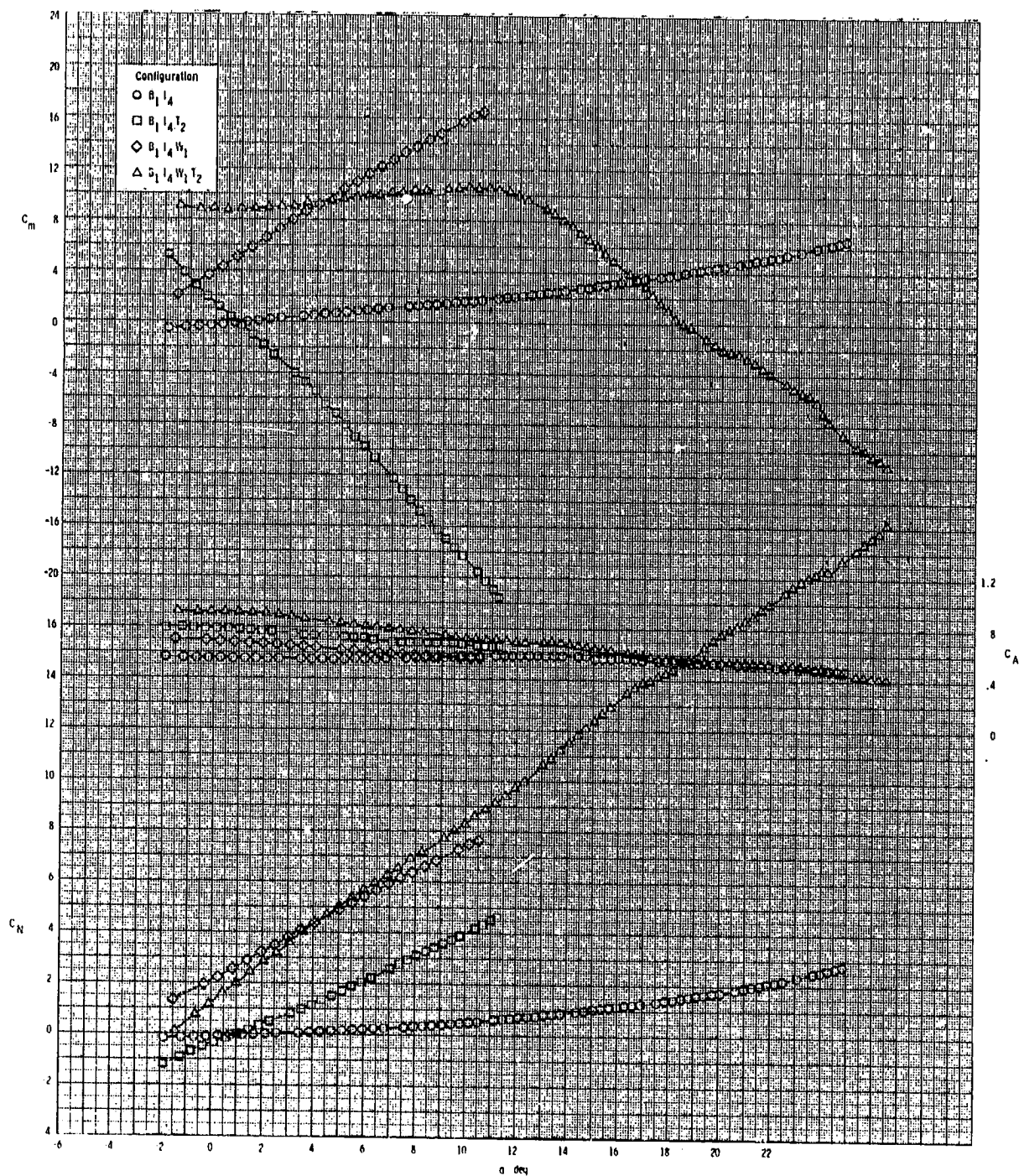
ORIGINAL PAGE IS
OF POOR QUALITY



(b) Concluded.

Figure 29.- Continued.

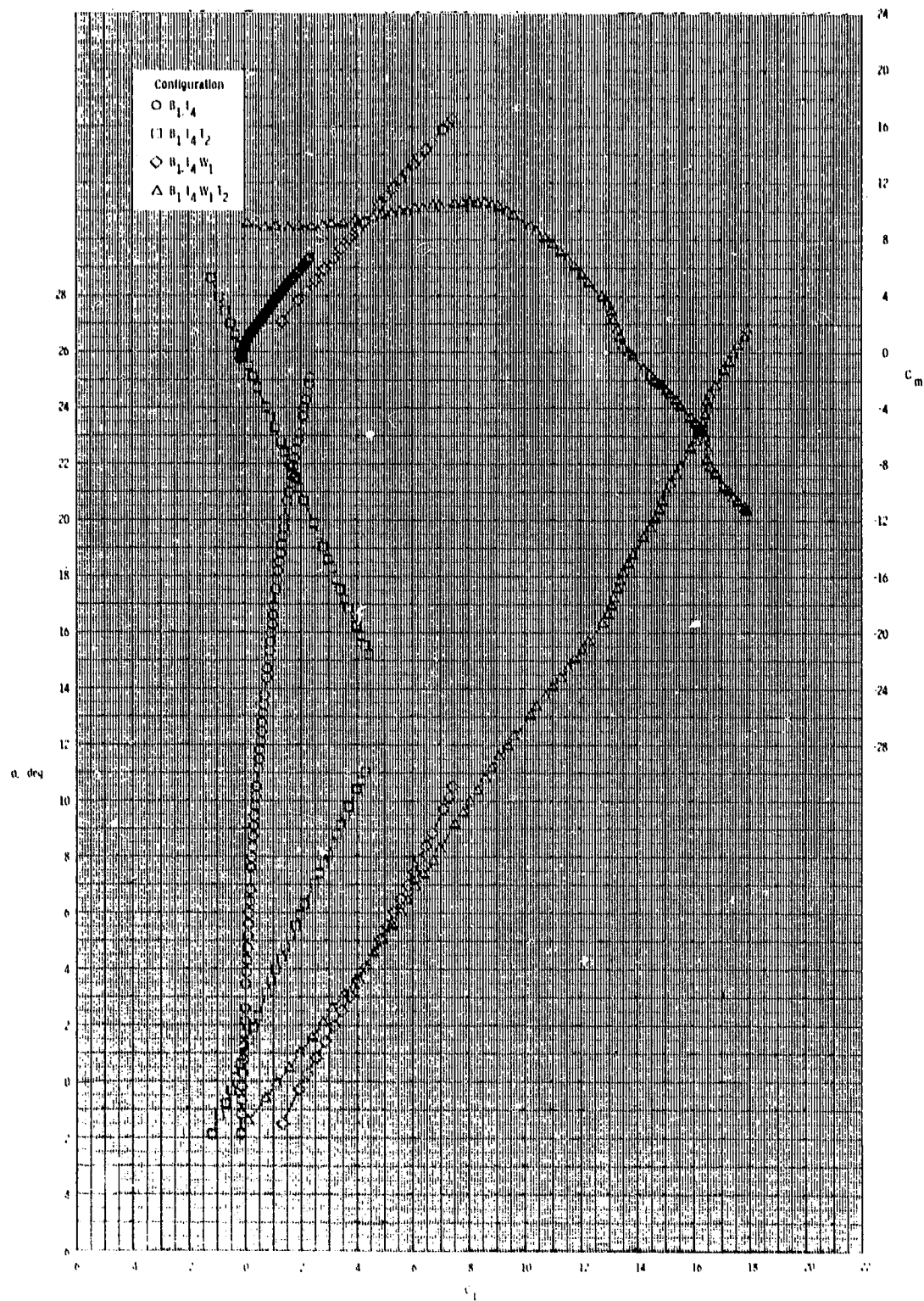
ORIGINAL PAGE IS
OF POOR QUALITY



(c) $M = 0.95$.

Figure 29.- Continued.

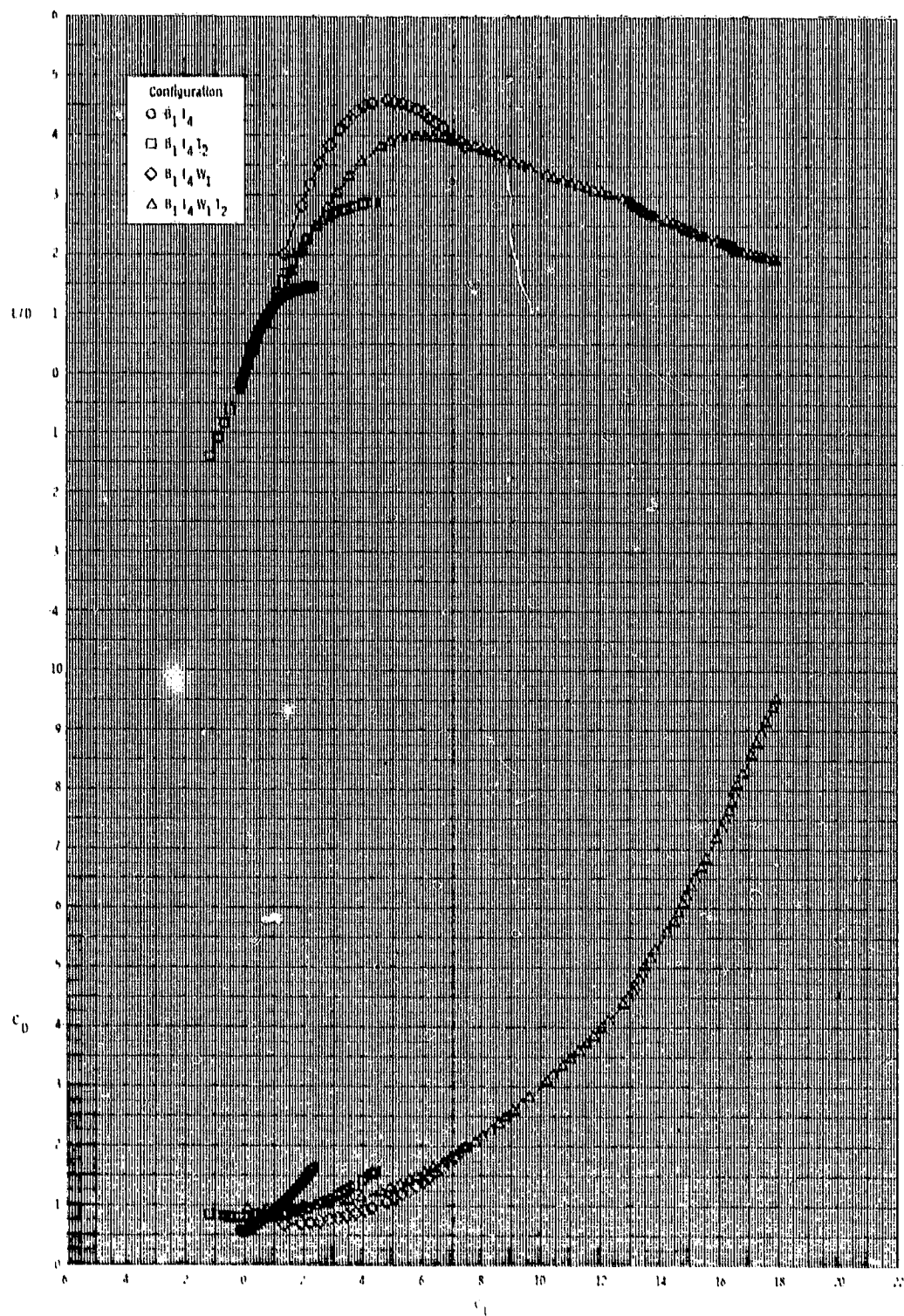
ORIGINAL PAGE IS
OF POOR QUALITY



(c) Continued.

Figure 29.- Continued.

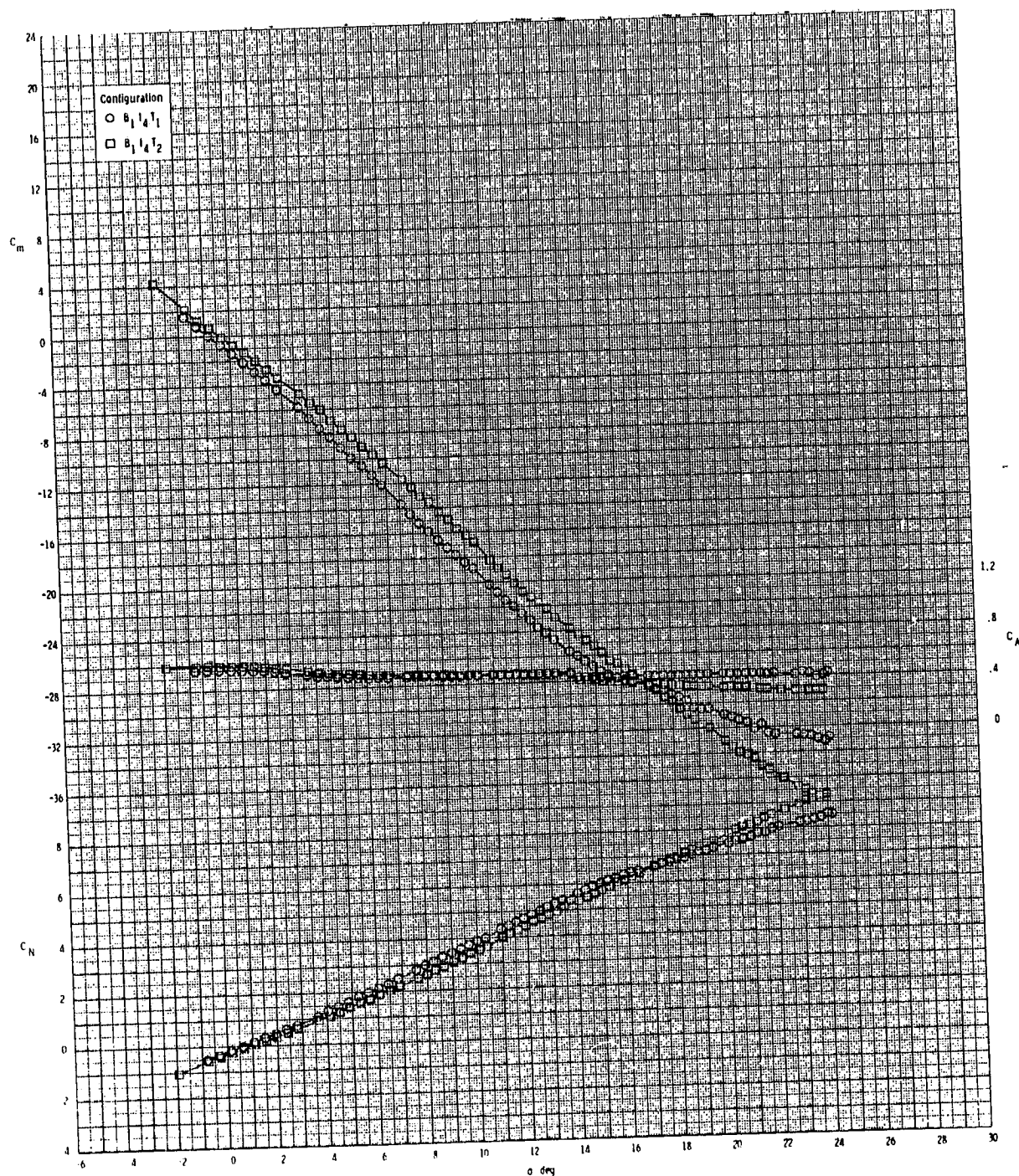
ORIGINAL PAGE IS
OF POOR QUALITY



(c) Concluded.

Figure 29.- Concluded.

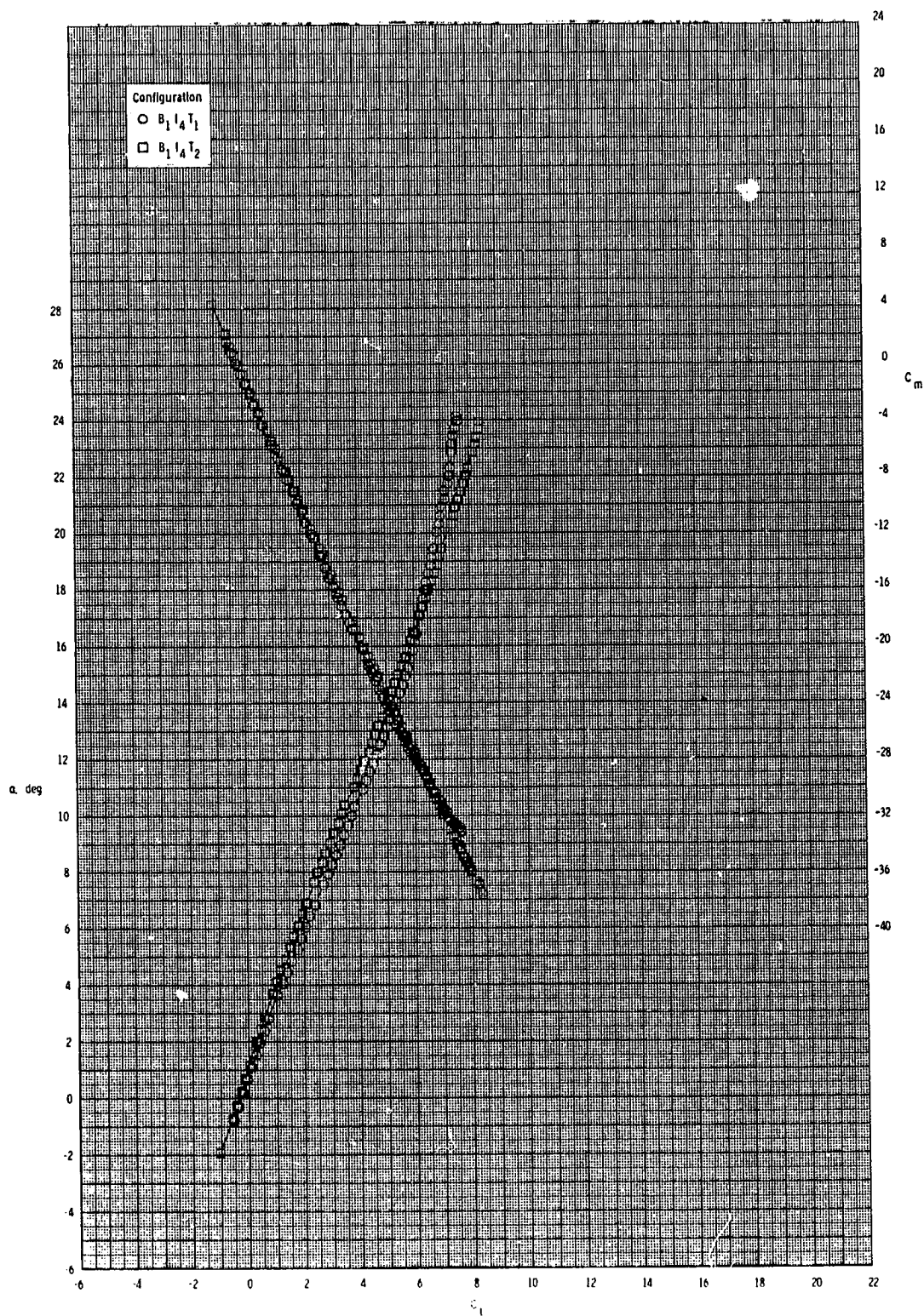
ORIGINAL PAGE IS
OF POOR QUALITY



(a) $M = 0.60$.

Figure 30.- Effect of tail configuration on longitudinal aerodynamic characteristics for axisymmetric inlet with wing off and internal duct closed.

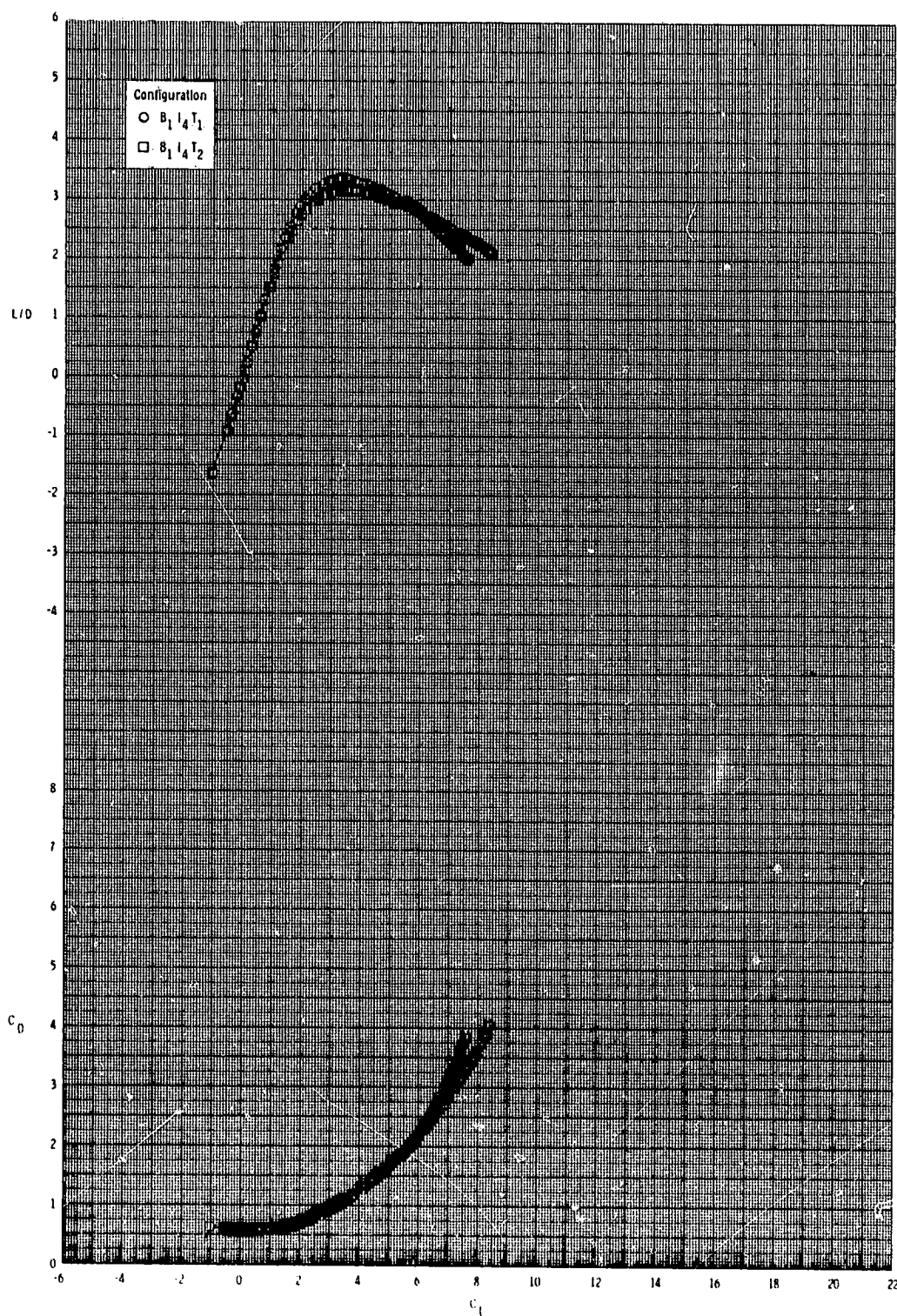
ORIGINAL PAGE IS
OF POOR QUALITY



(a) Continued.

Figure 30.- Continued.

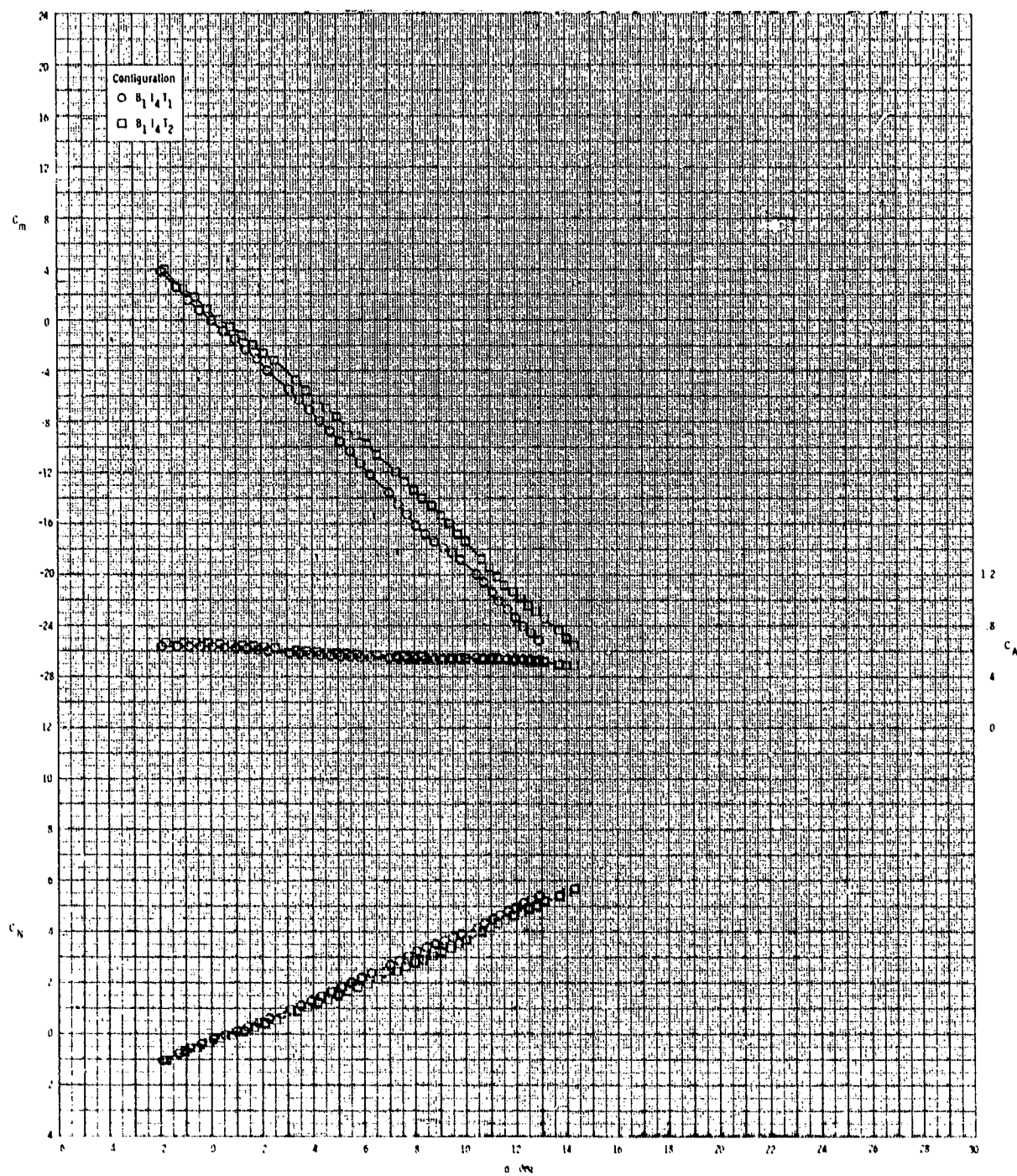
ORIGINAL PAGE IS
OF POOR QUALITY



(a) Concluded.

Figure 30.- Continued.

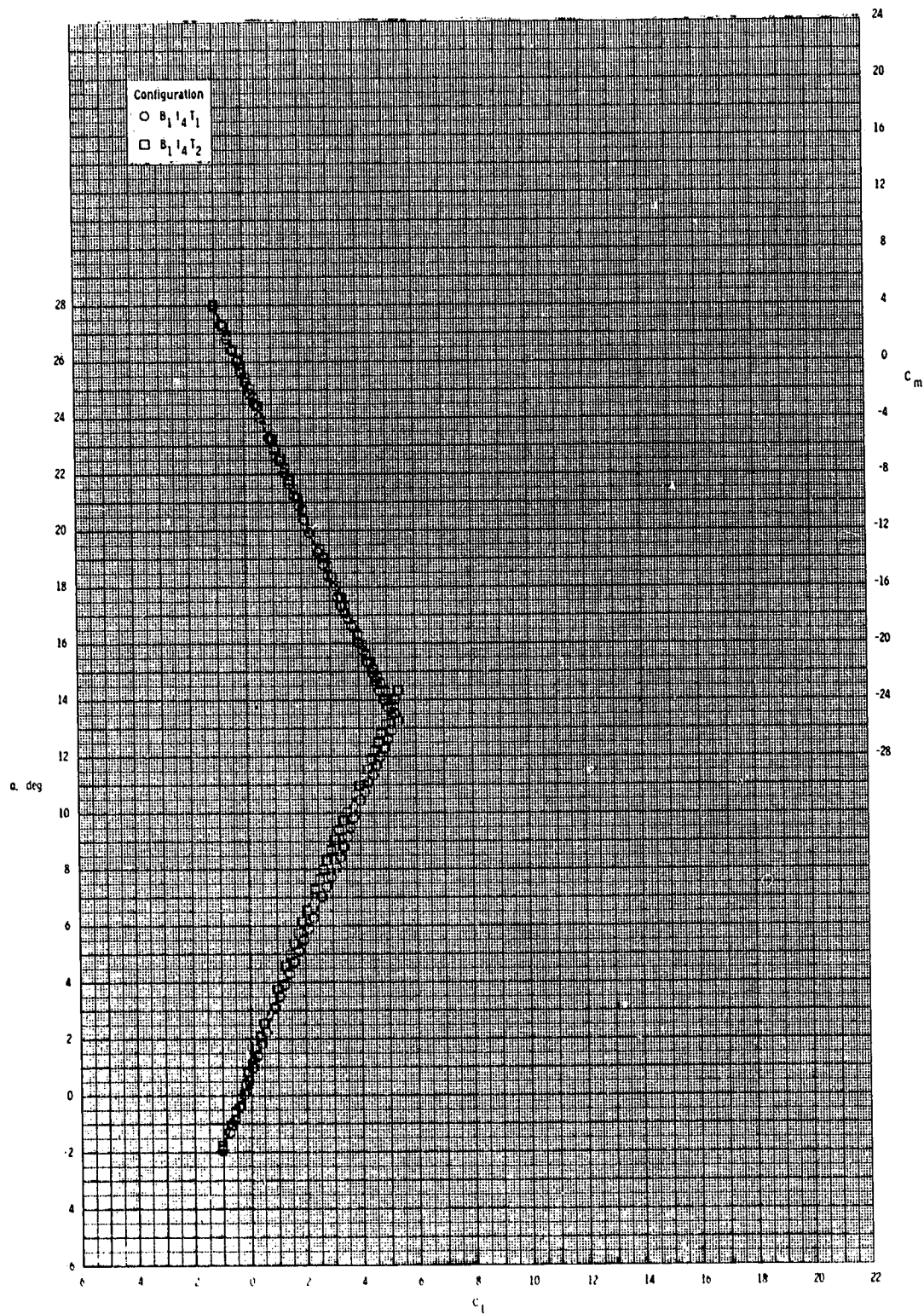
ORIGINAL PAGE IS
OF POOR QUALITY



(D) $M = 0.80$.

Figure 30.- Continued.

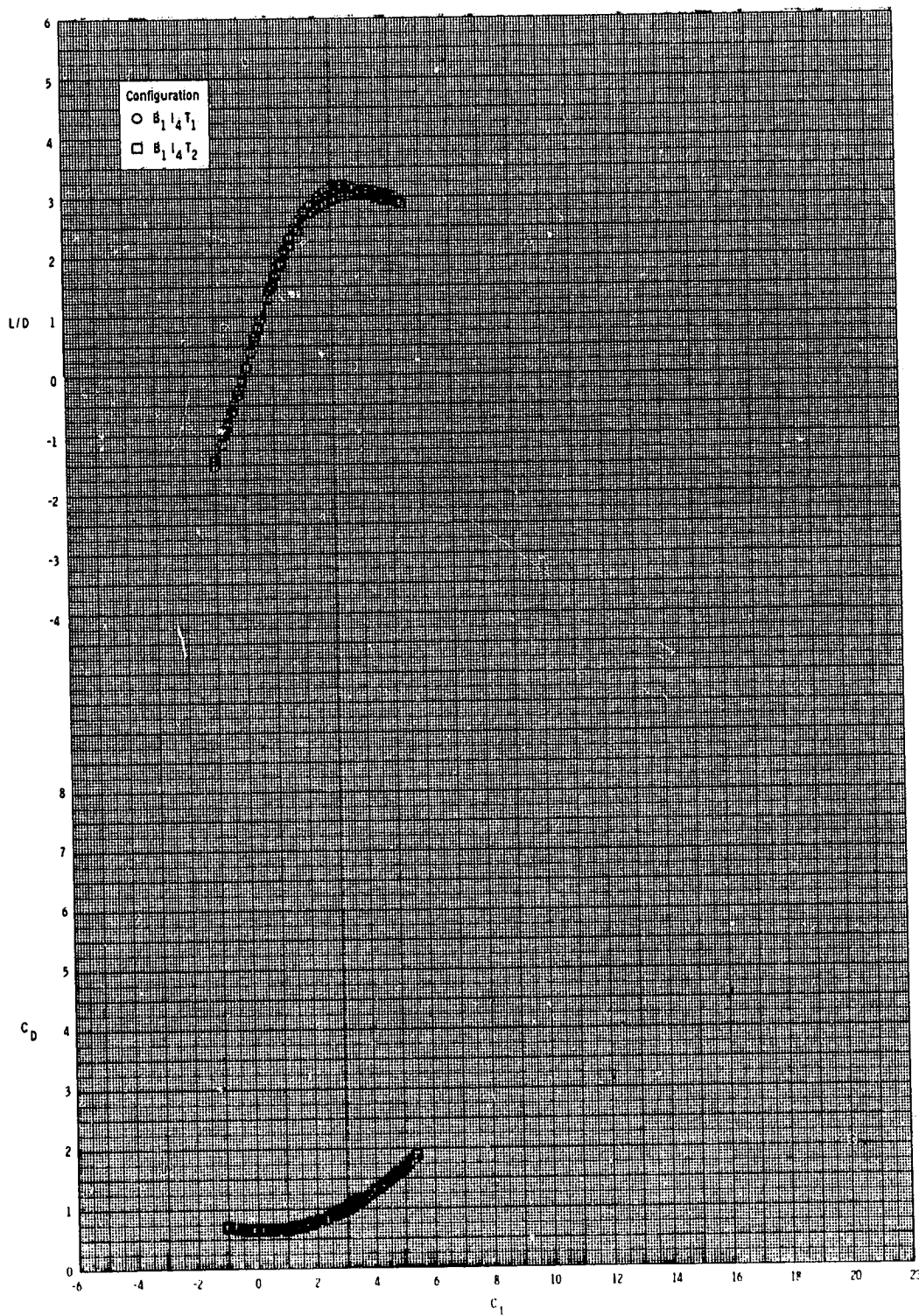
ORIGINAL PAGE IS
OF POOR QUALITY



(b) Continued.

Figure 30.- Continued.

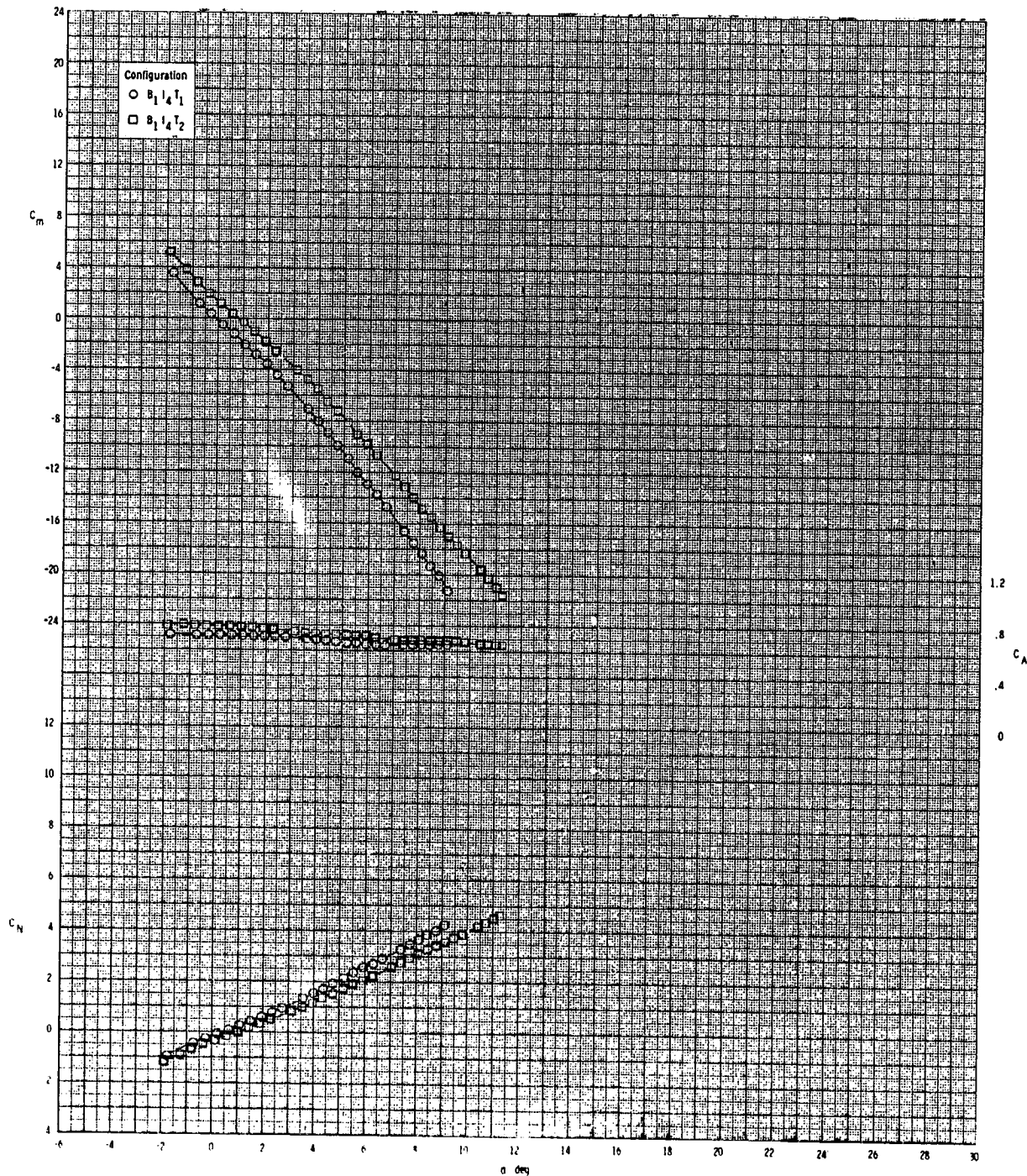
ORIGINAL PAGE IS
OF POOR QUALITY



(b) Concluded.

Figure 30.- Continued.

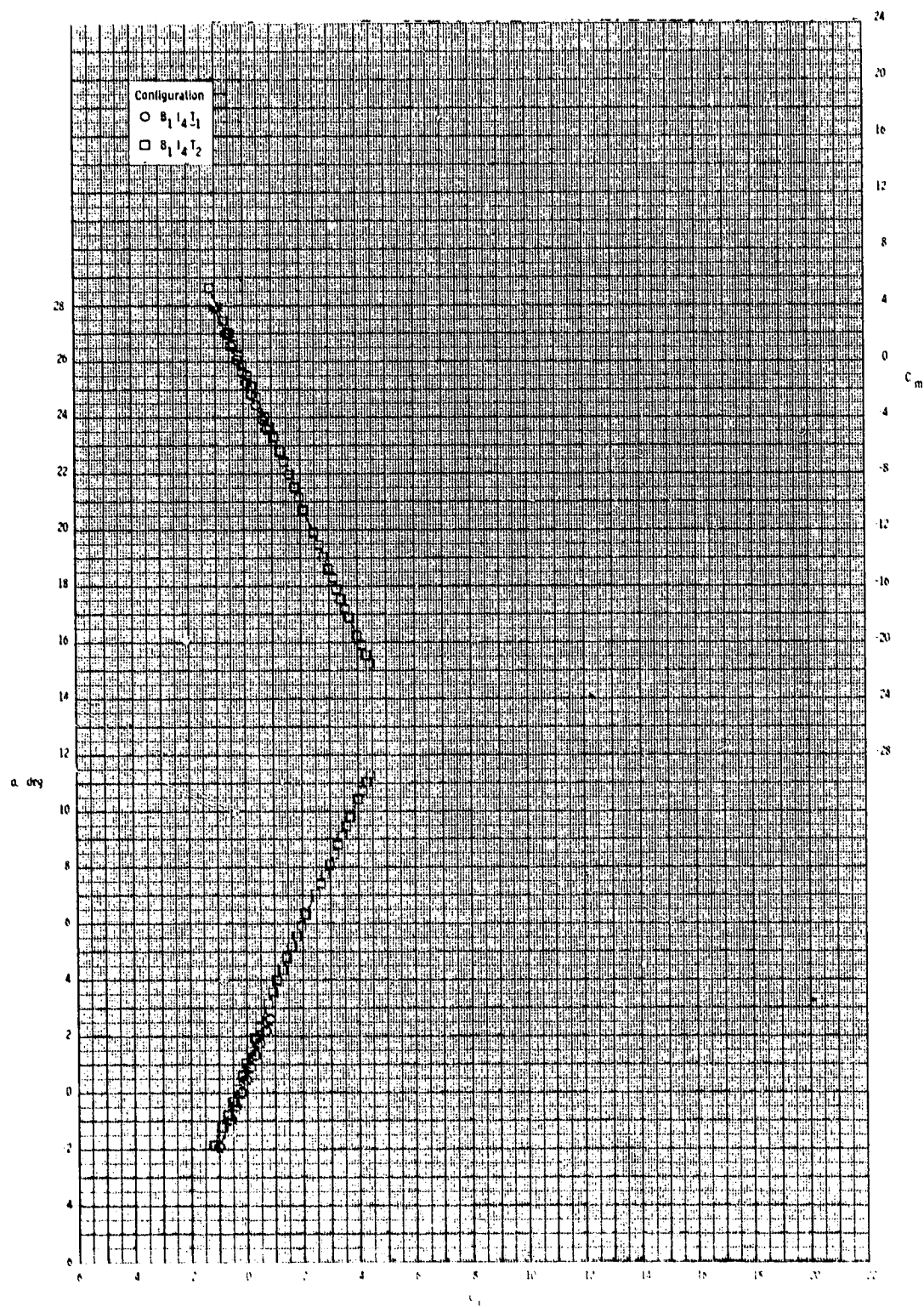
ORIGINAL PAGE IS
OF POOR QUALITY



(c) $M = 0.95$.

Figure 30.- Continued.

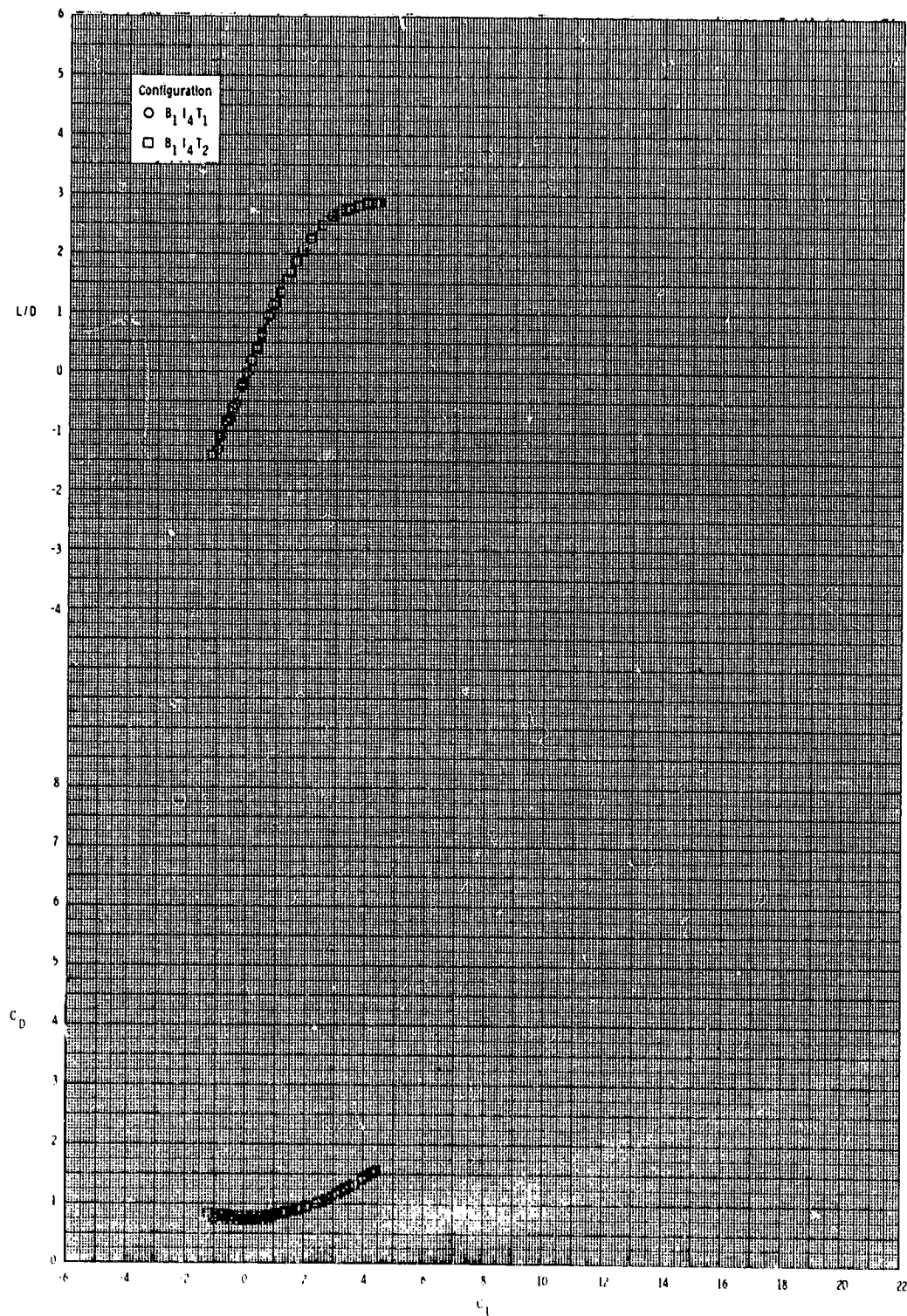
ORIGINAL PAGE IS
OF POOR QUALITY



(c) Continued.

Figure 30.- Continued.

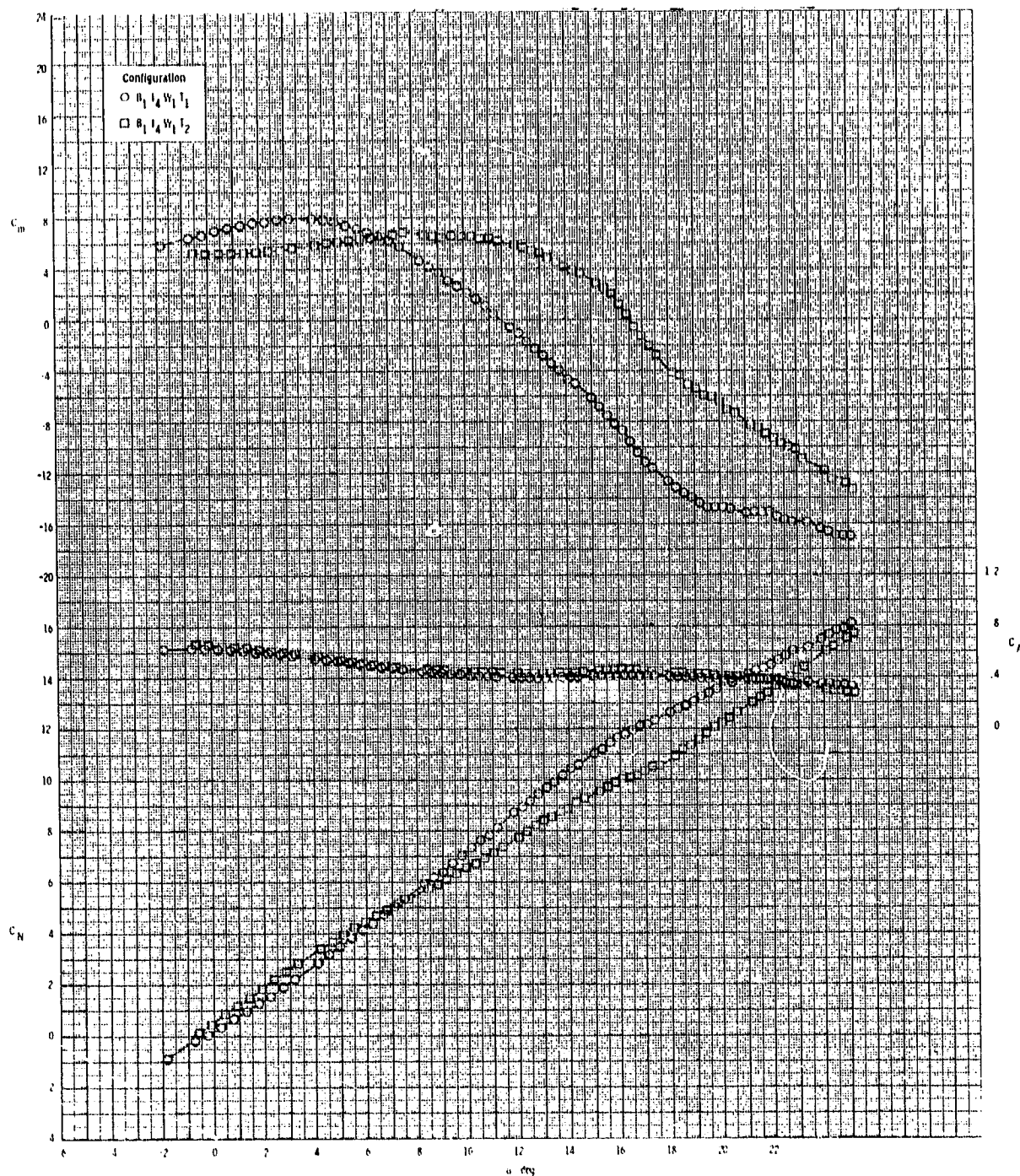
ORIGINAL PAGE IS
OF POOR QUALITY



(c) Concluded.

Figure 30.- Concluded.

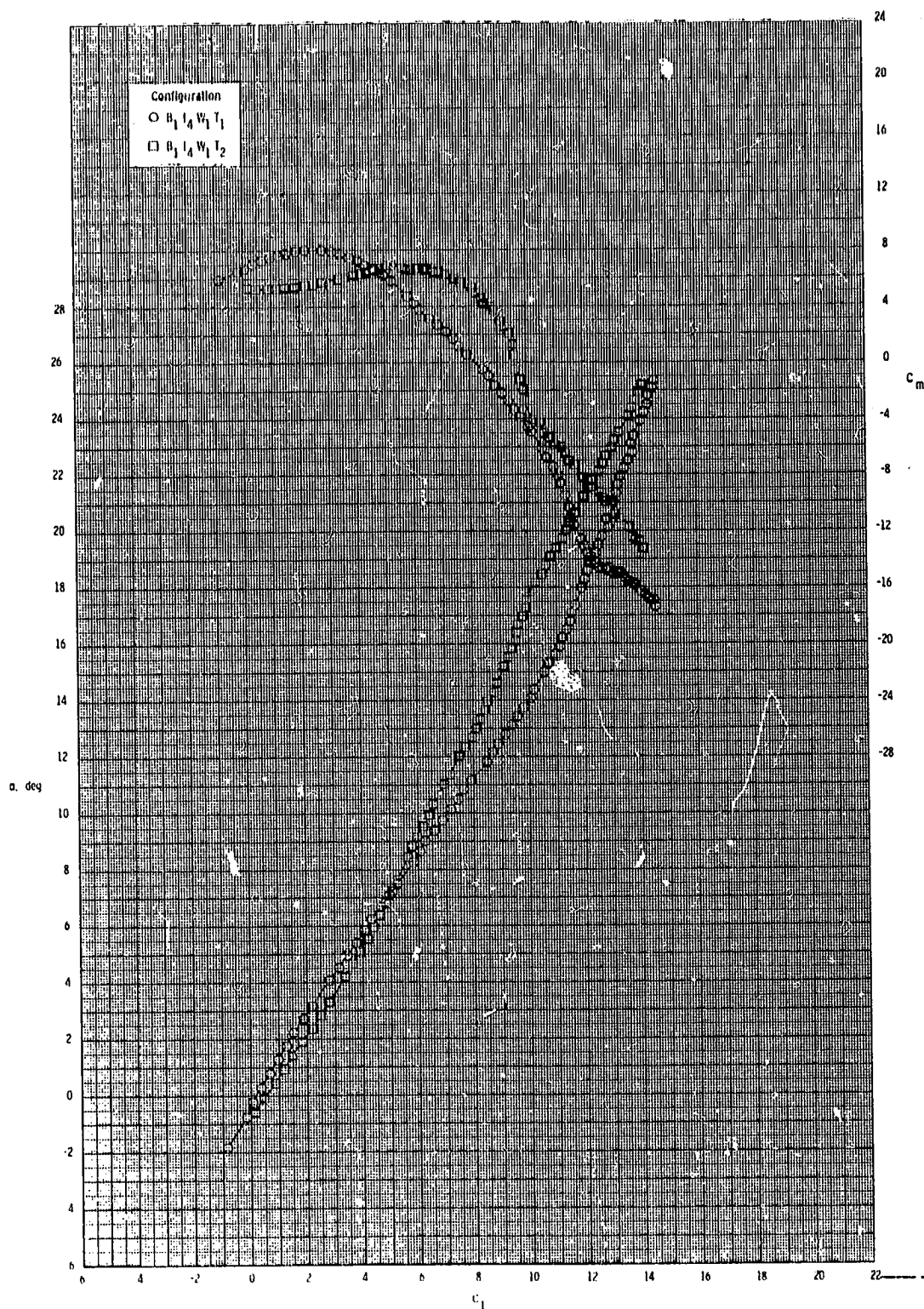
ORIGINAL PAGE IS
OF POOR QUALITY



(a) $M = 0.60$.

Figure 31.- Effect of tail configuration on longitudinal aerodynamic characteristics for axisymmetric inlet with wing on and internal duct closed.

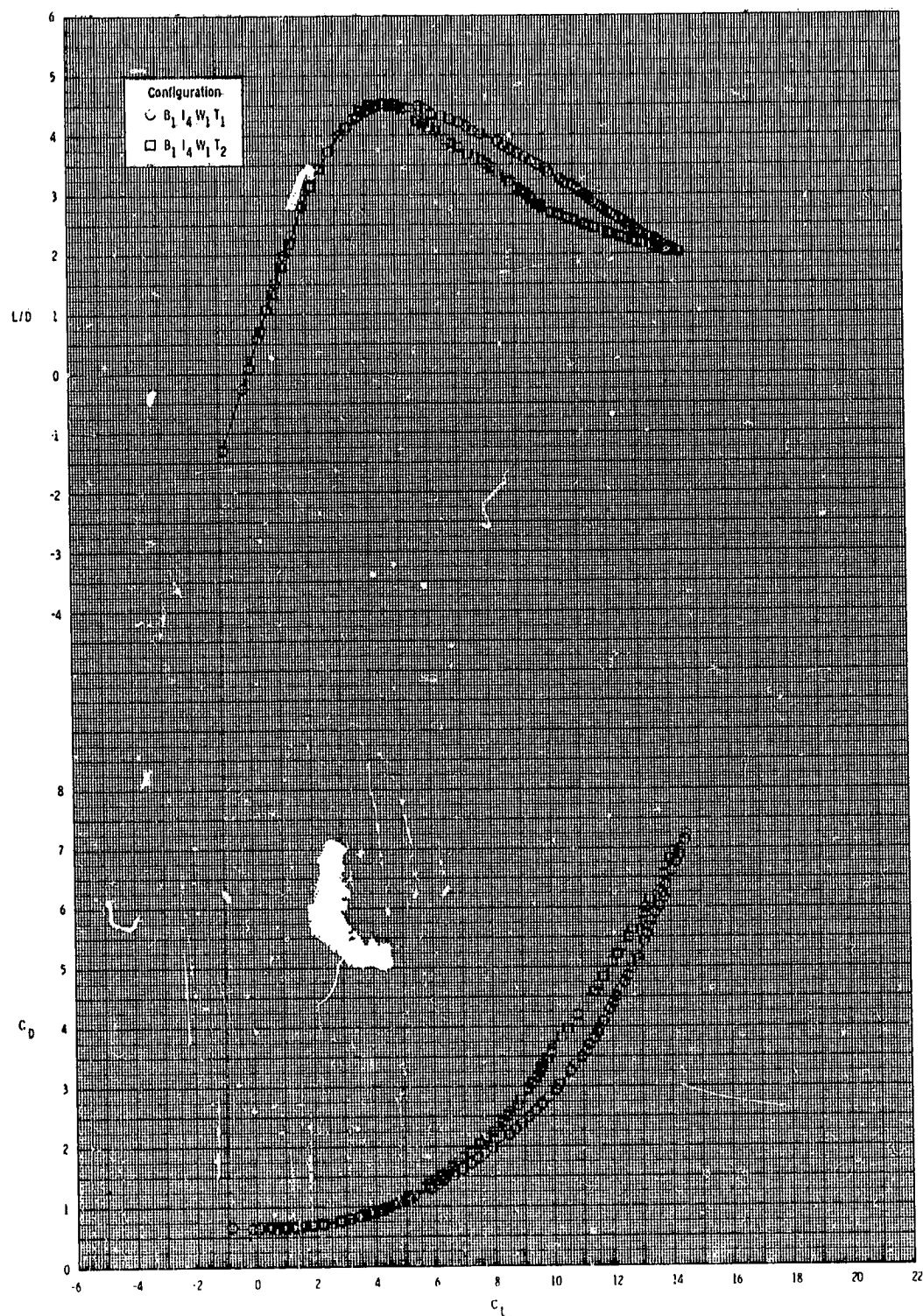
ORIGINAL PAGE 19
OF POOR QUALITY



(a) Continued.

Figure 31.- Continued.

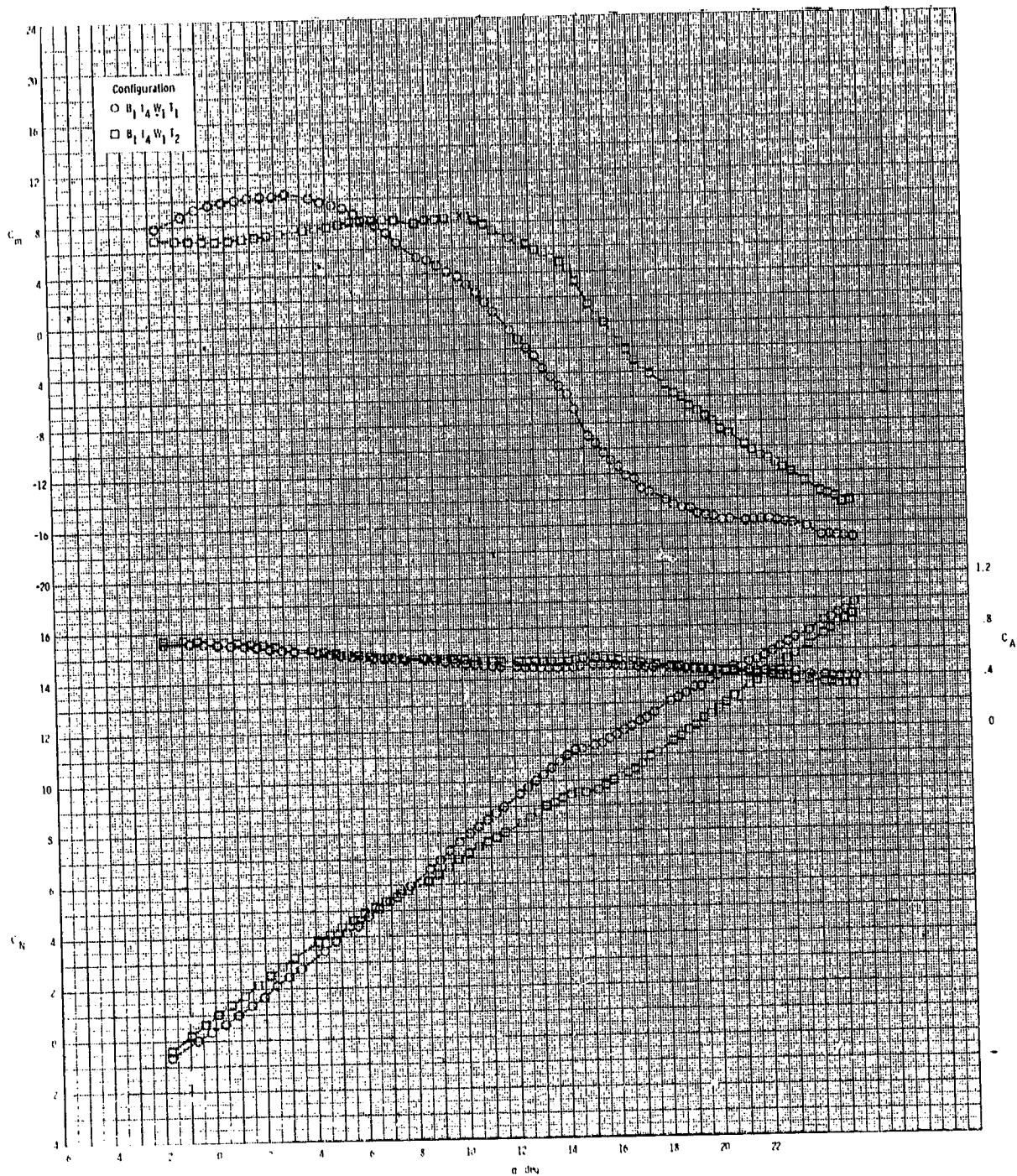
ORIGINAL PAGE IS
OF POOR QUALITY



(a) Concluded.

Figure 31.- Continued.

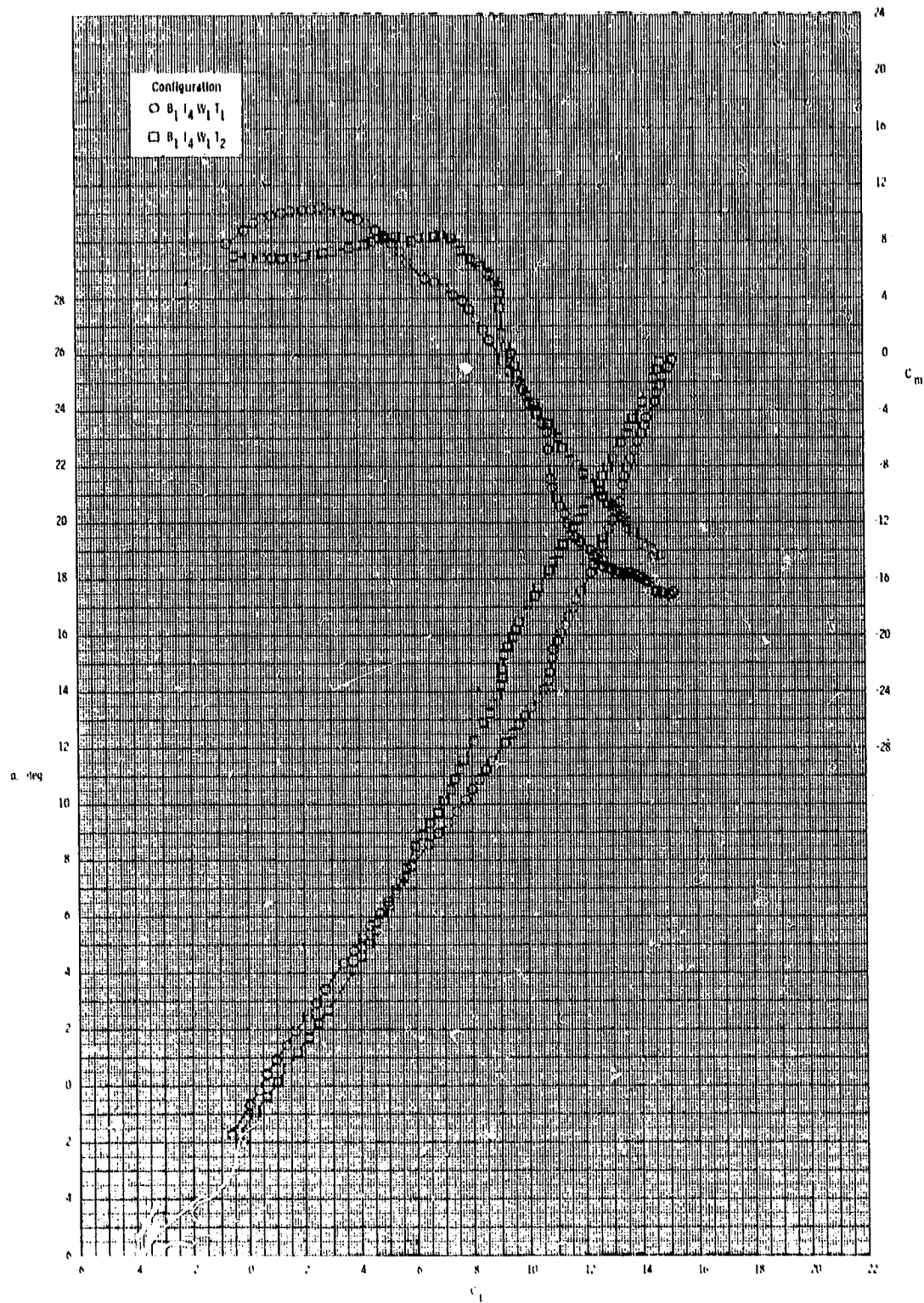
ORIGINAL PAGE IS
OF POOR QUALITY



(b) $M = 0.80$.

Figure 31.- Continued.

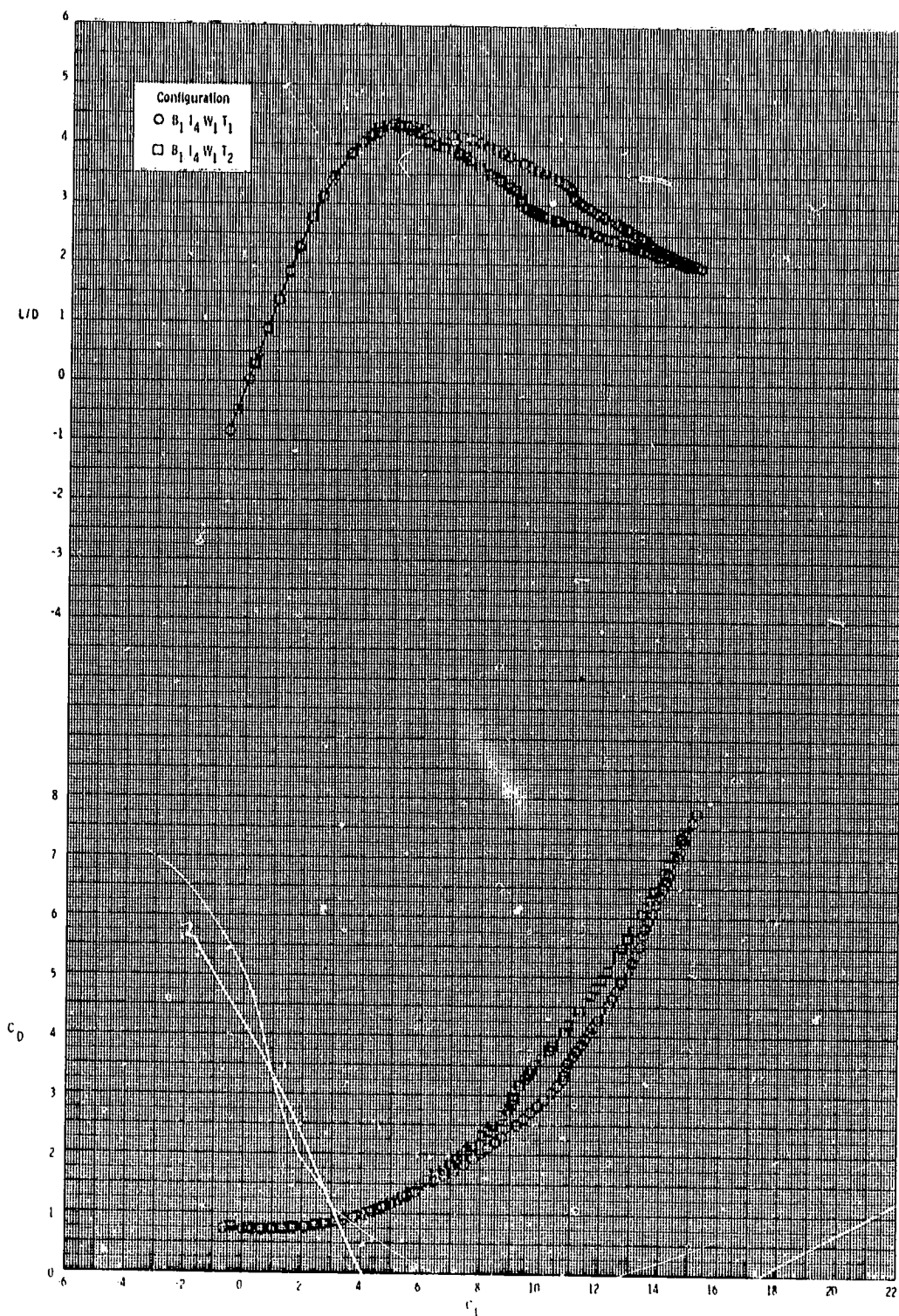
ORIGINAL PAGE IS
OF POOR QUALITY



(b) Continued.

Figure 31.- Continued.

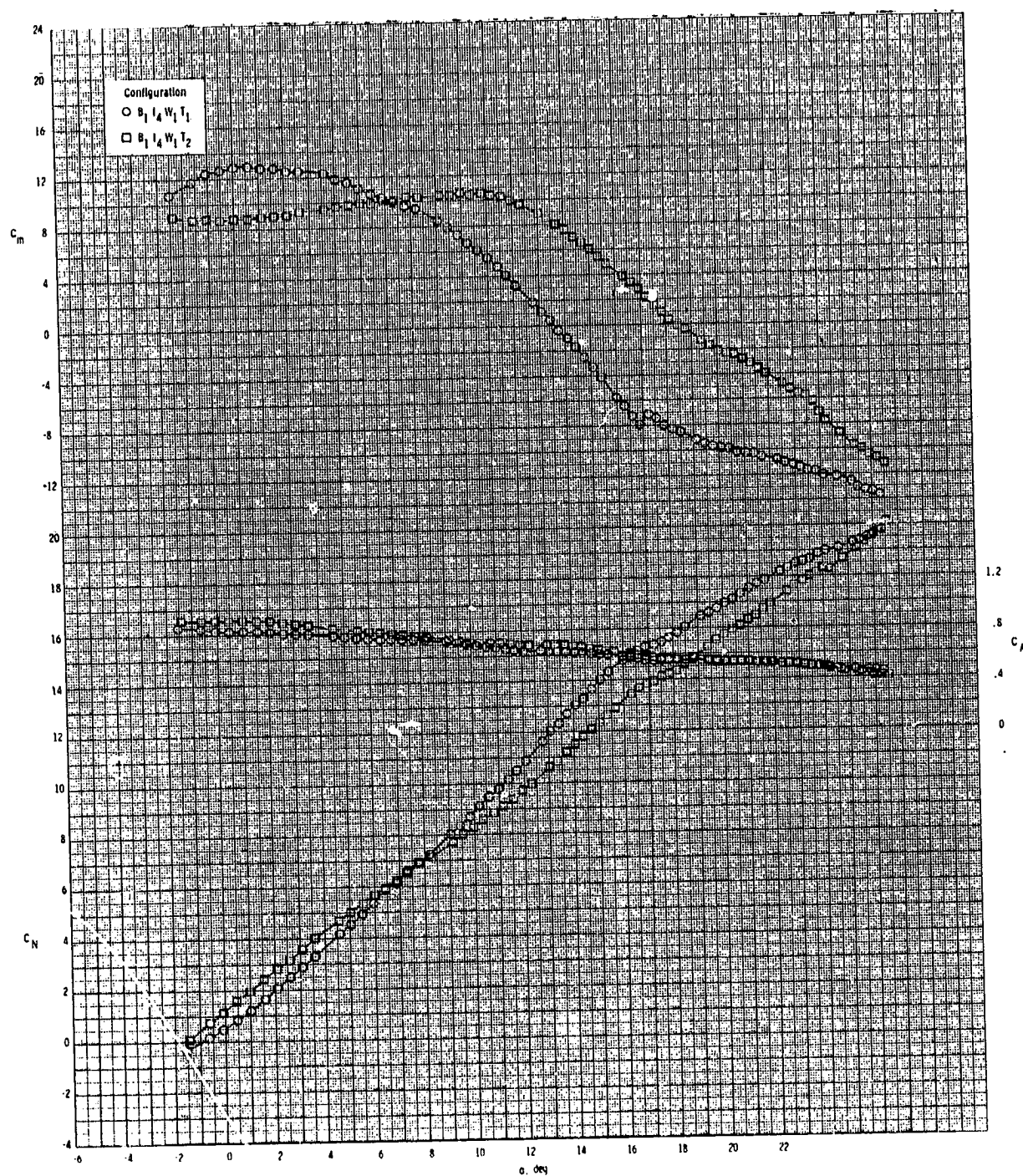
ORIGINAL PAGE IS
OF POOR QUALITY



(b) Concluded.

Figure 31.- Continued.

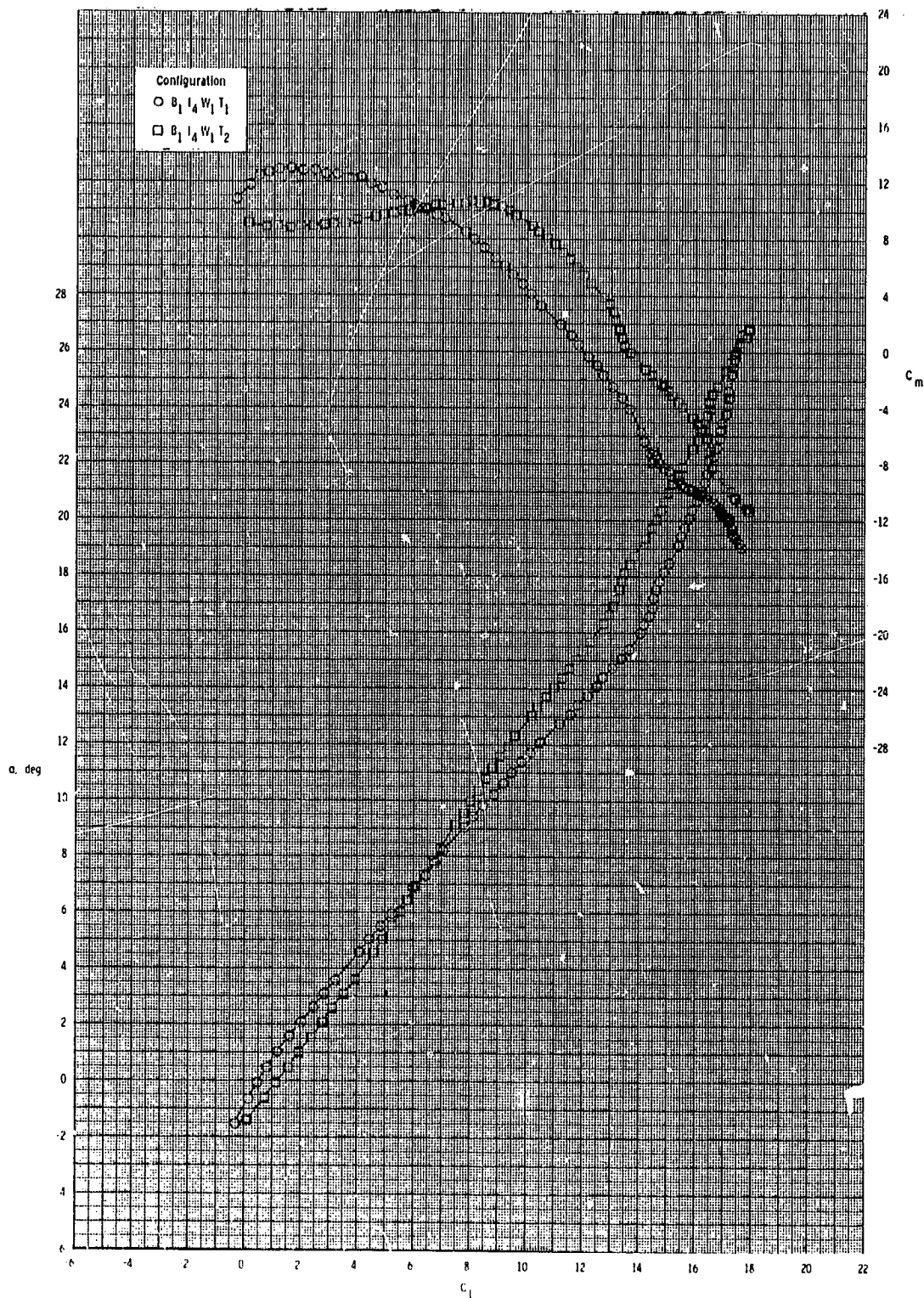
ORIGINAL PAGE IS
OF POOR QUALITY



(c) $M = 0.95$.

Figure 31.- Continued.

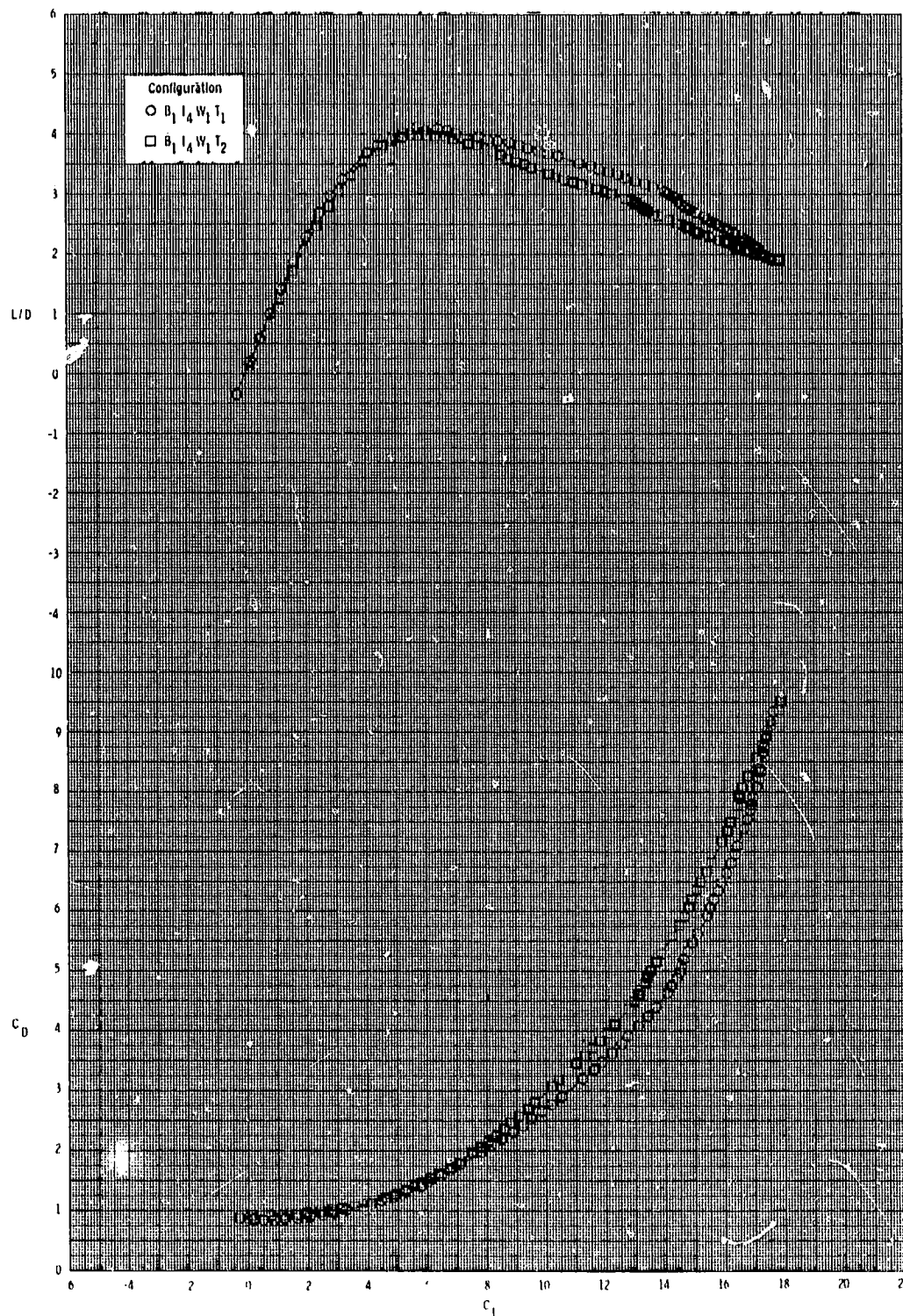
ORIGINAL PAGE IS
OF POOR QUALITY



(c) Continued.

Figure 31.- Continued.

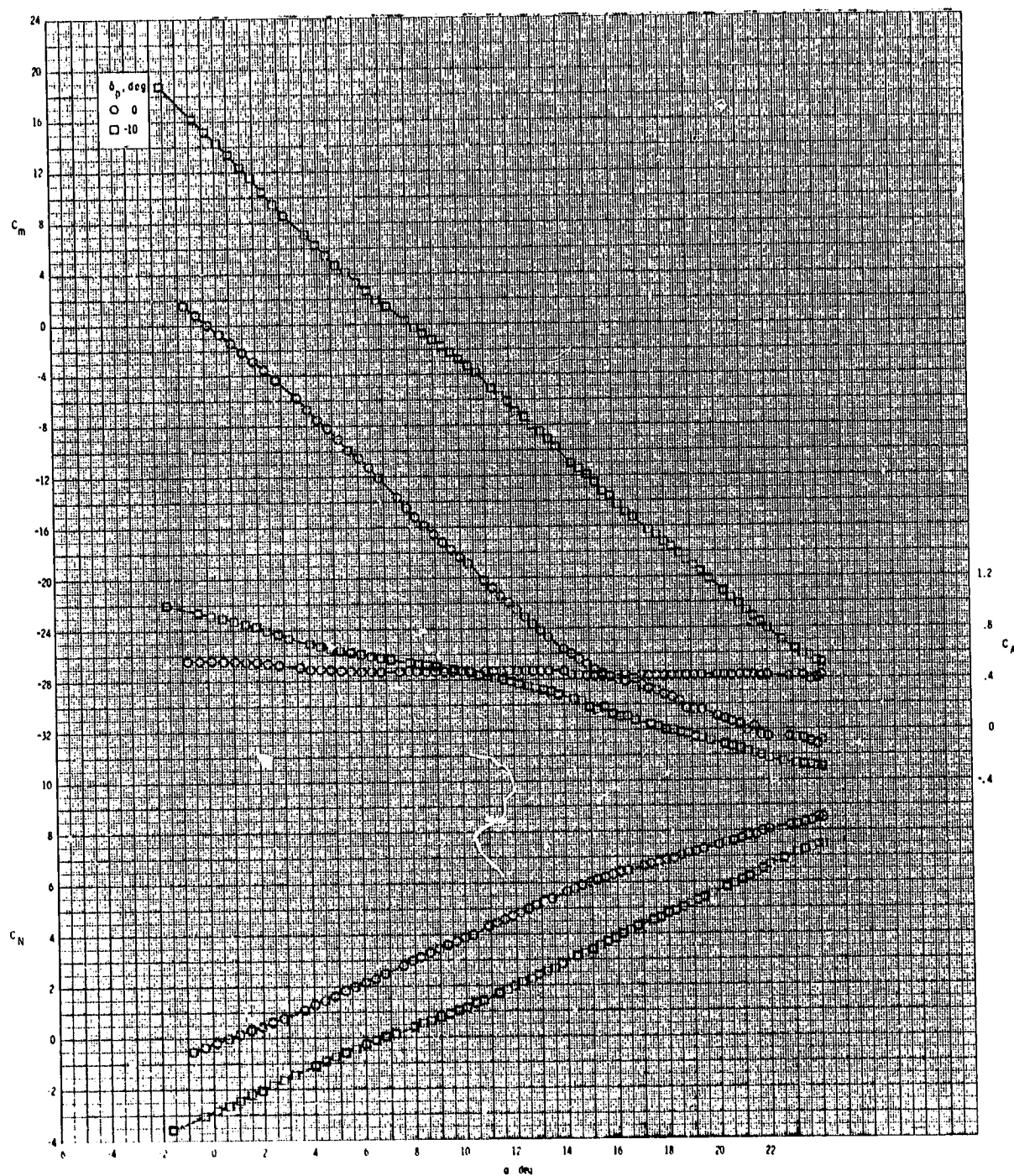
ORIGINAL PAGE IS
OF POOR QUALITY



(c) Concluded.

Figure 31.- Concluded.

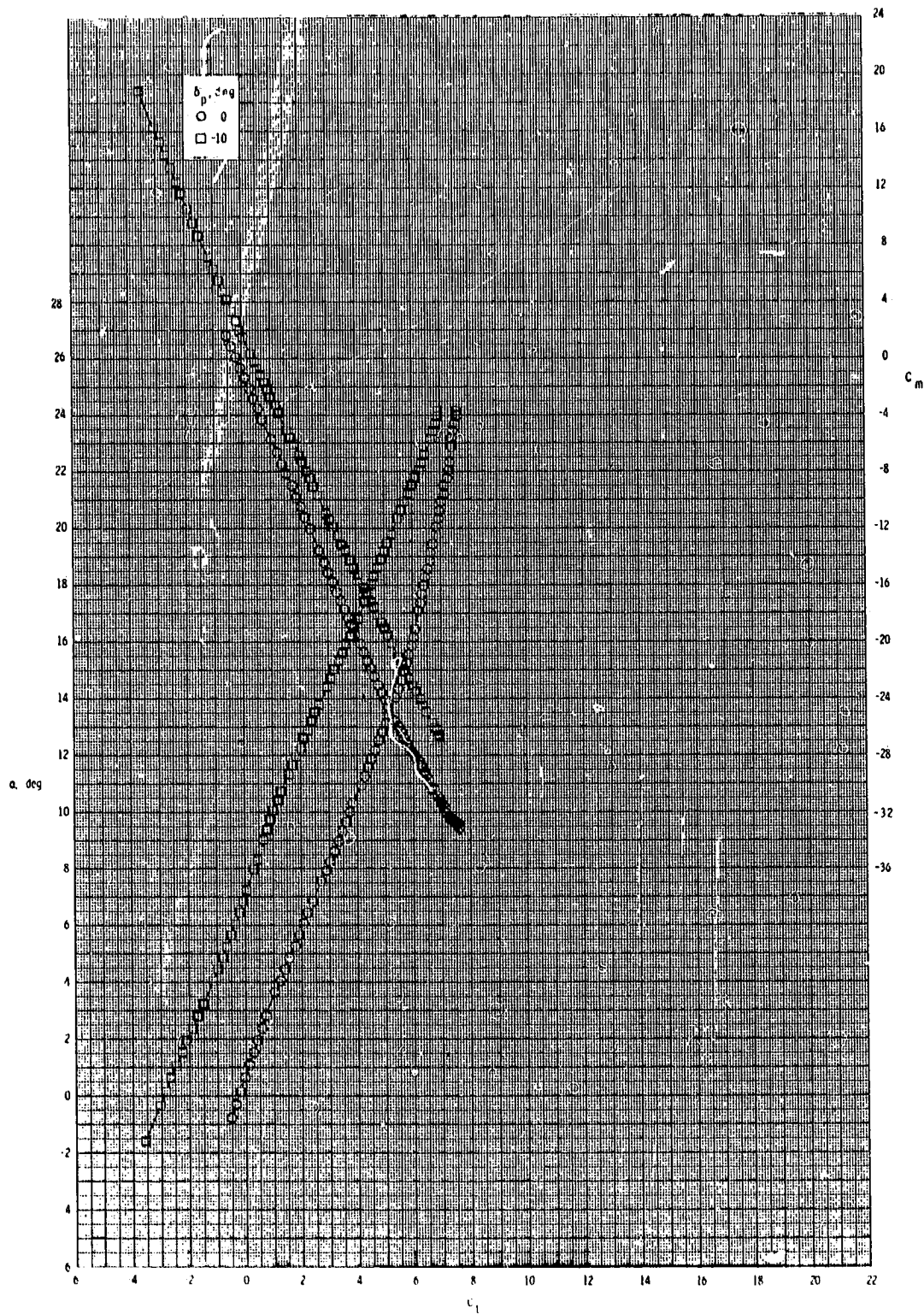
ORIGINAL PAGE IS
OF POOR QUALITY



(a) $M = 0.60$.

Figure 32.- Pitch-control effectiveness of configuration $B_1I_4T_1$ with internal duct closed.

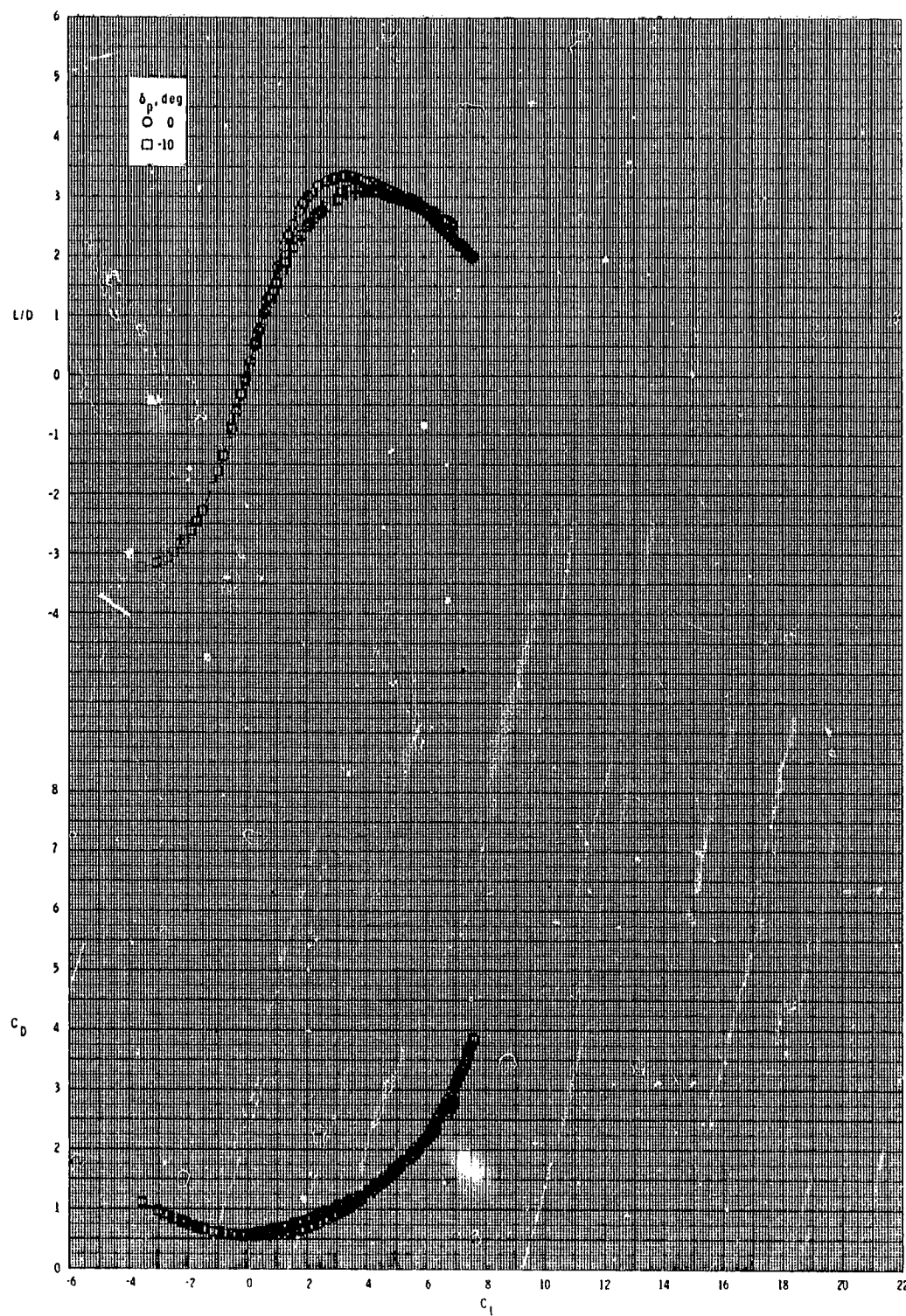
ORIGINAL PAGE IS
OF POOR QUALITY



(a) Continued.

Figure 32.- Continued.

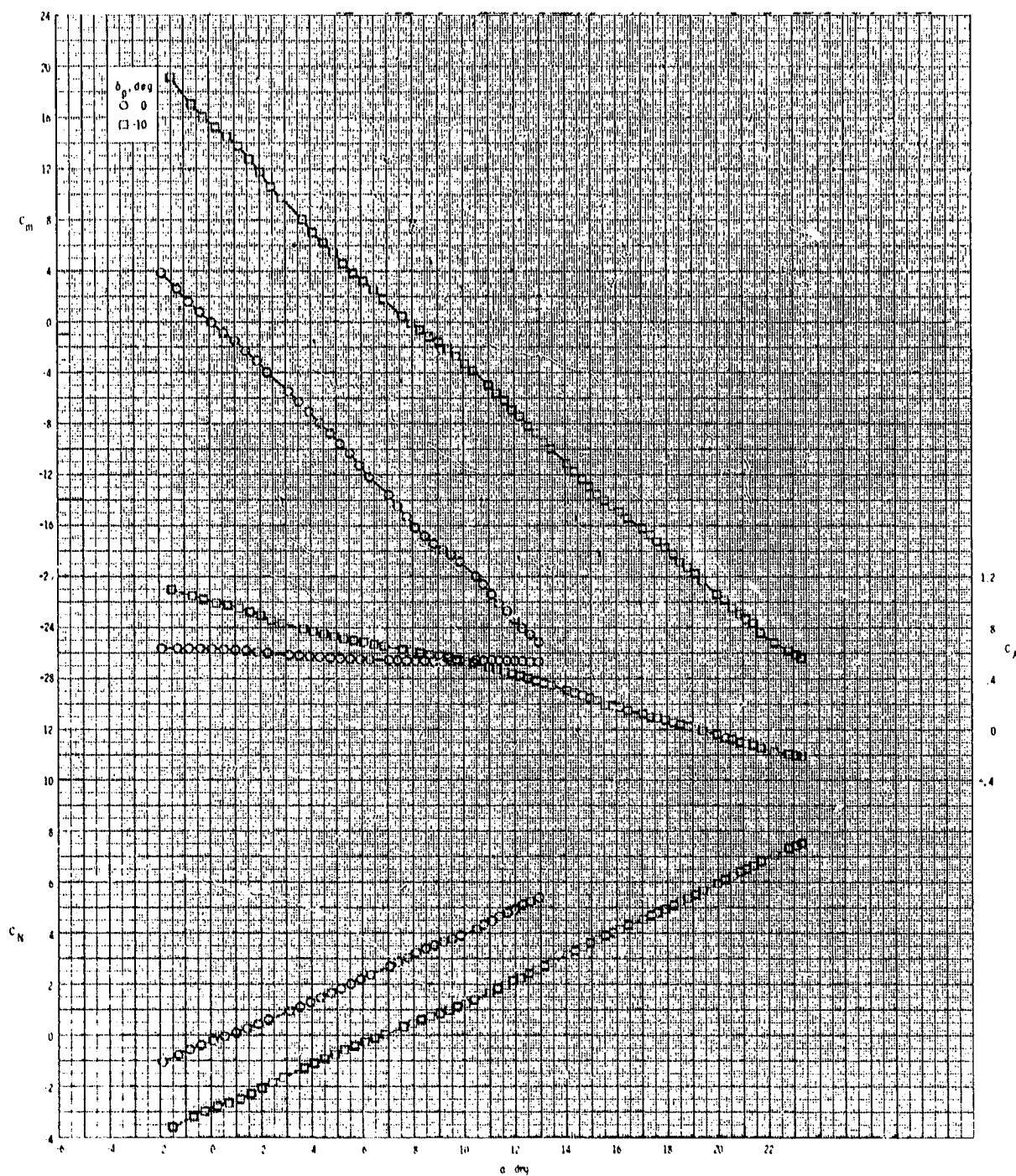
ORIGINAL PAGE IS
OF POOR QUALITY



(a) Concluded.

Figure 32.- Continued.

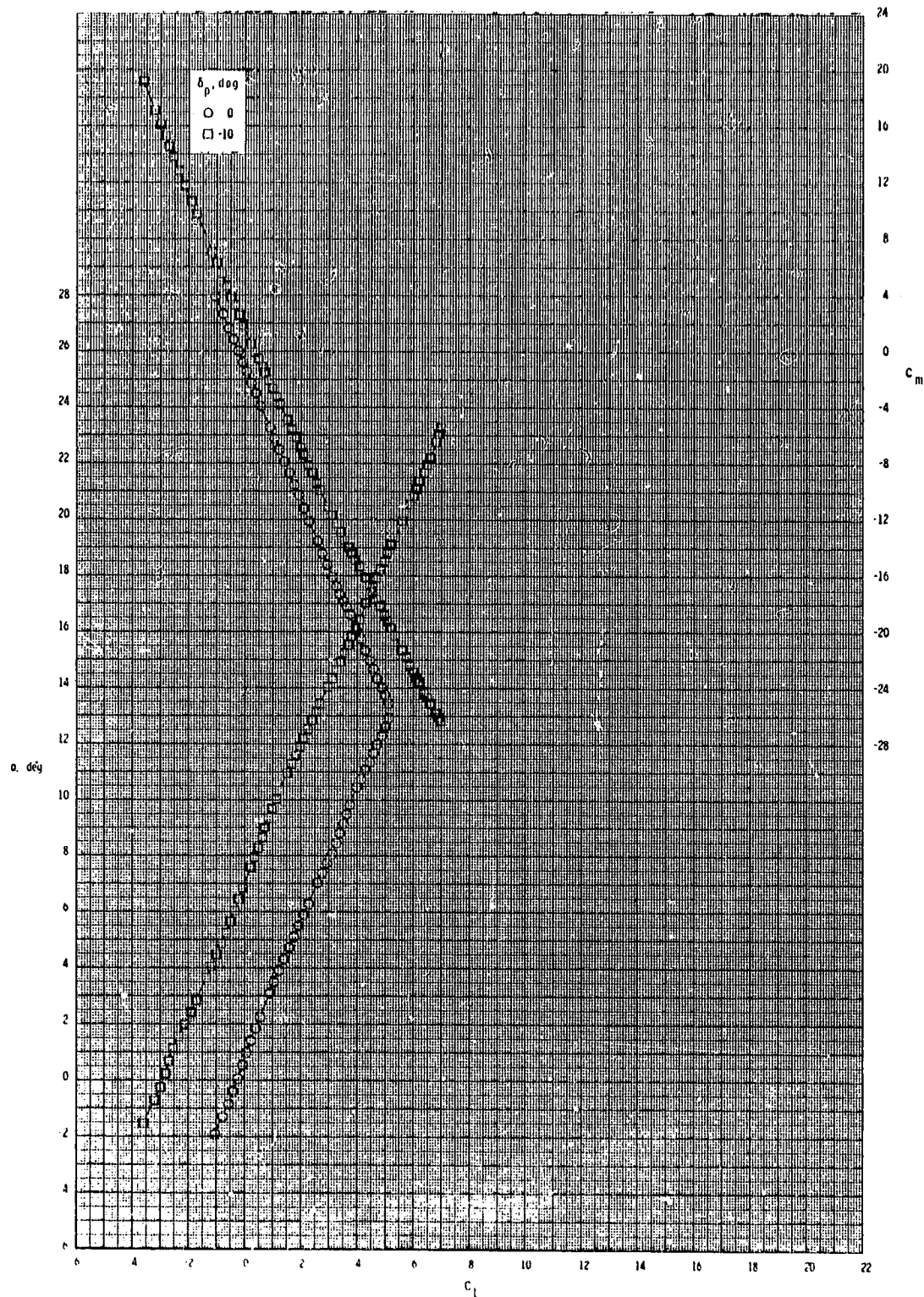
ORIGINAL PAGE IS
OF POOR QUALITY



(b) $M = 0.80$.

Figure 32.- Continued.

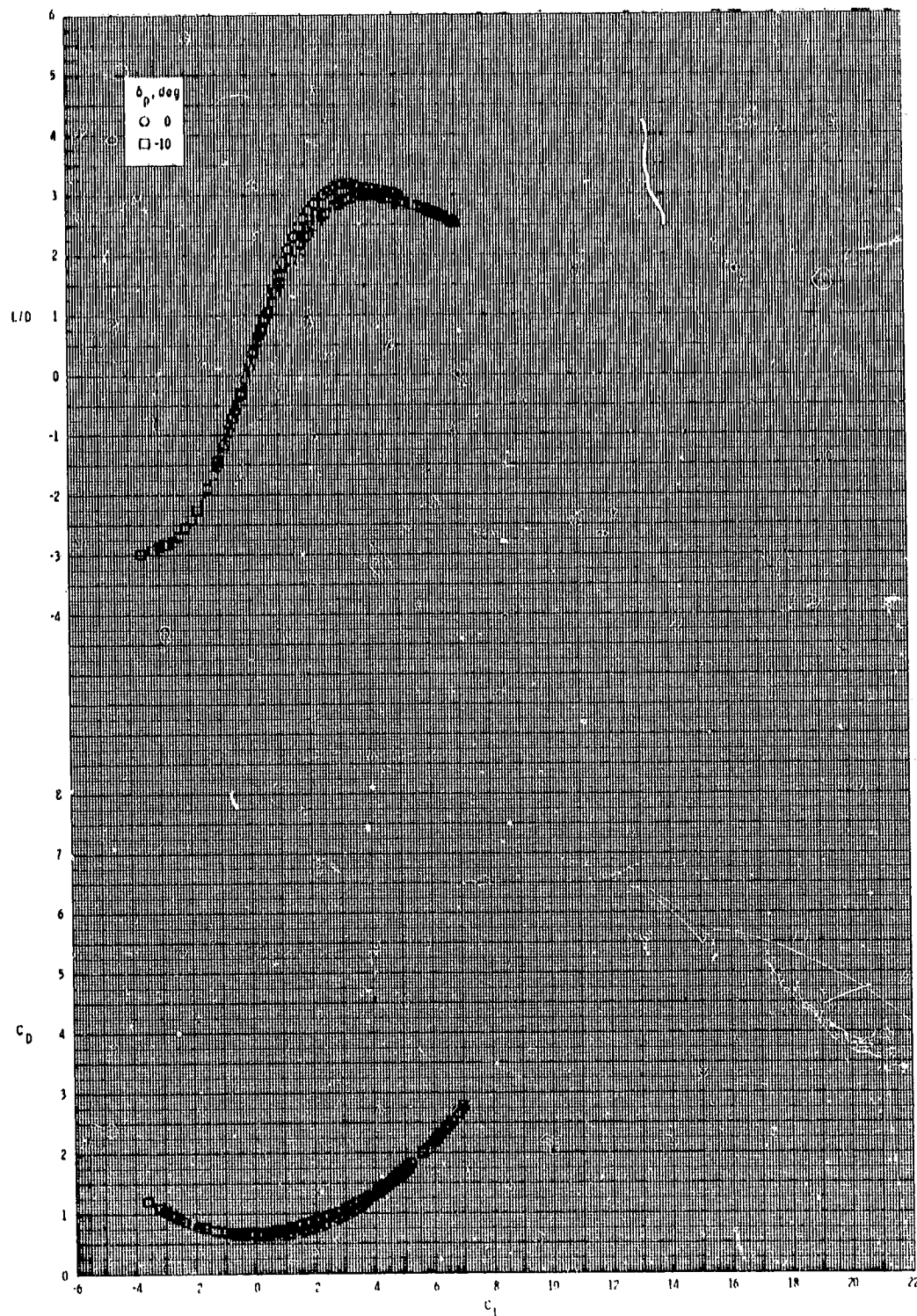
ORIGINAL PAGE IS
OF POOR QUALITY



(h) Continued.

Figure 32.- Continued.

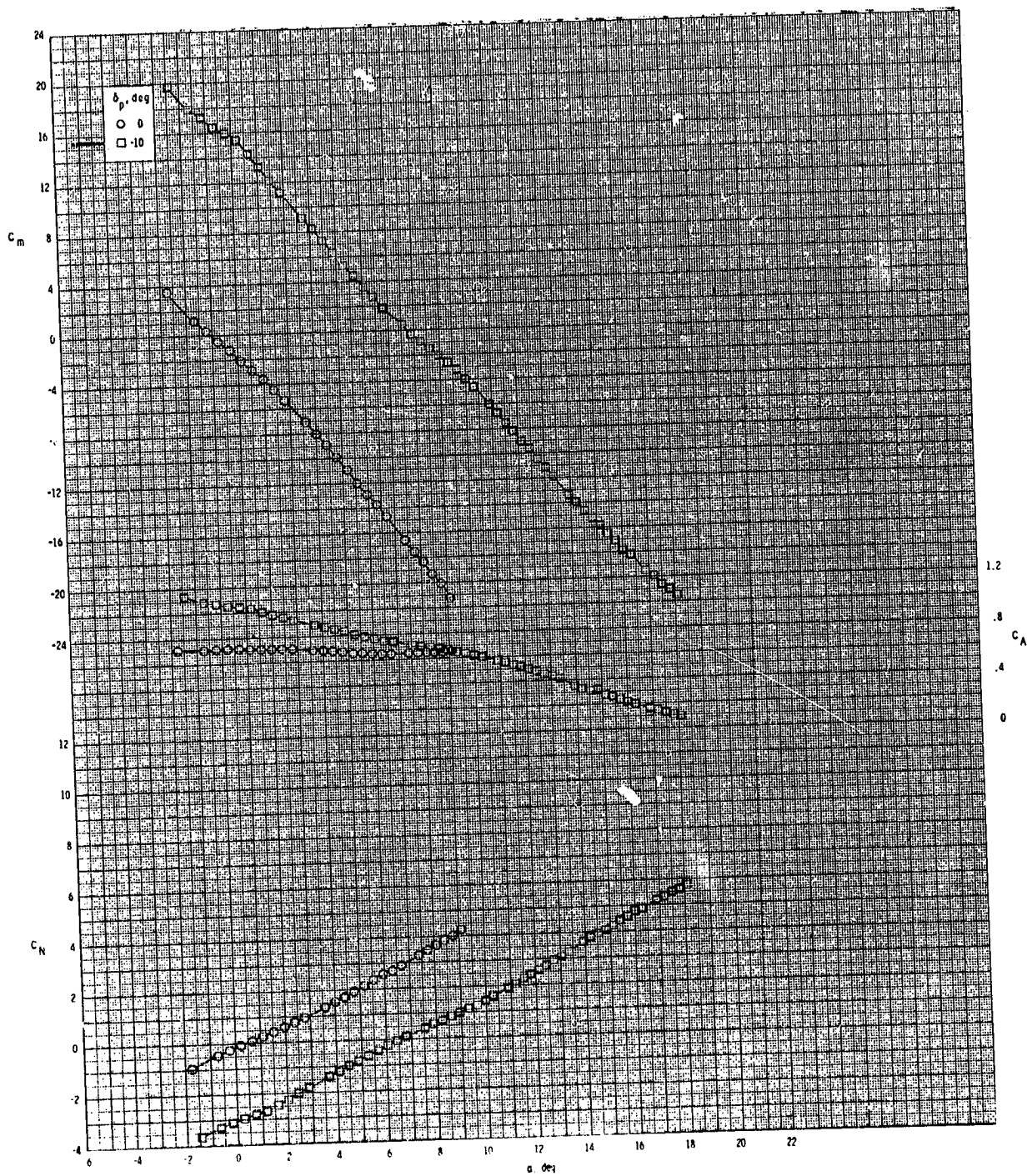
ORIGINAL PAGE IS
OF POOR QUALITY



(b) Concluded.

Figure 32.- Continued.

ORIGINAL PAGE IS
OF POOR QUALITY

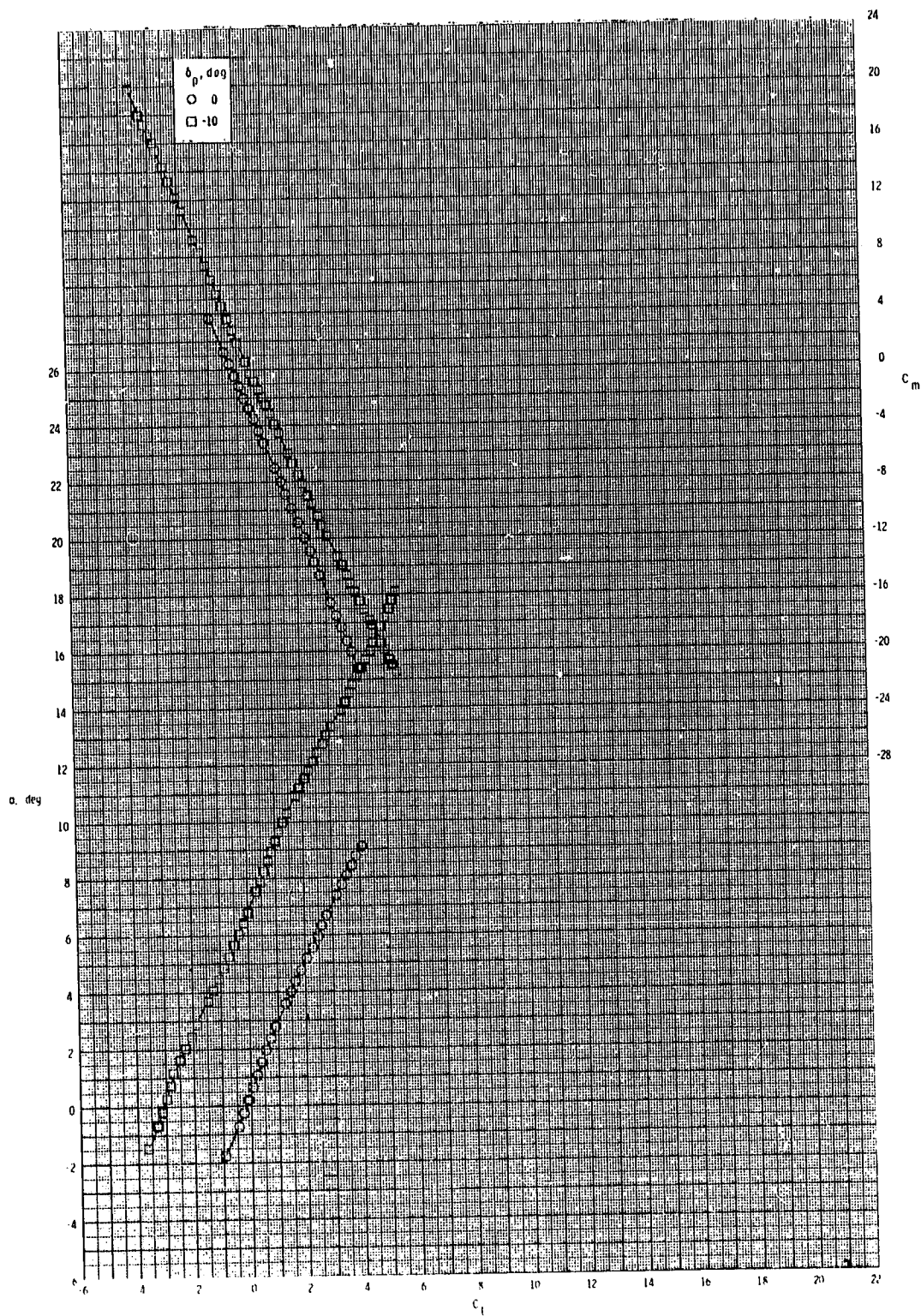


(c) $M = 0.95$.

Figure 32.- Continued.

C-4

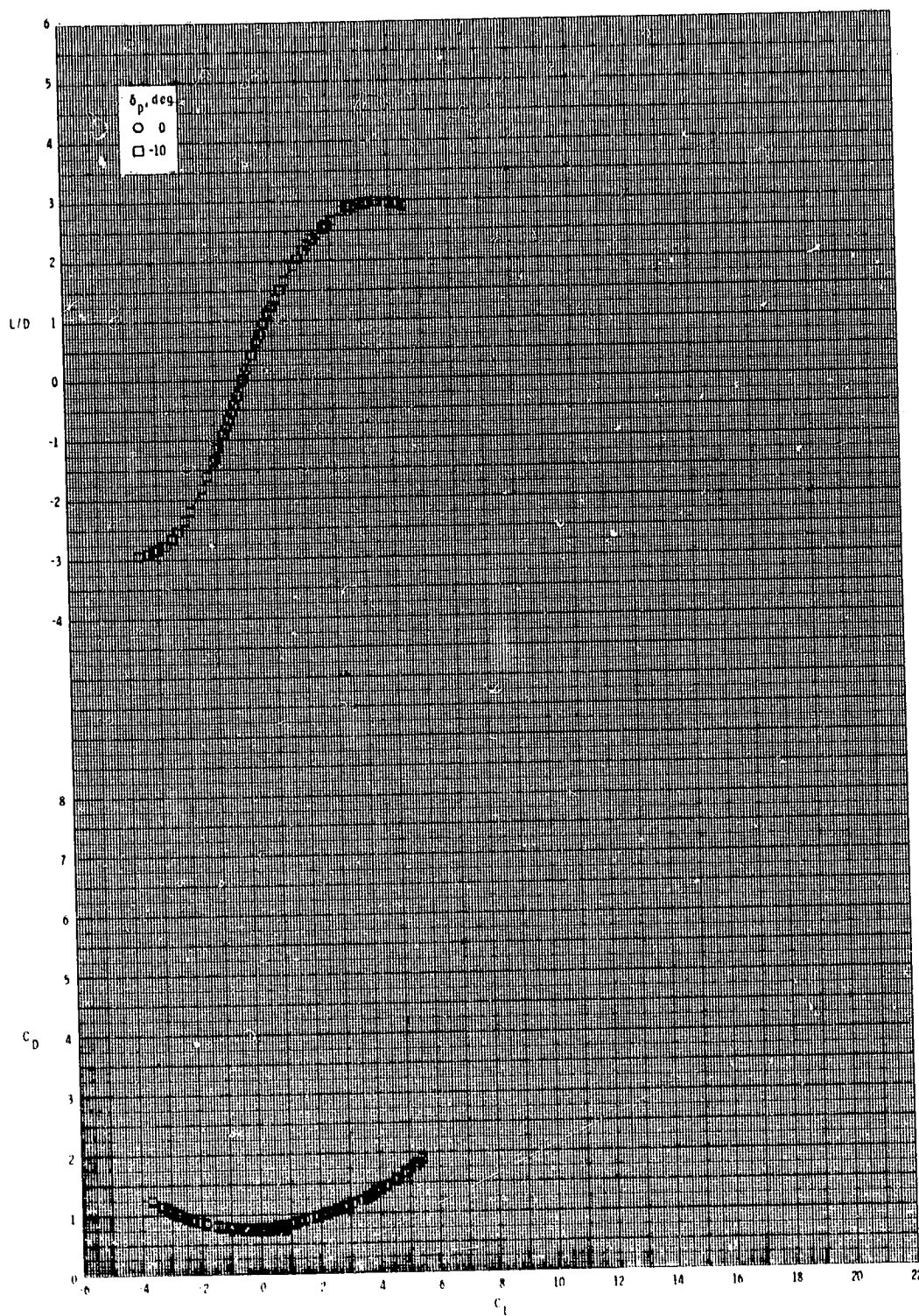
ORIGINAL PAGE 15
OF POOR QUALITY



(c) Continued.

Figure 32.- Continued.

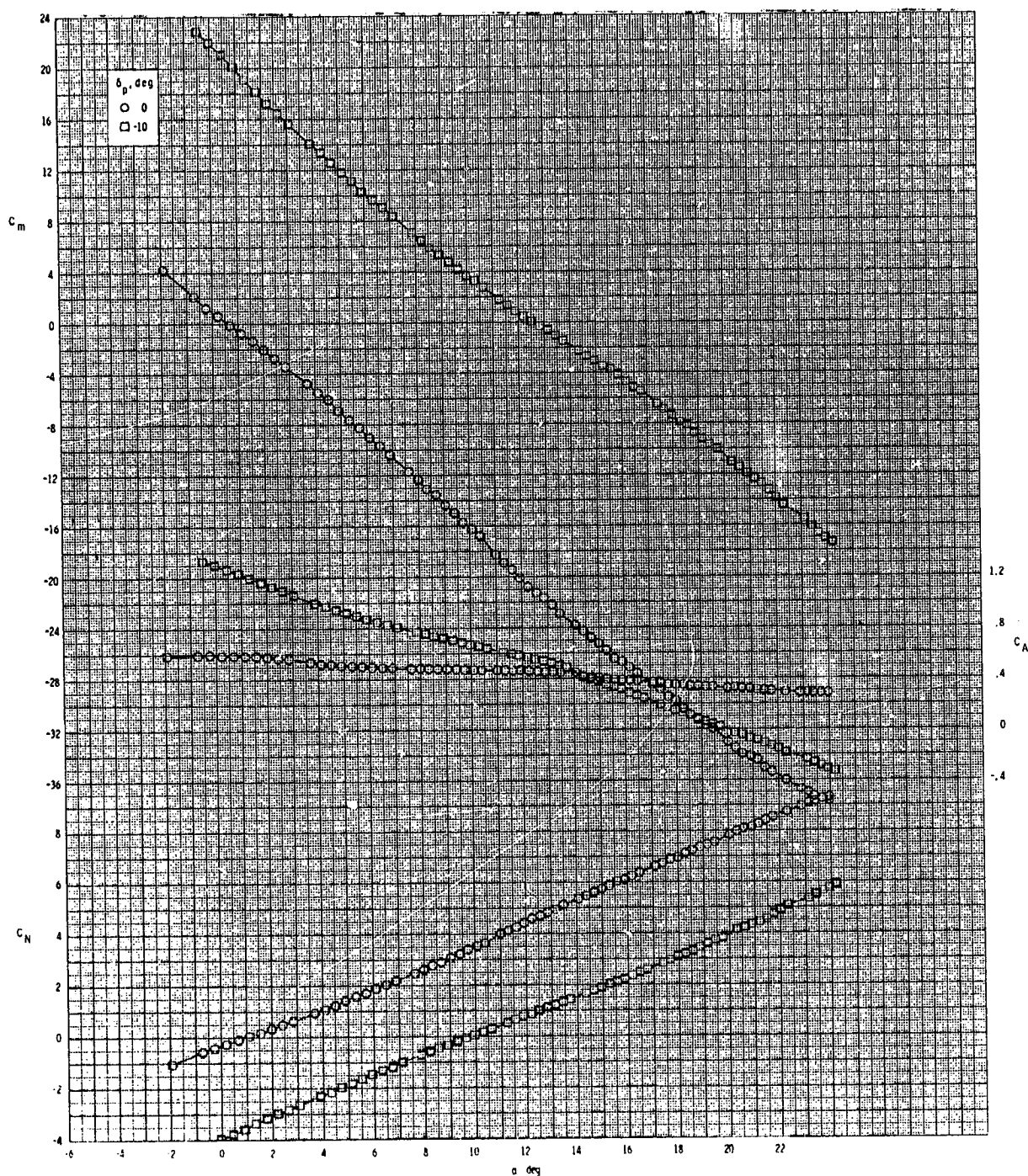
ORIGINAL PAGE IS
OF POOR QUALITY



(c) Concluded.

Figure 32.- Concluded.

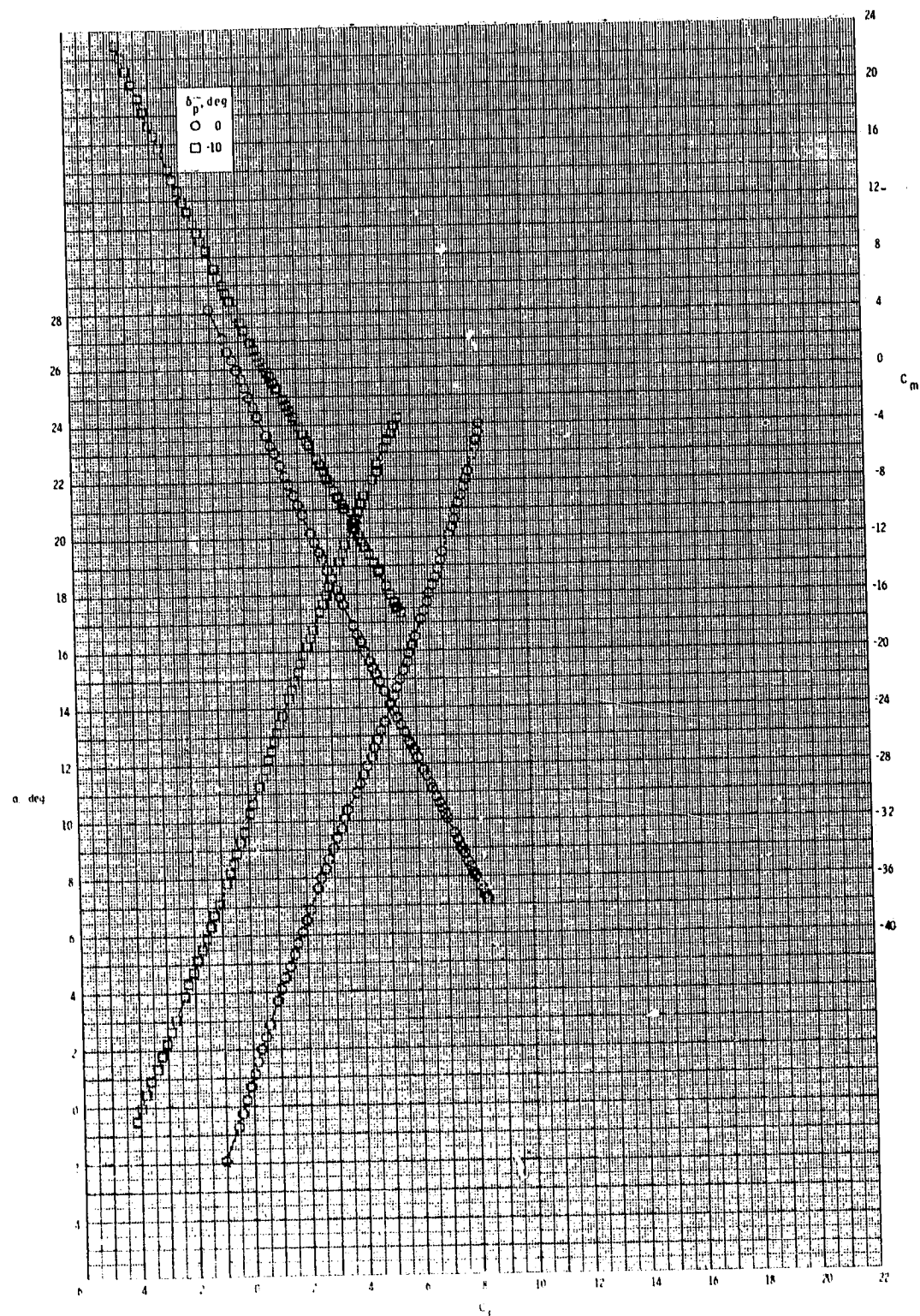
ORIGINAL PAGE IS
OF POOR QUALITY



(a) $M = 0.60$.

Figure 33.- Pitch-control effectiveness of configuration B₁I₄T₂ with internal duct closed.

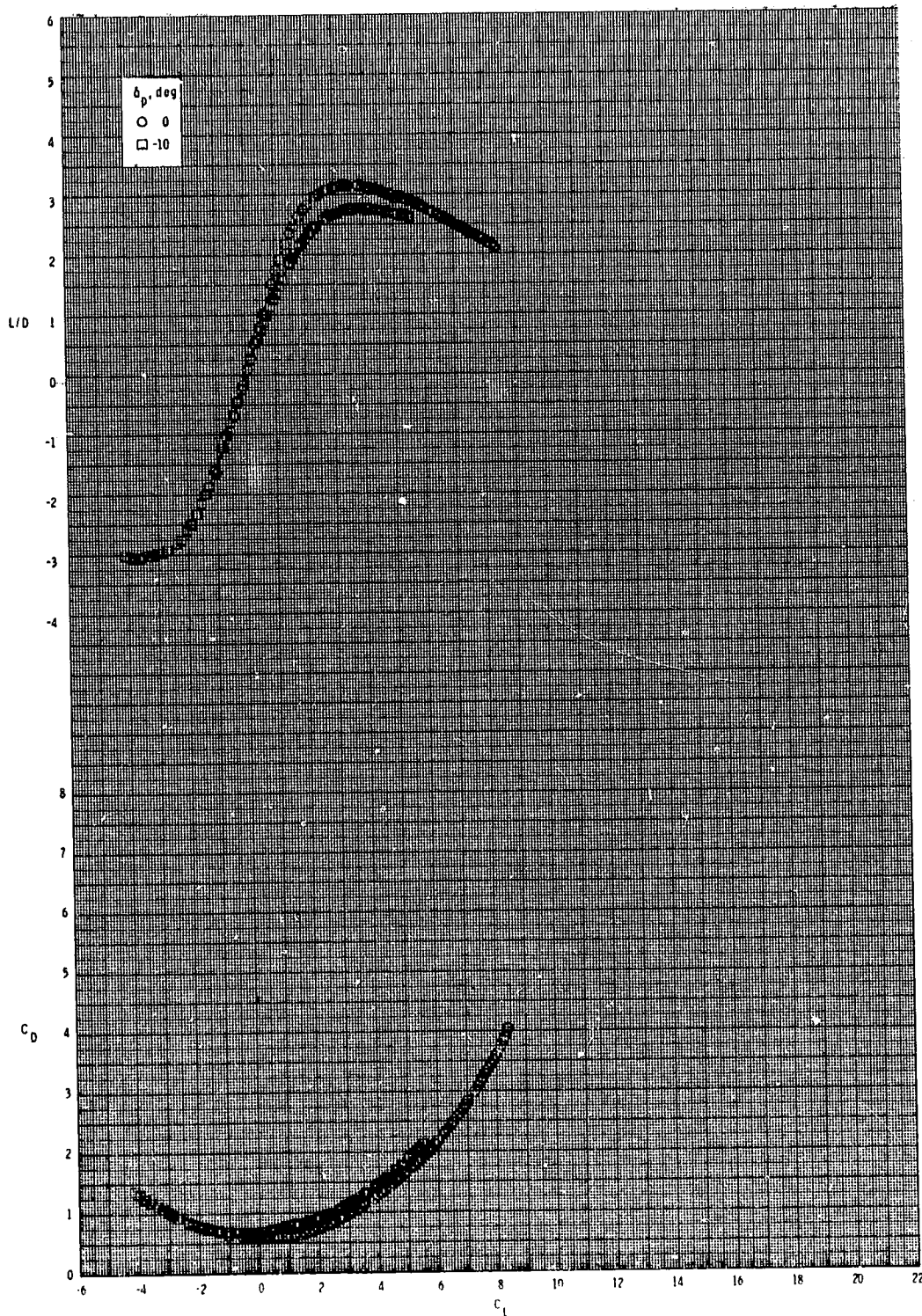
ORIGINAL PAGE IS
OF POOR QUALITY



(a) Continued.

Figure 33.- Continued.

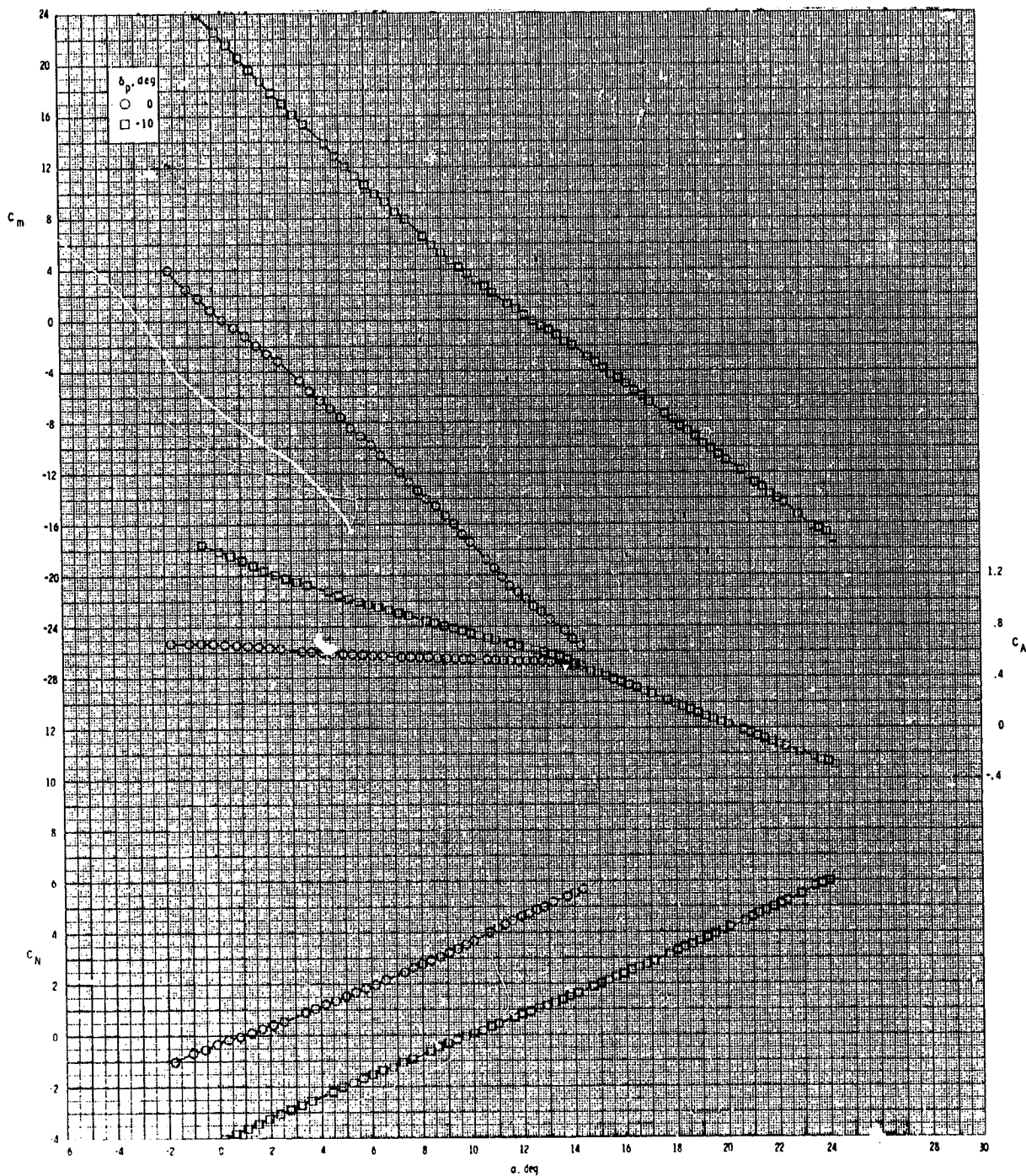
ORIGINAL PAGE IS
OF POOR QUALITY



(a) Concluded.

Figure 33.- Continued.

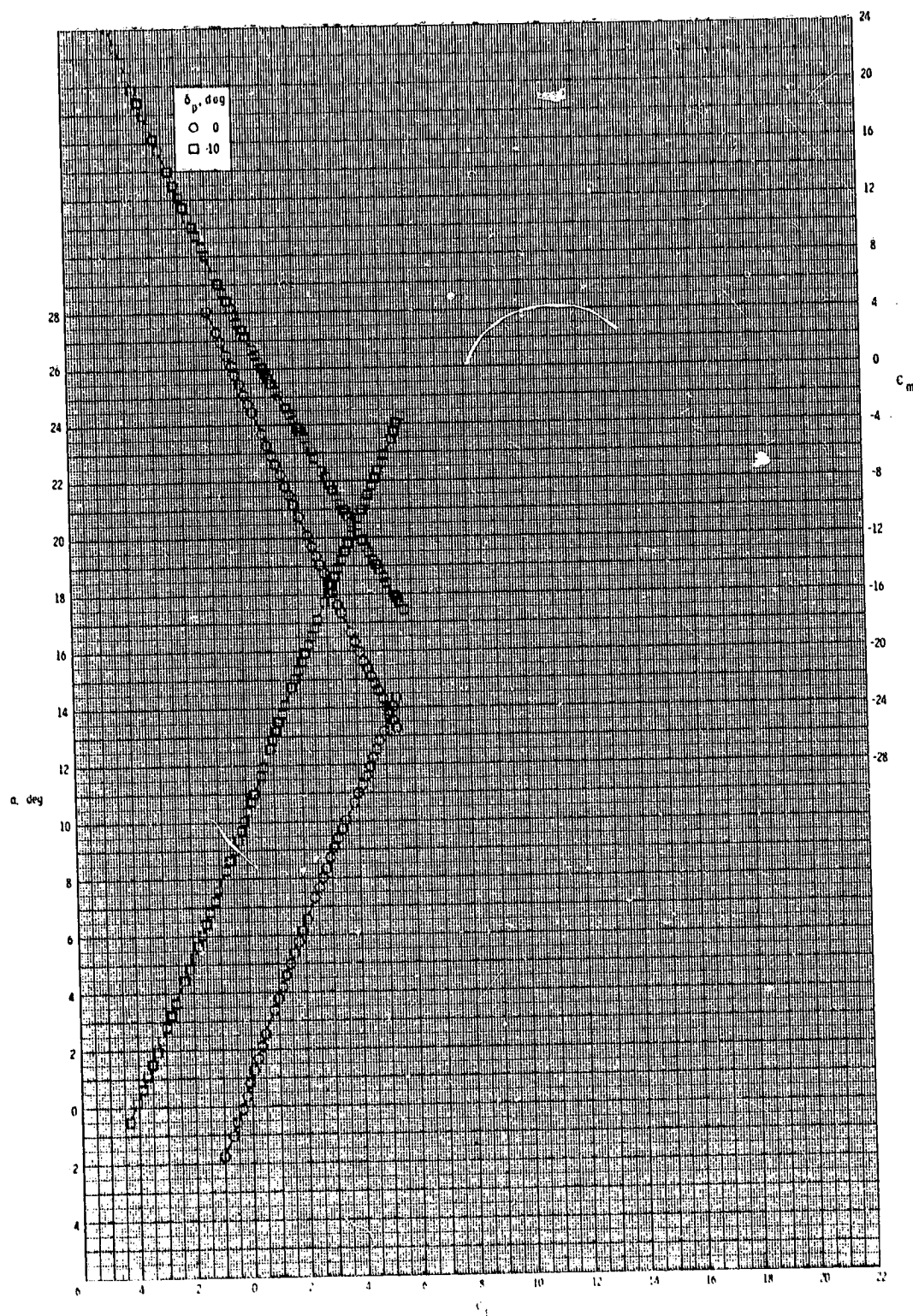
ORIGINAL PAGE IS
OF POOR QUALITY



(b) $M = 0.80$.

Figure 33.- Continued.

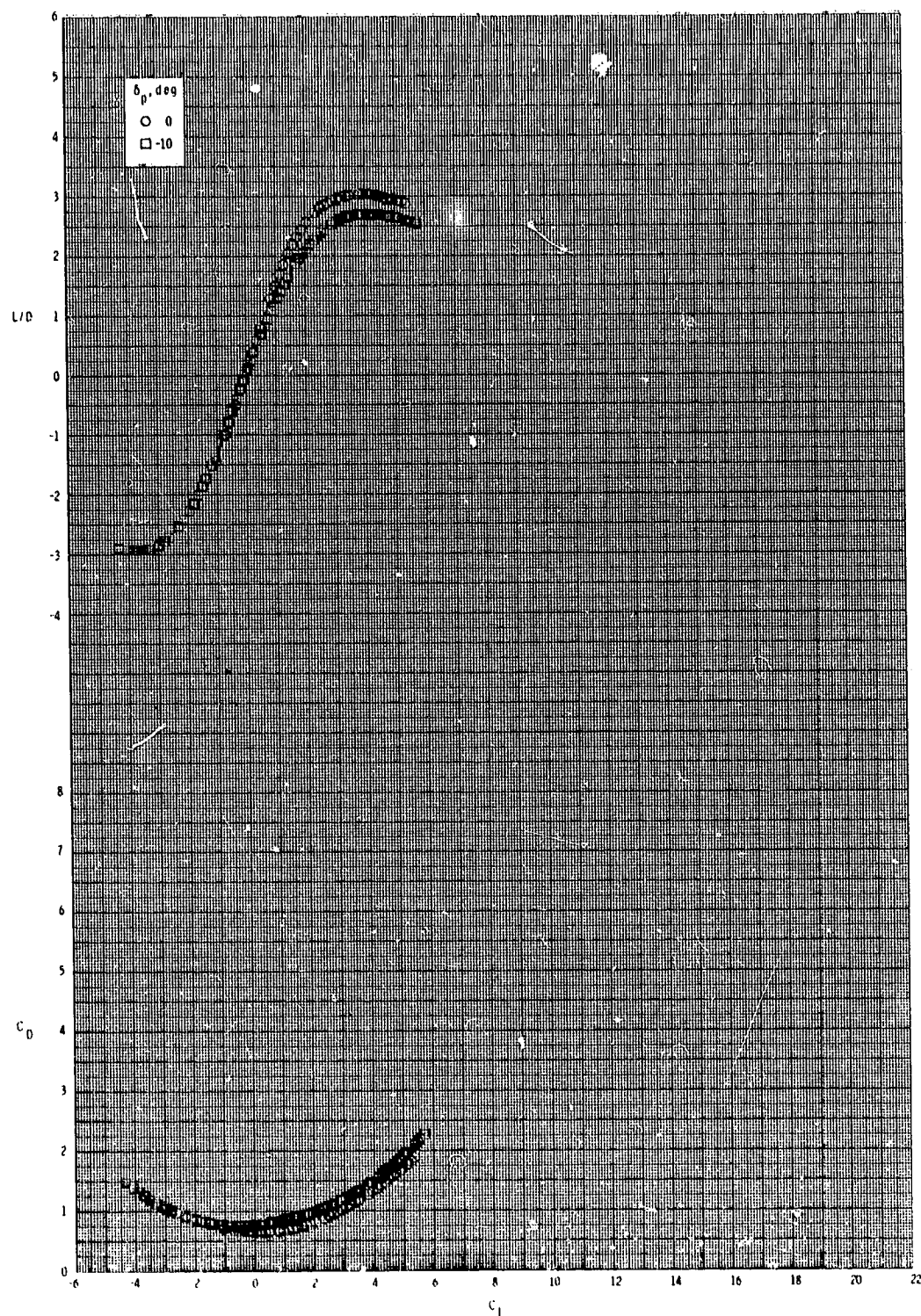
ORIGINAL PAGE IS
OF POOR QUALITY



(b) Continued.

Figure 33.- Continued.

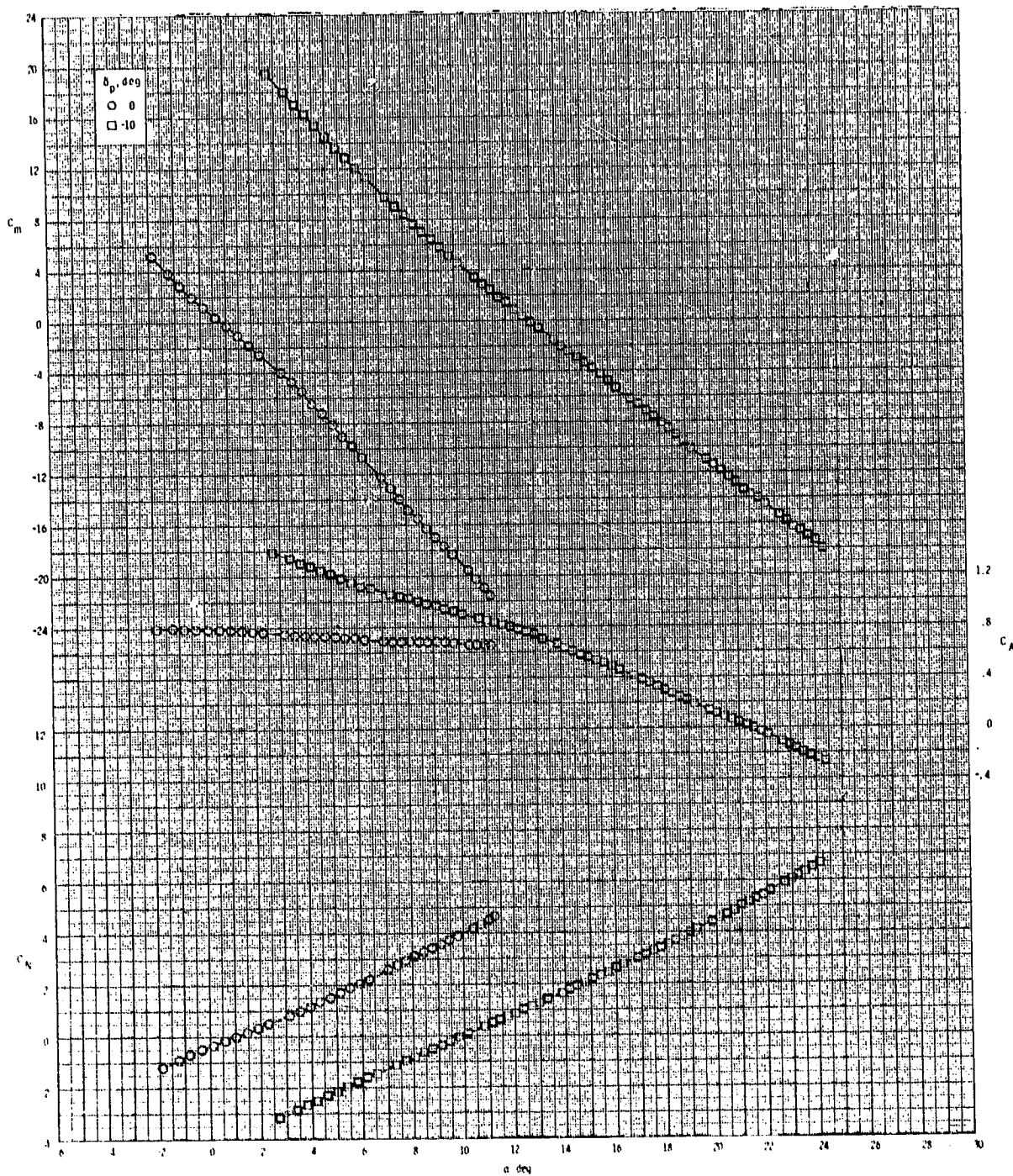
ORIGINAL PAGE IS
OF POOR QUALITY



(b) Concluded.

Figure 33.- Continued.

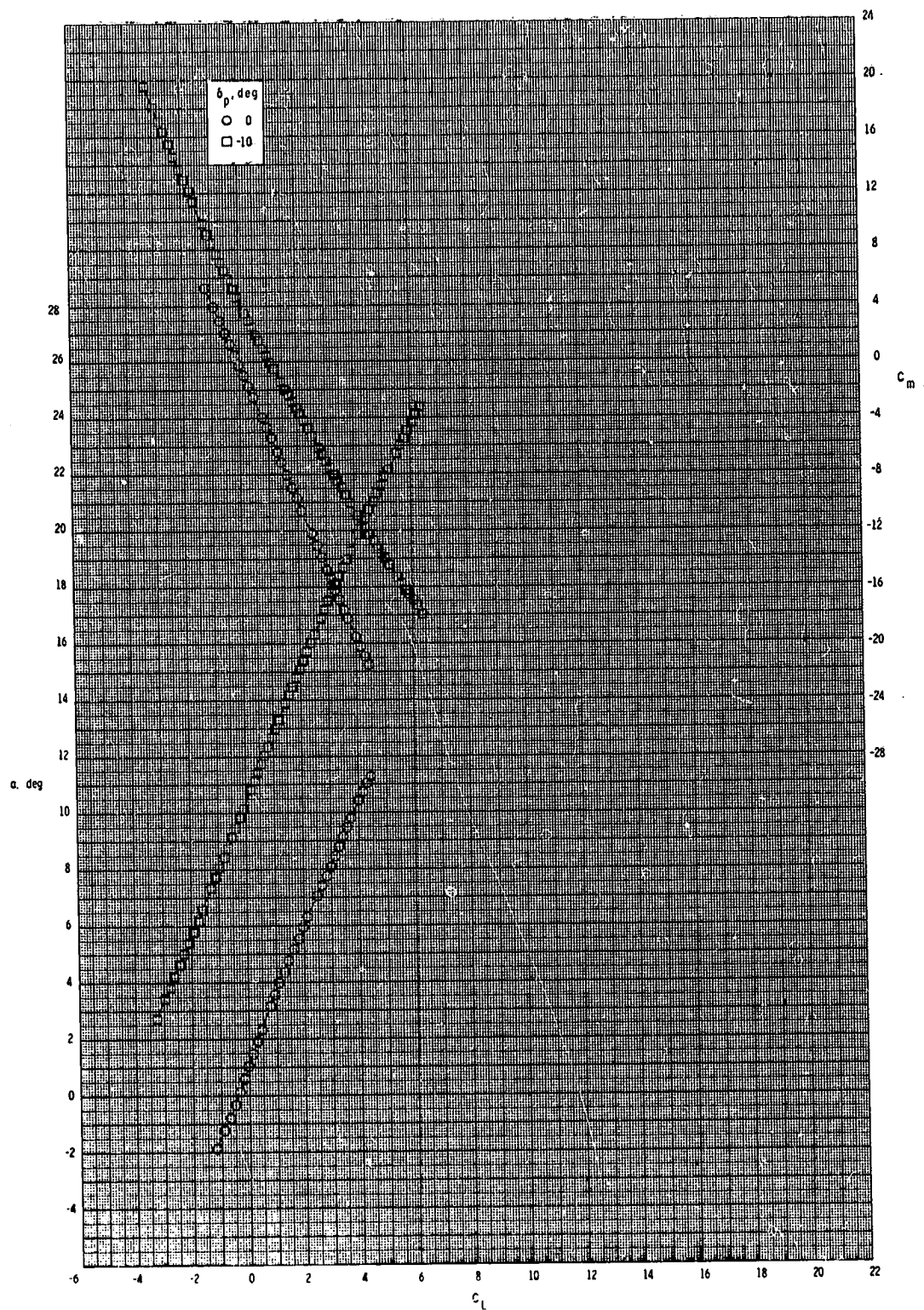
ORIGINAL PAGE IS
OF POOR QUALITY



(c) $M = 0.95$.

Figure 33.- Continued.

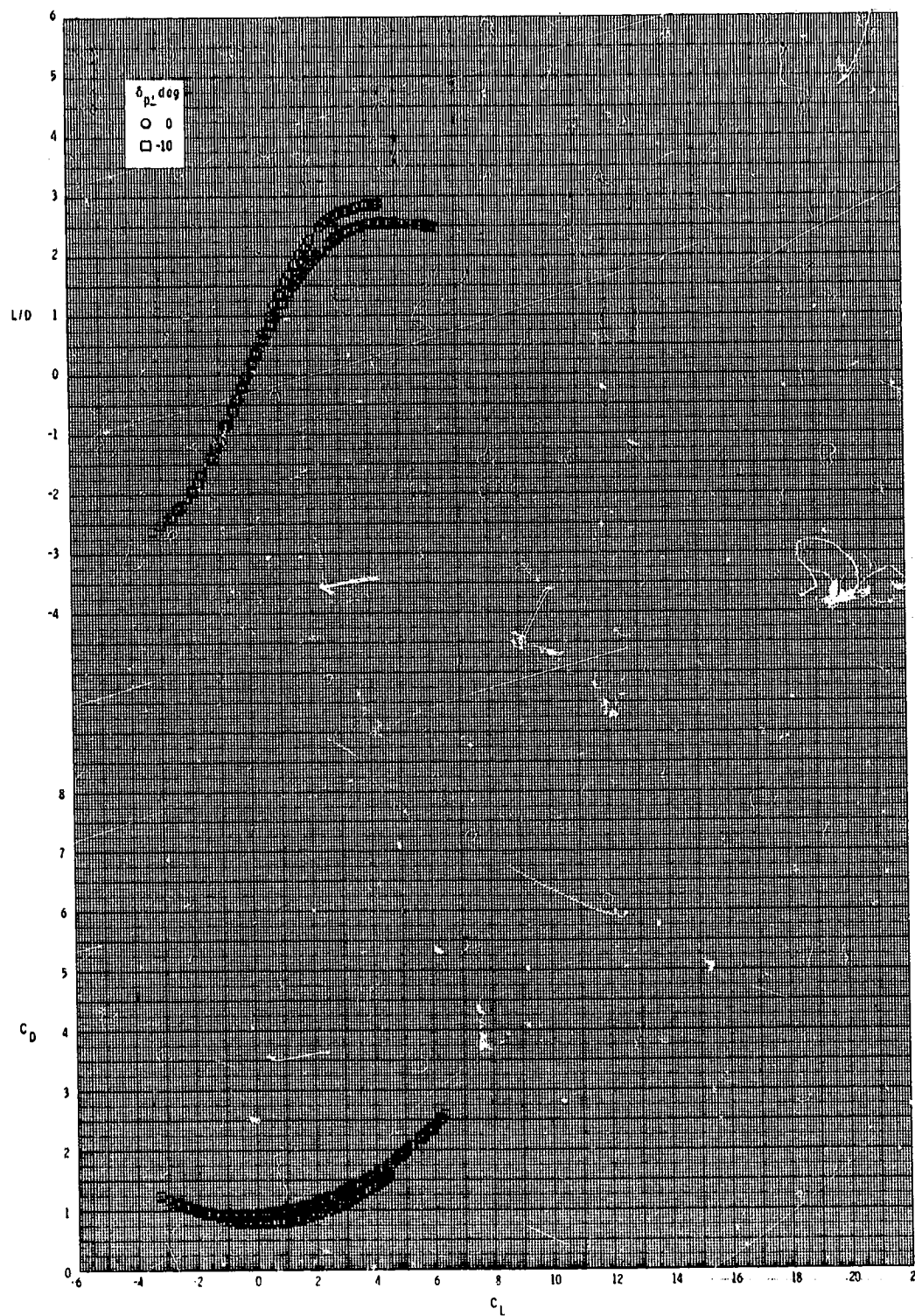
ORIGINAL PAGE IS
OF POOR QUALITY



(c) Continued.

Figure 33.- Continued.

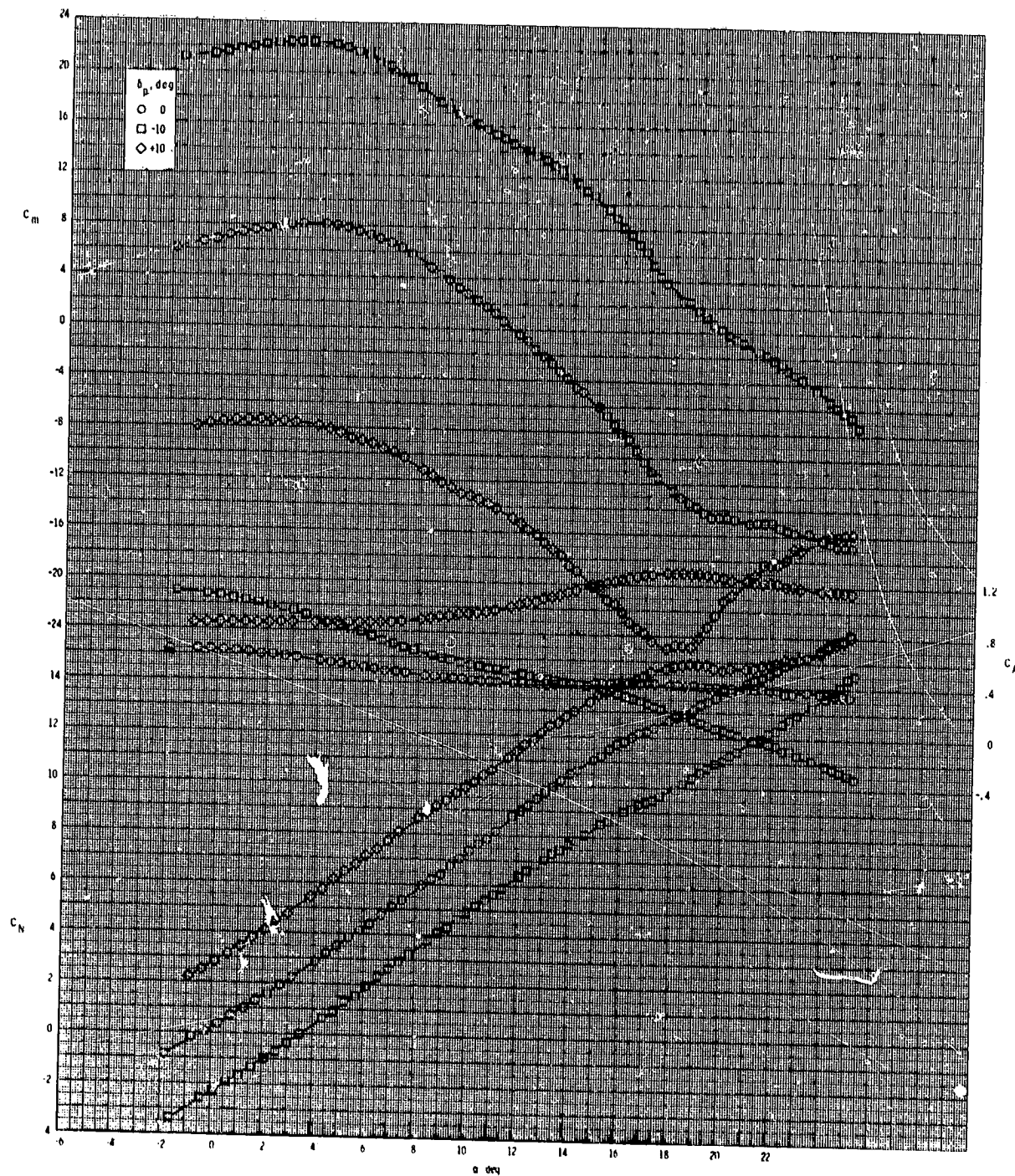
ORIGINAL PAGE IS
OF POOR QUALITY



(c) Concluded.

Figure 33.- Concluded.

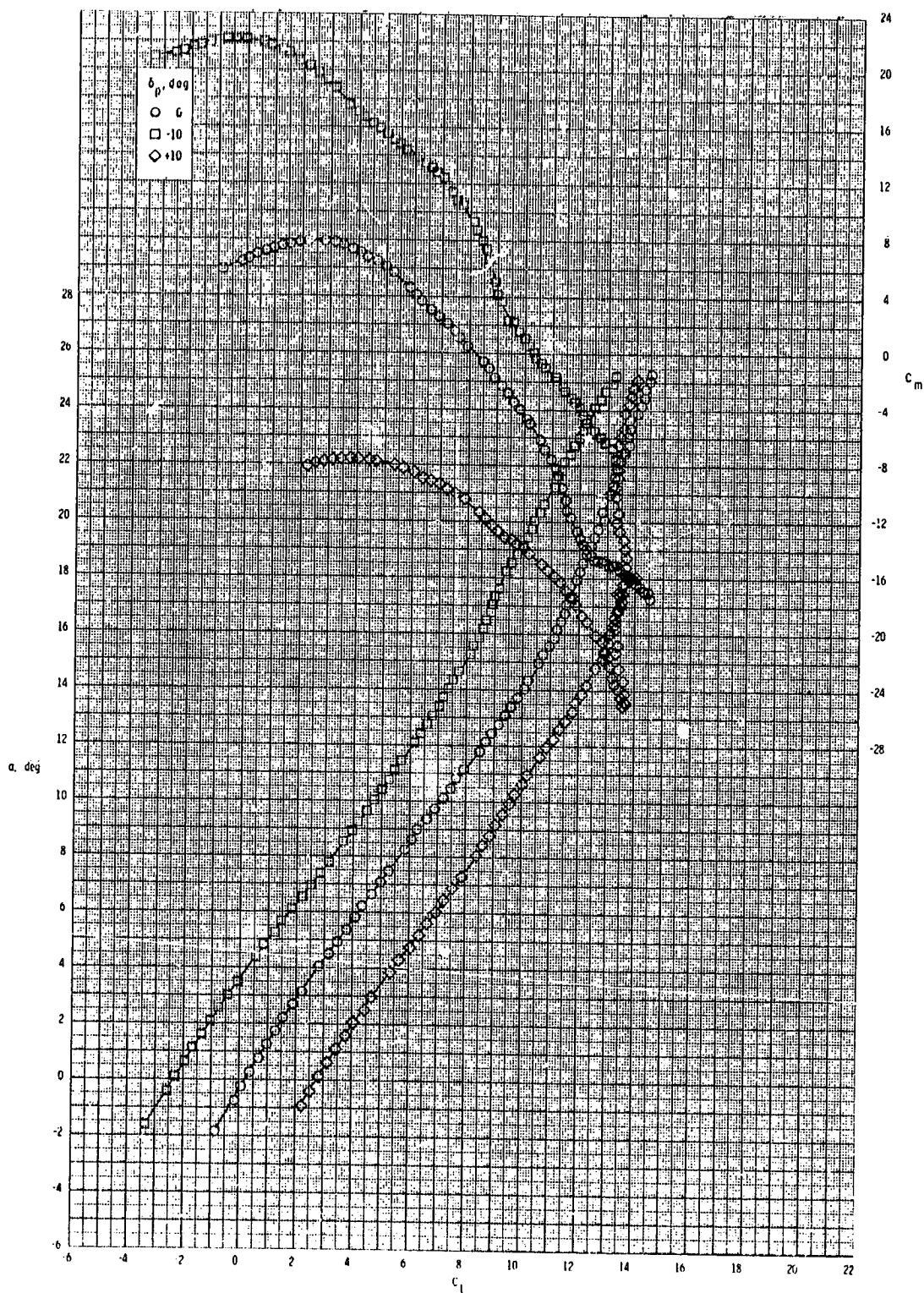
ORIGINAL PAGE IS
OF POOR QUALITY



(a) $M = 0.60$.

Figure 34.- Pitch-control effectiveness of configuration B₁I₄W₁T₁ with internal duct closed.

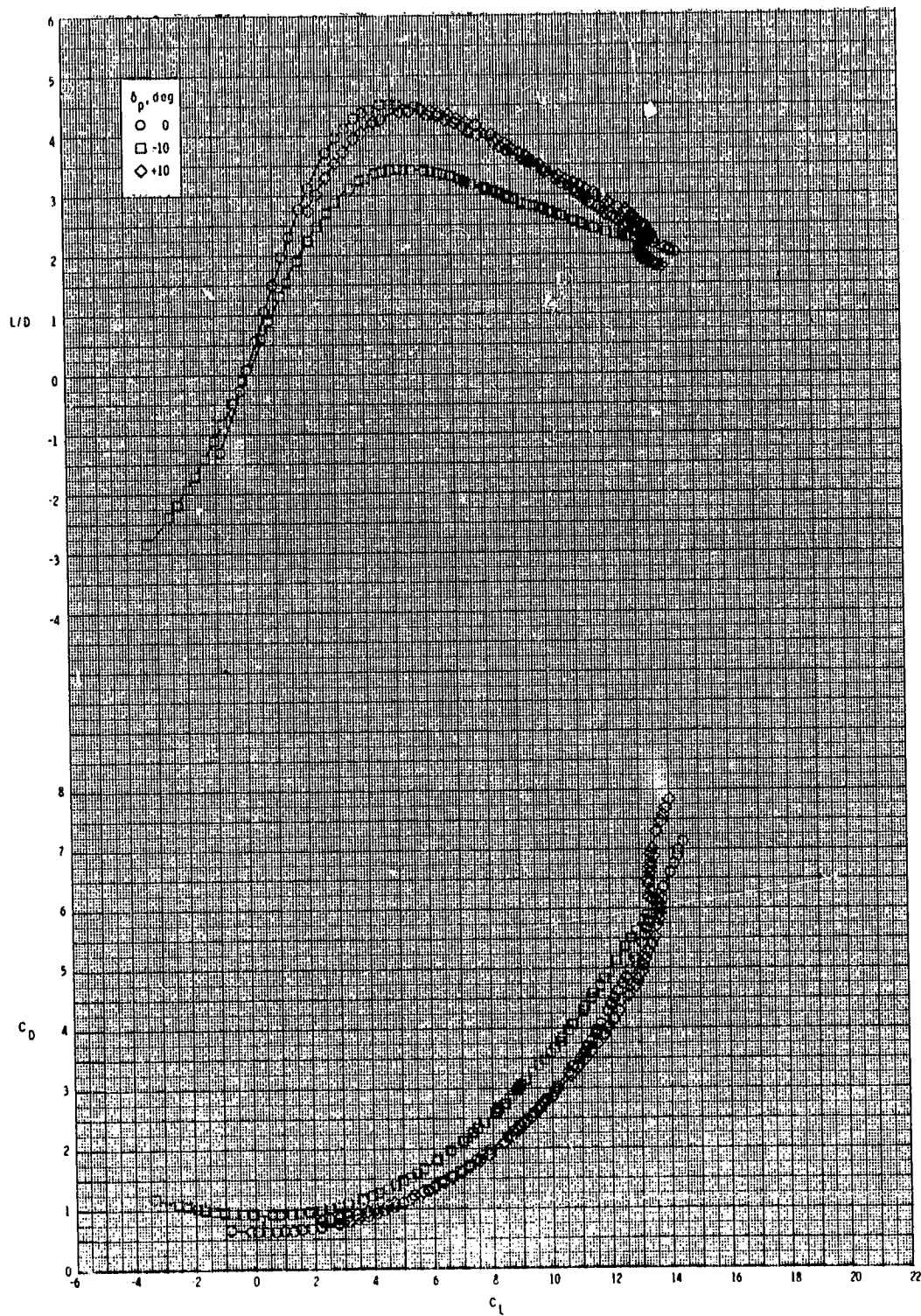
ORIGINAL PAGE IS
OF POOR QUALITY



(a) Continued.

Figure 34.- Continued.

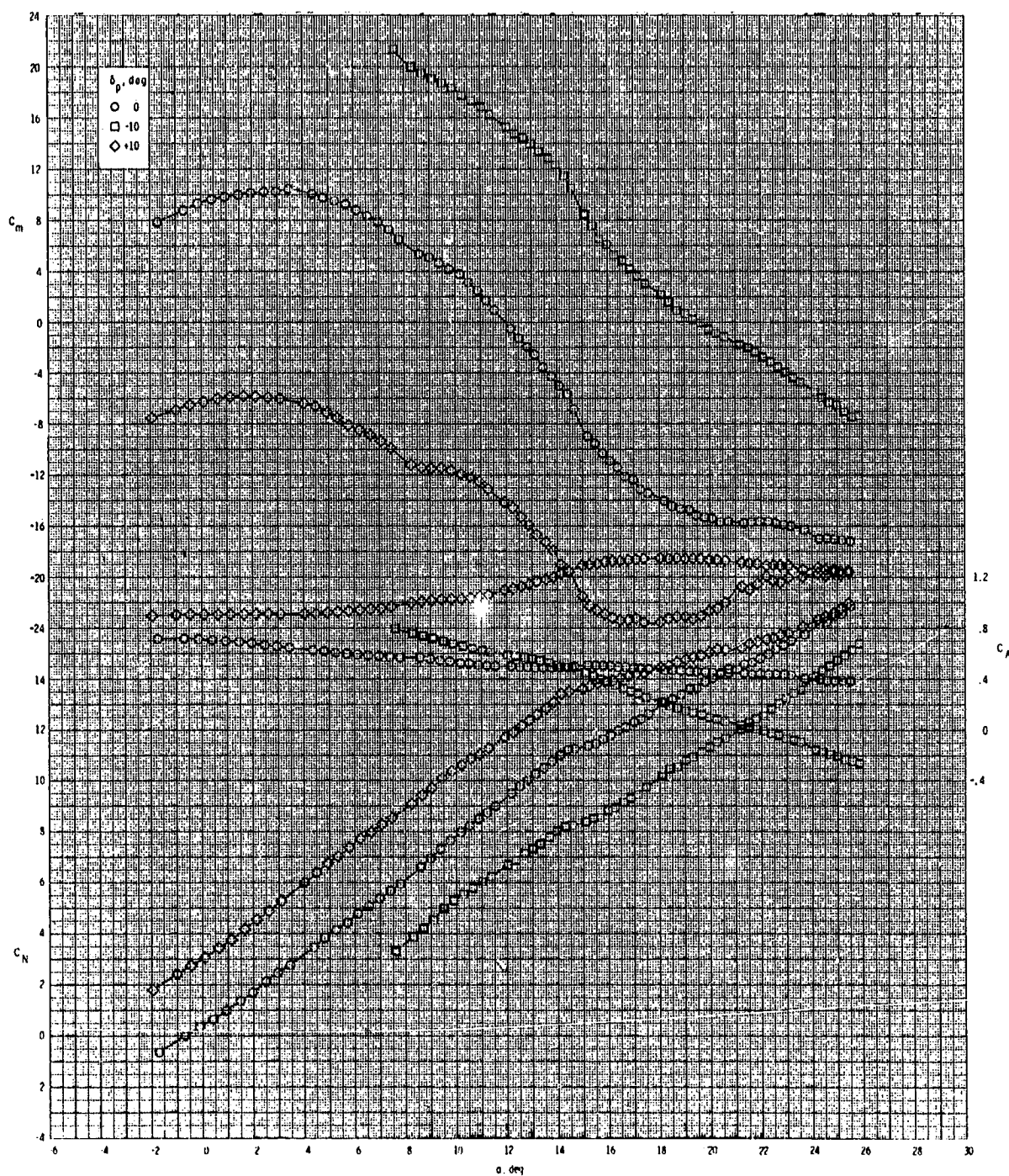
ORIGINAL PAGE 13
OF POOR QUALITY



(a) Concluded.

Figure 34.- Continued.

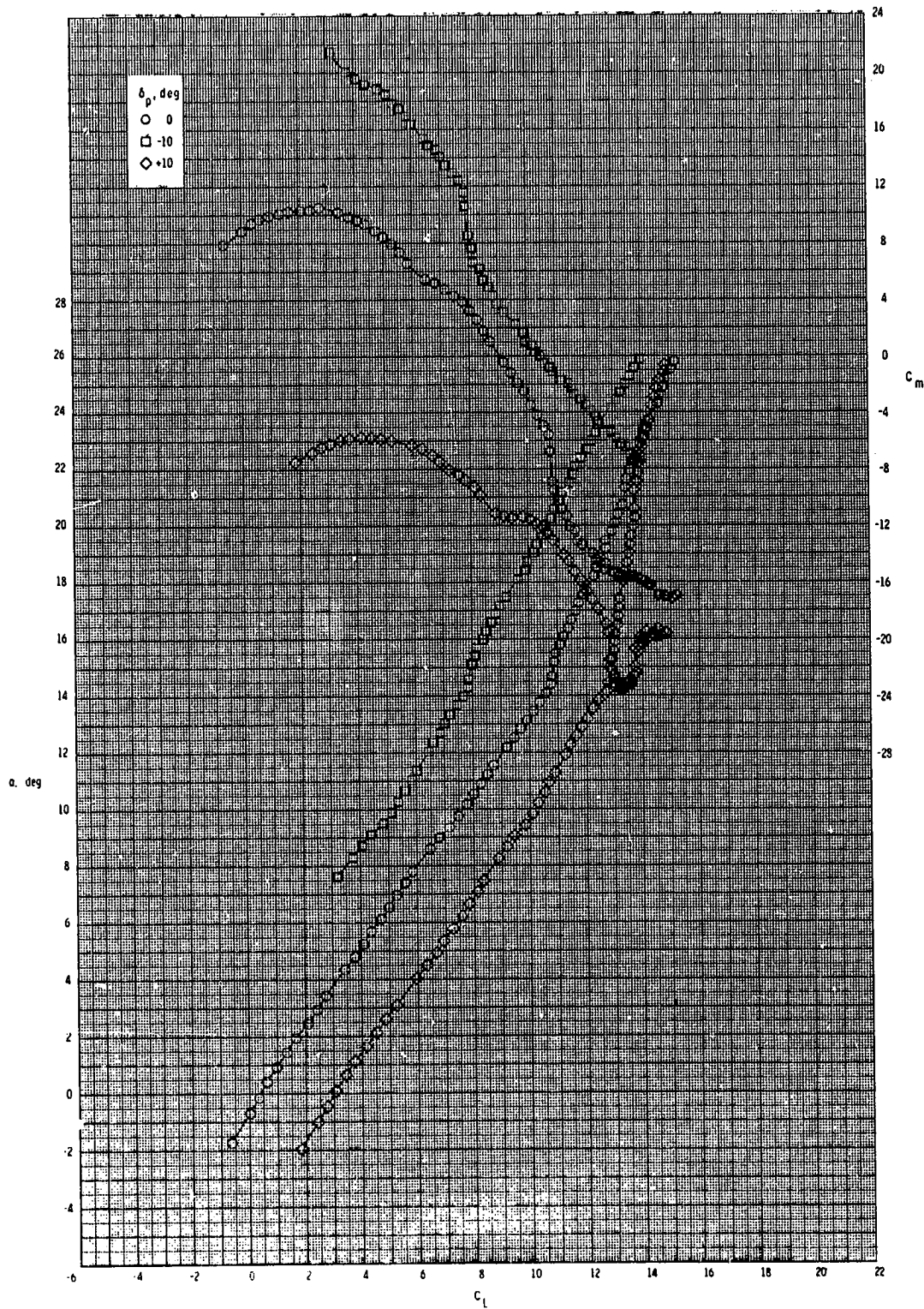
ORIGINAL PAGE IS
OF POOR QUALITY



(b) $M = 0.80$.

Figure 34.- Continued.

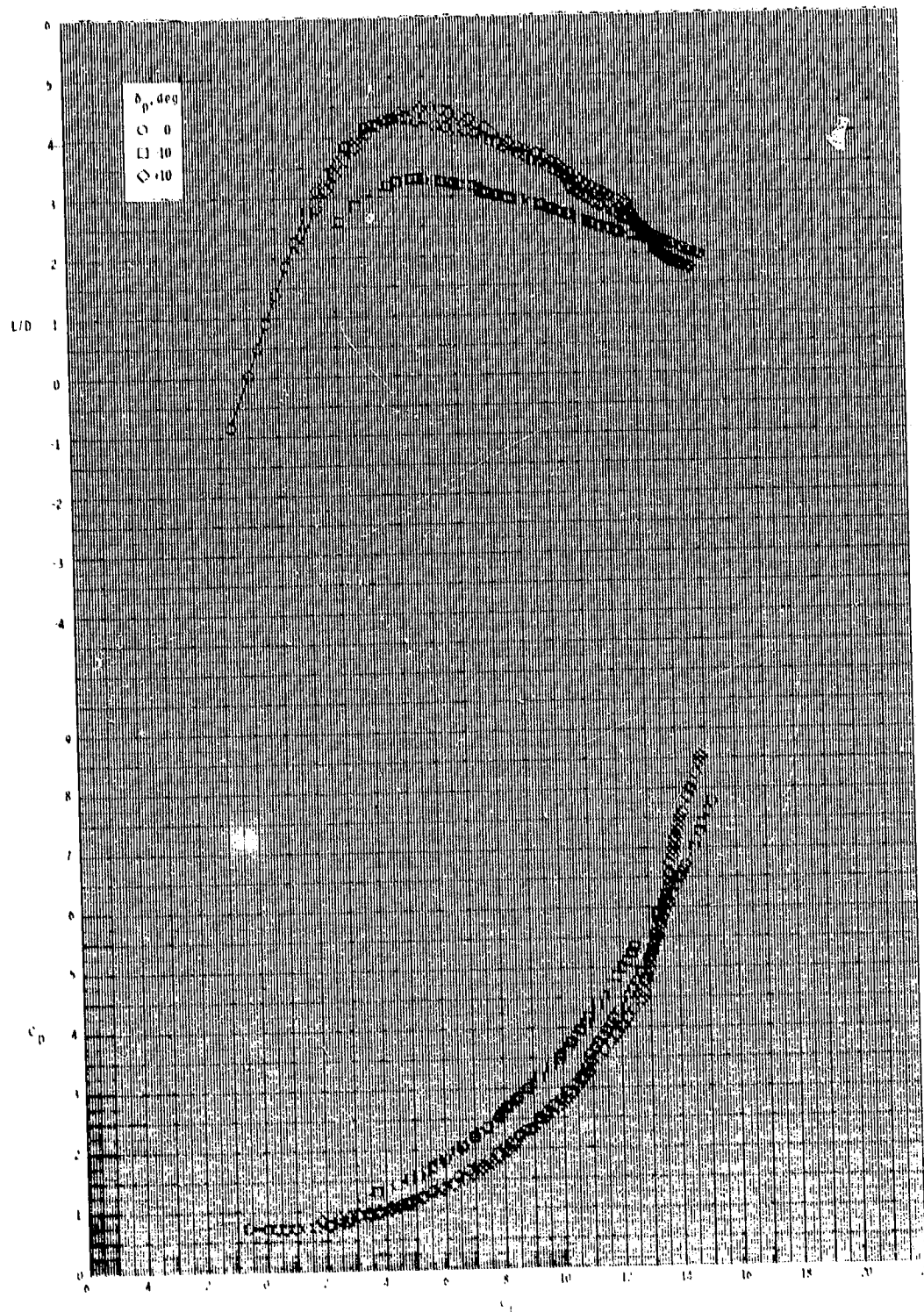
ORIGINAL PAGE IS
OF POOR QUALITY



(b) Continued.

Figure 34.- Continued.

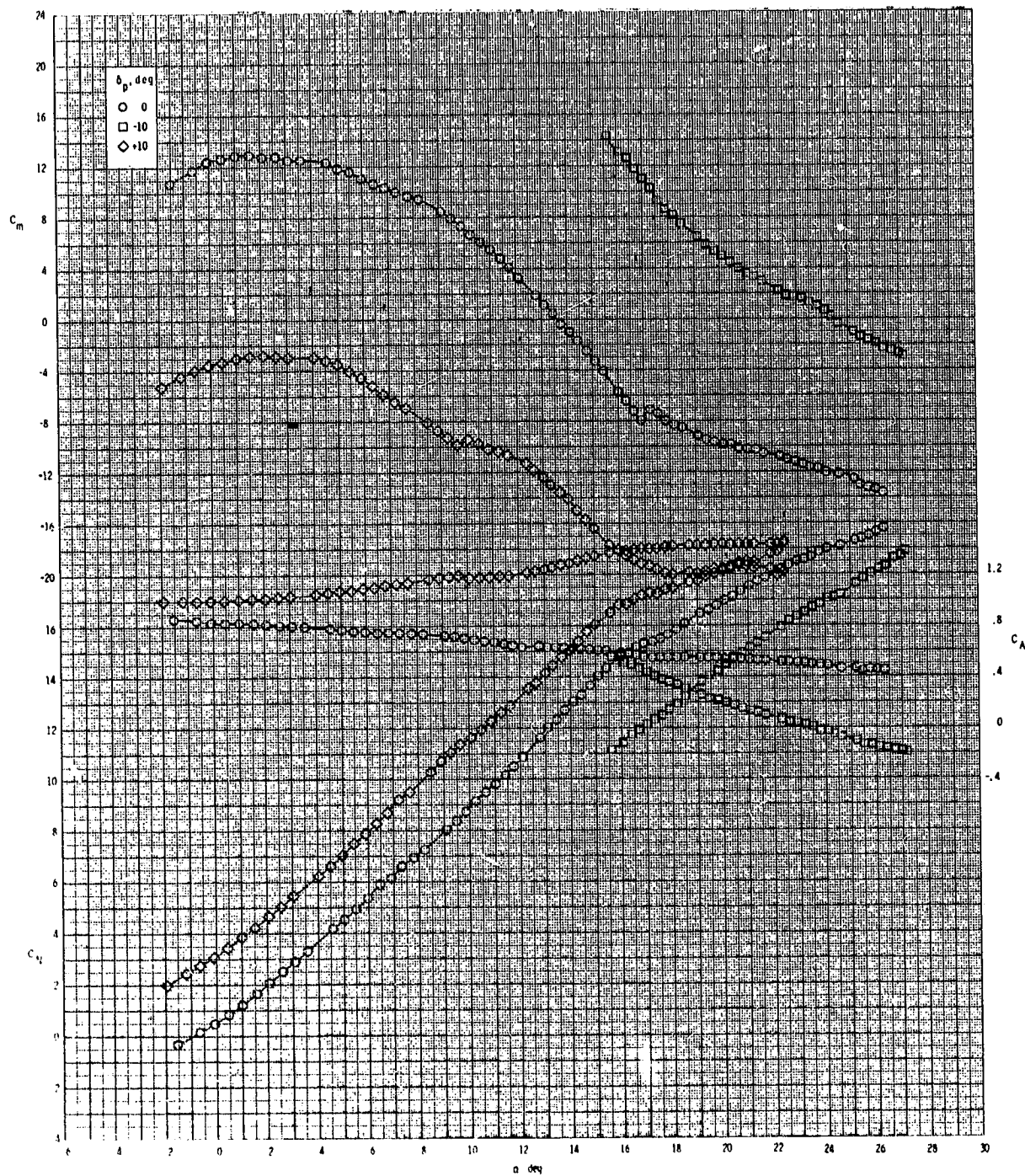
ORIGINAL PAGE IS
OF POOR QUALITY



(b) Concluded.

Figure 34.- Continued.

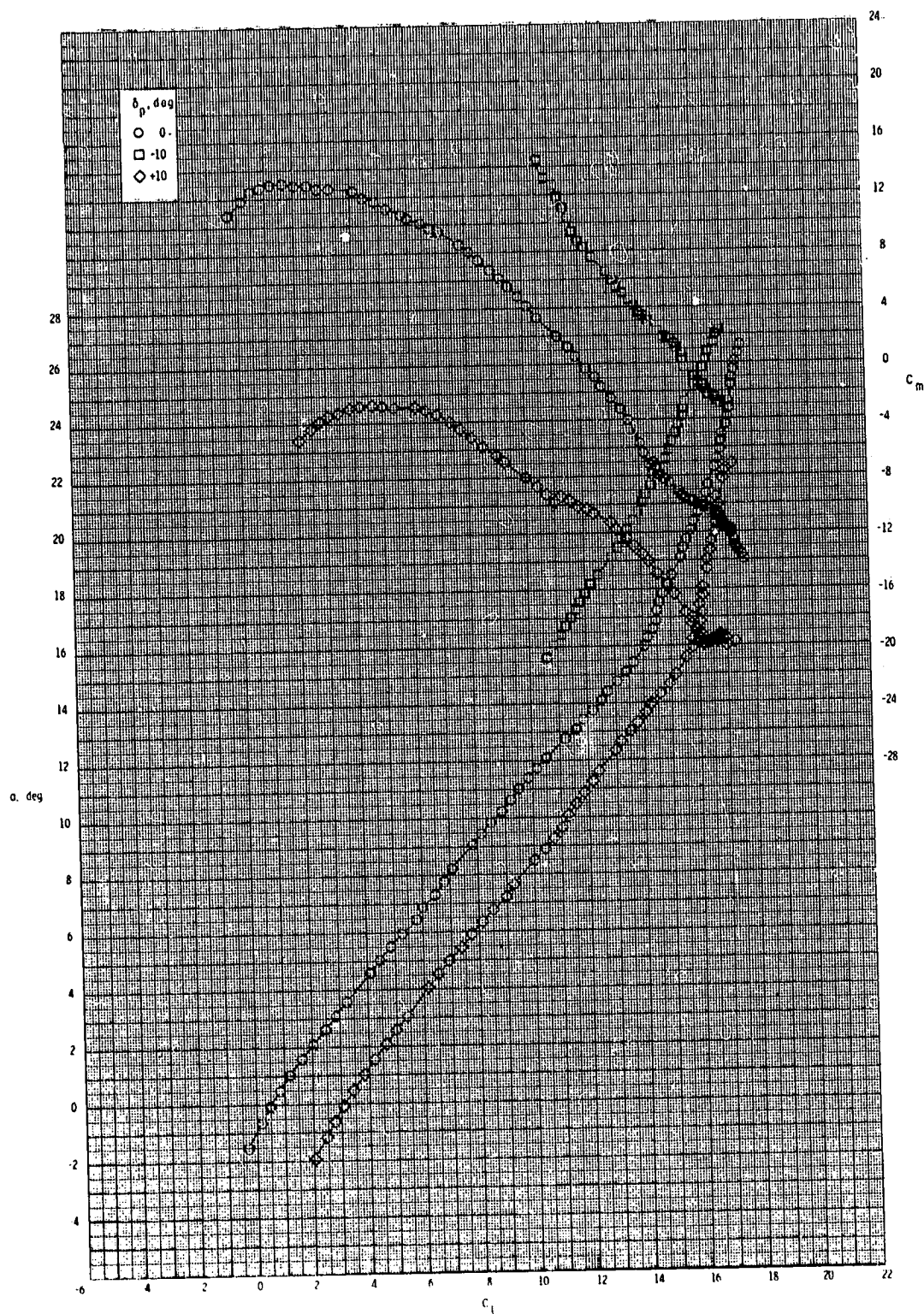
ORIGINAL PAGE 13
OF POOR QUALITY



(c) $M = 0.95$.

Figure 34.- Continued.

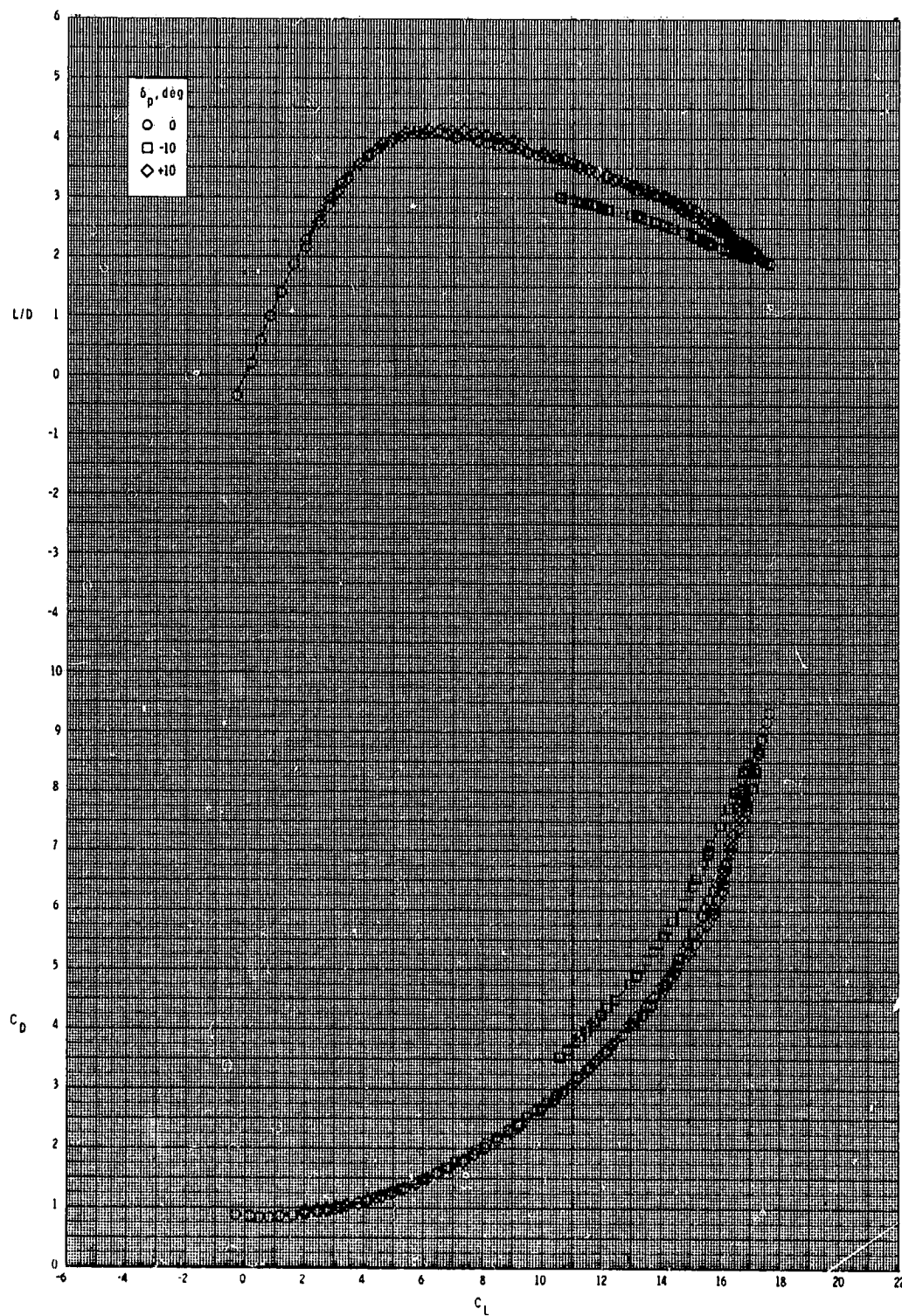
ORIGINAL PAGE IS
OF POOR QUALITY



(c) Continued.

Figure 34.- Continued.

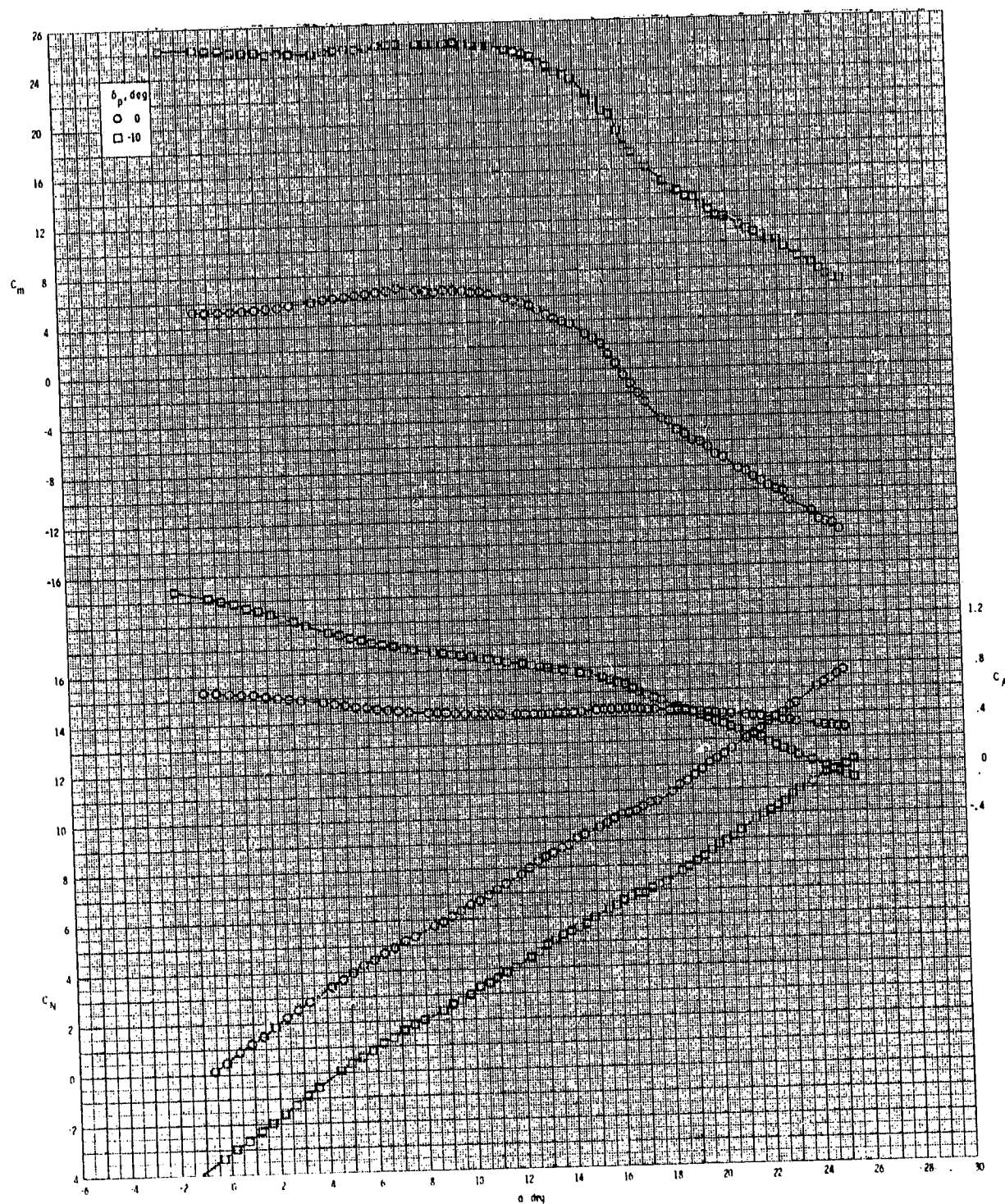
ORIGINAL PAGE IS
OF POOR QUALITY



(c) Concluded.

Figure 34.- Concluded.

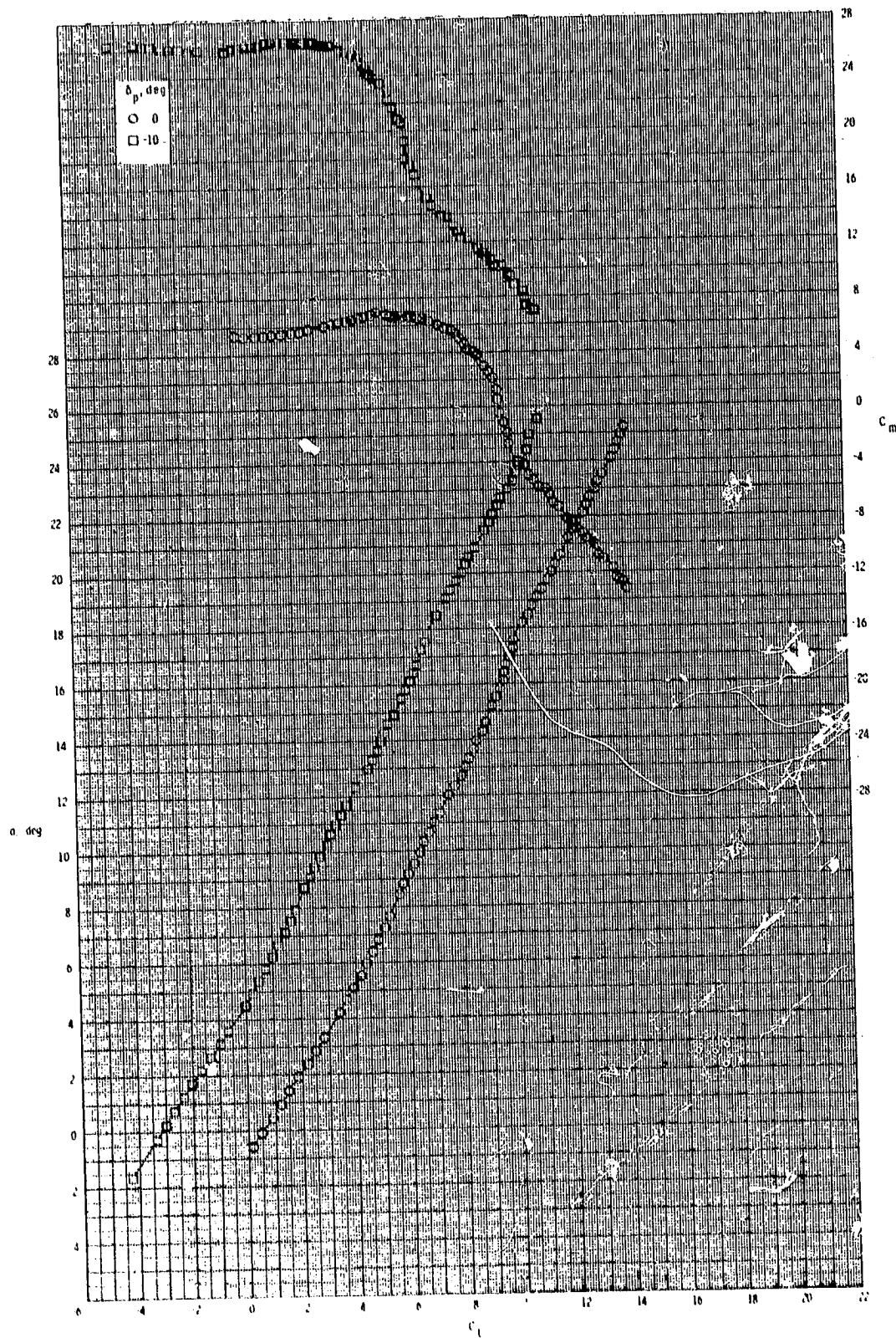
ORIGINAL PAGE IS
OF POOR QUALITY



(a) $M = 0.60$.

Figure 35.- Pitch-control effectiveness of configuration $B_1I_4W_1T_2$ with internal duct closed.

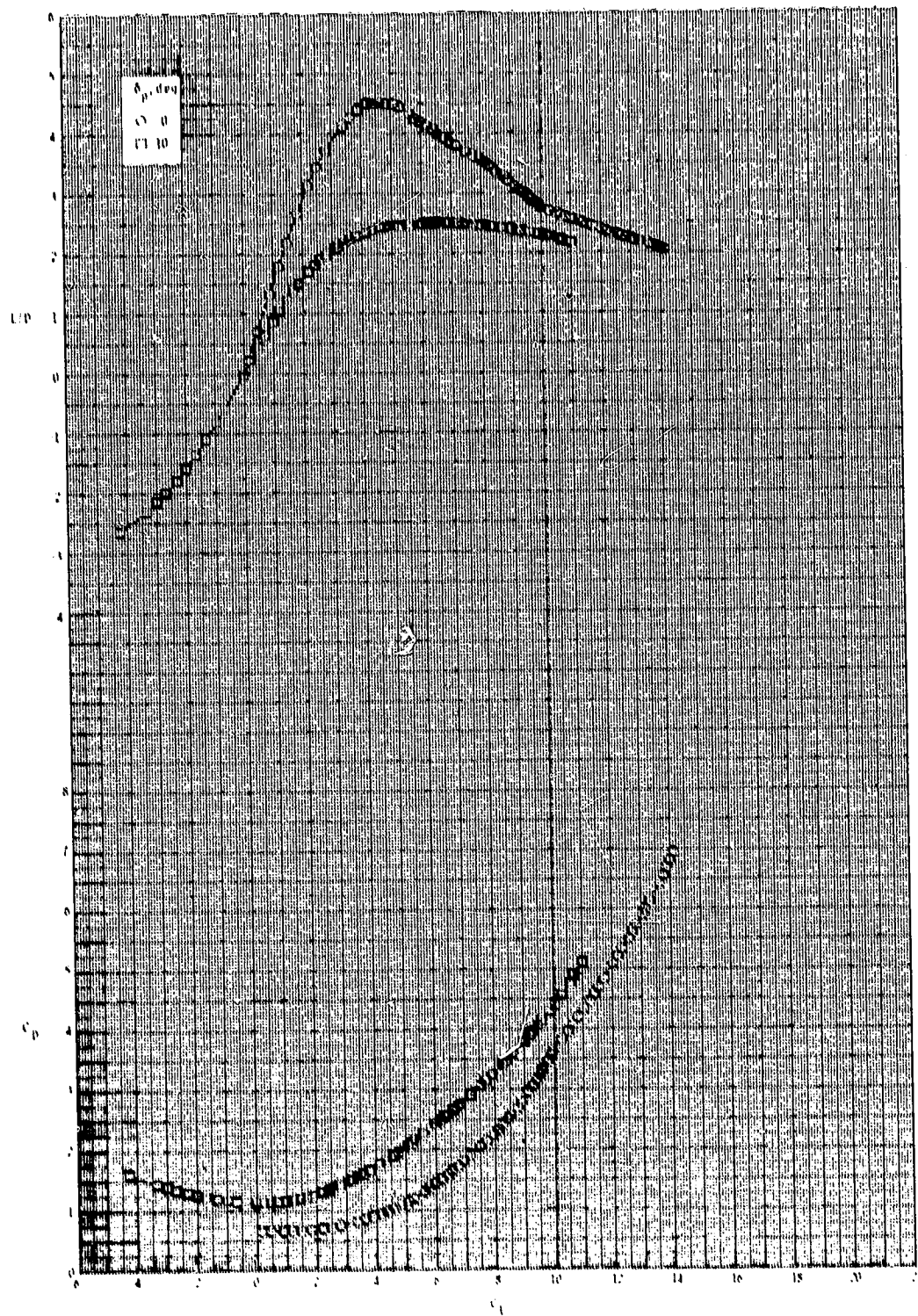
ORIGINAL PAGE IS
OF POOR QUALITY



(a) Continued.

Figure 35.- Continued.

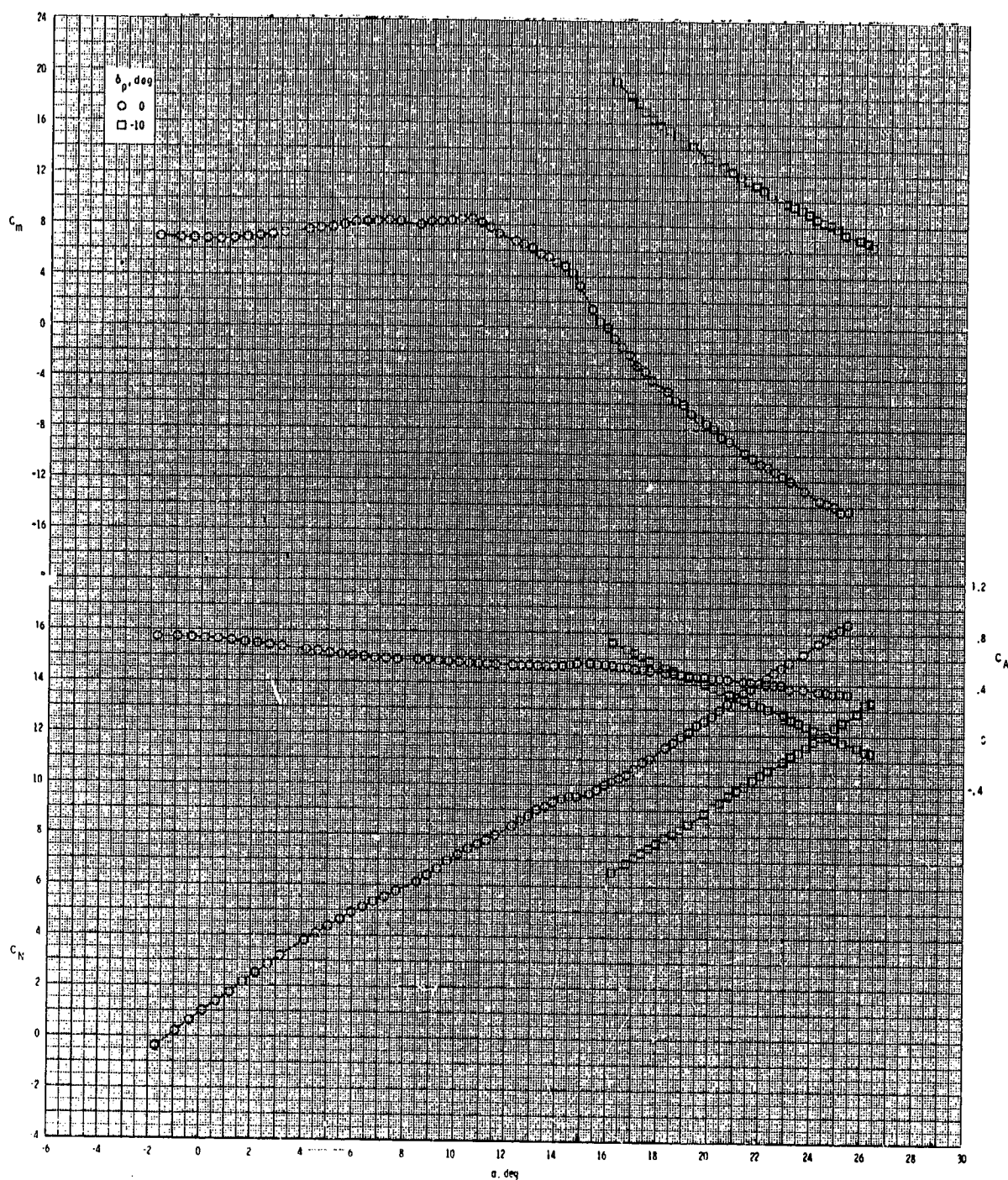
ORIGINAL PAGE IS
OF POOR QUALITY



(a) Concluded.

Figure 35.- Continued.

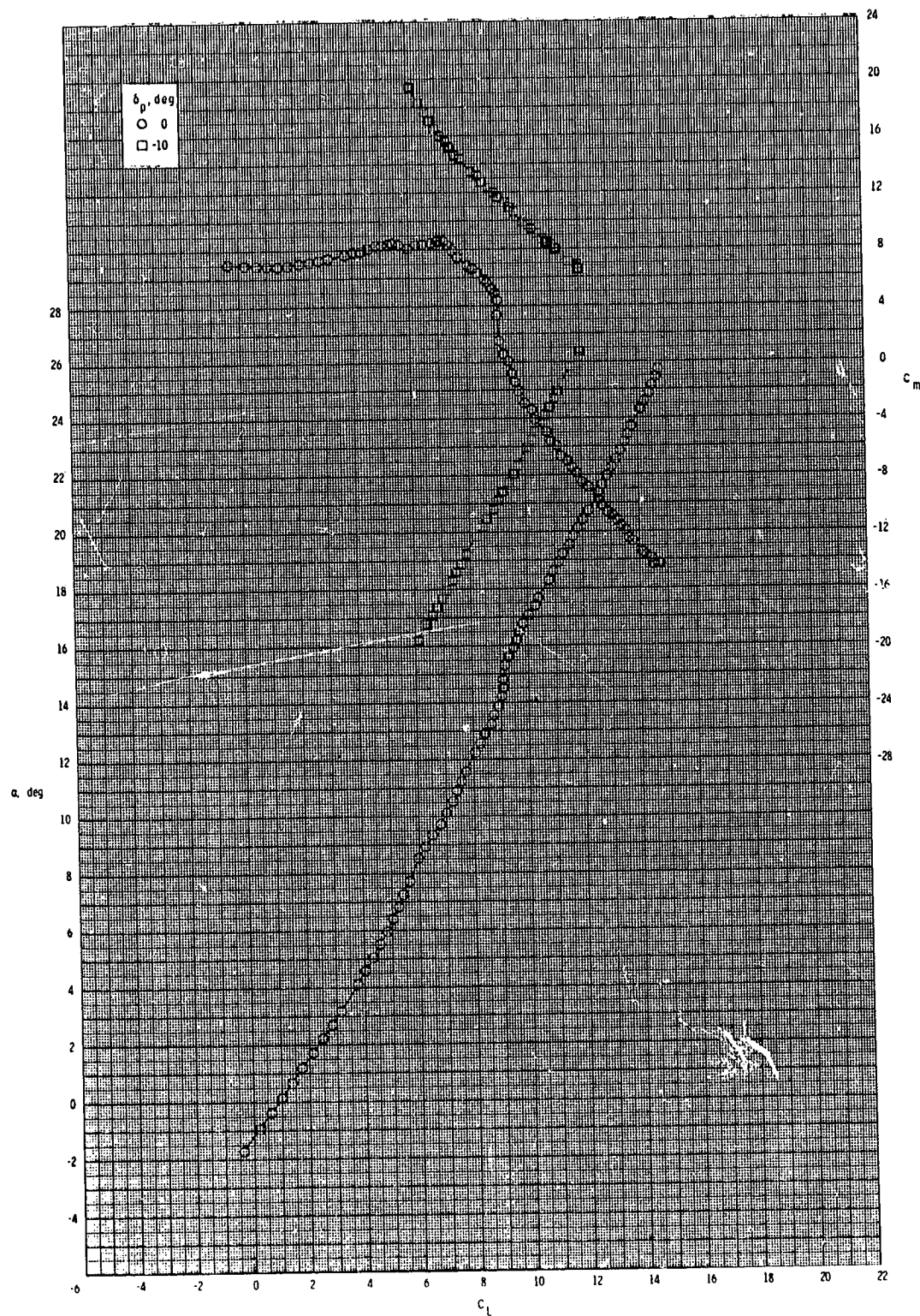
ORIGINAL PAGE IS
OF POOR QUALITY



(b) $M = 0.80$.

Figure 35.- Continued.

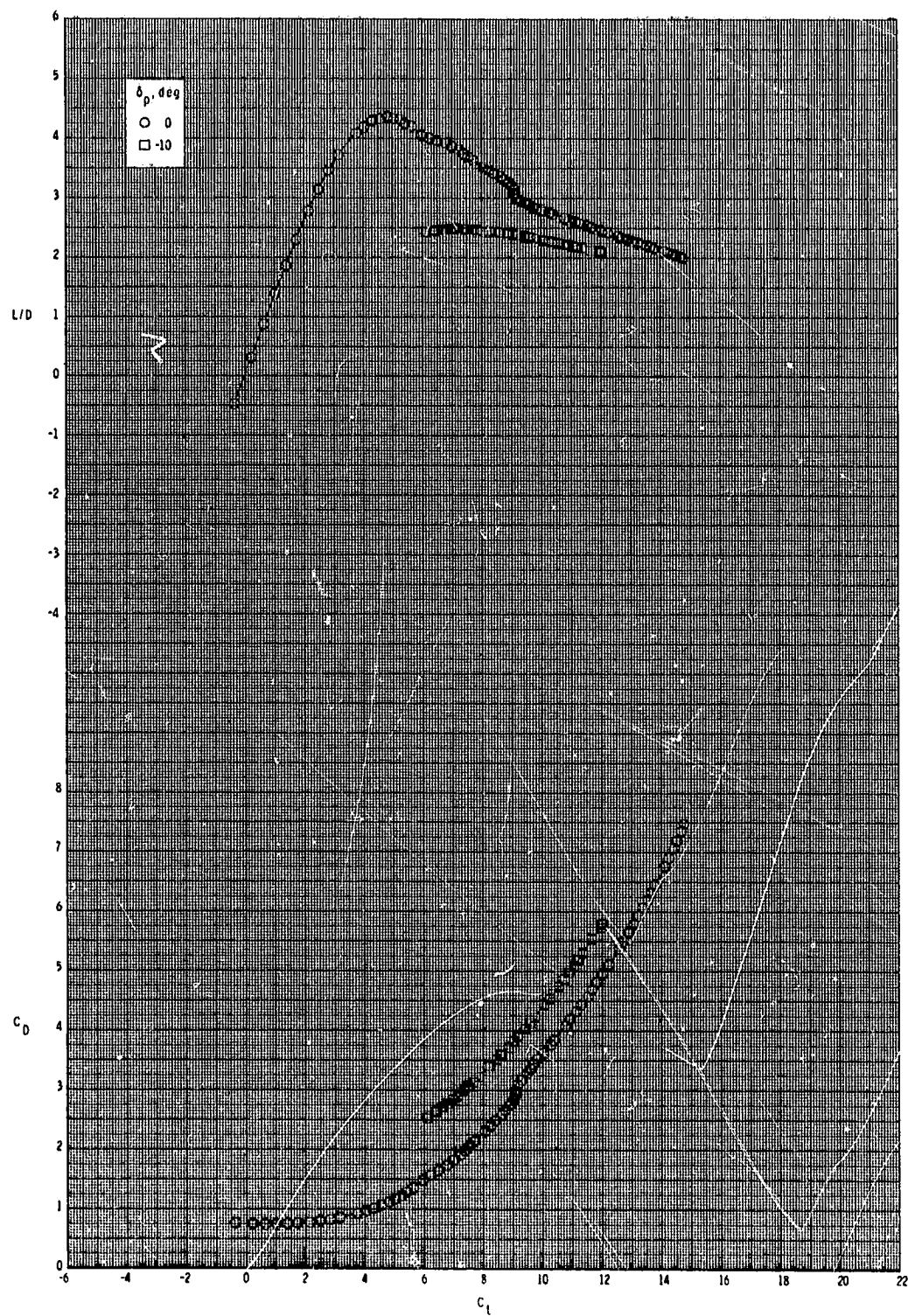
ORIGINAL PAGE IS
OF POOR QUALITY



(h) Continued.

Figure 35.- Continued.

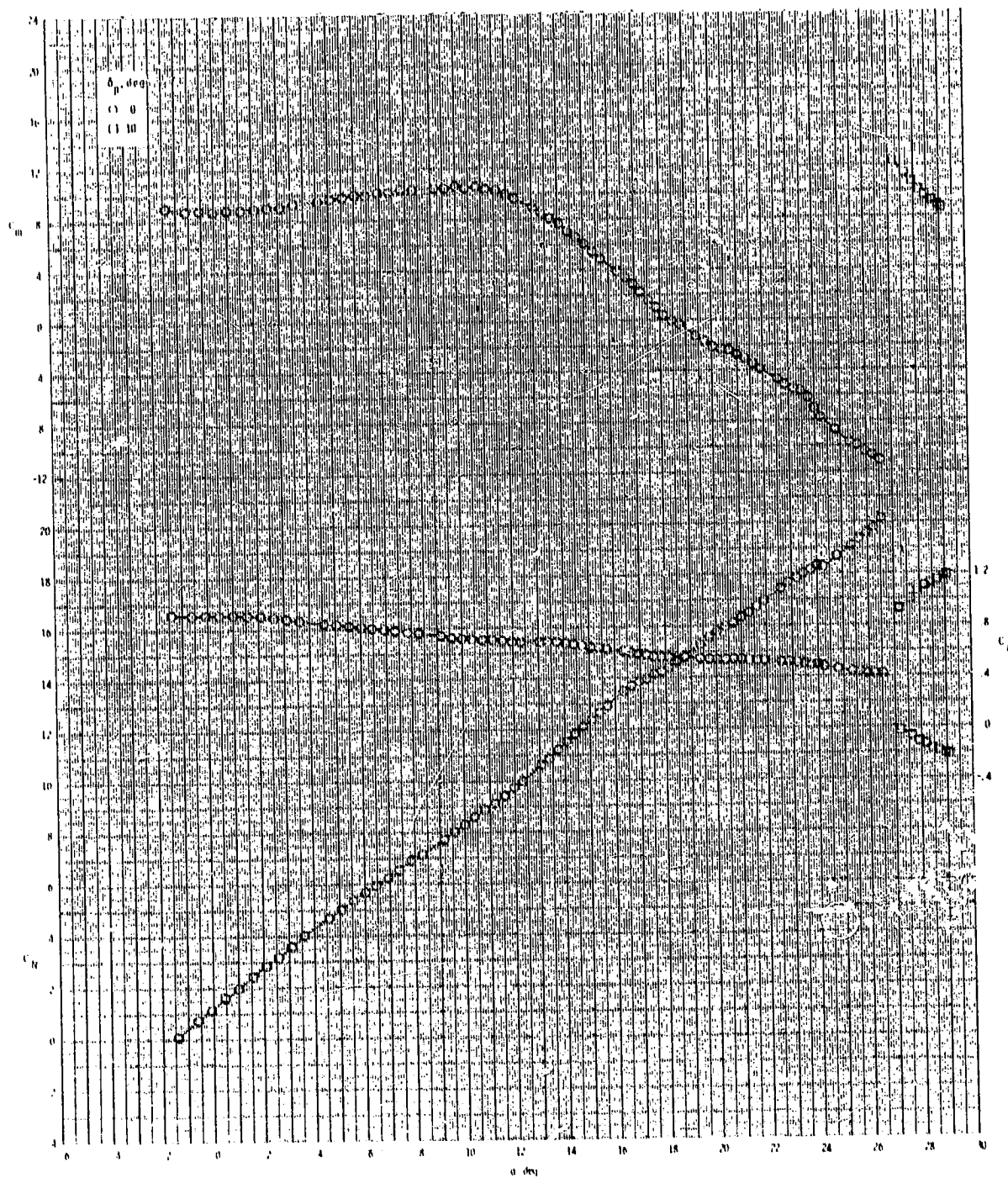
ORIGINAL PAGE IS
OF POOR QUALITY



(b) Concluded.

Figure 35.- Continued.

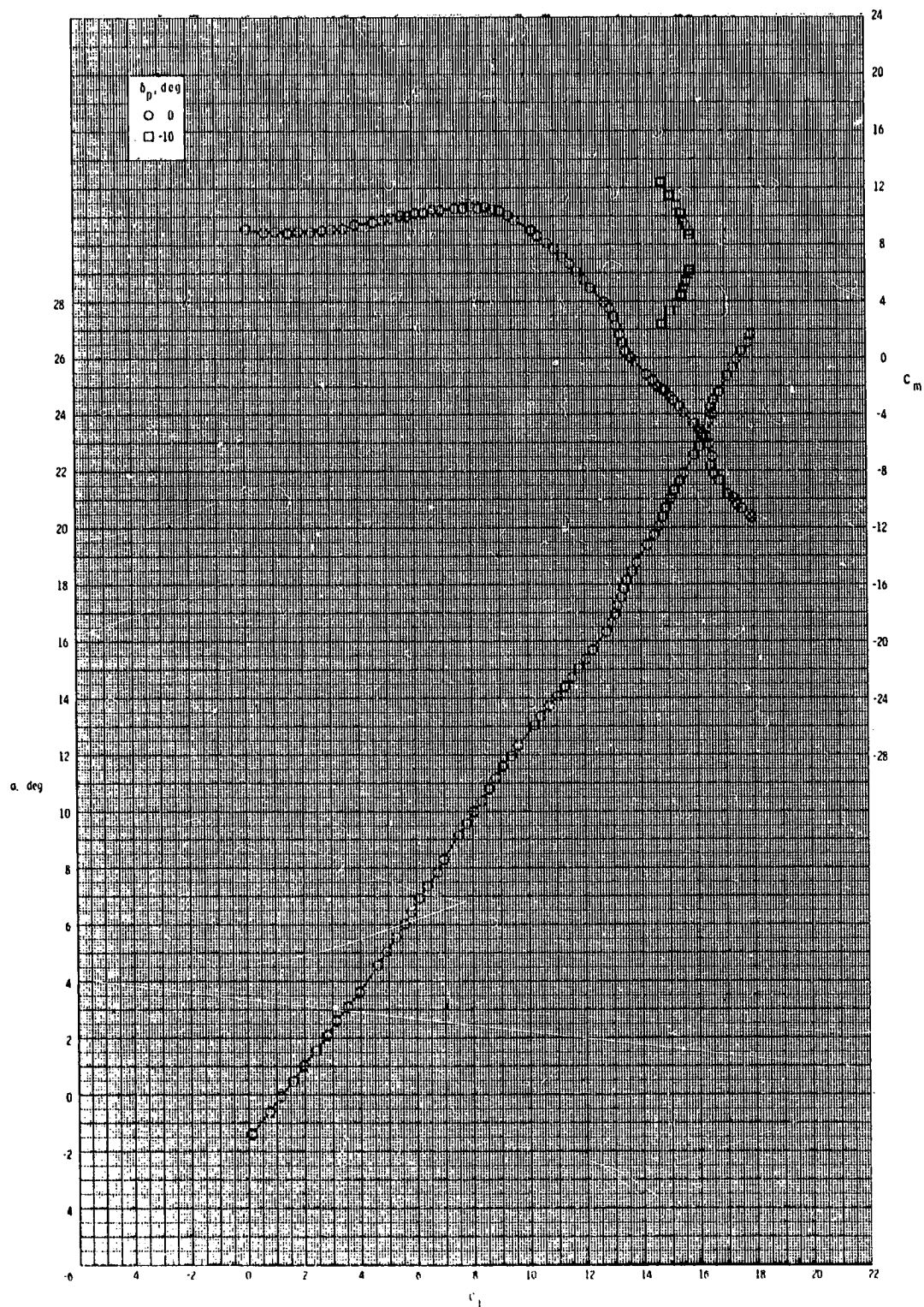
ORIGINAL PAGE IS
OF POOR QUALITY



(c) $M = 0.95$.

Figure 35.- Continued.

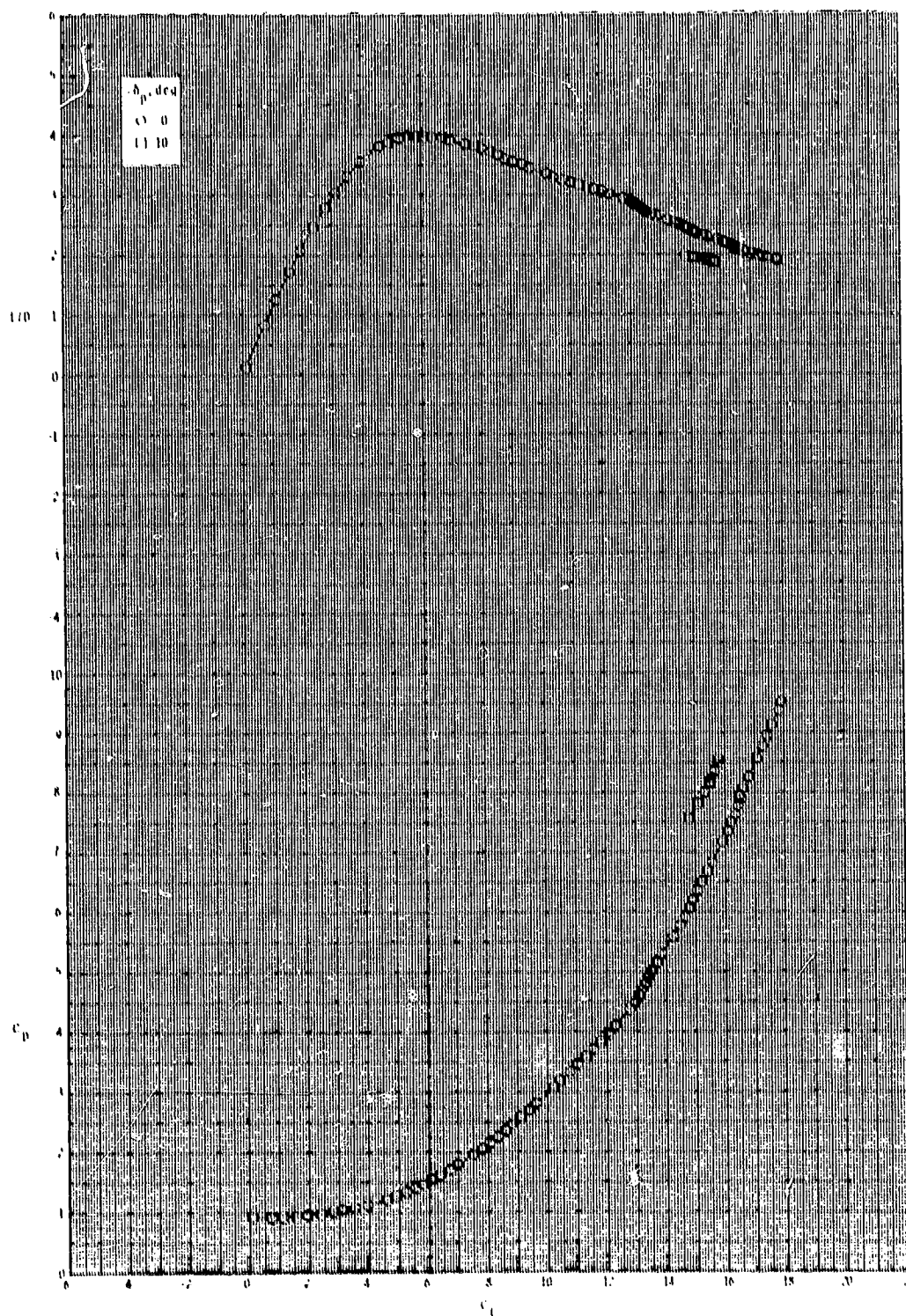
ORIGINAL PAGE IS
OF POOR QUALITY



(c) Continued.

Figure 35.- Continued.

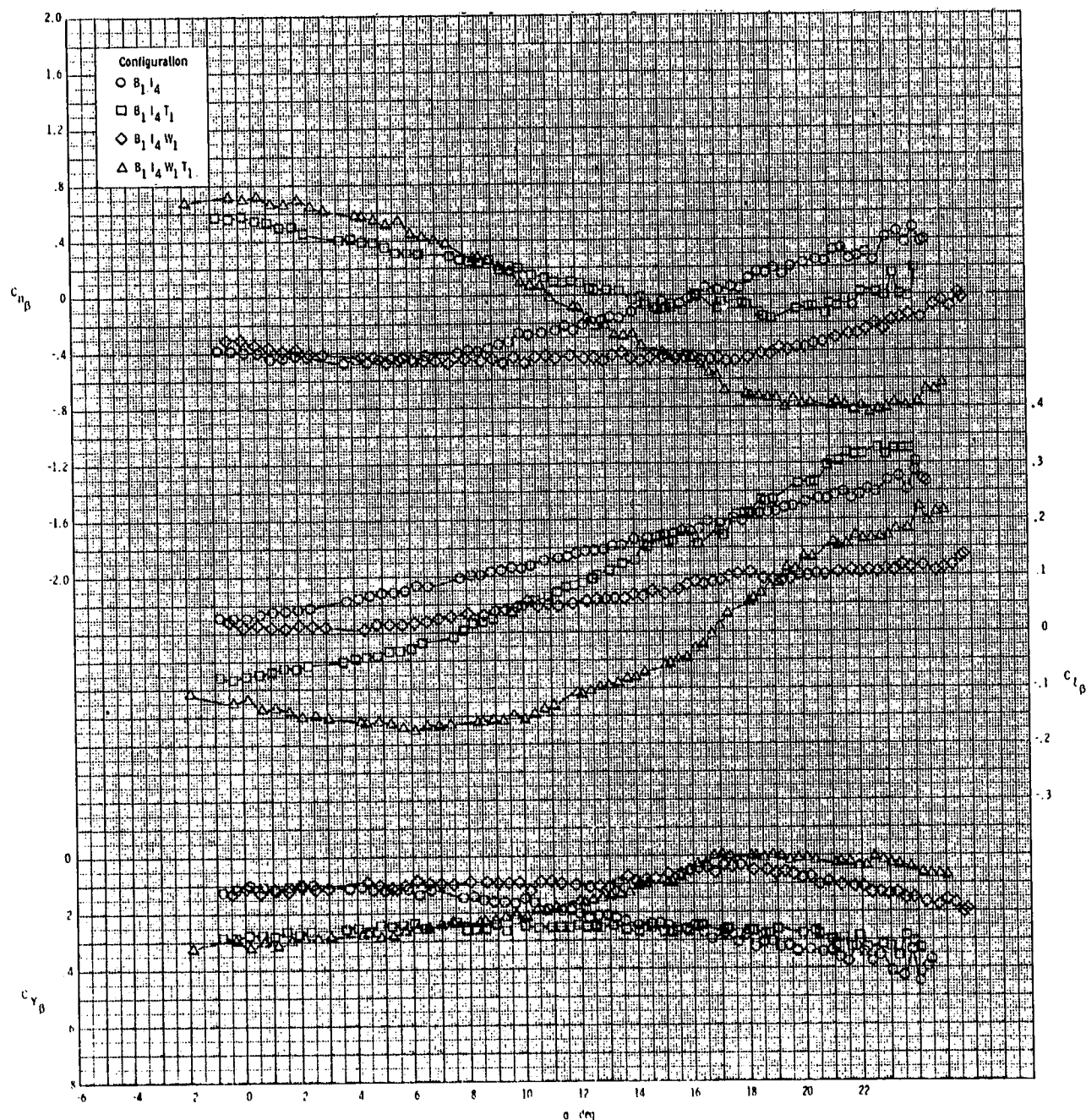
ORIGINAL PAGE IS
OF POOR QUALITY



(c) Concluded.

Figure 35.- Concluded.

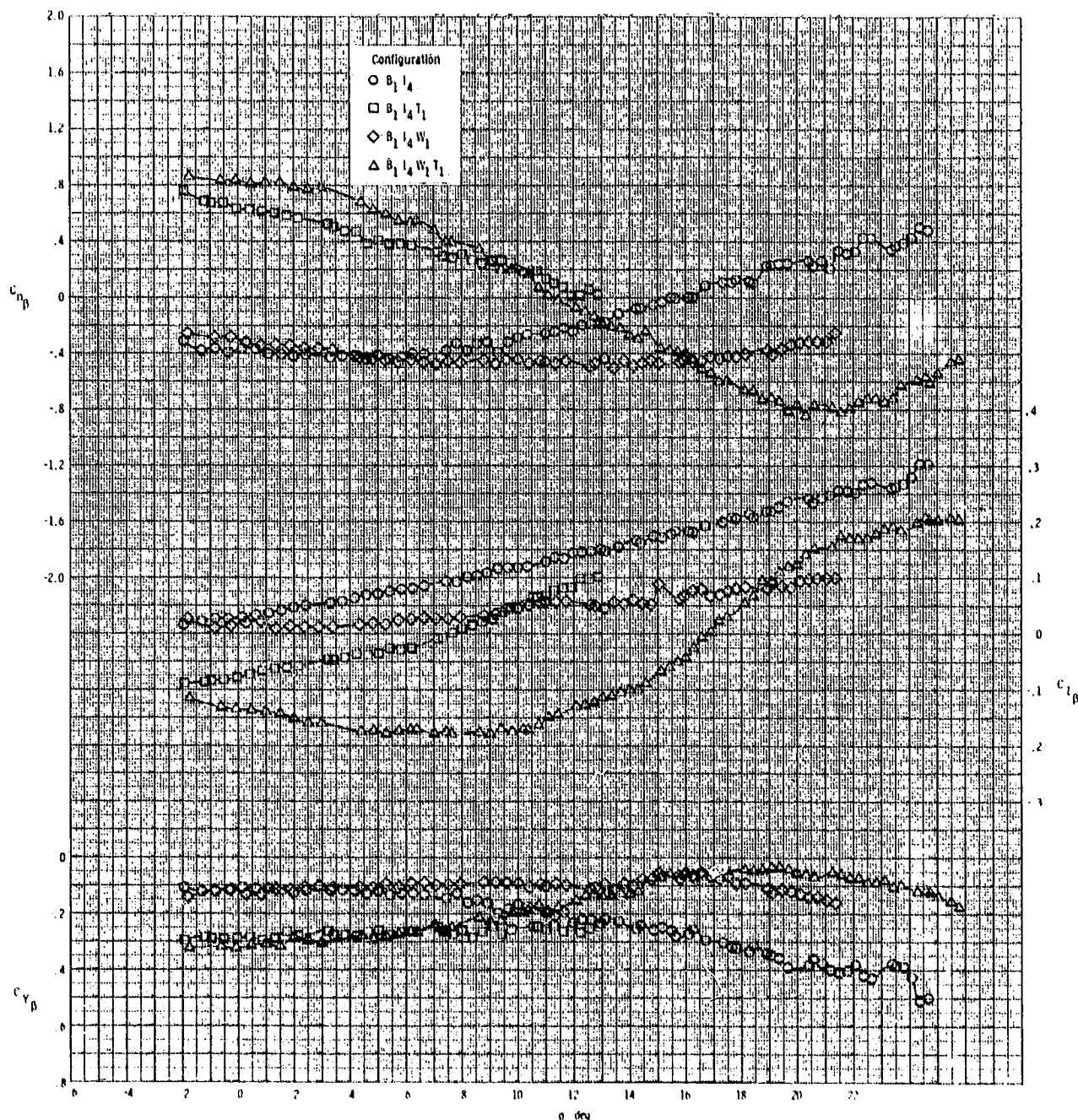
ORIGINAL PAGE IS
OF POOR QUALITY



(a) $M = 0.60$.

Figure 36.- Effect of various model components on lateral-directional stability for axisymmetric inlet with T_1 and internal duct closed.

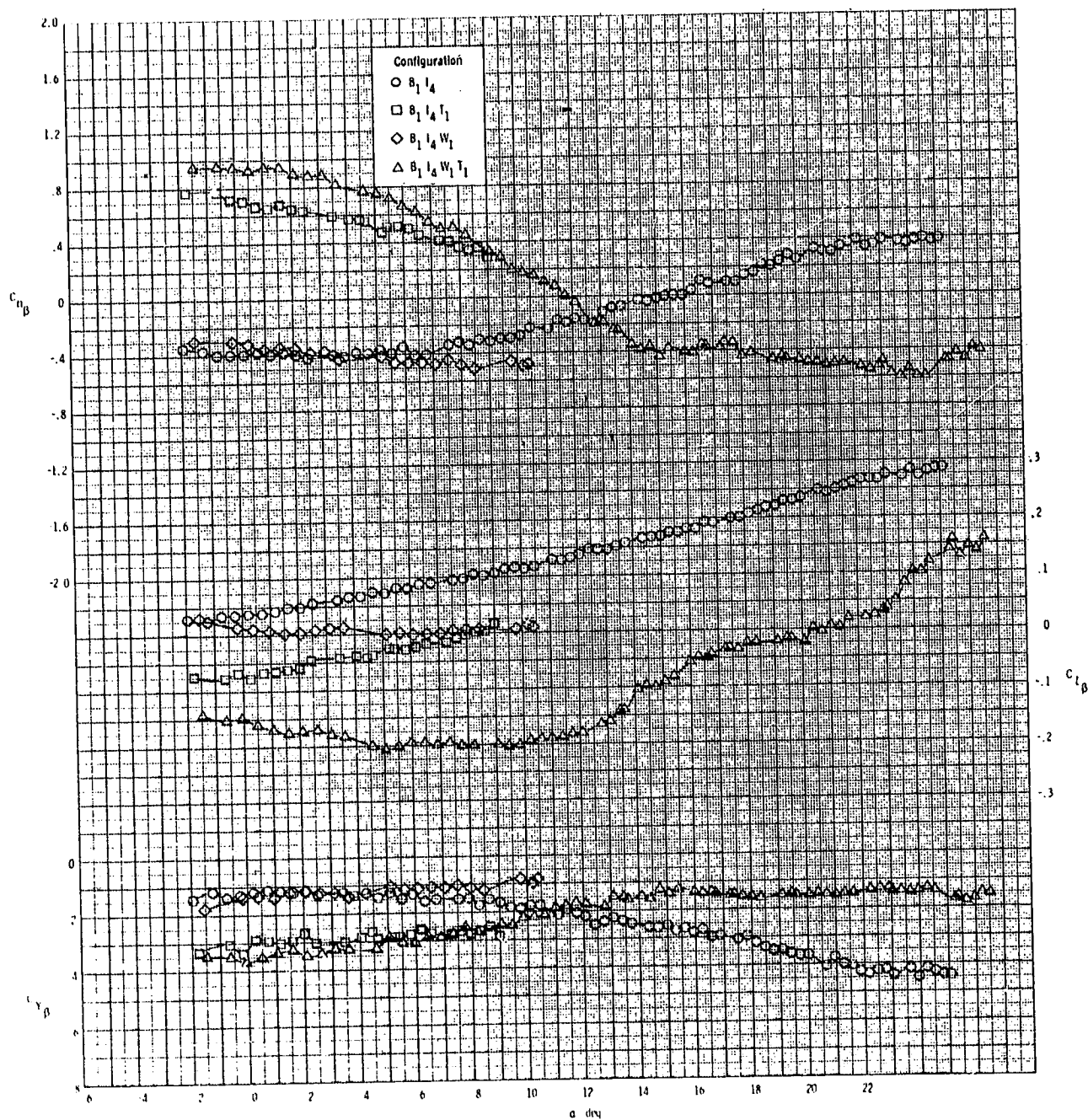
ORIGINAL PAGE IS
OF POOR QUALITY



(b) $M = 0.80$.

Figure 36.- Continued.

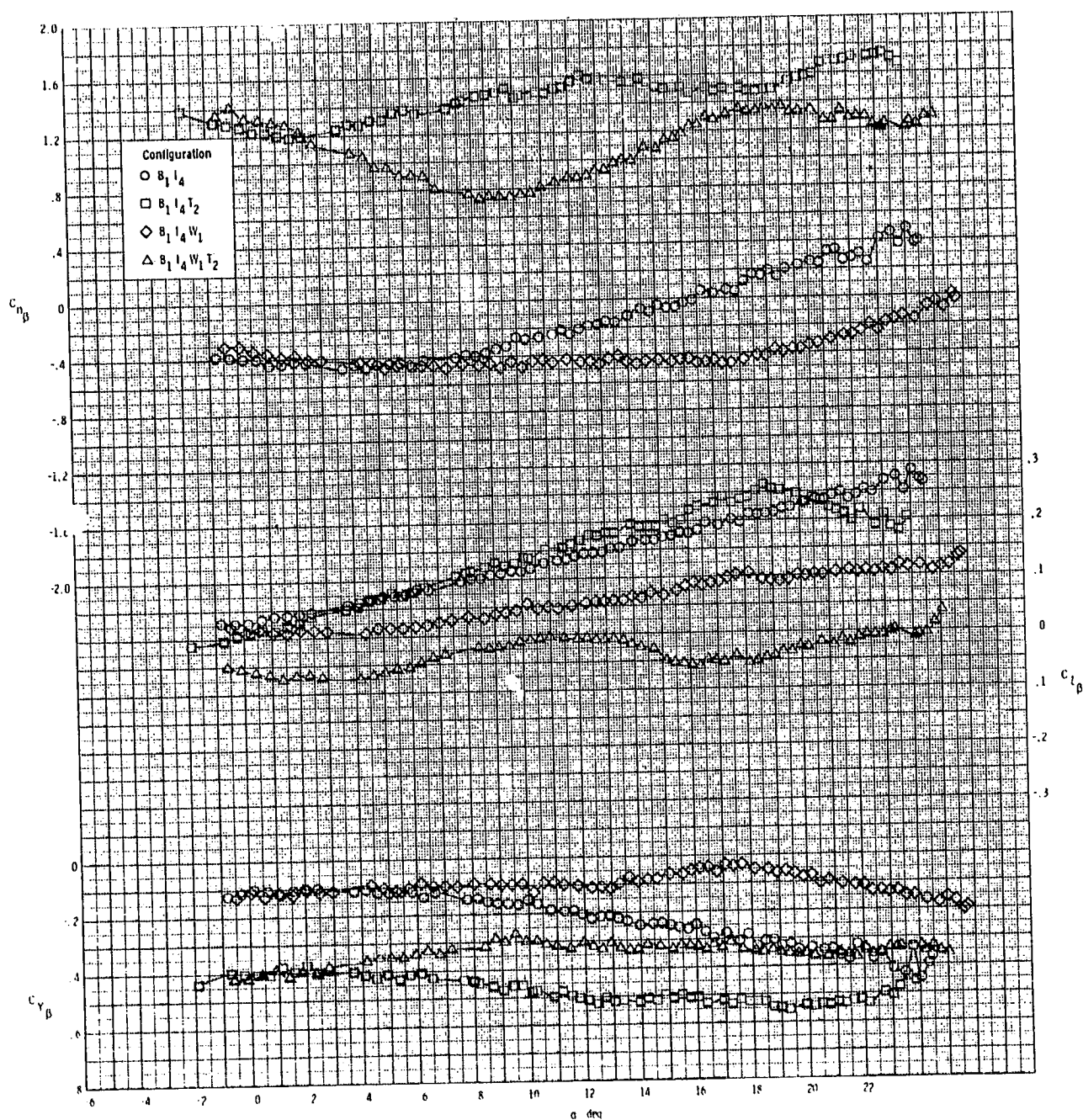
ORIGINAL PAGE IS
OF POOR QUALITY



(c) $M = 0.95$.

Figure 36.- Concluded.

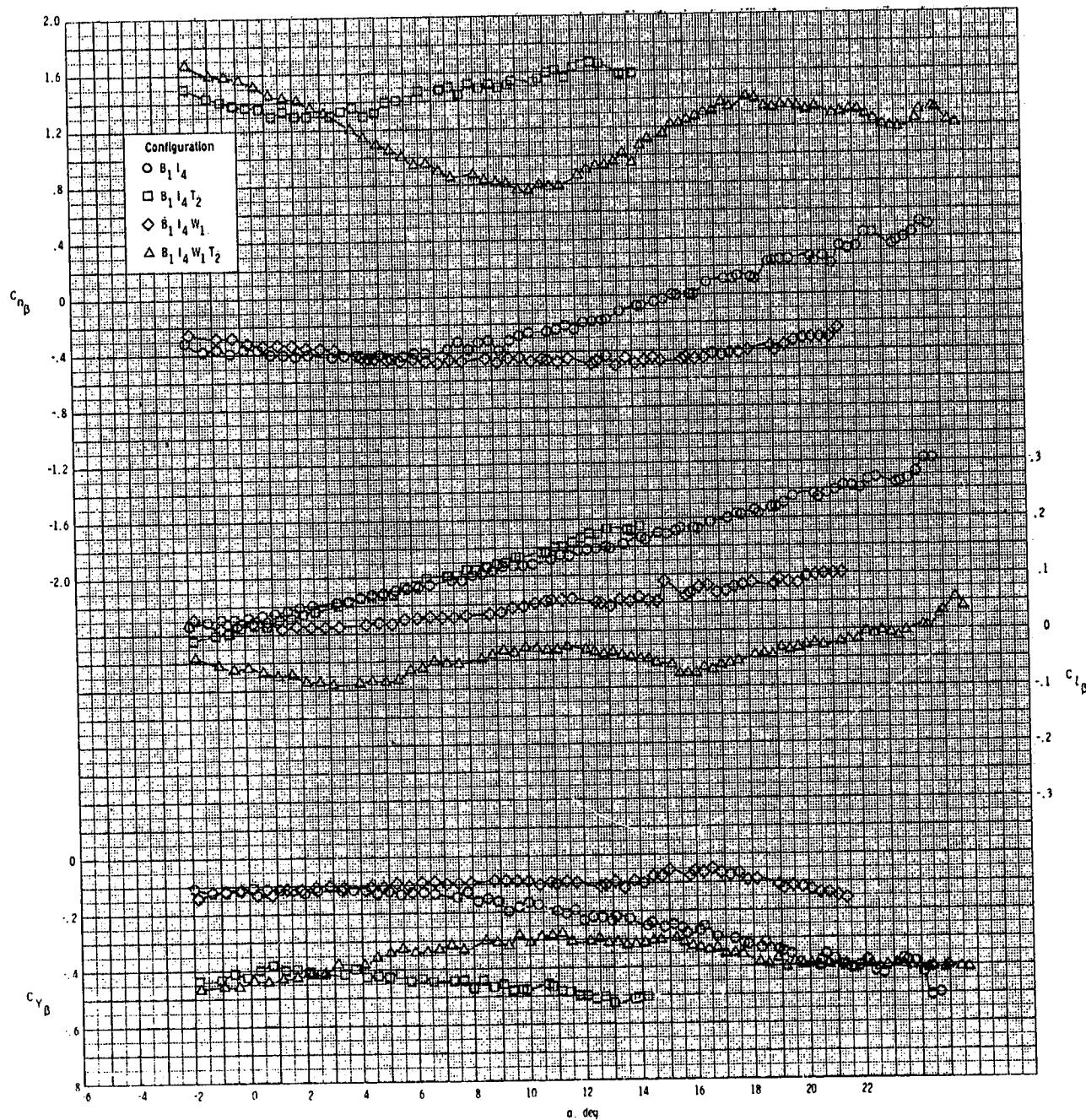
ORIGINAL PAGE IS
OF POOR QUALITY



(a) $M = 0.60$.

Figure 37.- Effect of various model components on lateral-directional stability for axisymmetric inlet with T_2 and internal duct closed.

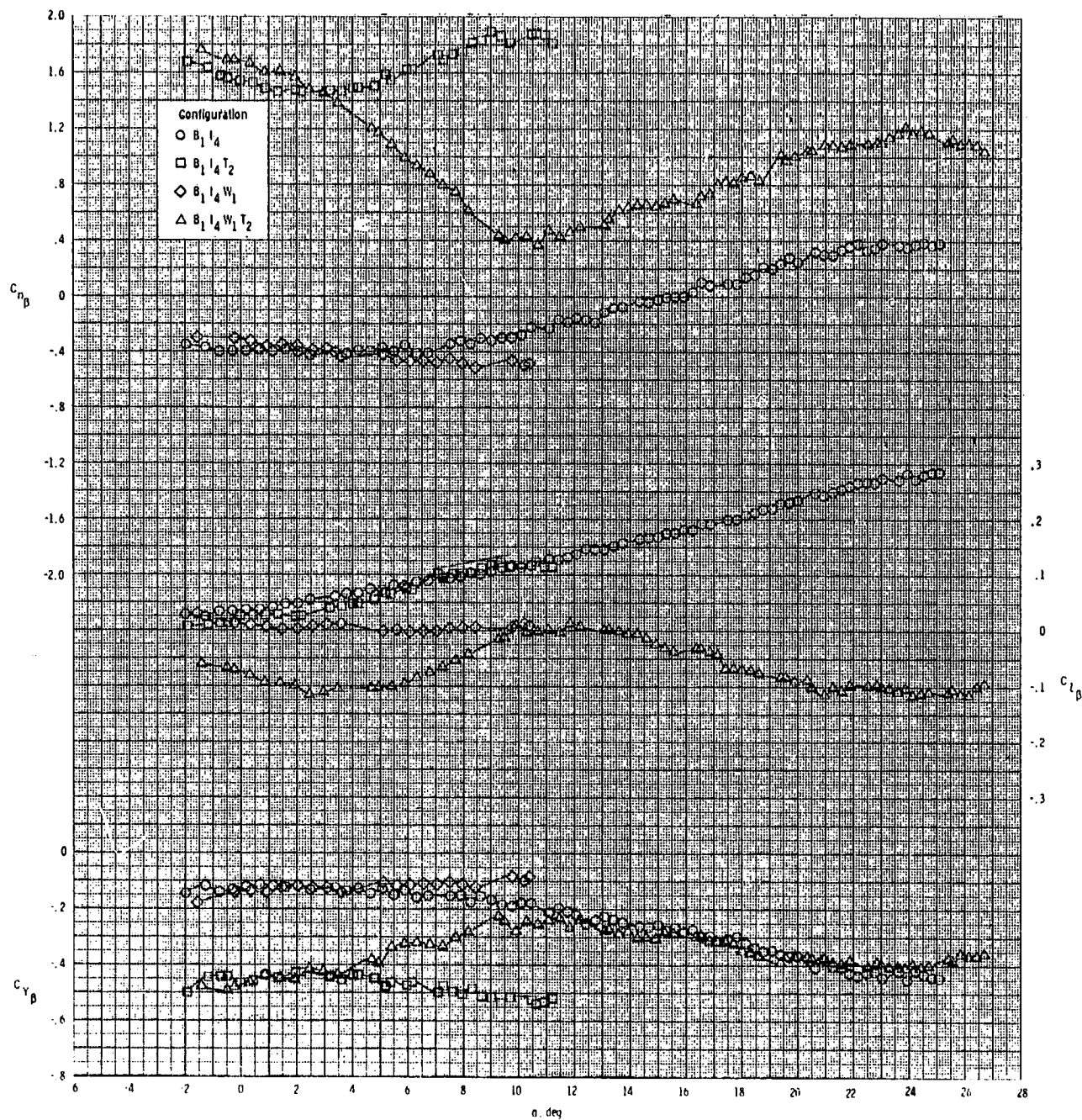
ORIGINAL PAGE IS
OF POOR QUALITY



(b) $M = 0.80$.

Figure 37.- Continued.

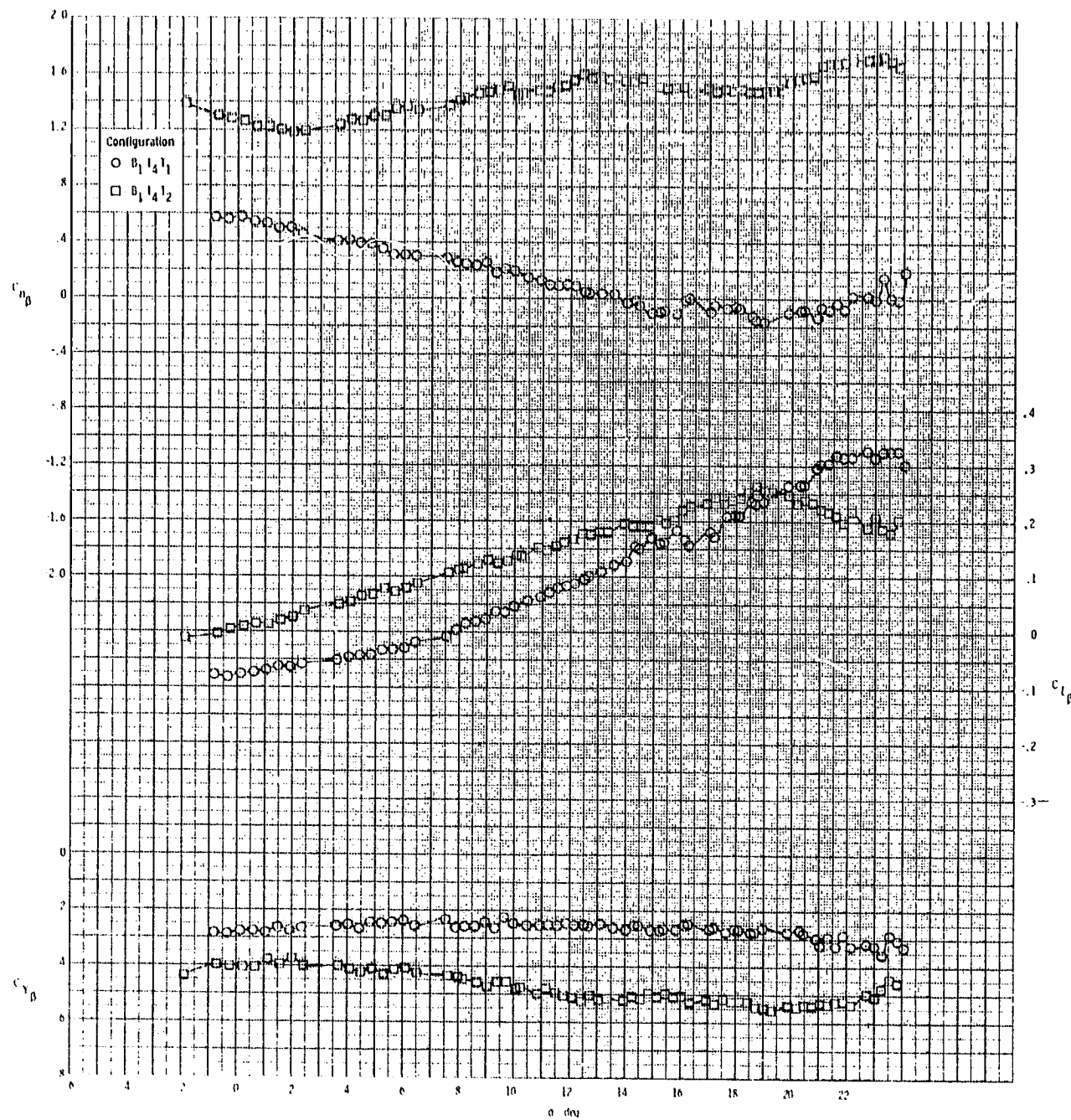
ORIGINAL PAGE IS
OF POOR QUALITY



(c) $M = 0.95$.

Figure 37.- Concluded.

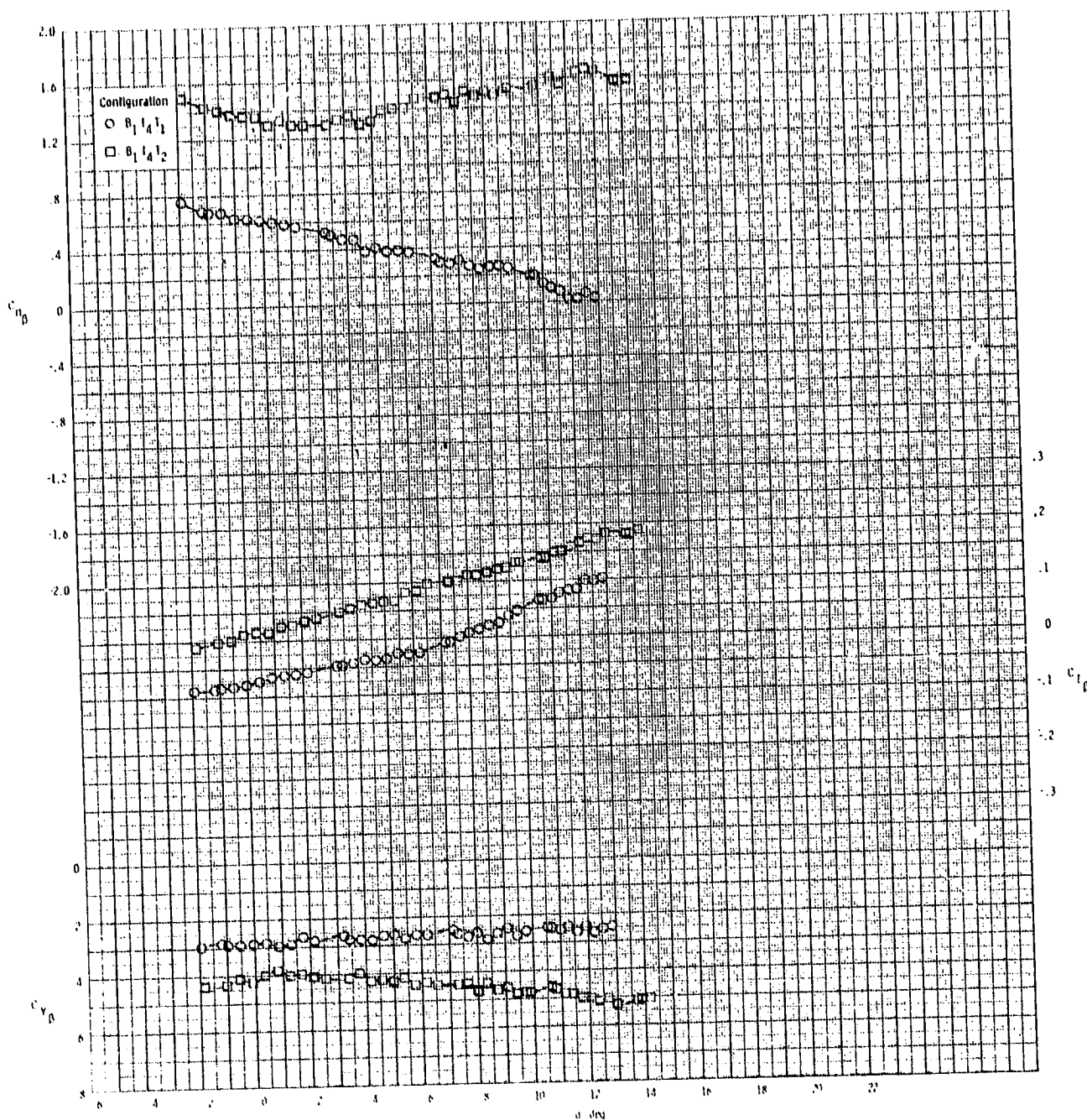
ORIGINAL PAGE IS
OF POOR QUALITY



(a) $M = 0.60$.

Figure 38.- Effect of tail configuration on lateral-directional stability for axisymmetric inlet with wing off and internal duct closed.

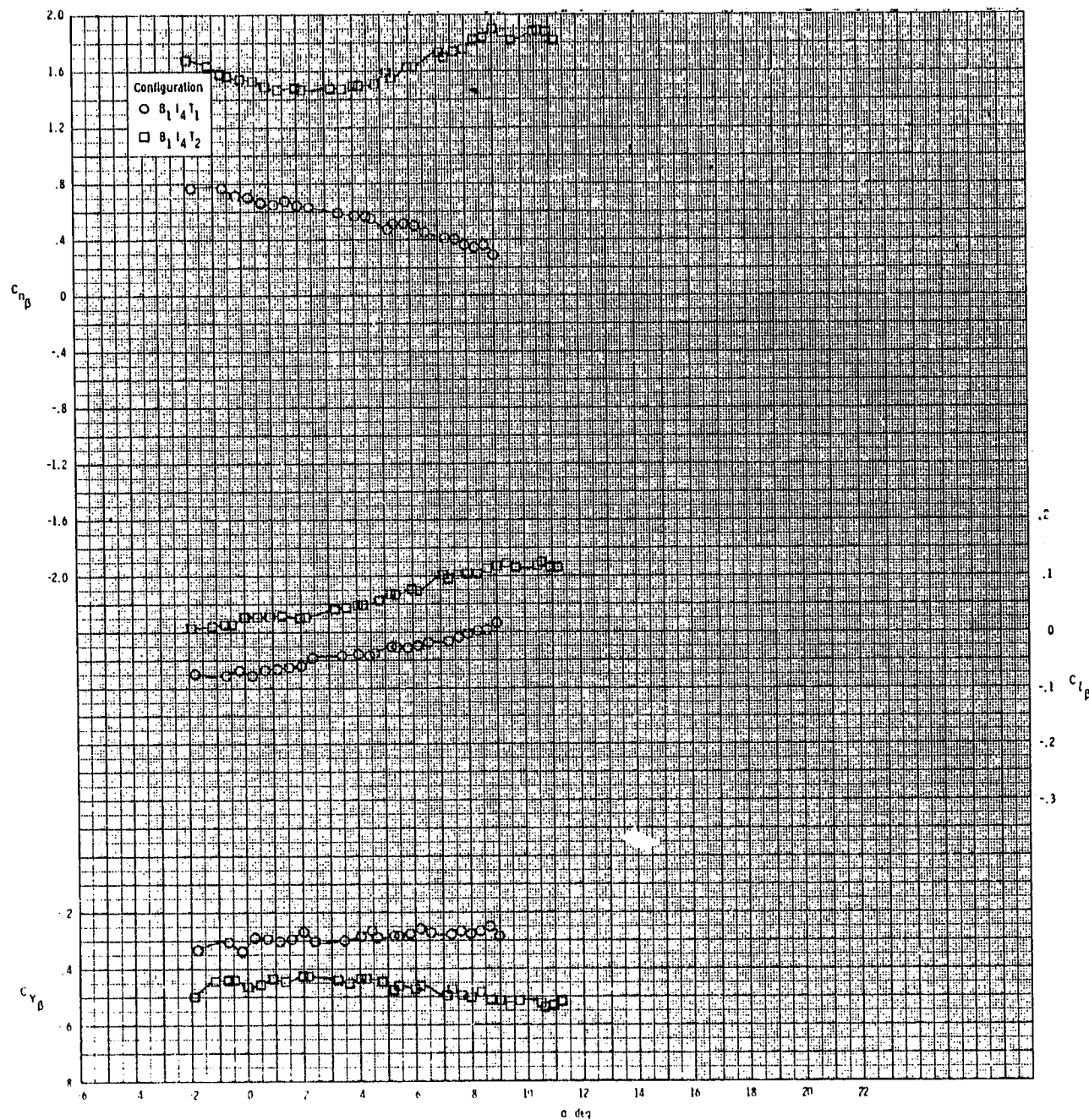
ORIGINAL PAGE IS
OF POOR QUALITY



(b) $M = 0.80$.

Figure 38.- Continued.

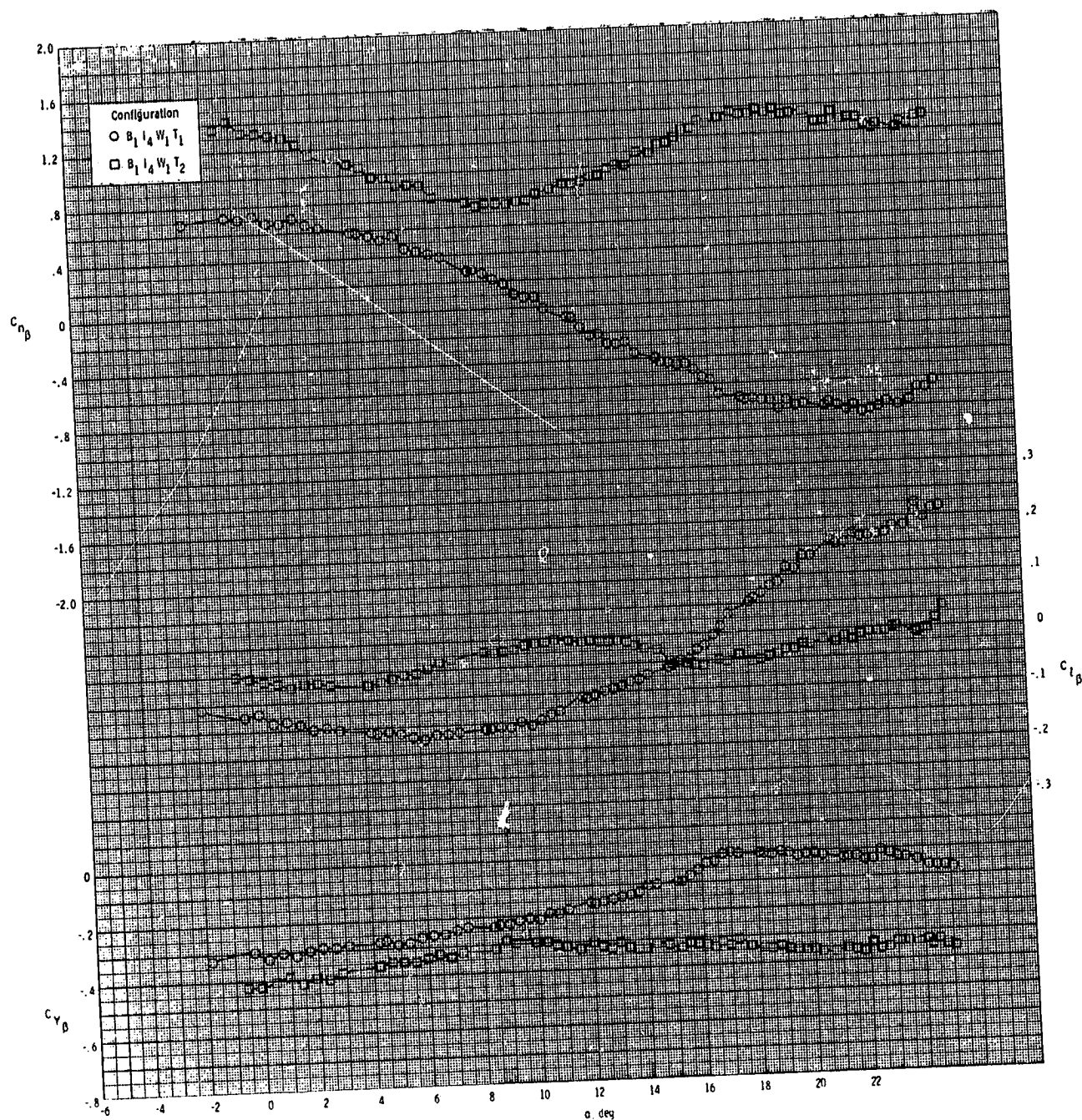
ORIGINAL PAGE IS
OF POOR QUALITY



(c) $M = 0.95$.

Figure 38.- Concluded.

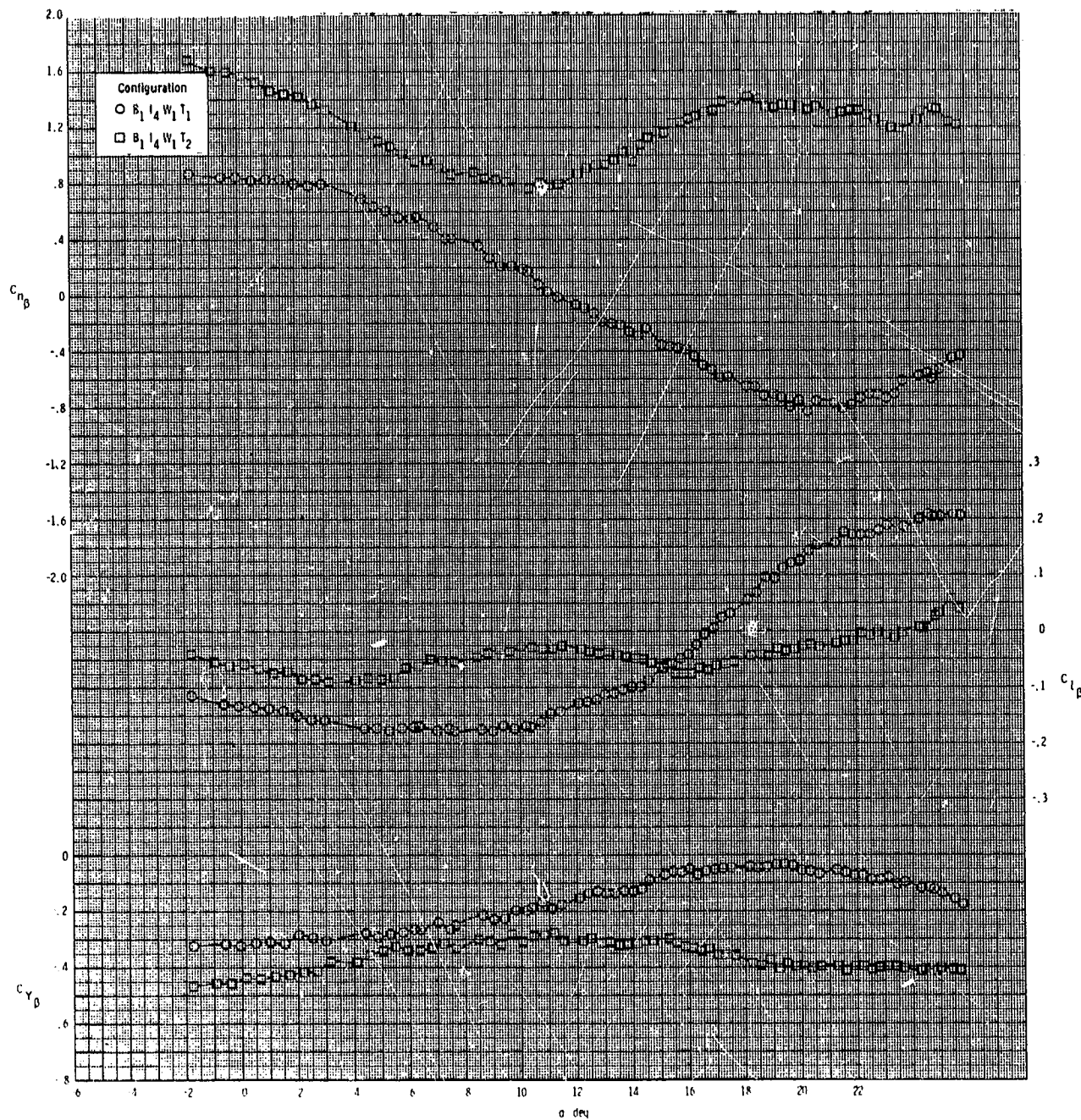
ORIGINAL PAGE IS
OF POOR QUALITY



(a) $M = 0.60$.

Figure 39.- Effect of tail configuration on lateral-directional stability for axisymmetric inlet with wing on and internal duct closed.

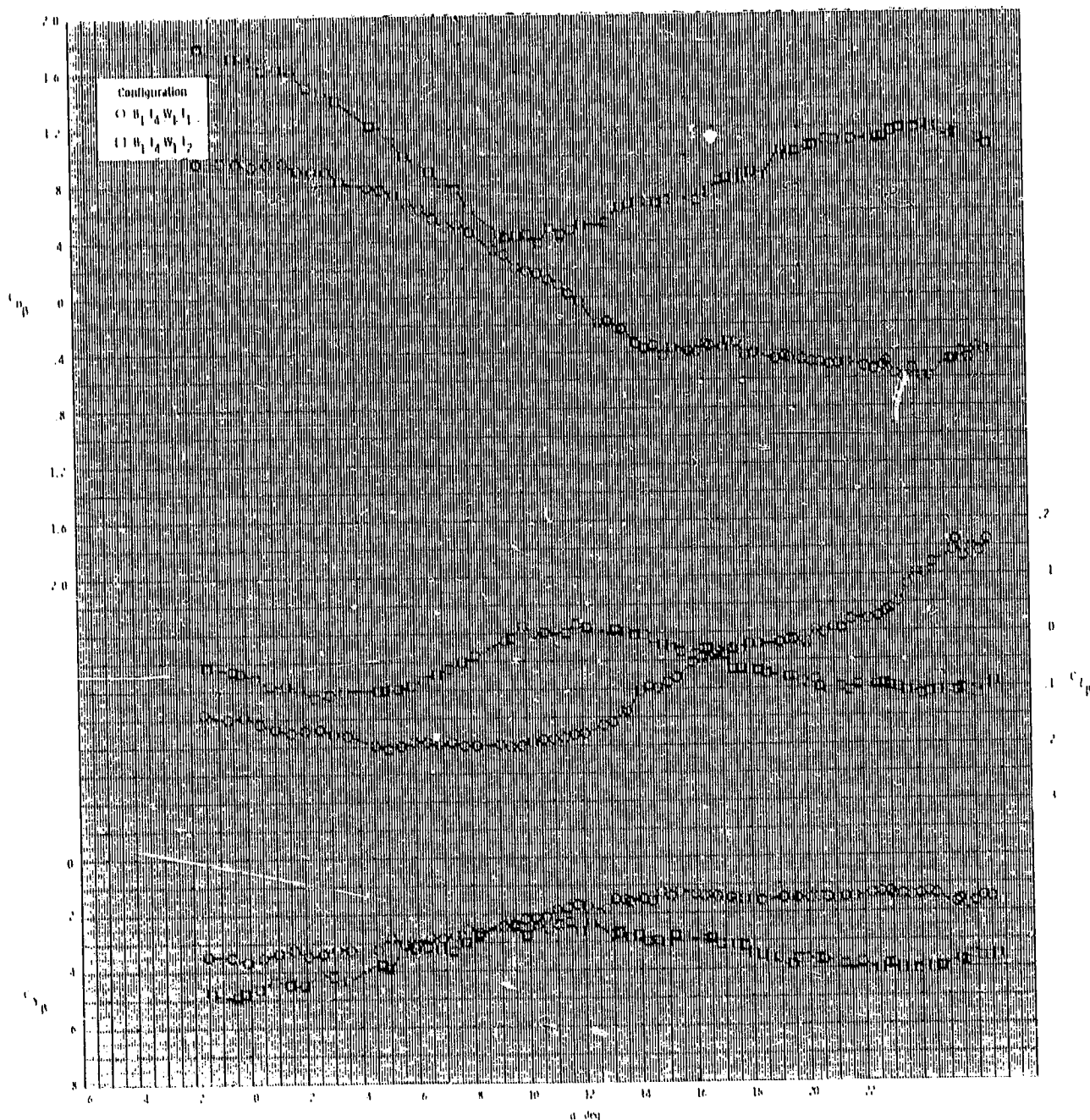
ORIGINAL PAGE IS
OF POOR QUALITY



(b) $M = 0.80$.

Figure 39.- Continued.

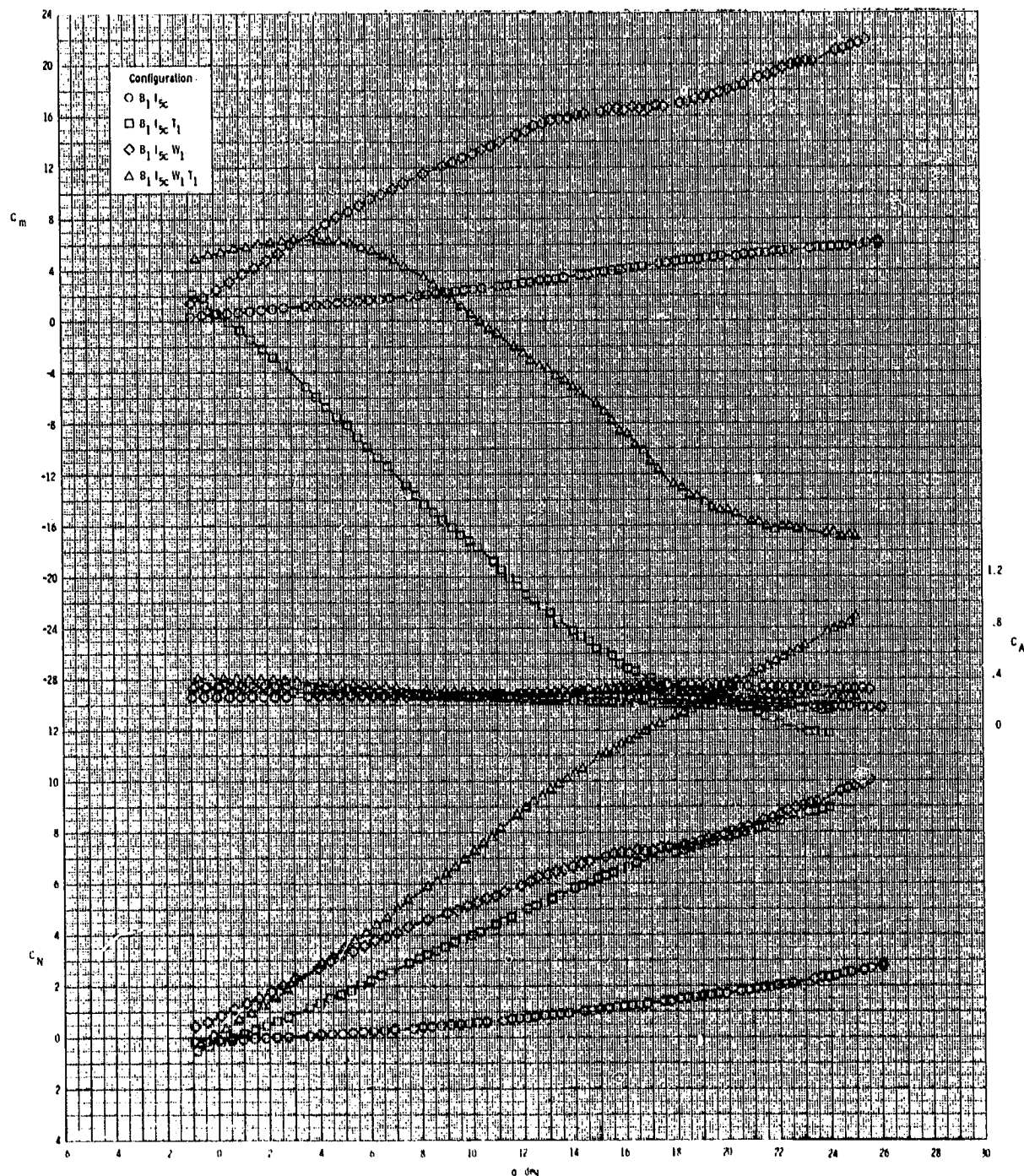
ORIGINAL PAGE IS
OF POOR QUALITY



(c) $M = 0.95$.

Figure 39.- Concluded.

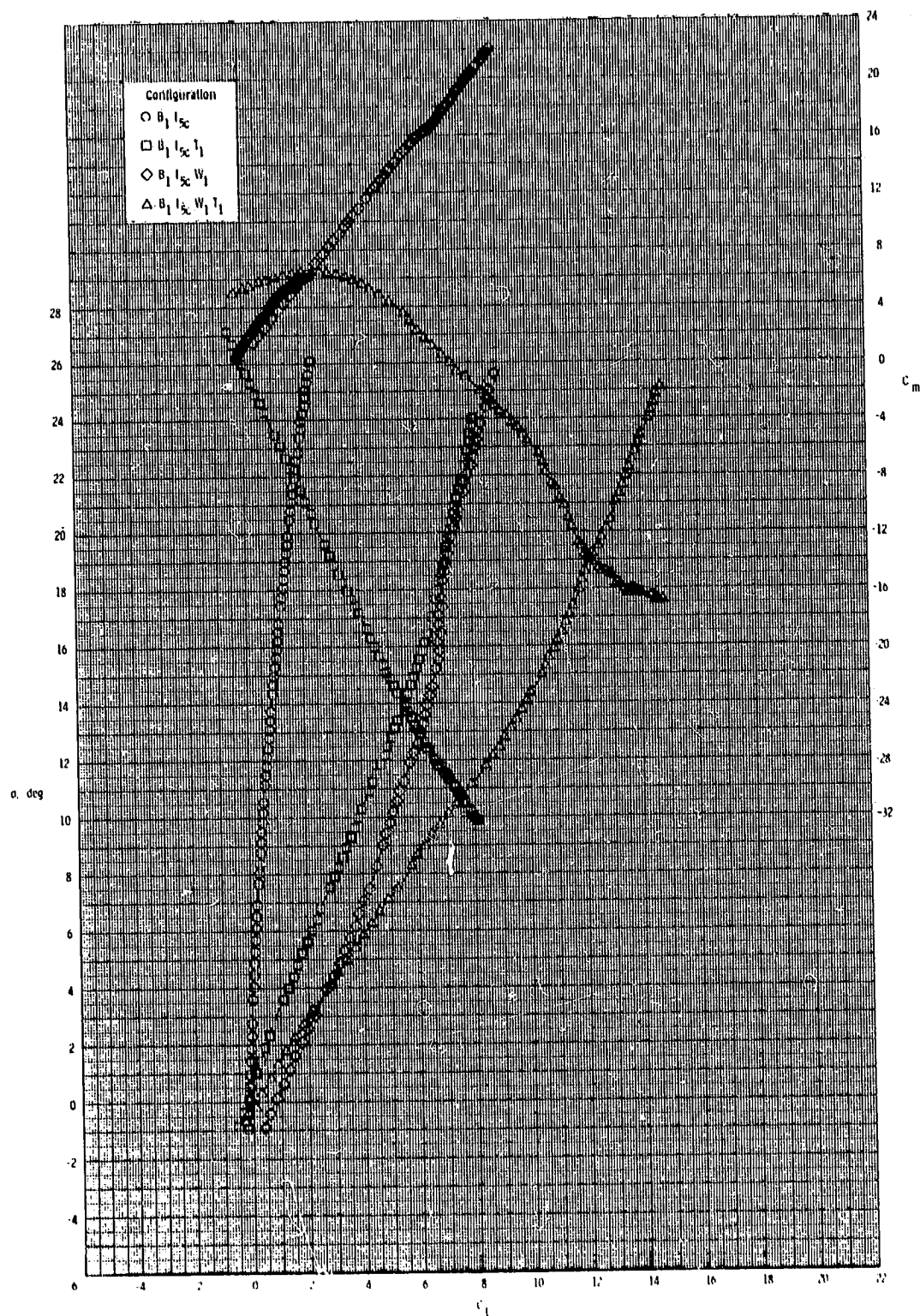
ORIGINAL PAGE IS
OF POOR QUALITY



(a) $M = 0.60$.

Figure 40.- Effect of various model components on longitudinal aerodynamic characteristics for 2-D inlet with T_1 and internal duct closed.

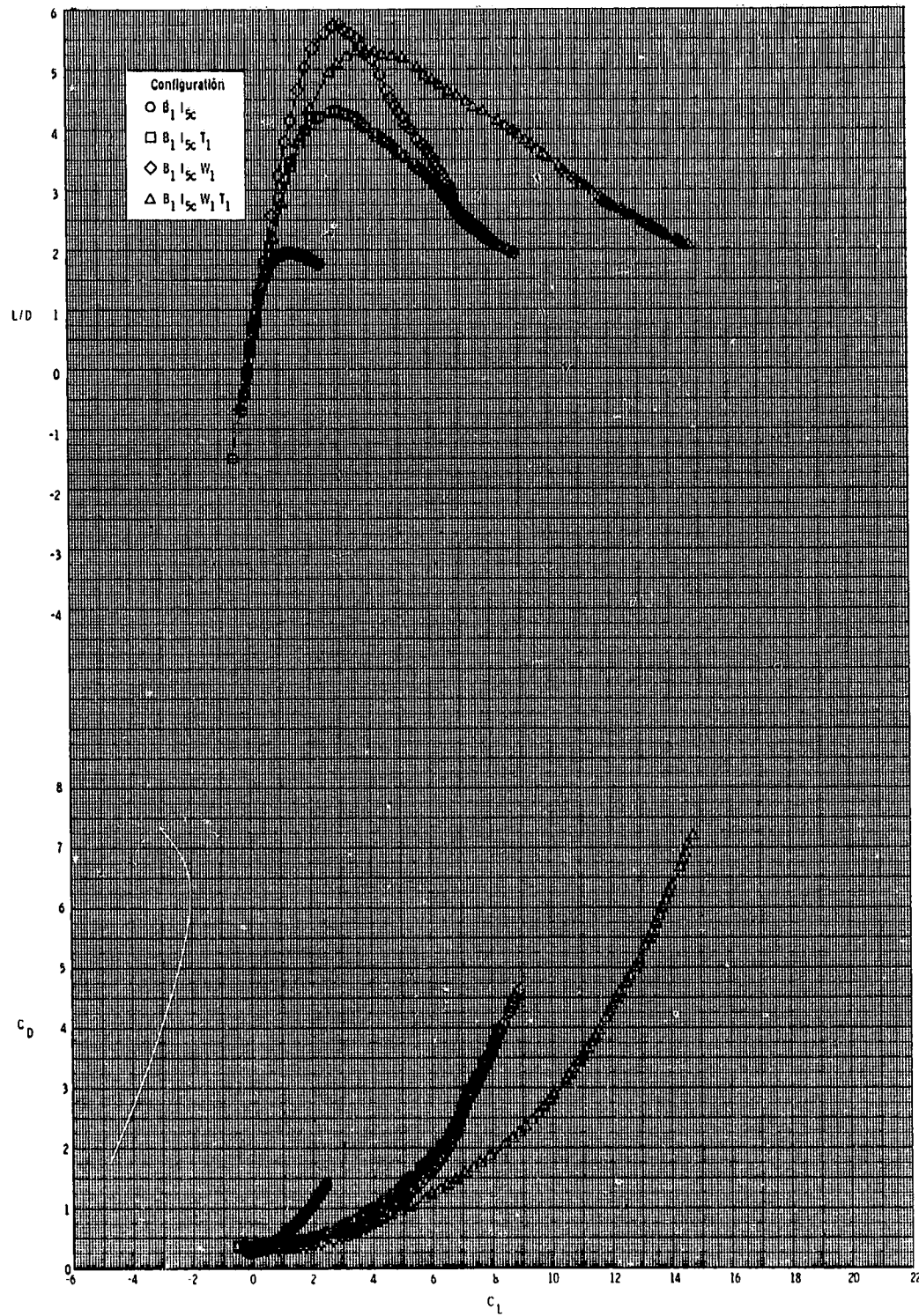
ORIGINAL PAGE IS
OF POOR QUALITY.



(a) Continued.

Figure 40.- Continued.

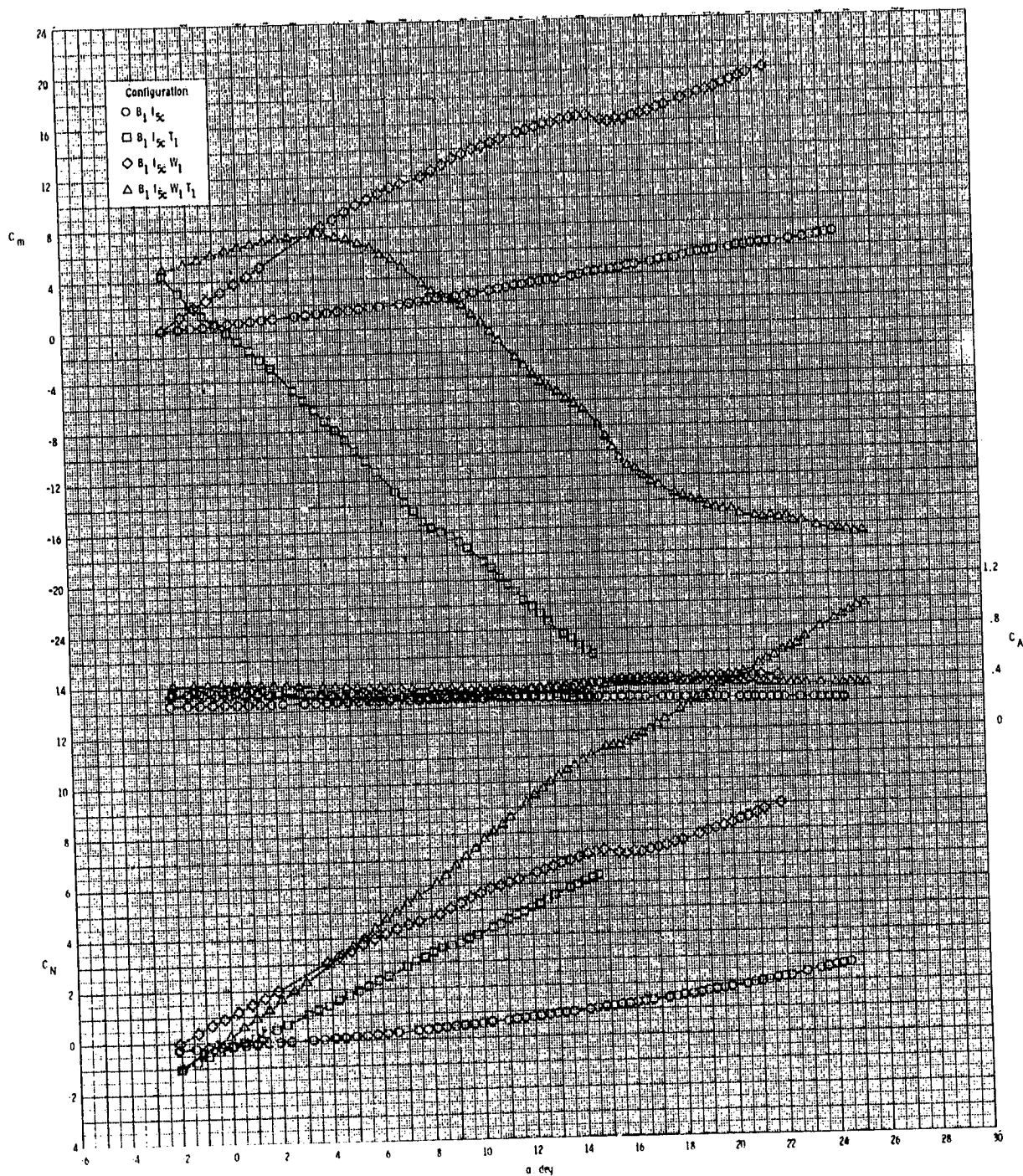
ORIGINAL PAGE IS
OF POOR QUALITY



(a) Concluded.

Figure 40.- Continued.

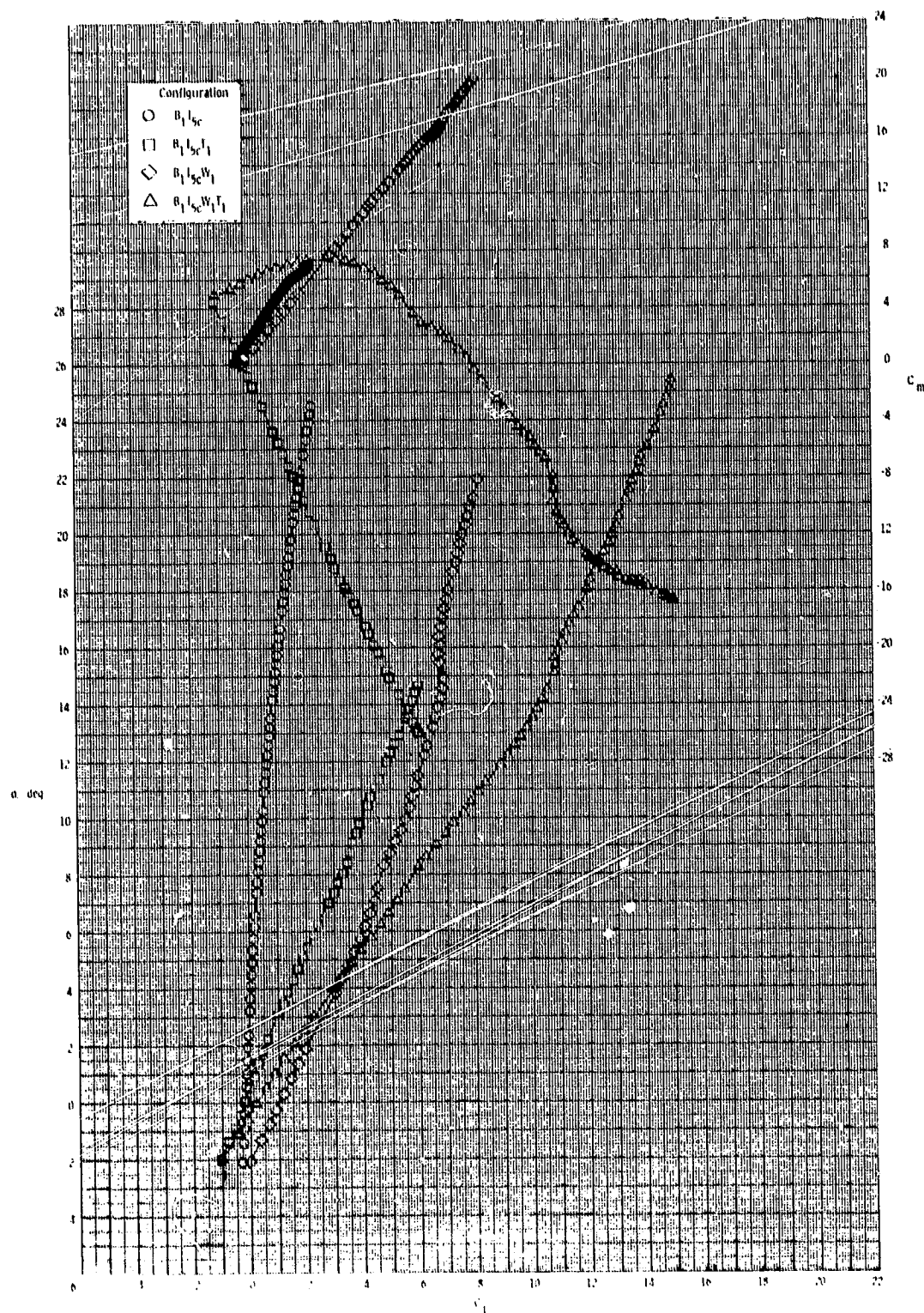
ORIGINAL PAGE IS
OF POOR QUALITY



(b) $M = 0.80$.

Figure 40.- Continued.

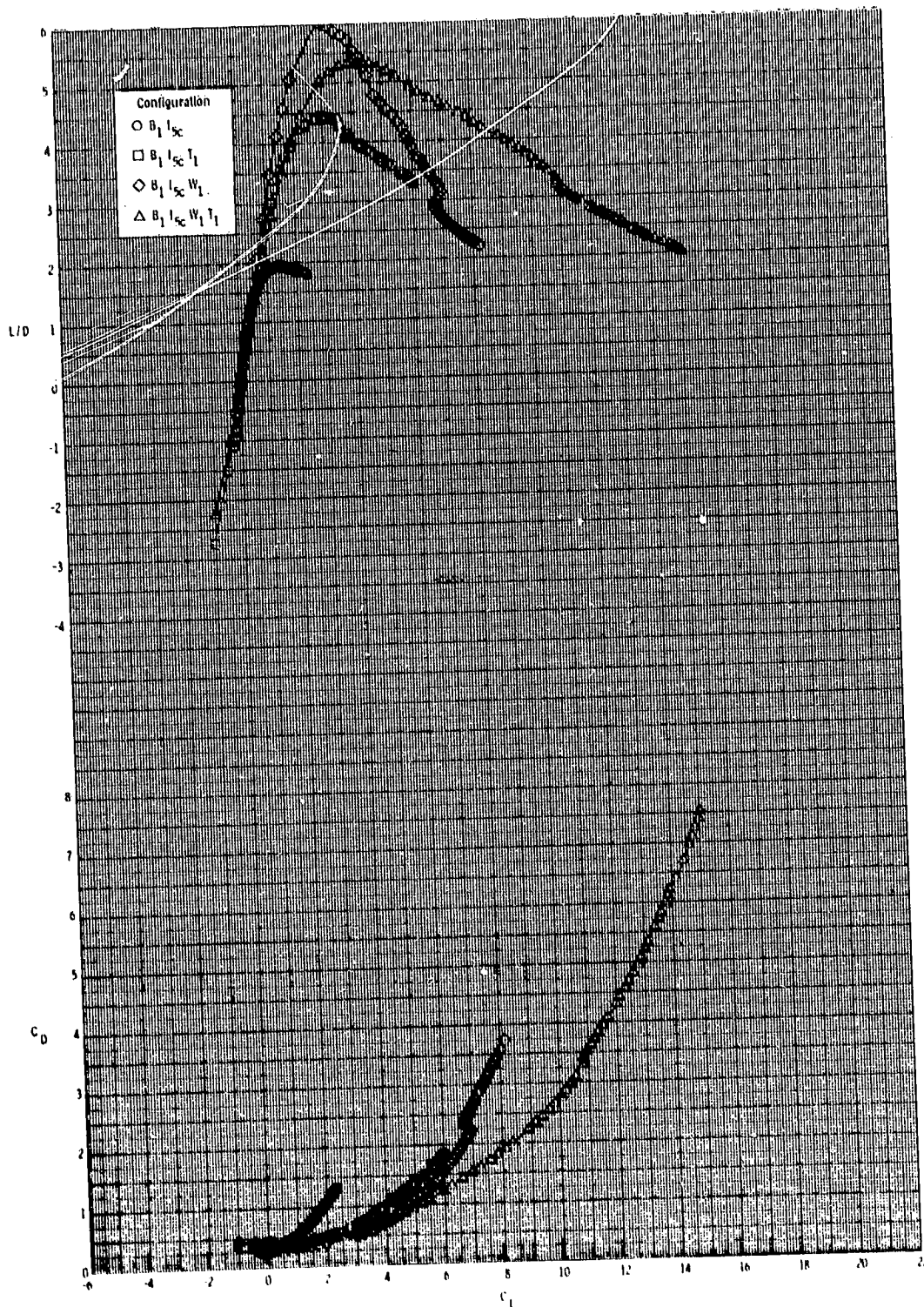
ORIGINAL PAGE IS
OF POOR QUALITY



(b) Continued.

Figure 40.- Continued.

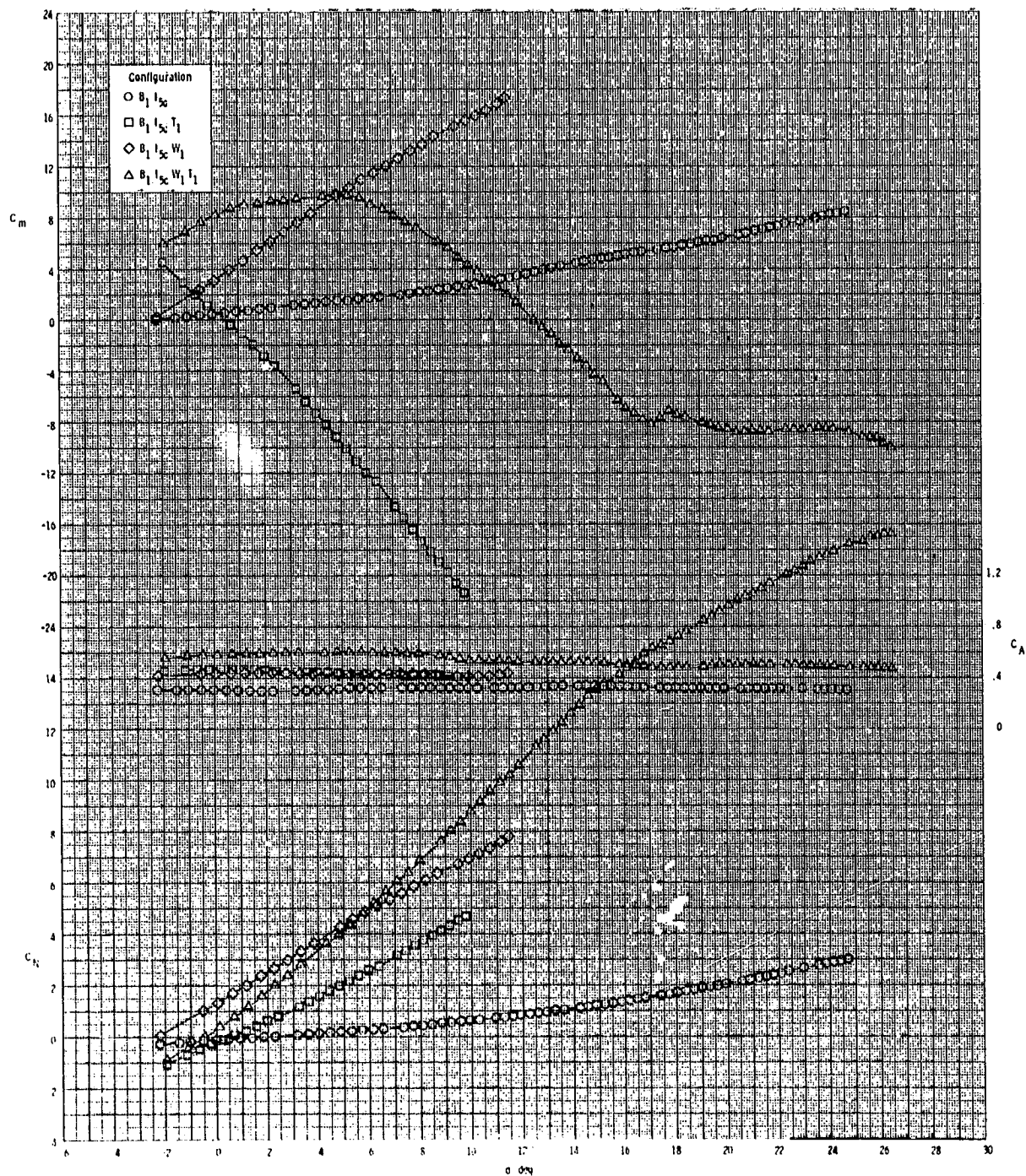
ORIGINAL PAGE IS
OF POOR QUALITY



(b) Concluded.

Figure 40.- Continued.

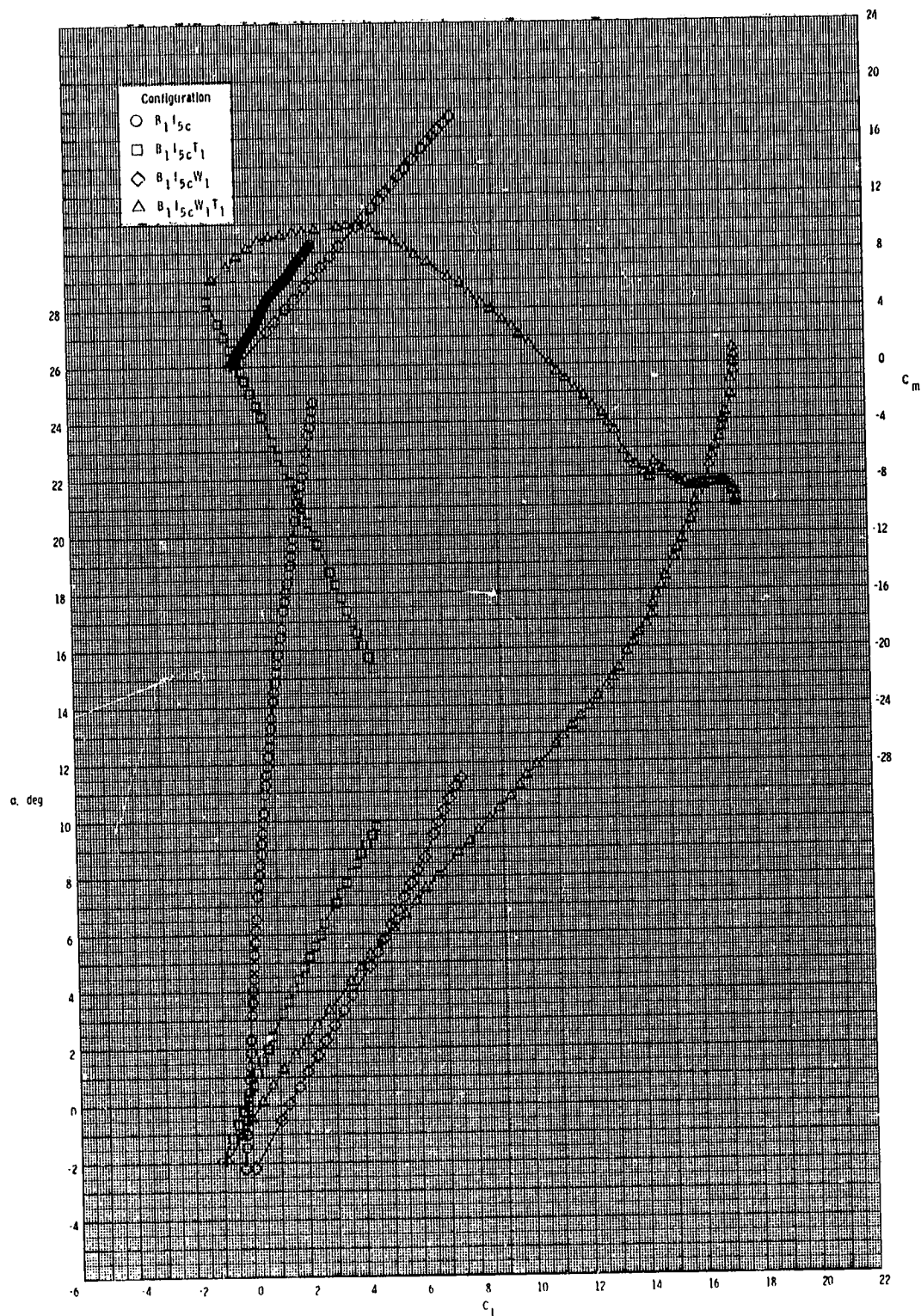
ORIGINAL PAGE IS
OF POOR QUALITY



(c) $M = 0.95$.

Figure 40.-Continued.

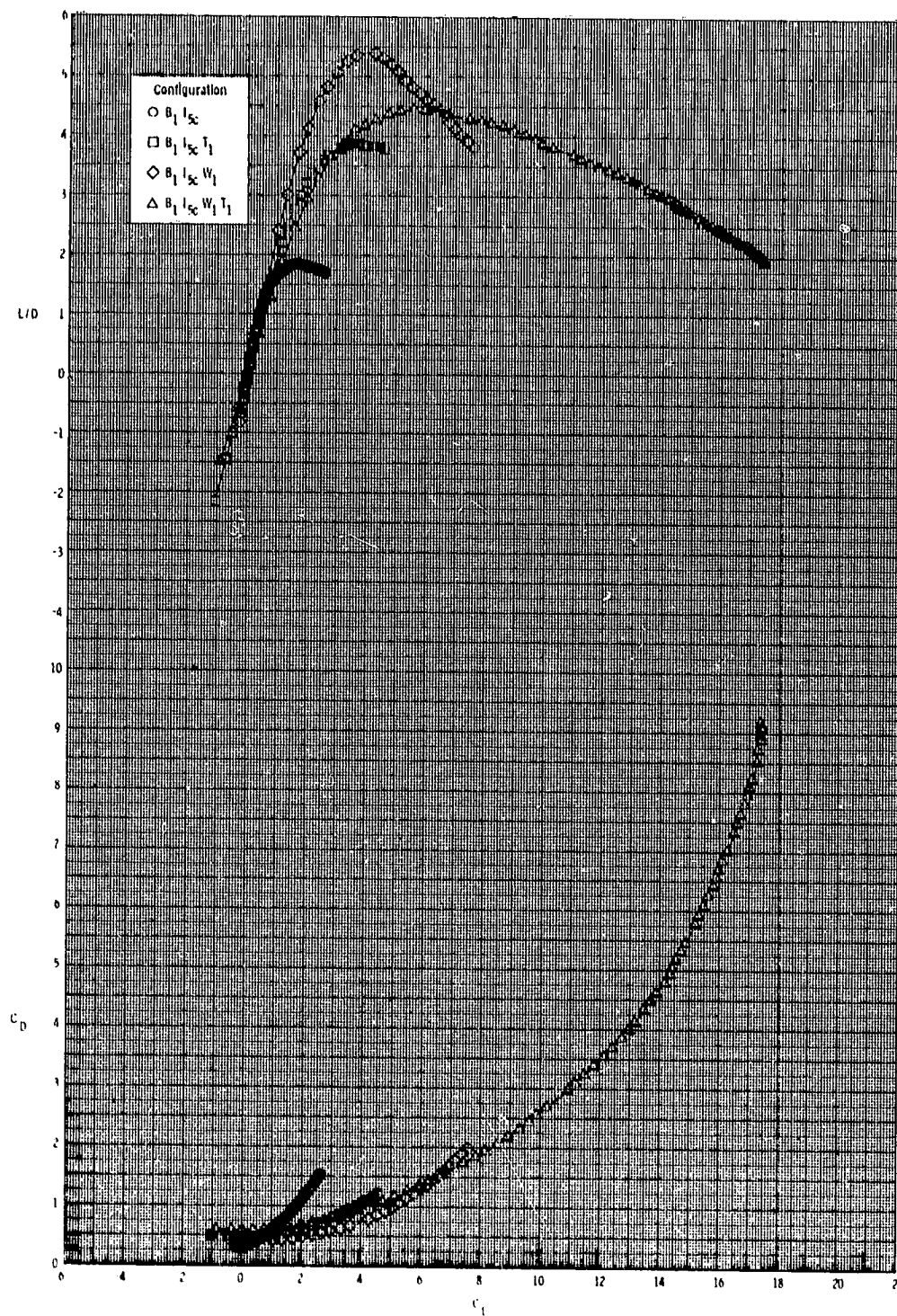
ORIGINAL PAGE IS
OF POOR QUALITY



(c) Continued.

Figure 40.- Continued.

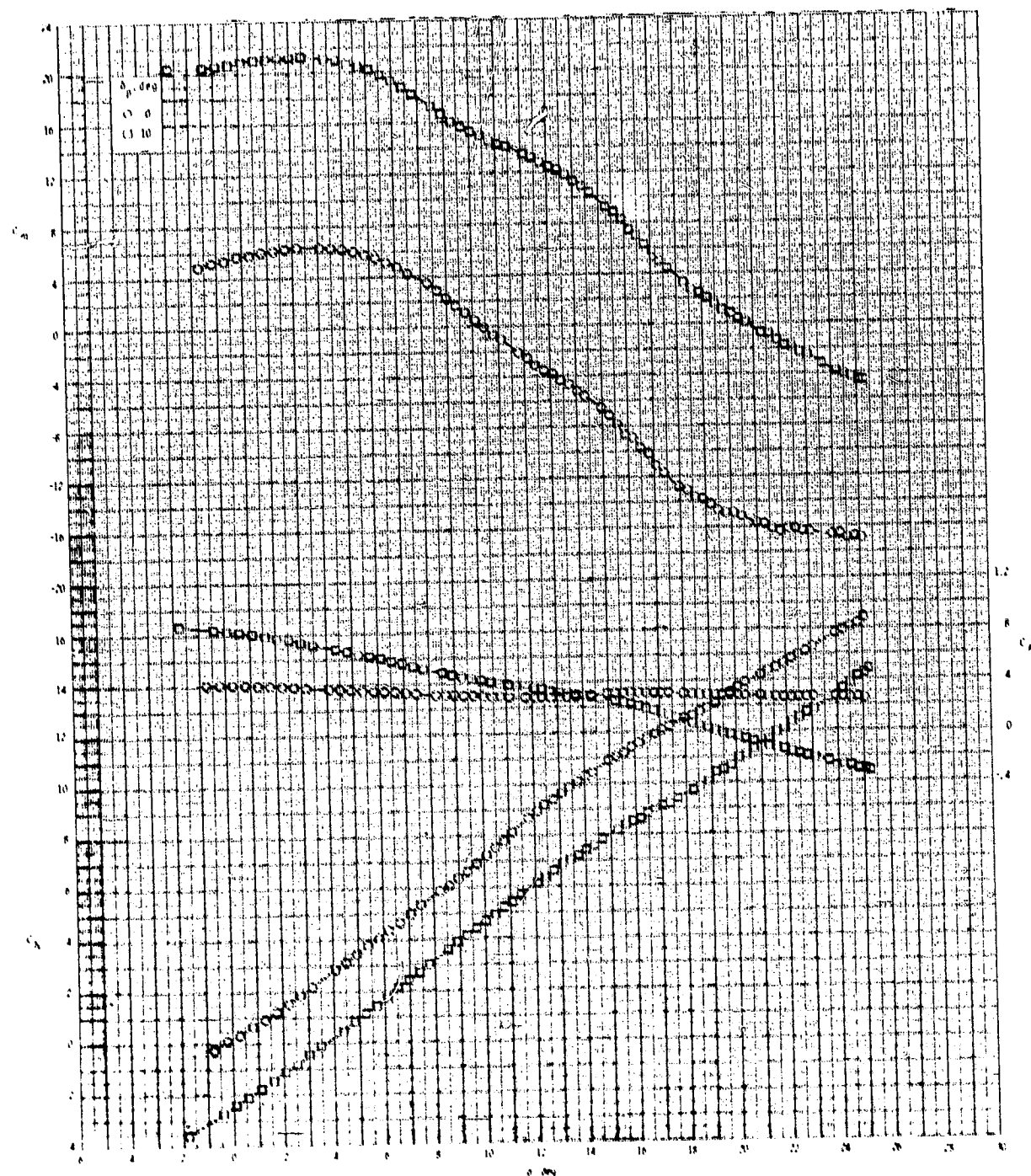
ORIGINAL PAGE IS
OF POOR QUALITY



(c) Concluded.

Figure 40.- Concluded.

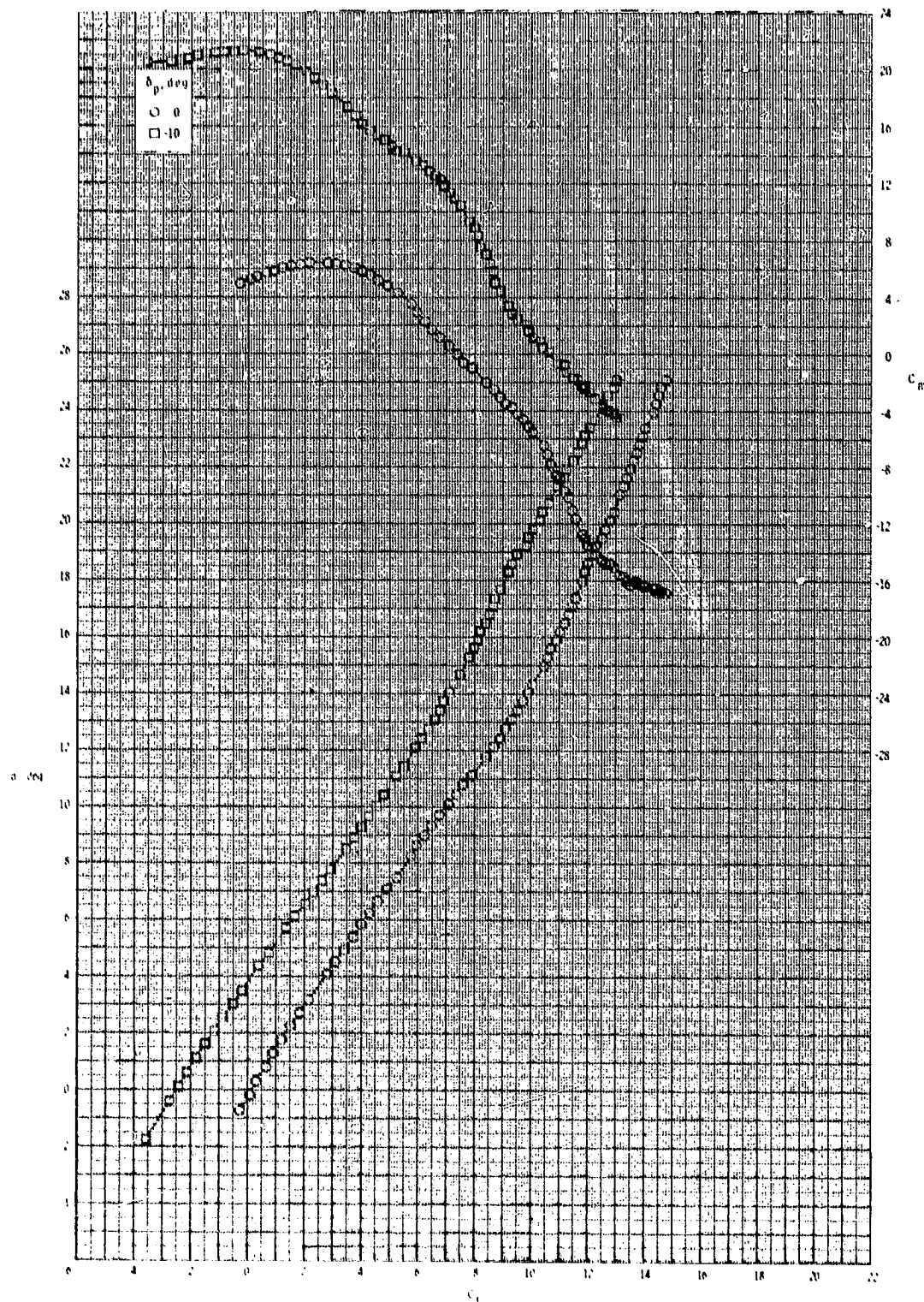
ORIGINAL PAPER
OF POOR QUALITY



(a) $M = 0.60$.

Figure 41.- Pitch-control effectiveness of configuration $B_1I_{5C}W_1T_1$ with internal duct closed.

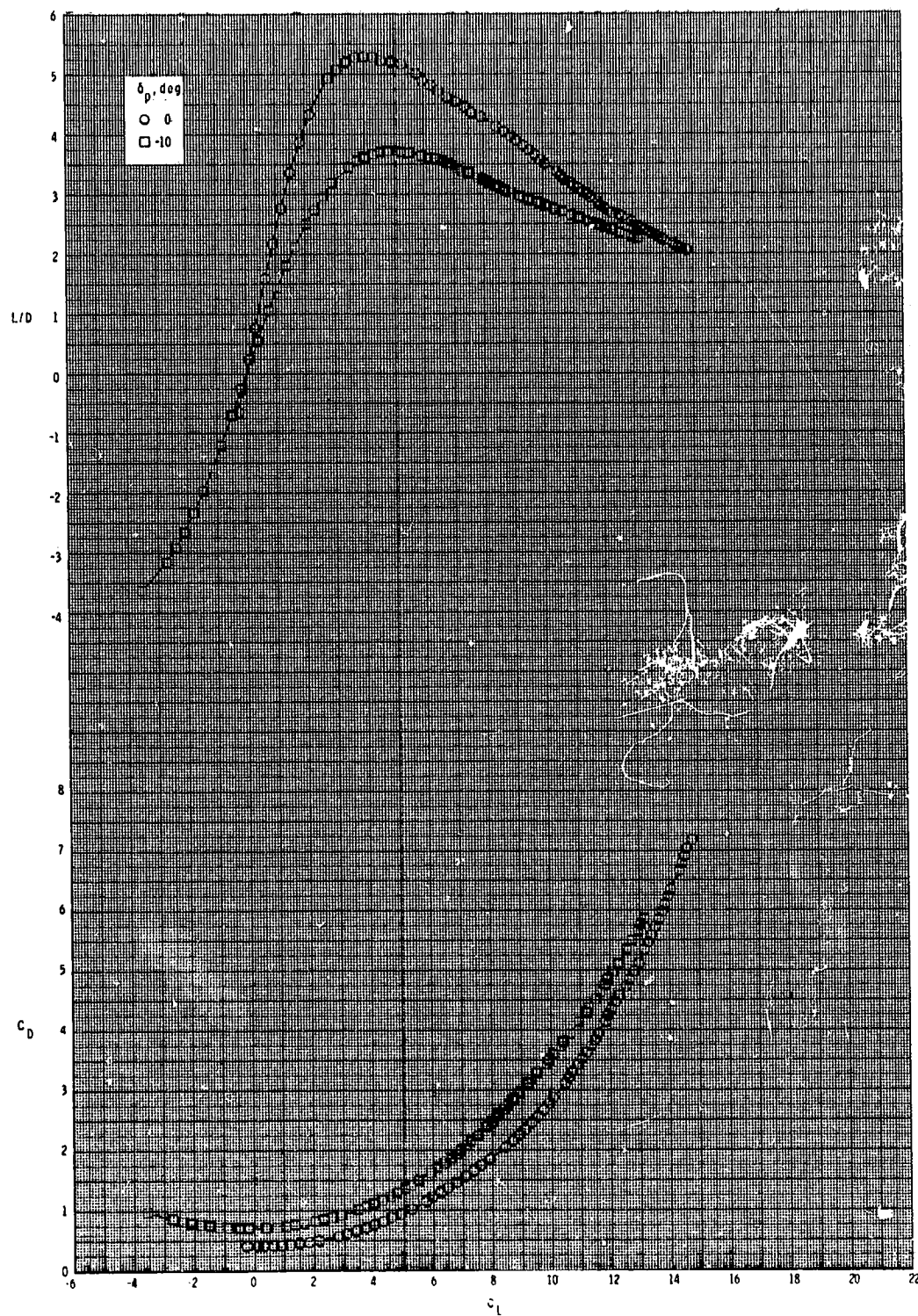
ORIGINAL PAGE IS
OF POOR QUALITY



(a) Continued.

Figure 41.- Continued.

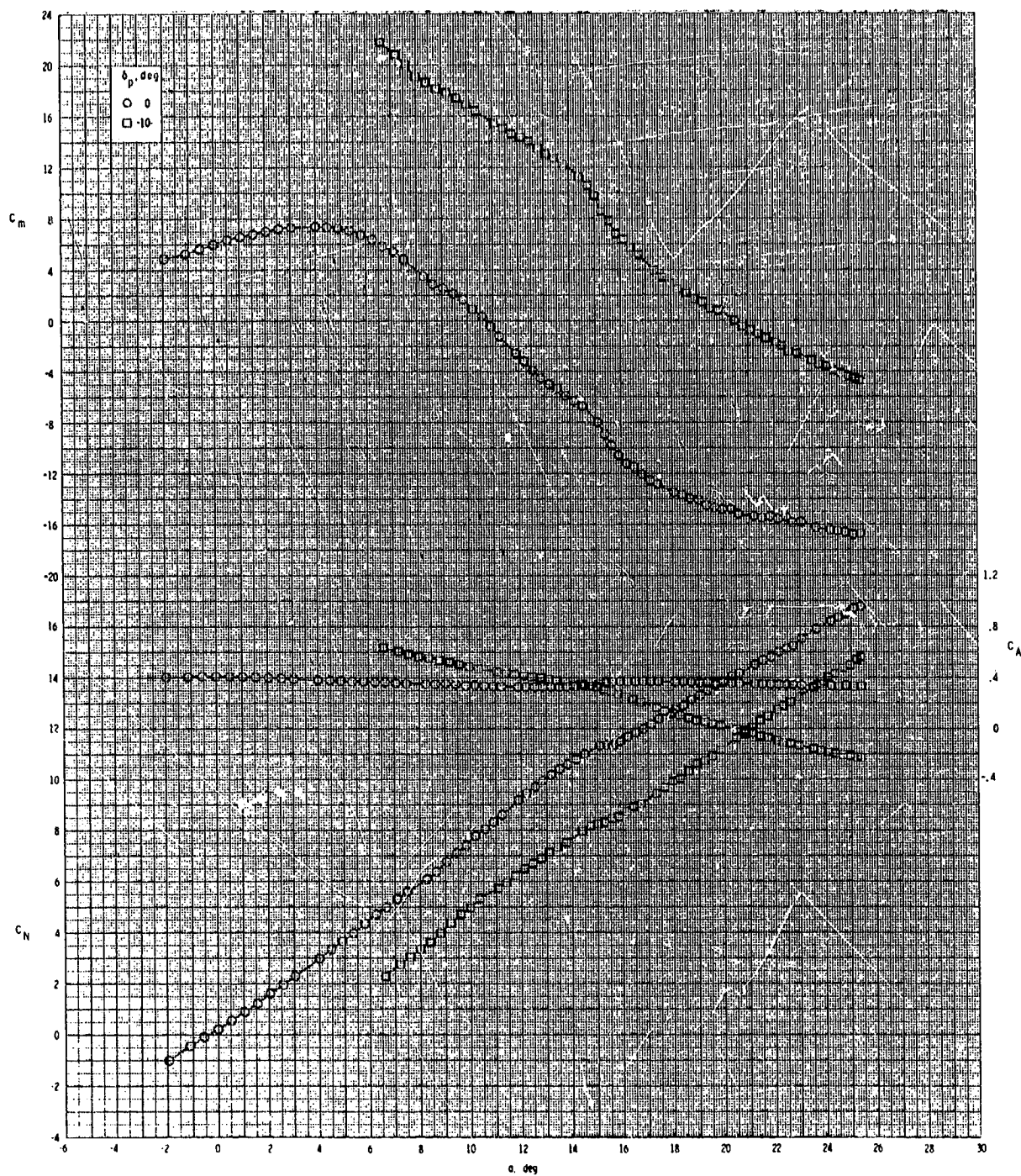
ORIGINAL PAGE IS
OF POOR QUALITY



(a) Concluded.

Figure 41.- Continued.

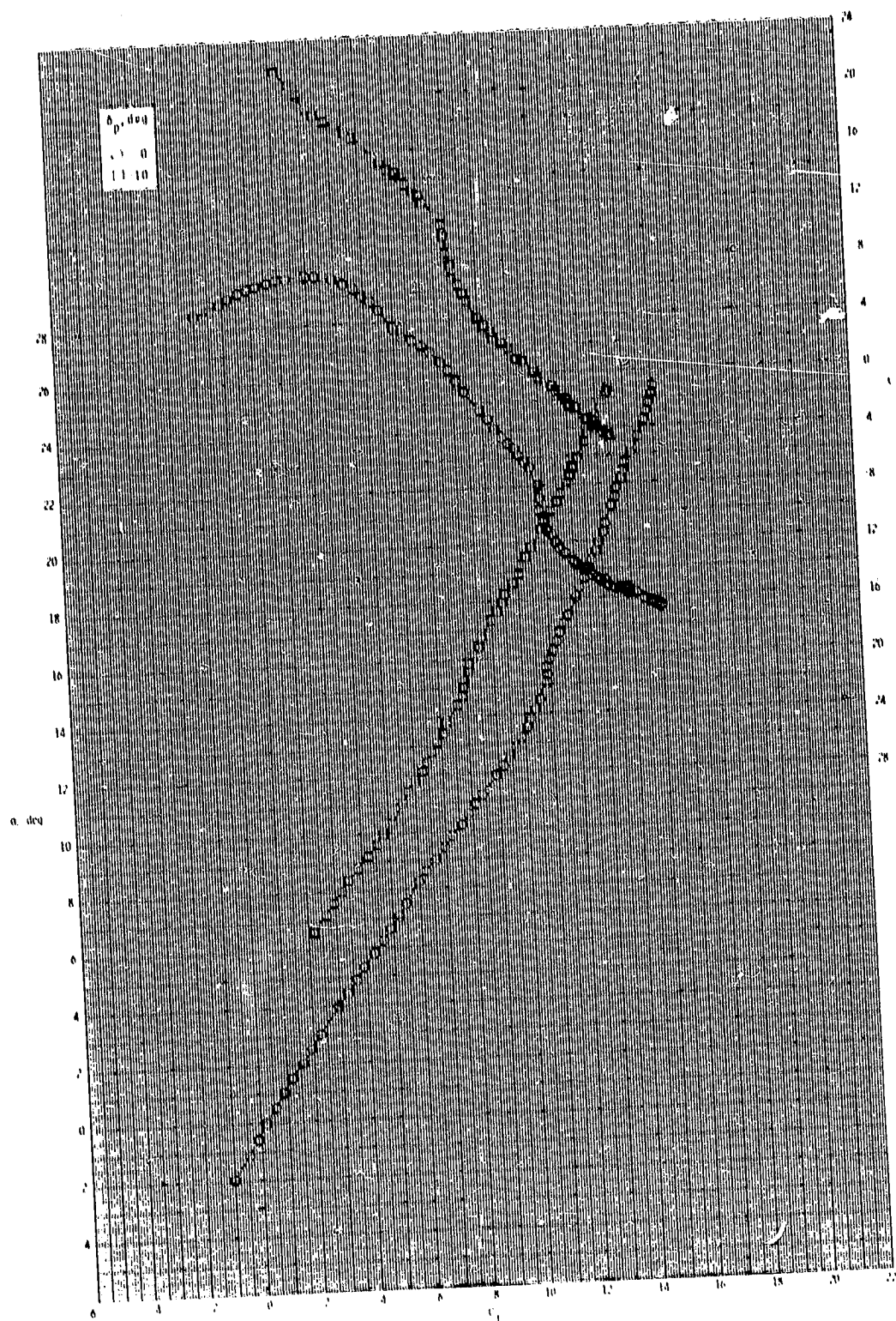
ORIGINAL PAGE IS
OF POOR QUALITY



(b) $M = 0.80$.

Figure 41.- Continued.

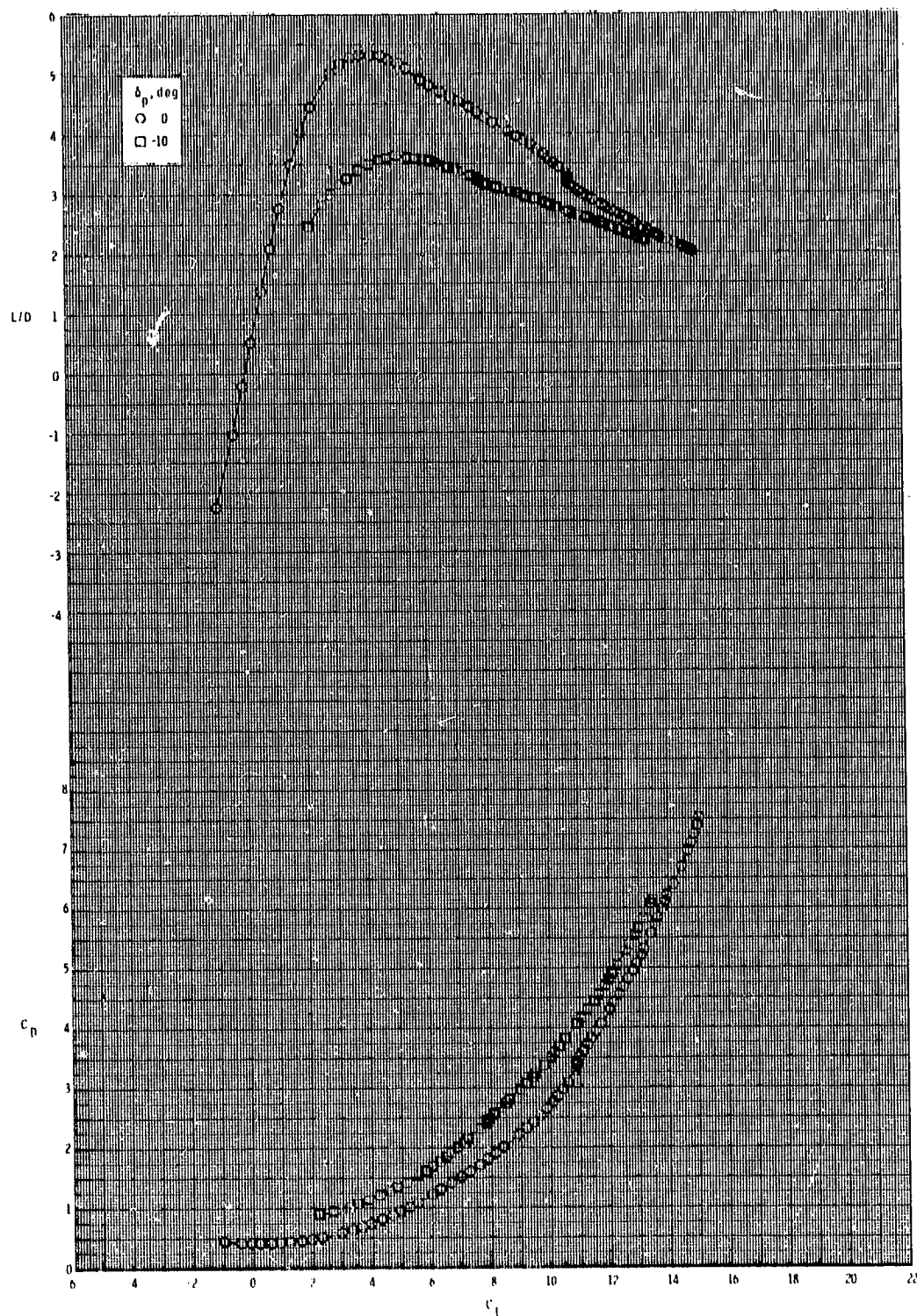
ORIGINAL PAGE IS
OF POOR QUALITY



(b) Continued.

Figure 41.- Continued.

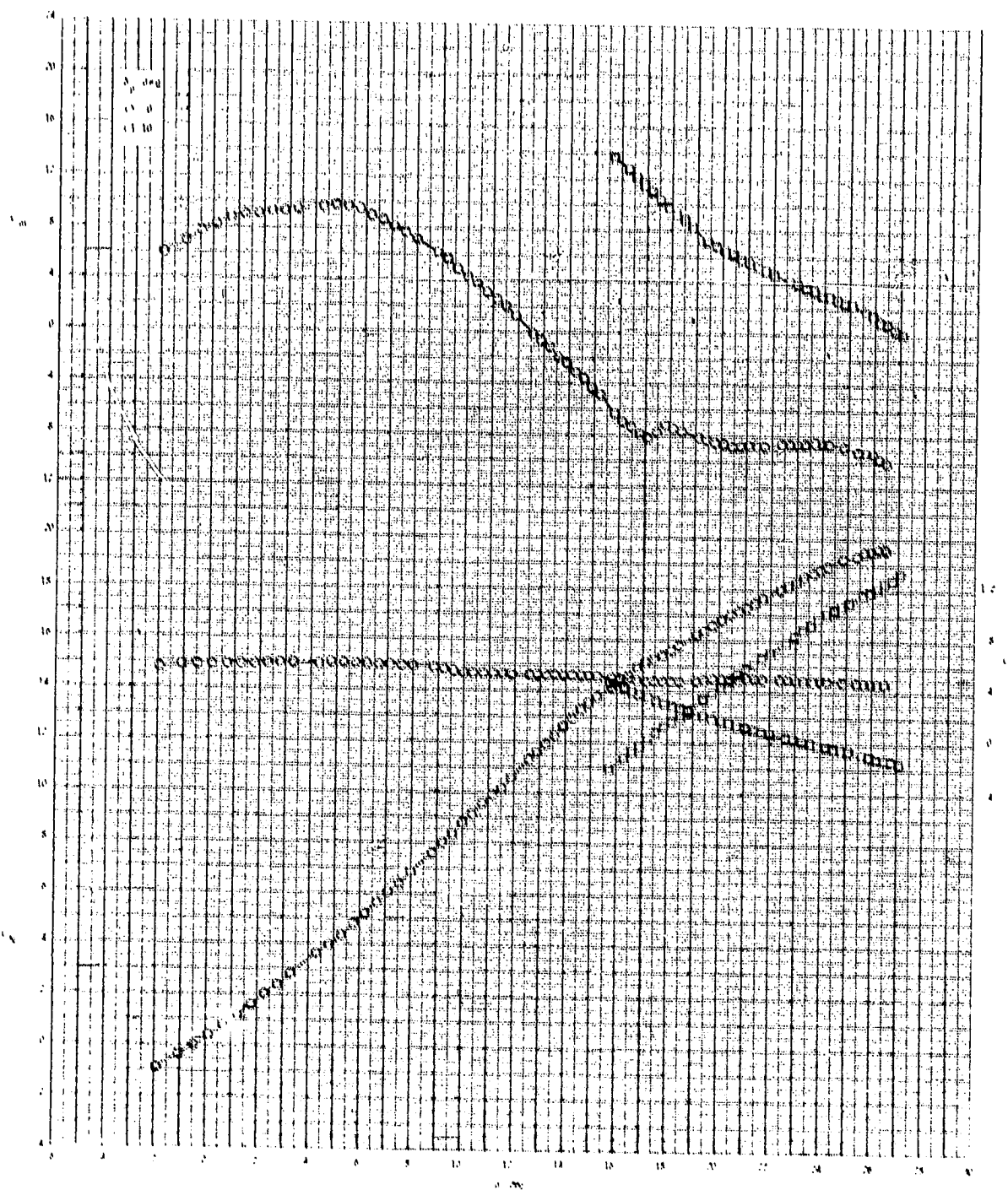
ORIGINAL PAGE IS
OF POOR QUALITY.



(b) Concluded.

Figure 41.- Continued.

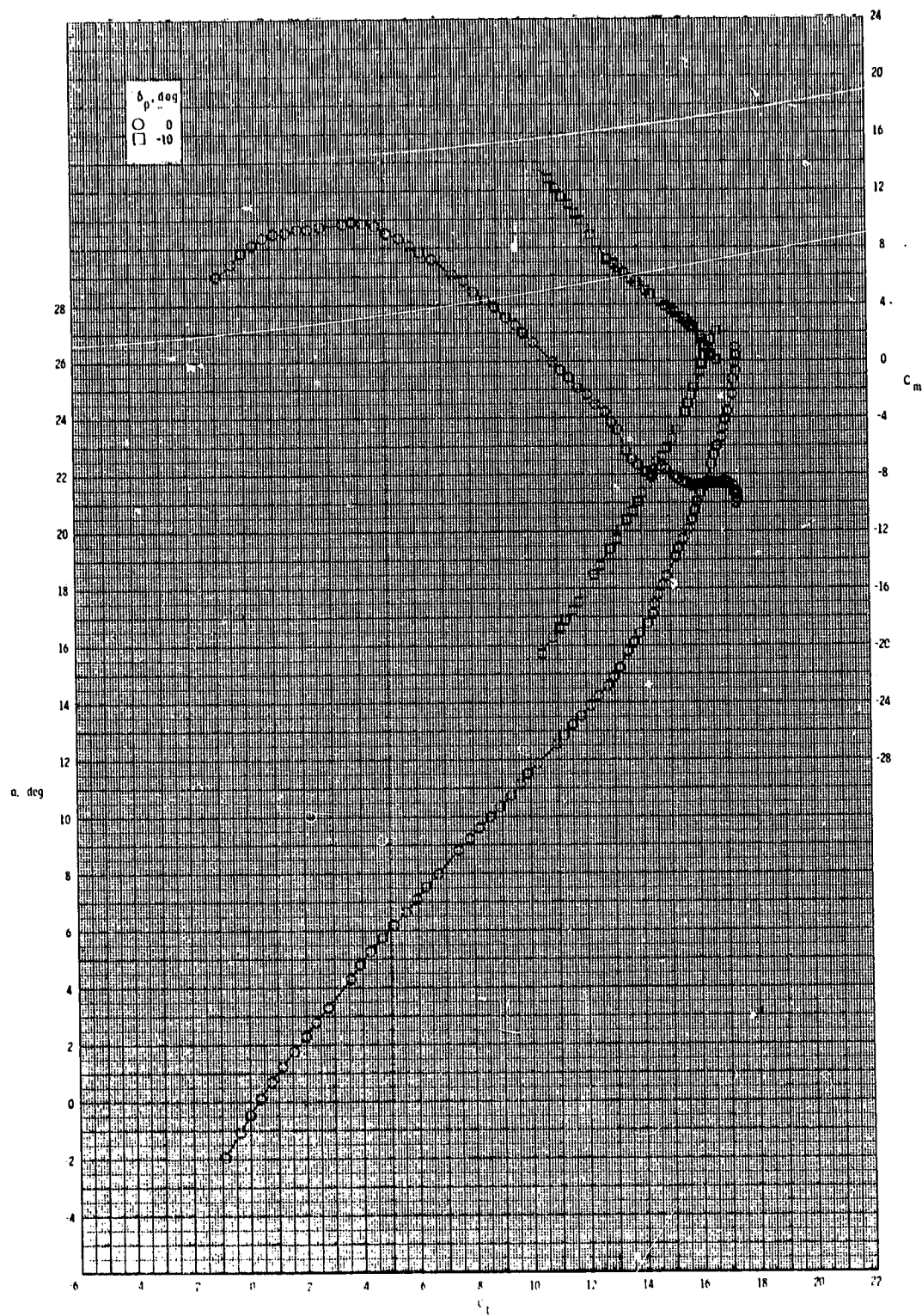
ORIGINAL PAGE IS
OF POOR QUALITY



(c) M 0.95

Figure 41.- Continued.

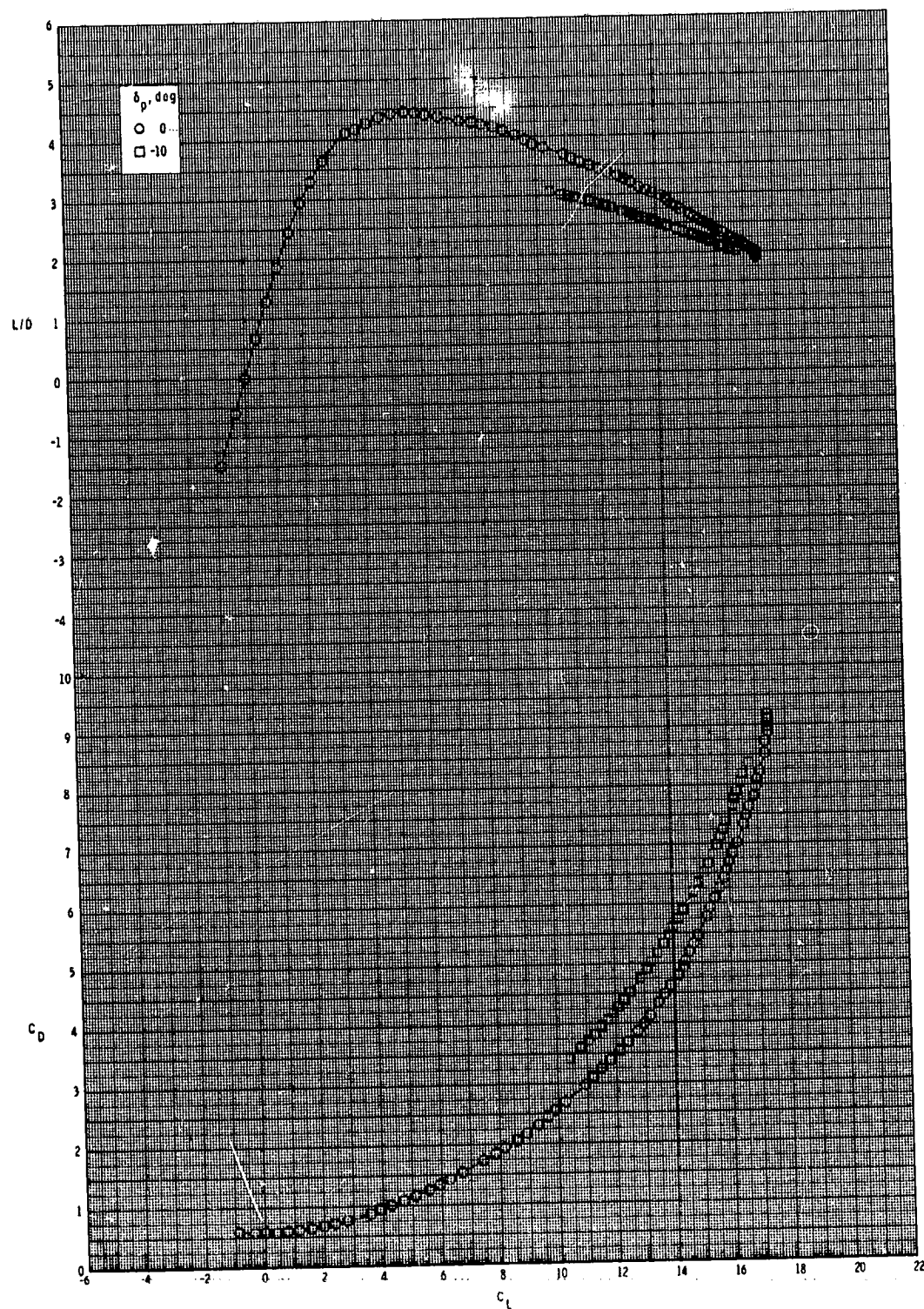
ORIGINAL PAGE IS
OF POOR QUALITY



(c) Continued.

Figure 41.- Continued.

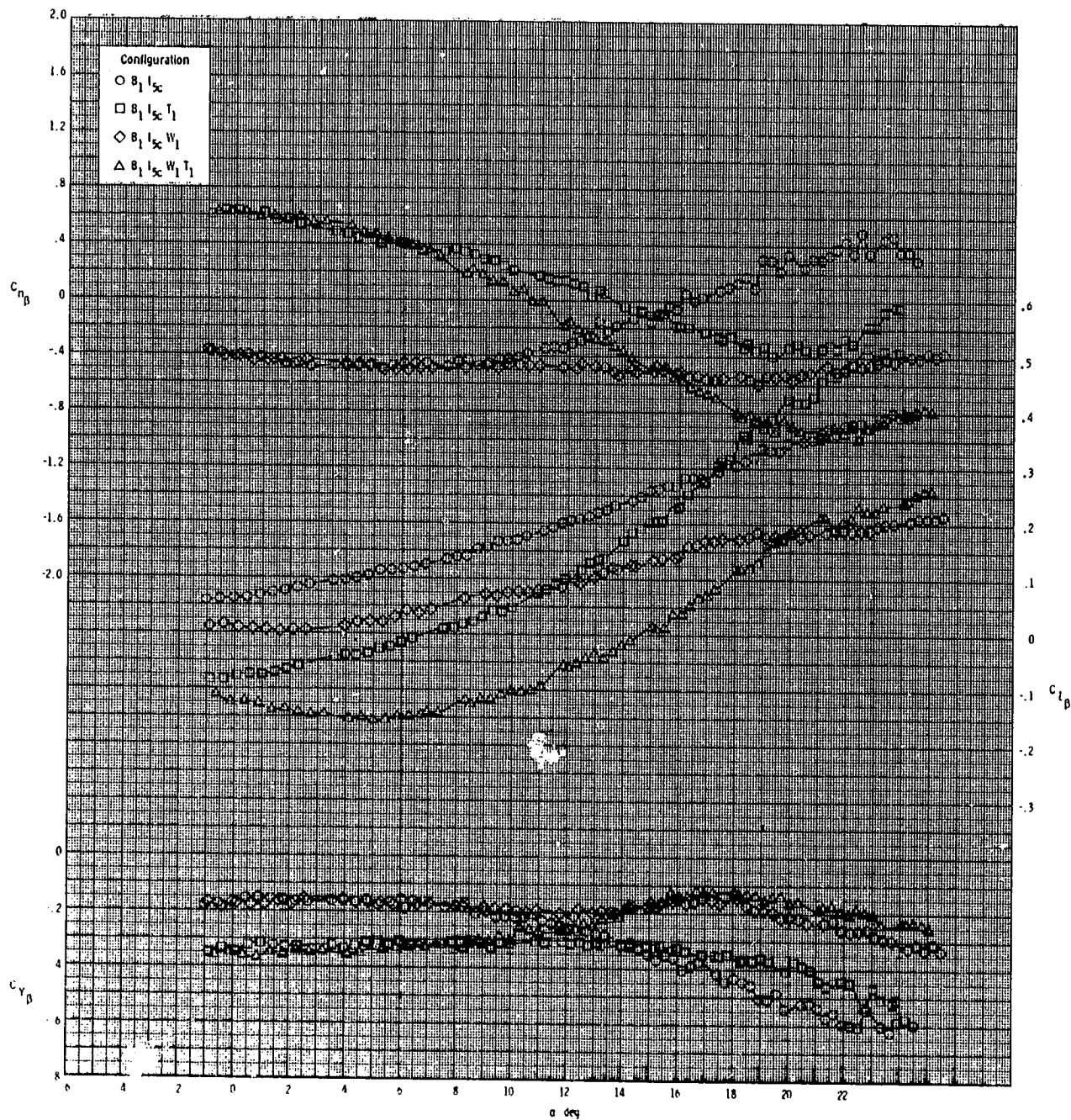
ORIGINAL PAGE 13
OF POOR QUALITY



(c) Concluded.

Figure 41.- Concluded.

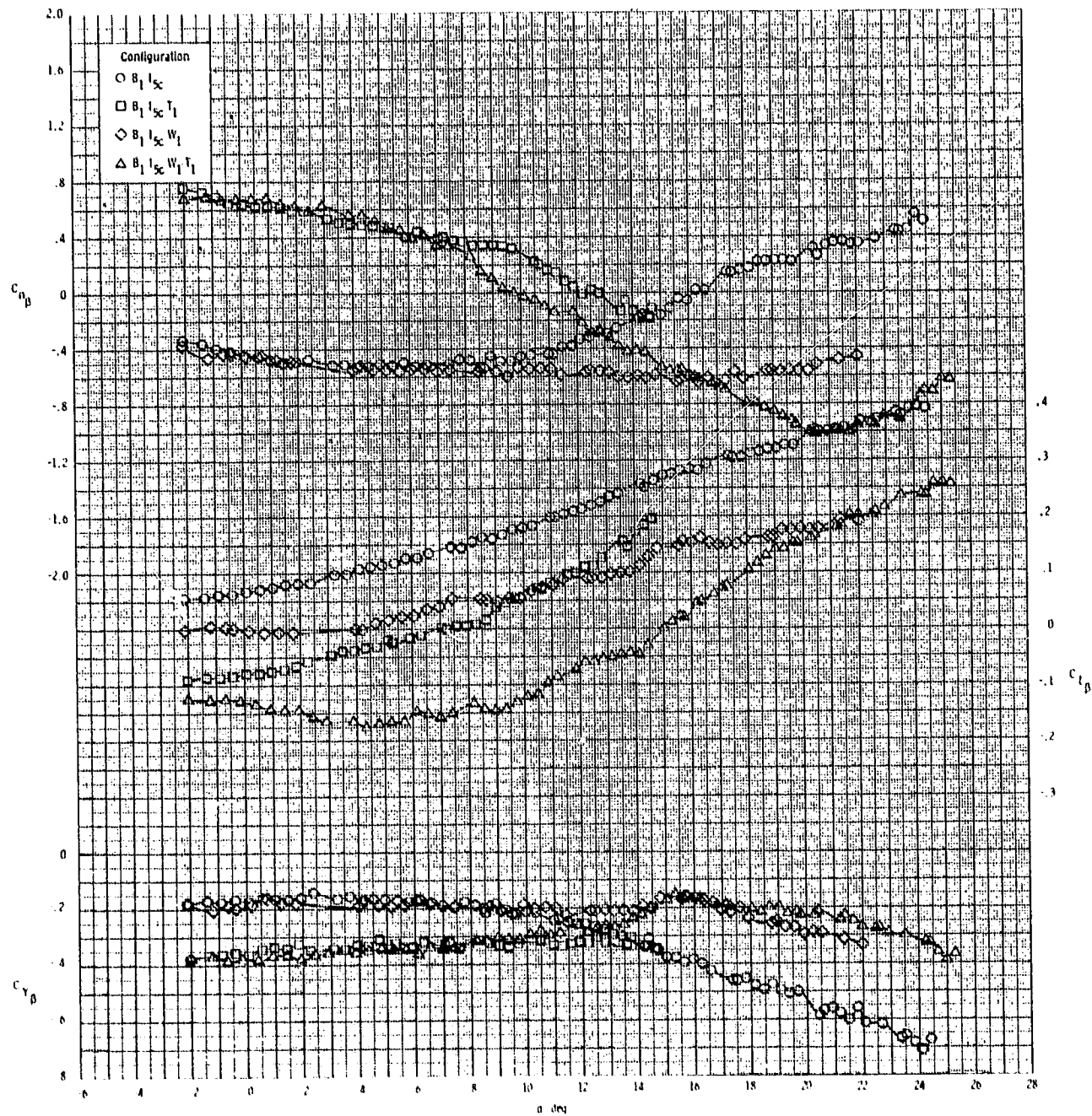
ORIGINAL PAGE IS
OF POOR QUALITY



(a) $M = 0.60$.

Figure 42.- Effect of various model components on lateral-directional stability for 2-D inlet with T_1 and internal duct closed.

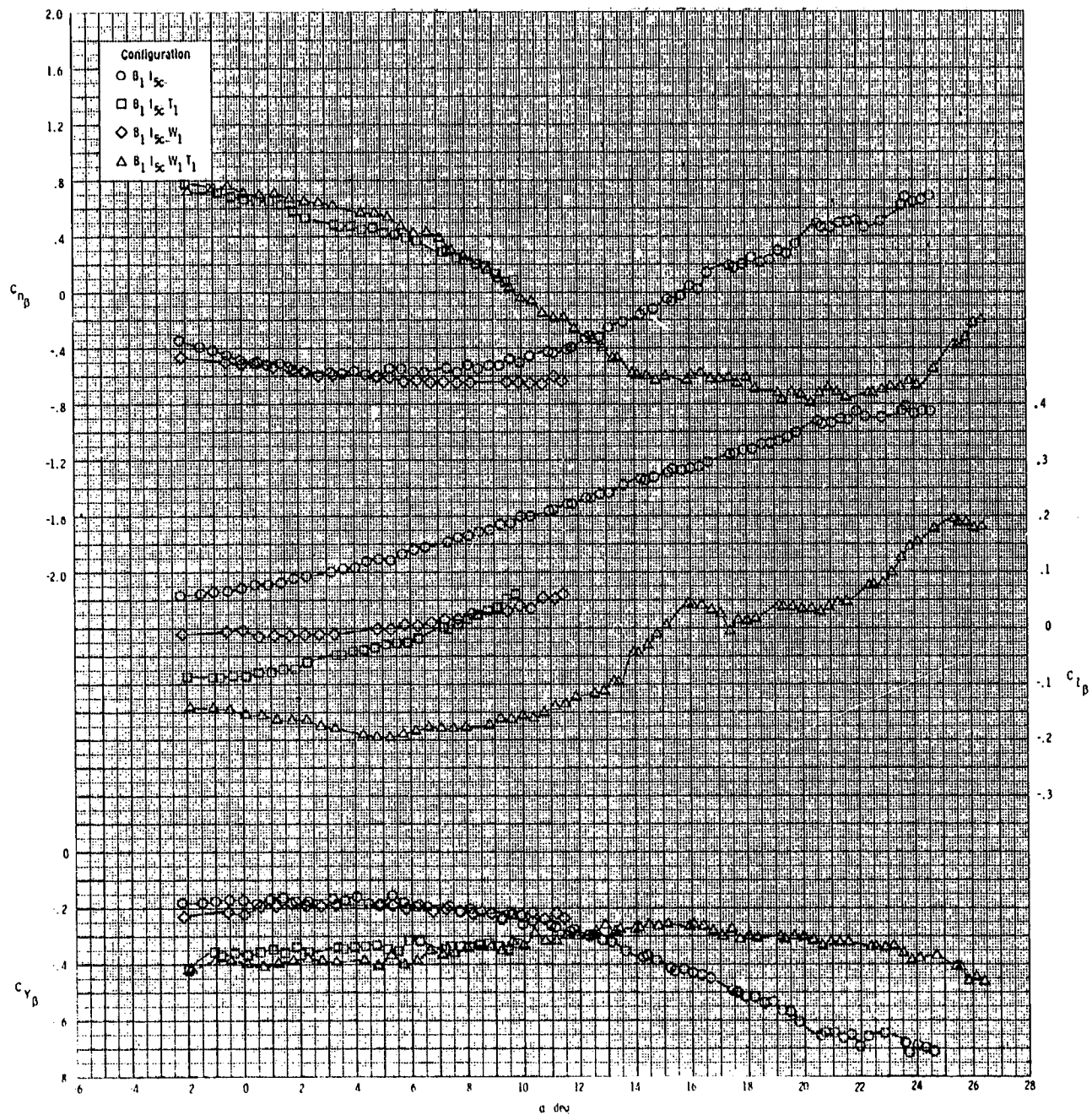
ORIGINAL PAGE IS
OF POOR QUALITY



(b) $M = 0.80$.

Figure 42.- Continued.

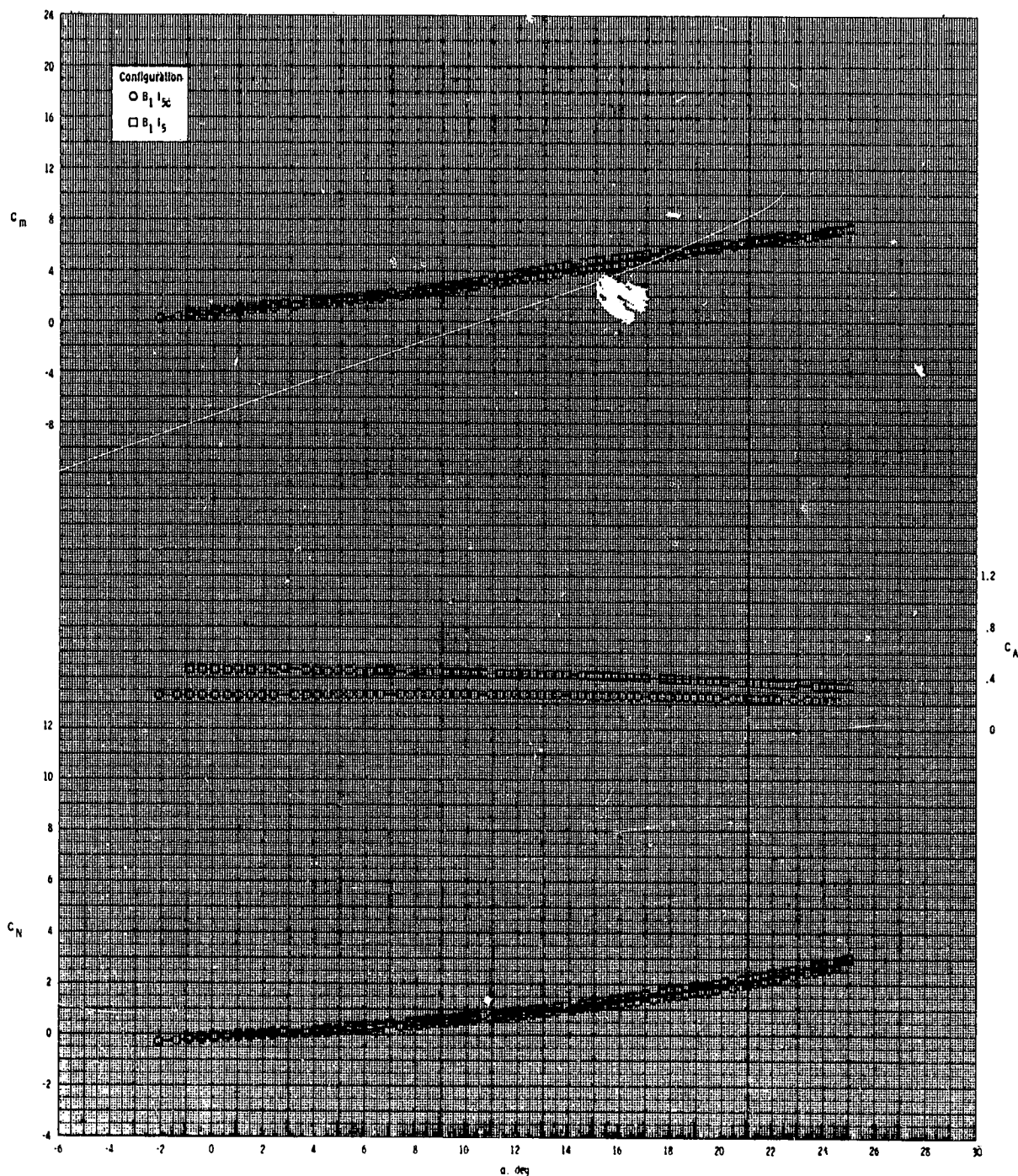
ORIGINAL PAGE IS
OF POOR QUALITY



(c) $M = 0.95$.

Figure 42.- Concluded.

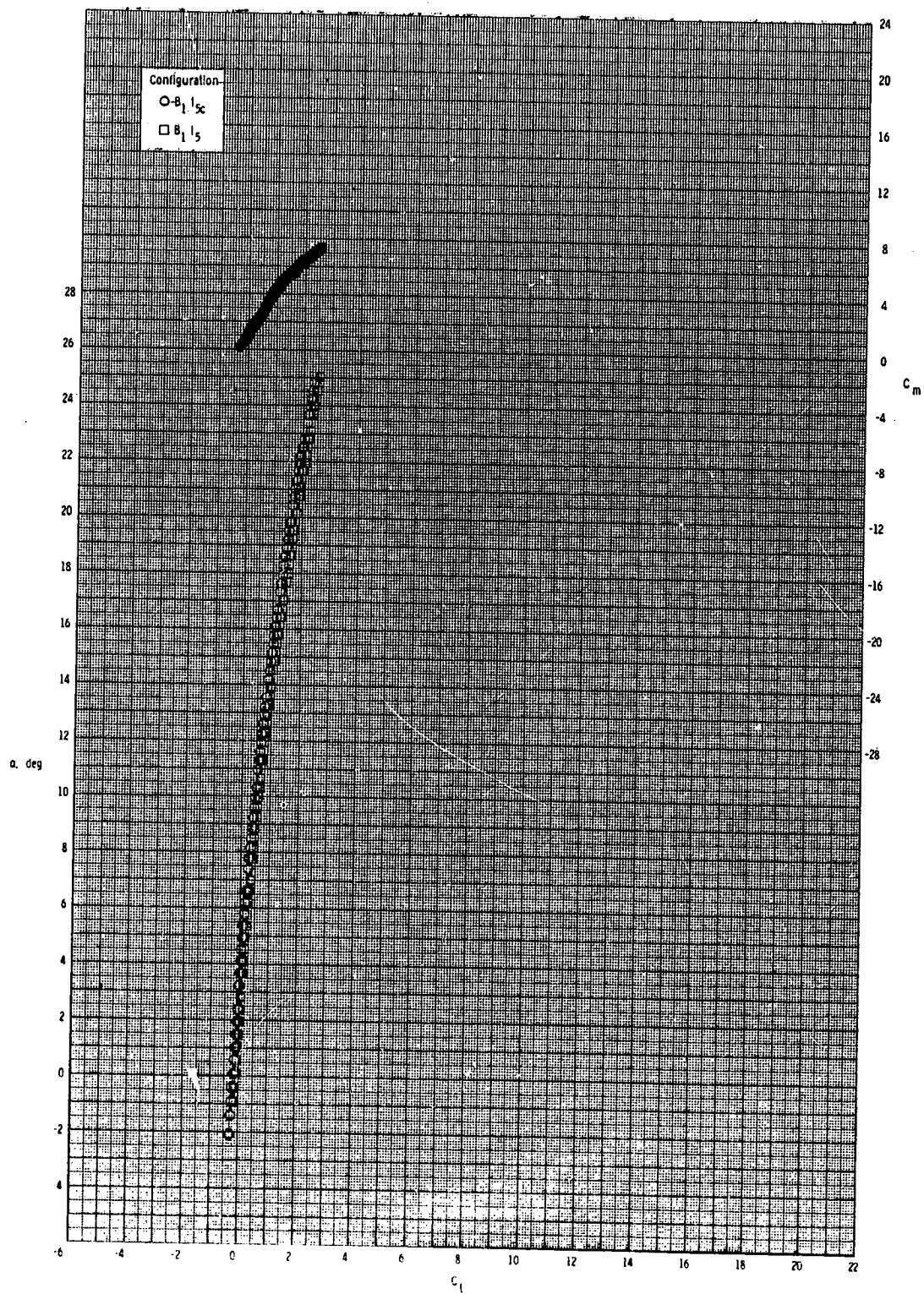
ORIGINAL PAGE IS
OF POOR QUALITY



(a) $M = 0.80$.

Figure 43.- Effect of inlet covers on longitudinal aerodynamic characteristics for 2-D inlet with internal duct closed.

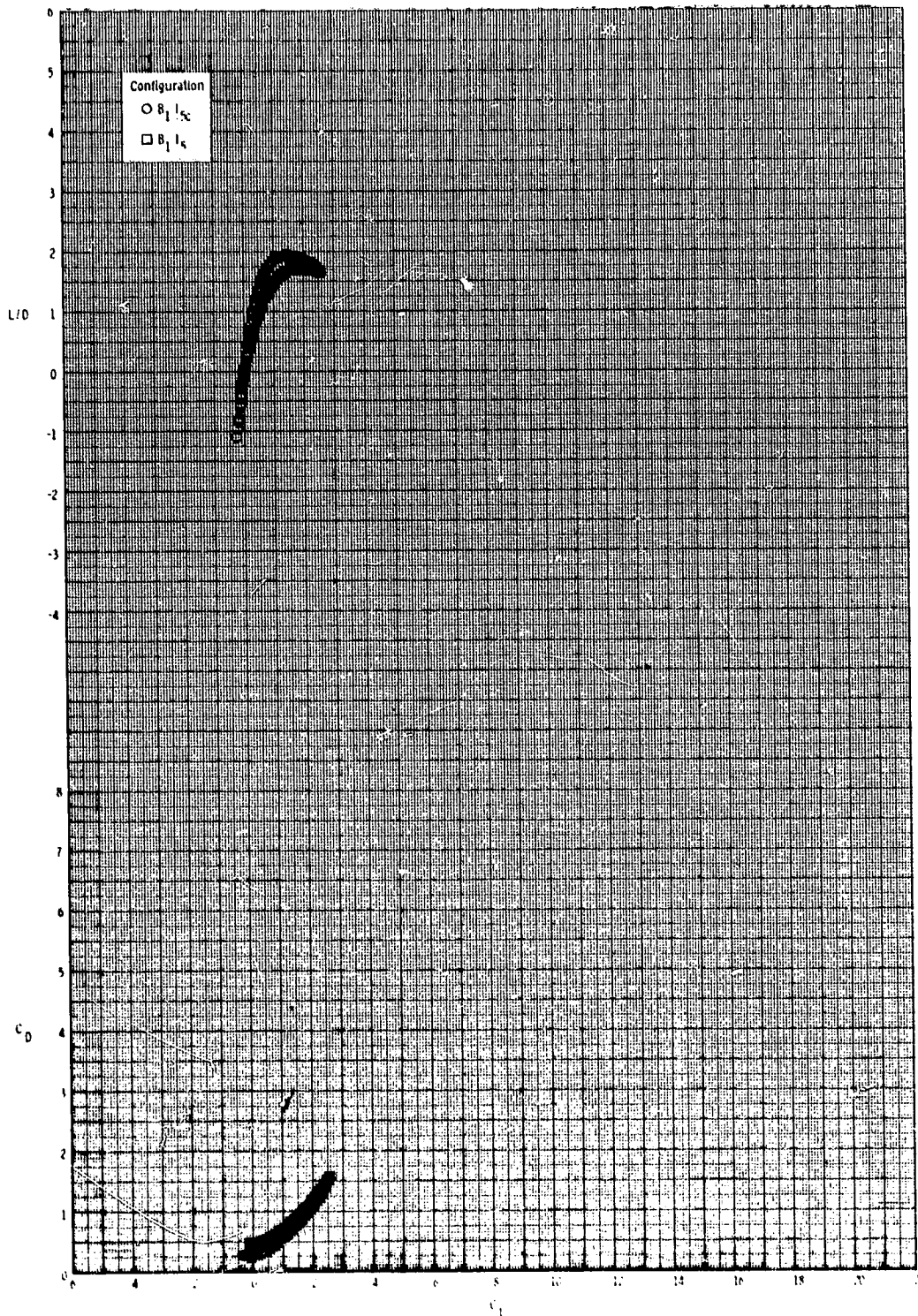
ORIGINAL PAGE IS
OF POOR QUALITY



(a) Continued.

Figure 43.- Continued.

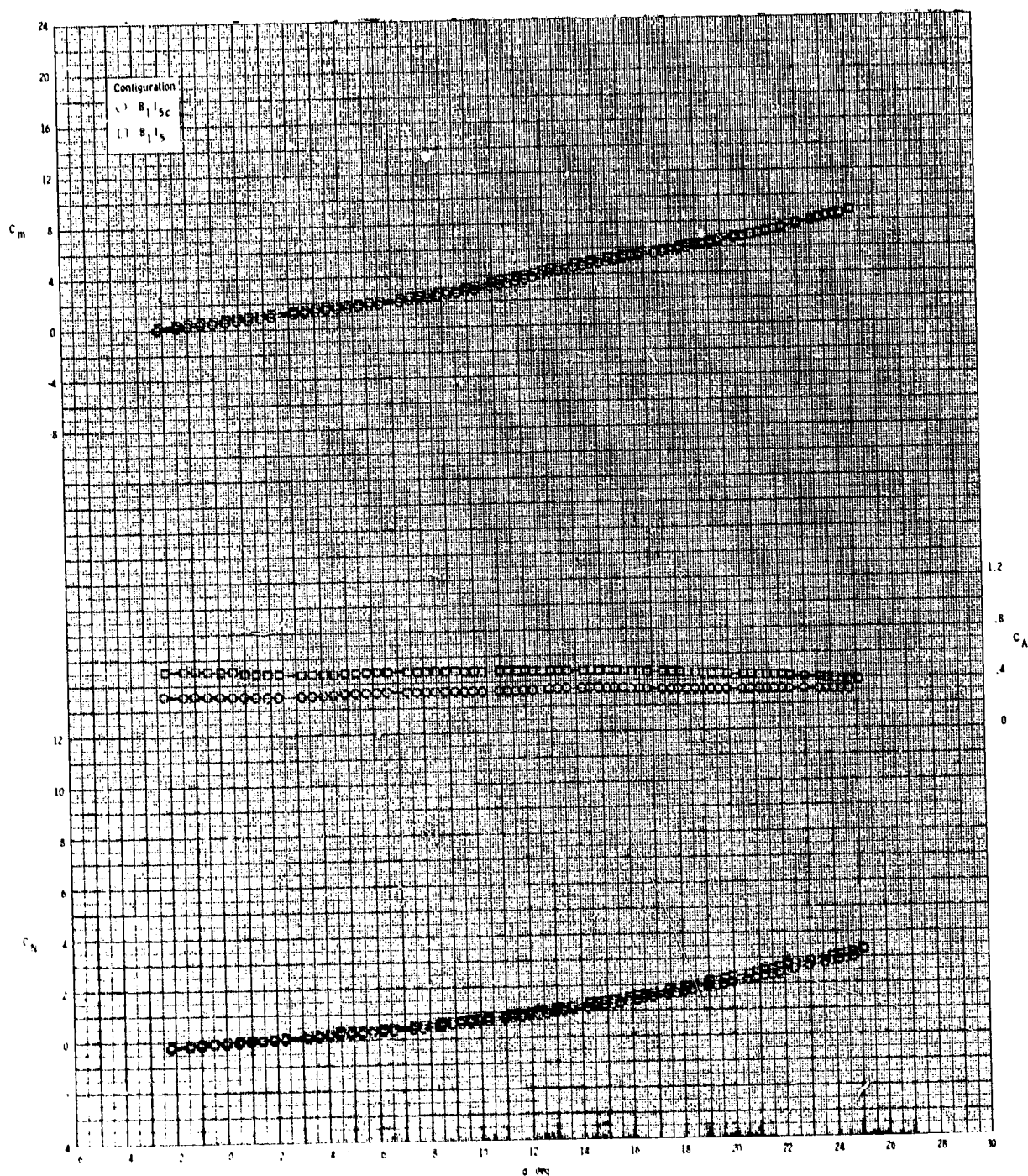
ORIGINAL PAGE IS
OF POOR QUALITY



(a) Concluded.

Figure 43.- Continued.

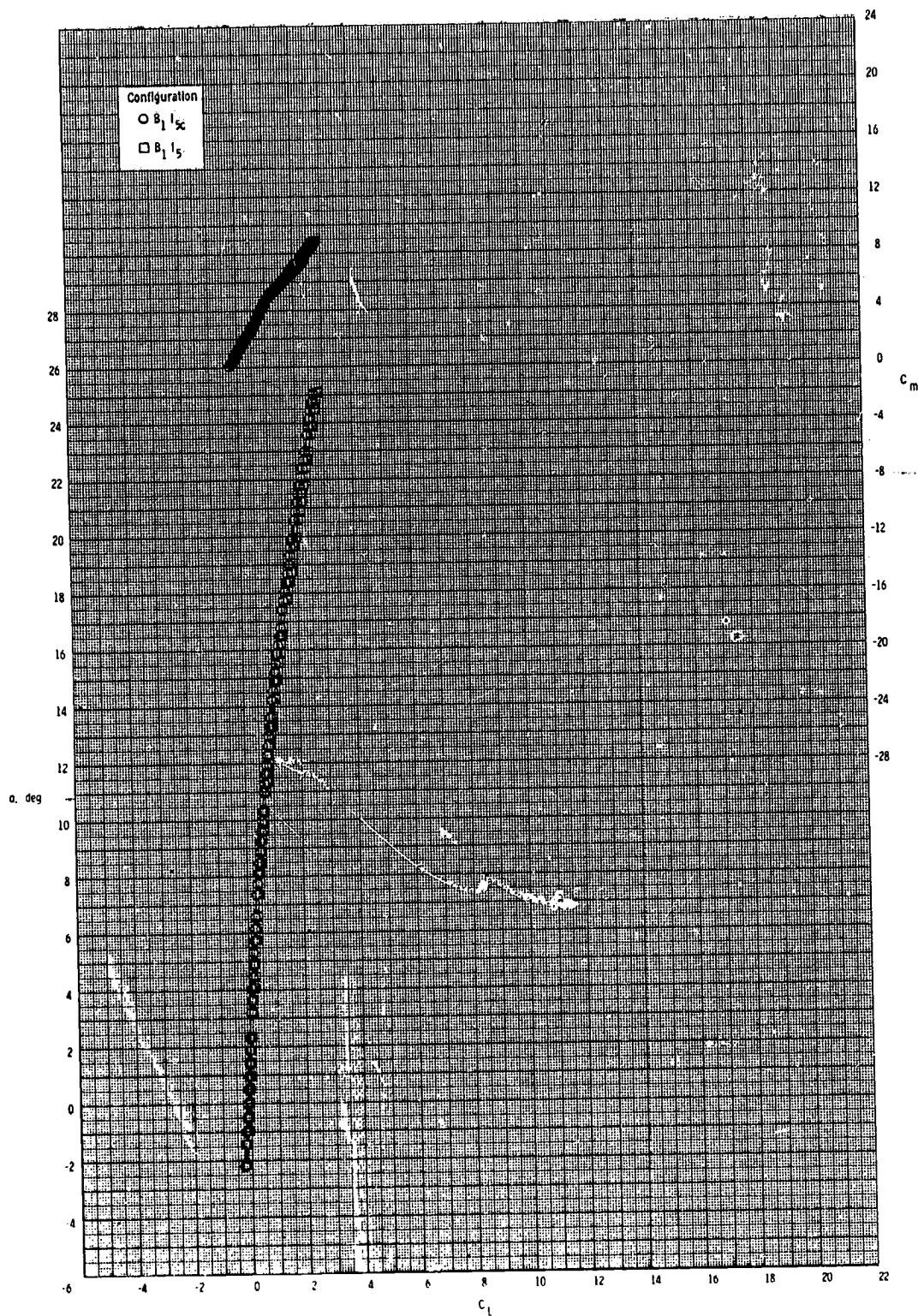
ORIGINAL PAGE IS
OF POOR QUALITY



(b) $M = 0.95$.

Figure 43.- Continued.

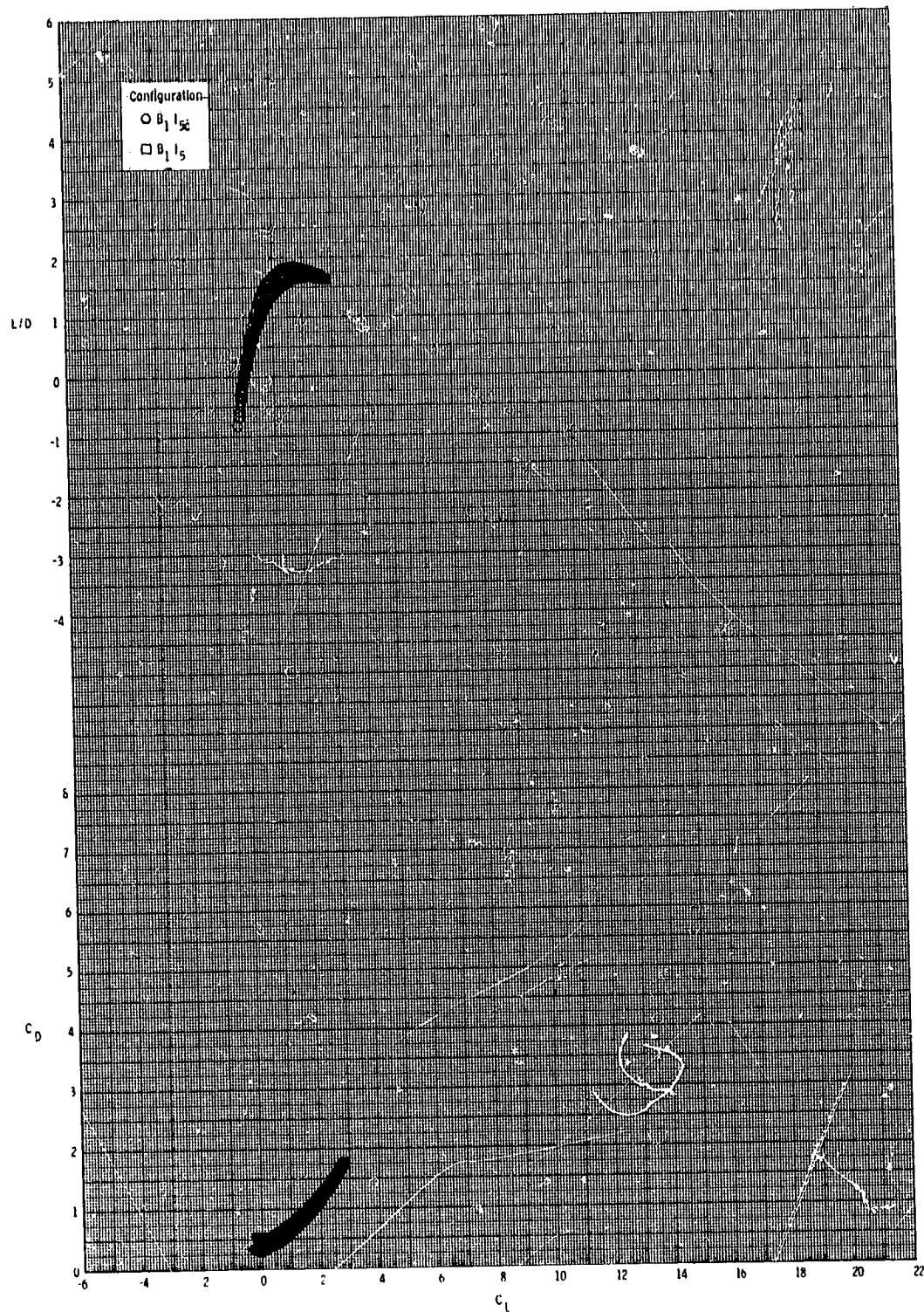
ORIGINAL PAGE IS
OF POOR QUALITY



(b) Continued.

Figure 43.- Continued.

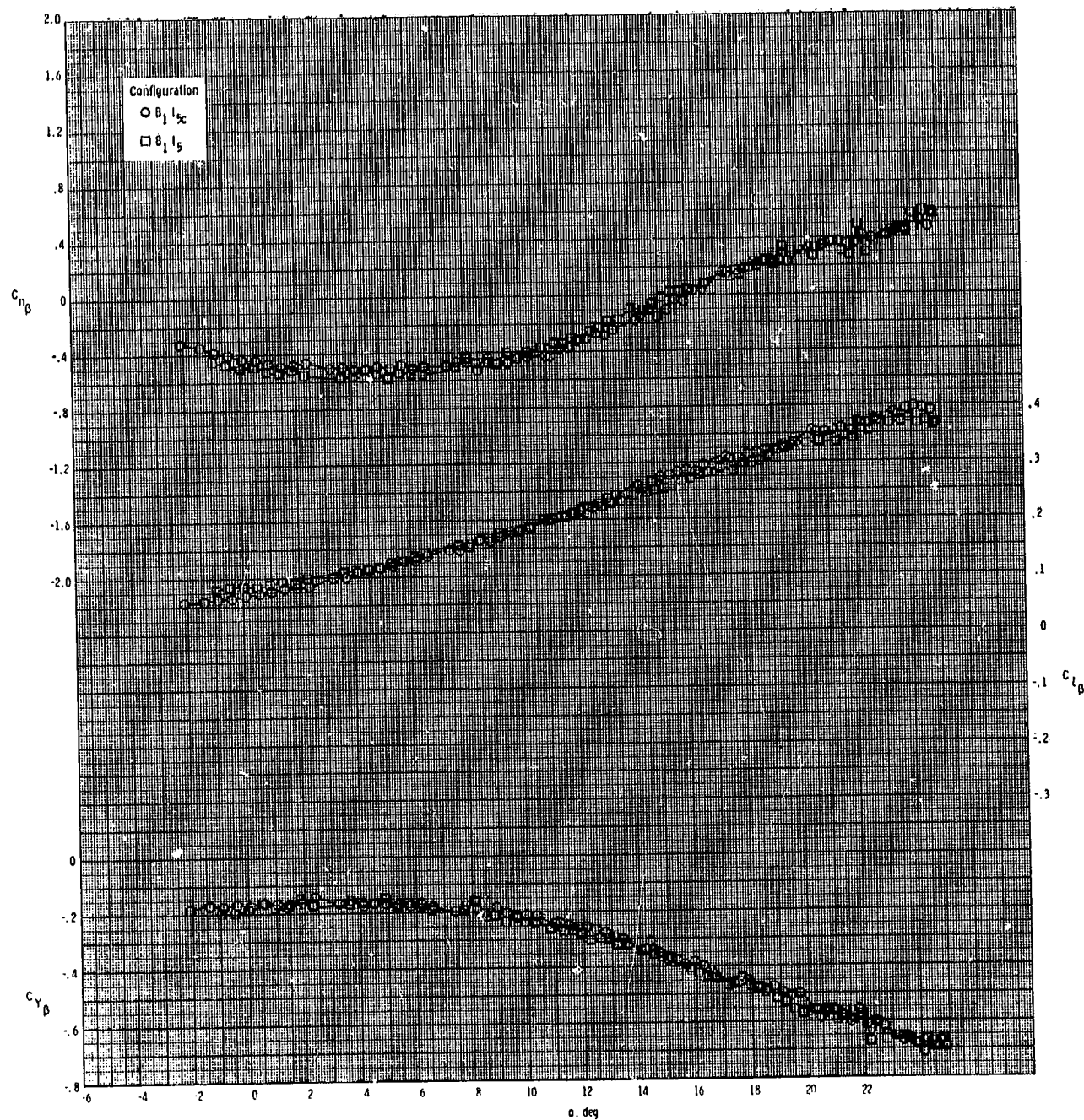
ORIGINAL PAGE IS
OF POOR QUALITY



(b) Concluded.

Figure 43.- Concluded.

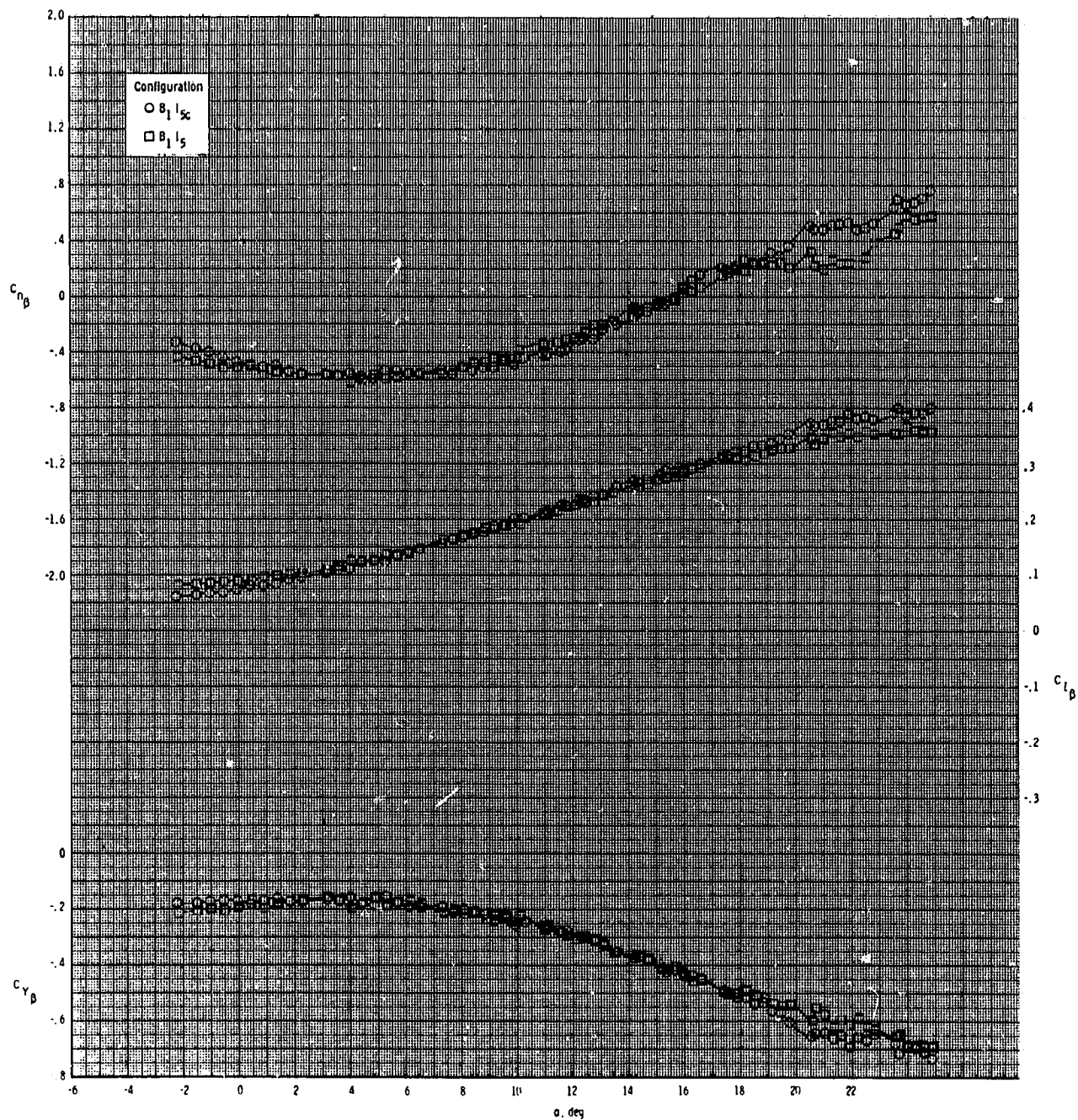
ORIGINAL PAGE IS
OF POOR QUALITY



(a) $M = 0.80$.

Figure 44.- Effect of inlet covers on lateral-directional stability for 2-D inlet with internal duct closed.

ORIGINAL PAGE IS
OF POOR QUALITY



(b) $M = 0.95$.

Figure 44.- Concluded.